

# UNCLASSIFIED

AD NUMBER
AD870734
NEW LIMITATION CHANGE
TO Approved for public release, distribution unlimited
FROM Distribution authorized to U.S. Gov't. agencies and their contractors; Critical Technology; MAY 1970. Other requests shall be referred to Air Force Research Labs., Hanscom AFB, MA.
AUTHORITY
AFCRL ltr, 22 Dec 1971

THIS PAGE IS UNCLASSIFIED

# Airborne Measurements Of Optical Atmospheric Properties

## At Night

AD 870734

AD No. \_\_\_\_\_  
DDC FILE COPY

Seibert Q. Duntley

Richard W. Johnson

Jacqueline I. Gordon

Almerian R. Boileau

This document is subject to special export controls and each transmittal to foreign governments or foreign nations may be made only with prior approval of AFCRL (CROA), L. G. Hanscom Field, Bedford, Massachusetts 02173.

FINAL REPORT MAY 1970

Period covered: January 19, 1967 through April 30, 1970

CONTRACT NO. F 19628-67-C-0181

Project No. 7621

Task No. 762107

Work Unit No. 76210701

MULTIPLE REPRINTS INCLUDED

Contract Monitor: Leo J. Sheehan, Major, USAF  
Optical Physics Laboratory

Prepared for

Air Force Cambridge Research Laboratories, Office of Aerospace Research  
United States Air Force, Bedford, Massachusetts 01730

UNIVERSITY  
OF  
CALIFORNIA  
SAN DIEGOSCRIPPS  
INSTITUTION  
OF  
OCEANOGRAPHY

VISIBILITY LABORATORY San Diego, California 92152

AFCRL-70-0137

UNIVERSITY OF CALIFORNIA, SAN DIEGO  
SCRIPPS INSTITUTION OF OCEANOGRAPHY  
VISIBILITY LABORATORY  
SAN DIEGO, CALIFORNIA 92152

## AIRBORNE MEASUREMENTS OF OPTICAL ATMOSPHERIC PROPERTIES AT NIGHT

Seibert Q. Duntley, Richard W. Johnson,  
Jacqueline I. Gordon, and Almerian R. Boileau

CONTRACT NO. F 19628-67-C-0181

Project No. 7621

Task No. 762107

Unit No. 76210701

### FINAL REPORT

Period Covered: January 19, 1967 through April 30, 1970

SIO Ref. 70-7

May 1970

Contract Monitor: Leo J. Sheehan, Major, USAF  
Optical Physics Laboratory

### MULTIPLE REPRINTS INCLUDED

This document is subject to special export controls and each transmittal to foreign governments or foreign nationals may be made only with prior approval of AFCRL (CROA), L. G. Hanscom Field, Bedford, Massachusetts 02173.

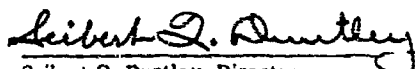
Prepared for

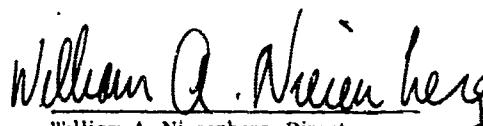
AIR FORCE CAMBRIDGE RESEARCH LABORATORIES  
OFFICE OF AEROSPACE RESEARCH  
UNITED STATES AIR FORCE  
BEDFORD, MASSACHUSETTS 01730

Approved:

REPRODUCED FROM COLOR STOCK

Approved for Distribution:

  
Seibert Q. Duntley, Director  
Visibility Laboratory

  
William A. Nierenberg, Director  
Scripps Institution of Oceanography

# Abstract

This report presents atmospheric optical data collected at night in Thailand chiefly with airborne instruments during two field expeditions, one trip made during the wet monsoon season and one during the dry season. Results from eighteen flights are presented. The data include irradiance, directional reflectance of backgrounds, total scattering coefficients, atmospheric beam transmittance, path radiance, and directional path reflectance. Data for starlight, moonlight, and overcast conditions were derived for downward-looking paths of sight inclined at seven zenith angles ( $93^\circ$ ,  $95^\circ$ ,  $100^\circ$ ,  $105^\circ$ ,  $120^\circ$ ,  $150^\circ$ , and  $180^\circ$ ) from altitudes of 1524 m and lower in five spectral regions, as follows: four narrow band optical filters with maximum transmittances at 475, 515, 660, and 745 nm; one broad band sensitivity representing the S-20 multiplier phototubes fitted with UV reflection filter. Simultaneous photoelectric (Royco) measurements of the distributions of atmosphere particle sizes are reported.



# Summary

This is the Final Report prepared in compliance with AFCRL contract F 19628-67-C-0181. The principal task was to make nighttime atmospheric optical measurements in Thailand and Puerto Rico by sensors developed at the Visibility Laboratory and installed in Air Force C-130 aircraft No. 50022, and from these measurements to determine several important optical properties of various downward inclined paths of sight. These properties include the atmospheric beam transmittance, path radiance, path reflectance, background reflectance, background radiance, and contrast transmittance.

Two field trips were made to Thailand, the first during September and October in 1968, the second during February, March, and April of 1969. The first trip coincided with the wet monsoon season; the second trip was during the relatively dry season. During both trips data were recorded over the Khorat Plateau forested area, over cultivated areas of the Chao Phraya River delta, over the Gulf of Siam, and over land areas adjacent to the Gulf in the vicinity of Rayong. The Puerto Rico trip was made in July of 1969; nighttime data were recorded over the Atlantic Ocean north of Puerto Tortuguero.

The instrumentation carried by the C-130 aircraft for recording optical data consisted of a total scattering meter (or nephelometer) for determining the total scattering coefficient, two sky scanning radiometers for recording upper and lower sky radiances, a fixed large aperture radiometer for recording nadir radiances, and a dual irradiator for recording alternately the downwelling and upwelling irradiances. The meteorological instrumentation included a Royco particle counter, pressure transducers, a dewpoint hygrometer, and an AN/AMQ-17 aerograph for measuring ambient temperature and humidity. The installation of the above equipment in Air Force C-130 aircraft No. 50022 was performed by Hayes International Corp. under Air Force Contract F 19650-68-C-0315.

Each optical instrument was fitted with five optical filters causing it to measure at four different narrow band wavelengths of the spectrum. The fifth filter permitted the sensor to record in accordance with the sensitivity of the S-20 multiplier phototube from 400 nm to approximately 800 nm. The wavelength selection for the four narrow band filters was based on the expected changes in the chlorophyll and xanthophyll content of the vegetation during seasonal change or after crop harvesting.

Data were recorded on magnetic tape in the aircraft by means of a 42 channel magnetic tape data logger, except for the data from the Royco particle counter which were recorded on paper tape. The data tapes, both magnetic and paper, were returned to the Visibility Laboratory at San Diego for processing. The magnetic tape was then processed by the computer facilities at University of California, San Diego, and the paper tapes processed manually at the Visibility Laboratory.

Analogous optical data were also obtained on the ground, sometimes simultaneously, by effectively duplicate instrumentation.

Simultaneous meteorological data were also obtained in the aircraft and at the ground installations. These data include atmospheric pressure, temperature, humidity, and particle size distribution. They are not included in this report.

# Contents

ABSTRACT	iii
SUMMARY (S.Q.D.)	v
LIST OF ILLUSTRATIONS	ix
CONTRIBUTORS TO THE REPORTED RESEARCH	xi
LIST OF RELATED CONTRACTS AND PUBLICATIONS	xiii
1. INTRODUCTION (S.Q.D.)	1-1
1.1 Background of the Project	1-2
1.2 Earlier Airborne Optical Atmospheric Measurements	1-2
1.3 Visibility Laboratory In-Flight Atmospheric Measurement Program	1-2
1.4 Project SHED LIGHT	1-3
2. THEORY (J.I.G.)	2-1
2.1 Contrast Transmittance	2-1
2.2 Directional Path Reflectance	2-1
2.3 Background Reflectance	2-2
2.4 Downwelling Irradiance	2-2
2.5 Beam Transmittance	2-3
2.6 Earth Curvature	2-4
2.7 Path Radiance	2-5
2.8 Equilibrium Radiance	2-5
2.9 Proportional Directional Scattering Coefficient	2-6
3. INSTRUMENTATION (R.W.J.)	3-1
3.1 Radiometric Systems	3-1
3.2 Meteorological Systems	3-17
3.3 Control and Communications	3-21
3.4 Radiometric Calibration Procedures	3-29

4. DATA COLLECTION METHODS (R.W.J.)	4-1
4.1 Airborne System	4-1
4.2 Ground-Based System	4-6
5. DATA PROCESSING (R.W.J.)	5-1
5.1 Airborne Data	5-1
5.2 Ground-Based Data	5-5
6. AIRBORNE DATA	6-1
6.1 Flight Descriptions (A.R.B.)	6-1
6.2 Presentation of Data (A.R.B.)	6-6
6.3 Data Tables (J.I.G.)	6-14
6.4 Data Interpretation (J.I.G.)	6-189
7. GROUND-BASED DATA (J.I.G. and R.W.J.)	7-1
7.1 Description of Ground Operation	7-1
7.2 Presentation of Ground-Based Data	7-3
7.3 Ground-Based Data Interpretation	7-21
8. ROYCO DATA (R.W.J.)	8-1
9. ACKNOWLEDGEMENTS	9-1
10. REFERENCES	10-1

#### APPENDIX A

Image Transmission by the Troposphere I

#### APPENDIX B

Visibility, Applied Optics, Vol. 3, No. 5, May 1964

- I. Introduction
- II. Summary
- III. Optical Properties of Objects and Backgrounds

#### APPENDIX C

Visibility, Applied Optics, Vol. 3, No. 5, May 1964

- VI. Atmospheric Properties

#### APPENDIX D

Directional Reflectance of Atmospheric Paths of Sight

#### APPENDIX E

Model for a Clear Atmosphere

#### APPENDIX F

Scattering Functions of Light in the Atmospheric Boundary Layer

#### APPENDIX G

Glossary and Notation

# List Of Illustrations

Figure	Title	Page
1-1.	Contrast Transmittance for Two Model Atmospheres	1-9
1-2.	Improved Computer-Generated Pictures	1-16
1-3.	Reflection Spectrum of a Typical Leaf	1-22
1-4.	Standardized Sensitivity-Transmittance $\overline{S_{\lambda}T_{\lambda}}$ of the Five Narrow Band Filter-Phototube Combinations	1-23
2-1.	Path Length Geometry	2-3
2-2.	Incremental Path Length $\Delta r$ for Near Horizontal Slant Paths at Paths of Sight Zenith Angle $\theta$	2-4
3-1.	Typical Multiplier Phototube Assembly	3-3
3-2.	Temperature Control Housing Assembly	3-4
3-3.	Typical Optical Filter Assembly	3-5
3-4.	Typical Visibility Laboratory Model 5 Photometer Circuit	3-6
3-5.	Photometer Slide Subassembly	3-7
3-5A.	Photometer Power Supply	3-7
3-6.	Automatic $2\pi$ Scanner Assembly	3-8
3-7.	$2\pi$ Scanner Installation for Lower Hemisphere Measurement	3-9
3-7A.	Ground-Based Instrument Enclosure Used During TDY-1	3-10
3-7B.	Ground-Based Instrument Enclosure Setup at Lop Buri Site During TDY-2	3-10
3-8.	Integrating Nephelometer Aircraft Installation	3-11
3-9.	Integrating Nephelometer Mode Selector Head Subassembly	3-11
3-10.	Artist's Rendition of Integrating Nephelometer	3-12
3-11.	Air and Ground Nephelometer Shrouds	3-13

## LIST OF ILLUSTRATIONS (CONT.)

Figure	Title	Page
3-12.	Dual Irradiometer Assembly	3-14
3-12A.	Dual Irradiometer Installation	3-14
3-13.	Large Aperture Telescope Assembly	3-15
3-14.	Ground Goniophotometer Assembly	3-16
3-14A.	Vertical Path Function Meter Installed on C-130 No. 50022 (Horizontal Configuration)	3-16
3-14B.	Vertical Path Function Meter Installed on C-130 No. 50022 (Inclined Configuration)	3-16
3-15.	Meteorological Fin	3-17
3-16.	Airborne Royco Plumbing	3-19
3-17.	Rack A: Cambridge 137-C3 (Lower Right); AN/AMQ-17 Aerograph Set (Lower Left); Royco System (Top)	3-19
3-18.	Cambridge Model 137-C3 Probe Housing	3-20
3-19.	Rack B: Automatic $2\pi$ Scanner Control Console, 1: Scanner Control Panels, 1 and 2; Programmer Panel; Gyro Control Panel; Power Distribution Panel; Programmer Control Panel	3-22
3-20.	Rack C: Photometer Temperature Control Panel; Defroster Panel; Ten Slide Photometer Module; Nephelometer Power Supply	3-24
3-21.	Visibility Studies Control Console Left and Right: Optical Filter Control Panel; Accessory Control Panel; Flight Dynamics Display Panel; Camera Control Panel; Remote Scanner and Data Logger Control	3-25
3-22.	Complete Aircraft Rack Installation	3-26
3-23.	42 Channel Data Logger	3-27
3-24.	20 Channel Data Logger	3-28
3-25.	Typical Linearity Calibration Curve	3-30
3-26.	Typical Absolute Calibration Form	3-30
4-1.	Typical Airborne Data Profile	4-2
4-2.	Irradiometer Cap	4-10
5-1.	Project SHED LIGHT Data Flow Schedule	5-2
6-1.	Relative Irradiance Due to the Moon as a Function of Phase Angle	6-189
6-2.	Starlight and Overcast Sky Radiances for Filter 5 at the Lowest Flight Altitude	6-191
6-3.	Mie Proportional Directional Volume Scattering Functions Used in the Calculations of Equilibrium Radiance	6-196
6-4.	Equilibrium Radiance and Apparent Radiance for the Vertical Downward Path of Sight from Ground Level to Altitude, for Filter 5, Flight 82 I	6-197
6-5.	Contrast Transmittance for the Vertical Path of Sight between Ground Level and Altitude, for Filter 5, Flight 82 I	6-198
6-6.	Contrast Transmittance Nomogram	6-200
7-1.	Rice Field and Dirt Road at Lop Buri Site During TDY-1	7-3
7-2.	Lop Buri Area with Location of Ground Station and Flight Path	7-5
7-3.	Sandy Beach and Road (E and W), Scrub and Sand (N), Ocean (S), and Wild Sweet Peas and Grass Nearby at Rayong Site During TDY-1	7-7
7-4.	Rayong Area with Location of Ground Station and Flight Paths for TDY-1 and TDY-2	7-8
7-5.	Views of Harvested Rice Fields at Lop Buri Site During TDY-2	7-16

# Contributors To The Reported Research

The following scientists and engineers of the Visibility Laboratory, in addition to the authors of this report, contributed directly or indirectly to the research being reported in this Final Report:

Mr. James L. Harris, Sr., Associate Director of the Laboratory.

Mr. Roswell W. Austin, Manager of the Laboratory.

Mr. T. J. Petzold, Chief, Engineering Branch.

Mr. Gary C. Barnett, Assistant Development Engineer, in charge  
of Airborne Section of Scientific Party (now with the Santa  
Barbara Research Center).

Mr. Gerald D. Edwards, Senior Development Engineer,

Mr. Floyd D. Miller, Associate Development Engineer, and

Mr. George H. Tate, Associate Development Engineer, all three  
of whom contributed to the design of the optical instrumentation.

Mrs. Catharine Edgerton, Associate Development Engineer,  
Meteorologist, and

Mrs. Peggy V. Church, Assistant Development Engineer, coordinator  
during the preliminary preparation of this report.

# **Related Contracts And Publications**

**Related Contracts:** None

**Publications:**

Interim Progress Report No. 1 (1967)

Boileau, A. R., "Determination of Path Radiance for Downward Path of Sight from Ground-Based or Low-Altitude Measurement," J. Opt. Soc. Am. **58**, April 1968, p. 586.

Boileau, A. R., "Determination of Path Radiance for Downward Path of Sight from Ground-Based or Low-Altitude Measurement," AF CRL-68-0394. SIO Ref. 68-24, (October 1968).

Interim Progress Report No. 2 (December 1968).

Interim Report No. 3, "Project SHED LIGHT Contrast Transmittance Data," (October 1969).

# 1. Introduction

This final report under Air Force Contract No. F 19628-67-C-0181 is part of the research program of Air Force Project OPERATION SHED LIGHT. That project, initiated in 1965, seeks to improve Air Force capability for close support operations at night. The advent of electro-optical night vision devices, potentially capable of enabling crews of low flying aircraft to view terrains by starlight, resulted in a requirement for optical data on the atmospheric limitations on the operation of such devices, particularly along shallowly inclined paths of sight. Optimization of the engineering design of such night viewing devices also requires information concerning the nighttime optical properties of typical backgrounds against which objects of interest are expected to appear. In short, the requirement is for all of the data that are necessary to predict the magnitude and character of nighttime optical signals available at an aircraft. Such data were collected and are presented in this report.

Optical properties of atmospheres and terrains were measured from a specially instrumented C-130 aircraft and an associated ground station at several selected locations in Thailand during the wet monsoon season in the Fall of 1968 and the dry monsoon season during the Spring of 1969. Supplementary in-flight meteorological measurements were also recorded. These may provide a link with more conventional meteorological records. The optical data cover four selected wavelength intervals in the visible spectrum and the near infrared. Numerical examples are provided to illustrate some uses of the data which may be made by engineers concerned with the design of improved electro-optical night viewing devices for specialized applications.



## **1.1 BACKGROUND OF THE PROJECT**

The difficult experimental task described in this report was carried out successfully within the time requirements of Project SHED LIGHT only because most of the experimental techniques and some of the necessary instruments were already in existence. Airborne research in atmospheric optics under Air Force sponsorship has been a continuous activity at the Visibility Laboratory of the University of California since 1952, but the work has its roots in similar airborne experiments conducted by some of the Laboratory's scientific personnel during World War II and thereafter.

The Visibility Laboratory was established jointly by the United States Air Force and the United States Navy to develop a capability for predicting, by calculation from physical data, the probabilities with which any object of military importance can be visually detected, recognized, or identified under operational conditions of any kind, anywhere, any time, with or without the aid of optical instruments, photographic systems, or electro-optical devices. Techniques for accomplishing this mission are under continuing development. The bank of necessary physical data is constantly growing. The experiments conducted in Thailand for Project SHED LIGHT are part of the Laboratory's on-going program of environmental measurements.

## **1.2 EARLIER AIRBORNE OPTICAL ATMOSPHERIC MEASUREMENTS**

A few airborne optical atmospheric measurements were made by U.S. military and industrial scientists during World War I and, to a limited extent, throughout the years that followed. A small amount of similar work was also carried out by other nations. In 1940 some of the authors of this report undertook airborne optical and terrain measurements from aircraft at the request of the United States Army. The first of these measurements were made in December of 1940 from a military aircraft operated by the Massachusetts National Guard. The equipment consisted of battery-operated, laboratory-type visual photometers poorly suited to the needs of the task. After the United States entered World War II, new specialized in-flight spectroradiometric equipment was constructed, based chiefly on photographic photometry. It was used in B-17 and B-24 aircraft by personnel of the present Visibility Laboratory.

Similar studies by the same individuals continued after the war under various military sponsorships. Data were obtained from an instrumented Air Force B-47, an instrumented Navy F2H2, and an instrumented Navy R4D. In this period experimental procedures shifted from reliance on photographic photometry to automatic, recording photoelectric devices employing multiplier phototubes. Data flights were made in continental United States and in Puerto Rico. Many of the data served highly specialized, specific needs. Other data were of low reliability compared with today's standards and have been superseded by newer work. Some, however, had wide applicability and are still in use.

## **1.3 VISIBILITY LABORATORY IN-FLIGHT ATMOSPHERIC MEASUREMENT PROGRAM**

The Air Force/Visibility Laboratory in-flight atmospheric measurement program was initiated in 1952 in response to requirements of the Strategic Air Command of the U. S. Air Force. The initial needs were for data under night conditions. None of the preceding airborne measurements had been made during darkness. No existing airborne equipment had sufficient sensitivity for operation in starlight. A preliminary attempt to obtain the needed data was made in B-36 aircraft from Fairchild Air Force Base near Spokane, Washington. Although some marginally applicable information was secured, it was clear that the task required an

aircraft permanently instrumented with photoelectric equipment of advanced design. Early in 1953 a B-29 assigned to the Air Research and Development Command was made available to the Visibility Laboratory for instrumentation at Edwards Air Force Base, California. The installation included two large aperture (12-inch diameter) reflecting type, scanning telephotometers for mapping the night sky above and below the aircraft and a variety of other photoelectric optical measuring devices capable of use at night. The same instruments also functioned in daylight.

Even before the original nighttime data requirements were fulfilled, new military requirements for optical atmospheric data appeared. Eventually the B-29 aircraft was replaced by a C-130 and the original instruments were updated. Because there was no longer any requirement for airborne measurements at night and because the large scanners had severe aerodynamic problems, new smaller and faster scanners were constructed. All of the new equipment for the C-130 was designed solely for use at daytime light levels. That restriction proved to be unfortunate when, in January, 1966, Air Force Project OPERATION SHED LIGHT produced a requirement for low altitude optical atmospheric data at night. There was neither time nor funds to reinstrument the C-130 completely.

#### 1.4 PROJECT SHED LIGHT\*

Fortunately, new developments in multiplier phototubes enabled the sensitivity of the small scanners and other in-flight optical instruments to be increased significantly. Samples of the new detectors were used to demonstrate that the existing small scanners and other optical sensors could be converted for successful night operation. The subsequent conversion required both the use of expensive, state-of-the-art, selected multiplier phototubes and drastic reductions in data acquisition rates (scan rates), but no other feasible option was found within the constraints of time and funds. Even so, extensive changes in experimental methodology, electronic circuitry, and data processing procedures had to be made. Some additional instrumentation and extensive aircraft modification was required. New ground station equipment was built. All of this was accomplished within a time span acceptable to Project OPERATION SHED LIGHT.

This report describes the equipment and overseas deployments, and presents the best of the resulting data.

#### FIRST AND SECOND OVERSEAS DEPLOYMENTS

At the request of the Air Force, data were obtained first during two overseas deployments in Thailand. All arrangements were made by the Contract Monitors. They also selected sites for the experiments. One of the Project Monitors, Dr. Robert W. Fenn, has provided an account of the planning of the field measurement program in Thailand; it is quoted verbatim immediately below.

"Planning of Field Measurement Program.

"Very limited data on atmospheric visibility exist for the Indochina area. Climatic data are primarily based on Weather Services' compilations and are restricted to ground surface visibility observations.

"An analysis of such data, for instance for Thailand, reveals that there are considerable local variations in surface visibility, even in yearly average values. The annual average visibilities

---

\* See also SHED LIGHT management report.

vary between 8 km (Khlong Yai on the east coast of the Gulf of Siam 11°47' N, 102°53' E) and 25 km (Phrach Unla Chomklao in the Chao Phraya Delta, 13°32' N, 100°35' E) with the majority of values between 9 and 15 km.

"The weather of Southeast Asia is controlled by the monsoon regime. The southwest monsoon during the summer months brings the warm and moist air from the Gulf of Siam and the Gulf of Bengal with heavy rain showers into the Southeast Asia Peninsula. The northeast monsoon from the interior of Asia is dry, except where it picks up moisture on its way across the Gulf of Tonkin and the South China Sea, causing 'chrachin' condition with drizzle along the Vietnam coastal region.

"The visibility conditions are characterized also by the monsoon regime. Heavy rain showers during the summer monsoon tend to washout dust and haze from the air resulting in good visibilities under the generally overcast sky. During the dry winter monsoon period dry dust from the ground is picked up by winds to form haze layers, frequently enhanced by smoke from burning rice fields. In general visibilities during the dry season range from about 6-10 km, whereas they improve to 10-15 km during the rainy season.

"No quantitative data existed on the vertical structure of the atmosphere with regard to its turbidity characteristics.

"From these considerations it is quite apparent that a limited field measurement program should as a minimum cover the two major seasons, namely summer and winter monsoon and possibly reach into the transitional periods in April-May and October-November.

"A study of the Southeast Asia area shows that a number of rather typical areas exist with regard to their geographical features as well as atmospheric features.

"As such areas one may define: (a) the River Delta areas, with their canals and rice fields, (b) the heavily wooded highlands of the interior areas, and (c) the Coastal strips. All these areas are found in various locations in Southeast Asia.

"The meteorological conditions vary considerably for these locations. The exposure of land areas to oceans has a significant effect on the monsoon influence. The geographical location of the Thai Peninsula with regard to the Gulf of Siam produces a similar effect on the northeast monsoon as for the coastal range of Vietnam. On the other hand the southwest monsoon during the summer months transports air over large land masses before it reaches the Vietnam east coastal areas, a condition which is similar to that for central Thailand during the northeast monsoon. One therefore might expect some airmass similarity between the northeast monsoon region in Thailand and the southwest monsoon region in Vietnam. The large scale airmass circulation patterns in addition are strongly affected by local phenomena as the burning of rice fields. Apparently early morning hazes and smoke prevail near populated areas, this effect being enhanced by the hazy nature of the equatorial air mass.

"The adequacy of a particular field site for the purposes of this project depends on many factors such as terrain representativeness, atmospheric-meteorological conditions, air mass circulation (and here particularly local effects may disturb the representativeness of an area), logistical aspects regarding ground operation and aircraft operation and the combination of both.

"Based on these considerations and on observations during a preliminary survey trip, three areas in Thailand were selected for the measurement program:

1. The Chao Phraya Lowlands in the vicinity of Lop Buri north of Bangkok
2. The Khorat Plateau in the general vicinity of Nakhon Ratchasima
3. The coast along the Gulf of Siam east of U-Taphao near Rayong

"The location and general characteristics of these three areas is shown in Figures 1 through 4.

"As will be pointed out later in the report, one difficulty with regard to representativeness in nighttime measurements in all these locations is the presence of artificial lights. Otherwise the terrain was very homogeneous within the measurement area. Some comments on the specific terrain features for individual flights are given in the description of the airborne data packages (Section 6-1)."



Fig. 1. Three Thailand Areas Selected for Measurement Program

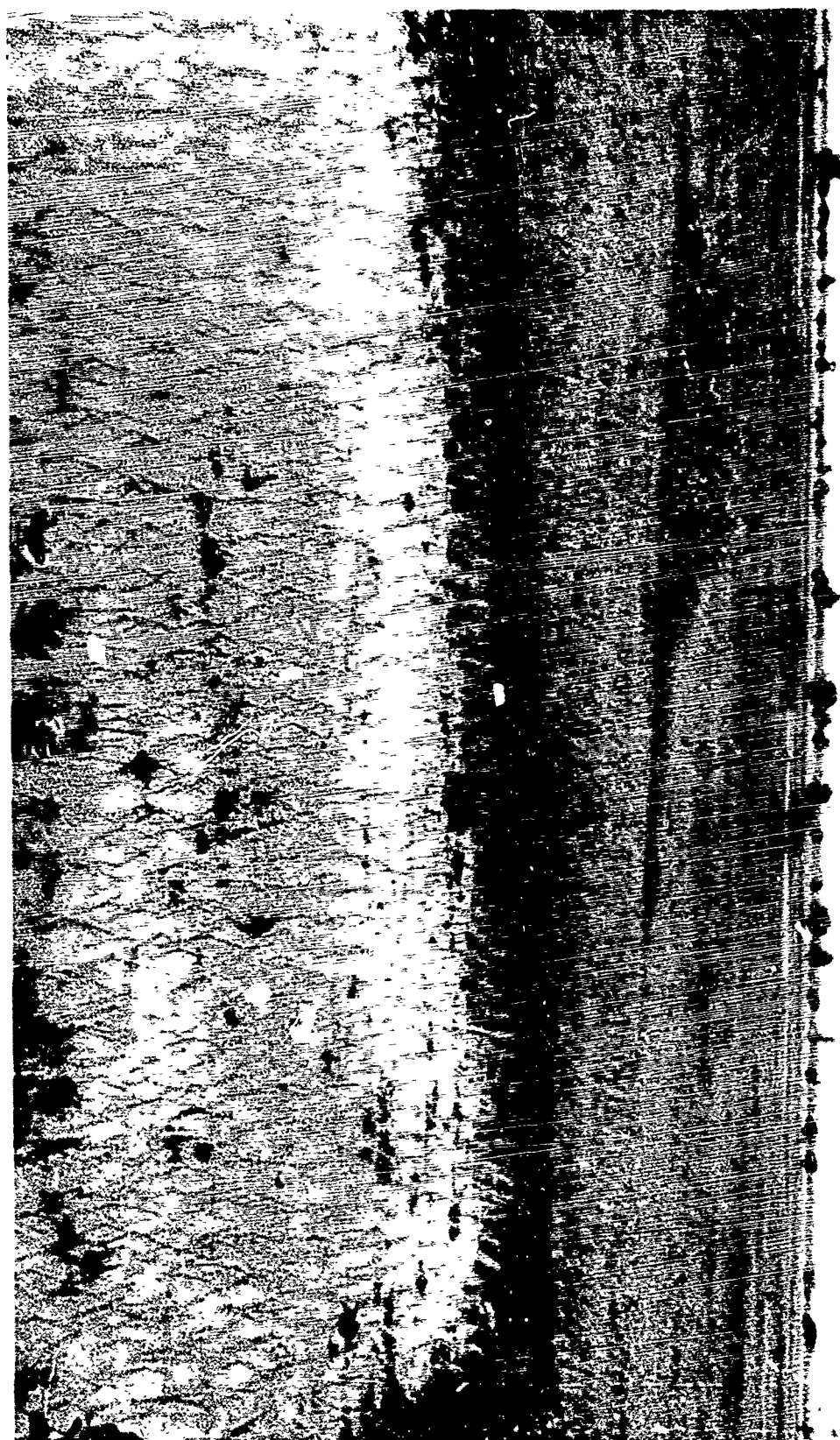


Fig. 2. Lop Bari, River Delta Area



Fig. 3. Khorat Plateau, Evergreen Forest



Fig. 4. Rayong Coastal Region

## PROJECT OBJECTIVE

The objective of project OPERATION SHED LIGHT is to improve the capability of the Air Force to operate at night. The ability of the human eye to discriminate objects is severely reduced at nighttime light levels. This can be partially overcome in two ways: (1) by illuminating the terrain, or (2) by using image intensifier devices. These are well described by Morton (1964), whose analysis demonstrates the critical role of apparent object contrast among those factors which determine the limiting performance of such visual aids\*. Accurate knowledge of the spectral characteristics of the apparent contrast of objects when viewed against typical backgrounds is vital to the optimization of systems for operational use. Thus, detailed knowledge of the reduction of contrast by the atmosphere is essential for proper engineering design. The nighttime in-flight data collected in Thailand and presented in this report are intended to fulfill that need.

Prior to the experiments described by this report, nighttime atmospheric contrast transmittance from air to ground was virtually unknown. Limited previous experimental (Duntley, et al., 1964) and theoretical (Duntley, et al., 1957, and Wells, et al., 1968) analyses of daytime contrast transmittance and its dependence on altitude, look angle, atmospheric light scattering properties, illumination and ground albedo have shown that the inherent contrast of an object against its background can be reduced by several orders of magnitude if viewed along a path through the atmosphere. Figure 1-1, which is based on theoretical work from Wells, et al. (1968), shows contrast transmittance (or ratio of apparent to inherent contrast) as a function of altitude for two model atmospheres; the results show a strong dependence on atmospheric properties.

### CONTRAST TRANSMISSION VERSUS RECEIVER ALTITUDE

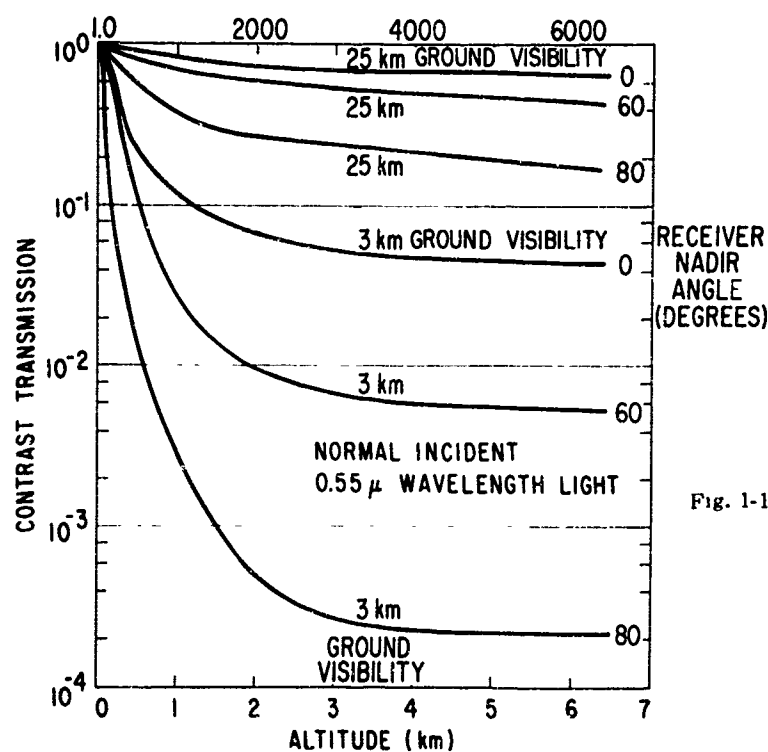


Fig. 1-1. Contrast Transmittance for Two Model Atmospheres

\* See pages 666 and 667 of Morton (1964) reference, note that contrast appears as  $C^2$  in these equations.



Theoretical and experimental studies also indicated that there exists a strong wavelength dependence for contrast transmittance. This wavelength dependence is not only a function of atmospheric properties but also of the spectral reflectance characteristics of the background immediately adjacent to the object. One of the important atmospheric properties, the *spectral path radiance*, although ordinarily unaffected by the spectral nature of the target and its immediately adjacent background, may nevertheless exhibit a mild but rarely negligible wavelength dependence on the average spectral reflectance of the terrain beneath the path of sight. Thus, it was clear that all of the new nocturnal measurements must be made at appropriately selected spectral bands.

The previous studies also showed a significant difference in contrast attenuation between cases with directional illumination (sun or moon) and diffuse illumination (overcast sky or starlight night sky).

The results from the theoretical analyses and the fact that these computations were based only on general model atmospheres indicated that a requirement exists for experimental field measurements in a variety of environmental conditions

#### FLIGHT REQUIREMENTS

From the outset it was clear that crews of fast, low altitude aircraft must view the terrain along shallowly inclined paths of sight. When flying over verdant countryside they are confronted with exceedingly complex scenes containing hundreds of visible objects. Among all of these the observer must find some particular object of interest and make positive identification before it passes from his field of view. Obviously, no mechanism should be overlooked to aid the observer in his task. Various means for making specific objects more conspicuous were suggested by the authors and by Air Force personnel. Some of these were explored in preliminary studies.

#### PRELIMINARY STUDIES

The detailed design of the experimental equipment and the data collection procedure was preceded by sample calculations using dummy data in order to explore the requirements for optimizing the design of night viewing systems for particular seeing tasks. During April 1966 a letter describing some of these preliminary studies was sent to the Air Force. Part of that letter, quoted almost verbatim, is as follows:

"... the results are interesting even though they are based upon assumed input data and despite the fact that they represent only a very small sample of the type of study which could and should be made in order to optimize the performance of future night viewing systems.

"Two kinds of sample calculations were made. The first illustrates how spectral data on objects and backgrounds can be used to select the filters for multispectral systems. It also explores the potential capability of one method for combining and displaying the resulting multispectral images. The second type of calculation illustrates how data on the contrast transmitting properties of the atmosphere can be combined with object and background data and with the modulation transfer function of the night viewing system to predict maximum sighting and recognition ranges for various atmospheric conditions. The latter type of calculation necessarily involves assumptions concerning magnification (focal length); extension of this type of calculation to the case of dynamic search would involve the question of field of view. In fact, every one of the parameters which specifies the performance of a night viewing system is involved in these calculations in such a way that parametric studies can be made and all of the trade-offs explored.

"The sample calculations were not intended to be the ultimate in completeness or sophistication. They were done as preliminary trials and without the expenditure of any major amount

of time on the part of those who participated in them. They must be regarded merely as illustrative examples. Fortunately a great deal of new knowledge and a great many new tools for calculations of this kind have been developed here comparatively recently. Many of the operations which have in the past been time consuming when done by hand have been programmed for computers. There is, in fact, an active project supported by NASA in our laboratory for developing computer programs for such purposes in order that large scale parametric studies of dynamic search, detection, and recognition can be carried out quickly and economically. All of these new developments contribute to a potential for the utilization of data such as the type under consideration to be obtained with the C-130 in a night operating configuration. Exploration of design compromises and system performance of night vision systems could be performed rapidly and thoroughly.

"The illustrative calculations referred to above were made by James L. Harris of the Visibility Laboratory who has written an internal memorandum about the work. His memorandum says, in part:

"... The purpose of the calculation is *not* to predict real scotoscope performance but rather to show the type of calculations which could be made if the appropriate input data are obtained.

"The calculation is divided into two parts. Part I deals with the question of the inherent optical signal, i.e., the nature of the object and its environment, the spectral properties of each, and the utilization of spectral filtering to improve system performance. Part II deals with the calculation of the object image as displayed by the system, accounting for the effect on the inherent optical signal of the contrast transmittance of the atmosphere, the modulation transfer function of the image intensifier system, and the noise level of the intensifier system. The fundamental limitations on detection and recognition imposed by these combined properties are calculated.

#### Part I - Inherent Optical Signal

"A background consisting of vegetation has a spectral characteristic differing considerably from that associated with the painted surfaces of most man-made objects. Figure 1 shows a crude plot of a typical object and background (ERDL data January 1964). My reference for this data did not show the curves below 0.5 microns and I truncated the graph at 0.8 microns since this is the approximate cutoff of sensitivity of the S-20 photocathode.

"Figure 1 also shows the relative response of the S-20 photocathode over this region and a plot of the product of the sensitivity curve with both the object and background spectral radiance curves. It is apparent from these curves that for the conditions under which these data were taken, there is a region below 0.68 microns in which the object would have positive contrast (i.e., appear brighter than the background) and a region above 0.68 microns in which the object would have negative contrast (i.e., appear darker than the background). For an unfiltered S-20 surface, the contrast of the displayed image would be determined by an integral over the whole spectral region. Since this combines the positive and negative contrast regions it would be reasonable to expect that the display contrast might be improved by appropriate spectral filtering.

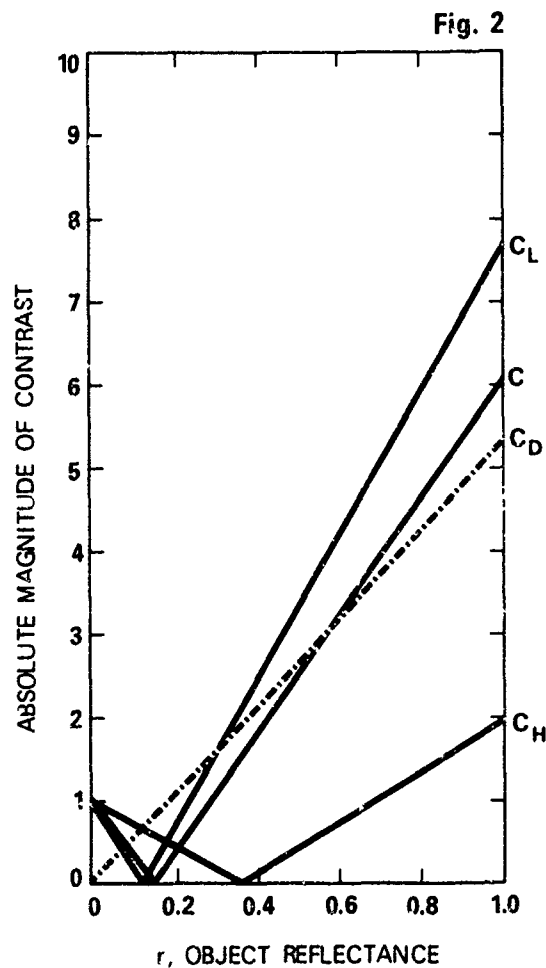
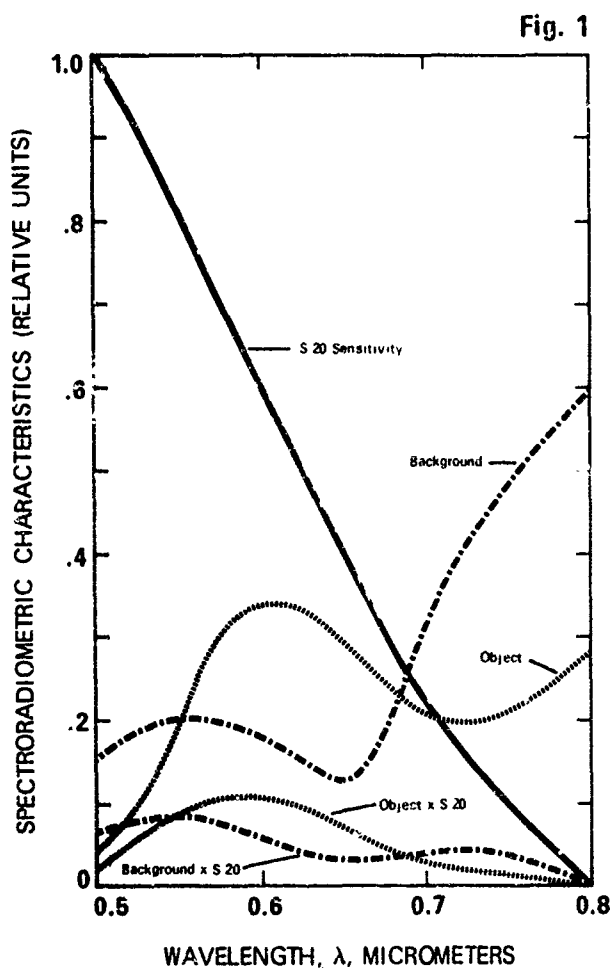
"The reference from which I extracted the ERDL data implied that the curves were drawn for an object having an average reflectance on the order of 20%. A different value of reflectance would of course result in a different contrast and a different crossover point.

"By numerical integration of the composite object and background curves of Fig. 1, the inherent contrast of the object against the background as viewed by an unfiltered S-20 photocathode is given by the equation

$$C_o = 7.03r - 1, \quad (1)$$

where  $r$  is the average reflectance of the object.

"A plot of the absolute magnitude of Eq. 1 is shown in Fig. 2. The contrast is zero at  $r = 0.14$ , negative for lesser reflectance values and positive for object reflectances greater than 0.14.



If, on the other hand, we were to filter spectrally, passing only the band from 0.68 to 0.8 microns, then by numerical integration over that region (the "high wavelength" region)

$$C_H = 2.95r - 1 \quad (2)$$

This curve is also shown in Fig. 2. The reflectance for zero contrast now is  $r = 0.34$ .

If we spectrally filtered to pass only that band of frequencies between 0.5 and 0.68 microns then the contrast for that region (the "low wavelength" region) is

$$C_L = 8.65r - 1 \quad (3)$$

so that the reflectance for zero contrast is  $r = 0.12$  (see Fig. 2). A comparison of the  $C_H$  and  $C_L$  curves shown in Fig. 2 verifies the observation from the spectral plots of Fig. 1 that for a reflectance of .20, the object contrast would be positive for the spectral region below 0.68 and negative for the spectral region above 0.68.

The simple observations made above made it clear that proper spectral filtering depends upon the reflectance of the object for which we are searching, and this piece of information may not exist a priori. We can, however, take advantage of the fact that the contrast cannot be zero simultaneously in both spectral regions. Suppose that we alternately filtered 0.5 to 0.68 and 0.68 to 0.8, repeating the operation at a repetition rate well below the critical flicker fusion frequency for the human visual system. By the appropriate addition of neutral density filters

we could balance the two systems so that the background flux was equal for each. The contrast for either of the two filterings would be as given by Eqs. 2 and 3, however the object would "flicker" between two luminance values whose difference would never be zero for any non-zero value of object reflectance. We can make this quantitative by noting the values of the numerical integrations which were performed on the effective spectral distribution curves of Fig. 1. These numerical evaluations of the integral were

$$\begin{aligned} I_{TL} &= 580r \\ I_{BL} &= 67 \\ I_{TH} &= 80r \\ I_{BH} &= 27 \end{aligned} \quad (4)$$

where the B and T subscripts refer to background and object and the L and H subscripts refer to the "low" (0.5 to 0.68 micron) and "high" (0.68 to 0.8 micron) spectral regions. To make the background flux equal for the two regions we must attenuate the "low" region by a factor 27/67. This would give a new set of values.

$$\begin{aligned} I_{TL} &= 234r \\ I_{BL} &= 27 \\ I_{TH} &= 80r \\ I_{BH} &= 27 \end{aligned} \quad (5)$$

A measure of the visual effectiveness of the flicker display is to specify the quantity

$$C_D = \frac{B_{TH} - B_{TL}}{B_B} = \frac{154r}{27} = 5.72r \quad (6)$$

This quantity is also shown in Fig. 2. Over the region of practical reflectance values, say 0.1 to 0.4, the "dynamic" display contrast compares favorably with the contrast obtainable from either of the static spectral filterings, and of course it is never zero contrast in this region.

One very important fact that is not apparent in the calculations made above is that the dynamic display may offer invaluable aid in the very difficult problem of attempting to recognize quickly an object of interest located in a very cluttered background. The flickering of the object would be very effective in calling the observer's attention to the object. It is my opinion that the problem of recognition of the object in the cluttered background may be the most serious problem to be faced in the practical use of these devices.

The illustrative calculations which have been made relative to spectral filtering and dynamic display techniques illustrate that *much profitable analysis of the optimization of the device can be made providing the basic spectral data on objects and backgrounds are obtained.*

## Part II - Detection and Recognition Ranges

Three basic mechanisms operate to reduce the quality of the object image which will be displayed at the image intensifier. These are the contrast reduction imposed by the atmosphere, the resolution limitations of the image intensifier, and the photon-shot-noise inherent in the display. The contrast transmittance of the atmosphere may be expressed by the equation<sup>1</sup>

$$\tau_c = \frac{1}{1 + N^* \frac{1}{b} N_o T} \quad (7)$$

1. A. R. Boileau, J. Appl. Opt. 3, 571 (1964).

where the path radiance  $N^*$  is the radiance of flux scattered into the path of sight,  ${}_bN_o$  is the inherent background radiance, i.e., that which would be measured close to the background, and  $T$  is the beam transmittance of the path of sight, i.e., the transmittance for an image-forming ray from the object. All three quantities  $N^*$ ,  ${}_bN_o$ , and  $T$  are a function of wavelength, and contrast transmittance is therefore a function of wavelength. Any realistic analysis of optimum spectral filtering must consider the wavelength dependence of contrast transmittance. Unfortunately the data required to evaluate contrast transmittance as a function of wavelength do not exist for the nighttime environment.

For the purpose of this illustrative calculation we will assume the simple exponential form of contrast transmittance,

$$T = e^{-r/L} \quad (8)$$

where  $r$  is the slant range to the object and  $L$  is the attenuation length in the same units as the slant range. For the purpose of this analysis we will assume attenuation lengths of 625 ft, 5000 ft, and 20 000 ft.

The resolution of the image intensifier can be specified in terms of the modulation transfer function of the device, i.e., the transmission encountered by each spatial frequency. Since I did not have actual modulation transfer function data, I assumed the analytic form

$$T = \frac{1}{1 + (Kf)^2} \quad (9)$$

which typifies many image-forming systems. I further assumed that the resolution of the system was defined in the conventional manner to be 20 line pairs per millimeter and that this meant that  $T = 0.02$  at a frequency of 20 cycles per millimeter. The assumption was made that the image intensifier used a 12 inch focal length lens system. Equation 9 together with the assumption of the focal length allows an interpretation as to the modulation transfer function mapped into object space, i.e., cycles per foot at the object, for operation at a specific slant range  $r$ .

Equipments and computer programs developed in the course of the image processing research sponsored by ARPA<sup>2,3</sup> were used to generate both numerical descriptions and corresponding pictures of two different but somewhat similar objects of interest as they would appear in the display when viewed at ranges of 2500, 5000, 10 000, 20 000, 40 000, and 80 000 ft. The two objects were selected on the basis of their availability in our file and consisted of a Patton tank and a Mechanical Mule. One aspect of the choice was the desire to have two objects having approximately equal detection ranges but ones which are readily distinguishable given sufficient resolution.

The steps in the process were as follows:

(1) The film transparencies for the two objects were run through the image processing film scanner which generates a deck of IBM cards containing information on the transmission of the film at each of 3600 points (a 60 x 60 grid of points). This deck of cards is processed at the UCSD Computer Center using the CDC-3600 digital computer. The processing consists of making a Fourier analysis of the object, applying the modulation transfer function for each of the object ranges, and then obtaining the inverse Fourier transform which is a description, over the 60 x 60 grid, of the relative luminance values for the displayed image. In addition to tabulated data, the computer furnishes a deck of "picture" cards which can be played back through the scanner electronics, displayed on a cathode ray tube, and photographed by a Polaroid scope camera to obtain a picture of the image degraded by the modulation transfer function.

A set of the pictures obtained in this way is shown in Fig. 3. The bottom picture was obtained directly from the film scanner with no degradation imposed. The rest of the set shows the image quality for target ranges of 2500, 5000, 10 000, 20 000, 40 000, and 80 000 feet. The

2. J. L. Harris, SIO Ref. 63-10 (April 1963).

3. J. L. Harris, J. Opt. Soc. Am., **56**, 569 (1966).

pictures show the image degradation due to the modulation transfer function but do not show either the noise or the contrast reduction by the atmosphere. Pictures showing the combination of all three image degradation components can be made but the time available for this calculation did not permit that step to be performed. (Atmospheric properties and noise effects were, however, included in the calculations which led to the curves appearing later in this discussion).

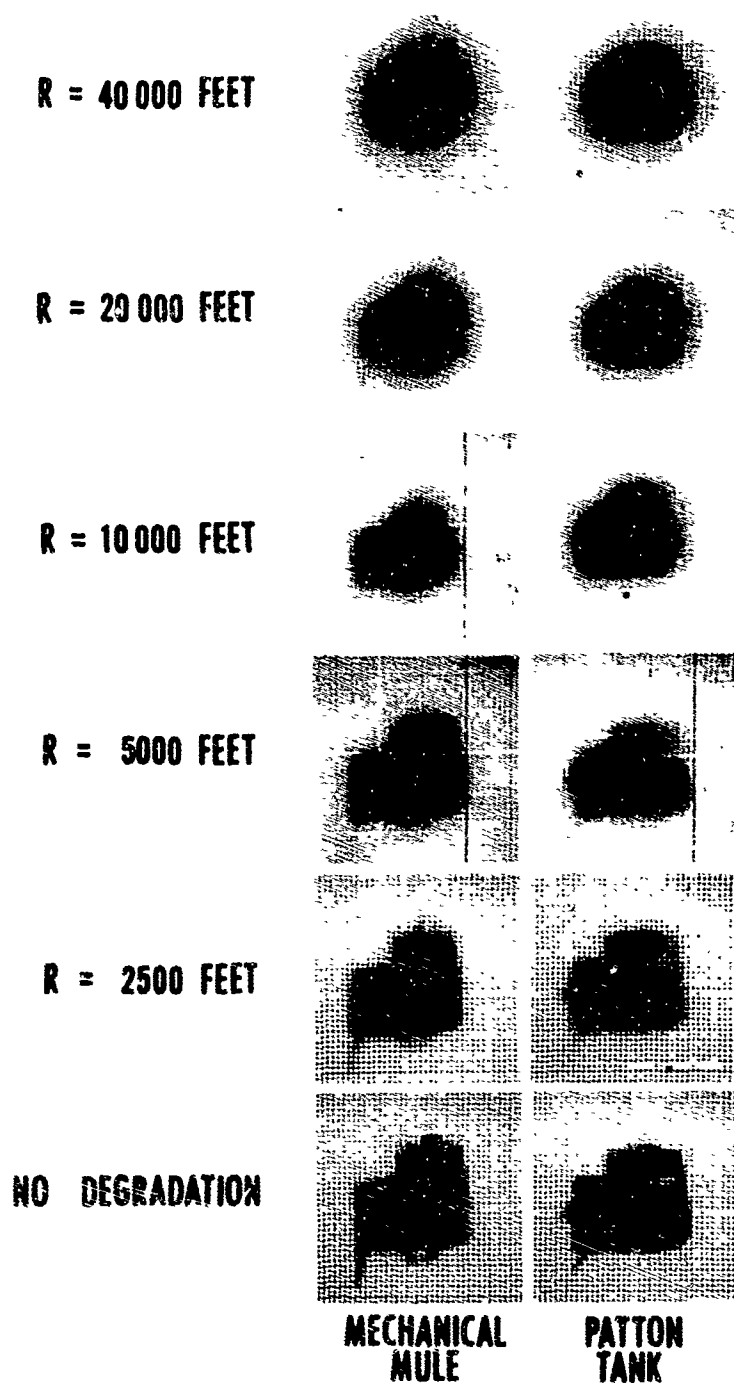


**Fig. 3**

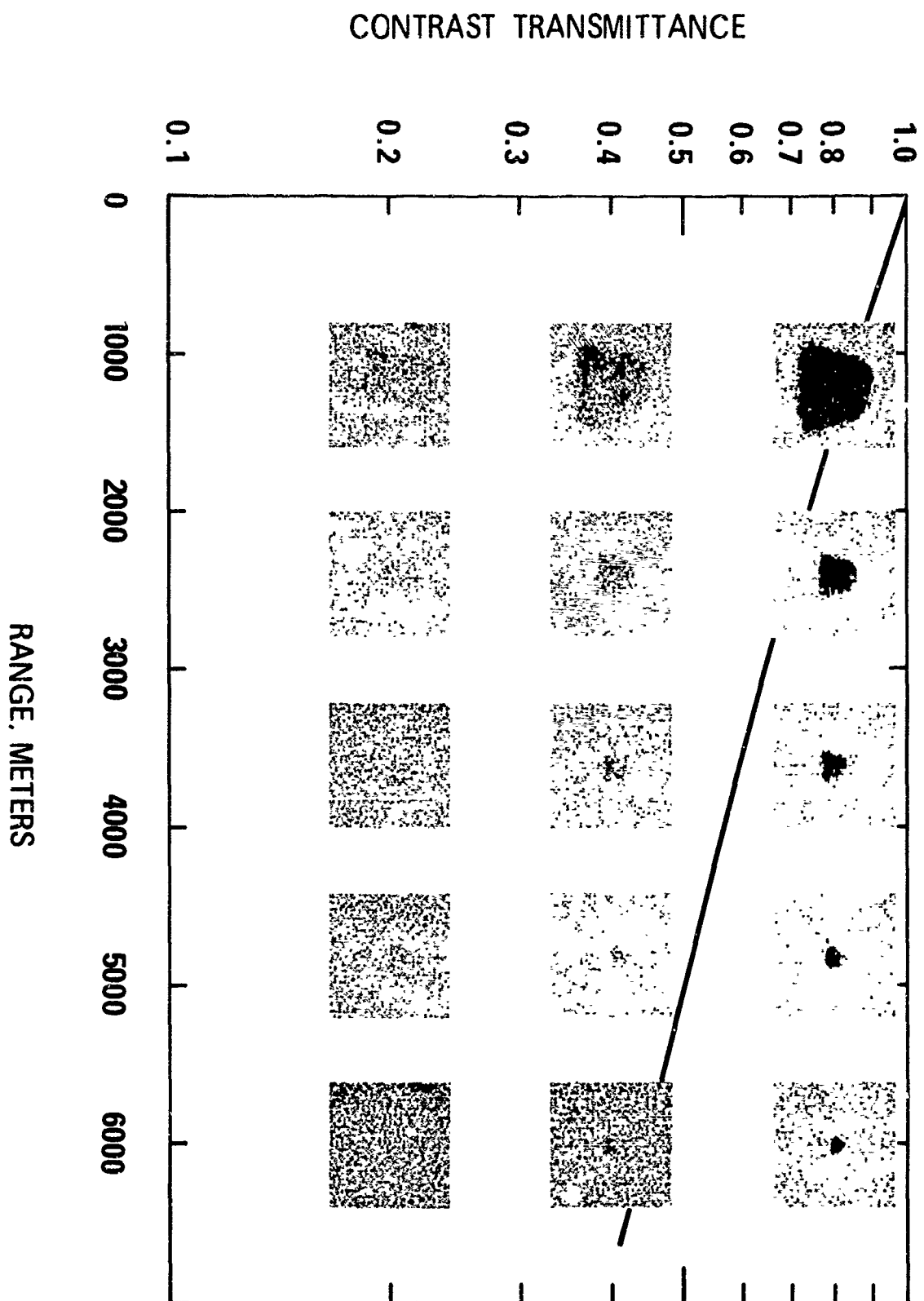


Fig. 1-2. Improved Computer-Generated Pictures

(See Page 1-20)

The next step in the analysis was to predict the range at which each of the objects can be detected and the range at which the two objects can be distinguished from one another. The calculations are based on the quadratic content concepts derived in the paper "Resolving Power and Decision Theory"<sup>4</sup>. Specifically the probability of detection and recognition are determined from Eqs. 11 and 14 in that paper. For detection, the difference image is the difference between the object image and the background image. For recognition the difference image is the difference between the tank image and the mechanical mule image.

As a preliminary to performing the calculation it was necessary to estimate the noise level associated with an element of the display. It was assumed that the limiting noise would be photon-shot-noise and that due to the atmospheric contrast reduction the display contrast at threshold range would be quite low, so that the photon-shot-noise variance could be assumed constant over the entire image.

For an area increment  $\Delta A$  on the photocathode of the image intensifier, the incident flux would be

$$F = \frac{\Delta A}{f^2} A_L \quad (10)$$

where  $F$  is the flux in lumens,  $B$  is the scene luminance in lumens  $\text{ster}^{-1} \text{ft}^{-2}$ ,  $f$  is the focal length, and  $A_L$  is the area of the entrance pupil of the optical system. Photopic units were used for this estimate because the proper radiometric values to correspond to various lighting conditions were not known. By multiplying Eq. 10 by  $n$ , the number of photons per second in each lumen, the number of photons per second was obtained, i.e.,

$$N = B \frac{\Delta A}{f^2} A_L n \quad (11)$$

For an observation time  $T$ , the number of photons is

$$N = B \frac{\Delta A}{f^2} A_L n T \quad (12)$$

Multiplying Eq. 12 by the quantum efficiency,  $q$ , of the photosensitive surface gives the number of photoelectrons,  $m$ ,

$$m = B \frac{\Delta A}{f^2} A_L n T q \quad (13)$$

The photoelectrons will follow a Poisson distribution which has the property that the variance  $\sigma^2$  is equal to the mean, i.e.,

$$\sigma^2 = m = B \frac{\Delta A}{f^2} A_L n T q \quad (14)$$

Equation 14 in reference 4 requires the noise variance per unit area which is

$$v = \frac{\sigma^2}{\Delta A} = \frac{B A_L n T q}{f^2} \quad (15)$$

---

4. J. L. Harris, J. Opt. Soc. Am., 54, 606 (1964).



The numerical values used for the noise estimate were

$$B = 10^{-5} \text{ lumens ster}^{-1} \text{ ft}^{-2}$$

$$A_L = 0.2 \text{ ft}^2$$

$$n = 4 \times 10^{15} \text{ photons sec}^{-1} \text{ per lumen}$$

$$T = 0.1 \text{ second}$$

$$q = 0.20$$

$$f^2 = 1 \text{ ft}^2$$

Calculation of quadratic content from the degraded images and noise variance per unit area from Eq. 15 resulted in the detection and recognition probability curves shown in Figs. 4 and 5. For the detection case, Eq. 14 of reference 4 was modified to insert a threshold which results in a false alarm probability of  $10^{-3}$ . Figure 4 shows the probability of detection as a function of range for the three values of meteorological range. Figure 5 shows the probability of distinguishing between the two objects as a function of range for each of the meteorological ranges. For the recognition case, the probability at long ranges approaches a value of 0.5 which is the probability of making a correct binary decision on the basis of chance alone.

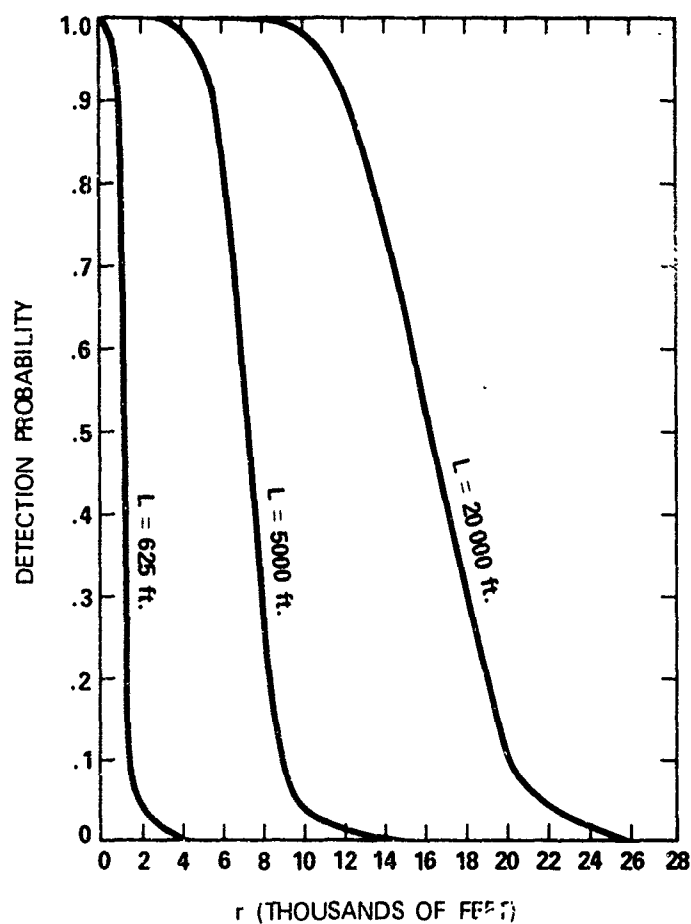
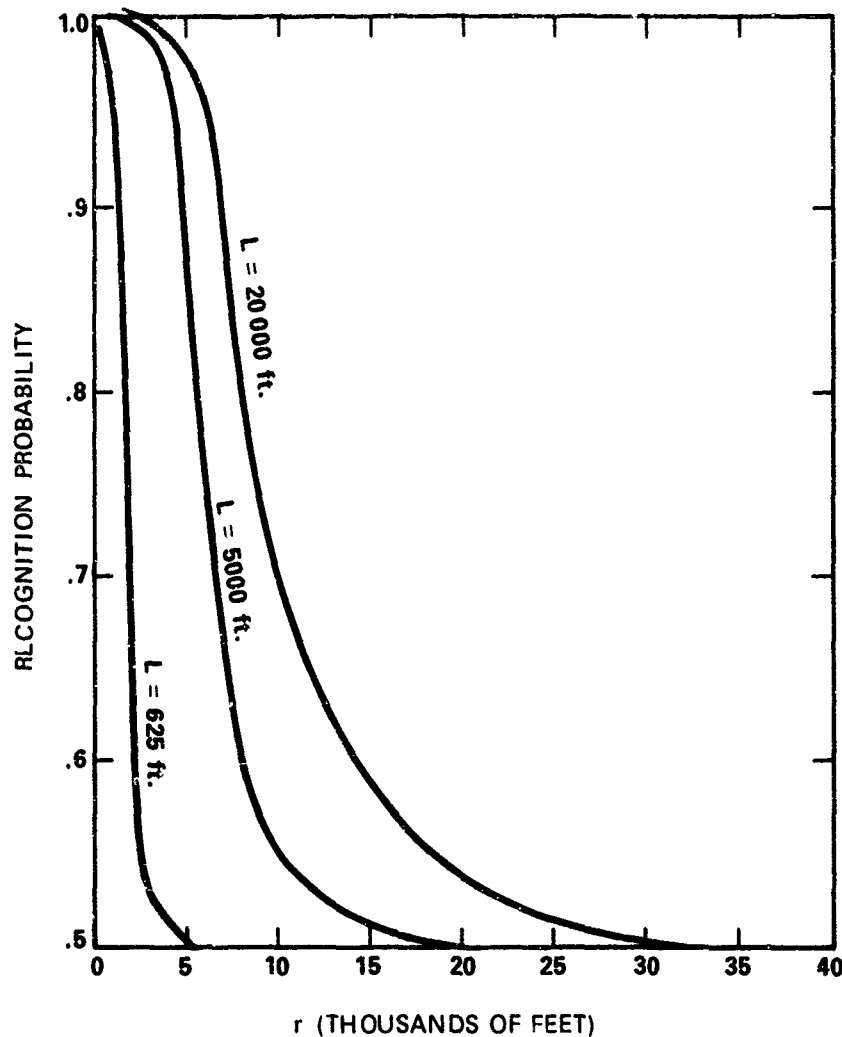


Fig. 4

Fig. 5



'As indicated in the quadratic content derivations of reference 4, calculations of this type represent upper limits to performance since the equations are based on complete extraction of information from the degraded image. While the human system may approach this limit in the case of detection, it is likely that in attempting to perform recognition of these low resolution, low contrast, noisy images, the human visual system may be quite inefficient in the extraction of information and the performance would then be significantly less than that predicted in Fig. 5.

#### Conclusion

'The purpose of performing this illustrative calculation was to indicate the techniques of problem analysis which are presently in existence. It is my personal belief that these tools can be profitably employed both in the optimization of the design of image intensifier systems and in the optimization of doctrine for the use of such apparatus. To make such analysis meaningful it is necessary to have reliable data on the spectral radiance of objects and backgrounds and spectral data required for calculation of contrast transmittance, i.e., spectral path radiance and spectral beam transmittance.'

.....

"It must be remembered that the foregoing examples are the results of dummy calculations based upon assumed input data which have been prepared solely for the purpose of illustrating some of the uses which would be served by data on nighttime atmospheric effects and nighttime directional reflectance properties of terrains and man-made objects."

## IMPROVED COMPUTER-GENERATED PICTURES

The computer-generated pictures in the preceding quotation (Fig. 3) omit the effects of contrast reduction by the atmosphere and the inescapable spatial photon-shot-noise which characterizes the images produced by image intensifier devices when used under full-night conditions. Also omitted was the effect of range on image size. Subsequent advances in computer technology at the Visibility Laboratory now enable all of these effects to be incorporated accurately. In order to reproduce the dynamic aspect of photon-shot-noise, computer-generated motion pictures are prepared for projection at the rate of 16 frames per second. Although such movies cannot be used in this report, an example composed of single frames appears as Fig. 1-2.

The object selected for Fig. 1-2 was the same tank used in the 1966 pictures. Its background is white concrete pavement having a directional reflectance of 0.60. An overcast starlight condition was assumed by specifying that the luminance of this background is  $1 \times 10^{-5} \text{ lu } \Omega^{-1} \text{ ft}^{-2}$ . This photometric specification is used reluctantly instead of a radiometric one in deference to conventional practice with respect to night vision devices.

The objective lens was chosen to be 750 mm focal length,  $f/4$ . This choice is such that each picture element in the  $64 \times 64$  tank image is  $0.1 \text{ mm} \times 0.1 \text{ mm}$ . Calculation shows that on the average 40 photons arrive each  $1/16$  second on every picture element which depicts the background. The mean number of photoelectrons was also calculated for each of the other picture elements in the  $64 \times 64$  array. A software program then replaced each mean value in the picture with a random selection from a Poisson distribution having that mean. The calculation of mean photoelectrons requires an assumed time of observation, which in this case was chosen to be  $1/16$  second. The time choice is associated with the generation of 16 frames per second movies in which the dynamic noise pattern can be fully seen. Perceptually, the viewing of single frames such as those shown in Fig. 1-2 makes the noise level appear greater than it would be in the dynamic situation.

The modulation transfer function (mtf) for the image intensifier was chosen to be of the form

$$\left[ 1 + \frac{49}{400} f^2 \right]^{-1}$$

where  $f$  is in cycles  $\text{mm}^{-1}$ . This corresponds to the mtf having a value of 0.02 at 20 cycles  $\text{mm}^{-1}$ .

The atmospheric conditions were assumed to be those of Flight 82I. Contrast transmittance values were calculated from the tabulated directional path reflectances and the directional reflectance of the concrete background (0.60). The ranges assumed were 1200, 2400, 3600, 4800, and 6000 m. For simplicity the zenith angle of the path of sight was assumed to be  $105^\circ$  for all ranges so that range and altitude are linearly related by a single constant for all ranges. The resulting contrast transmittances for the corresponding slant ranges are listed in Table 1-1.

Table 1-1. Contrast Transmittances

Slant Range (meters)	Atmospheric Contrast Transmittance
1177.3	0.84
2354.6	0.70
3531.9	0.60
4709.2	0.52
5886.5	0.45

Figure 1-2 contains five columns of photographs depicting the appearance of the tank at each of these five ranges as seen through the image intensifier under the assumed starlight conditions when the atmospheric contrast transmittance of the slant paths of sight are 0.80, 0.40, and 0.20. The curve through this matrix of pictures was plotted from Table 1-1 and depicts the atmospheric effect on the image under the atmospheric and lighting conditions which prevailed at the time of Flight 82 I.

The pictures give a direct intuitive means of evaluating the image quality for any specified set of conditions. The computer software produces, however, much more than pictorial information. Numerical evaluation of quadratic content of the image (detection) and quadratic content of difference images (recognition) serve as a basis for analytic treatment of performance expectations. By splitting the object and background into separate images for a number of spectral bands, the analysis is easily extended to include strategies with respect to spectral filtering.

For use in any future work, a more rigorous computer model than the one used in this example is available for the image intensifier. A software package which has been developed here for a Navy project takes the optical signal through the lens mtf and then through each stage of a multistage image intensifier so that for each stage the mtf, nonlinearity of phosphors, and noise accumulation can be appropriately handled.

#### SPECTRAL FILTERING

All verdant terrains appear green. Despite minor differences among plant species, the green color results from the presence of chlorophyll, a red-absorbing (blue) substance, and xanthophyll, a blue-absorbing (yellow) substance. These two compounds are intimately associated in green plant materials. Chlorophyll is, in fact, responsible for the important ability of plants to convert solar energy into chemical potential energy (e.g., sugars) with release of oxygen into the atmosphere. The reflection spectrum of a typical leaf is shown in Fig. 1-3. The spectral regions of low reflectance (valleys) in the curve are due to strong absorption by xanthophyll in the blue (left) and chlorophyll in the red (right) at these wavelengths. Between these two regions of strong spectral absorption is a reflectance peak which results from the scattering of light by colorless, nearly absorption-free mechanical structures within the leaf. This green reflectance is

responsible for the color of the leaf as viewed by human eyes. At the far right of Fig. 1-3 beyond 680 nm, the reflectance of the leaf rises abruptly and remains high throughout the near infrared region of the spectrum. This high reflectance is, again, the result of light scattering by absorption-free mechanical structures within the leaf; it signifies that none of the substances in the leaf absorbs the near infrared strongly. Thus, infrared photography of terrains shows the foliage to be highly reflecting, somewhat as if covered by snow. Ordinarily, this is not visually apparent because the dramatic increase in reflectance occurs at the extreme red end of the visual sensitivity. From a color standpoint, it is completely masked by the green reflectance peak which, although lower in absolute value, is vastly more effective in stimulating vision because it occupies the spectral region where the eye is most sensitive. Observers equipped with tight-fitting, very deep red goggles can, after sufficient dark adaption, see foliage as highly reflecting, much as in an infrared photograph.

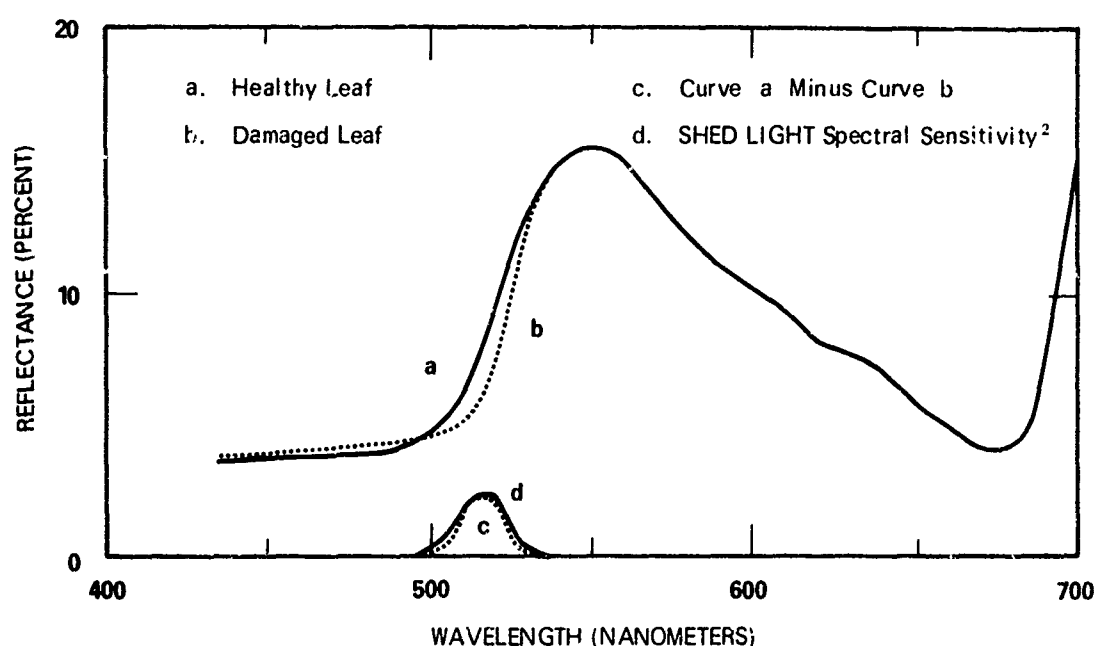


Fig. 1-3. Reflection Spectrum of a Typical Leaf

*Classical Camouflage Detection.* Most green paints which derive their color from mixtures of blue and yellow inorganic pigments do not exhibit high reflectance in the near infrared. Therefore, infrared photographs can often distinguish between visually similar green plants and green paints by showing the former as light and the latter as dark.

A common photographic technique for this form of camouflage detection uses a special color film in which the three spectral sensitivities are green, red, and infrared rather than blue, green, and red as in conventional color films. Such pictures show foliage as red because of high infrared reflectance of the foliage but reproduce conventional green paints as blue-green. This product, developed during World War II as a camouflage detection film, has subsequently been put to many other valuable uses. In agriculture and forestry, for example, it detects crop and forest areas where plant diseases are beginning to destroy vital

chlorophyll structures. In oceanography and hydrography the "color-infrared" film prominently displays silt distributions and some forms of pollution in rivers, harbors, lakes, and oceans.

*Foliage Changes.* The foregoing well-known facts have been summarized only to illustrate one way of causing certain man-made objects to have increased conspicuity when viewed by multispectral, electro-optical night vision devices. The above example is by no means the only way in which spectral differences can be exploited. In fact, from the standpoint of Project SHED LIGHT interests, much more subtle and possibly more important spectral discriminations involve the spectral changes which occur in leaf materials after they have been cut or damaged. The spectral details and time history of such changes depend upon such factors as the species, the nature of the plant injury, and its condition. Very intensive studies show that in many cases the first significant change in the reflection spectrum of injured leaves occurs in a narrow spectral region centering at approximately 515 nm. An additional absorption soon occurs which lowers the reflectance there before changes have occurred elsewhere in the spectrum. In some cases the reflectance at 515 nm may be reduced to half its original value before any other significant spectral change takes place. In the hope of exploiting this early change in the reflection spectrum of injured foliage, one of the four spectral sensitivities selected for the airborne data collection program in Project SHED LIGHT was a comparatively narrow spectral region centered at 515 nm. For comparison purposes, another SHED LIGHT filter was centered at 475 nm in the wavelength region of the xanthophyll absorption because the reflectance of leaves in this spectral region may change only slightly while, by comparison, the reflectance at 515 nm changes by a factor of 2. These two filters are referred to in this report as filters 1 and 2. The corresponding spectral sensitivities are illustrated in Fig. 1-4 and tabulated in Section 6.2.

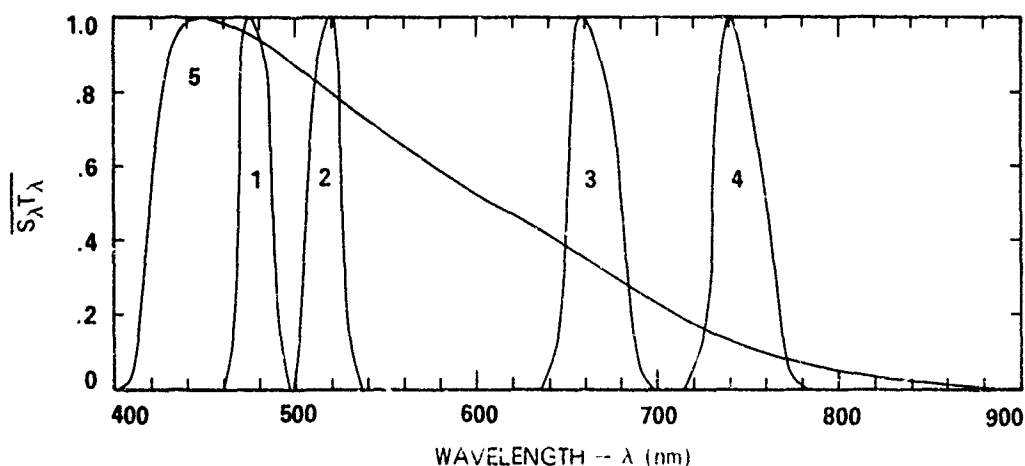


Fig. 1-4. Standardized Sensitivity-Transmittance  $\overline{S_{\lambda}T_{\lambda}}$  of the Four Narrow Band Filter-Phototube Combinations

Later in the history of an injured plant chlorophyll decomposes so that absorption in the red and orange spectral region below 680 nm is lessened. The leaf becomes progressively more reflectant in this spectral region, i.e., the reflectance curve rises. To take advantage of this reflectance change, the third filter in the SHED LIGHT data was chosen to transmit the spectral region just below 680 nm, as shown in Fig. 1-4.

Initially at least, reflectance in the adjacent near infrared (above 720 nm) changes very little. Thus, the fourth narrow band sensitivity began just above 720 nm and peaked at 745 nm. When properly compared, these two spectral regions sensitively display a second stage of plant damage.

It must be noted that the decomposition products of chlorophyll and other leaf materials are sometimes colored; i.e., they may have absorption bands in the visible spectrum or near-infrared. Therefore, complex changes in spectrum and color are sometimes seen in the later stages of plant damage, depending upon the manner in which the foliage was injured and upon peculiarities of particular plant species. The year-to-year variability in deciduous autumn foliage illustrates that the situation is not simple. Fortunately, the spectral reflectance of dead foliage is of less concern than the more subtle changes that occur during the first hours or days following leaf damage.

*Filter Selection.* The four narrow band SHED LIGHT filters were chosen in part on the basis of the above considerations, but two other requirements were also important. First, the spectral character of light scattered by the atmosphere should be revealed by the SHED LIGHT data. To do this, the narrow band sensitivities should be widely distributed across the spectrum. Filters 1 through 4 fulfill this requirement, as shown in Fig. 1-4. Since atmospheric scattering exhibits no spectral fine-structure, the exact positions of the sensitivities are not critical. It is believed that the choice of filters based upon foliage considerations was satisfactory.

Second, the spectral bands should be as narrow as possible, consistent with sensor sensitivity. The four filters selected were recognized as too narrow for some starlight measurements and occasionally sub-marginal under moonlight conditions. Since the existing filter changing mechanisms and other considerations limited the maximum number of filters to five, it was decided to let the fifth filter expose the S-20 photocathodes to the entire spectrum above the ultraviolet. Thus, as shown in Fig. 1-4, the sensitivity of Filter 5 was that of the phototube covered only by an ultraviolet rejection filter (Wratten 2A). Data were obtained by Filter 5 when all other filters were light starved and these data served several practical purposes that are explained later in this report.

#### RELIABILITY OF THE DATA

No effort was spared to maximize the reliability of the data contained in this report. Experience accumulated during more than 25 years of in-flight optical measurements dictated many precautions. Even under optimum daylight conditions with full home-base laboratory support, data of high reliability are not easy to achieve. Night operations overseas, often under adverse weather conditions and with no technical support beyond the resources of the field party, are more difficult.

Not all of the data taken in Thailand are tabulated in this report, only those believed to be highly reliable are included. It is possible that portions of the remaining data can be brought up to a useful level of reliability by further study, but neither time nor funds were available under the contract to accomplish this. There are three principal reasons why these additional data are presently judged insufficiently reliable for inclusion in this report.

### (1) Insufficient Light

In some instances there was insufficient light to make one or more of the key measurements. Missing vital components of data prevented the end-product quantities (e.g.,  $N^*$ ,  $T$ ,  $R^*$ ) from being calculated. There were marginal cases in which the signal-to-noise ratio made the end-product quantities uncertain. The criteria used as the basis of judgement in such cases are discussed later in this report.

### (2) Aircraft Movement

The airborne data could not all be taken in one place, because the aircraft is a moving platform. Thus, on some occasions, clouds overhead, patterns of lights on the ground, or the glow of cities and villages caused distortions of the basic data which made the calculated end-product quantities unusable (e.g., negative values). Some correction and smoothing of the basic data were readily possible. For example, lightning flashes (a common occurrence) are recognizable in the records and interpolation from adjacent data was usually possible. Occasionally, however, when the quantity being measured was changing rapidly, the "settling time" of the photoelectric photometer was too great to permit reliable interpolations to be made. Corresponding effects sometimes occurred when a scanner swept across the moon or over an unusually bright light on the ground.

### (3) Temporal Changes in the Atmosphere

The data collection sequences required considerable time, as detailed in the flight plans given in Section 4. The movement of clouds high overhead, always difficult to see at night, was a frequent cause of data which could not be usefully interpreted. This was particularly true on moonlight flights when the upper clouds were scattered or broken. On one occasion, Flight 100, a complete change in the weather occurred. Fortunately, the lighting conditions were stable before and after the change so that the resulting data formed two reliable sets. These sets are given in this report as Flights 100 I and 100 II.

No data were rendered unreliable due to in-flight malfunction of the aircraft, the measuring equipment it carried, or to imperfection of performance on the part of the Air Force flight crew or the scientific party.

*Precision.* Information pertinent to estimating the reproducibility (precision) of the data presented here will be found throughout this report in descriptions of the apparatus, the flight procedures, the calibrations, the methods of data reduction, and the weather conditions. It will be no surprise that the fundamental sources of noise associated with photoelectric systems were more prominent in the measurements made at night than in corresponding measurements by day. No single precision figure applies uniformly throughout the data. In fact, it is all but impossible to associate a meaningful precision figure with such final quantities as path radiance, directional path reflectance, terrain reflectance, etc., since these are composite values derived from many interlocking measurements by various sensors whose own precision differed from moment to moment depending upon light level at the photocathode. Precision is discussed in more detail later in this section and some best estimates are given.

*Accuracy.* Reliability of the data involves much more than the precision of the measurements. Correctness of absolute values (accuracy) always depends upon the validity of calibrations and the stability of each measuring system with respect to its calibration. Accurate photoelectric measurements of natural lighting over enormous dynamic ranges is a difficult matter even when a single phototube is used, but the problems are compounded when, as in the case of the SHED LIGHT program, many separate phototubes



were required, since all radiometric systems had to have closely identical spectral sensitivities and compatible calibrations.

*Phototube Selection.* It is an inescapable fact that phototubes of the same make and model are not created equal. To the contrary, it is probable that no two phototubes are identical in all measurable respects. Even the state-of-the-art phototubes used for Project SHED LIGHT, procured under stringent specifications requiring careful selection by the manufacturers, were all significantly different. Each was subjected to a long series of tests and further selection at the Visibility Laboratory. These tests, devised over many years of work on airborne photoelectric measurement systems, explore many electrical characteristics, including sensitivity, dark current, and noise. The spectral sensitivity of each tube and all its electrical and mechanical properties was measured over wide ranges of temperature.

The characteristics of all photocathodes are temperature dependent in a complex manner (Murray and Manning, 1960, Boileau and Miller, 1967). The effect is not only a simple change of sensitivity with temperature; it is also a function of wavelength. For example, lowering the temperature of the cathode may increase the sensitivity by 10% in the short wavelength part of the visible spectrum, while the sensitivity in the long wavelength part of the spectrum is decreased by 50%. It is essential, therefore, that the phototube cathode be maintained at a constant temperature. In each SHED LIGHT instrument a thermister bead attached to the photocathode provided the input to an electronic servosystem which maintained the photocathode temperature within  $\pm 0.5^\circ\text{C}$  of a selected temperature by means of a thermoelectric heater/cooler within the housing of the phototube.

Microphonic properties of each phototube were measured. Their dynamic responses were also studied; it is not uncommon to find otherwise closely identical tubes that differ in the times they require to return to their normal sensitivity after receiving a burst of light. The light might be due to a lightning flash somewhere in the night sky or to a scanner sweeping past the moon or over some bright light on the ground. Long term drifts and many other characteristics were measured until, finally, tubes were selected for specific instruments.

*Final Calibrations.* It is necessary to make the final absolute calibrations and, where possible, to also make the final spectral sensitivity checks after the phototube has been mounted in the appropriate instrument. In every case the final radiometric calibration was performed on the entire instrument. When necessary, the filters were altered to make all spectral sensitivities conform with the standard chosen for the whole system.

*In-Flight Calibrations.* Each SHED LIGHT phototube housing contained a highly stable, self-luminous, radioactive button which served as a midrange radiance standard. Upon command, light from this button was presented to the photocathode and all other light was blocked. Checks of absolute sensitivity could be made in flight by means of this internal radiance standard. This was done at frequent intervals throughout all the in-flight measurement sequences, as shown by the charts in Section 4.

*Stability of Calibrations.* A full battery of the calibrations described above was performed on each of the aircraft and ground station instruments immediately before the overseas deployments. They were repeated immediately after the equipment had returned to the Laboratory. It was heartening to find that no significant changes in the shape of calibration curves had occurred. This was true in the case of both ex-

peditions to Thailand in view of the frequent in-flight calibration checks made with the internal radioactive radiance standards, there is strong reason to believe that every system performed in accordance with its Laboratory calibration at all times. Thus, from the standpoint of instrument calibration, the reliability of the data is excellent.

*Radiometric Standards.* All of the radiometric data are reported in absolute units. The calibrations upon which these numbers are based made use of incandescent lamps calibrated in the Visibility Laboratory from several standard lamps purchased from the U. S. National Bureau of Standards. The techniques and equipments used for making these secondary standards and for operating the incandescent standard lamps purchased from the Bureau of Standards were developed with great care over a period of several years. Every effort was made to make our standard lamp facility represent the latest state of the art.

In preparation for building the best possible facility for operating primary standard lamps and making secondary standards, an experienced Visibility Laboratory engineer, thoroughly versed in the theory and practice of lamp standardization, photometry, and radiometry, visited the National Bureau of Standards in Washington, D. C. to observe the equipment and procedures used there. He then visited the corresponding government standardizing laboratories of Canada, Great Britain, France, and Germany to learn firsthand the techniques employed by those countries as well. The lamp standardization facilities subsequently set up at the Visibility Laboratory were based upon all this information. These facilities represent the best ones presently achievable for visible spectrum radiometric calibration.

It is important to note that all radiometric calibrations involved in the SHED LIGHT measurements were based on incandescent standard lamps and attenuations by means of inverse square law techniques involving every precaution and refinement. Each SHED LIGHT instrument had absolute calibrations at a minimum of five different light levels throughout its operating range and linearity checks at 0.1 log intervals. The reliability of the SHED LIGHT data is believed to be excellent with respect to both linearity and absolute calibration.

Additional discussion of the SHED LIGHT data reliability is in Section 6.2.

## SHED LIGHT DATA

Designers of SHED LIGHT electro-optical night vision devices need to know the optical signal available at the sensor. Two quantities are required. (1) the apparent contrast of the object of interest and (2) the approximate apparent radiance of its background. These can be calculated from the data in this report. Ideally, the data should be monochromatic and known throughout the spectral range of the sensor. The SHED LIGHT data are not monochromatic, but they are as narrow band as sensitivity constraints permitted (see Fig. 1-4). They range from blue to very-near infrared. Illustrative examples of their use are in Section 6.2.

The experimental procedures used to collect the data are based upon theory described in the following section. A unified system of mathematical notation is applied throughout this report, it has been developed with great care over many years and has been used in many publications and reports. Some of these reports are reproduced as Appendices A through E. A tabulation of the notation is given in the glossary at the end of this report.

## 2. Theory

### 2.1 CONTRAST TRANSMITTANCE

Contrast transmittance  ${}_b\tau_r(z, \theta, \phi)$  is defined as the ratio of the apparent contrast  $C_r(z, \theta, \phi)$  to the inherent contrast  $C_o(z_t, \theta, \phi)$ :

$${}_b\tau_r(z, \theta, \phi) = C_r(z, \theta, \phi) / C_o(z_t, \theta, \phi) . \quad (2-1)$$

The parenthetical modifiers indicate the altitude  $z$  of the sensor and the zenith angle  $\theta$  and azimuth  $\phi$  of the path of sight. The path length  $r$  in the direction of the path of sight is between the altitude of the target  $z_t$  and the sensor altitude  $z$ . For the inherent contrast the path length is zero. The presubscript  $b$  on the contrast transmittance  ${}_b\tau_r(z, \theta, \phi)$  indicates background. The contrast transmittance is a function of the inherent background radiance  ${}_bN_o(z_t, \theta, \phi)$ , the atmospheric beam transmittance  $T_r(z, \theta)$ , and the path radiance  $N_r^*(z, \theta, \phi)$  of the path of sight shown in Eq. 2-2 (refer to Appendix B Eq. 2.4 on p. 555):

$${}_b\tau_r(z, \theta, \phi) = [1 + N_r^*(z, \theta, \phi) / {}_bN_o(z_t, \theta, \phi) T_r(z, \theta)]^{-1} . \quad (2-2)$$

### 2.2 DIRECTIONAL PATH REFLECTANCE

The concept of directional path reflectance (refer to Appendix D p. 3) is utilized in an alternate form of Eq. 2-2,

$${}_b\tau_r(z, \theta, \phi) = [1 + R_r^*(z, \theta, \phi) / {}_bR_o(z_t, \theta, \phi)]^{-1} , \quad (2-3)$$

where  ${}_bR_p(z, \theta, \phi)$  is the directional background reflectance. By definition, the directional path reflectance is

$$R_p^*(z, \theta, \phi) = \pi N_p^*(z, \theta, \phi) / H(z, d) T_p(z, \theta) , \quad (2-4)$$

where  $H(z, d)$  is the downwelling irradiance. We have chosen to present the atmospheric data in the form of directional path reflectance since, in this form, it can be easily utilized with the directional reflectance of a variety of backgrounds smaller in extent but different from the heterogeneous background which contributed to the path radiance and downwelling irradiance. The directional path reflectance is also the most convenient form of presenting the atmospheric data for easy use to obtain contrast transmittance.

## 2.3 BACKGROUND REFLECTANCE

The inherent background reflectance is defined as

$${}_bR_o(z, \theta, \phi) = \pi {}_bN_o(z, \theta, \phi) / H(z, d) , \quad (2-5)$$

where  $H(z, d)$  is the downwelling irradiance at the target altitude (refer to Appendix B, p. 558 or Boileau and Gordon, p. 805 (1966)). The inherent background reflectance may be obtained from either (1) a measurement by a ground-based telephotometer<sup>†</sup> (refer to Section 7 and Appendix B), or (2) measurements by an airborne telephotometer. In this report airborne telephotometer data from the lowest altitude of flight not interpolated to ground level were used to obtain the terrain reflectances reported in Section 6.3 for each flight.

## 2.4 DOWNWELLING IRRADIANCE

The irradiance used to compute the directional path reflectance  $R_p^*(z, \theta, \phi)$  and the airborne terrain reflectance is computed from data at the lowest altitude of flight by the equation

$$H(z, d) = \int_{2\pi} N(z, \theta', \phi') \cos \theta' d\Omega , \quad (2-6)$$

where  $N(z, \theta', \phi')$  is the sky radiance at direction  $\theta', \phi'$ . Using the same equation, the upwelling irradiance  $H(z, u)$  is computed by replacing the sky radiances with apparent terrain radiances from the lower hemisphere scanner. The  $\theta'$  would then be the nadir angle so that  $\cos \theta'$  is positive. The albedo  $A(z)$  is the ratio of the upwelling to downwelling irradiance  $H(z, u)/H(z, d)$ .

---

<sup>†</sup> Although the measurements are radiometric as opposed to photometric the instrument used to perform these measurements is referred to herein as a "telephotometer" in lieu of the more precise term "teledradiometer". This is in keeping with the practice established in previous publications.

A second type of irradiance is the scalar or nondirectional irradiance.

$$h(z,d) = \int_{4\pi} N(z,\theta',\phi') d\Omega. \quad (2-7)$$

The scalar irradiance is *not* weighted by the cosine. The upwelling irradiance from zenith angles between  $90^\circ$  and  $180^\circ$  is designated by  $h(z,u)$  and computed by using Eq. 2-7 also. The total scalar irradiance is the sum of the upwelling and downwelling scalar irradiances  $h(z) = h(z,u) + h(z,d)$ . The scalar albedo is defined as the ratio of upwelling to downwelling scalar irradiance,  $h(z,u)/h(z,d)$ . For a full discussion of scalar irradiance and scalar albedo users refer to Appendix E.

## 2.5 BEAM TRANSMITTANCE

The beam transmittance  $T_r(z,\theta)$  is obtained directly from the total scattering coefficient  $s(z)$  by means of Eq. 2-8. (Refer also to Appendix C, p. 570). When there is no significant atmospheric absorption in the passbands of the measurements, e.g., from smoke, dust, or smog, the attenuation coefficient  $a(z)$  is equivalent to the scattering coefficient  $s(z)$ . Therefore,

$$T_r(z,\theta) = \text{EXP} \left[ - \sum_{i=1}^n a(z_i) \Delta r \right] = \text{EXP} \left[ - \sum_{i=1}^n s(z_i) \Delta r \right]. \quad (2-8)$$

The incremental path length  $\Delta r$  used was 30.5 m (100 ft). The measured total scattering coefficient data were extrapolated to ground level by assuming an optical standard atmosphere, Duntley (1948), for the interval between the lowest altitude of measurement and ground level:

$$s(0) = s(z) \exp(z/9140 \text{ m}). \quad (2-9)$$

Similarly, upward extrapolations were made to 1829 m (6000 ft) above ground level when the highest flight altitude was less than 1829 m.

All altitudes reported herein are between ground level and 1524 m (5000 ft). For all paths of sight at zenith angles  $\geq 94^\circ$   $\Delta r$  equals  $\Delta z \sec \theta$ , for these altitudes. The  $\Delta r$  is always nonnegative since  $\Delta z$  is defined as  $z_1 - z_2$  (the subscripts increase with the flux direction). See Fig. 2-1.

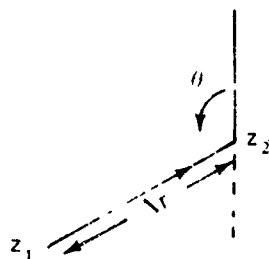


Fig. 2-1. Path Length Geometry

For zenith angles  $94^\circ$ , the beam transmittance can also be expressed as a function of the vertical beam transmittance  $T_r(z, 180)$  as follows:

$$T_r(z, \theta) = T_r(z, 180)^{|\sec \theta|} \quad (2-10)$$

## 2.6 EARTH CURVATURE

For the path of sight at  $93^\circ$  zenith angle, the  $\Delta r$  for  $\Delta z = 30.5$  m (100 ft) is 10% longer at ground level than at 1524 m due to the curvature of the earth. Therefore, for this path of sight, the incremental path length  $\Delta r$  is computed from

$$\Delta r = (\zeta + z_1) \sin(\theta'' + \theta - 180^\circ) / \sin(180^\circ - \theta) \quad (2-11)$$

The  $\zeta$  is the radius of the earth and  $\theta''$  is the zenith angle for the upward path initiating at  $z_1$  from the opposite direction to the downward path at zenith angle  $\theta$ . See Fig. 2-2.

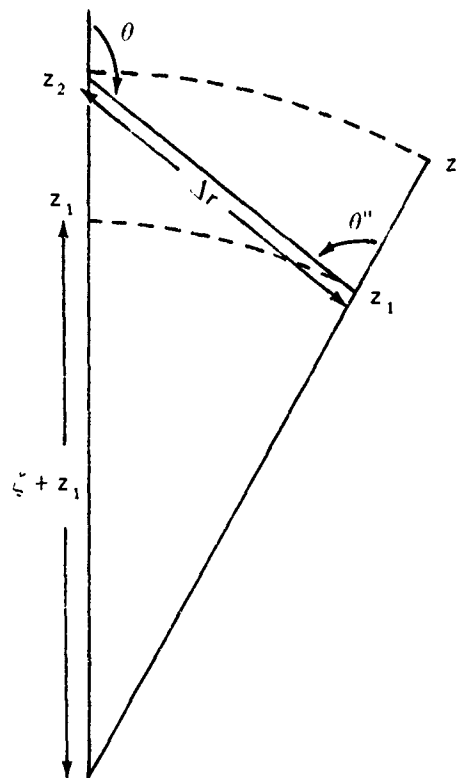


Fig. 2-2. Incremental path length  $\Delta r$  for near horizontal slant paths at paths of sight zenith angle  $\theta$ . Zenith angle  $\theta''$  is the flux direction of the same path. The angle  $\theta''$  is not equal to  $180^\circ - \theta$  due to the curvature of the earth.

The zenith angle  $\theta''$  is found by

$$\sin \theta'' = (\Delta z + \zeta + z_1) / (\zeta + z_1) \sin(180^\circ - \theta) . \quad (2-12)$$

## 2.7 PATH RADIANCE

Path radiance  $N_r^*(z, \theta, \phi)$  for the downward-looking path of sight is the integration or summation of the path function  $N_*(z, \theta, \phi)$  weighted by the beam transmittance  $T_{r_i}(z, \theta)$ . Path length  $r_i$  is from the incremental path  $\Delta r$  to the sensor at  $z$ :

$$N_r^*(z, \theta, \phi) = \sum_{i=1}^m N_*(z_i, \theta, \phi) T_{r_i}(z, \theta) \Delta r . \quad (2-13)$$

(Refer to Appendix A, Eq. 17 on p. 502.) The path function  $N_*(z_i, \theta, \phi)$  is the product of the equilibrium radiance  $N_q(z_i, \theta, \phi)$  and total scattering coefficient  $s(z_i)$  [refer to Appendix A, Eq. 11 on p. 502, since  $s(z) = 1/L(z)$ ]:

$$N_*(z_i, \theta, \phi) = N_q(z_i, \theta, \phi) s(z_i) . \quad (2-14)$$

## 2.8 EQUILIBRIUM RADIANCE

The equilibrium radiance (refer to Appendix A, p. 502, and Appendix E, p. 15) is first computed from the measurements made at each of the altitudes of level flight (at approximately 305 m [1000 ft] intervals) and then interpolated and extrapolated to obtain values at each 30.5 m (100 ft) interval  $z_i$ . To compute the equilibrium radiance the following equation is used (refer to Appendix E, Eq. 16<sup>⊕</sup> on p. 16):

$$N_q(z, \theta, \phi) = \int_{4\pi} N(z, \theta', \phi') \frac{\sigma(z, \beta')}{s(z)} d\Omega , \quad (2-15)$$

where  $N(z, \theta', \phi')$  is the apparent radiance of the sky, moon, or ground for direction  $\theta'$  and  $\phi'$ . The ratio  $\sigma(z, \beta')/s(z)$  is the proportional directional scattering coefficient at angle  $\beta'$  and altitude  $z$ . The  $\beta'$  is the angle between the path of sight at  $\theta, \phi$  and the radiance at  $\theta', \phi'$ . It is found by

$$\cos \beta' = \sin \theta \sin \phi \sin \theta' \sin \phi' + \sin \theta \cos \phi \sin \theta' \cos \phi' + \cos \theta \cos \theta' . \quad (2-16)$$

<sup>⊕</sup>Since the moon radiance was included in the sky measurements, the separate term for the scalar irradiance of the sun (or full moon)  $h_s$  (the first term of the right member of Eq. 16) reduces to zero. Equation 16 applies equally well to real and model atmospheres.

It is the scalar irradiance which designates the flux that enters into the computations of equilibrium radiance and path function when the directional radiances are not known or used. It is the directionality of that flux combined with the directionality of the volume scattering function which produces the unique equilibrium radiance associated with each path of sight.

## 2.9 PROPORTIONAL DIRECTIONAL SCATTERING COEFFICIENT

The proportional directional scattering function is found by combining the Rayleigh scattering component and the Mie scattering component:

$$\sigma(z, \beta') s(z) = \left\{ {}_R s(z) \left[ \frac{\sigma(\beta')}{s} \right] + {}_M s(z) \left[ \frac{\sigma(z, \beta')}{s(z)} \right] \right\} s(z) . \quad (2-17)$$

The Rayleigh scattering coefficient  ${}_R s(z)$  is computed from the values of Rayleigh volume scattering coefficient taken from Penndorf (1957) for 0°C sea level pressure at the mean wavelength of each passband and corrected to ambient temperature and pressure by the ideal gas law equation. Since the Rayleigh scattering is a direct function of density,

$${}_R s(z) = {}_R s(0) P(z) / [T(z) 3.71 \text{E } 3] , \quad (2-18)$$

where  $P(z)$  is pressure in dynes  $\text{cm}^{-2}$ ,  $T(z)$  is temperature in degrees Kelvin, and  $3.71\text{E } 3^*$  has units of dynes  $\text{cm}^{-2} \text{ } ^\circ\text{K}^{-1}$  and is the density at standard sea level pressure and 0°C temperature times the universal gas constant. The proportional directional scattering function for Rayleigh scattering  ${}_R[\sigma(\beta)/s]$  is not a function of altitude so the parenthetical modifier is not used; it is found by

$${}_R[\sigma(\beta)/s] = (1 + \cos^2 \beta) 3 \cdot (16 \pi) . \quad (2-19)$$

The Mie scattering coefficient at measurement altitude  $z$  is the measured scattering coefficient minus the Rayleigh coefficient computed from Eq. 2-18 above:

$${}_M s(z) = s(z) - {}_R s(z) . \quad (2-20)$$

---

\*The form of 3.71E 3 is the computer way of writing  $3.71 \times 10^3$ . This computer form is used throughout the report.



The Mie volume scattering function  $\{ \sigma(z, \beta) / s(z) \}$  is taken from a catalog of values derived from data on photopic volume scattering functions published by Barteneva (1960) (refer to Appendix F) for a range of total scattering coefficients from near Rayleigh atmosphere to heavy fog. The Barteneva volume scattering functions show a good correlation with total scattering coefficient in the range of scattering below the limit for visual flight rules ( $6.2E-4/m$ ). Good correlation is also shown for the Barteneva functions with the ratio of directional scattering coefficients at scattering angles,  $\beta = 30^\circ$  and  $150^\circ$ ,  $\{ \sigma(z, 30) / \sigma(z, 150) \}$ . Since reliable airborne data on volume scattering function were not available, the total scattering coefficient for Filter 5 was assumed to be reasonably similar to the photopic coefficient and the selection from the Barteneva catalog made accordingly<sup>‡</sup>. The Mie volume scattering functions thus selected were used for all five filters at that altitude.

---

<sup>‡</sup> Volume scattering functions were recorded at Lop Buri and Khorat during the period of 10 March to 2 April 1960 by AFCRL personnel for wavelengths of 475, 515, 660, and 745 nm. One AFCRL station date coincides with SHED LIGHT ground station No. 2.9 and two dates correspond with Flights 96 and 99. The AFCRL relative volume scattering function data are currently being extrapolated to  $\beta = 0^\circ$  and  $\beta = 180^\circ$  by following Barteneva's method of graphing volume scattering function vs  $\cos \beta$  and extrapolating the function to  $\beta = 0^\circ$  and  $\beta = 180^\circ$ . The AFCRL relative volume scattering functions will then be integrated to provide a relative  $s(0)$  and be divided by that value to obtain values of  $\sigma(0, \beta) / s(0)$ . These proportional volume scattering functions will then be compared to values of  $\sigma(0, 30^\circ) / s(0)$  and  $\sigma(0, 150^\circ) / s(0)$  for ground station 2.9 and to the values of  $\sigma(z, \beta) / s(z)$  obtained by the method described above and used for the lowest altitude of measurement for Flights 96 and 99.

## 3. Instrumentation

The scientific instrumentation utilized for the SHED LIGHT task falls into three basic categories: (1) radiometric, (2) meteorological, and (3) control and communication. Each of these categories contains several different types of instrument systems. For convenience, all significant instrument systems are tabulated in Table 3-1. Each system and its peculiarities are discussed in the following paragraphs.

### 3.1 RADIOMETRIC SYSTEMS

A standardized radiometer has been developed by the Visibility Laboratory and has been used as the basic detector configuration of all Project SHED LIGHT activities. A typical standardized radiometer consists of five major assemblies, as noted in Table 3-1 and listed below.

1. Multiplier Phototube Assembly
2. Temperature Control Housing Assembly
3. Optical Filter Assembly
4. Radiometer Measuring Circuit Assembly
5. Optical Collector Assembly

These assemblies are generally interchangeable, allowing easy field cannibalization in the event of a catastrophic failure of any assembly in a key system. All assemblies mate in pressure seals which allows each section to be purged with dry nitrogen and maintained at approximately 5 psi positive pressure.

**Table 3-1. Project SHED LIGHT Instrumentation**

**I Radiometric**

- A. Multiplier Phototube Assembly
- B. Temperature Control Housing Assembly
- C. Optical Filter Assembly
- D. Radiometer Measuring Circuit Assembly
- E. Optical Collector Assembly
  - 1. Automatic  $2\pi$  Scanner Assembly
  - 2. Integrating Nephelometer Mode Selector Head Subassembly
  - 3. Dual Irradiometer Assembly
  - 4. Large Aperture Telescope Assembly
  - 5. Vertical Path Function Meter Assembly

**II Meteorological**

- A. Royco Model 220 Particle Counter
- B. Cambridge Model 137-C3 Aircraft Hygrometer System
- C. AN/AMQ-17 Aerograph Set
- D. Bourns Model 430/530 Absolute Pressure Transducer
- E. Bourns Model 509 Differential Pressure Transducer
- F. Bendix Model 566 Aspirated Hygrometer
- G. Science Associates Windspeed and Direction Set
- H. Taylor Model SMT-5-51 Aneroid Barometer

**III Control and Communication**

- A.  $2\pi$  Scanner Control Console
- B. Photometer Temperature Control Panel
- C. Optical Filter Control Panel
- D. Ten Slide Photometer Module
- E. Camera Control Panel
- F. Flight Dynamics Display Panel
- G. 42 Channel Data Logger
- H. 20 Channel Data Logger

**MULTIPLIER PHOTOTUBE ASSEMBLY**

The basic detector in all these systems is a multiplier phototube. A typical assembly is illustrated in Fig. 3-1. Several functions are performed by this assembly. The cylindrical aluminum slug acts as a mechanical support for the multiplier phototube, the emitter/follower circuit, the temperature control thermostats, and an Isolite photometric standard source. The slug also acts as a thermal dashpot to aid in maintaining a constant cathode temperature on the multiplier phototube.

Two types of multiplier phototubes were used during the SHED LIGHT program. The primary detector was an EMR 541E fourteen-stage, end-on tube having an S-20 spectral response. Nine assemblies containing the 541E tube were built for this program. The secondary detector was an EMR 543C fourteen-stage, end-on tube having an S-1 spectral response. Six assemblies containing the 543C tube were built.



Fig. 3-1. Typical Multiplier Phototube Assembly

The thermostats which are mounted in this assembly are the control elements for the photometer temperature control panel system listed in Table 3-1. These Philadelphia Scientific Glass Co. TM 802 mercury column thermostats are selected to maintain the multiplier phototube assembly at 25°C for the S-20 housings and at 10°C for the S-1 housings.

The Isolite photometric reference sources are mounted on this assembly to ensure their temperature stability. These sources utilize a Kr85 gas exciter and a USRC-L-1614 phosphor. They generate approximately 1200  $\mu$ l as a luminous reference source. In some systems, the small amount of alpha radiation escaping from these sources generated an undesirable false signal in the detector circuit. In these cases the substitution of a C-14 exciter was made. This reduced the luminous output to about 8  $\mu$ l but eliminated the alpha radiation problems.

#### TEMPERATURE CONTROL HOUSING ASSEMBLY

The temperature control housing is illustrated in Fig. 3-2. This assembly mechanically surrounds the multiplier phototube assembly and provides the heat pumping necessary for maintaining temperature stability. The active elements are Cambion model 3951 thermoelectric junctions. Two of these junctions located symmetrically about the multiplier phototube assembly ensure efficient thermal control. To optimize thermal pumping in the high ambient temperatures anticipated during the SHED LIGHT mission, the outer surface of the temperature control housing was finned and shrouded for forced air-cooling. On systems assigned to an airborne application the shroud is ducted to collect ram air induced by the velocity of the aircraft. On systems assigned to ground-based applications, an alternate shroud containing an integral muffin fan is utilized.

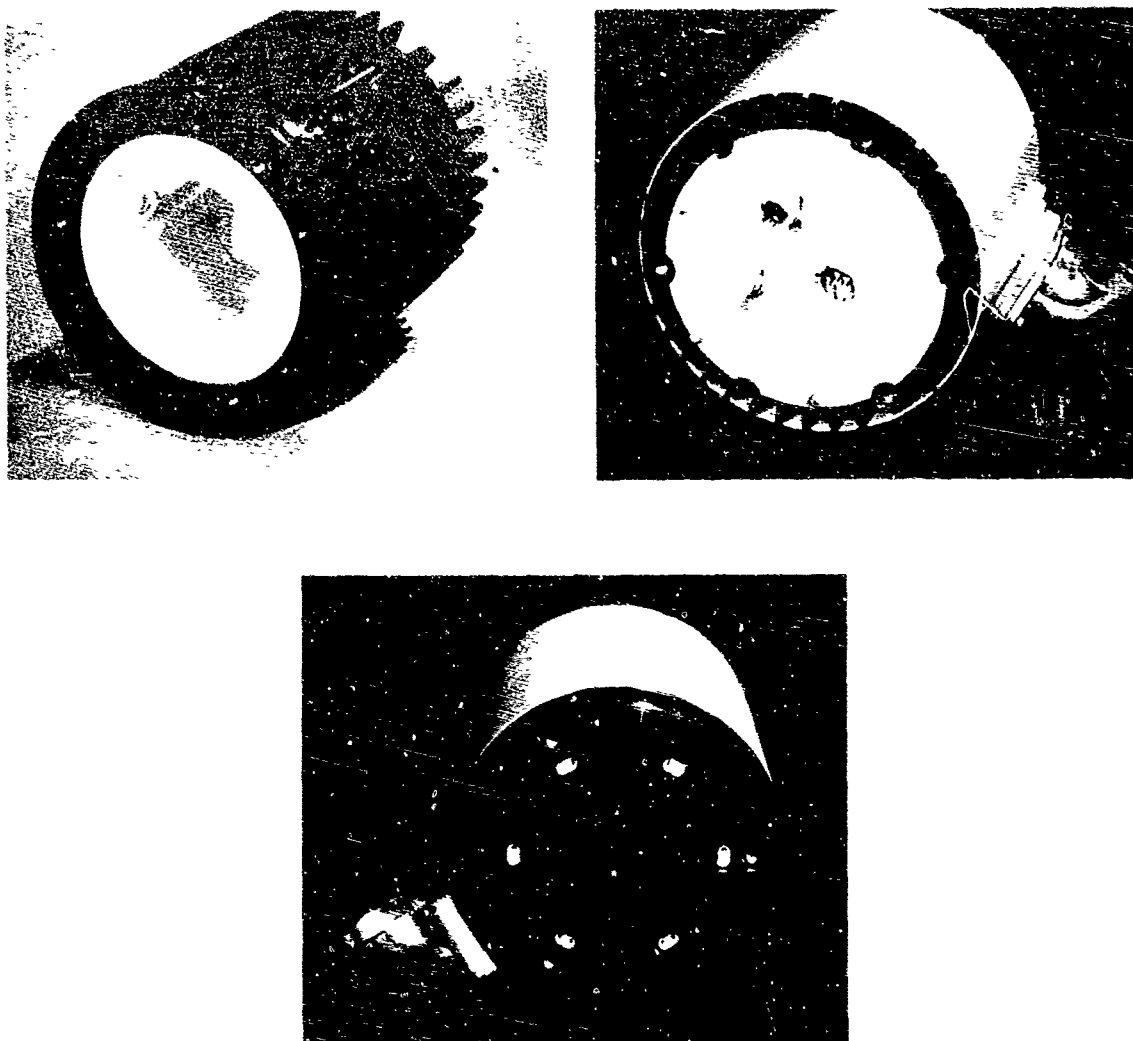


Fig. 3-2. Temperature Control Housing Assembly

#### OPTICAL FILTER ASSEMBLY

A typical optical filter assembly is illustrated in Fig. 3-3. These filter changing mechanisms are designed to mechanically and optically interface with all temperature control housings and optical collector assemblies. Each is an electrically independent device which can, upon electrical command, interpose any one of six optical filter holders into the optical path.

For the SHED LIGHT missions, each of these filter changers contained four Baird-Atomic type B-3 visible spectrum interference filters, one UV rejection filter, and one memory reference system mirror. The type B-3 filters had center wavelengths of 475 nm, 515 nm, 660 nm, and 745 nm. A filter changer of this type was assigned to each of the eight primary S-20 detector systems.

An alternate filter changer, one with three filter holders, was assigned to each of the five secondary S-1 detector systems. These assemblies are mechanically, electrically, and optically interchangeable with the six-holder model. Each of these three-holder assemblies contains one visible rejection filter, one inactive holder, and one memory reference system mirror.

The electrical control circuit for the filter holder carrying the memory system mirror is the electrical inverse of those circuits controlling the optical filters. Thus whenever filter control system power is off, the memory mirror automatically drops into place. This mirror completes the optical path between the Isolite standard source and the multiplier phototube cathode, providing a constant-flux storage and standby condition.

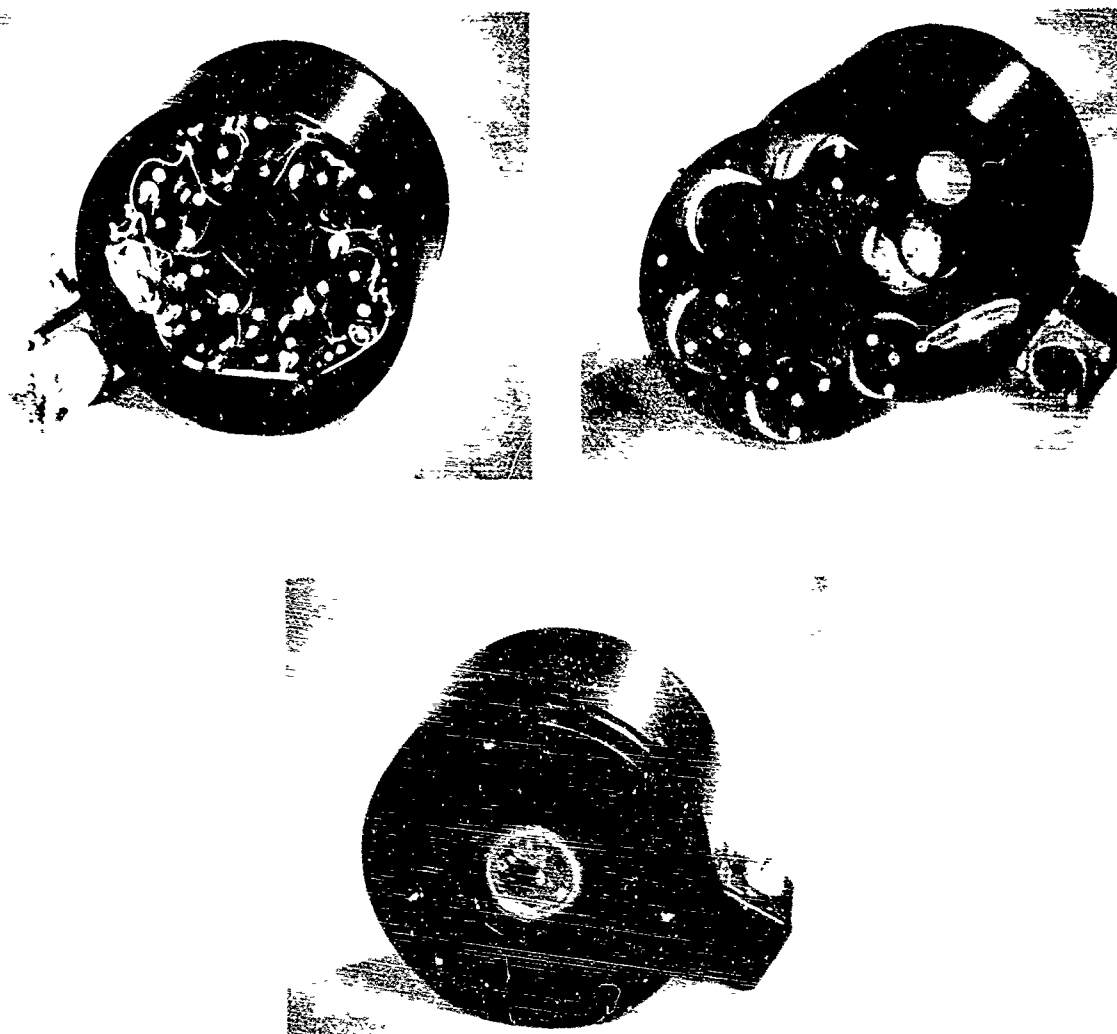


Fig. 3-3. Typical Optical Filter Assembly

## RADIOMETER MEASURING CIRCUIT ASSEMBLY

A standardized radiometer measuring circuit has been utilized with all systems described in this section. It is a solid state package designed for use on the 28 vdc aircraft power. It consists of three basic subassemblies: a multiplier phototube and emitter follower stage, a high voltage and readout section, and a general purpose power supply. In the operational mode, all three subassemblies are linked in a closed loop feedback circuit which serves the high voltage applied to the multiplier phototube. The feedback loop maintains a constant anode current by inversely varying the high voltage with the flux incident at the photocathode. A typical electrical schematic of the Visibility Laboratory model 5 photometer circuit is illustrated in Fig. 3-4 and typical subassemblies are shown in Figs. 3-5 and 3-5A.

This particular circuit is readily adaptable for use with any multiplier phototube. Anode current levels and therefore basic radiometric sensitivity can be easily altered by changing only the anode load resistor. For the SHED LIGHT program this circuit was used with a 1000 megohm anode load in all 541E circuits and with a 100 megohm load in the 543C circuits.

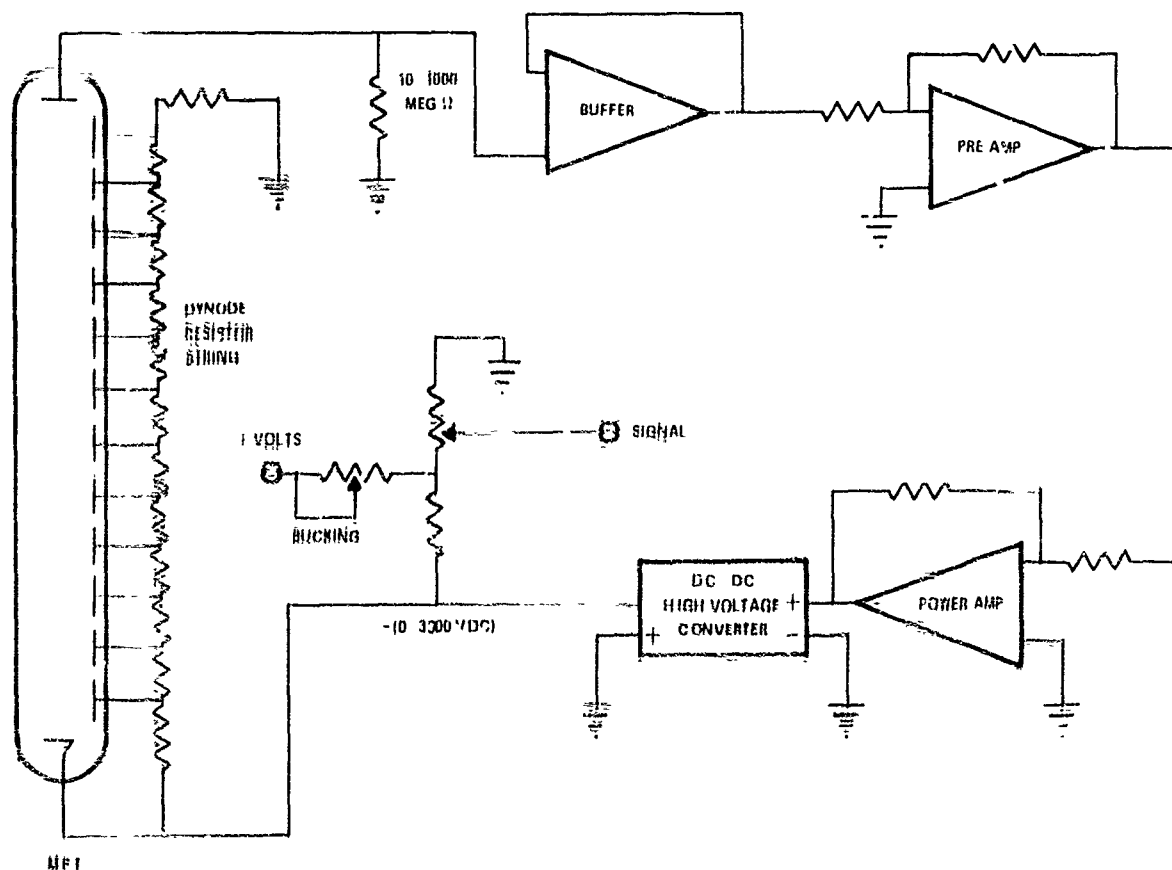


Fig. 1-1 Schematic of Visibility Laboratory Model 5 Photometer Circuit

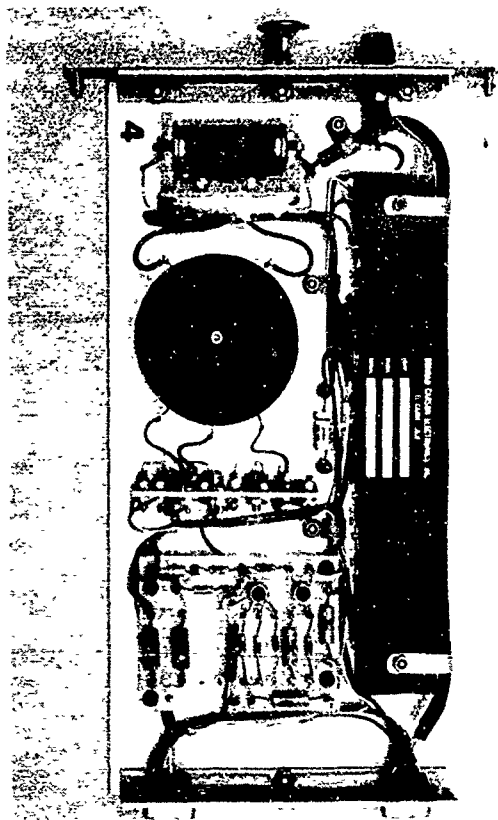


Fig. 3-5. Photometer Slide Subassembly

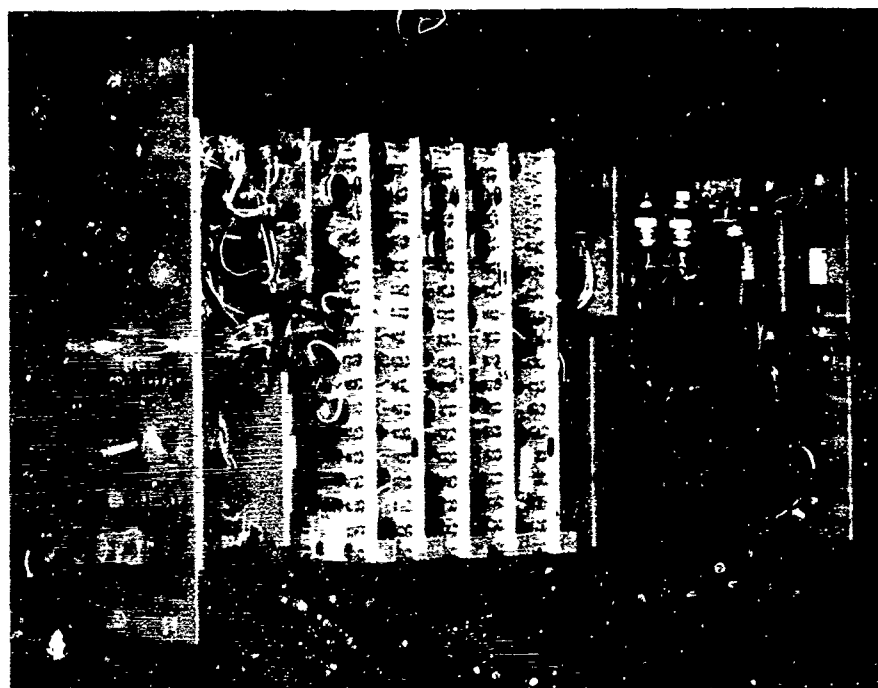


Fig. 3-5A. Photometer Power Supply



For packaging convenience, nine high voltage and readout sections plus a single shared power supply are grouped into a single module. This composite assembly is referred to in the Control and Communications Section as the ten slide photometer module. Two ten slide modules and 14 high voltage and readout sections were provided for the SHED LIGHT activity.

#### OPTICAL COLLECTOR ASSEMBLY

Five basic collector assemblies were used in combination with the basic detector configurations described in the preceding sections. The only major differences between the various radiometer systems described in this report are the differences in these five collector assemblies. The basic assemblies tabulated in Table 3-1 are listed below for convenience.

1. Automatic  $2\pi$  Scanner Assembly
2. Integrating Nephelometer Mode Selector Head Subassembly
3. Dual Irradiometer Assembly
4. Large Aperture Telescope Assembly
5. Vertical Path Function Meter Assembly

These typical assemblies are described briefly below.

*Automatic  $2\pi$  Scanner Assembly* (See Figs. 3-6 and 3-7.) This collector assembly is essentially a small telescope that can be directed to optically scan any point within a  $2\pi$  steradian field of view. The telescope itself has only a  $5^\circ$  field of view with an objective lens 9.5 mm in diameter.

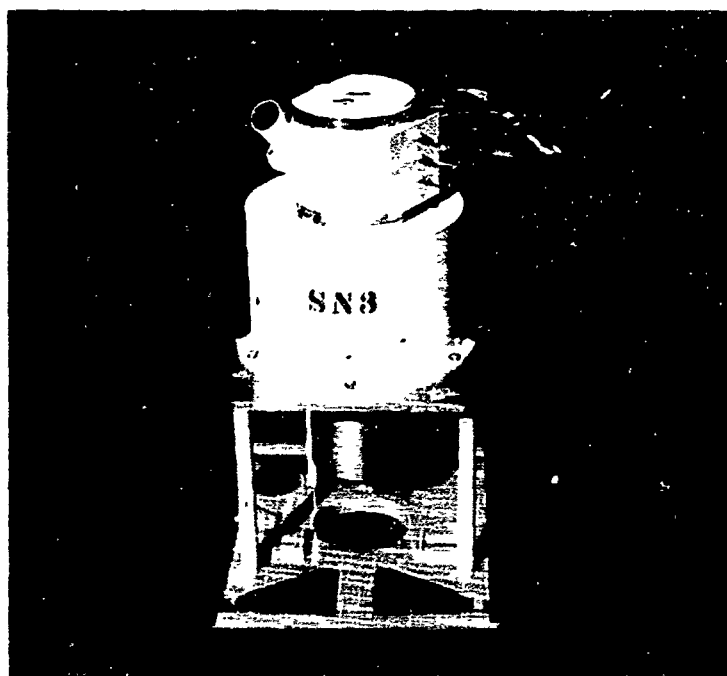


Fig. 16. Automatic  $2\pi$  Scanner Assembly

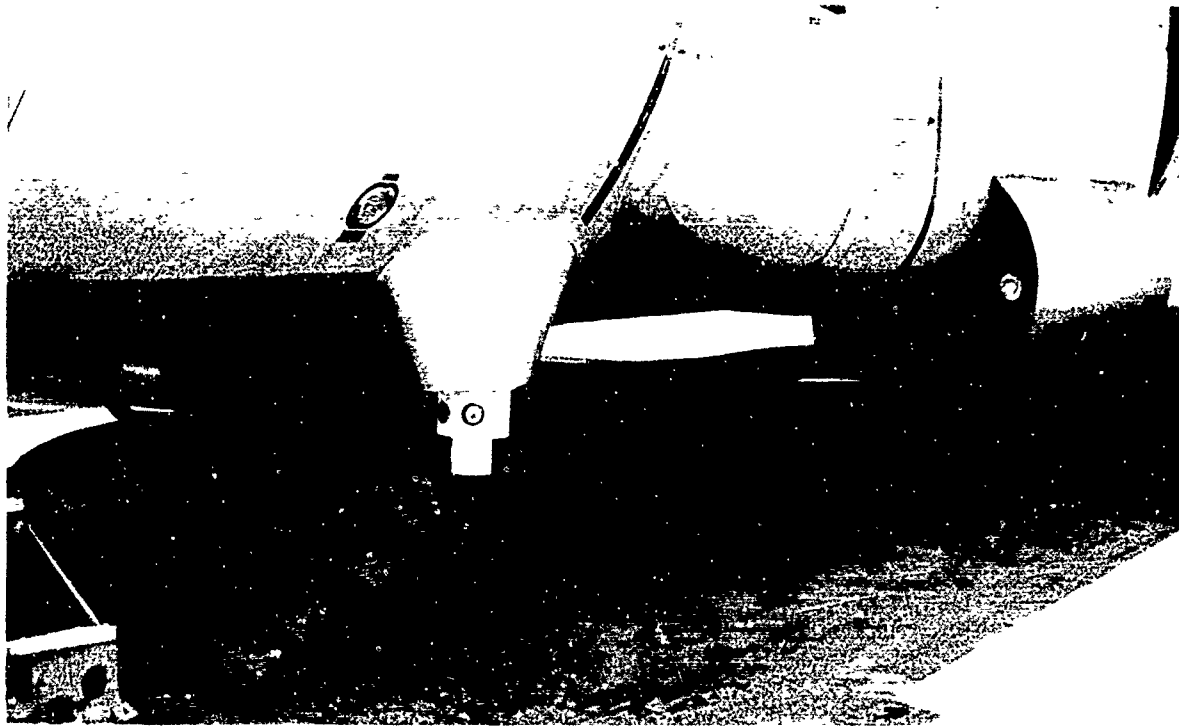


Fig. 3-7.  $2\pi$  Scanner Installation for Lower Hemisphere Measurement

The telescope subassembly is integrally mounted in an azimuth and elevation drive subassembly which is remotely controlled by servo transmitter follower circuits. The sweep pattern for the field of view is determined by a solid state logic circuit contained in the  $2\pi$  scanner control console. For the SHED LIGHT mission the airborne scanners were directed to rotate in the azimuth at a constant rate of  $360^\circ$  per second. The elevation drive simultaneously followed a variable rate ramp function. The resultant sweep pattern covered a full  $2\pi$  steradian in 32 seconds. An alternate scan rate was available for selection at the discretion of the system operator. This alternate scan covered the  $2\pi$  steradian field in 160 seconds.

Since the  $2\pi$  scanner azimuth and elevation drive subassembly is a slaved unit, it may also be driven by manually controlled servo transmitters. This enables the system operator to manually direct the pointing of the telescope line of sight at his discretion. This option is also accomplished at the  $2\pi$  scanner control console.

Four telescope and azimuth and elevation drive subassemblies were built for this project mission. They are reasonably identical and can be readily interchanged in the field. They interface mechanically and optically with any of the optical filter assemblies discussed previously.

Two of these  $2\pi$  scanner assemblies are normally mounted on the project aircraft. One is located on the top of the fuselage for scanning the upper hemisphere radiance distributions and the other is located on the bottom of the fuselage for scanning the lower hemisphere radiance distributions.

The two remaining automatic  $2\pi$  scanners are normally assigned to the project ground station. (See Figs. 3-7A and 3-7B for ground station instrument setups.) In this application they may be oriented to scan either upper hemisphere radiances or inherent terrain radiances at the discretion of the system operator.

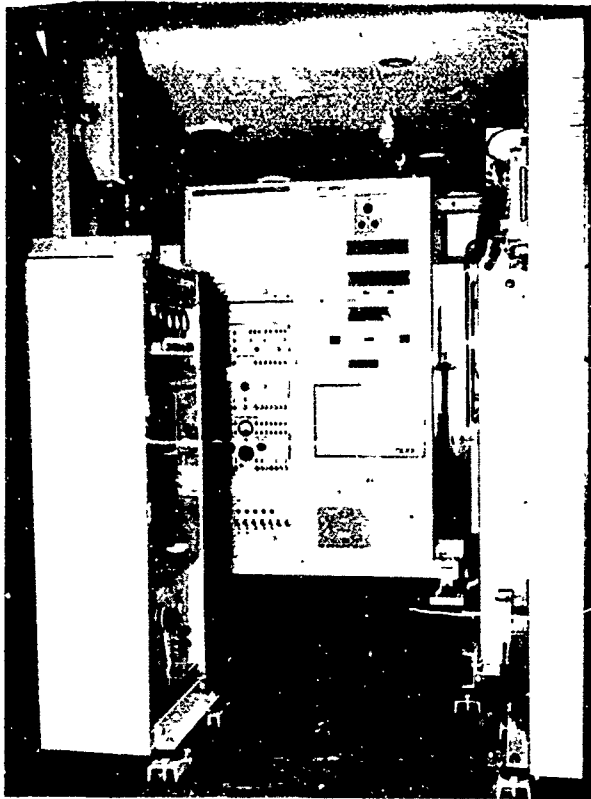


Fig. 3-7A. Ground-Based Instrument Enclosure used During TDY-1

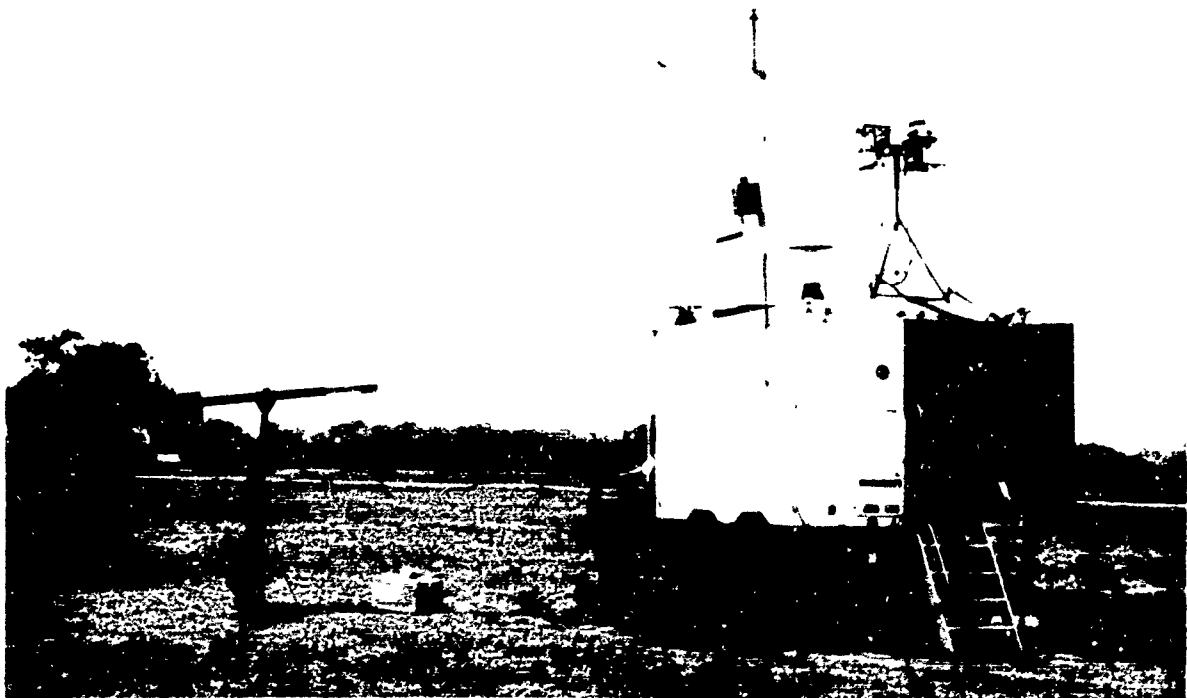


Fig. 3-7B. Ground-Based Instrument Enclosure Setup at Lop Buri Site During TDY-2

*Integrating Nephelometer Mode Selector Head Subassembly.* (See Figs. 3-8 and 3-9.) In order to measure and evaluate the total scattering coefficient of typical real aerosols, the Visibility Laboratory has devised and built an instrument referred to as an integrating nephelometer. This device measures the radiant flux scattered from the well-defined flux beam of a high-intensity projector. The scattered flux is collected simultaneously through three different optical channels, sorted, and routed to the detector assembly for measurement.

The mode selector head is the subassembly which collects, sorts, and identifies this flux prior to its arrival at the detector.

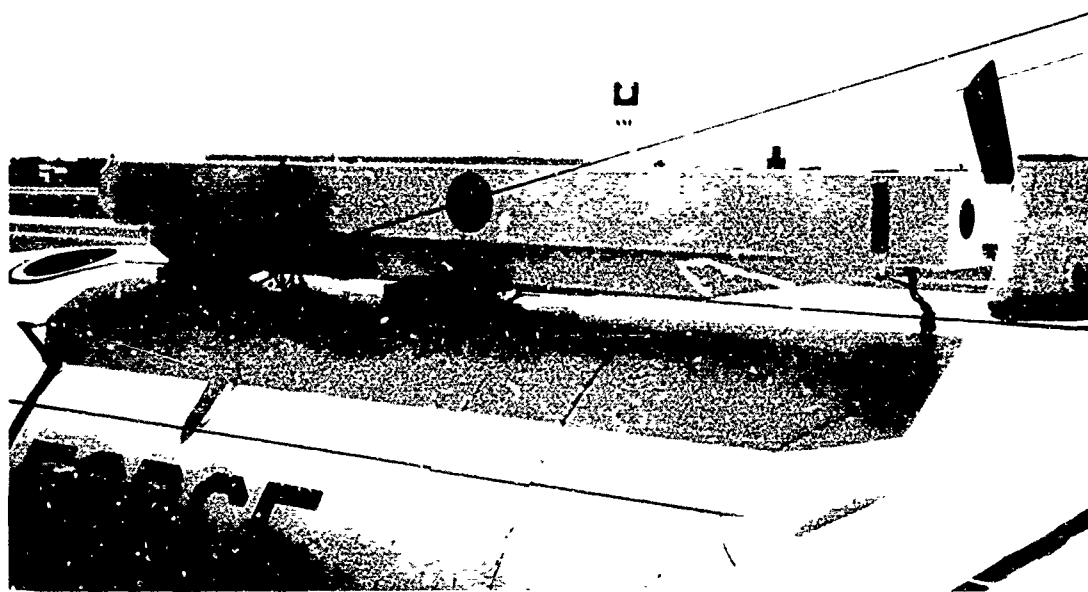


Fig. 3-8. Integrating Nephelometer Aircraft Installation

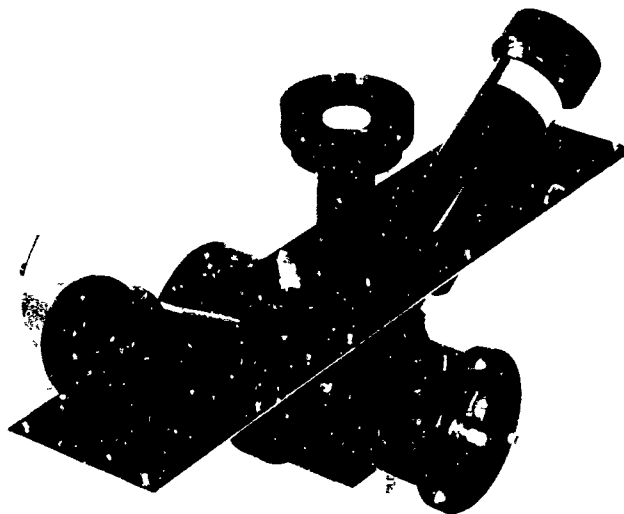


Fig. 3-9. Integrating Nephelometer Mode Selector Head Subassembly

The mode selector head contains three optical input channels but only one optical output. A rotating prism subassembly allows the system operator to select any one input channel for optical coupling with the output channel, while simultaneously occulting the remaining two. The resultant time-sharing of a single detector assembly yields a device optimized for ratio type measurements.

The two outermost input channels of the mode selector head are simple telescope subassemblies, while the centrally located third is an irradiometer subassembly. The complete three channel collector is oriented adjacent to the flux beam of the projector as illustrated in Fig. 3-10. In this orientation, one telescope collects flux scattered from the beam at the forward scattering angle of  $30^\circ$ , while the other collects flux from the beam at the back scattering angle of  $150^\circ$ . The collection apertures are 4.79 cm in diameter and the telescope has a  $2^\circ$  field of view. The irradiometer, which is mechanically corrected to yield a nearly cosine acceptance, collects flux scattered from the beam at all scattering angles between  $5^\circ$  and  $170^\circ$ .

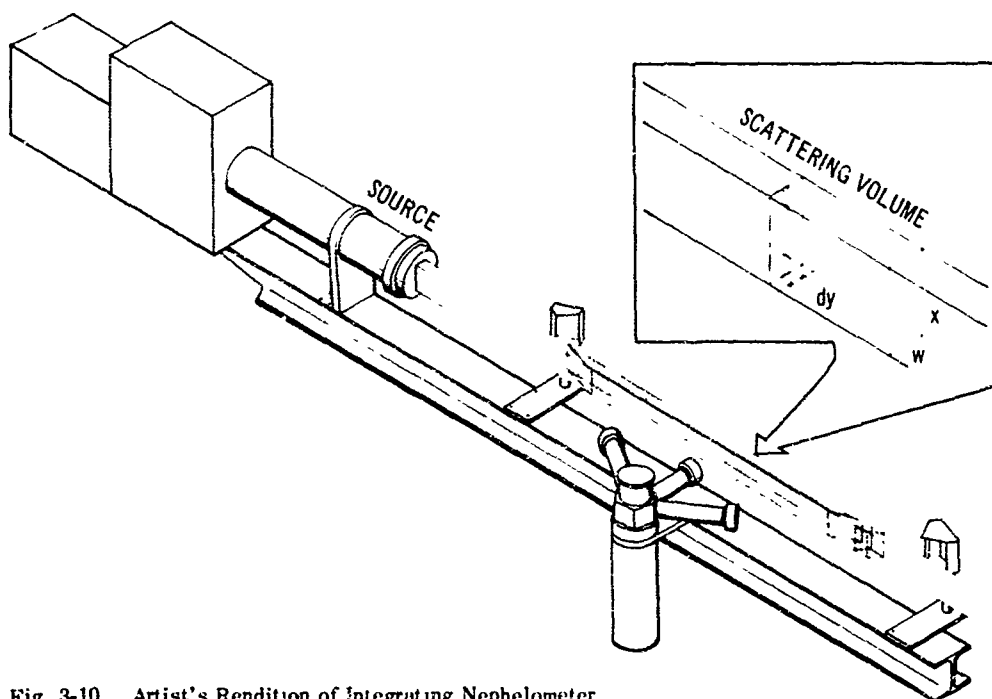


Fig. 3-10. Artist's Rendition of Integrating Nephelometer

From properly calibrated measurements of the scattered flux made through the two telescope channels, one may derive a value for the directional scattering coefficient of the aerosol within the scattering volume.

In a similar manner, properly calibrated measurements of the scattered flux made through the irradiometer channel yield values for the total scattering coefficient of the sample aerosol.

The details of the operational concept and calibration technique for this instrument are covered more thoroughly in two separate memoranda currently being prepared for publication.

Two complete integrating nephelometer instruments were fabricated for the SHED LIGHT mission. Each instrument was made up of two mode selector head subassemblies complete with detector and filter subassemblies (one for the S-20 multiplier phototube, the other for the S-1 multiplier phototube), one high-intensity projector, and an ambient light shroud.

All four of the mode selector head subassemblies are identical and interchangeable. The two projectors and shrouds were customized according to whether they were for airborne or ground-based operation. See Fig. 3-11.

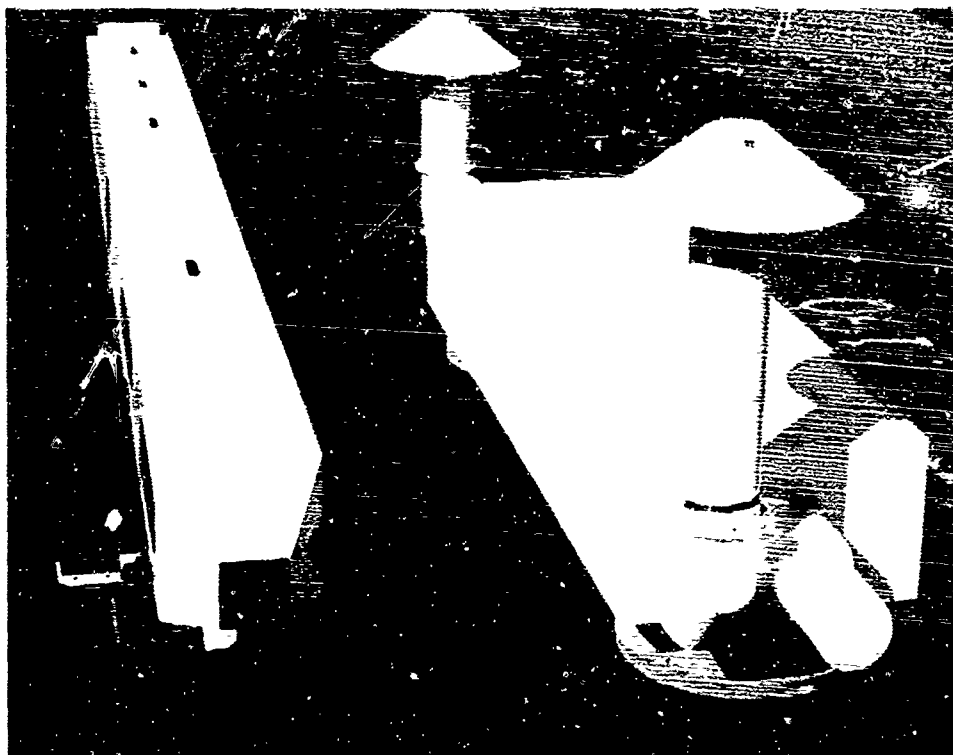


Fig. 3-11. Air and Ground Nephelometer Shrouds

**Dual Irradiometer Assembly.** (See Figs. 3-12 and 3-12A.) The dual irradiometer assembly is a two channel irradiometer. It has two optical input channels but only one optical output. A rotating prism sub-assembly allows the system operator to select either input channel for optical coupling with the output channel, while simultaneously occulting the other. The resultant time-sharing of a single detector assembly yields a device optimized for ratio type measurements.

The flat plate diffuse collector surfaces used in this assembly are mechanically corrected to yield a cosine collection characteristic within  $\pm 2\%$  for all angles of incidence between  $0^\circ$  and  $80^\circ$ .

The dual irradiometer assembly is mounted in the aircraft wingtip so that the flat plate collectors are horizontal. In this configuration the upper channel receives radiant flux from the entire hemisphere above the aircraft and the lower channel receives radiant flux from the entire hemisphere below the aircraft. These measurements of downwelling and upwelling irradiance can be used both in the calculation of directional terrain reflectances and in inter-system data validation checks.

Two dual irradiometer assemblies were fabricated for the SHED LIGHT mission. Both were assigned to the aircraft, one using an S-20 detector assembly and the other using an S-1 detector assembly.

Fig. 3-12. Dual Irradiometer Assemb



Fig. 3-12A. Dual Irradiometer Installation

*Large Aperture Telescope Assembly.* (See Fig. 3-13 ) This telescope assembly is used in the radiometer system which functions as a backup system for measuring very low flux levels. The airborne telescope assembly has a  $5^\circ$  circular field of view and an objective lens 6.2 cm in diameter. With this larger collection aperture, flux levels significantly lower than the detection threshold of the  $2\pi$  scanner assembly can be reached and adequately measured. The ground-based large aperture telescope field of view is  $2^\circ$  by  $5^\circ$ .

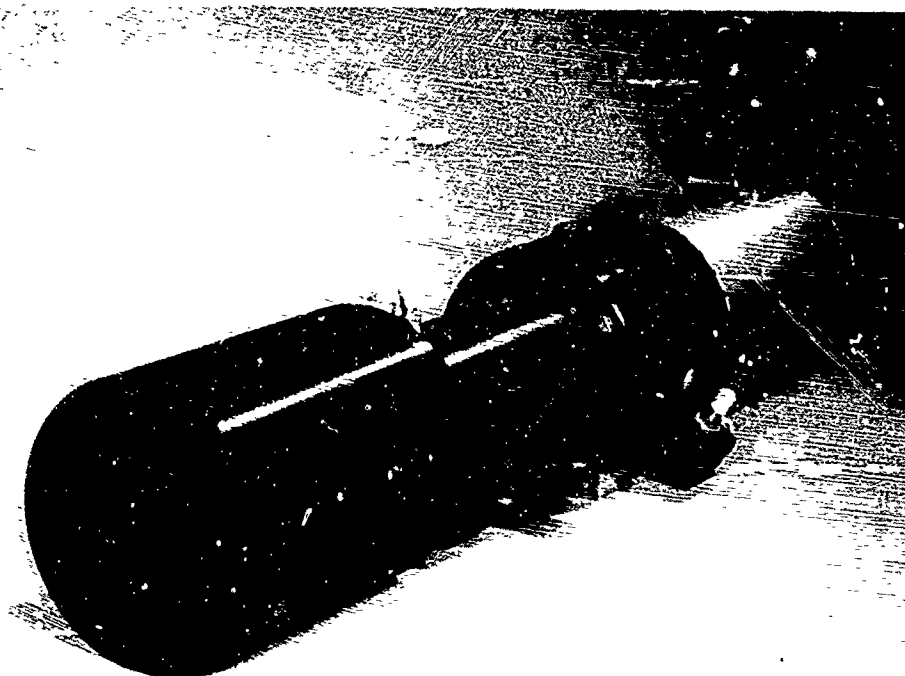


Fig. 3-13. Large Aperture Telescope Assembly

Three large aperture telescope assemblies were fabricated for the SHED LIGHT mission. Two were assigned to the aircraft for monitoring apparent nadir terrain radiances. The third was assigned to the ground station for measurement of inherent terrain radiance.

Several special purpose ground-based frames and tripods were used with this radiometer. They were primarily aids in making measurements of directional terrain reflectance. In all cases they were manually operated devices that functioned to ensure high reproducibility in aiming the telescope optical axis. One such device, referred to as the ground goniophotometer assembly, is illustrated in Fig. 3-14.

*Vertical Path Function Meter Assembly.* The vertical path function meter is a radiometer and shroud assembly designed to measure the radiant flux scattered from a small, well-defined volume of aerosol. The device is illustrated in Figs. 3-14A and 3-14B. Earlier models of airborne path function meters and their utilization are referred to in Appendix A.



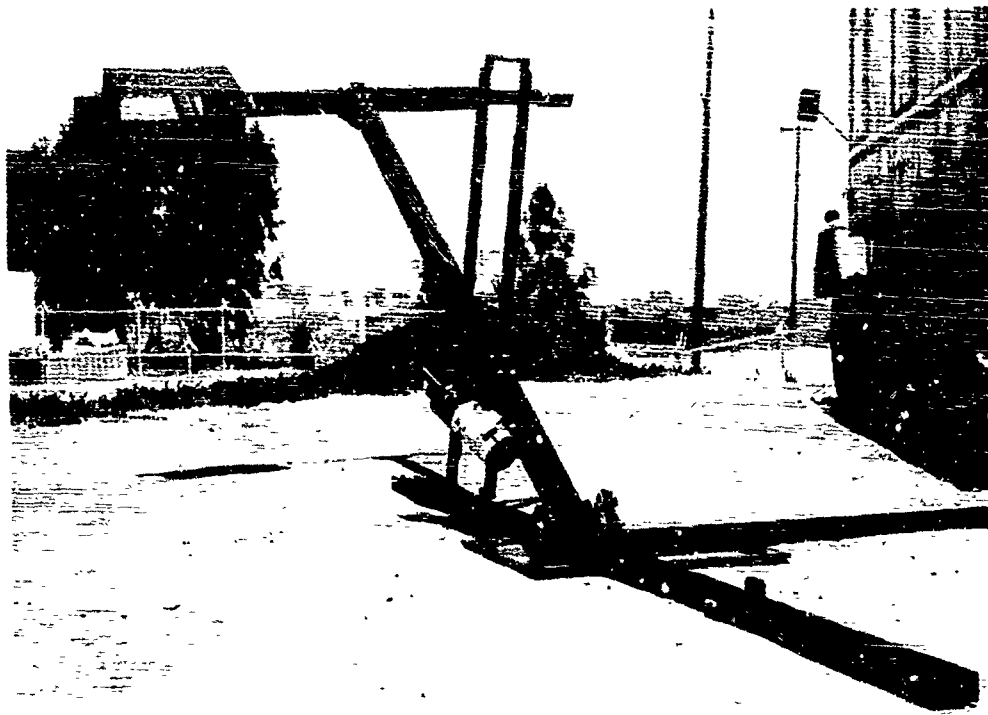


Fig. 3-14. Ground Goniophotometer Assembly

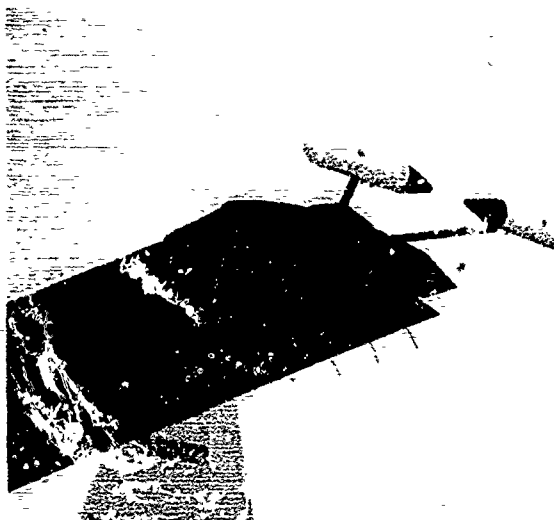


Fig. 3-14A. Vertical Path Function Meter Installed on C-130 No. 50022. This horizontal configuration is used in the determination of horizontal attenuation lengths.



Fig. 3-14B. Vertical Path Function Meter Installed on C-130 No. 50022. This inclined configuration is used in the determination of inclined path radiances.

The most significant feature of the current model is that its orientation can be changed during flight. The scattering volume is 2.5 cm in diameter and 30.5 cm long. It is defined by the cylindrically limited field of view of the component telephotometer and the two tapered sunshades shown in the illustration. The entire assembly can be rotated 180° in approximately 1 minute. When the aircraft is flying straight and level, this plane of rotation is vertical. Measurements of path function can be made at zenith angles between 0° and 180° at azimuths corresponding to the aircraft heading.

The ability to make direct measurements of path function at inclined lines of sight during ascending and descending daytime flight patterns is essential for validating the data processing technique used with the nighttime data packages.

### 3.2 METEOROLOGICAL SYSTEMS

All of the meteorological systems utilized in this project were purchased items. The operating characteristics of each are available in their manufacturer's brochures. Only a summary of their main features and characteristics are presented in this report.

The airborne meteorological package consists of one Royco model 220 particle counter, one Cambridge model 137-C3 aircraft hygrometer system, one AN/AMQ-17 aerograph set, and two Bourns aneroid pressure transducers.

All the airborne meteorological transducers and sampling probes are located on an external fin which extends outward from the aircraft fuselage. The fin is located on the right side of the aircraft and forward of the propellers. It is illustrated in Fig. 3-15.



Fig. 3-15. Meteorological Fin

The ground-based meteorological package was less extensive, consisting only of one Royco model 220 particle counter (discussed in the following paragraph), one Bendix model 566 aspirated hygrometer, one Science Associates windspeed and direction set, and one Taylor model SMT-5-51 aneroid barometer.

#### AIRBORNE METEOROLOGICAL PACKAGE

*Royco Model 220 Particle Counter.* This device is used to determine the number and size of aerosol particles which are present in a sample volume of air. To do this a controlled flow of air is passed through a brightly-illuminated sampling chamber. The illuminated air sample is observed by a sensitive telephotometer system. Whenever an aerosol particle passes through the chamber, it causes a burst of scattered flux which is sensed by the telephotometer. This scattered flux is related to the particle size; with adequate calibration, the device can therefore determine the number of particles per unit volume which pass through the sampling chamber and their approximate size.

The size spectrum measurable with this device is somewhat variable at the discretion of the operator. For the SHED LIGHT mission, both airborne and ground-based systems were calibrated to count particle sizes occurring between 0.3  $\mu\text{m}$  and 26.0  $\mu\text{m}$  effective diameters. At the normal operating flow rate of 0.1 cubic foot of air per minute, satisfactory particle distributions were accumulated in 4-minute sampling intervals.

The Royco system is the only major system used in this task which does not have its output recorded digitally on magnetic tape. Instead, the particle count is recorded on printed paper tape. As a result, the Royco data is processed independently from the bulk of the project raw data and is not included in the automatic data processing technique discussed in Section 5. The Royco data is normally punched on IBM cards and stored in this format until a demand for its further processing is levied. For this report, only total particles per unit volume are listed. Size distribution information is being deferred for later publication.

Two Royco systems were provided for this task. They are identical systems, with the exception of their inlet plumbing. One system was assigned to the project aircraft for airborne measurements and the other was assigned to the project ground station.

The airborne Royco system inlet plumbing is designed to pick up ram air outside the aircraft, route it at low velocity to the system sensor subassembly, and dump the unused portion plus the system exhaust outside the aircraft. The entire inlet, sample, and exhaust plumbing loop is sealed to prevent contamination of the outside aerosol sample with the pressurized cabin air. The airborne Royco system plumbing is illustrated in Fig. 3-16. Also see Fig. 3-17 for airborne rack A.

The ground station Royco system is located immediately adjacent to the ground station integrating nephelometer. The Royco inlet plumbing in this instance is simply a 15 cm piece of straight tubing which connects the system inlet to the integrating nephelometer shroud. In this application, the Royco system samples a portion of the same aerosol that passes through the nephelometer chamber.

*Cambridge Model 137-C3 Aircraft Hygrometer System.* (See Fig. 3-17.) The Cambridge model 137-C3 hygrometer is a device used for determining the dewpoint of the aerosol surrounding an aircraft during flight. The sensor for this device is located in a restricted flow chamber mounted outside the aircraft beneath the fin assembly and is illustrated in Fig. 3-18.

The physical concept upon which the operation of this device is based is the chilled mirror. A thermoelectric heat pump reduces the temperature of the gold plated mirror until moisture from the ambient air

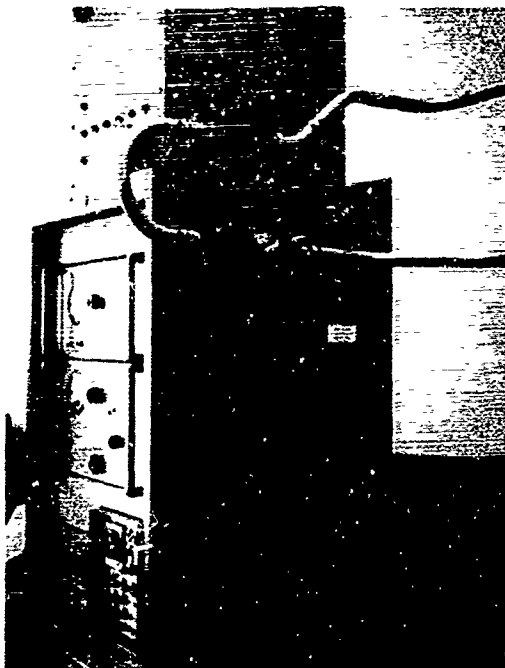
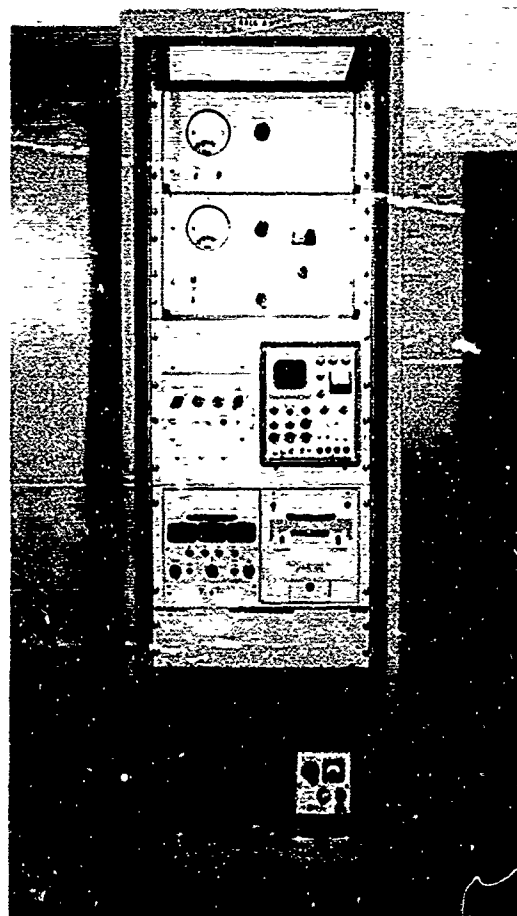


Fig. 3-16. Airborne Royco Plumbing

Fig. 3-17. Rack A: Cambridge 137-C3 (Lower Right);  
AN/AMQ-17 Aerograph Set (Lower Left);  
Royco System (Top)



flowing past it begins to condense on the mirrored surface. The photoelectric detection of this condensation is used as a control signal to the heat pump. A closed loop servo link is established so that the temperature of the mirror surface is maintained at the nominal dewpoint. An integrally mounted platinum resistance thermometer is used to measure the actual temperature of the mirror. From this measure of the dewpoint temperature and the air temperature, the calculation of aerosol relative humidity is direct and straightforward.

*AN/AMQ-17 Aerograph Set.* (See Fig. 3-17.) This aerograph set is a standard military inventory item. Its operating characteristics and technical description are covered in USNAF TP-133. Its general function is to automatically measure and record ambient temperature, pressure, and relative humidity in typical airborne applications. It is suitable for use on aircraft operating at flight speeds between 144 and 518 knots (74 and 267 m/sec) and at altitudes up to 67,000 feet (20 km).

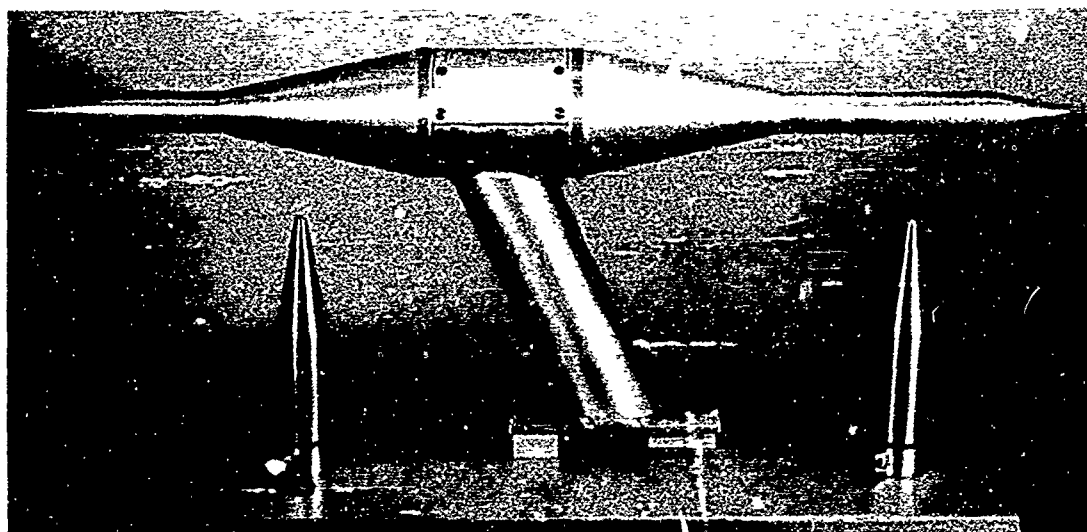


Fig. 3-18. Cambridge Model 137-C3 Probe Housing

*Bourns Model 430/530 Absolute Pressure Transducer.* This transducer is an aneroid/potentiometer device used to provide pressure altitude data. The static probe located on the meteorological fin is the inlet. The transducer is calibrated over a range of 0 to 15 psia, with a static error band of  $\pm 1.0\%$  or approximately  $\pm 10$  mb.

*Bourns Model 509 Differential Pressure Transducer.* This transducer is an aneroid/potentiometer device used to provide indicated airspeed. The pitot and static probes located on the meteorological fin are the inlets. The transducer is calibrated over a range of 0 to 5 psid.

#### GROUND-BASED METEOROLOGICAL PACKAGE

*Bendix Model 566 Aspirated Hygrometer.* This device is a handheld, battery powered, self-aspirating, wet/dry bulb thermometer. The operator wets the wick of the wet bulb thermometer and turns on the ducted fan. When the wet and dry bulb thermometers stabilize, he reads the two temperatures and calculates dewpoint and relative humidity. Two of these devices were provided for this project. One is assigned to the aircraft for ground checkout. The other is assigned to the ground station for data collection.

*Science Associates Windspeed and Direction Set.* This battery powered device is assigned to the ground station for determining local surface wind conditions. Data readings are manually recorded on a standardized meteorological observation sheet.

*Taylor Model SM-T-5-51 Aneroid Barometer.* This handheld device is assigned to the ground station for determining local atmospheric pressure. It is temperature-compensated and adjustable for true ground elevation. The dial face is calibrated in inches of mercury.

### 3.3 CONTROL AND COMMUNICATIONS

The control panels, consoles, data loggers, and other support facilities described in this section are the backbone of the project instrumentation. Without them, all of the elegant and expensive transducers described in Sections 3.1 and 3.2 would be, for all practical purposes, useless. Unless the assorted data channels are properly selected and identified and unless these data-identifying analogs are accurately logged, no information retrieval is possible from the mass of analog data presented to the logger.

#### AUTOMATIC $2\pi$ SCANNER CONTROL CONSOLE

There are two automatic  $2\pi$  scanner control consoles associated with this project. One is assigned to the aircraft system and the other to the ground station. In each case, their operational function is the same: to power and direct the automatic  $2\pi$  scanner azimuth and elevation drive subassemblies. However, their internal designs and performance capabilities are quite different.

The airborne scanner control console is illustrated in Fig. 3-19. It consists of six individual panels mounted in the standard 19 inch rack B, plus a remote start/stop function located in the right control console. The component panels are: (1) scanner control panels, two each, (2) programmer control panel, (3) programmer panel, and (4) gyro control panel. An alternate programmer panel is available for use in the less sophisticated ground-based system. The functional description of each panel is outlined briefly below.

*Scanner Control Panels.* As mentioned earlier the scanner azimuth and elevation drive subassembly is essentially a simple servo follower; for each of the four scanner drive subassemblies there is an individual demodulator and servo transmitter circuit. These circuits plus drive power distribution circuits are located in each scanner control panel.

*Programmer Control Panel.* In order to direct an automatic  $2\pi$  scanner in any given direction, transmitter instructions may be generated in either of two ways: (1) manually, via graduated hand operated dials on the programmer control panel face, or (2) automatically, via the solid state control circuits located in the programmer panel. Selector switches for choosing either of these two control modes are located on the programmer control panel. Transfer of the automatic mode start/stop control to the remote panel in the right control console is also included on the programmer control panel. Synchronization of the scanner search program with the 42 channel data logger is also accomplished through this control panel.

*Programmer Panel.* The actual automatic pattern that the scanner field of view traverses is established by a solid state logic control array located in the programmer panel. In the early development stages of

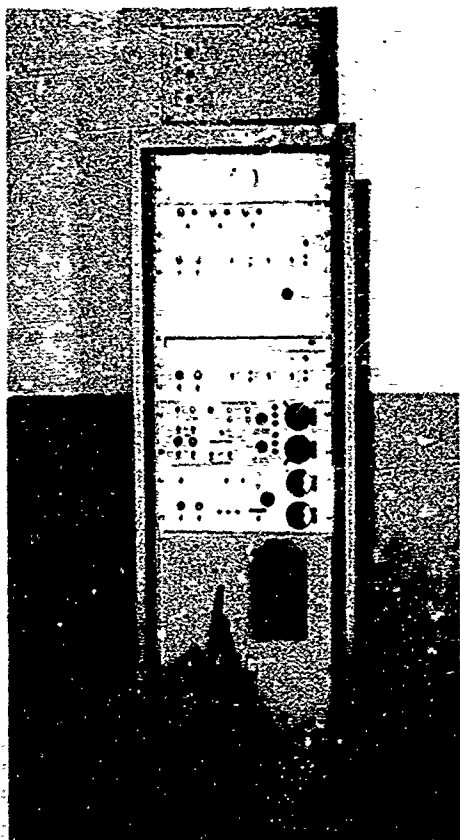


Fig. 3-19. Rack B: Automatic  $2\pi$  Scanner Control Console, 1: Scanner Control Panels, 1 & 2; Programmer Panel; Gyro Control Panel; Power Distribution Panel; Programmer Control Panel

the automatic  $2\pi$  scanner assembly, there was a strong demand for a flexible, high speed pattern control assembly. The most appropriate technique available at the time involved the development of an in-house design utilizing a standardized logic card and rack assembly available from Computer Control Co., Inc.

The original pattern called for a full  $2\pi$  steradian search plus reset in 32 seconds. The azimuth drive was constant at 1 revolution per second. The elevation drive followed a variable rate ramp function. The elevation sequence was as follows:

Azimuth Revolution	$\Delta$ Elevation/Rev	Upper Hemisphere Zenith Angles	Lower Hemisphere Zenith Angles
0 through 12	1°	92° to 80°	88° to 100°
13 through 18	2.5°	80° to 65°	100° to 115°
19 through 31	5°	65° to 0°	115° to 180°
32	Reset	0° to 92°	180° to 88°

This scan rate was too fast for many night applications due to the dynamic response characteristics of the radiometer detector circuits (refer to Section 6). Consequently, a timing modification was inserted to slow the entire routine down to one fifth its original speed. In this mode the full  $2\pi$  steradian search, plus reset, required 160 seconds with the azimuth sweep constant at 5 seconds per revolution. The selection of either scan rate is available to the operator via a rotary selector switch on the face of the programmer panel.

*Gyro Control Panel.* All azimuth and elevation analogs generated by the  $2\pi$  scanner orientation potentiometers are related to the aircraft frame. If the aircraft is flying straight and level, all scanner orientation data is relatively true. Aircraft bearing is recorded on the project data logger so that corrections can be made during data processing for bearing variations during flight. However, since no corrections are made for orientation errors induced by pitch or roll, a reliable monitoring of these maneuvers, if any, was desirable. As a result, a Sperry system SP-40 vertical gyroscope was rigidly mounted to the floor of the aircraft directly below the upper hemisphere  $2\pi$  scanner. Using this gyro as a vertical reference, aircraft pitch and roll analogs were generated and fed to the 42 channel data logger. The erection and control circuits required to drive and monitor the project gyro are contained in the gyro control panel.

Auxiliary circuits related to the equilibrium radiance telephotometer, a system not utilized for the night phases of this program, are included in both the gyro control panel and programmer control panel.

*Ground-Based Programmer.* The automatic  $2\pi$  scanner control console assigned to the ground station is not as sophisticated as the airborne unit. It consists of two scanner control panels, as in the airborne system, and a simplified programmer panel.

The ground-based programmer panel drives two automatic  $2\pi$  scanners in either an automatic search routine or a manually controlled search pattern. In the manual mode, the control dials drive servo transmitters just as in the airborne system. However, in the automatic mode, the ground programmer is significantly different from the airborne.

The ground programmer automatic mode does not use electronic control logic. It is an electromechanical system using synchronous motors, cams, and cam followers as the pattern control elements. It is designed to drive the  $2\pi$  scanners in a stylized search routine which requires 160 seconds to map a  $2\pi$  steradian field of view. The azimuth drive is at a constant speed of 1 revolution per 12 seconds. Each azimuth revolution is run at a fixed elevation angle (zenith angle) in accordance with the listing below. The program time is 120 seconds for pattern scan plus 24 seconds for reset.

Rev No.	Elevation Angle	Zenith Angle
1	$2\frac{1}{2}^{\circ}$	$87\frac{1}{2}^{\circ}$
2	$7\frac{1}{2}^{\circ}$	$82\frac{1}{2}^{\circ}$
3	$12\frac{1}{2}^{\circ}$	$77\frac{1}{2}^{\circ}$
4	$17\frac{1}{2}^{\circ}$	$72\frac{1}{2}^{\circ}$
5	$22\frac{1}{2}^{\circ}$	$67\frac{1}{2}^{\circ}$
6	$27\frac{1}{2}^{\circ}$	$62\frac{1}{2}^{\circ}$
7	$42\frac{1}{2}^{\circ}$	$47\frac{1}{2}^{\circ}$
8	$57\frac{1}{2}^{\circ}$	$32\frac{1}{2}^{\circ}$
9	$72\frac{1}{2}^{\circ}$	$17\frac{1}{2}^{\circ}$
10	$87\frac{1}{2}^{\circ}$	$2\frac{1}{2}^{\circ}$

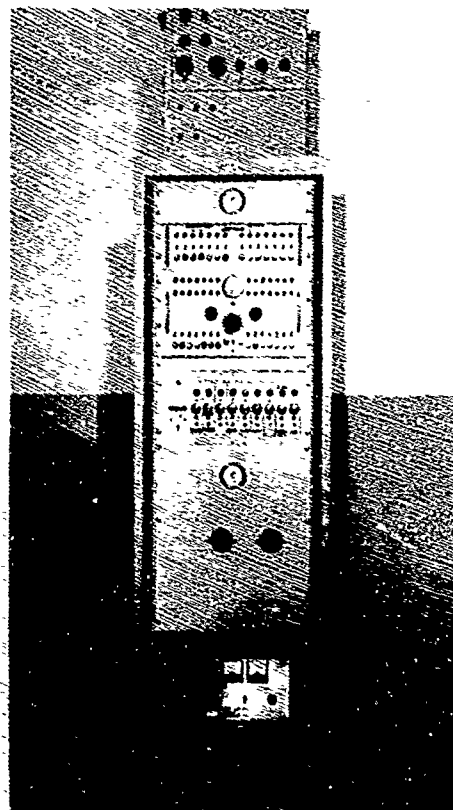
This scan pattern has proved to be inadequate as a general purpose routine. It was established to concentrate its data collection near the horizon. Since that time, more sophisticated data processing techniques have dictated the need for a finer search grid; the scan pattern will be altered in the near future to satisfy this new requirement.



### PHOTOMETER TEMPERATURE CONTROL PANEL

The photometer temperature control system consists of the temperature control housing discussed briefly in Section 3.1, the temperature control thermostat also mentioned in Section 3.1, and the photometer temperature control panel illustrated in Fig. 3-20.

Fig. 3-20. Rack C: Photometer Temperature Control Panel; Defroster Panel; Ten Slide Photometer Module; Nephelometer Power Supply



This panel is a 28 vdc power distribution and readout circuit. It is wired to control and monitor 14 independent temperature control systems. It contains the primary power switch and power distribution relays for each system. These relays, under the automatic control of the temperature control thermostats, reverse the flow of current through the circuit to either heat or cool the inside of the temperature control housing. The resultant temperature of the multiplier phototube cathode is monitored by a Yellow Springs Industry 44011 thermistor bead which is cemented directly upon the glass envelope of the tube.

The performance of each of the 14 available circuits controlled by this panel can be monitored in two ways. The resistance of each thermistor bead can be read on the panel meter, which is calibrated in degrees Centigrade. Also, the current flow in each circuit is monitored by individual lights in both the heat and cool legs. The alternate blinking of the indicator lights indicates proper circuit performance and allows the operator to estimate the system duty cycles at each transducer location.

### OPTICAL FILTER CONTROL PANEL

The optical filter control panel is illustrated in Fig. 3-21. It is a 28 vdc power distribution circuit al-

lowing the ganged control of up to 14 individual optical filter changers. The individual optical filter changer assemblies were described in Section 3.1.

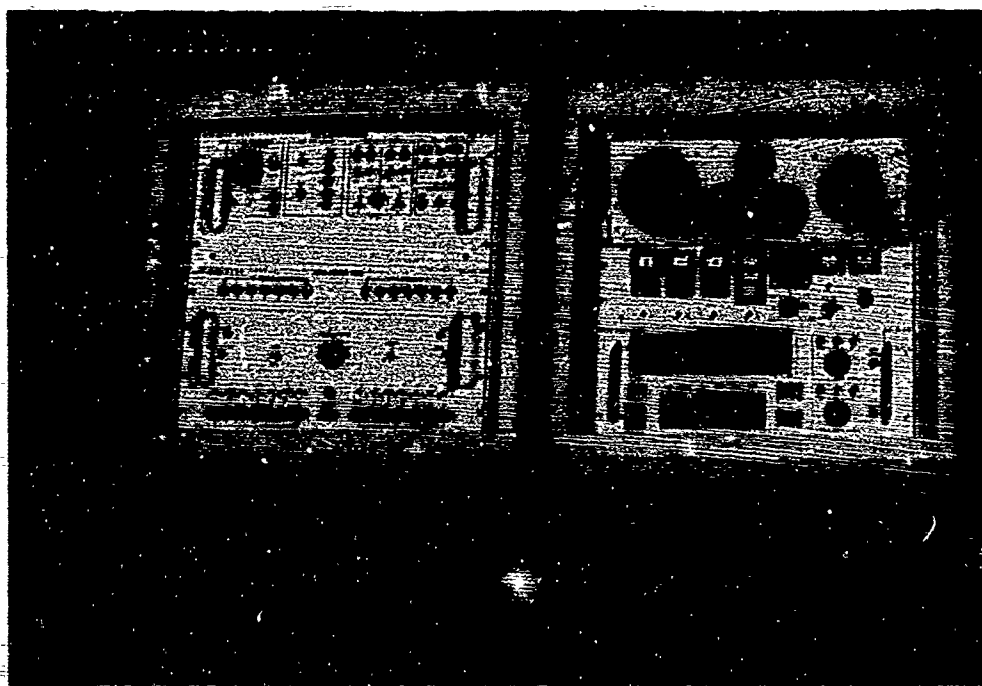


Fig. 3-21. Visibility Studies Control Console Left and Right: Optical Filter Control Panel; Accessory Control Panel; Flight Dynamics Display Panel; Camera Control Panel; Remote Scanner and Data Logger Control

A common selector switch in the center of the panel simultaneously drives each of the activated filter changing assemblies into the selector mode. All 14 circuits are individually switched so that any circuit not activated, i.e., power off, leaves its associated filter changer in the power off, or "memory position".

The system operator is able to interpose any one of six filter holders, and its enclosed optical element, into the optical path of any radiometer. The operational compromise in this system is that *all* activated filter changers follow the selector switch together. The only alternative condition is power off. In the power off condition the memory flux mirror is automatically inserted into that system optical path and the radiometer is relegated to a standby status.

Each of the 14 individual circuits has its own verification light. In each filter changing assembly there are six micro switches which are mechanically actuated by the insertion of a filter holder into the optical path. These switches are electrically "anded" with the selector switch and the verification light. Thus, when a filter selection is made and the verification light comes on, the operator knows with certainty that the optical filter he called for is in fact fully inserted into the optical path.

A supplementary wafer on the filter select switch generates an identifying dc voltage which is transmitted to the 42 channel data logger. In this way the radiometric data can be recovered even if the operator inadvertently calls for an optical filter in an incorrect sequence, or if he forgets to change filters between two successive data collection elements.

#### TEN SLIDE PHOTOMETER MODULE

The ten slide photometer module is illustrated in Fig. 3-20. It is merely a standardized frame which has been prewired to accept the radiometer high voltage and measuring circuits discussed in Section 3.1 and illustrated in Fig. 3-5.

The heavy-duty frame is designed for rack and panel disconnect of all component slide assemblies. The first slide contains the power supply section. It drives up to nine individual radiometer high voltage and readout sections. Each of the nine remaining slides contains one high voltage and readout section. Since for most project activities only six to eight radiometers are ever on line at any given time, there is always at least one slide assembly on standby and available as a spare.

#### CAMERA CONTROL PANEL

This panel, illustrated as part of the right control console in Fig. 3-21, was not used during the night phases of this project.

Its daytime function is to control and trigger the three project cameras. Normally there is an Automax G-10 in each wingtip and a KS-17 Strike camera in the ramp. The cameras are for descriptive documentation of the test environment only. No photogrammetry is attempted.

#### FLIGHT DYNAMICS DISPLAY PANEL

It is essential that the project scientific crew and the USAF flight crew are fully coordinated throughout each data collection mission. To aid in this coordination, to minimize intercom chatter, and to help prevent altitude disorientation of the project crew, several flight instruments have been located at the project control console. This group of instruments is referred to as the flight dynamics display panel and is illustrated in Figs. 3-21 and 3-22.

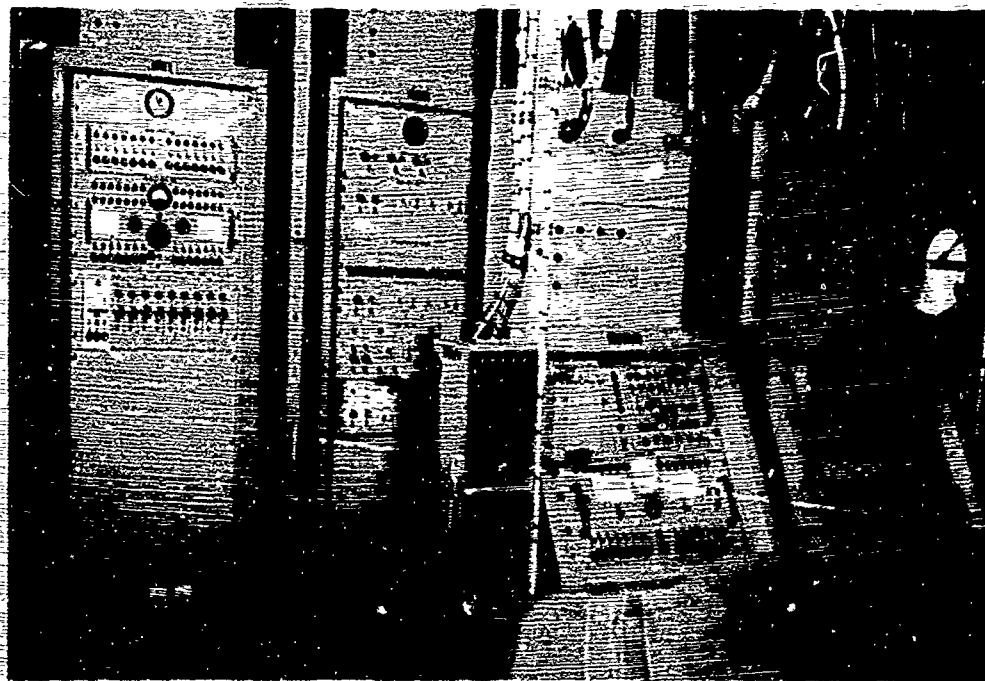


Fig. 3-22. Complete Aircraft Rack Installation

The panel contains the following instruments: (1) gyro magnetic compass indicator, (2) airspeed indicator, (3) altimeter, (4) artificial horizon, and (5) stopwatch and elapsed time clock. All project flight instruments are completely independent of the aircraft flight instrument systems, except for the compass indicator which is linked to the aircraft system through a repeater and amplifier circuit.

#### 42 CHANNEL DATA LOGGER

The heart of the airborne data collection system is the data logger illustrated in Fig. 3-23. This system is designed to accept up to 42 independent analog inputs. The input voltages are specified between 0.000 vdc and  $\pm 0.999$  vdc. The system has three modes of operation: (1) normal, (2) calibrate, and (3) manual.

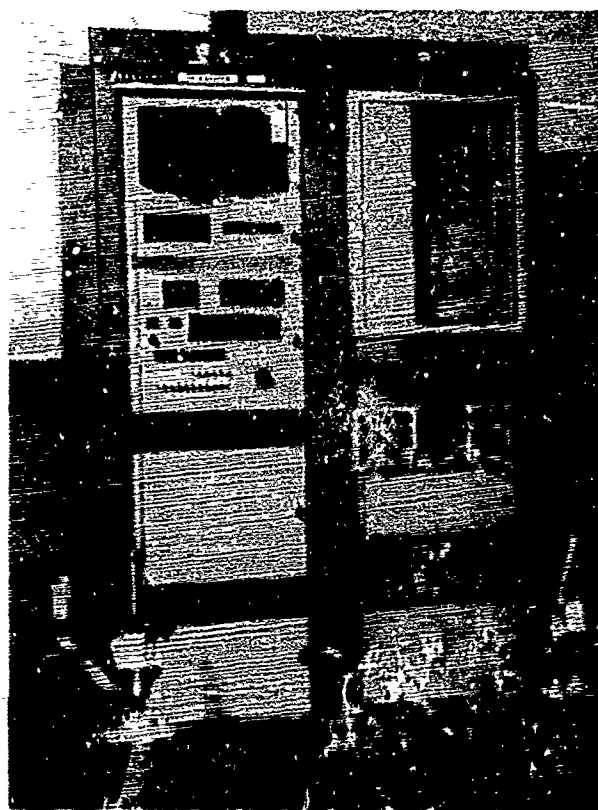


Fig. 3-23. 42 Channel Data Logger

In the NORMAL mode, all 42 input signals are multiplexed into a 240 sample per second array, sequentially converted to digital format, and serially recorded on magnetic tape. Tape speed is 3.56 ips. In this mode the system records continuously until it is stopped either manually by the operator, or by the low tape cutoff. The multiplex array is externally patchable for complete sample rate flexibility. The current sample rate per channel is illustrated in Table 5-1 of the Data Processing Section. The length of one block of data on the tape is 3840 computer words; each word contains 48 bits.

In the CALIBRATE mode, the system starts upon manual command, records one pass through the multiplexer, i.e., 1 second at 240 samples per second, and stops automatically. This mode is normally used for recording dc calibration checks. At one time it was used for monitoring radiometer "memory flux" levels, but that has been abandoned in favor of a longer recording interval.

In the MANUAL mode the system works as a multi-input digital voltmeter (DVM). Selector buttons on the front panel allow the operator to select any one of the 42 input channels for visual display. Upon selecting a specific channel, the channel identification number is displayed on a two-digit nixie display and the digital value of the signal voltage on that channel is shown on a separate three-digit plus sign nixie display. In this mode, the operator can monitor the input signals at any time from each transducer system for either calibration checks or troubleshooting.

The data logger also contains the project clock. Project time is displayed in six digits (hours, minutes, and seconds) on both the data logger panel and its remote panel in the right control console. Project time may or may not be set at real time, according to the operator's selection.

The data logger provides synchronizing pulses to the  $2\pi$  scanner control console. These pulses permit convenient remote control functions to be "anded" at the right control console and establish synchronous data logging for improved data processing efficiencies.

Twelve thumbwheel potentiometers are available on the front panel for the insertion of fixed identification data. This information is automatically recorded each time the tape is started.

#### 20 CHANNEL DATA LOGGER

The ground-based data logger is illustrated in Fig. 3-24. This incremental logger is less sophisticated than the airborne system. It accepts up to 20 independent analog signals. Its input DVM is manually adjusted to accept signals between 0.0000 vdc and  $\pm 1.2000$  vdc; however, the actual input analogs are identical with those in the airborne instrument systems.

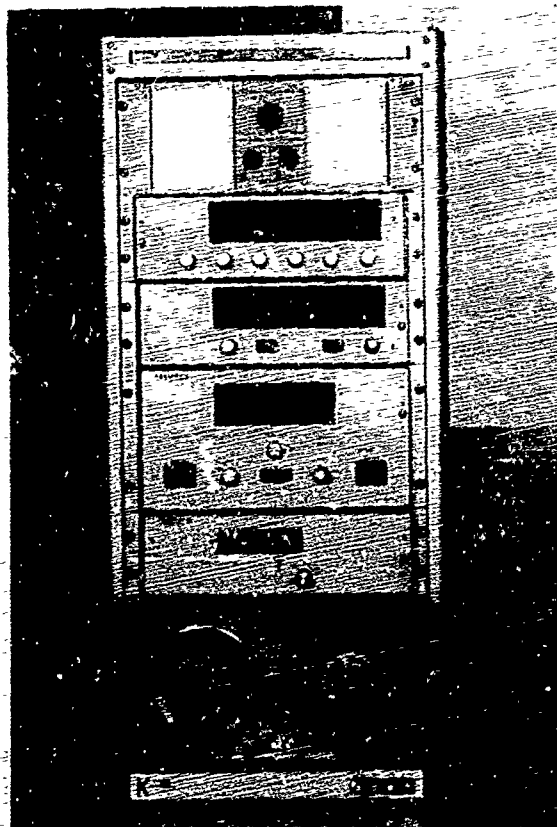


Fig. 3-24. 20 Channel Data Logger

This system has two modes of operation: (1) normal and (2) manual.

In the NORMAL mode the analog signals are measured, serialized, and recorded digitally on magnetic tape. In this mode the system incrementally records channel by channel at about eight channels per second. Once started, it cycles continuously through the channel sequence until manually stopped by the operator.

In the MANUAL mode the system operates as a multi-input DVM. A manual channel selection is available with an associated nixie type display.

Project time is displayed on the logger front panel. It is normally synchronized with GMT, local, or, when practical, airborne project time.

Ten thumbwheel potentiometers are available on the front panel for the insertion of fixed identification data.

### 3.4 RADIOMETRIC CALIBRATION PROCEDURES

All the radiometers used in this project are calibrated in essentially the same manner. In each case the system is calibrated by first determining its relative flux versus high voltage characteristics over the anticipated operating span and second by establishing known absolute flux levels on this voltage curve. The entire calibration procedure is conducted using standard photometric practices, a 3-meter optical bench, and incandescent standards of luminous intensity traceable to the National Bureau of Standards.

The process of establishing the relative flux versus high voltage characteristic curve for each system is simple and direct. The radiometer system is positioned on the optical bench and irradiated with flux from a stabilized incandescent lamp. The mechanical and optical arrangement is such that the amount of flux presented to the detector can be readily varied in increments of 0.10 log units. The mechanical constraints on positioning the movable lamp housing ensure compliance with the desired inverse square relationship between lamp position and flux at the detector. Therefore, through an iterative process of relocating the lamp housing at a predetermined set of locations on the optical bench and recording the resulting radiometer output signal, one can generate a set of data illustrating the system electrical response to known changes of input radiance. This set of data is commonly referred to as the system linearity calibration.

The linearity calibrations for all radiometers employed in the SHED LIGHT task extended over a radiance span of 5 log cycles. The electrical circuitry was adjusted to yield an output signal which swung from +250 mv to -1000 mv for this five decade swing in radiant input. The pseudo-logarithmic characteristic of the radiometer measuring circuit results in a linearity calibration typified in Fig. 3-25.

Since it was desirable to run these radiometers at maximum sensitivity, the linearity calibrations were extended beyond the normally specified limits of system precision. Each system was forced to the point where dark current considerations resulted in an uncertainty equivalent to 50% of the calibration incremental least count; i.e., if a 0.10 log (26%) change in flux results in a 20 mv change in output signal, the calibration cutoff point occurs when the uncertainty in the output signal reaches  $\pm 10$  mv.

Due to the characteristic rolloff of the typical linearity calibration curve plus the dark current cutoff specification, the overall system precision index is variable. This is a factor which must be well understood by those involved in any final data analysis.

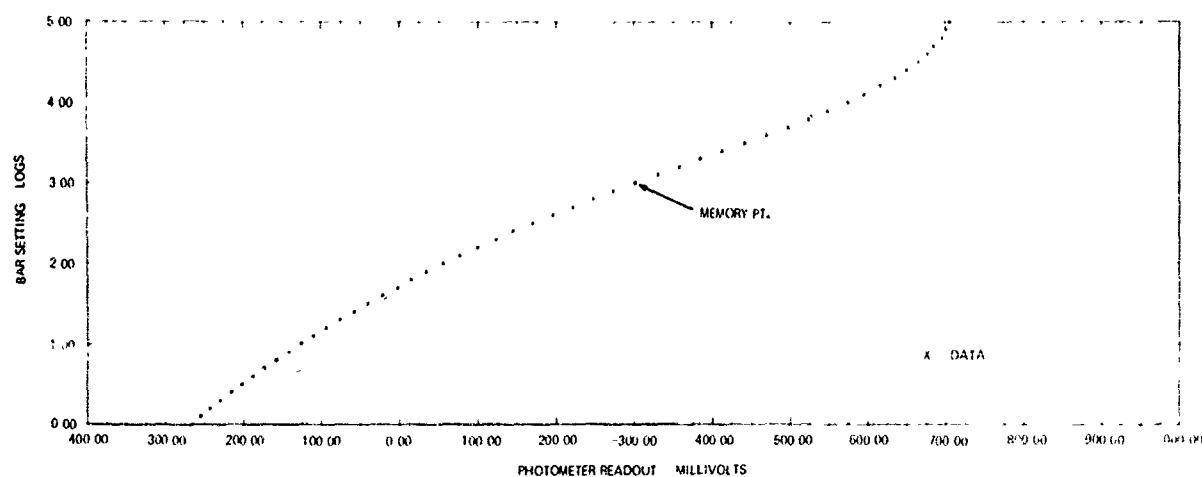


Fig. 3-25. Typical Linearity Calibration Curve

For example, in the center of the span, readout uncertainties of  $\pm 1$  mv are typical and linearity slopes of 30 mv per 0.1 log change in flux are common. Thus a readout precision of  $\pm 0.003$  log unit or  $\pm 1\%$  of the reading is typical. However, near the dark current cutoff, readout uncertainties of  $\pm 10$  mv are encountered with accompanying linearity slopes of 20 mv per 0.1 log change in flux. Under these conditions, a readout precision of only  $\pm 0.050$  log unit or  $\pm 12\%$  of the reading is achievable. Extreme caution must be maintained in the evaluation of measurements made near the dark current cutoff.

Once the linearity calibration for the radiometer system has been established, a similar procedure is followed to convert the calibration into absolute units. For this portion of the calibration sequence, an incandescent standard of luminous intensity is used as the flux source. Then absolute levels of irradiance can be presented to the radiometer either directly or via a calibrated reflectance standard.

A typical data sheet for the absolute calibration of a SHED LIGHT radiometer is shown in Fig. 3-26. Five different levels of input radiance are used in the determination of the calibration constant for the system. The calibration constant is referred to as the zero scale value and is labeled ZSV on the calibration forms.

ABSOLUTE CALIBRATION DATA FOR 2 PI SCANNER 10-1							FILTER NO. 1	4750 ANGSTROMS			
DATE 81122 TASK ASSIGNMENT 2ND S20							INSTRUMENT TYPE		RADIOMETER		
REFLECTANCE OF CALIBRATION TARGET 21.0 PERCENT											
SPAN 10	LAMP NO.	TOTAL DIST. CM.	TOTAL DIST. SQ. CM. SQ.	CALC. TGT. R OR F	DETC. REL OUTPUT	LOG OF (K0/K)	RAW ZSV	1V. RAW ZSV	1V. LUM. TO RAD. WATTS/LUM.	1V. LUM. TO RAD. WATTS/LUM.	CORRECTED ZSV
1	200	519.400	2.698E+05	1.097E-07	-5.24	4.291	2.129E-03	2.075E-03	1.176E-04	1.176E-04	2.327E-04
2	210	449.400	2.020E+05	1.495E-07	-5.17	4.150	2.097E-03				
3	100	309.400	9.573E+04	1.844E-07	-5.15	4.041	2.024E-03				
4	110	349.400	1.221E+05	2.403E-07	-5.14	3.921	2.011E-03				
5	70	309.400	9.573E+04	1.072E-07	-5.15	3.775	1.877E-03				
6	110	349.400	1.221E+05	2.403E-07	-5.14	3.895	1.891E-03				
7	100	309.400	9.573E+04	1.844E-07	-5.15	4.041	2.024E-03				
8	210	449.400	2.020E+05	1.495E-07	-5.17	4.150	2.097E-03				
9	200	519.400	2.698E+05	1.097E-07	-5.11	4.297	2.161E-03				
STANDARD DEVIATION = 1.159E-04											
FRACTIONAL STANDARD DEVIATION = 5.45 PERCENT											
RADIOMETER UNITS											
CALCULATED TARGET LUMINANCE EXPRESSED AS LUMENS/STERADIAN SQ. CM.											
CORRECTED ZERO SCALE VALUE EXPRESSED AS WATTS/STERADIAN SQ. CM.											

Fig. 3-26. Typical Absolute Calibration Form

Nine determinations of the calibration constant are made during each calibration run. The average value of the nine determinations is assumed to be the most probable value for the calibration constant. Due to precision limitations, stray light, and related procedural errors, typical standard deviations for the calibration constant are on the order of  $\pm 5\%$ . Table 3-2 illustrates the quality of typical calibration constants associated with data tabulated in Section 6. It should be noted that the term standard deviation is not rigorously correct in this application since the calibration data set includes some obvious systematic errors due to detector dynamic response as well as some procedural stray light errors. These systematic errors are not removed from the calibration data and as a result the standard deviation of the calibration constant determination represents a worst-case type of index.

Table 3-2. Calibration Constants and Related Fractional Standard Deviations (%)

Radiometer	FILTER 1		FILTER 2		FILTER 3		FILTER 4		FILTER 5		Average $\delta$ for System
	ZSV	$\delta$	ZSV	$\delta$	ZSV	$\delta$	ZSV	$\delta$	ZSV	$\delta$	
2 $\pi$ Scanner No. 1	2.32 E-7	$\pm 6$	2.28 E-7	$\pm 6$	6.35 E-7	$\pm 2$	1.12 E-6	$\pm 5$	7.06 E-8	$\pm 3$	$\pm 4$
2 $\pi$ Scanner No. 3	1.72 E-7	$\pm 2$	2.00 E-7	$\pm 3$	5.00 E-8	$\pm 3$	1.82 E-6	$\pm 3$	5.10 E-8	$\pm 4$	$\pm 3$
2 $\pi$ Scanner No. 4	1.57 E-7	$\pm 2$	1.89 E-7	$\pm 2$	5.23 E-7	$\pm 2$	1.90 E-6	$\pm 3$	5.04 E-8	$\pm 5$	$\pm 3$
Integrating Nephelometer No. 1	4.67 E-7	$\pm 10$	6.42 E-8	$\pm 10$	1.19 E-7	$\pm 7$	6.15 E-7	$\pm 9$	1.34 E-8	$\pm 5$	$\pm 8$
Integrating Nephelometer No. 3	1.70 E-7	$\pm 2$	2.34 E-7	$\pm 2$	3.89 E-7	$\pm 2$	1.72 E-6	$\pm 3$	4.27 E-8	$\pm 3$	$\pm 2$
Dual Irradiometer No. 1	1.39 E-7	$\pm 4$	1.56 E-7	$\pm 4$	2.83 E-7	$\pm 3$	4.29 E-7	$\pm 3$	2.81 E-8	$\pm 3$	$\pm 3$
Large Aperture Telephotometer No. 1	9.01 E-9	$\pm 4$	1.17 E-8	$\pm 5$	2.09 E-8	$\pm 4$	5.46 E-8	$\pm 2$	2.87 E-9	$\pm 4$	$\pm 4$
Large Aperture Telephotometer No. 3	2.12 E-8	$\pm 4$	2.23 E-8	$\pm 3$	5.94 E-8	$\pm 12$	1.46 E-7	$\pm 5$	4.87 E-9	$\pm 4$	$\pm 6$

Obviously these procedural and precision uncertainties are independent of the absolute accuracy of the standard lamp calibration, which is assumed to be  $\pm 3\%$ .

At regular intervals during the calibration procedure the radiometer is automatically exposed to its internal reference source, i.e., Isolite standard of luminous intensity. Since this integral, exceptionally stable source is always available for reinspection by the radiometer during subsequent measurement activities, the long term stability of the detector can be monitored and, when necessary, automatic adjustments to the calibration constant can be readily effected.

#### CALIBRATION CORRECTION FACTOR

The basic standard from which all these calibrations are derived is an incandescent lamp. Since this lamp is supplied with its calibration in luminous units, a luminance-to-radiance conversion is required. This unit conversion is applied to the calibration constant as a multiplicative factor of the form

$$F_1 = \frac{\sum W_{\lambda} \epsilon_{\lambda} (\overline{S_{\lambda} T_{\lambda}}) \Delta \lambda}{680 \sum W_{\lambda} \epsilon_{\lambda} \bar{y} \Delta \lambda} \quad (3-1)$$



where

$W_{\lambda}$  = Spectral emittance of the calibration source

$(\bar{S}_{\lambda}T_{\lambda})$  = Spectral response of the standard detector

$\bar{y}$  = Photopic response of the eye

$\epsilon_{\lambda}$  = Emmissivity of tungsten filament

The unit conversion factors applicable to the five spectral responses used during this project are tabulated below in Table 3-3.

Table 3-3. Unit Conversion Factors

Filter No.	Spectral Band	Luminance-to-Radiance Factor ( $F_1$ )
		(Watts/Lumen)
1	475 nm	1.31 E-4
2	515 nm	1.97 E-4
3	660 nm	6.96 E-4
4	745 nm	8.37 E-4
5	S-20	2.11 E-3

The application of these luminance-to-radiance conversion factors to the calibration data enables the radiometer to be used as a direct reading device. This feature makes it simple for the operator to accomplish quick field evaluation of the measured data.

Once the measured data is returned to the Laboratory for processing, further adjustment factors are applied to yield the engineering units presented in this report.

#### SPECTRAL CORRECTION FACTOR

If all the photoelectric systems had precisely the same spectral sensitivities, there would be no requirement for corrections beyond the conversion made by factor  $F_1$ . However, since there is a wide latitude in the spectral characteristics of individual multiplier phototubes, small mismatches among systems remain even after extensive optical filtering.

The Visibility Laboratory procedure is to carefully measure the spectral sensitivity of each multiplier phototube and then select groups of phototubes having similar spectral characteristics. Therefore the required spectral filtering is also similar. Even in these selected groups, there remain small differences in the spectral sensitivity. These differences are then minimized by use of slightly different filters for each tube so that, finally, all the photoelectric systems are closely matched in spectral sensitivity.

This second factor,  $F_2$ , corrects the small remaining spectral difference between the response of any given phototube and the standard response of the system for both the spectral distribution used during calibration and the spectral distribution of the final field targets. This factor,  $F_2$ , is also applied to the absolute calibration

$$F_2 = \frac{\sum W_\lambda (\overline{S_\lambda T_\lambda}) \Delta \lambda}{\sum W_\lambda (S_\lambda T_\lambda) \Delta \lambda} \times \frac{\sum W_\lambda \epsilon_\lambda (S_\lambda T_\lambda) \Delta \lambda}{\sum W_\lambda \epsilon_\lambda (\overline{S_\lambda T_\lambda}) \Delta \lambda}, \quad (3-2)$$

where

$\epsilon_\lambda$  = Spectral emittance of tungsten lamp at some color temperature

$W_\lambda$  = Spectral emittance of target in field

$(\overline{S_\lambda T_\lambda})$  = Standardized spectral response ( $\bar{y}$  for photopic case)

$(S_\lambda T_\lambda)$  = Spectral response of individual system

For radiometric calibrations, when the  $S_\lambda T_\lambda$  of a particular instrument is used as the standard  $\overline{S_\lambda T_\lambda}$  for the experiment  $F_2$  equals 1.0 for that instrument.

The combined use of the two factors,  $F_1$  and  $F_2$ , for the radiometric calibrations is equivalent to using a single factor defined below

$$F_1 F_2 = \frac{\sum W_\lambda \epsilon_\lambda (S_\lambda T_\lambda) \Delta \lambda}{680 \sum W_\lambda \epsilon_\lambda \bar{y}_\lambda \Delta \lambda} \times \frac{\sum W_\lambda (\overline{S_\lambda T_\lambda}) \Delta \lambda}{\sum W_\lambda (S_\lambda T_\lambda) \Delta \lambda} \quad (3-3)$$

In  $F_2$ , the spectral emittance of the target in the field,  $W_\lambda$ , depends upon the instrument being calibrated. Since the term appears in the numerator and the denominator of the factor, the exact spectral emittance does not need to be used. A relative spectral curve may be substituted so long as the same function is used for both numerator and denominator. For the SHED LIGHT project a spectral emittance curve is used from Johnson, et al (1965) to approximate the nighttime sky.

#### COLOR BALANCE AND MEAN WAVELENGTH

Color balance is defined as the radiance measure obtained when a sensor is measuring a spectrally neutral radiance, where a radiance  $N_\lambda$  of  $1 \text{ watt } \Omega^{-1} \text{ m}^{-2} \text{ nm}^{-1}$  is assumed. Color balance is then equivalent to the area under the relative spectral response curve.

$$N = \sum_0^{\infty} S_{\lambda} T_{\lambda} N_{\lambda} \Delta \lambda. \quad (3-4)$$

Mean wavelength is computed by the equation

$$\bar{\lambda} = \frac{\sum (\lambda (S_{\lambda} T_{\lambda})) \Delta \lambda}{\sum (S_{\lambda} T_{\lambda}) \Delta \lambda} \quad (3-5)$$

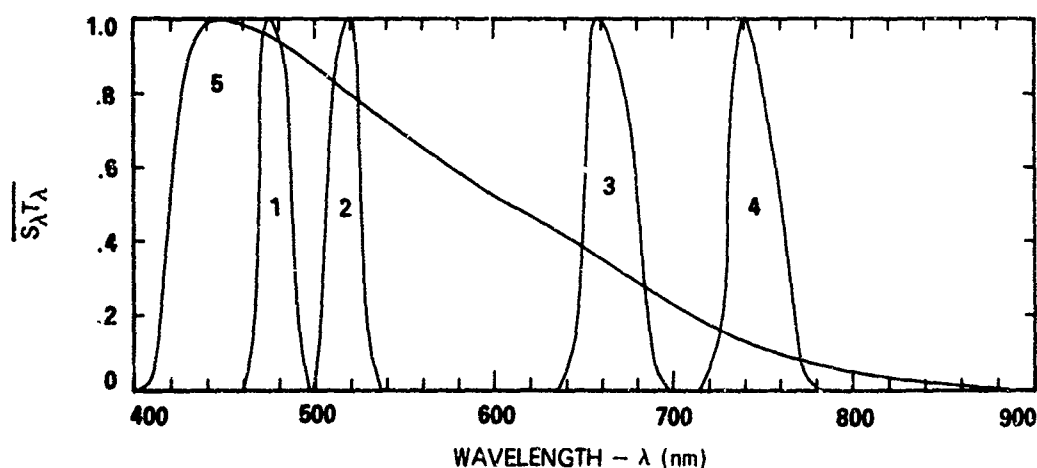
The color balance or area under the spectral response curves and the mean wavelength for each SHED LIGHT filter is presented in Table 3-4.

Table 3-4. Filter Color Balance and Mean Wavelength

Filter	Color Balance (nm)	Mean Wavelength (nm)
1	20.09	477.8
2	20.27	514.9
3	20.83	663.2
4	29.95	740.1
5	170.2	525.1

Conversion is made from units of watts  $m^{-2}$  to watts  $m^{-2} \mu m^{-1}$  and watts  $\Omega^{-1} m^{-2}$  to watts  $\Omega^{-1} m^{-2} \mu m^{-1}$  by dividing by the color balance and multiplying by 1000.

The normalized spectral response curves for the five cathode sensitivity-filter transmittance combinations used in this project are shown in Fig. 1-4, which is repeated below.



Standardized Sensitivity-Transmittance  $\overline{S_{\lambda} T_{\lambda}}$  of the Five Narrow Band Filter-Phototube Combinations

## 4. Data Collection Methods

During the field portion of this SHED LIGHT task, two independent activities were maintained simultaneously. The airborne instrument system was one activity and the ground-based instrument system was the other. Although the basic concept of the experiment was built around the joint operation of these two systems in a highly coordinated and simultaneous measurement routine, the realities of weather and distance forced an early modification to the plan. The compromise routine was for each system to run data collection sequences at every opportunity, on a nightly schedule. If weather permitted, simultaneous measurements at the same test area were assigned top priority. If for any reason the joint sequences were aborted, both systems were to automatically revert to independent operation.

### 4.1 AIRBORNE SYSTEM

The data collection sequence for the airborne system was broken into five standardized elements: (1) preflight warmup and calibration check, (2) straight and level sequences, (3) vertical profile sequences, (4) in-flight calibration checks, and (5) post-flight calibration check.

A typical mission sequence is illustrated in Fig. 4-1 and described chronologically below.

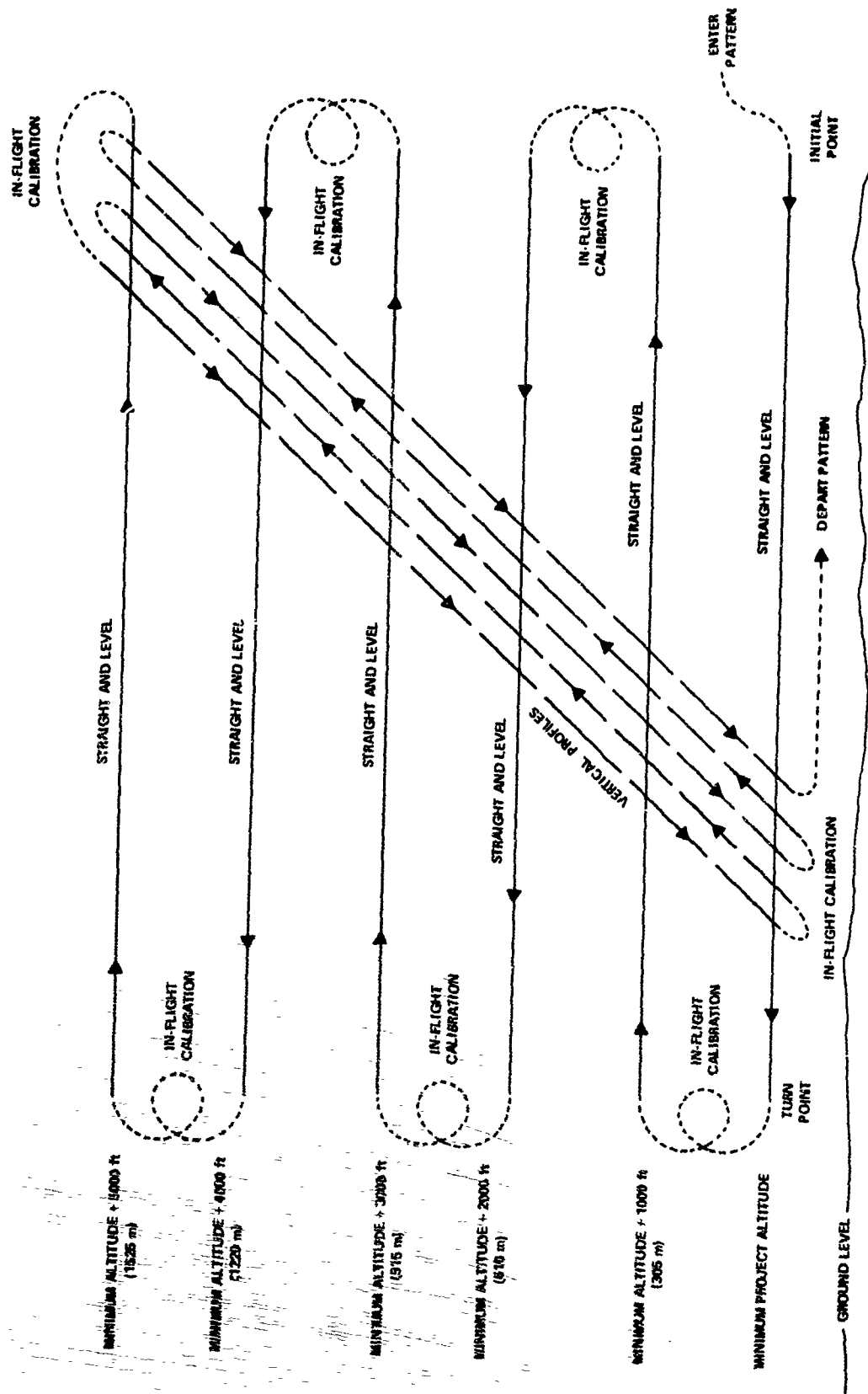


Fig. 4-1. Typical Airborne Data Profile

Mission Sequence	Typical Altitude
1. Preflight warmup, equipment operation, and calibration check	
2. Ferry from staging airbase to test area	
3. In-flight calibration check	
4. Straight and level sequence	At minimum project altitude
5. In-flight calibration check	Climb to minimum altitude + 1000 ft
6. Straight and level sequence	At minimum altitude + 1000 ft
7. In-flight calibration check	Climb to minimum altitude + 2000 ft
8. Straight and level sequence	At minimum altitude + 2000 ft
9. In-flight calibration check	Climb to minimum altitude + 3000 ft
10. Straight and level sequence	At minimum altitude + 3000 ft
11. In-flight calibration check	Climb to minimum altitude + 4000 ft
12. Straight and level sequence	At minimum altitude + 4000 ft
13. In-flight calibration check	Climb to minimum altitude + 5000 ft
14. Straight and level sequence	At minimum altitude + 5000 ft
15. In-flight calibration check	
16. Vertical profile	Descending at 1500 ft/min to minimum altitude
17. In-flight calibration check	
18. Vertical profile	Ascending at 1000 ft/min to minimum altitude + 5000 ft
19. In-flight calibration check	
20. Vertical profile	Descending at 1500 ft/min to minimum altitude
21. In-flight calibration check	
22. Vertical profile	Ascending at 1000 ft/min to minimum altitude + 5000 ft
23. In-flight calibration check	
24. Vertical profile	Descending at 1500 ft/min to minimum altitude
25. In-flight calibration check	
26. Post-flight calibration check	
27. Ferry from test area to staging airbase	
28. Termination	

The total elapsed time required for completion of items 3 through 26 was normally 2 hours and 30 minutes. In special situations where faster scan rates were appropriate, the elapsed time could be reduced to 1 hour and 10 minutes.

## PREFLIGHT WARMUP AND CALIBRATION CHECK

Just as the air crew must make a preflight check of the aircraft in order to ensure a successful mission, so must the scientific party "preflight" the technical equipment. During this technical preflight, which begins about 2 hours before takeoff, several activities must occur. (1) External protective covers are removed from all transducers and probes. Each external appurtenance is checked for visible signs of damage or contamination. (2) All electrical circuits are energized and test sequences are run to ensure proper operation of drive and control circuits. (3) All transducer circuits are energized and quiescent signals checked and evaluated for normal ground level readings. (4) Data logger multiplexing, A/D conversion, and tape transport operation are verified. (5) Flight plan details and alternate site selections are confirmed with USAF flight crew.

A primary consideration during the preflight phase is the temperature stabilization of the various multiplier phototube systems. If the aircraft has been subjected to high daytime temperatures during the interval preceding the proposed flight, the dark currents in the detectors will be at relatively high levels. Although only 20 or 30 minutes is required for the thermoelectric heat pumps to stabilize the multiplier phototubes at their control temperatures, approximately 60 minutes at the control temperature is required before the detector dark currents have stabilized adequately to begin reliable data collection. For this reason, temperature stabilization is always achieved prior to takeoff. This preflight stabilization allows the system to be ready for data collection immediately upon arrival at the test area, regardless of the duration of the ferry flight.

## IN-FLIGHT CALIBRATION CHECKS

Probably the single most important feature of the airborne radiometer systems is the internal calibration source which is built into each detector assembly. Through the use of this source, a regularly scheduled monitoring of the detector radiant sensitivity is easily accomplished. At the turn of a switch on the filter control panel, each radiometer optical path is interrupted by a memory mirror and radiant flux from its Isolite source is routed to the detector. The detector response to this "memory flux" should be stable and repeatable throughout the mission. Assuming no optical, electrical, or mechanical malfunction, any variation in a radiometer response to its "memory flux" may be attributed to a shift in system radiant sensitivity. Since the "memory flux" response for each radiometer is also recorded during the radiometer absolute calibration sequence, the calibration constant can be updated to compensate for any moderate drift in the system radiant sensitivity.

In order to maintain control of data quality, all radiometer systems have their "memory flux" responses monitored at regular intervals. During the airborne data collection profiles, a special block of "memory flux" response is recorded before and after every major profile element, i.e., straight and level sequences and/or vertical profile ascents and descents.

In addition to the "memory" calibration check, a second in-flight calibration is regularly employed. The integrating nephelometer designed and built for this project is calibrated by inserting a well-defined reflecting surface into the projector flux beam and measuring the amount of flux reflected back into the detector irradiometer channel. This calibration scheme is devised to accomplish two procedural goals. First, it allows the integrating nephelometer to function as a ratio measuring device, independent of absolute radiometric calibration. This implies operation at an accuracy equivalent to the precision level of the linearity calibration. Second, it offers a method of indirectly monitoring the stability of the projector output. The more stable the projector output, the less often a calibration is required. However, since this nephe-

lometer is a direct flow device, the projector lens is exposed to the sample aerosol flowing through the instrument. There is no guarantee that the projector output will not be attenuated by a contamination of the lens surface. Therefore a regular calibration check is desirable. During the airborne data collection a special block of nephelometer calibration response is recorded before and after every vertical profile element.

Immediately preceding the first "memory" calibration, a special multiplex input board is inserted into the data logger. This "A/D calibration" board applies internally generated, predetermined, calibrated dc voltages to each of the 42 data logger input channels. A 32 second block of these "A/D calibration" voltages is recorded. This information allows subsequent data processing routines to check for and correct any variations in the A/D converter operations.

#### STRAIGHT AND LEVEL SEQUENCES

During each straight and level element of the data collection sequence the pilot maintains a straight and level flight attitude at a maximum indicated airspeed of 150 knots. If weather and terrain permit, the aircraft heading is established crosswind. The ideal pattern for the straight and level sequences would result in all six ground tracks falling on a single line between the initial point and the turn point. See Fig. 4-1. The six straight and level elements are actually stacked in a vertical slab of atmosphere approximately 30 miles long, 0.5 mile wide, and 1 mile high.

While the aircraft is traversing the approximately 15-minute long straight and level element, the following types of data collection occur.

1. Automatic  $2\pi$  scanners map upper and lower hemisphere radiance distributions. Complete radiance maps of both hemispheres are sequentially completed in five spectral bands.
2. Integrating nephelometer measures the total scattering coefficient and directional scattering coefficients at  $\beta 30^\circ$  and  $\beta 150^\circ$ . All three measurements are sequentially completed in five spectral bands.
3. Dual irradiator measures the total upwelling and total downwelling irradiance. Both upwelling and downwelling measurements are sequentially completed in five spectral bands.
4. Large aperture telephotometer measures apparent nadir terrain radiance. This measurement is also made sequentially in five spectral bands.
5. Royco particle counter runs a standard 4-minute accumulation cycle and automatically prints out the accumulated particle distribution.
6. Peripheral data are recorded continuously. These data include airspeed, pitch, roll, altitude, outside temperature, outside pressure, outside dewpoint temperature, control panel selector settings, and project time.

#### VERTICAL PROFILE SEQUENCES

During each vertical profile element of the data collection sequence the pilot maintains an approximately level attitude, a straight heading, a maximum indicated airspeed of 150 knots, and an average rate of descent or ascent of 1000 ft per minute. Five vertical profile elements are run during each data collection sequence. These elements are conducted in the same vertical slab of atmosphere that was defined by the preceding six straight and level elements.



While the aircraft is traversing the approximately 5-minute long climb or descent leg, the following types of data collection occur.

1. Integrating nephelometer measures total scattering coefficient only. Each ascent and descent is run continuously from top to bottom in the same spectral band in order not to miss the fine structure in the scattering coefficient versus altitude profile. Thus a complete 5000 ft climb or descent is required for the measurement in each of the five spectral bands.
2. Dual irradiator measures total upwelling irradiance only. The selection of spectral bands is matched with the integrating nephelometer.
3. Large aperture telephotometer monitors apparent nadir terrain radiance. These measurements are for control and intercomparison only. The selection of spectral bands is matched with the integrating nephelometer.
4. Peripheral data are recorded continuously. These data are the same as during the straight and level sequences.

#### POST-FLIGHT CALIBRATION CHECK

Immediately following the last "memory" calibration and just before terminating the data collection sequence, the "A/D calibration" multiplex input board is again inserted into the data logger. Another 32 second block of "A/D calibration" voltages is recorded. The combined preflight and post-flight "A/D calibration" data provide reliable insight into data logger performance throughout the data collection sequence. This performance is continuously monitored throughout the entire data collection sequence via several selected "A/D calibration" voltages which are hard-wired into the data multiplex array.

#### FLIGHT PLANNING

The general mission plan was to perform several standard data collection profiles over each of the pre-selected ground sites, under both moonlight and starlight conditions, during both wet and dry monsoon conditions. There were three different ground sites, each chosen for its particularly unique terrain and meteorological characteristics.

The three geographic areas were: (1) the inland and relatively high Khorat plateau, (2) the lower delta regions near Lop Buri, and (3) the southern seacoast in the vicinity of Rayong. The several listings of data flights, contained in Section 6, illustrate the degree of success attained in fulfilling the general plan.

During every mission, top priority was given to those systems essential for the recovery of beam transmission and path radiance data. Thus the primary systems used were the integrating nephelometer and the upper and lower hemisphere scanners. All other systems were either peripheral or backup and were therefore subject to cannibalization or abandonment in the event of any malfunction which affected a primary system.

#### 4.2 GROUND-BASED SYSTEM

The ground-based data collection sequence was designed to supplement the airborne data whenever the aircraft was operating in the immediate vicinity. However, it was also complete enough to stand alone when the aircraft mission was diverted or aborted.

The ground-based instrument system has several operational responsibilities. First, it must supply a ground level data base to allow interpolation of various measurements between ground altitude and the lowest attainable aircraft altitude. Second, it must supply long term temporal sampling of those meteorological and radiometric quantities which relate to the project task. The ground station has run several 24-hour data sequences to monitor temporal variations in particle concentrations and scattering coefficients. This long term continuous measurement capability may in fact be the most significant capability inherent in the system. Third, the ground system serves as a spare parts and repair facility for the entire air/ground operation. In the event of a catastrophic failure in a primary airborne instrument or assembly, the equivalent piece of instrumentation is reassigned to the aircraft from the ground-based system. The aircraft can then return to service with a minimum of "down time" and repairs can be accomplished under the more convenient ground station conditions.

#### DATA COLLECTION SEQUENCE

The ground-based system was assigned three radiometer systems, three meteorological instruments, a Royco particle counter system, and communications equipment. The ground-based data collection sequence is not as automatic as the airborne sequence, but is otherwise quite similar. However, there is a basic difference in priorities. During each ground-based data sequence, top priority was given to those systems essential for the recovery of inherent background radiances. Consequently the primary systems used were the large aperture telephotometer and the automatic  $2\pi$  scanner.

The ground-based data collection sequence was broken into five standardized elements: (1) warmup and calibration check, (2)  $2\pi$  scanner data set, (3) integrating nephelometer data set, (4) large aperture telephotometer data set, and (5) Royco particle counter and meteorological data set.

A typical data collection sequence involving items 2, 3, 4, and 5 in the preceding paragraph required approximately 1 hour and 30 minutes elapsed time.

During each of the ground-based standard data elements the following type activities occur.

*Warmup and Calibration Check.* Since the radiometric systems at the ground station are identical with those on the aircraft, a similar warmup and calibration check is essential. Approximately 2 hours prior to the anticipated data collection interval, a ground station "preflight" is initiated as follows. (1) All external protective covers are removed and each device is checked for visible signs of damage or contamination. (2) All electrical circuits are energized and test sequences run. (3) All transducer circuits are energized and quiescent signal levels checked. And (4) Data logger multiplexing, A/D conversion, and tape transport operation are verified.

*$2\pi$  Scanner Data Set.* The ground-based  $2\pi$  scanner is mounted on a swivel-head tripod on the top of the ground system enclosure. In this configuration it can be manually oriented to scan either the upper hemisphere sky or the lower hemisphere terrain. When the scanner is oriented in the inverted position so that it is scanning the lower hemisphere, its field of view is obviously occulted by the tripod and enclosure. However, for many applications, the terrain view angles of greatest interest are those with zenith angles between  $90^\circ$  and  $120^\circ$ . In these cases, the inverted scanner clear field of view is adequate.

For a  $2\pi$  scanner data set, the scanner is first oriented to map the upper hemisphere sky radiance. A complete radiance map is sequentially completed in five spectral bands. Following these five sky maps, the scanner is inverted and oriented to map the lower hemisphere terrain radiance. A complete radiance

map is sequentially completed in five spectral bands.

Immediately prior to and following each radiance map, the scanner is directed to monitor its internal "memory flux" and a "memory" calibration is recorded on the data tape. In this manner, as in the airborne system, a tight control is maintained over data quality.

Since each  $2\pi$  scanner map takes  $2\frac{1}{2}$  minutes elapsed time for completion (and we run a total of ten), the total  $2\pi$  scanner data set takes a minimum of 30 minutes to complete.

*Integrating Nephelometer Data Set.* The ground-based integrating nephelometer is the optical equivalent of the airborne system. The only differences are in the projector lamps and in the ambient light shrouds. Operationally they are identical. The detector assemblies are completely interchangeable. The ground shroud is larger than the airborne, allowing more efficient interior stray light control. It is also exhaust-fan ventilated through trapped inlet and exhaust ports, allowing continuous operation during both daylight and nighttime ambient illumination levels.

For an integrating nephelometer data set, the sequence of events is as follows. (1) "Memory flux" and calibration reflected flux values are measured and recorded. (2) The irradiometer channel is selected and the scattered flux measurement representing total scattering coefficient is recorded. (3) The  $\beta_{30}$  radiometer channel is selected and the scattered flux measurement representing the directional scattering coefficient at  $30^\circ$  is recorded. (4) The  $\beta_{150}$  radiometer channel is selected and the scattered flux measurement representing the directional scattering coefficient at  $150^\circ$  is recorded. And (5) "memory flux" and calibration reflected flux values are again measured and recorded.

The five step sequence described in the preceding paragraph is repeated five times, once in each of the five spectral bands under investigation. Ten seconds of recording time is allotted to each measurement. Thus approximately 1 minute elapsed time per spectral band is required for a total of about 5 minutes for the complete set. Switching and control activities generally inflate the necessary elapsed time to about 7 or 8 minutes for an integrating nephelometer data set.

The ground-based Royco particle counter draws its aerosol sample from inside the integrating nephelometer shroud. As a result the two systems produce a large data set of closely coupled measurements relating optical scattering coefficients and particulate particle counts.

*Large Aperture Telephotometer Data Set.* The large aperture telephotometer assigned to the ground station is a multipurpose device which is used in a variety of configurations. Its primary aim is to guarantee the acquisition of reliable inherent terrain radiance data under the most severe low flux conditions.

The large aperture telephotometer is generally used as the detector assembly on a large swinging arm goniophotometer, or as a scanning telephotometer on a panhead tripod. Both schemes are devised to yield inherent terrain radiance data.

In the goniophotometer configuration, the assembly is devised so that the telephotometer optical line of sight is directed downward toward the target terrain. The line of sight is rotated vertically about the ground intercept so that the zenith angle of the line of sight swings between  $92^\circ$  (nearly horizontal) and  $180^\circ$  (vertically downward). The terrain radiance at the ground intercept is measured at several predetermined zenith angles. For this project the selected angles were  $93^\circ$ ,  $95^\circ$ ,  $100^\circ$ ,  $105^\circ$ ,  $120^\circ$ ,  $135^\circ$ , and  $180^\circ$ .

The goniophotometer frame allows the line of sight to swing through the vertical so that zenith angles on pairs of reciprocal azimuths can be covered with one setup. The normal azimuthal orientations are par-

allel to and at right angles to the lunar azimuth. The ground intercept for a zenith angle of  $180^\circ$  is rectangular (30.5 cm x 61 cm) and is the center point of the target area in all orientations.

In the tripod configuration, the telephotometer optical line of sight can be pointed in any direction. Normally the same zenith angle and azimuth orientations are used in this configuration as in the gonio-photometer configuration. The basic difference is that in the tripod configuration the center of the target area is different in each new orientation. Also, due to the difference in optical lever arms involved, the rectangular intercept is much smaller than for the gonio configuration. The advantage of the tripod configuration is its ease of portability. It can be located anywhere within 35 meters of the ground enclosure and picked up and moved by one man.

For a large aperture telephotometer data set the following sequence of events takes place. (1) The internal "memory flux" is monitored and recorded and (2) the optical line of sight is set to zenith angle  $180^\circ$ . A calibration target is inserted into the line of sight and its radiance measured and recorded. The calibration target is a flat plywood panel, 91.5 cm x 91.5 cm, painted with 3M Series 100 velvet coating white, No. 100-A10. (3) At each of the seven desired zenith angles the optical line of sight is oriented and the terrain radiance is measured and recorded. (4) The calibration target measurement is repeated and the "memory flux" is remonitored and recorded.

The four steps above are repeated in each of the five spectral bands and in each of the four cardinal azimuths. All azimuths are relative to the lunar azimuth.

*Royco Particle Counter and Meteorological Data Set.* The Royco particle counter is fortunately an automatic system. Once the operator selects the accumulation interval, the device can be set to accumulate and print out at regular sample intervals without further attention.

The ground-based Royco system was set up to accumulate particle counts for 10 minutes. After this interval it printed out the cumulative count per channel, cleared its memory, and immediately began a new 10-minute accumulation. This sample rate continued throughout the entire mission time of approximately 4 hours. At selected sites, the Royco system was allowed to run for 24 hours.

At the beginning and end of each mission, during the later deployments, standardized measurements of wet and dry bulb temperature, atmospheric pressure, and surface windspeed and direction were taken and recorded.

*Irradiometer Attachments.* Total downwelling irradiance is always a highly desired measurable in any field situation. Frequently the quantity is not only used alone as flux level monitoring parameter but is also used in ratio with some other measured radiance to calculate a reflectance value.

All of the radiometer telescopes used in the Visibility Laboratory field systems are provided with manually fitted irradiometer attachments. The same detector system can then be used to make measurements of both the total downwelling irradiance upon a surface and the directional radiance reflected from the surface. These joint measurements combine into reflectance values with an accuracy that approaches the precision level of the detector readout. The standard irradiometer cap attachment is illustrated in Fig. 4-2.

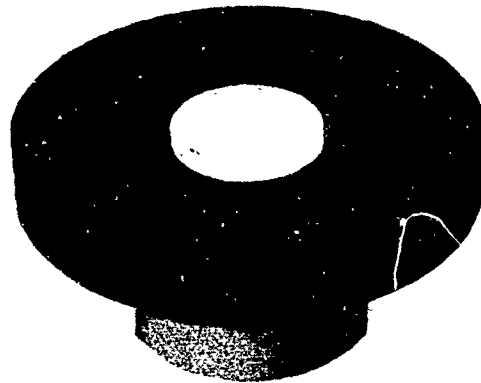


Fig. 4-2. Irradiometer Cap

In a typical ground-based data sequence, the cap is attached to the  $2\pi$  scanner before and after each upper hemisphere radiance map is completed. This provides a convenient calculative check, inasmuch as the proper integration of the  $2\pi$  scanner upper hemisphere radiance data should yield the same value of downwelling irradiance as the measurement when using the irradiometer attachment. More important, the irradiometer cap is used to obtain simultaneous measurements when the large aperture telephotometer is in operation.

The irradiometer attachment is also used in conjunction with the large aperture telephotometer. Before and after each set of directional terrain radiance measurements the large aperture telephotometer is oriented vertically and the irradiometer cap attached to its sunshade. In this configuration the telephotometer can measure a total downwelling irradiance immediately applicable to its directional radiance measurements, yielding highly reliable directional reflectance data.

## 5. Data Processing

As in any reasonably complex, multi-input sample data system, there is a large amount of data handling required before the scientific analyst ever sees the package. The degree of sophistication utilized for this portion of Project SHED LIGHT data is illustrated in Fig. 5-1. In this generalized flow chart, the step-by-step processing of the raw field data is illustrated for the convenience of project organization and control and does not include the details of the actual computer programming.

The airborne data and ground-based data are processed separately as illustrated in the data flow schedule. There are two primary reasons for this approach. First, the recording format of the two data loggers is significantly different. Second, each data collection sequence, airborne and ground-based, is considered to be a completely independent activity and therefore must be reduced to usable format in the most direct manner possible.

### 5.1 AIRBORNE DATA

As noted in Table 5-1 several classes of data are recorded during an airborne data set (1) radiometer outputs, (2) selector control codes, (3) transducer orientation and flight attitude signals, and (4) calibration voltages, etc. All systems, regardless of type have been designed for an electrical output between 0 and  $\pm 1$  vdc for full scale. The data logger has a least count of  $\pm 1$  mv and records in digital format at a multiplex rate of 240 samples per second and a tape rate of 200 bits per inch (bpi) and 3.56 inches per second.

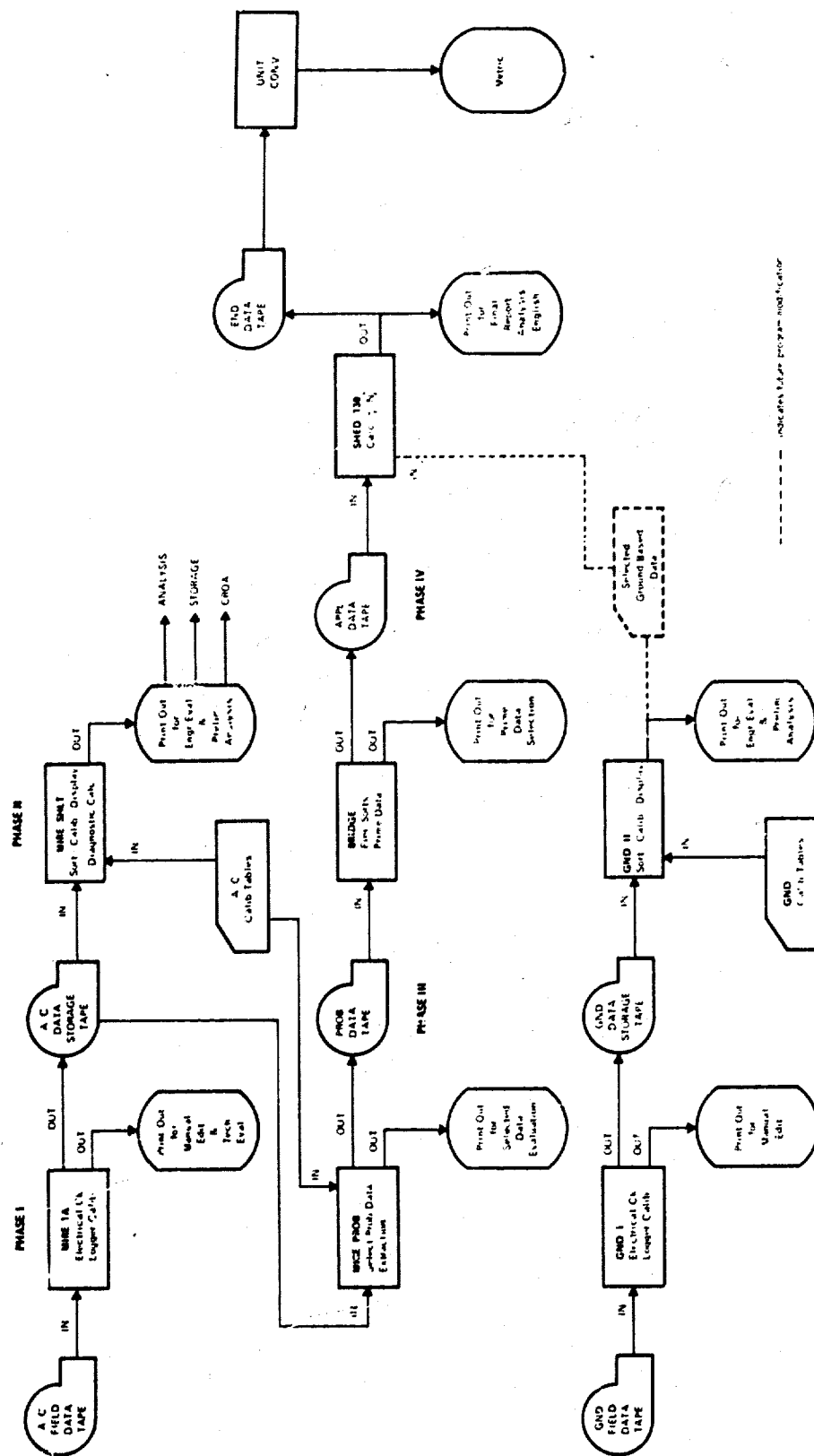


Fig. 5.1. Project SLED LIGHT Data Flow Schedule

Table 5-1. Airborne Data Classifications

Analog Input Channel	Signal Class	Samples Per Sec	Item Description
1	R	60	Upper Hemisphere Radiance
2	O/C	15	Upper Hemisphere $2\pi$ Scanner Azimuth
3	O/C	3	Upper Hemisphere $2\pi$ Scanner Elevation
4	R	60	Lower Hemisphere Radiance
5	O/C	15	Lower Hemisphere $2\pi$ Scanner Azimuth
6	O/C	3	Lower Hemisphere $2\pi$ Scanner Elevation
7	R	2	Irradiance, Left Dual
8	R	2	Irradiance, Right Dual
9	K	2	Calibration Reference
10	R	4	Integrating Nephelometer (right)
11	K	4	Integrating Nephelometer (left)
12	R	4	Nadir Radiance (aft)
13	K	4	Calibration Reference
14	M	1	AN/AMQ-17 Relative Humidity
15	K	2	Calibration Reference
16	K	2	Calibration Reference
17	K	2	Calibration Reference
18	K	2	Calibration Reference
19	K	2	Calibration Reference
20	K	2	Calibration Reference
21	O/C	2	Integrating Nephelometer Mode Selector (left)
22	M	1	Cambridge 137-C3 Dewpoint Temperature
23	O/C	3	Optical Filter Identification
24	O/C	2	Integrating Nephelometer Mode Selector (right)
25	K	2	Calibration Reference
26	O/C	2	Altitude
27	O/C	3	Roll
28	O/C	2	Pitch
29	O/C	1	Magnetic Heading
30	O/C	1	Indicated Airspeed
31	K	1	Calibration Reference
32	O/C	2	Source Check +990 mv
33	O/C	2	Source Check -990 mv
34	O/C	3	A/D Zero Check 000 mv
35	M	3	AN/AMQ-17 Temperature
36	R	2	Nadir Radiance (fwd)
37	M	3	AN/AMQ-17 Static Pressure
38	K	3	Calibration Performance
39	O/C	2	A/D Span Check +950 mv
40	O/C	2	Irradiometer Prism Identification
41	K	3	Calibration Reference
42	K	2	Calibration Reference

R = Radiometer Signal  
 O/C = Orientation and Control Signal  
 M = Meteorological Signals  
 K = Internal Calibration Signal



## PHASE I

The first phase in the airborne data processing schedule, program MIRE 1A, is designed to verify the electrical quality of the recorded data and build in some insurance against data loss through mishandling. Program MIRE 1A operates on the raw field tape in the following manner:

1. Examines data channels 34 and 39 which monitor A/D calibration input voltages of 0.000 vdc and 0.950 vdc.
2. Corrects all channels for errors due to minor variations in A/D zero and or span calibration. Rejects all data blocks having A/D zero or span variations exceeding 10 mv.
3. Examines each 3480-word data block and tabulates its status, i.e., electrical calibration and parity.
4. Prints out block status tally for editing and evaluation.
5. Sorts data which is stored in original A/D multiplex array into ordered sets by analog input channel. This operation in effect gets all  $2\pi$  scanner data into one set, all dewpoint data into another set, and all pitch and roll data into another, etc. All data is ordered chronologically by project time.
6. Transfers validated and corrected data to 800 bpi storage tapes. Writes two identical storage tapes to protect against future data loss due to mishandling. All data is stored in corrected millivolt values in the original field tape format.

## PHASE II

The second phase of the data processing schedule, program MIRESHLT, is designed to convert the myriad of raw millivolt values on the data storage tape into interpretable tables of calibrated engineering quantities. Program MIRESHLT is the most comprehensive and expensive routine in the entire schedule. However, it is the application of this routine which allows the results of a 3-hour data collection flight to be available for preliminary analysis within 48 hours of the tape arrival at the computer center.

Program MIRESHLT operates on the data storage tape in the following manner.

1. Applies the appropriate calibration values to each set of data. This operation, depending upon the system, involves the application of multiplicative factors, the interpolation between tabular values, or the calculation of inter-set ratios.
2. Calculates and applies calibration updates to all radiometer channels based upon "memory calibration" readings interspersed within the basic data.
3. Performs sample calculations to illustrate data quality. Compares results against pre-determined standards of maximum and minimum allowable values. Flags all data falling outside allowable limits. Tallies percentage offscale data in critical channels.
4. Puts out printout sheets tabulating results of all operations performed. These sheets contain tables of all measured values as a function of time and/or altitude. In addition to the tabular presentation, all quantities can be plotted upon demand. These general purpose displays are used for in-house analysis and delivery to authorized outside users, etc. They are complete, including all calibration values used.

### PHASE III

Because the output from MIRESHLT is quite voluminous, special sorting routines have been written to retrieve selected portions of the data from any given flight. Program MIREPROB is one of these extraction routines. The function of program MIREPROB, however, goes slightly beyond a simple re-sort in that it performs the following functions.

1. Extracts from the data storage tape all raw data required for the specified task.
2. Applies appropriate calibration values in the same manner as program MIRESHLT.
3. Reorders data into an array suitable for more efficient processing.
4. Calculates some intermediate derived quantities and sorts by tighter specifications on data quality.
5. Puts out printout sheets tabulating the results of all operations performed.
6. Puts out problem data tape for use in final calculations.

It is anticipated that the basic functions of the MIREPROB program can be absorbed in MIRESHLT and the final program, SHEDC130, after this report is completed.

### PHASE IV

The final step in the processing of a typical airborne data tape is the generation of the desired end data. This has been the goal of the entire project. All that has gone before – the development of the theoretical approach, the design and fabrication of the instrumentation, and the deployment of the field data collection exercises – has been directed toward feeding this final computational phase.

The final calculation routine, program SHEDC130, was an experimental program where several methods of data retrieval were attempted. This complicated the program by creating storage problems. Consequently an intermediate program, BRIDGE, was developed to precede SHEDC130 in order to handle minor interface and format problems, correct the scanner data for known errors, and eliminate the effects of excessive external lights for the starlight flights. Program BRIDGE generates the intermediate applications data tape.

Program SHEDC130 computes the data in Section 6 from the selected measured and derived quantities stored on the application data tape according to the equations in Section 2. Since the basic method described in Section 2 is the most effective, much can be eliminated in program SHEDC130, allowing programs BRIDGE and UNIT CONV (refer to Fig. 5-1) to be absorbed in the single program SHEDC130 after completion of this report.

## 5.2 GROUND-BASED DATA

The data processing associated with the ground-based data set is similar in concept to that applied to the airborne data. The primary differences are the result of a different recording format between the two data loggers and the significantly lesser amount of data resulting from the ground station. As noted in Table 5-2 the same general classes of data are handled, but in much smaller quantities. Again, all systems, regardless of type, have been designed for an electrical output between 0 and  $\pm 1$  vdc for full scale.

The data logger is normally adjusted for a least count of  $\pm 0.1$  mv. It also records in digital format; however, the normal incremental sample rate is only approximately eight samples per second.

**Table 5-2. Ground-Based Data Classifications**

Analog Input Channel	Signal Class	Measured Quantity
00	O/C	Automatic $2\pi$ Scanner Elevation
01	R	Automatic $2\pi$ Scanner Radiance
02	O/C	Automatic $2\pi$ Scanner Azimuth
03	R	Automatic $2\pi$ Scanner Radiance
04	O/C	Automatic $2\pi$ Scanner Azimuth
05	R	Automatic $2\pi$ Scanner Radiance
06	O/C	Automatic $2\pi$ Scanner Elevation
07	R	Automatic $2\pi$ Scanner Radiance
08	O/C	Automatic $2\pi$ Scanner Azimuth
09	R	Automatic $2\pi$ Scanner Radiance
10	O/C	Automatic $2\pi$ Scanner Azimuth
11	R	Automatic $2\pi$ Scanner Radiance
12	R	Large Aperture Telephotometer
13	R	Automatic $2\pi$ Scanner, w/irradiance attachment
14	O/C	Large Aperture Telephotometer, Zenith Angle
15	O/C	Calibration Reference
16	R	Automatic $2\pi$ Scanner, w/irradiance attachment
17	R	Integrating Nephelometer (left)
18	R	Integrating Nephelometer (right)
19	O/C	Integrating Nephelometer Mode

R = Radiometer Signal

O/C = Orientation and Control Signal

## PHASE I

The first phase of the ground-based data processing schedule, program GND I, has the same general function as in the airborne case. It is designed to verify the quality of the recorded data, determine the usable quantity of data available, and provide data storage tapes for further processing.

Program GND I operates on the raw field tape in the following manner.

1. Examines each ten character word and identifies and tabulates its classification and parity.
2. Prints out tape status tally and data classification summary for editing and evaluation.
3. Sorts the data, which is stored in the original multiplex array, into ordered sets by analog input channel.
4. Transfers acceptable data to storage tapes. All data is stored in millivolt values in the original field tape format.

## PHASE II

The second phase of the ground-based data processing, program GND II, is designed to convert the raw millivolt values on the storage tape into interpretable tables of calibrated engineering quantities.

Program GND II operates on the data storage tape in the following manner.

1. Applies the appropriate calibration values to each set of data.
2. Calculates and applies calibration updates to all radiometer channels.
3. Performs sample calculations to illustrate data quality. Flags all data falling outside pre-established allowable limits.
4. Reorders automatic  $2\pi$  scanner data into a stylized array suitable for manual analysis.
5. Puts out printout sheets tabulating results of all operations performed. These sheets contain tables of all measured values as a function of project time. These general purpose displays are used for in-house analysis, delivery to authorized outside users, and selection of ground data to be card-inputted into phases III and IV of the airborne data processing flow, etc.

Due to the reasonably small quantities involved and the sometimes very specialized utilization of the ground-based data, there was no automatic processing beyond GND II.

## 6. Airborne Data

### 6.1 FLIGHT DESCRIPTIONS

Data-gathering flights were made in three general areas in Thailand: the Khorat Plateau; the lowlands adjacent to the Chao Phraya River, and over the land and the Gulf of Siam near Rayong. The flight descriptions which follow identify the general area of each flight by reference to a fixed geographical location. For the Khorat Plateau area the references are the TREND site and the city of Khorat. For the lowlands adjacent to the Chao Phraya River the reference is the city of Lop Buri (with Sing Buri as secondary reference). And for the flights over the Gulf of Siam and adjacent land the reference is the city of Rayong. The latitude and longitude coordinates and approximate elevation above sea level of the foregoing geographical locations are given in Table 6-1.

Table 6-1. Location and Elevation of Geographical References

Reference	Latitude	Longitude	Approximate Elevation (Meters)
TREND Site	14.5° N	102.0° E	600
Khorat	15.0° N	102.1° E	200
Lop Buri	14.8° N	100.6° E	25
Sing Buri	14.9° N	100.5° E	25
Rayong	12.7° N	101.3° E	5

Table 6-2 is a summary of pertinent data for the flights being reported. In the table flight numbers are sequential. Flights 82 and 88 are reported as two flights because each flight was, in effect, two flights with data recorded over two geographical locations. Flight 100 is reported as two flights because of a distinct change in atmospheric conditions which occurred during the flight. The date of each flight is the Greenwich date. The times under the Total Time of Data-Taking column are Greenwich mean times (GMT) and in parentheses local civil times (LCT), which is GMT plus 7 hours. The site for each flight is the fixed geographical location to which the flight is referenced. The moon phase angle can be defined as the angle between two lines from the center of the moon, one to the center of the sun and the other to the center of the earth (Russell 1916). The moon zenith angles are tabulated from the time when sky radiance data-taking began, at the time of moon transit (minimum zenith angle) when applicable, and at the conclusion of sky radiance data-taking.

Table 6-2. Flight Data

Flight No.	Date 1968	Total Time of Data-taking				Site	Moon Phase Angle	Moon Zenith Angle		
		Start		End				Start	Transit	End
		GMT	LCT	GMT	LCT					
82 I	15 Sep	1748	(0048)	1856	(0156)	TREND	101°	82°		75°
82 II	15 Sep	1926	(0226)	2027	(0327)	Khorat	102°	59°		53°
86	7 Oct	1612	(2312)	1839	(0139)	Khorat	14°	23°	2°	5°
87	12 Oct	1226	(1926)	1337	(2037)	Rayong	67°	Before Moonrise		
88 I	19 Oct	1411	(2111)	1526	(2226)	Rayong	152°	Before Moonrise		
88 II	19 Oct	1542	(2242)	1632	(2332)	Rayong	152°	Before Moonrise		
89	21 Oct	1320	(2020)	1410	(2110)	Lop Buri	176°	Before Moonrise		
1969										
91	28 Feb	1352	(2052)	1621	(2321)	Lop Buri	40°	15°	11°	18°
92	9 Mar	1731	(0031)	1953	(0253)	Lop Buri	70°	74°		54°
93	10 Mar	1811	(0111)	2034	(0334)	Khorat	83°	77°		58°
96	25 Mar	1347	(2047)	1614	(2314)	Khorat	95°	42°		65°
97	27 Mar	1432	(2132)	1700	(0000)	Rayong	71°	29°		54°
98	30 Mar	1412	(2112)	1625	(2325)	Lop Buri	37°	12°	1°	12°
99	2 Apr	1339	(2039)	1606	(2306)	Khorat	2°	54°		30°
100 I	3 Apr	1338	(2038)	1444	(2144)	Khorat	11°	67°		53°
100 II	3 Apr	1449	(2149)	1521	(2221)	Khorat	11°	52°		49°
101	6 Apr	1330	(2030)	1440	(2140)	Rayong	50°	Before Moonrise		
102	7 Apr	1334	(2034)	1437	(2137)	Lop Buri	64°	Before Moonrise		

The first seven flights being reported, No. 82I to 89, were made during the wet season in the Fall of 1968. The balance of the flights being reported, No. 91 to 102, eleven in all, were made during the dry season in the Spring of 1969. There was a distinct difference in ground lighting between those two seasons. During the wet season the ground lights were primarily electric lights around homes or small settlements with a few small trash fires scattered throughout the area. During the dry season, in addition to the electric lights, there were many areas where the dried vegetation was being burned following the harvesting of the crops. These areas were extensive, especially in the Lop Buri/Sing Buri area, with the color of the fire varying from yellowish flames to deep red of the embers.

#### FLIGHT 82I

Overcast moonlight. This flight was conducted over the TREND site shortly after midnight local time and soon after moonrise. The TREND site was situated in the northern foothills of the Dangrek Mountains. The ground cover consisted of random areas of small deciduous trees and tall grass. The area was cut through just north of the TREND site by a hard-surface road with bare reddish soil areas on either side. There were very few ground lights in the vicinity of the TREND site, but there was a river dam with many electric lights a few miles beyond the southwest end of the flight path. High scattered cirrus clouds covered the sky, partially obscuring the moon, and low stratus clouds were located southwest of the flight area. Moon phase angle was  $101^\circ$ ; moon zenith angle was  $82^\circ$  at start of sky radiance data-taking and  $75^\circ$  at completion.

#### FLIGHT 82II

Moonlight. This part of the flight started at 0226 local time, over an area approximately 65 km east of Khorat, and ended at 0327. The terrain was flat. The vegetation consisted of forested areas of small deciduous trees with flooded rice paddies scattered among the trees. The cloud cover had changed sufficiently from that of Flight 82I to reveal the moon. In addition, a considerable number of lightning flashes were observed in the northwest direction. Moon phase angle was  $102^\circ$ ; moon zenith angle ranged from  $59^\circ$  to  $53^\circ$  during sky radiance data-taking.

#### FLIGHT 86

Moonlight. Data were gathered in the same general area as in Flight 82II, approximately 34 km east southeast of Khorat. The data-taking started at 2312 local time and continued until 0139. The vegetation consisted of forested areas of small deciduous trees and flooded rice paddies. The sky was clear except for high thin cirrus clouds. The moon phase angle was  $14^\circ$ ; the moon zenith angle ranged from  $23^\circ$  to  $5^\circ$  during sky radiance data-taking. The moon zenith angle was  $2^\circ$  at time of transit.

#### FLIGHT 87

Starlight before moonrise. Data were recorded over the Gulf of Siam approximately 8 km south of Rayong. The water depth was approximately 20 m (10 fm). Data-taking started at 1926 local time and was completed at 2037, before moonrise. At the beginning of the flight there were high cirrus clouds to the north. Near the end of the flight some stratus was seen along the beachline at an estimated altitude of 1000 to 1200 m.

#### FLIGHT 88 I

Starlight before moonrise with a cloud overcast. Data were gathered over the Gulf of Siam approximately 8 km south of Rayong. Depth of water was approximately 20 m (10 fm). Weather was described as clear with some clouds at 600 m. A thick overcast was seen approximately 30 km south of the flight area. A thunderstorm with bright lightning flashes was in the northwest direction. Data-taking started at 2111 local time and ended at 2226.

#### FLIGHT 88 II

Starlight before moonrise with scattered clouds. The location for this flight was a valley about 40 km east of Rayong. The terrain was relatively flat, cultivated (but not with rice paddies), and interspersed with small tree-covered knolls. In addition to the scattered clouds at 600 m, there was an overcast 140 km to the south and thunderstorms were seen in the northwest direction. Data-taking started at 2242 local time and ended at 2332.

#### FLIGHT 89

Starlight before moonrise with thick overcast at 1500 m. The flight pattern was from Lop Buri to approximately 40 km west of Sing Buri. The terrain was flat (river delta country) and cultivated with rice paddies and other crops; there were also small scattered settlements. The illumination from ground lights on the surface of the overcast was readily discernible. Data-taking started at 2020 local time and ended at 2110. Data-taking terminated at 1372 m, just below the overcast.

#### FLIGHT 91

Moonlight. The flight pattern was from Lop Buri to approximately 40 km west of Sing Buri. The terrain was flat (river delta country) and cultivated with rice paddies and other crops, there were also small scattered settlements. This was the dry season (March) when crops had been harvested, ground cover had yellowed, rice paddies were dry, and the stubble was being burned off. Water was still present in some of the fields however and reflected moonlight was observed at the beginning of the flight. The atmosphere was free of clouds but quite hazy, especially near the ground, and there was very little wind. Data were recorded from 2052 local time to 2321. The moon phase angle was  $40^\circ$ , the moon zenith angle was  $15^\circ$  at the start of sky radiance data-taking,  $11^\circ$  at transit, and  $18^\circ$  when sky radiance data-taking ended.

#### FLIGHT 92

Moonlight (approximately one and one-half days before the quarter moon). The flight pattern was from Lop Buri to approximately 40 km west of Sing Buri. The terrain was flat (river delta country) and cultivated with rice paddies; and there were also small scattered settlements. This was the dry season (March) when crops had been harvested, ground cover had yellowed, rice paddies were dry, and the stubble was being burned off. The atmosphere was free of clouds but hazy at the lower altitudes. Data were recorded from just after midnight, 0031 local time, until 0253. The moon phase angle was  $70^\circ$ , the moon zenith angle during sky radiance data-taking ranged from  $74^\circ$  to  $54^\circ$ .

#### FLIGHT 93

Quarter moon. Data were gathered over the wooded terrain of the Khorat Plateau some 60 km east of Khorat. There were very few artificial lights under the flight pattern. The terrain consisted primarily of



dry rice paddies and deciduous trees. This was the dry season (March) and the vegetation (tree leaves and ground cover) had lost the green color of the wet season. The atmosphere was very hazy at low altitudes. Some clouds at an undetermined altitude occasionally obscured the moon. Data-taking started at 0111 local time and ended at 0334. The moon phase angle was  $83^\circ$ ; the moon zenith angle ranged from  $77^\circ$  at the start of sky radiance data-taking to  $58^\circ$  at the end.

#### FLIGHT 96

Quarter moon. Data were gathered over the wooded terrain about 60 km east of Khorat. There were very few artificial lights under the flight pattern. The terrain consisted primarily of dry rice paddies and deciduous trees. This was the dry season (although it had rained in this area during the afternoon) and the vegetation (leaves on trees and ground cover) had lost the green color of the wet season. The atmosphere was very hazy at low altitudes. There was considerable thin cirrus estimated at 6000 m. The data-taking started at 2047 local time and ended at 2314. The moon phase angle was  $95^\circ$ ; the moon zenith angle was  $42^\circ$  at the start of sky radiance data-taking and was  $65^\circ$  at the end.

#### FLIGHT 97

Moonlight. The flight was made over the Gulf of Siam, approximately 130 km south of Rayong, where water depth was about 55 m (30 fm). The atmosphere was essentially clear except for small scattered clouds at about a 450-meter altitude. Data-gathering started at 2132 local time and ended at 2400. The moon phase angle was  $71^\circ$ ; the moon zenith angle was  $29^\circ$  when sky radiance data-taking started and  $54^\circ$  when data-taking ended.

#### FLIGHT 98

Moonlight. This flight was made in the Lop Buri area. Away from the city of Lop Buri the ground cover consisted of harvested-crop areas. There was considerable artificial ground lighting in the area. There were high thin cirrus clouds with haze near the ground. Data-taking started at 2112 local time and ended at 2325. The moon phase angle was  $37^\circ$ ; the moon zenith angle during sky radiance data-taking ranged from  $12^\circ$  to  $1^\circ$  at transit, to  $12^\circ$ .

#### FLIGHT 99

Full moon. This flight was made approximately 60 km east of Khorat. The terrain was relatively flat and forested with deciduous trees and rice paddies. During this season (dry season) the tree foliage was sparse, dry, and yellowed and the rice paddies between the trees were dry. There were a few artificial ground lights. Particularly near the ground the atmosphere was hazy and there were some cirrus clouds remaining after a local thunderstorm had dissipated. Data-taking started at 2039 local time and ended at 2306. The moon phase angle was  $2^\circ$ , the moon zenith angle was  $54^\circ$  at the start of sky radiance data-taking and  $30^\circ$  at the end.

#### FLIGHT 100I

Moonlight. This flight was made approximately 60 km east of Khorat. The terrain was relatively flat and consisted of deciduous trees and rice paddies. During this season (dry season) the tree foliage was sparse, dry, and yellowed and the rice paddies between the trees were dry. There were a few artificial ground lights. The atmosphere was hazy near the ground, with no clouds except a thunderstorm toward the

east. Data-taking started at 2038 local time and continued until 2144. The moon phase angle was  $11^\circ$ , the moon zenith angle during sky radiance data-taking was  $67^\circ$  at the start and  $53^\circ$  at the end.

#### FLIGHT 100 II

Overcast moonlight. This flight was a continuation of Flight 100 I, after the formation of a cloud overcast and in the same area approximately 60 km east of Khorat. The terrain was relatively flat and consisted of deciduous trees and rice paddies. During this season (dry season) the foliage was sparse, dry, and yellowed and the rice paddies among the trees were dry. There were a few artificial ground lights. There was a continuous cloud overcast at 1500 m. Data-taking started at 2149 LCT and terminated at 2221. The moon was completely obscured by the overcast.

#### FLIGHT 101

Starlight before moonrise. This flight was made over the Gulf of Siam, approximately 95 km south of Rayong, where the depth of the water was 60 m (33 fm). The sky was free of clouds but the atmosphere was very hazy at low altitudes, presumably because of an offshore (north) wind. Data-taking started at 2030 LCT and ended at 2140.

#### FLIGHT 102

Starlight before moonrise. The flight pattern was from 15 to 90 km south of Lop Buri. The terrain was flat, cultivated with rice paddies, and included small settlements. During this dry season the rice paddies were dry and other vegetation had lost its lush, green appearance. There were no clouds but the atmosphere was very hazy at low altitude, presumably from the burning off of stubble in the dried rice paddies. Data-taking started at 2034 and ended before moonrise at 2137.

## 6.2 PRESENTATION OF DATA

Data are presented in tables in Section 6.3, one set of tables for each flight with the table sets arranged sequentially by flight number. Each table set consists of a flight description followed by tables of

- Irradiance,
- Directional Reflectance of Background,
- Total Scattering Coefficient,
- Beam Transmittance from Ground to Altitude,
- Path Radiance from Ground to Altitude, and
- Directional Path Reflectance from Ground to Altitude.

The table sets are color-coded. Each set of tables is printed on paper of one color and two colors are used alternately so that the tables from one flight are readily distinguishable from the table sets of the flight preceding and following.

Each optical property is tabulated in the tables as a function of altitude except for the Directional Reflectance of Background which is tabulated as a function of zenith angle. The data are further subdivided

by optical filters. Additionally, for those flights when the moonlight was sufficiently intense to cause directional effects, tables of Directional Reflectance of Background, Path Radiance from Ground to Altitude, and Directional Path Reflectance from Ground to Altitude are presented in four sets for the four azimuths, with respect to the moon, of 0°, 90°, 180°, and 270°.

The data tables are not complete. There are two reasons for this. First, during some of the flights the scattered flux (by which the total scattering coefficient is determined) was below the sensitivity threshold of the nephelometer Filter 4. Accordingly, for those flights the Filter 4 data are not included. And because beam transmittance is computed directly from the total scattering coefficient, the beam transmittances and two optical properties which include the beam transmittance in their derivation, Path Radiance from Ground to Altitude and Directional Path Reflectance from Ground to Altitude, cannot be included.

The second reason was the very low radiance values sometimes encountered during data-taking, values below the sensitivity threshold of the sky scanning radiometers. And because sky radiances are used in computing Irradiance, Directional Reflectance of Background, Path Radiance from Ground to Altitude, and Directional Path Reflectance from Ground to Altitude, those properties for the filters in question cannot be included.

The numerical values in the tables are expressed either as decimal numbers or as the products of decimal numbers and a power of 10. For example, in the Irradiance table for Flight 82I the irradiance values are written in the form of 3.144 E-05, the computer way of writing  $3.144 \times 10^{-5}$ . If the number were 3.144 E 05, that is, with no minus sign, it would be equivalent to  $3.144 \times 10^5$ . In the same table the albedos are decimal numbers in the form of .049.

In all these tables the data are tabulated by optical filters. The spectral responses of the filtered phototubes for Filters 1 through 4 are shown in Table 6-2A. These data are plotted in Fig. 1-4 in the Introduction.

**Table 6-2A. Standardized Sensitivity-Transmittance  $\overline{S\lambda T\lambda}$  of the Four Narrow Band Filter-Phototube Combinations**

$\lambda^*$	Filter No. 1	$\lambda$	Filter No. 2 <sup>†</sup>	$\lambda$	Filter No. 3	$\lambda$	Filter No. 4
460	0.007	500	0.067	635	0.002	715	0.008
465	0.149	505	0.415	640	0.049	720	0.054
470	0.848	510	0.815	645	0.180	725	0.149
475	1.000	515	0.964	650	0.553	730	0.447
480	0.933	520	1.000	655	0.995	735	0.881
485	0.830	525	0.621	660	1.000	740	1.000
490	0.179	530	0.135	665	0.942	745	0.903
495	0.029	535	0.029	670	0.863	750	0.798
				675	0.748	755	0.658
				680	0.477	760	0.509
				685	0.159	765	0.295
				690	0.050	770	0.103
				695	0.017	775	0.029
						780	0.009

\* Wavelength is in nanometers.

<sup>†</sup> A peak transmittance of 515 nm was desired. This required excessive trimming. A peak transmittance of 520 nm was accepted as a compromise.

## DATA RELIABILITY

This report presents the results of a major effort to obtain meaningful atmospheric optical data. Certain aspects of the data reliability are discussed in Section I of this report; additional information is given in the paragraphs which follow.

The taking of atmospheric optical data during moonlight and starlight presented problems of what optical instruments to use and how to achieve the necessary sensitivity to use them. The nephelometer was designed and constructed for this project. The sky scanning radiometers were already designed and being constructed before the night requirement arose so that the problem in this case was how to achieve maximum sensitivity. This was also the situation in the case of the irradiometers and the large aperture telephotometers.

Following this paragraph are several subheadings describing separate problems and how these problems were handled. The solutions to some of the problems were very straightforward. The solutions to others were compromises. The inevitable result of compromise is a reduction in the reliability of the data. We think, however, that in general these data are good and in most cases quite reliable. In other cases the data suffer from the compromises.

*Thermal Control.* The spectral sensitivity of multiplier phototube cathodes varies as a function of their temperature (Murray and Manning, 1960, and Boileau and Miller, 1967). This variation is not only a simple change of sensitivity with temperature; it is also a function of wavelength. For example, lowering the temperature of the cathode may increase the sensitivity by 10% in the short wavelength part of the visible spectrum while the sensitivity in the long wavelength part of the spectrum is decreased by 50%. Accordingly, for measurement accuracy it is essential that the phototube cathode be maintained at a constant temperature. Thermoelectric junction temperature control units, developed at the Visibility Laboratory and capable of maintaining the temperature of the cathodes at a selected temperature,  $\pm 0.5^\circ\text{C}$ , were used in all airborne and ground-based optical instruments during Project SHED LIGHT data-taking.

*Instrument Calibrations.* Calibrations of the optical instruments were carried out in the radiometric calibration facility at the Visibility Laboratory (refer to Section 3.4, Radiometric Calibration Procedures). Several different secondary standards of luminous flux were used as the radiometric standards. The instruments were calibrated as units, that is, with optical components assembled in normal operational configuration. Because of the high sensitivity of the equipments (the maximum possible sensitivity for operating at very low flux levels), special precautions were made to preclude stray light. The standard deviations resulting from the calibrations were usually  $\pm 3\%$  with some instruments going as high as  $\pm 5\%$ .

*Field Calibrations.* Each optical instrument is fitted with an optical filter changer mechanism. Each of the filter changer mechanisms has one filter position fitted with an angled front surface mirror which reflects flux from a radioactive flux source to the cathode of the phototube. During the calibration of each instrument the radiance of this flux source was recorded. This flux source was used in the field as a calibrating device and the flux from this source was recorded before and after each data-gathering run.

*Data Reduction.* All data reduction has been done by computer. Instructions put into the data reduction program were to identify the voltages related to the radiance of each radioactive flux source, to average these voltages, and to print out the maximum, minimum, and average voltage values. The computer then compared the average voltage value with the voltage value recorded during calibration and adjusted

the instrument calibration to bring the two corresponding radiance values into agreement. If the intensity of the radioactive flux source is constant, and it is assumed to be so, this procedure corrects (within the range of the voltage variation) any error caused by small changes of multiplier phototube sensitivity.

The data recorded on the airborne magnetic tape data logger are voluminous, far too many to be studied individually. Accordingly, another instruction in the data reduction program was to time-average the radiometric data or, as in the case of the sky scanning radiometers, to get one average value for each  $360^\circ$  scan (this averaging was done only for the starlight cases). This procedure tended to reduce, or even eliminate, the random fluctuations in radiance values due to the small changes of phototube sensitivity. Thus the radiance values reported and used in deriving other atmospheric properties in this report are believed to be accurate within the standard deviations reported above.

*Phototube Noise.* A multiplier phototube has a high degree of precision when operating at relatively high flux levels. It retains this relatively high precision as the flux level lowers until the flux level nears the limiting sensitivity of the phototube. At this time the precision starts to lessen because of phototube noise. Continued lowering of the flux level is accompanied by rapidly increasing noise and loss of precision in the phototube signal until a flux level is eventually reached where the signal from the phototube is too imprecise to be of value. Therefore a level of precision had to be established below which the data were unacceptable. The criterion used in SHED LIGHT data reduction was: when the phototube signal for a 20% change in flux varied  $20 \pm 10\%$ , the data were discarded. It must be realized that the above criterion indicates only the data to be discarded. The data retained are better, higher precision data.

*Data Interpretation.* Lightning flashes were observed during some of the data-gathering runs and these were often recorded by the upper sky scanning radiometer. During all of the flights over land and some of the flights over water, artificial lights were present on the ground or on boats at sea. These lights were steady lights and were, of course, recorded by the lower sky scanning radiometer. It was believed the lightning flashes and ground lights were artificialities that should be eliminated from the data, if possible. Accordingly, for starlight skies the computer was programmed to compare all upper and lower sky radiances with the radiance of the zenith sky and to reject all radiances one order of magnitude greater than the zenith radiance. While this procedure eliminated the radiances one order of magnitude greater than the zenith radiance, it did not eliminate the radiances from small lights of lesser intensities. The above procedure could not be used in moonlight flights because of the high value of the moon's radiance compared to the radiance of the zenith sky. In those cases all data are included. Fortunately, during moonlight the general flux level is approximately two orders of magnitude above that of starlight, so the effect of the lightning flashes and ground lights for the moonlight cases was reduced by a factor of approximately two orders of magnitude from that of starlight.

## OPTICAL PROPERTIES

*Irradiance.* The irradiances  $H(z,d)$  and  $H(z,u)$ , albedos  $H(z,u)/H(z,d)$ , scalar irradiances  $h(z,d)$ ,  $h(z,u)$ , and  $h(z)$ , and scalar albedos  $h(z,u)/h(z,d)$  are presented in columnar form as a function of altitude. The altitudes are given in meters above ground level at intervals of approximately 300 m. The lowest reported values are those computed from data taken at minimum aircraft altitude. Because of data fluctuations with altitude it was impractical to extrapolate the data to zero altitude.

There are five tables of irradiance for each flight, one table for each optical filter. The dimensions and units for the irradiances are "watt  $m^{-2} \mu m^{-1}$ ". Albedos are, of course, dimensionless.

Some albedo values appear to be excessively great indeed, some are greater than unity. As stated in the Theory Section, irradiances are calculated from upper and lower sky radiances. The *measured* lower sky radiances included the effect of ground lights. The computer program designed to eliminate the effect of those lights during the calculation of the irradiances was not always successful. Thus some values of the upwelling irradiance and, consequently, the albedo values calculated from those irradiance values, are too great.

**Directional Reflectance of Background.** The Directional Background Reflectance  ${}_bR_o(z, \theta, \phi)$  is tabulated by zenith angle in five columns for the five optical filters. For the starlight flights, or equivalent, one table of data is presented. For the moonlight flights four tables of data are presented, one for each of the four azimuthal points. Reflectance is dimensionless.

**Background Radiance.** Background radiance is not included in these tables. It may be computed from the foregoing Irradiance and Directional Reflectance of Background by the equation

$${}_bN_o(0, \theta, \phi) = \frac{1}{\pi} {}_bR_o(0, \theta, \phi) H(0, d) \quad (6-1)$$

**Examples.** For Flight 82 I, Filter 1: the irradiance at the lowest altitude is  $3.14E-5 \text{ watt m}^{-2} \mu\text{m}^{-1}$ , the directional background reflectance for a zenith angle of  $93^\circ$  is 1.04

Then

$${}_bN_o(0, 93^\circ) = \frac{1}{\pi} \times 1.04 \times 3.14E-5$$

and

$${}_bN_o(0, 93^\circ) = 1.04E-5 \text{ watt } \Omega^{-1} \text{ m}^{-2} \mu\text{m}^{-1}$$

**Example.** For Flight 82 II, Filter 1: the irradiance at the lowest altitude is  $7.49E-5 \text{ watt m}^{-2} \mu\text{m}^{-1}$ , the directional background reflectances for a zenith angle of  $93^\circ$  and for the different azimuthal angles with respect to the moon are

$$\phi = 0^\circ \quad {}_bR_o(0, 93^\circ, 0^\circ) = 0.433,$$

$$\phi = 90^\circ \quad {}_bR_o(0, 93^\circ, 90^\circ) = 0.566,$$

$$\phi = 180^\circ \quad {}_bR_o(0, 93^\circ, 180^\circ) = 0.578,$$

and

$$\phi = 270^\circ \quad {}_bR_o(0, 93^\circ, 270^\circ) = 0.312.$$

With the above reflectances, the radiances computed with Eq. 6-1 are

$${}_bN_o(0, 93^\circ, 0^\circ) = 1.03E-5 \text{ watt } \Omega^{-1} \text{ m}^{-2} \mu\text{m}^{-1},$$

$${}_bN_o(0, 93^\circ, 90^\circ) = 1.35E-5 \text{ watt } \Omega^{-1} \text{ m}^{-2} \mu\text{m}^{-1},$$

$${}_bN_o(0, 93^\circ, 180^\circ) = 1.38E-5 \text{ watt } \Omega^{-1} \text{ m}^{-2} \mu\text{m}^{-1},$$

and

$${}_bN_o(0, 93^\circ, 270^\circ) = 0.744E-5 \text{ watt } \Omega^{-1} \text{ m}^{-2} \mu\text{m}^{-1}.$$

**Total Scattering Coefficient.** The total scattering coefficient  $s(z)$  is tabulated by altitude in five columns for the five optical filters. The altitude is given in meters, above ground level, at approximately 30.5 m (100 ft) increments. The dimension and unit for the total scattering coefficient are "per meter".

The total scattering coefficient is used for the calculation of atmospheric beam transmittance. It was so used in the various equations of the Theory Section to calculate the values of atmospheric beam transmittance in the tables which follow in Section 6.3.

**Beam Transmittance from Ground to Altitude.** Atmospheric beam transmittance is tabulated for the slant paths of sight, between the ground and altitudes shown, for the seven zenith angles from  $93^\circ$  to  $180^\circ$ . There are five tables, one for each optical filter. This property is dimensionless.

The symbol for atmospheric beam transmittance is  $T_r(z, \theta)$ , where  $r$  is the length of the path of sight,  $z$  is the altitude of the observer or sensor, and  $\theta$  is the zenith angle of the path of sight. The path of sight geometry is illustrated in Fig. 2-1 shown in Section 2 (also refer to Appendix A, p. 501). Thus the beam transmittance for Flight 82 I, Filter 1, zenith angle of  $105^\circ$ , from an altitude of 305 m, where because of the secant relationship  $r = 1178$ , is

$$T_{1178}(305, 105^\circ) = 0.804.$$

The secant relationship illustrated in Fig. 2-1 does not hold for the zenith angle of  $93^\circ$  because of the earth's curvature. (Refer to Earth Curvature in Theory Section.) In this case the path length  $r$ , when the earth curvature is considered, is 5880 m instead of 5828 m calculated by the secant relationship. Thus the transmittance is

$$T_{5880}(305, 93^\circ) = 0.337.$$

**Path Radiance from Ground to Altitude.** Path radiance  $N_r^*(z, \theta, \phi)$  is tabulated for the slant paths of sight, between the ground and the altitude shown, for the seven zenith angles from  $93^\circ$  to  $180^\circ$ . There are five tables, one for each optical filter. For moonlight flights there are four such sets of data, one set for each of the four azimuthal directions of  $0^\circ$ ,  $90^\circ$ ,  $180^\circ$ , and  $270^\circ$ . The dimensions and units are "watt  $\Omega^{-1} \text{ m}^{-2} \mu\text{m}^{-1}$ ".

**Examples.** For Flight 82 I, Filter 1, zenith angle of  $105^\circ$ , from an altitude of 305 m, and path length  $r$  of 1178 m, the path radiance is

$$N_{1178}^*(305, 105^\circ, \phi) = 1.04\text{E-}6 \text{ watt } \Omega^{-1} \text{ m}^{-2} \mu\text{m}^{-1}.$$

Similarly, for Flight 82 II using the same filter, zenith angle, and altitude, the path radiances are

$$N_{1178}^*(305, 105^\circ, 0^\circ) = 5.06\text{E-}6 \text{ watt } \Omega^{-1} \text{ m}^{-2} \mu\text{m}^{-1},$$

$$N_{1178}^*(305, 105^\circ, 90^\circ) = 2.50\text{E-}6 \text{ watt } \Omega^{-1} \text{ m}^{-2} \mu\text{m}^{-1},$$

$$N_{1178}^*(305, 105^\circ, 180^\circ) = 2.68\text{E-}6 \text{ watt } \Omega^{-1} \text{ m}^{-2} \mu\text{m}^{-1},$$

and 
$$N_{1178}^*(305, 105^\circ, 270^\circ) = 2.47\text{E-}6 \text{ watt } \Omega^{-1} \text{ m}^{-2} \mu\text{m}^{-1}.$$

Note that the path radiance for the path of sight in the direction of the moon is greater than the other path radiance values by a factor of 2.

**Directional Path Reflectance from Ground to Altitude.** Directional path reflectance  $R_p^*(z, \theta, \phi)$  is tabulated for the slant paths of sight, for the path length between the ground and the indicated altitude, and for the seven zenith angles from  $93^\circ$  to  $180^\circ$ . There are five tables, one for each optical filter, and in the case of the moonlight flights there are four data sets, one for each of the four azimuthal angles, with respect to the moon, of  $0^\circ$ ,  $90^\circ$ ,  $180^\circ$ , and  $270^\circ$ . This property is dimensionless.

The user of these tables is urged to read Appendix D for a clearer understanding of the concept of directional path radiance.

**Contrast Transmittance.** Contrast transmittance  ${}_b\tau_r(z, \theta, \phi)$  is not tabulated. This optical property is a function of atmospheric beam transmittance, path radiance, and the inherent background radiance against which an object is viewed. The background radiance measured by the airborne radiometer was the average radiance of many individual areas integrated into one value by the  $5^\circ$  circular field of the radiometer. The inherent background radiance against which the object is viewed will probably never be the same as the measured average radiance. If the area of that background is sufficiently small, its radiance will have no appreciable effect on the measured average background radiance and thus will have no appreciable effect on the path radiance. In this case *decoupling* exists between the object background area and the path radiance and under this circumstance of decoupling the contrast transmittance may be calculated by Eq. 3 of Appendix D:

$${}_b\tau_r(z, \theta, \phi) = \left\{ 1 + [R_p^*(z, \theta, \phi) / {}_bR_o(z, \theta, \phi)] \right\}^{-1}.$$

It is suggested that the user of this report read the discussion of *decoupling* on page 554 of Appendix B.

**Examples.** On a night similar to that of Flight 82I, assume that the contrast transmittance is needed for a slant path of sight  $15^\circ$  below the horizon (zenith angle of  $105^\circ$ ), from an aircraft flying at an altitude of 1220 m, and for an object located on a concrete pad (surrounded by vegetation) which has a known reflectance in the direction of the path of sight of 0.600. Assume further that the sensor sensitivity is very close to 515 nm. From the tables of Flight 82I the directional path reflectance for a zenith angle of  $105^\circ$ , Filter 2, and an altitude of 1219 m is  $6.10\text{E-}1$ . Then by using the above equation

$${}_b\tau_{4710}(1219, 105^\circ, \phi) = [1 + (0.610/0.600)]^{-1} = 0.496.$$

When the aircraft has proceeded to the point where the zenith angle is  $120^\circ$ , the corresponding directional path reflectance is  $1.98\text{E-}1$ . Now, assuming there is no change in inherent background reflectance with change of the reflectance angle, then

$${}_b\tau_{2438}(1219, 120^\circ, \phi) = [1 + (0.198/0.600)]^{-1} = 0.752.$$

When the aircraft is directly above the object, the directional path reflectance is  $5.40\text{E-}2$  and the contrast transmittance would be

$${}_b\tau_{1219}(1219, 180^\circ, \phi) = [1 + (0.054/0.600)]^{-1} = 0.917.$$



Now, instead of a concrete pad let us assume the object is located on a black macadam road (surrounded by vegetation) with a reflectance of 0.125, which is again independent of reflection angle. The corresponding contrast transmittance values for the different zenith angles would be

$$b_{\tau_{4710}}(1219, 105^\circ, \phi) = 0.170 ,$$

$$b_{\tau_{2438}}(1219, 120^\circ, \phi) = 0.387 ,$$

and

$$b_{\tau_{1219}}(1219, 180^\circ, \phi) = 0.698 .$$

Now assume that it is after moonrise and the night is similar to that of Flight 8211. From the tables of that flight the directional path reflectances for zenith angle of  $105^\circ$ , altitude of 1219 m, and Filter 2 are

$$R_{4710}^*(1219, 105^\circ, 0^\circ) = 1.20 ,$$

$$R_{4710}^*(1219, 105^\circ, 90^\circ) = 0.795 ,$$

$$R_{4710}^*(1219, 105^\circ, 180^\circ) = 0.819 ,$$

and

$$R_{4710}^*(1219, 105^\circ, 270^\circ) = 0.906 .$$

The resulting contrast transmittances for an object against a background reflectance of 0.600, still independent of angle of reflection, for the four azimuths would be

$$b_{\tau_{4710}}(1219, 105^\circ, 0^\circ) = 0.333 ,$$

$$b_{\tau_{4710}}(1219, 105^\circ, 90^\circ) = 0.430 ,$$

$$b_{\tau_{4710}}(1219, 105^\circ, 180^\circ) = 0.423 ,$$

and

$$b_{\tau_{4710}}(1219, 105^\circ, 270^\circ) = 0.398 .$$

When the aircraft has proceeded to the point when the zenith angle is  $120^\circ$ , the four directional path reflectances would be

$$R_{2438}^*(1219, 120^\circ, 0^\circ) = 0.344 ,$$

$$R_{2438}^*(1219, 120^\circ, 90^\circ) = 0.276 ,$$

$$R_{2438}^*(1219, 120^\circ, 180^\circ) = 0.299 ,$$

and

$$R_{2438}^*(1219, 120^\circ, 270^\circ) = 0.298 .$$

Now the resulting contrast transmittances of the object against a background reflectance of 0.600 for the four azimuths would be

$$b_{\tau_{2438}}(1219, 120^\circ, 0^\circ) = 0.636 ,$$

$$b_{\tau_{2438}}(1219, 120^\circ, 90^\circ) = 0.685 ,$$

$$b_{\tau_{2438}}(1219, 120^\circ, 180^\circ) = 0.667 ,$$

and

$$b_{\tau_{2438}}(1219, 120^\circ, 270^\circ) = 0.668 .$$

When the aircraft is directly above the object, the directional path reflectance would be 0.0904 without regard to the azimuth. Then the contrast transmittance would be

$$b_{1219}^{\tau}(1219, 180^{\circ}, \phi) = 0.869 .$$

A similar treatment for an object against the macadam road with a reflectance of 0.125 would be

$$b_{4710}^{\tau}(1219, 105^{\circ}, 0^{\circ}) = 0.0943 ,$$

$$b_{4710}^{\tau}(1219, 105^{\circ}, 90^{\circ}) = 0.136 ,$$

$$b_{4710}^{\tau}(1219, 105^{\circ}, 180^{\circ}) = 0.132 ,$$

$$b_{4710}^{\tau}(1219, 105^{\circ}, 270^{\circ}) = 0.121 ,$$

$$b_{2438}^{\tau}(1219, 120^{\circ}, 0^{\circ}) = 0.267 ,$$

$$b_{2438}^{\tau}(1219, 120^{\circ}, 90^{\circ}) = 0.312 ,$$

$$b_{2438}^{\tau}(1219, 120^{\circ}, 180^{\circ}) = 0.295 ,$$

$$b_{2438}^{\tau}(1219, 120^{\circ}, 270^{\circ}) = 0.296 ,$$

and

$$b_{1219}^{\tau}(1219, 180^{\circ}, \phi) = 0.580 .$$

The foregoing examples are based on two reflectances of 0.600 and 0.125 which are assumed to have no change with the angle of reflection. The purpose of the examples is to show how the contrast transmittance changes with variation of the factors in the contrast transmittance equation, especially the background reflectance. In real life the inherent background reflectance is seldom, if ever, a constant value independent of angle of reflection and the user of these tables is urged to read Appendix B, particularly the part entitled "III. Optical Properties of Objects and Backgrounds".

### 6.3 DATA TABLES

Each set of tables is printed on paper of one color and two colors are used alternately so that the tables from one flight are readily distinguishable from the tables of the flight preceding and following.

#### FLIGHT 82I

Overcast moonlight. This flight was conducted over the TREND site shortly after midnight local time and soon after moonrise. The TREND site was situated in the northern foothills of the Dangrek Mountains. The ground cover consisted of random areas of small, deciduous trees and tall grass. The area was cut through just north of the TREND site by a hard-surface road with bare, reddish soil areas on either side. There were very few ground lights in the vicinity of the TREND site, but there was a river dam with many electric lights a few miles beyond the southwest end of the flight path. High scattered cirrus clouds covered the sky, partially obscuring the moon, and low stratus clouds were located southwest of the flight area. Moon phase angle was  $101^\circ$ ; moon zenith angle was  $82^\circ$  at start of sky radiance data-taking and  $75^\circ$  at completion.

FLIGHT NO. 82 I FILTER NO. 1  
IRRADIANCE(WATTS/SQ.M.MICRO M.)

ALTITUDE (METERS)	DOWN- WELLING	UP- WELLING	ALBEDO	SCALAR DOWNWELLING	SCALAR UPWELLING	SCALAR TOTAL	SCALAR ALBEDO
378	3.144E-05	1.542E-06	.049	7.133E-05	7.511E-06	7.884E-05	.105
654	3.085E-05	1.932E-06	.063	7.454E-05	1.068E-05	8.522E-05	.143
965	2.800E-05	1.048E-06	.066	6.486E-05	9.380E-06	7.424E-05	.145
1364	2.643E-05	2.133E-06	.081	6.523E-05	1.133E-05	7.657E-05	.174
1603	2.449E-05	1.898E-06	.077	6.016E-05	9.886E-06	7.004E-05	.164
1857	2.104E-05	2.290E-06	.109	5.112E-05	1.035E-05	6.146E-05	.202

FLIGHT NO. 82 I FILTER NO. 2  
IRRADIANCE(WATTS/SQ.M.MICRO M.)

ALTITUDE (METERS)	DOWN- WELLING	UP- WELLING	ALBEDO	SCALAR DOWNWELLING	SCALAR UPWELLING	SCALAR TOTAL	SCALAR ALBEDO
356	3.169E-05	2.644E-06	.083	7.543E-05	1.061E-05	8.604E-05	.141
639	2.867E-05	2.695E-06	.094	6.829E-05	1.383E-05	8.212E-05	.203
964	2.703E-05	2.995E-06	.111	6.360E-05	1.304E-05	7.664E-05	.205
1278	2.624E-05	3.029E-06	.115	5.977E-05	1.414E-05	7.391E-05	.237
1586	2.439E-05	3.444E-06	.140	5.915E-05	1.394E-05	7.309E-05	.236
1859	2.141E-05	3.272E-06	.153	4.869E-05	1.368E-05	6.236E-05	.281

FLIGHT NO. 82 I FILTER NO. 3  
IRRADIANCE(WATTS/SQ.M.MICRO M.)

ALTITUDE (METERS)	DOWN- WELLING	UP- WELLING	ALBEDO	SCALAR DOWNWELLING	SCALAR UPWELLING	SCALAR TOTAL	SCALAR ALBEDO
353	3.131E-05	3.134E-06	.100	7.525E-05	1.533E-05	9.058E-05	.204
637	2.885E-05	3.368E-06	.117	6.876E-05	1.918E-05	8.794E-05	.279
965	2.856E-05	3.992E-06	.140	6.870E-05	2.065E-05	8.935E-05	.301
1279	2.737E-05	3.776E-06	.138	6.414E-05	2.174E-05	8.589E-05	.339
1586	2.617E-05	3.437E-06	.131	6.172E-05	1.968E-05	8.140E-05	.319
1869	2.369E-05	4.035E-06	.170	5.553E-05	2.243E-05	7.795E-05	.404

FLIGHT NO. 82 I FILTER NO. 4  
IRRADIANCE(WATTS/SQ.M.MICRO M.)

ALTITUDE (METERS)	DOWN- WELLING	UP- WELLING	ALBEDO	SCALAR DOWNWELLING	SCALAR UPWELLING	SCALAR TOTAL	SCALAR ALBEDO
353	1.255E-05	8.479E-06	.676	3.357E-05	2.540E-05	5.898E-05	.757
635	1.261E-05	6.402E-06	.508	3.455E-05	2.191E-05	5.646E-05	.634
965	1.305E-05	6.758E-06	.518	3.445E-05	2.455E-05	5.900E-05	.713
1279	1.188E-05	6.730E-06	.567	3.233E-05	2.233E-05	5.465E-05	.591
1585	1.089E-05	6.458E-06	.593	2.845E-05	2.449E-05	5.294E-05	.861
1868	9.940E-06	6.040E-06	.608	2.697E-05	2.213E-05	4.910E-05	.821

FLIGHT NO. 82 I FILTER NO. 5  
IRRADIANCE(WATTS/SQ.M.MICRO M.)

ALTITUDE (METERS)	DOWN- WELLING	UP- WELLING	ALBEDO	SCALAR DOWNWELLING	SCALAR UPWELLING	SCALAR TOTAL	SCALAR ALBEDO
344	3.351E-05	2.590E-06	.077	7.853E-05	1.076E-05	8.929E-05	.137
646	3.019E-05	3.149E-06	.104	6.895E-05	1.268E-05	8.163E-05	.184
965	3.087E-05	3.234E-06	.105	6.989E-05	1.416E-05	8.405E-05	.203
1278	2.824E-05	3.592E-06	.127	6.558E-05	1.521E-05	8.079E-05	.232
1585	2.806E-05	3.577E-06	.127	6.240E-05	1.524E-05	7.763E-05	.244
1871	2.552E-05	3.811E-06	.149	6.246E-05	1.476E-05	7.721E-05	.236

FLIGHT NO. 82 I  
DIRECTIONAL REFLECTANCE OF BACKGROUND  
FILTERS

ZENITH ANGLE	1	2	5	3	4
93	1.03537	1.16497	.83400	2.06282	4.26376
95	.47917	.79348	.67530	.78943	1.71599
100	.09171	.20225	.14182	.12576	.97000
105	.05422	.11571	.09780	.10195	.78459
120	.04585	.08268	.06956	.08668	.66564
150	.03388	.05945	.05211	.07724	.59214
180	.02940	.04951	.04608	.07397	.56671

DATE 91568 FLIGHT NO. 02 I GROUND LEVEL ALTITUDE ( M.)= 629 IUP=1

ALTITUDE (METERS)	TOTAL SCATTERING COEFFICIENT (PER METER)				
	FILTERS	1	2	3	4
0		1.882E-04	1.688E-04	9.926E-05	8.185E-05
30		1.876E-04	1.682E-04	9.893E-05	8.158E-05
61		1.869E-04	1.676E-04	9.860E-05	8.131E-05
91		1.863E-04	1.671E-04	9.827E-05	8.104E-05
122		1.857E-04	1.665E-04	9.794E-05	8.077E-05
152		1.851E-04	1.660E-04	9.751E-05	8.050E-05
183		1.845E-04	1.654E-04	9.729E-05	8.023E-05
213		1.838E-04	1.649E-04	9.697E-05	7.996E-05
244		1.832E-04	1.643E-04	9.664E-05	7.970E-05
274		1.826E-04	1.638E-04	9.632E-05	7.943E-05
305		1.820E-04	1.632E-04	9.600E-05	7.917E-05
335		1.814E-04	1.627E-04	9.568E-05	7.890E-05
366		1.801E-04	1.621E-04	9.427E-05	7.690E-05
396		1.795E-04	1.616E-04	9.178E-05	7.557E-05
427		1.789E-04	1.612E-04	8.973E-05	7.916E-05
457		1.793E-04	1.601E-04	8.881E-05	7.777E-05
480		1.794E-04	1.602E-04	8.856E-05	7.772E-05
518		1.780E-04	1.595E-04	8.611E-05	7.687E-05
549		1.755E-04	1.592E-04	8.552E-05	7.693E-05
579		1.730E-04	1.608E-04	8.576E-05	7.687E-05
610		1.728E-04	1.585E-04	8.506E-05	7.610E-05
640		1.724E-04	1.569E-04	8.465E-05	7.593E-05
671		1.718E-04	1.543E-04	8.441E-05	7.549E-05
701		1.669E-04	1.553E-04	8.460E-05	7.491E-05
732		1.651E-04	1.551E-04	8.353E-05	7.439E-05
762		1.650E-04	1.564E-04	8.437E-05	7.449E-05
792		1.631E-04	1.554E-04	8.361E-05	7.266E-05
823		1.599E-04	1.503E-04	8.270E-05	7.194E-05
853		1.599E-04	1.442E-04	8.270E-05	7.227E-05
884		1.607E-04	1.399E-04	8.210E-05	6.928E-05
914		1.599E-04	1.406E-04	8.202E-05	6.818E-05
945		1.611E-04	1.380E-04	8.197E-05	6.547E-05
975		1.621E-04	1.359E-04	8.175E-05	6.496E-05
1006		1.616E-04	1.338E-04	8.104E-05	6.378E-05
1036		1.594E-04	1.360E-04	7.943E-05	6.389E-05
1067		1.561E-04	1.371E-04	7.839E-05	6.434E-05
1097		1.542E-04	1.352E-04	7.783E-05	6.496E-05
1128		1.535E-04	1.300E-04	7.761E-05	6.463E-05
1158		1.522E-04	1.260E-04	7.697E-05	6.317E-05
1189		1.510E-04	1.241E-04	7.639E-05	6.173E-05
1219		1.509E-04	1.217E-04	7.635E-05	6.124E-05
1250		1.501E-04	1.150E-04	7.624E-05	6.032E-05
1280		1.500E-04	1.156E-04	7.566E-05	5.935E-05
1311		1.504E-04	1.138E-04	7.459E-05	5.881E-05
1341		1.488E-04	1.125E-04	7.371E-05	5.829E-05
1372		1.465E-04	1.119E-04	7.291E-05	5.838E-05
1402		1.446E-04	1.093E-04	7.205E-05	5.827E-05
1433		1.449E-04	1.092E-04	7.194E-05	5.815E-05
1463		1.455E-04	1.083E-04	7.197E-05	5.820E-05
1494		1.451E-04	1.062E-04	7.121E-05	5.693E-05
1524		1.438E-04	1.052E-04	7.140E-05	5.598E-05
1554		1.429E-04	1.042E-04	7.053E-05	5.560E-05
1585		1.425E-04	1.022E-04	7.014E-05	5.499E-05
1615		1.421E-04	1.022E-04	6.983E-05	5.492E-05
1646		1.402E-04	9.986E-05	7.059E-05	5.442E-05
1676		1.378E-04	9.879E-05	7.063E-05	5.376E-05
1707		1.357E-04	9.799E-05	6.983E-05	5.232E-05
1737		1.360E-04	9.660E-05	6.964E-05	5.329E-05
1768		1.340E-04	9.655E-05	6.847E-05	5.225E-05
1798		1.317E-04	9.681E-05	6.693E-05	5.196E-05
1829		1.287E-04	9.681E-05	6.602E-05	5.196E-05

FIRST DATA ALT.	12	14	12	12	12
LAST DATA ALT.	61	61	61	61	61

		FLIGHT NO. 82 I		FILTER NO. 1					
		BEAM TRANSMITTANCE FROM GROUND TO ALTITUDE							
ALTITUDE		ZENITH ANGLE OF PATH OF SIGHT (DEGREES)							
METERS		93	95	100	105	120	150	180	
305		.3370547	.5234828	.7226273	.8041593	.8933085	.9369376	.9451500	
610		.1159389	.2806586	.5284861	.6518946	.8013295	.8799649	.8951701	
914		.0422149	.1575429	.3955182	.5366967	.7245984	.8302850	.8512335	
1219		.0158330	.0910835	.3004224	.4462699	.6585949	.7857407	.8115386	
1524		.0061482	.0544126	.2319717	.3751927	.6020296	.7460403	.7759057	

		FLIGHT NO. 82 I		FILTER NO. 2					
		BEAM TRANSMITTANCE FROM GROUND TO ALTITUDE							
ALTITUDE		ZENITH ANGLE OF PATH OF SIGHT (DEGREES)							
METERS		93	95	100	105	120	150	180	
305		.3770828	.5596400	.7472620	.8224505	.9037693	.9432566	.9506678	
610		.1439827	.3188860	.5634686	.6805378	.8193660	.8913463	.9051884	
914		.0569415	.1875764	.4317186	.5691768	.7469760	.8449938	.8642777	
1219		.0247212	.1179173	.3419917	.4868098	.6889144	.8064263	.8300087	
1524		.0119479	.0798352	.2811903	.4268945	.6436353	.7753864	.8022688	

		FLIGHT NO. 82 I		FILTER NO. 3					
		BEAM TRANSMITTANCE FROM GROUND TO ALTITUDE							
ALTITUDE		ZENITH ANGLE OF PATH OF SIGHT (DEGREES)							
METERS		93	95	100	105	120	150	180	
305		.5634881	.7107790	.8425276	.8913998	.9422272	.9662261	.9706839	
610		.3292118	.5194398	.7190207	.8020625	.8921020	.9362068	.9445115	
914		.1972976	.3877316	.6215552	.7268426	.8477665	.9090553	.9207424	
1219		.1202245	.2940761	.5410217	.6622272	.8078792	.8841103	.8988210	
1524		.0749418	.2274632	.4755841	.6073565	.7725066	.8615497	.8789236	

		FLIGHT NO. 82 I		FILTER NO. 4					
		BEAM TRANSMITTANCE FROM GROUND TO ALTITUDE							
ALTITUDE		ZENITH ANGLE OF PATH OF SIGHT (DEGREES)							
METERS		93	95	100	105	120	150	180	
305		.6231177	.7546311	.8682281	.9095528	.9521114	.9720651	.9757619	
610		.3908037	.5746085	.7572276	.8297934	.9079371	.9457656	.9528574	
914		.2495651	.4445969	.6657495	.7611229	.8682334	.9216622	.9317904	
1219		.1667307	.3552343	.5948384	.7057301	.8349291	.9010821	.9137445	
1524		.1141753	.2894800	.5367611	.6587238	.8056640	.8827096	.8975879	

		FLIGHT NO. 82 I		FILTER NO. 5					
		BEAM TRANSMITTANCE FROM GROUND TO ALTITUDE							
ALTITUDE		ZENITH ANGLE OF PATH OF SIGHT (DEGREES)							
METERS		93	95	100	105	120	150	180	
305		.3994168	.5791376	.7602174	.8319902	.9091805	.9465131	.9535096	
610		.1621544	.3420573	.5836595	.6968040	.8294459	.8976608	.9107392	
914		.0668092	.2058659	.4523790	.5873107	.7592018	.8529513	.8713219	
1219		.0258243	.1287118	.3573622	.5013827	.6995137	.8135665	.8363694	
1524		.0127858	.0826522	.2861273	.4319088	.6475377	.7780771	.8046973	

FLIGHT NO. 82 I      FILTER NO. 1  
 PATH RADIANCE FROM GROUND TO ALTITUDE(WATTS/STER.SQ.M MICRO M.)  
 ALTITUDE      ZENITH ANGLE OF PATH OF SIGHT (DEGREES)  
 METERS      93      95      100      105      120      150      180

305	4.439E-06	3.076E-06	1.625E-06	1.035E-06	4.192E-07	1.681E-07	1.305E-07
610	6.155E-06	4.796E-06	2.840E-06	1.890E-06	7.992E-07	3.253E-07	2.527E-07
914	6.746E-06	5.723E-06	3.718E-06	2.570E-06	1.131E-06	4.661E-07	3.622E-07
1219	6.703E-06	6.023E-06	4.243E-06	3.043E-06	1.398E-06	5.893E-07	4.596E-07
1524	6.709E-06	6.230E-06	4.657E-06	3.446E-06	1.647E-06	7.102E-07	5.563E-07

FLIGHT NO. 82 I      FILTER NO. 2  
 PATH RADIANCE FROM GROUND TO ALTITUDE(WATTS/STER.SQ.M MICRO M.)  
 ALTITUDE      ZENITH ANGLE OF PATH OF SIGHT (DEGREES)  
 METERS      93      95      100      105      120      150      180

305	4.698E-06	3.209E-06	1.681E-06	1.071E-06	4.356E-07	1.745E-07	1.350E-07
610	6.412E-06	4.940E-06	2.896E-06	1.924E-06	8.166E-07	3.323E-07	2.573E-07
914	6.852E-06	5.759E-06	3.711E-06	2.562E-06	1.133E-06	4.681E-07	3.626E-07
1219	6.776E-06	6.039E-06	4.193E-06	2.993E-06	1.377E-06	5.811E-07	4.519E-07
1524	6.658E-06	6.142E-06	4.502E-06	3.301E-06	1.572E-06	6.782E-07	5.296E-07

FLIGHT NO. 82 I      FILTER NO. 3  
 PATH RADIANCE FROM GROUND TO ALTITUDE(WATTS/STER.SQ.M MICRO M.)  
 ALTITUDE      ZENITH ANGLE OF PATH OF SIGHT (DEGREES)  
 METERS      93      95      100      105      120      150      180

305	3.569E-06	2.288E-06	1.139E-06	7.118E-07	2.867E-07	1.087E-07	8.344E-08
610	5.475E-06	3.799E-06	2.028E-06	1.299E-06	5.354E-07	2.049E-07	1.572E-07
914	6.563E-06	4.853E-06	2.752E-06	1.804E-06	7.555E-07	2.928E-07	2.241E-07
1219	7.186E-06	5.600E-06	3.350E-06	2.245E-06	9.534E-07	3.780E-07	2.895E-07
1524	7.421E-06	6.053E-06	3.804E-06	2.602E-06	1.129E-06	4.571E-07	3.514E-07

FLIGHT NO. 82 I      FILTER NO. 4  
 PATH RADIANCE FROM GROUND TO ALTITUDE(WATTS/STER.SQ.M MICRO M.)  
 ALTITUDE      ZENITH ANGLE OF PATH OF SIGHT (DEGREES)  
 METERS      93      95      100      105      120      150      180

305	2.128E-06	1.365E-06	7.023E-07	4.579E-07	2.053E-07	9.453E-08	7.644E-08
610	3.419E-06	2.352E-06	1.284E-06	8.530E-07	3.878E-07	1.785E-07	1.442E-07
914	4.216E-06	3.069E-06	1.761E-06	1.189E-06	5.455E-07	2.491E-07	2.003E-07
1219	4.672E-06	3.558E-06	2.133E-06	1.463E-06	6.803E-07	3.110E-07	2.499E-07
1524	4.860E-06	3.857E-06	2.408E-06	1.678E-06	7.938E-07	3.657E-07	2.941E-07

FLIGHT NO. 82 I      FILTER NO. 5  
 PATH RADIANCE FROM GROUND TO ALTITUDE(WATTS/STER.SQ.M MICRO M.)  
 ALTITUDE      ZENITH ANGLE OF PATH OF SIGHT (DEGREES)  
 METERS      93      95      100      105      120      150      180

305	4.664E-06	3.157E-06	1.641E-06	1.042E-06	4.185E-07	1.688E-07	1.307E-07
610	6.327E-06	4.826E-06	2.799E-06	1.852E-06	7.859E-07	3.208E-07	2.495E-07
914	6.848E-06	5.684E-06	3.615E-06	2.482E-06	1.110E-06	4.571E-07	3.565E-07
1219	7.086E-06	6.203E-06	4.230E-06	3.000E-06	1.385E-06	5.837E-07	4.563E-07
1524	7.044E-06	6.427E-06	4.659E-06	3.405E-06	1.624E-06	7.054E-07	5.541E-07

FLIGHT NO. 82 I		FILTER NO. 1					
DIRECTIONAL PATH REFLECTANCE FROM GROUND TO ALTITUDE		ZENITH ANGLE OF PATH OF SIGHT (DEGREES)					
ALTITUDE METERS	93	95	100	105	120	150	180
305	1.316E 00	5.872E-01	2.247E-01	1.287E-01	4.689E-02	1.793E-02	1.380E-02
610	5.305E 00	1.708E 00	5.370E-01	2.897E-01	9.945E-02	3.694E-02	2.821E-02
914	1.601E 01	3.630E 00	9.393E-01	4.784E-01	1.559E-01	5.609E-02	4.251E-02
1219	4.230E 01	6.608E 00	1.411E 00	6.813E-01	2.121E-01	7.493E-02	5.659E-02
1524	1.090E 02	1.144E 01	2.006E 00	9.178E-01	2.734E-01	9.512E-02	7.164E-02

FLIGHT NO. 82 I		FILTER NO. 2					
DIRECTIONAL PATH REFLECTANCE FROM GROUND TO ALTITUDE		ZENITH ANGLE OF PATH OF SIGHT (DEGREES)					
ALTITUDE METERS	93	95	100	105	120	150	180
305	1.235E 00	5.685E-01	2.231E-01	1.291E-01	4.779E-02	1.834E-02	1.408E-02
610	4.416E 00	1.536E 00	5.096E-01	2.803E-01	9.881E-02	3.696E-02	2.818E-02
914	1.193E 01	3.044E 00	8.523E-01	4.463E-01	1.504E-01	5.492E-02	4.160E-02
1219	2.718E 01	5.078E 00	1.216E 00	6.096E-01	1.981E-01	7.145E-02	5.398E-02
1524	5.525E 01	7.627E 00	1.587E 00	7.667E-01	2.422E-01	8.672E-02	6.546E-02

FLIGHT NO. 82 I		FILTER NO. 3					
DIRECTIONAL PATH REFLECTANCE FROM GROUND TO ALTITUDE		ZENITH ANGLE OF PATH OF SIGHT (DEGREES)					
ALTITUDE METERS	93	95	100	105	120	150	180
305	6.356E-01	3.230E-01	1.356E-01	8.012E-02	3.053E-02	1.129E-02	8.626E-03
610	1.649E 00	7.338E-01	2.827E-01	1.626E-01	6.023E-02	2.196E-02	1.670E-02
914	3.338E 00	1.256E 00	4.443E-01	2.491E-01	8.942E-02	3.232E-02	2.442E-02
1219	5.997E 00	1.911E 00	6.214E-01	3.402E-01	1.184E-01	4.291E-02	3.232E-02
1524	9.936E 00	2.670E 00	8.025E-01	4.299E-01	1.466E-01	5.324E-02	4.012E-02

FLIGHT NO. 82 I		FILTER NO. 4					
DIRECTIONAL PATH REFLECTANCE FROM GROUND TO ALTITUDE		ZENITH ANGLE OF PATH OF SIGHT (DEGREES)					
ALTITUDE METERS	93	95	100	105	120	150	180
305	8.549E-01	4.529E-01	2.025E-01	1.260E-01	5.396E-02	2.434E-02	1.961E-02
610	2.190E 00	1.025E 00	4.243E-01	2.573E-01	1.069E-01	4.725E-02	3.787E-02
914	4.229E 00	1.728E 00	6.622E-01	3.912E-01	1.573E-01	6.745E-02	5.301E-02
1219	7.014E 00	2.507E 00	8.974E-01	5.189E-01	2.040E-01	8.640E-02	6.845E-02
1524	1.066E 01	3.335E 00	1.123E 00	6.377E-01	2.466E-01	1.037E-01	8.203E-02

FLIGHT NO. 82 I		FILTER NO. 5					
DIRECTIONAL PATH REFLECTANCE FROM GROUND TO ALTITUDE		ZENITH ANGLE OF PATH OF SIGHT (DEGREES)					
ALTITUDE METERS	93	95	100	105	120	150	180
305	1.095E 00	5.111E-01	2.024E-01	1.174E-01	4.315E-02	1.672E-02	1.285E-02
610	3.658E 00	1.323E 00	4.496E-01	2.492E-01	8.883E-02	3.350E-02	2.568E-02
914	9.610E 00	2.588E 00	7.489E-01	3.963E-01	1.370E-01	5.024E-02	3.836E-02
1219	2.305E 01	4.518E 00	1.110E 00	5.610E-01	1.856E-01	6.726E-02	5.115E-02
1524	5.165E 01	7.290E 00	1.527E 00	7.391E-01	2.351E-01	8.499E-02	6.455E-02



#### FLIGHT 82II

Moonlight. This part of the flight started at 0226 local time, over an area approximately 65 km east of Khorat, and ended at 0327. The terrain was flat. The vegetation consisted of forested areas of small deciduous trees with flooded rice paddies scattered among the trees. The cloud cover had changed sufficiently from that of Flight 82I to reveal the moon. In addition, a considerable number of lightning flashes were observed in the northwest direction. Moon phase angle was  $102^\circ$ ; moon zenith angle ranged from  $59^\circ$  to  $53^\circ$  during sky radiance data-taking.

FLIGHT NO. 42 II FILTER NO. 1  
IRRADIANCE (WATTS/SQ.M. MICRO M.)

ALTITUDE (METERS)	DOWN- WELLING	UP- WELLING	ALBEDO	SCALAR DOWNWELLING	SCALAR UPWELLING	SCALAR TOTAL	SCALAR ALBEDO
331	7.494E-05	5.781E-06	.077	1.733E-04	1.071E-05	1.872E-04	.09%
601	9.664E-05	5.409E-06	.056	1.999E-04	1.915E-05	2.190E-04	.09%
921	1.516E-04	8.334E-06	.055	1.910E-04	2.512E-05	2.261E-04	.083
1235	1.672E-04	7.315E-06	.044	2.306E-04	2.466E-05	2.552E-04	.075
1523	1.977E-04	7.346E-06	.065	2.183E-04	2.522E-05	2.435E-04	.116

FLIGHT NO. 42 II FILTER NO. 2  
IRRADIANCE (WATTS/SQ.M. MICRO M.)

ALTITUDE (METERS)	DOWN- WELLING	UP- WELLING	ALBEDO	SCALAR DOWNWELLING	SCALAR UPWELLING	SCALAR TOTAL	SCALAR ALBEDO
331	4.903E-05	8.432E-06	.172	1.087E-04	2.281E-05	1.315E-04	.21%
600	5.343E-05	7.763E-06	.128	1.436E-04	3.003E-05	1.706E-04	.214
921	7.453E-05	1.163E-05	.153	1.581E-04	3.063E-05	1.888E-04	.194
1231	9.366E-05	9.204E-06	.098	1.983E-04	2.914E-05	2.254E-04	.148
1528	1.200E-04	1.010E-05	.084	2.467E-04	2.957E-05	2.763E-04	.120

FLIGHT NO. 42 II FILTER NO. 3  
IRRADIANCE (WATTS/SQ.M. MICRO M.)

ALTITUDE (METERS)	DOWN- WELLING	UP- WELLING	ALBEDO	SCALAR DOWNWELLING	SCALAR UPWELLING	SCALAR TOTAL	SCALAR ALBEDO
332	5.819E-05	9.112E-06	.157	1.785E-04	2.721E-05	1.537E-04	.215
600	7.247E-05	8.650E-06	.117	1.553E-04	2.879E-05	1.841E-04	.185
922	4.629E-05	8.140E-06	.176	1.049E-04	2.826E-05	1.331E-04	.264
1237	7.410E-05	1.039E-05	.146	1.550E-04	3.320E-05	1.882E-04	.214
1529	1.756E-04	9.212E-06	.052	3.435E-04	3.151E-05	3.750E-04	.092
1831	9.531E-05	8.709E-06	.091	2.124E-04	3.127E-05	2.437E-04	.147

FLIGHT NO. 42 II FILTER NO. 4  
IRRADIANCE (WATTS/SQ.M. MICRO M.)

ALTITUDE (METERS)	DOWN- WELLING	UP- WELLING	ALBEDO	SCALAR DOWNWELLING	SCALAR UPWELLING	SCALAR TOTAL	SCALAR ALBEDO
332							
594							
921							
1236							
1529							
1831							

FLIGHT NO. 42 II FILTER NO. 5  
IRRADIANCE (WATTS/SQ.M. MICRO M.)

ALTITUDE (METERS)	DOWN- WELLING	UP- WELLING	ALBEDO	SCALAR DOWNWELLING	SCALAR UPWELLING	SCALAR TOTAL	SCALAR ALBEDO
332	9.046E-05	8.920E-06	.099	1.747E-04	2.313E-05	1.978E-04	.132
605	5.216E-05	8.440E-06	.108	1.703E-04	2.435E-05	1.946E-04	.143
912	4.638E-05	1.123E-05	.254	1.060E-04	7.037E-05	1.364E-04	.286
1237	9.311E-05	1.467E-05	.135	1.711E-04	3.400E-05	2.251E-04	.178
1530	1.324E-04	1.179E-05	.088	2.647E-04	3.186E-05	2.968E-04	.120
1832	1.634E-04	1.602E-05	.095	3.075E-04	4.054E-05	4.081E-04	.110

FLIGHT NO. 82 II  
AZIMUTH OF PATH OF SIGHT = 0  
DIRECTIONAL REFLECTANCE OF BACKGROUND

ZENITH ANGLE	FILTERS				
	1	2	5	3	4
93	.43339	.74216	.32070	.66526	
95	.20871	.39534	.18790	.46956	
100	.11694	.28303	.15859	.16188	
105	.10300	.24070	.12665	.13676	
120	.07847	.14301	.09017	.11544	
150	.04979	.13701	.08942	.13022	
180	.12847	.12941	.06594	.10770	

FLIGHT NO. 82 II  
AZIMUTH OF PATH OF SIGHT = 90  
DIRECTIONAL REFLECTANCE OF BACKGROUND

ZENITH ANGLE	FILTERS				
	1	2	5	3	4
93	.56597	1.16664	.61488	1.56846	
95	.28193	.51550	.32304	2.30101	
100	.12893	.27337	.14001	.21015	
105	.11844	.24587	.11920	.14126	
120	.08092	.15113	.10322	.12137	
150	.06490	.13635	.07597	.09526	
180	.12847	.12941	.06594	.10770	

FLIGHT NO. 82 II  
AZIMUTH OF PATH OF SIGHT = 180  
DIRECTIONAL REFLECTANCE OF BACKGROUND

ZENITH ANGLE	FILTERS				
	1	2	5	3	4
93	.57767	1.21153	.63432	1.77753	
95	.18547	.44970	.30215	.61315	
100	.10780	.25626	.12896	.17460	
105	.08175	.22246	.11954	.13355	
120	.06123	.19551	.11240	.12948	
150	.05351	.14564	.08373	.12041	
180	.12847	.12941	.06594	.10770	

FLIGHT NO. 82 II  
AZIMUTH OF PATH OF SIGHT = 270  
DIRECTIONAL REFLECTANCE OF BACKGROUND

ZENITH ANGLE	FILTERS				
	1	2	5	3	4
93	.51198	.54898	.29033	.69929	
95	.17374	.30835	.15812	.26609	
100	.05362	.22098	.12264	.14102	
105	.07417	.19534	.11833	.15783	
120	.06771	.17501	.10492	.11859	
150	.05570	.13810	.08236	.11349	
180	.12847	.12941	.06594	.10770	

DATE 9156Z FLIGHT NO. 82 11 GROUND LEVEL ALTITUDE (M.) 223 102-1

ALTITUDE (METERS)	FILTERS	TOTAL SCATTERING COEFFICIENT (PER METER)				
	1	2	3	4	5	
0	2.555E-04	1.894E-04	1.224E-04	1.067E-04	1.993E-04	
30	2.547E-04	1.884E-04	1.220E-04	1.059E-04	1.991E-04	
61	2.538E-04	1.874E-04	1.216E-04	1.055E-04	1.985E-04	
91	2.529E-04	1.874E-04	1.212E-04	1.052E-04	1.978E-04	
122	2.521E-04	1.869E-04	1.208E-04	1.048E-04	1.971E-04	
152	2.513E-04	1.863E-04	1.204E-04	1.045E-04	1.965E-04	
183	2.504E-04	1.857E-04	1.200E-04	1.041E-04	1.958E-04	
213	2.496E-04	1.850E-04	1.196E-04	1.038E-04	1.952E-04	
244	2.488E-04	1.844E-04	1.192E-04	1.034E-04	1.945E-04	
274	2.480E-04	1.837E-04	1.188E-04	1.031E-04	1.939E-04	
305	2.471E-04	1.833E-04	1.184E-04	1.028E-04	1.932E-04	
335	2.463E-04	1.826E-04	1.180E-04	1.024E-04	1.926E-04	
366	2.342E-04	1.794E-04	1.141E-04	1.029E-04	1.920E-04	
396	2.266E-04	1.819E-04	1.115E-04	1.007E-04	1.883E-04	
427	2.235E-04	1.817E-04	1.120E-04	1.011E-04	1.853E-04	
457	2.157E-04	1.823E-04	1.118E-04	1.003E-04	1.822E-04	
488	2.057E-04	1.848E-04	1.130E-04	9.431E-05	1.734E-04	
518	1.995E-04	1.865E-04	1.138E-04	9.743E-05	1.692E-04	
549	1.979E-04	1.933E-04	1.143E-04	8.906E-05	1.687E-04	
579	1.959E-04	1.972E-04	1.163E-04	8.777E-05	1.650E-04	
610	1.958E-04	1.881E-04	1.121E-04	8.829E-05	1.650E-04	
640	1.977E-04	1.785E-04	1.115E-04	9.119E-05	1.579E-04	
671	1.990E-04	1.777E-04	1.080E-04	9.137E-05	1.673E-04	
701	2.021E-04	1.759E-04	1.064E-04	9.123E-05	1.672E-04	
732	2.022E-04	1.737E-04	1.061E-04	9.123E-05	1.662E-04	
762	2.016E-04	1.631E-04	1.057E-04	9.030E-05	1.654E-04	
792	1.993E-04	1.553E-04	1.013E-04	8.830E-05	1.655E-04	
823	1.948E-04	1.539E-04	9.802E-05	8.604E-05	1.649E-04	
853	1.931E-04	1.549E-04	9.802E-05	8.543E-05	1.618E-04	
884	1.908E-04	1.571E-04	9.856E-05	8.283E-05	1.599E-04	
914	1.896E-04	1.570E-04	9.903E-05	8.086E-05	1.560E-04	
945	1.837E-04	1.569E-04	9.842E-05	7.923E-05	1.527E-04	
975	1.805E-04	1.611E-04	9.920E-05	7.795E-05	1.519E-04	
1006	1.774E-04	1.566E-04	1.001E-04	7.603E-05	1.467E-04	
1036	1.770E-04	1.512E-04	9.944E-05	7.500E-05	1.447E-04	
1067	1.739E-04	1.452E-04	9.603E-05	7.325E-05	1.431E-04	
1097	1.722E-04	1.419E-04	9.343E-05	7.111E-05	1.399E-04	
1128	1.704E-04	1.369E-04	9.122E-05	6.954E-05	1.370E-04	
1158	1.665E-04	1.230E-04	8.953E-05	6.847E-05	1.361E-04	
1189	1.673E-04	1.261E-04	8.729E-05	6.593E-05	1.337E-04	
1219	1.667E-04	1.210E-04	8.540E-05	6.442E-05	1.312E-04	
1250	1.634E-04	1.166E-04	8.456E-05	6.360E-05	1.299E-04	
1280	1.591E-04	1.117E-04	8.376E-05	6.290E-05	1.288E-04	
1311	1.561E-04	1.095E-04	8.224E-05	6.222E-05	1.273E-04	
1341	1.559E-04	1.079E-04	8.070E-05	6.067E-05	1.259E-04	
1372	1.530E-04	1.085E-04	8.052E-05	6.025E-05	1.243E-04	
1402	1.559E-04	1.075E-04	8.022E-05	5.962E-05	1.270E-04	
1433	1.522E-04	1.064E-04	8.009E-05	5.963E-05	1.262E-04	
1463	1.497E-04	1.059E-04	7.951E-05	5.900E-05	1.248E-04	
1494	1.486E-04	1.047E-04	7.916E-05	5.880E-05	1.237E-04	
1524	1.491E-04	1.022E-04	7.834E-05	5.819E-05	1.222E-04	
1554	1.473E-04	1.009E-04	7.436E-05	5.649E-05	1.244E-04	
1585	1.471E-04	9.710E-05	7.417E-05	5.431E-05	1.201E-04	
1615	1.453E-04	9.354E-05	7.234E-05	5.489E-05	1.145E-04	
1646	1.413E-04	9.273E-05	7.097E-05	5.512E-05	1.124E-04	
1676	1.333E-04	7.357E-05	7.016E-05	5.433E-05	1.112E-04	
1707	1.313E-04	6.394E-05	6.974E-05	5.331E-05	1.103E-04	
1737	1.317E-04	6.498E-05	6.794E-05	5.144E-05	1.101E-04	
1768	1.312E-04	6.555E-05	6.732E-05	5.320E-05	1.092E-04	
1798	1.305E-04	6.428E-05	7.004E-05	5.293E-05	1.085E-04	
1829	1.293E-04	6.305E-05	6.981E-05	5.231E-05	1.082E-04	

FIRST DATA ALT. 11 12 12 12 12

LAST DATA ALT. 31 31 31 31 31

		FLIGHT NO. 82 II		FILTER NO. 1				
		BEAM TRANSMITTANCE FROM GROUND TO ALTITUDE		ZENITH ANGLE OF PATH OF SIGHT (DEGREES)				
ALTITUDE	METERS	93	95	100	105	120	150	180
305		.2284094	.4152668	.6433312	.7438305	.8579659	.9153536	.9262645
610		.0623783	.1949400	.4401435	.5766051	.7520065	.8482747	.8671831
914		.0185829	.0977741	.3113030	.4570503	.6667828	.7913659	.8165677
1219		.0061671	.0530282	.2289905	.3719508	.5993313	.7441080	.7741649
1524		.0022380	.0307818	.1742850	.3097008	.5451203	.7044721	.7383226

		FLIGHT NO. 82 II		FILTER NO. 2				
		BEAM TRANSMITTANCE FROM GROUND TO ALTITUDE		ZENITH ANGLE OF PATH OF SIGHT (DEGREES)				
ALTITUDE	METERS	93	95	100	105	120	150	180
305		.3346653	.5212710	.7210932	.8030135	.8926494	.9365385	.9448013
610		.1102467	.2723603	.5205867	.6453393	.7971482	.8773110	.8928316
914		.0398208	.1522530	.3887959	.5305594	.7202974	.8274360	.8487034
1219		.0159900	.0917477	.3015201	.4473632	.6594796	.7863155	.8120527
1524		.0077692	.0626304	.2489399	.3933913	.6169725	.7566759	.7854760

		FLIGHT NO. 82 II		FILTER NO. 3				
		BEAM TRANSMITTANCE FROM GROUND TO ALTITUDE		ZENITH ANGLE OF PATH OF SIGHT (DEGREES)				
ALTITUDE	METERS	93	95	100	105	120	150	180
305		.4929703	.6564124	.8095417	.8678315	.9292484	.9585194	.9639753
610		.2437267	.4402224	.6624536	.7585928	.8667382	.9207455	.9309878
914		.1314613	.3058876	.5518212	.6710673	.8134437	.8876210	.9019112
1219		.0725139	.2196631	.4673275	.6002618	.7678223	.8585295	.8762547
1524		.0427677	.1653653	.4052560	.5455266	.7307451	.8343441	.8548363

		FLIGHT NO. 82 II		FILTER NO. 4				
		BEAM TRANSMITTANCE FROM GROUND TO ALTITUDE		ZENITH ANGLE OF PATH OF SIGHT (DEGREES)				
ALTITUDE	METERS	93	95	100	105	120	150	180
305		.5411923	.6939041	.8324279	.8842164	.9382891	.9638924	.9686532
610		.3036113	.4952396	.7027888	.7892797	.8847138	.9317225	.9405923
914		.1768357	.3637793	.6019774	.7114016	.8383956	.9032402	.9156395
1219		.1114655	.2618877	.5296487	.6521547	.8019402	.8803520	.8955112
1524		.0747243	.2278948	.4760368	.6077444	.7727619	.8617140	.8790688

		FLIGHT NO. 82 II		FILTER NO. 5				
		BEAM TRANSMITTANCE FROM GROUND TO ALTITUDE		ZENITH ANGLE OF PATH OF SIGHT (DEGREES)				
ALTITUDE	METERS	93	95	100	105	120	150	180
305		.3151721	.5029812	.7082614	.7934131	.8871091	.9331781	.9418647
610		.1074079	.2664105	.5167837	.6421725	.7951209	.8760221	.8916955
914		.0391608	.1509121	.3870735	.5289813	.7191876	.8266997	.8480493
1219		.0158977	.0915463	.3011877	.4470322	.6591770	.7861416	.8118972
1524		.0069904	.0588920	.2413677	.3853221	.6103890	.7520037	.7812740

AZIMUTH OF PATH OF SIGHT = 0  
 FLIGHT NO. 82 II FILTER NO. 1  
 PATH RADIANCE FROM GROUND TO ALTITUDE (WATTS/STER.SQ.M MICRO M.)  
 ALTITUDE ZENITH ANGLE OF PATH OF SIGHT (DEGREES)  
 METERS 93 95 100 105 120 150 180

305	2.368E-05	1.630E-05	8.275E-06	5.061E-06	1.747E-06	5.754E-07	4.348E-07
610	2.889E-05	2.279E-05	1.323E-05	8.471E-06	3.098E-06	1.049E-06	8.025E-07
914	3.901E-05	3.103E-05	1.890E-05	1.232E-05	4.631E-06	1.587E-06	1.228E-06
1219	4.880E-05	3.958E-05	2.486E-05	1.644E-05	6.309E-06	2.194E-06	1.723E-06
1524	4.615E-05	4.043E-05	2.744E-05	1.871E-05	7.479E-06	2.680E-06	2.134E-06

FLIGHT NO. 82 II FILTER NO. 2  
 PATH RADIANCE FROM GROUND TO ALTITUDE (WATTS/STER.SQ.M MICRO M.)  
 ALTITUDE ZENITH ANGLE OF PATH OF SIGHT (DEGREES)  
 METERS 93 95 100 105 120 150 180

305	9.680E-06	6.409E-06	3.331E-06	2.106E-06	8.438E-07	3.505E-07	2.847E-07
610	1.522E-05	1.127E-05	6.436E-06	4.192E-06	1.719E-06	7.060E-07	5.696E-07
914	2.021E-05	1.578E-05	9.542E-06	6.328E-06	2.634E-06	1.067E-06	8.540E-07
1219	2.492E-05	1.998E-05	1.250E-05	8.395E-06	3.537E-06	1.429E-06	1.145E-06
1524	3.008E-05	2.416E-05	1.528E-05	1.031E-05	4.352E-06	1.754E-06	1.413E-06

FLIGHT NO. 82 II FILTER NO. 3  
 PATH RADIANCE FROM GROUND TO ALTITUDE (WATTS/STER.SQ.M MICRO M.)  
 ALTITUDE ZENITH ANGLE OF PATH OF SIGHT (DEGREES)  
 METERS 93 95 100 105 120 150 180

305	1.059E-05	6.372E-06	3.066E-06	1.831E-06	6.699E-07	2.529E-07	1.997E-07
610	1.694E-05	1.131E-05	5.838E-06	3.564E-06	1.323E-06	4.947E-07	3.893E-07
914	1.850E-05	1.370E-05	7.657E-06	4.814E-06	1.838E-06	6.912E-07	5.442E-07
1219	1.903E-05	1.504E-05	8.954E-06	5.788E-06	2.289E-06	8.813E-07	6.986E-07
1524	2.790E-05	2.089E-05	1.208E-05	7.740E-06	3.023E-06	1.152E-06	9.190E-07

FLIGHT NO. 82 II FILTER NO. 4  
 PATH RADIANCE FROM GROUND TO ALTITUDE (WATTS/STER.SQ.M MICRO M.)  
 ALTITUDE ZENITH ANGLE OF PATH OF SIGHT (DEGREES)  
 METERS 93 95 100 105 120 150 180

305							
610							
914							
1219							
1524							

FLIGHT NO. 82 II FILTER NO. 5  
 PATH RADIANCE FROM GROUND TO ALTITUDE (WATTS/STER.SQ.M MICRO M.)  
 ALTITUDE ZENITH ANGLE OF PATH OF SIGHT (DEGREES)  
 METERS 93 95 100 105 120 150 180

305	1.746E-05	1.149E-05	5.727E-06	3.491E-06	1.267E-06	4.824E-07	3.944E-07
610	2.326E-05	1.746E-05	9.768E-06	6.188E-06	2.341E-06	8.964E-07	7.293E-07
914	2.105E-05	1.816E-05	1.158E-05	7.719E-06	3.121E-06	1.233E-06	9.970E-07
1219	2.727E-05	1.946E-05	1.311E-05	9.068E-06	3.860E-06	1.569E-06	1.262E-06
1524	3.051E-05	2.501E-05	1.649E-05	1.133E-05	4.850E-06	1.970E-06	1.585E-06

AZIMUTH OF PATH OF SIGHT = 00

FLIGHT NO. 82 II

FILTER NO. 1

PATH RADIANCE FROM GROUND TO ALTITUDE(WATTS/STER.SQ.M MICRO M.)

ALTITUDE METERS	93	95	100	105	120	150	180
305	9.143E-06	6.544E-06	3.729E-06	2.505E-06	1.154E-06	5.470E-07	4.348E-07
610	1.130E-05	9.279E-06	5.988E-06	4.229E-06	2.052E-06	9.966E-07	8.025E-07
914	1.416E-05	1.205E-05	8.272E-06	6.042E-06	3.059E-06	1.514E-06	1.228E-06
1219	1.660E-05	1.454E-05	1.044E-05	7.833E-06	4.121E-06	2.100E-06	1.723E-06
1524	1.639E-05	1.516E-05	1.159E-05	8.963E-06	4.896E-06	2.569E-06	2.134E-06

FLIGHT NO. 82 II

FILTER NO. 2

PATH RADIANCE FROM GROUND TO ALTITUDE(WATTS/STER.SQ.M MICRO M.)

ALTITUDE METERS	93	95	100	105	120	150	180
305	6.871E-06	4.643E-06	2.549E-06	1.689E-06	7.583E-07	3.478E-07	2.847E-07
610	9.453E-06	7.368E-06	4.536E-06	3.139E-06	1.473E-06	6.926E-07	5.696E-07
914	1.101E-05	9.241E-06	6.159E-06	4.419E-06	2.173E-06	1.040E-06	8.540E-07
1219	1.227E-05	1.069E-05	7.524E-06	5.553E-06	2.841E-06	1.394E-06	1.145E-06
1524	1.349E-05	1.192E-05	8.623E-06	6.474E-06	3.397E-06	1.707E-06	1.413E-06

FLIGHT NO. 82 II

FILTER NO. 3

PATH RADIANCE FROM GROUND TO ALTITUDE(WATTS/STER.SQ.M MICRO M.)

ALTITUDE METERS	93	95	100	105	120	150	180
305	5.863E-06	3.698E-06	1.934E-06	1.264E-06	5.606E-07	2.532E-07	1.997E-07
610	8.600E-06	6.103E-06	3.468E-06	2.334E-06	1.068E-06	4.899E-07	3.893E-07
914	9.780E-06	7.554E-06	4.606E-06	3.178E-06	1.486E-06	.823E-07	5.442E-07
1219	1.051E-05	8.525E-06	5.526E-06	3.898E-06	1.867E-06	8.701E-07	6.986E-07
1524	1.261E-05	1.033E-05	6.743E-06	4.819E-06	2.358E-06	1.130E-06	9.190E-07

FLIGHT NO. 82 II

FILTER NO. 4

PATH RADIANCE FROM GROUND TO ALTITUDE(WATTS/STER.SQ.M MICRO M.)

ALTITUDE METERS	93	95	100	105	120	150	180
305							
610							
914							
1219							
1524							

FLIGHT NO. 82 II

FILTER NO. 5

PATH RADIANCE FROM GROUND TO ALTITUDE(WATTS/STER.SQ.M MICRO M.)

ALTITUDE METERS	93	95	100	105	120	150	180
305	6.354E-06	5.622E-06	3.153E-06	2.107E-06	9.758E-07	4.758E-07	3.944E-07
610	1.048E-05	8.292E-06	5.172E-06	3.618E-06	1.760E-06	8.775E-07	7.298E-07
914	1.059E-05	9.314E-06	6.404E-06	4.604E-06	2.371E-06	1.198E-06	9.970E-07
1219	1.154E-05	1.033E-05	7.496E-06	5.620E-06	2.967E-06	1.520E-06	1.262E-06
1524	1.335E-05	1.189E-05	8.802E-06	6.715E-06	3.647E-06	1.904E-06	1.585E-06

AZIMUTH OF PATH OF SIGHT = 100  
 FLIGHT NO. 82 II FILTER NO. 1  
 PATH RADIANCE FROM GROUND TO ALTITUDE (WATTS/STER.SQ.M MICRO M.)  
 ZENITH ANGLE OF PATH OF SIGHT (DEGREES)

ALTITUDE METERS	93	95	100	105	120	150	180
305	9.279E-06	6.696E-06	3.902E-06	2.678E-06	1.299E-06	5.822E-07	4.348E-07
610	1.165E-05	9.620E-06	6.345E-06	4.575E-06	2.310E-06	1.078E-06	8.025E-07
914	1.407E-05	1.222E-05	8.688E-06	6.315E-06	3.511E-06	1.670E-06	1.228E-06
1219	1.675E-05	1.490E-05	1.115E-05	8.51E-06	5.001E-06	2.385E-06	1.723E-06
1524	1.710E-05	1.597E-05	1.271E-05	9.018E-06	6.109E-06	2.977E-06	2.134E-06

FLIGHT NO. 82 II FILTER NO. 2  
 PATH RADIANCE FROM GROUND TO ALTITUDE (WATTS/STER.SQ.M MICRO M.)  
 ZENITH ANGLE OF PATH OF SIGHT (DEGREES)

ALTITUDE METERS	93	95	100	105	120	150	180
305	7.25E-06	4.617E-06	2.544E-06	1.695E-06	7.803E-07	3.626E-07	2.847E-07
610	7.421E-06	7.359E-06	4.561E-06	3.183E-06	1.553E-06	7.279E-07	5.696E-07
914	1.083E-05	9.153E-06	6.177E-06	4.478E-06	2.277E-06	1.097E-06	8.540E-07
1219	1.225E-05	1.071E-05	7.648E-06	5.720E-06	3.078E-06	1.486E-06	1.145E-06
1524	1.391E-05	1.220E-05	9.020E-06	6.886E-06	3.844E-06	1.862E-06	1.413E-06

FLIGHT NO. 82 II FILTER NO. 3  
 PATH RADIANCE FROM GROUND TO ALTITUDE (WATTS/STER.SQ.M MICRO M.)  
 ZENITH ANGLE OF PATH OF SIGHT (DEGREES)

ALTITUDE METERS	93	95	100	105	120	150	180
305	5.598E-06	3.547E-06	1.886E-06	1.250E-06	5.857E-07	2.629E-07	1.997E-07
610	8.285E-06	5.906E-06	3.416E-06	2.337E-06	1.137E-06	5.154E-07	3.893E-07
914	9.417E-06	7.327E-06	4.538E-06	3.184E-06	1.587E-06	7.236E-07	5.442E-07
1219	1.021E-05	8.375E-06	5.474E-06	3.929E-06	2.011E-06	9.276E-07	6.986E-07
1524	1.235E-05	1.022E-05	6.851E-06	5.018E-06	2.683E-06	1.242E-06	9.190E-07

FLIGHT NO. 82 II FILTER NO. 4  
 PATH RADIANCE FROM GROUND TO ALTITUDE (WATTS/STER.SQ.M MICRO M.)  
 ZENITH ANGLE OF PATH OF SIGHT (DEGREES)

ALTITUDE METERS	93	95	100	105	120	150	180
305							
610							
914							
1219							
1524							

FLIGHT NO. 82 II FILTER NO. 5  
 PATH RADIANCE FROM GROUND TO ALTITUDE (WATTS/STER.SQ.M MICRO M.)  
 ZENITH ANGLE OF PATH OF SIGHT (DEGREES)

ALTITUDE METERS	93	95	100	105	120	150	180
305	6.227E-06	5.662E-06	3.203E-06	2.199E-06	1.113E-06	5.348E-07	3.944E-07
610	1.351E-05	8.364E-06	5.330E-06	3.825E-06	2.024E-06	9.848E-07	7.298E-07
914	1.571E-05	9.333E-06	6.582E-06	4.893E-06	2.673E-06	1.322E-06	9.970E-07
1219	1.600E-05	1.043E-05	7.707E-06	5.997E-06	3.322E-06	1.660E-06	1.267E-06
1524	1.700E-05	1.224E-05	9.253E-06	7.211E-06	4.215E-06	2.103E-06	1.585E-06



FLIGHT NO. 82 II

FILTER NO. 1

ALTITUDE METERS	93	95	100	105	120	150	180
305	9.201E-06	6.563E-06	3.710E-06	2.471E-06	1.113E-06	5.248E-07	4.348E-07
610	1.168E-05	9.514E-06	6.076E-06	4.249E-06	2.016E-06	9.698E-07	8.075E-07
914	1.382E-05	1.189E-05	8.197E-06	5.956E-06	2.971E-06	1.478E-06	1.228E-06
1219	1.581E-05	1.399E-05	1.015E-05	7.604E-06	3.975E-06	2.059E-06	1.723E-06
1524	1.593E-05	1.475E-05	1.134E-05	8.749E-06	4.762E-06	2.538E-06	2.134E-06

FLIGHT NO. 82 II

FILTER NO. 2

ALTITUDE METERS	93	95	100	105	120	150	180
305	7.189E-06	4.830E-06	2.615E-06	1.712E-06	7.551E-07	3.477E-07	2.847E-07
610	1.255E-05	9.374E-06	5.524E-06	3.714E-06	1.638E-06	7.152E-07	5.696E-07
914	1.418E-05	1.161E-05	7.665E-06	5.350E-06	2.444E-06	1.074E-06	8.540E-07
1219	1.370E-05	1.230E-05	8.638E-06	6.323E-06	3.062E-06	1.416E-06	1.145E-06
1524	1.442E-05	1.312E-05	9.648E-06	7.182E-06	3.615E-06	1.737E-06	1.413E-06

FLIGHT NO. 82 II

FILTER NO. 3

ALTITUDE METERS	93	95	100	105	120	150	180
305	5.671E-06	3.525E-06	1.838E-06	1.187E-06	5.122E-07	2.404E-07	1.997E-07
610	8.763E-06	6.143E-06	3.437E-06	2.283E-06	1.022E-06	4.735E-07	3.893E-07
914	1.003E-05	7.725E-06	4.636E-06	3.160E-06	1.448E-06	6.689E-07	5.442E-07
1219	1.092E-05	8.847E-06	5.505E-06	3.908E-06	1.837E-06	8.590E-07	6.986E-07
1524	1.267E-05	1.041E-05	6.776E-06	4.803E-06	2.324E-06	1.122E-06	9.190E-07

FLIGHT NO. 82 II

FILTER NO. 4

ALTITUDE METERS	93	95	100	105	120	150	180
305							
610							
914							
1219							
1524							

FLIGHT NO. 82 II

FILTER NO. 5

ALTITUDE METERS	93	95	100	105	120	150	180
305	5.531E-06	5.797E-06	3.130E-06	2.109E-06	9.690E-07	4.764E-07	3.944E-07
610	1.100E-05	4.636E-06	5.329E-06	3.696E-06	1.775E-06	8.835E-07	7.298E-07
914	1.142E-05	9.860E-06	6.669E-06	4.820E-06	2.405E-06	1.210E-06	9.970E-07
1219	1.209E-05	1.060E-05	7.74E-06	5.757E-06	2.975E-06	1.525E-06	1.262E-06
1524	1.354E-05	1.214E-05	3.774E-06	6.790E-06	3.61E-06	1.900E-06	1.585E-06

FLIGHT NO. 12 II      FILT NO. 1									
DIRECTIONAL PATH REFLECTANCE FROM GROUND TO ALTITUDE									
ALTITUDE	ZENITH ANGLE OF PATH OF SIGHT (DEGREES)								
METERS	33	45	60	75	90	105	120	135	150
305	4.447E-02	1.646E-01	5.393E-01	2.852E-01	4.536E-02	2.636E-02	1.468E-02		
610	1.249E-01	4.901E-02	1.200E-02	6.159E-01	1.727E-01	5.187E-02	3.880E-02		
914	1.101E-01	1.331E-01	2.445E-02	1.13E-02	1.912E-01	8.406E-02	6.305E-02		
1219	3.220E-01	3.129E-01	4.552E-02	1.3E-02	4.413E-01	1.236E-01	9.331E-02		
1524	3.440E-02	5.5E-02	3.600E-02	2.532E-02	3.752E-01	1.595E-01	1.212E-01		

FLIGHT NO. 12 II      FILT NO. 2									
DIRECTIONAL PATH REFLECTANCE FROM GROUND TO ALTITUDE									
ALTITUDE	ZENITH ANGLE OF PATH OF SIGHT (DEGREES)								
METERS	33	45	60	75	90	105	120	135	150
305	1.454E-02	7.679E-01	2.300E-01	1.681E-01	5.057E-02	2.394E-02	1.931E-02		
610	2.645E-02	2.652E-02	7.923E-01	4.163E-01	1.361E-01	5.157E-02	4.088E-02		
914	3.252E-01	6.642E-02	1.571E-02	7.642E-01	2.342E-01	8.265E-02	6.448E-02		
1219	9.483E-02	1.39E-01	2.656E-02	1.203E-02	3.437E-01	1.165E-01	9.035E-02		
1524	2.421E-02	2.472E-01	3.932E-02	1.679E-02	4.520E-01	1.486E-01	1.153E-01		

FLIGHT NO. 12 II      FILT NO. 3									
DIRECTIONAL PATH REFLECTANCE FROM GROUND TO ALTITUDE									
ALTITUDE	ZENITH ANGLE OF PATH OF SIGHT (DEGREES)								
METERS	33	45	60	75	90	105	120	135	150
305	1.100E-02	1.245E-01	2.047E-01	1.144E-01	3.895E-02	1.426E-02	1.119E-02		
610	3.579E-02	1.38E-02	4.751E-01	2.538E-01	8.245E-02	2.903E-02	2.299E-02		
914	7.002E-02	2.420E-02	7.497E-01	3.876E-01	1.721E-01	4.207E-02	3.260E-02		
1219	1.415E-01	2.699E-02	1.025E-02	5.210E-01	1.611E-01	5.546E-02	4.307E-02		
1524	3.220E-01	6.825E-02	1.610E-02	7.665E-01	2.255E-01	7.457E-02	5.808E-02		

FLIGHT NO. 12 II      FILT NO. 4									
DIRECTIONAL PATH REFLECTANCE FROM GROUND TO ALTITUDE									
ALTITUDE	ZENITH ANGLE OF PATH OF SIGHT (DEGREES)								
METERS	33	45	60	75	90	105	120	135	150
305									
610									
914									
1219									
1524									

FLIGHT NO. 12 II      FILT NO. 5									
DIRECTIONAL PATH REFLECTANCE FROM GROUND TO ALTITUDE									
ALTITUDE	ZENITH ANGLE OF PATH OF SIGHT (DEGREES)								
METERS	33	45	60	75	90	105	120	135	150
305	1.224E-02	7.935E-01	2.403E-01	1.528E-01	4.960E-02	1.795E-02	1.454E-02		
610	7.521E-02	2.260E-02	6.554E-01	3.446E-01	1.723E-01	3.553E-02	2.842E-02		
914	1.667E-01	4.180E-02	1.039E-02	5.667E-01	1.507E-01	5.178E-02	4.083E-02		
1219	4.864E-01	7.382E-02	1.517E-02	7.045E-01	2.033E-01	6.932E-02	5.400E-02		
1524	1.51E-02	1.375E-01	2.373E-02	1.021E-02	2.760E-01	9.100E-02	7.044E-02		

AZIMUTH OF PATH OF SIGHT = 90  
 FLIGHT NO. 82 II      FILTER NO. 1  
 DIRECTIONAL PATH REFLECTANCE FROM GROUND TO ALTITUDE  
 ZENITH ANGLE OF PATH OF SIGHT (DEGREES)

ALTITUDE METERS	93	95	100	105	120	150	180
305	1.678E-00	6.607E-01	2.430E-01	1.412E-01	5.641E-02	2.505E-02	1.968E-02
610	7.593E-00	1.996E-00	5.704E-01	3.075E-01	1.144E-01	4.926E-02	3.880E-02
914	3.195E-01	5.167E-00	1.114E-00	5.543E-01	1.923E-01	8.023E-02	3.305E-02
1219	1.122E-01	1.149E-01	1.911E-00	8.829E-01	2.883E-01	1.183E-01	9.331E-02
1524	3.070E-02	2.065E-01	2.783E-00	1.213E-00	3.766E-01	1.529E-01	1.121E-01

FLIGHT NO. 82 II      FILTER NO. 2  
 DIRECTIONAL PATH REFLECTANCE FROM GROUND TO ALTITUDE  
 ZENITH ANGLE OF PATH OF SIGHT (DEGREES)

ALTITUDE METERS	93	95	100	105	120	150	180
305	1.315E-00	5.707E-01	2.266E-01	1.348E-01	5.443E-02	2.380E-02	1.931E-02
610	5.494E-00	1.734E-00	5.583E-01	3.117E-01	1.184E-01	5.044E-02	4.088E-02
914	1.772E-01	3.890E-00	1.015E-00	5.337E-01	1.933E-01	8.051E-02	6.448E-02
1219	4.318E-01	7.470E-00	1.593E-00	7.994E-01	2.701E-01	1.136E-01	9.035E-02
1524	1.113E-02	1.219E-01	2.220E-00	1.055E-00	3.528E-01	1.446E-01	1.153E-01

FLIGHT NO. 82 II      FILTER NO. 3  
 DIRECTIONAL PATH REFLECTANCE FROM GROUND TO ALTITUDE  
 ZENITH ANGLE OF PATH OF SIGHT (DEGREES)

ALTITUDE METERS	93	95	100	105	120	150	180
305	6.429E-01	3.744E-01	1.292E-01	7.871E-02	3.260E-02	1.427E-02	1.119E-02
610	1.558E-00	7.490E-01	2.829E-01	1.662E-01	6.659E-02	2.875E-02	2.259E-02
914	4.019E-00	1.336E-00	4.509E-01	2.559E-01	9.867E-02	4.153E-02	3.260E-02
1219	7.329E-00	2.114E-00	6.388E-01	3.509E-01	1.313E-01	5.476E-02	4.307E-02
1524	1.593E-01	3.375E-00	8.996E-02	4.772E-01	1.743E-01	7.316E-02	5.808E-02

FLIGHT NO. 82 II      FILTER NO. 4  
 DIRECTIONAL PATH REFLECTANCE FROM GROUND TO ALTITUDE  
 ZENITH ANGLE OF PATH OF SIGHT (DEGREES)

ALTITUDE METERS	93	95	100	105	120	150	180
305							
610							
914							
1219							
1524							

FLIGHT NO. 82 II      FILTER NO. 5  
 DIRECTIONAL PATH REFLECTANCE FROM GROUND TO ALTITUDE  
 ZENITH ANGLE OF PATH OF SIGHT (DEGREES)

ALTITUDE METERS	93	95	100	105	120	150	180
305	9.216E-01	3.935E-01	1.546E-01	9.221E-02	3.820E-02	1.771E-02	1.454E-02
610	3.388E-00	1.073E-00	3.476E-01	1.957E-01	7.686E-02	3.479E-02	2.842E-02
914	9.482E-00	2.143E-00	5.746E-01	3.062E-01	1.145E-01	5.032E-02	4.083E-02
1219	2.522E-01	3.918E-00	8.643E-01	4.366E-01	1.563E-01	6.714E-02	5.400E-02
1524	6.638E-01	7.014E-00	1.266E-00	6.052E-01	2.075E-01	8.793E-02	7.044E-02

AZIMUTH OF PATH OF SIGHT = 100  
 FLIGHT NO. 82 II      FILTER NO. 1  
 DIRECTIONAL PATH REFLECTANCE FROM GROUND TO ALTITUDE  
 ALTITUDE      ZENITH ANGLE OF PATH OF SIGHT (DEGREES)  
 METERS      93      95      100      105      120      150      180

305	1.703E-00	6.76E-01	2.543E-01	1.509E-01	6.346E-02	2.666E-02	1.968E-02
610	7.833E-00	2.009E-00	6.044E-01	3.326E-01	1.310E-01	4.328E-02	4.880E-02
914	3.175E-01	5.239E-00	1.170E-00	5.476E-01	2.233E-01	8.849E-02	6.305E-02
1219	1.140E-02	1.178E-01	2.042E-00	9.751E-01	3.498E-01	1.344E-01	9.331E-02
1524	3.203E-02	2.175E-01	3.058E-00	1.376E-00	4.745E-01	1.771E-01	1.212E-01

FLIGHT NO. 82 II      FILTER NO. 2  
 DIRECTIONAL PATH REFLECTANCE FROM GROUND TO ALTITUDE  
 ALTITUDE      ZENITH ANGLE OF PATH OF SIGHT (DEGREES)  
 METERS      93      95      100      105      120      150      180

305	1.07E-00	5.676E-01	2.201E-01	1.353E-01	5.645E-02	2.481E-02	1.931E-02
610	1.476E-00	1.731E-00	5.614E-01	3.159E-01	1.249E-01	5.317E-02	4.088E-02
914	1.742E-01	3.842E-00	1.013E-00	5.438E-01	2.043E-01	8.492E-02	6.448E-02
1219	4.908E-01	7.431E-00	1.625E-00	3.193E-01	7.741E-01	1.211E-01	9.035E-02
1524	1.147E-02	1.256E-01	2.32E-00	1.122E-00	3.993E-01	1.577E-01	1.153E-01

FLIGHT NO. 82 II      FILTER NO. 3  
 DIRECTIONAL PATH REFLECTANCE FROM GROUND TO ALTITUDE  
 ALTITUDE      ZENITH ANGLE OF PATH OF SIGHT (DEGREES)  
 METERS      93      95      100      105      120      150      180

305	6.135E-01	2.913E-01	1.253E-01	7.779E-02	3.406E-02	1.482E-02	1.119E-02
610	1.800E-01	7.249E-01	2.790E-01	1.604E-01	7.096E-02	3.024E-02	2.259E-02
914	3.970E-00	1.293E-00	4.444E-01	2.564E-01	1.054E-01	4.404E-02	3.760E-02
1219	7.000E-00	2.000E-00	6.329E-01	3.536E-01	1.415E-01	5.838E-02	4.307E-02
1524	1.564E-02	3.339E-00	9.133E-01	4.909E-01	1.933E-01	6.042E-02	5.808E-02

FLIGHT NO. 82 II      FILTER NO. 4  
 DIRECTIONAL PATH REFLECTANCE FROM GROUND TO ALTITUDE  
 ALTITUDE      ZENITH ANGLE OF PATH OF SIGHT (DEGREES)  
 METERS      93      95      100      105      120      150      180

305							
610							
914							
1219							
1524							

FLIGHT NO. 82 II      FILTER NO. 5  
 DIRECTIONAL PATH REFLECTANCE FROM GROUND TO ALTITUDE  
 ALTITUDE      ZENITH ANGLE OF PATH OF SIGHT (DEGREES)  
 METERS      93      95      100      105      120      150      180

305	9.063E-01	3.909E-01	1.573E-01	9.625E-02	4.358E-02	1.990E-02	1.454E-02
610	3.395E-00	1.042E-00	3.586E-01	2.068E-01	8.839E-02	3.904E-02	2.842E-02
914	9.489E-00	2.159E-00	5.905E-01	3.212E-01	1.291E-01	5.555E-02	4.083E-02
1219	2.534E-01	3.955E-00	6.857E-01	4.574E-01	1.750E-01	7.331E-02	5.400E-02
1524	6.807E-01	7.213E-00	1.331E-00	6.499E-01	2.398E-01	9.711E-02	7.044E-02

AZIMUTH OF PATH OF SIGHT = 0°		FLIGHT NO. 12 II		FILTER NO. 1					
DIRECTIONAL PATH REFLECTANCE FROM GROUND TO ALTITUDE		ZENITH ANGLE OF PATH OF SIGHT (DEGREES)							
ALTITUDE METERS	93	95	100	105	120	150	180		
105	1.083E-01	0.676E-01	2.418E-01	1.392E-01	5.440E-02	2.404E-02	1.968E-02		
910	7.550E-02	2.045E-01	3.787E-01	3.089E-01	1.124E-01	4.111E-02	3.880E-02		
914	3.117E-01	2.099E-01	1.104E-00	5.464E-01	1.868E-01	7.821E-02	6.305E-02		
1219	1.075E-01	1.155E-01	1.058E-00	8.971E-01	2.781E-01	1.160E-01	9.331E-02		
1524	2.985E-01	2.009E-01	2.727E-00	1.164E-00	3.662E-01	1.510E-01	1.212E-01		

FLIGHT NO. 12 II		FILTER NO. 2							
DIRECTIONAL PATH REFLECTANCE FROM GROUND TO ALTITUDE		ZENITH ANGLE OF PATH OF SIGHT (DEGREES)							
ALTITUDE METERS	93	95	100	105	120	150	180		
105	1.377E-00	5.940E-01	2.324E-01	1.366E-01	5.421E-02	2.379E-02	1.931E-02		
910	7.315E-01	2.295E-00	6.799E-01	3.608E-01	1.317E-01	5.224E-02	4.088E-02		
914	2.242E-01	4.971E-00	1.263E-00	6.462E-01	2.174E-01	8.319E-02	6.448E-02		
1219	5.492E-01	9.088E-00	1.849E-00	3.058E-01	2.976E-01	1.156E-01	9.035E-02		
1524	1.190E-01	1.343E-01	2.433E-00	1.170E-00	3.754E-01	1.471E-01	1.153E-01		

FLIGHT NO. 12 II		FILTER NO. 3							
DIRECTIONAL PATH REFLECTANCE FROM GROUND TO ALTITUDE		ZENITH ANGLE OF PATH OF SIGHT (DEGREES)							
ALTITUDE METERS	93	95	100	105	120	150	180		
105	6.315E-01	2.925E-01	1.227E-01	7.389E-02	3.013E-02	1.355E-02	1.119E-02		
910	1.023E-00	7.539E-01	3.803E-01	1.626E-01	6.373E-02	2.778E-02	2.759E-02		
914	4.143E-00	1.364E-00	4.540E-01	2.545E-01	9.020E-02	4.072E-02	3.260E-02		
1219	2.139E-01	2.176E-00	6.490E-01	3.517E-01	1.273E-01	5.406E-02	4.307E-02		
1524	1.509E-01	3.402E-00	9.034E-01	4.757E-01	1.718E-01	7.267E-02	5.808E-02		

FLIGHT NO. 12 II		FILTER NO. 4							
DIRECTIONAL PATH REFLECTANCE FROM GROUND TO ALTITUDE		ZENITH ANGLE OF PATH OF SIGHT (DEGREES)							
ALTITUDE METERS	93	95	100	105	120	150	180		
105									
910									
914									
1219									
1524									

FLIGHT NO. 12 II		FILTER NO. 5							
DIRECTIONAL PATH REFLECTANCE FROM GROUND TO ALTITUDE		ZENITH ANGLE OF PATH OF SIGHT (DEGREES)							
ALTITUDE METERS	93	95	100	105	120	150	180		
105	9.441E-01	4.007E-01	1.559E-01	7.230E-02	3.793E-02	1.773E-02	1.454E-02		
910	3.555E-00	1.117E-00	3.581E-01	1.999E-01	7.751E-02	3.502E-02	2.842E-02		
914	1.313E-01	2.257E-02	3.091E-01	3.164E-01	1.161E-01	5.082E-02	4.083E-02		
1219	2.642E-01	4.077E-00	8.952E-01	4.473E-01	1.567E-01	6.736E-02	5.400E-02		
1524	6.729E-01	7.159E-00	1.291E-00	6.120E-01	2.059E-01	8.776E-02	7.044E-02		

#### FLIGHT 86

Moonlight. Data were gathered in the same general area as in Flight 82 II, approximately 34 km east of Khorat. The data-taking started at 2312 local time and continued until 0139. The vegetation consisted of forested areas of small deciduous trees and flooded rice paddies. The sky was clear except for high thin cirrus clouds. The moon phase angle was  $14^\circ$ ; the moon zenith angle ranged from  $23^\circ$  to  $5^\circ$  during sky radiance data-taking. The moon zenith angle was  $2^\circ$  at time of transit.

FLIGHT NO. 86 FILTER NO. 1  
IRRADIANCE(WATTS/SQ.M.MICRO M.)

ALTITUDE (METERS)	DOWN- WELLING	UP- WELLING	ALBEDO	SCALAR DOWNWELLING	SCALAR UPWELLING	SCALAR TOTAL	SCALAR ALBEDO
193	1.650E-03	3.177E-05	.019	2.232E-03	9.415E-05	2.326E-03	.042
485	6.851E-04	5.342E-05	.078	1.154E-03	1.555E-04	1.309E-03	.135
785	2.141E-03	6.633E-05	.031	2.605E-03	1.881E-04	2.793E-03	.072
1082	2.546E-03	9.515E-05	.037	2.949E-03	2.397E-04	3.188E-03	.081
1405	1.123E-03	9.111E-05	.081	1.486E-03	2.481E-04	1.735E-03	.167
1700	2.355E-03	1.119E-04	.046	2.767E-03	3.130E-04	3.020E-03	.116

FLIGHT NO. 86 FILTER NO. 2  
IRRADIANCE(WATTS/SQ.M.MICRO M.)

ALTITUDE (METERS)	DOWN- WELLING	UP- WELLING	ALBEDO	SCALAR DOWNWELLING	SCALAR UPWELLING	SCALAR TOTAL	SCALAR ALBEDO
191	1.886E-03	7.613E-05	.040	2.385E-03	1.640E-04	2.549E-03	.069
484	7.912E-04	9.154E-05	.116	1.183E-03	2.161E-04	1.399E-03	.183
785	2.046E-03	9.421E-05	.046	2.440E-03	2.332E-04	2.673E-03	.096
1082	2.053E-03	9.429E-05	.046	2.390E-03	2.369E-04	2.627E-03	.099
1408	7.320E-04	1.070E-04	.146	1.032E-03	2.671E-04	1.300E-03	.259
1702	1.728E-03	1.257E-04	.073	2.014E-03	3.007E-04	2.314E-03	.149

FLIGHT NO. 86 FILTER NO. 3  
IRRADIANCE(WATTS/SQ.M.MICRO M.)

ALTITUDE (METERS)	DOWN- WELLING	UP- WELLING	ALBEDO	SCALAR DOWNWELLING	SCALAR UPWELLING	SCALAR TOTAL	SCALAR ALBEDO
190	8.770E-04	6.516E-05	.072	1.174E-03	2.563E-04	1.430E-03	.218
484	1.327E-03	5.538E-05	.042	1.570E-03	1.330E-04	1.703E-03	.085
785	1.823E-03	9.247E-05	.051	2.055E-03	1.918E-04	2.247E-03	.093
1081	1.309E-03	1.775E-04	.136	1.489E-03	3.097E-04	1.798E-03	.208
1402	1.148E-03	2.009E-04	.175	1.309E-03	3.681E-04	1.677E-03	.281
1700	3.714E-03	1.528E-04	.041	3.885E-03	3.177E-04	4.203E-03	.082

FLIGHT NO. 86 FILTER NO. 4  
IRRADIANCE(WATTS/SQ.M.MICRO M.)

ALTITUDE (METERS)	DOWN- WELLING	UP- WELLING	ALBEDO	SCALAR DOWNWELLING	SCALAR UPWELLING	SCALAR TOTAL	SCALAR ALBEDO
173	1.600E-03	7.907E-04	.244	1.889E-03	7.591E-04	2.648E-03	.402
485	1.726E-03	3.547E-04	.206	1.942E-03	6.905E-04	2.632E-03	.356
785	1.635E-03	3.828E-04	.234	1.794E-03	7.286E-04	2.523E-03	.406
1082	2.146E-03	3.456E-04	.161	2.274E-03	6.630E-04	2.937E-03	.292
1401	7.022E-04	2.929E-04	.325	1.005E-03	7.369E-04	1.742E-03	.733
1704	3.064E-04	2.689E-04	.878	3.968E-04	5.476E-04	9.443E-04	1.380

FLIGHT NO. 86 FILTER NO. 5  
IRRADIANCE(WATTS/SQ.M.MICRO M.)

ALTITUDE (METERS)	DOWN- WELLING	UP- WELLING	ALBEDO	SCALAR DOWNWELLING	SCALAR UPWELLING	SCALAR TOTAL	SCALAR ALBEDO
173	1.029E-03	7.268E-05	.071	1.439E-03	1.575E-04	1.596E-03	.109
484	8.080E-04	1.042E-04	.129	1.184E-03	2.342E-04	1.418E-03	.198
785	1.114E-03	1.268E-04	.114	1.448E-03	2.726E-04	1.720E-03	.188
1082	1.081E-03	1.234E-04	.114	1.384E-03	2.868E-04	1.670E-03	.207
1703	7.107E-04	1.321E-04	.186	9.634E-04	3.218E-04	1.285E-03	.334

FLIGHT NO. 86					
AZIMUTH OF PATH OF SIGHT = 0					
DIRECTIONAL REFLECTANCE OF BACKGROUND					
ZENITH ANGLE	FILTERS				
	1	2	5	3	4
93	.08048	.05470	.21526	.15988	.18252
95	.05164	.03023	.11197	.08106	.16996
100	.03843	.02792	.08351	.06440	.16578
105	.02426	.03367	.06709	.05762	.20674
120	.02028	.03128	.04155	.05224	.22430
150	.01627	.04055	.09731	.07497	.16878
180	.01524	.03881	.06493	.08972	.27514

FLIGHT NO. 86					
AZIMUTH OF PATH OF SIGHT = 90					
DIRECTIONAL REFLECTANCE OF BACKGROUND					
ZENITH ANGLE	FILTERS				
	1	2	5	3	4
93	.07280	.05301	.12136	.28630	.18713
95	.04436	.03866	.09035	.10493	.19530
100	.03537	.02327	.07720	.07313	.19491
105	.02347	.03695	.07411	.06515	.21027
120	.01394	.03065	.04755	.05776	.22879
150	.01366	.03852	.08014	.06045	.19428
180	.01528	.03881	.06493	.08972	.27514

FLIGHT NO. 86					
AZIMUTH OF PATH OF SIGHT = 180					
DIRECTIONAL REFLECTANCE OF BACKGROUND					
ZENITH ANGLE	FILTERS				
	1	2	5	3	4
93	.08685	.09135	.11669	.13567	.24202
95	.05106	.05190	.10517	.07901	.23509
100	.03571	.04695	.09906	.07079	.25091
105	.03049	.04754	.08358	.07367	.24748
120	.02732	.05289	.07326	.06999	.25600
150	.02237	.04732	.09452	.06016	.26679
180	.01528	.03881	.06493	.08972	.27514

FLIGHT NO. 86					
AZIMUTH OF PATH OF SIGHT = 270					
DIRECTIONAL REFLECTANCE OF BACKGROUND					
ZENITH ANGLE	FILTERS				
	1	2	5	3	4
93	.08476	.09402	.13639	.25560	.19699
95	.04951	.04223	.09676	.11589	.19113
100	.03383	.04125	.08633	.07726	.22255
105	.02639	.04468	.06450	.07284	.23501
120	.02110	.04169	.05169	.07626	.26757
150	.01924	.04415	.07915	.06833	.18406
180	.01528	.03881	.06493	.08972	.27514



DATE 100768 FLIGHT NO. 86 GROUND LEVEL ALTITUDE ( M.)= 214 IUP=1

ALTITUDE (METERS)	TOTAL SCATTERING COEFFICIENT (PER METER)				
	FILTERS	1	2	3	4
0	4.041E-05	3.183E-05	1.764E-05	1.450E-05	4.189E-05
30	4.028E-05	3.172E-05	1.758E-05	1.445E-05	4.175E-05
61	4.014E-05	3.162E-05	1.752E-05	1.440E-05	4.161E-05
91	4.001E-05	3.151E-05	1.746E-05	1.435E-05	4.147E-05
122	3.988E-05	3.141E-05	1.741E-05	1.430E-05	4.134E-05
152	4.104E-05	3.215E-05	1.747E-05	1.446E-05	3.939E-05
183	3.966E-05	3.327E-05	1.737E-05	1.424E-05	3.809E-05
213	4.344E-05	3.269E-05	1.714E-05	1.413E-05	3.712E-05
244	4.192E-05	3.340E-05	1.666E-05	1.388E-05	3.637E-05
274	3.647E-05	3.091E-05	1.635E-05	1.380E-05	3.587E-05
305	3.345E-05	2.563E-05	1.631E-05	1.371E-05	3.568E-05
335	3.275E-05	2.475E-05	1.630E-05	1.366E-05	3.671E-05
366	3.207E-05	2.461E-05	1.626E-05	1.370E-05	3.669E-05
396	3.427E-05	2.432E-05	1.602E-05	1.367E-05	3.648E-05
427	3.306E-05	2.399E-05	1.610E-05	1.368E-05	3.587E-05
457	3.209E-05	2.365E-05	1.572E-05	1.355E-05	3.593E-05
488	3.159E-05	2.358E-05	1.534E-05	1.355E-05	3.535E-05
518	3.138E-05	2.355E-05	1.536E-05	1.356E-05	3.333E-05
549	3.114E-05	2.355E-05	1.527E-05	1.363E-05	3.236E-05
579	3.120E-05	2.331E-05	1.529E-05	1.351E-05	3.179E-05
610	3.114E-05	2.308E-05	1.522E-05	1.346E-05	3.185E-05
640	3.092E-05	2.287E-05	1.507E-05	1.353E-05	3.267E-05
671	3.086E-05	2.298E-05	1.514E-05	1.344E-05	3.294E-05
701	3.055E-05	2.299E-05	1.530E-05	1.348E-05	3.245E-05
732	3.026E-05	2.300E-05	1.518E-05	1.338E-05	3.215E-05
762	3.067E-05	2.302E-05	1.510E-05	1.331E-05	3.137E-05
792	3.020E-05	2.307E-05	1.493E-05	1.334E-05	3.110E-05
823	2.943E-05	2.299E-05	1.509E-05	1.335E-05	3.143E-05
853	2.917E-05	2.318E-05	1.503E-05	1.348E-05	3.191E-05
884	2.899E-05	2.308E-05	1.511E-05	1.356E-05	3.199E-05
914	2.898E-05	2.258E-05	1.506E-05	1.365E-05	3.348E-05
945	2.903E-05	2.261E-05	1.508E-05	1.364E-05	3.198E-05
975	2.929E-05	2.278E-05	1.497E-05	1.354E-05	3.063E-05
1006	3.016E-05	2.317E-05	1.492E-05	1.352E-05	3.077E-05
1036	3.110E-05	2.283E-05	1.488E-05	1.353E-05	3.069E-05
1067	3.120E-05	2.315E-05	1.512E-05	1.344E-05	3.069E-05
1097	3.117E-05	2.311E-05	1.524E-05	1.343E-05	3.027E-05
1128	3.144E-05	2.462E-05	1.503E-05	1.339E-05	3.005E-05
1158	3.331E-05	2.488E-05	1.484E-05	1.351E-05	2.925E-05
1189	3.320E-05	2.503E-05	1.492E-05	1.343E-05	2.956E-05
1219	3.237E-05	2.503E-05	1.523E-05	1.371E-05	3.128E-05
1250	3.299E-05	2.487E-05	1.479E-05	1.383E-05	3.206E-05
1280	3.458E-05	2.438E-05	1.447E-05	1.397E-05	3.168E-05
1311	3.548E-05	2.385E-05	1.443E-05	1.391E-05	3.113E-05
1341	3.378E-05	2.336E-05	1.437E-05	1.381E-05	3.064E-05
1372	3.427E-05	2.302E-05	1.439E-05	1.376E-05	3.037E-05
1402	3.752E-05	2.296E-05	1.443E-05	1.381E-05	3.028E-05
1433	3.589E-05	2.269E-05	1.443E-05	1.371E-05	3.152E-05
1463	3.461E-05	2.258E-05	1.435E-05	1.374E-05	3.185E-05
1494	3.295E-05	2.263E-05	1.441E-05	1.381E-05	3.064E-05
1524	3.419E-05	2.293E-05	1.437E-05	1.366E-05	3.085E-05
1554	3.382E-05	2.314E-05	1.450E-05	1.375E-05	3.033E-05
1585	3.244E-05	2.348E-05	1.449E-05	1.362E-05	3.049E-05
1615	3.090E-05	2.290E-05	1.489E-05	1.363E-05	3.011E-05
1646	3.093E-05	2.217E-05	1.508E-05	1.347E-05	2.960E-05
1676	3.024E-05	2.143E-05	1.480E-05	1.346E-05	2.876E-05
1707	2.952E-05	2.126E-05	1.448E-05	1.348E-05	2.949E-05
1737	2.942E-05	2.119E-05	1.443E-05	1.343E-05	3.013E-05
1768	2.932E-05	2.112E-05	1.438E-05	1.339E-05	3.003E-05
1798	2.922E-05	2.105E-05	1.434E-05	1.335E-05	2.993E-05
1829	2.912E-05	2.098E-05	1.429E-05	1.330E-05	2.983E-05
FIRST DATA ALT.		5	5	5	5
LAST DATA ALT.		57	57	57	50

FLIGHT NO. 86		FILTER NO. 1						
BEAM TRANSMITTANCE FROM GROUND TO ALTITUDE		ZENITH ANGLE OF PATH OF SIGHT (DEGREES)						
ALTITUDE		93	95	100	105	120	150	180
METERS								
305	.7906437	.8695283	.9322360	.9540127	.9759250	.9860288	.9878191	
610	.6516131	.7769680	.8810331	.9185312	.9569649	.9749230	.9782458	
914	.5416125	.6993135	.8356786	.8865316	.9395600	.9646460	.9693090	
1219	.4460619	.6273378	.7913415	.8546924	.9219370	.9541591	.9601765	
1524	.3584858	.5559661	.7447958	.8206284	.9027323	.9425316	.9501223	

FLIGHT NO. 86		FILTER NO. 2						
BEAM TRANSMITTANCE FROM GROUND TO ALTITUDE		ZENITH ANGLE OF PATH OF SIGHT (DEGREES)						
ALTITUDE		93	95	100	105	120	150	180
METERS								
305	.8298567	.8949382	.9458112	.9633112	.9808373	.9884912	.9903723	
610	.7183935	.8229836	.9068469	.9365015	.9666109	.9805846	.9831637	
914	.6237302	.7593759	.8709638	.9114746	.9531522	.9726785	.9762951	
1219	.5391405	.6992243	.8356251	.8864935	.9395391	.9646336	.9692981	
1524	.4633032	.6442063	.8019508	.8623634	.9262130	.9567114	.9623996	

FLIGHT NO. 86		FILTER NO. 3						
BEAM TRANSMITTANCE FROM GROUND TO ALTITUDE		ZENITH ANGLE OF PATH OF SIGHT (DEGREES)						
ALTITUDE		93	95	100	105	120	150	180
METERS								
305	.9039060	.9416462	.9702731	.9799566	.9895741	.9939673	.9947734	
610	.8225347	.8912127	.9438330	.9619589	.9801243	.9884761	.9900123	
914	.7499356	.8453451	.9191315	.9449942	.9711386	.9832338	.9854636	
1219	.6828738	.8021020	.8952243	.9284316	.9622903	.9780516	.9809640	
1524	.6225357	.7624767	.8727470	.9127262	.9538295	.9730775	.9766419	

FLIGHT NO. 86		FILTER NO. 4						
BEAM TRANSMITTANCE FROM GROUND TO ALTITUDE		ZENITH ANGLE OF PATH OF SIGHT (DEGREES)						
ALTITUDE		93	95	100	105	120	150	180
METERS								
305	.9198805	.9515131	.9753627	.9834025	.9913738	.9953106	.9956776	
610	.8478964	.9072871	.9523392	.9677670	.9831831	.9902560	.9915559	
914	.7811110	.8656240	.9301328	.9525681	.9751598	.9855823	.9875010	
1219	.7191267	.8256715	.9083323	.9375304	.9671605	.9809064	.9834443	
1524	.6579594	.7867617	.8865897	.9224139	.9590567	.9761528	.9793144	

FLIGHT NO. 86		FILTER NO. 5						
BEAM TRANSMITTANCE FROM GROUND TO ALTITUDE		ZENITH ANGLE OF PATH OF SIGHT (DEGREES)						
ALTITUDE		93	95	100	105	120	150	180
METERS								
305	.7943124	.8719530	.9335399	.9549077	.9763982	.9863051	.9881290	
610	.6445785	.7719616	.8791792	.9165329	.9558872	.9742889	.9776948	
914	.5295414	.6900665	.8301141	.8725666	.9373825	.9633546	.9681052	
1219	.4370096	.6179706	.7866635	.8512992	.9200425	.9530254	.9591885	
1524	.3581754	.5560336	.7448412	.8206620	.9027514	.9426431	.9501323	

AZIMUTH OF PATH OF SIGHT = 0								
FLIGHT NO. 86				FILTER NO. 1				
PATH RADIANCE FROM GROUND TO ALTITUDE(WATTS/STER.SQ.M MICRO M.)								
ALTITUDE	ZENITH ANGLE OF PATH OF SIGHT (DEGREES)							
METERS	93	95	100	105	120	150	180	
305	3.555E-05	2.022E-05	9.856E-06	6.326E-06	2.987E-06	1.803E-06	1.98E-06	
610	5.071E-05	3.053E-05	1.545E-05	1.008E-05	4.837E-06	2.909E-06	3.119E-06	
914	6.942E-05	4.345E-05	2.260E-05	1.496E-05	7.410E-06	4.668E-06	5.080E-06	
1219	8.734E-05	5.679E-05	3.035E-05	2.039E-05	1.039E-05	6.865E-06	7.589E-06	
1524	9.393E-05	6.419E-05	3.533E-05	2.417E-05	1.247E-05	8.622E-06	9.779E-06	

FLIGHT NO. 86			FILTER NO. 2					
PATH RADIANCE FROM GROUND TO ALTITUDE(WATTS/STER.SQ.M MICRO M.)								
ALTITUDE	ZENITH ANGLE OF PATH OF SIGHT (DEGREES)							
METERS	93	95	100	105	120	150	180	1 C
305	2.932E-05	1.649E-05	8.085E-06	5.259E-06	2.590E-06	1.548E-06	1.905E-06	
610	4.179E-05	2.458E-05	1.237E-05	8.126E-06	4.024E-06	2.582E-06	2.859E-06	
914	5.615E-05	3.423E-05	1.759E-05	1.166E-05	5.875E-06	3.849E-06	4.296E-06	
1219	6.815E-05	4.304E-05	2.264E-05	1.517E-05	7.770E-06	5.206E-06	5.957E-06	
1524	7.256E-05	4.764E-05	2.571E-05	1.738E-05	8.953E-06	6.085E-06	6.958E-06	

FLIGHT NO. 86			FILTER NO. 3					
PATH RADIANCE FROM GROUND TO ALTITUDE(WATTS/STER.SQ.M MICRO M.)								
ALTITUDE	ZENITH ANGLE OF PATH OF SIGHT (DEGREES)							
METERS	93	95	100	105	120	150	180	
305	1.011E-05	5.563E-06	2.664E-06	1.701E-06	7.926E-07	4.600E-07	4.987E-07	
610	1.456E-05	1.053E-05	5.119E-06	3.296E-06	1.566E-06	9.614E-07	1.112E-06	
914	2.705E-05	1.580E-05	7.812E-06	5.075E-06	2.468E-06	1.598E-06	1.921E-06	
1219	3.333E-05	2.006E-05	1.012E-05	6.652E-06	3.314E-06	2.247E-06	2.739E-06	
1524	3.848E-05	2.379E-05	1.223E-05	8.110E-06	4.098E-06	2.961E-06	3.627E-06	

FLIGHT NO. 86			FILTER NO. 4					
PATH RADIANCE FROM GROUND TO ALTITUDE(WATTS/STER.SQ.M MICRO M.)								
ALTITUDE	ZENITH ANGLE OF PATH OF SIGHT (DEGREES)							
METERS	93	95	100	105	120	150	180	
305	1.455E-05	8.023E-06	3.839E-06	2.535E-06	1.279E-06	8.109E-07	9.133E-07	
610	2.592E-05	1.470E-05	7.249E-06	4.789E-06	2.437E-06	1.582E-06	1.822E-06	
914	3.511E-05	2.053E-05	1.033E-05	6.872E-06	3.576E-06	2.380E-06	2.774E-06	
1219	4.341E-05	2.610E-05	1.337E-05	8.977E-06	4.739E-06	3.238E-06	3.942E-06	
1524	4.787E-05	2.962E-05	1.548E-05	1.043E-05	5.573E-06	3.884E-06	4.733E-06	

FLIGHT NO. 86			FILTER NO. 5					
PATH RADIANCE FROM GROUND TO ALTITUDE(WATTS/STER.SQ.M MICRO M.)								
ALTITUDE	ZENITH ANGLE OF PATH OF SIGHT (DEGREES)							
METERS	93	95	100	105	120	150	180	
305	2.472E-05	1.403E-05	6.839E-06	4.392E-06	2.068E-06	1.226E-06	1.325E-06	
610	4.036E-05	2.423E-05	1.226E-05	8.001E-06	3.843E-06	2.290E-06	2.445E-06	
914	5.253E-05	3.305E-05	1.726E-05	1.144E-05	5.634E-06	3.459E-06	3.726E-06	
1219	6.140E-05	4.029E-05	2.168E-05	1.457E-05	7.319E-06	4.589E-06	4.970E-06	
1524	6.741E-05	4.608E-05	2.556E-05	1.738E-05	8.873E-06	5.652E-06	6.180E-06	

AZIMUTH OF PATH OF SIGHT = 90							
FLIGHT NO. 86				FILTER NO. 1			
PATH RADIANCE FROM GROUND TO ALTITUDE(WATTS/STER.SQ.M MICRO M.)							
ZENITH ANGLE OF PATH OF SIGHT (DEGREES)							
ALTITUDE METERS	93	95	100	105	120	150	180
305	3.125E-05	1.820E-05	9.437E-06	6.424E-06	3.516E-06	2.407E-06	1.900E-06
610	4.568E-05	2.801E-05	1.490E-05	1.020E-05	5.598E-06	3.700E-06	3.119E-06
914	6.425E-05	4.079E-05	2.213E-05	1.529E-05	8.421E-06	5.791E-06	5.080E-06
1219	8.248E-05	5.421E-05	2.924E-05	2.043E-05	1.197E-05	8.124E-06	7.399E-06
1524	9.025E-05	6.211E-05	3.527E-05	2.469E-05	1.365E-05	9.791E-06	9.779E-06

FLIGHT NO. 86				FILTER NO. 2			
PATH RADIANCE FROM GROUND TO ALTITUDE(WATTS/STER.SQ.M MICRO M.)							
ZENITH ANGLE OF PATH OF SIGHT (DEGREES)							
ALTITUDE METERS	93	95	100	105	120	150	180
305	2.714E-05	1.561E-05	8.071E-06	5.491E-06	3.045E-06	2.174E-06	1.905E-06
610	3.881E-05	2.329E-05	1.230E-05	8.418E-06	4.630E-06	3.259E-06	2.859E-06
914	5.269E-05	3.267E-05	1.754E-05	1.209E-05	6.732E-06	4.782E-06	4.296E-06
1219	6.468E-05	4.143E-05	2.258E-05	1.565E-05	8.721E-06	6.250E-06	5.857E-06
1524	6.943E-05	4.612E-05	2.566E-05	1.787E-05	9.921E-06	7.163E-06	6.958E-06

FLIGHT NO. 86				FILTER NO. 3			
PATH RADIANCE FROM GROUND TO ALTITUDE(WATTS/STER.SQ.M MICRO M.)							
ZENITH ANGLE OF PATH OF SIGHT (DEGREES)							
ALTITUDE METERS	93	95	100	105	120	150	180
305	1.049E-05	5.895E-06	2.957E-06	1.955E-06	9.728E-07	5.963E-07	4.987E-07
610	1.816E-05	1.053E-05	5.379E-06	3.602E-06	1.871E-06	1.264E-06	1.112E-06
914	2.575E-05	1.535E-05	7.961E-06	5.385E-06	2.879E-06	2.082E-06	1.982E-06
1219	3.174E-05	1.943E-05	1.020E-05	6.943E-06	3.745E-06	2.778E-06	2.732E-06
1524	3.684E-05	2.310E-05	1.226E-05	8.973E-06	4.523E-06	3.551E-06	3.827E-06

FLIGHT NO. 86				FILTER NO. 4			
PATH RADIANCE FROM GROUND TO ALTITUDE(WATTS/STER.SQ.M MICRO M.)							
ZENITH ANGLE OF PATH OF SIGHT (DEGREES)							
ALTITUDE METERS	93	95	100	105	120	150	180
305	1.210E-05	6.865E-06	3.563E-06	2.466E-06	1.422E-06	1.057E-06	9.135E-07
610	2.207E-05	1.287E-05	6.767E-06	4.697E-06	2.727E-06	2.048E-06	1.822E-06
914	3.080E-05	1.843E-05	9.796E-06	6.824E-06	3.967E-06	3.037E-06	2.772E-06
1219	3.966E-05	2.428E-05	1.298E-05	9.046E-06	5.202E-06	3.979E-06	3.842E-06
1524	4.840E-05	3.028E-05	1.627E-05	1.127E-05	6.259E-06	4.711E-06	4.733E-06

FLIGHT NO. 86				FILTER NO. 5			
PATH RADIANCE FROM GROUND TO ALTITUDE(WATTS/STER.SQ.M MICRO M.)							
ZENITH ANGLE OF PATH OF SIGHT (DEGREES)							
ALTITUDE METERS	93	95	100	105	120	150	180
305	2.192E-05	1.269E-05	6.505E-06	4.380E-06	2.322E-06	1.591E-06	1.325E-06
610	3.643E-05	2.224E-05	1.175E-05	7.982E-06	4.258E-06	2.833E-06	2.445E-06
914	4.856E-05	3.094E-05	1.676E-05	1.150E-05	6.198E-06	4.189E-06	3.726E-06
1219	5.773E-05	3.824E-05	2.113E-05	1.465E-05	7.930E-06	5.387E-06	4.970E-06
1524	6.417E-05	4.417E-05	2.507E-05	1.749E-05	9.514E-06	6.515E-06	6.186E-06

FLIGHT NO. 86 FILTER NO. 1

PATH RADIANCE FROM GROUND TO ALTITUDE (WATTS/STER.SQ.M MICRO M.)

ALTITUDE METERS ZENITH ANGLE OF PATH OF SIGHT (DEGREES)

	93	95	100	105	120	150	180
305	3.101E-05	1.813E-05	9.477E-06	6.498E-06	3.606E-06	2.458E-06	1.988E-06
610	4.522E-05	2.781E-05	1.491E-05	1.027E-05	5.643E-06	3.755E-06	3.119E-06
914	6.345E-05	4.033E-05	2.193E-05	1.518E-05	8.368E-06	5.683E-06	5.080E-06
1219	8.153E-05	5.363E-05	2.967E-05	2.069E-05	1.148E-05	6.016E-06	7.589E-06
1524	8.915E-05	6.144E-05	3.497E-05	2.455E-05	1.362E-05	9.216E-06	9.779E-06

FLIGHT NO. 86 FILTER NO. 2

PATH RADIANCE FROM GROUND TO ALTITUDE (WATTS/STER.SQ.M MICRO M.)

ALTITUDE METERS ZENITH ANGLE OF PATH OF SIGHT (DEGREES)

	93	95	100	105	120	150	180
305	2.661E-05	1.538E-05	8.038E-06	5.520E-06	3.115E-06	2.270E-06	1.905E-06
610	3.819E-05	2.300E-05	1.226E-05	8.454E-06	4.739E-06	3.310E-06	2.859E-06
914	5.190E-05	3.224E-05	1.736E-05	1.201E-05	6.709E-06	4.715E-06	4.296E-06
1219	6.592E-05	4.033E-05	2.236E-05	1.554E-05	8.680E-06	6.168E-06	5.857E-06
1524	6.859E-05	4.557E-05	2.541E-05	1.774E-05	9.879E-06	7.112E-06	6.952E-06

FLIGHT NO. 86 FILTER NO. 3

PATH RADIANCE FROM GROUND TO ALTITUDE (WATTS/STER.SQ.M MICRO M.)

ALTITUDE METERS ZENITH ANGLE OF PATH OF SIGHT (DEGREES)

	93	95	100	105	120	150	180
305	8.202E-06	4.630E-06	2.361E-06	1.597E-06	8.669E-07	6.004E-07	4.987E-07
610	1.452E-05	9.012E-06	4.639E-06	3.148E-06	1.715E-06	1.229E-06	1.112E-06
914	2.330E-05	1.387E-05	7.186E-06	4.889E-06	2.664E-06	1.955E-06	1.922E-06
1219	2.949E-05	1.802E-05	9.446E-06	6.456E-06	3.531E-06	2.647E-06	2.739E-06
1524	3.488E-05	2.183E-05	1.158E-05	7.945E-06	4.254E-06	3.462E-06	3.827E-06

FLIGHT NO. 86 FILTER NO. 4

PATH RADIANCE FROM GROUND TO ALTITUDE (WATTS/STER.SQ.M MICRO M.)

ALTITUDE METERS ZENITH ANGLE OF PATH OF SIGHT (DEGREES)

	93	95	100	105	120	150	180
305	1.255E-05	7.159E-06	3.763E-06	2.628E-06	1.547E-06	1.155E-06	9.133E-07
610	2.296E-05	1.344E-05	7.134E-06	4.987E-06	2.931E-06	2.208E-06	1.822E-06
914	3.208E-05	1.924E-05	1.027E-05	7.174E-06	4.171E-06	3.125E-06	2.772E-06
1219	4.054E-05	2.487E-05	1.335E-05	9.335E-06	5.367E-06	4.061E-06	3.842E-06
1524	4.521E-05	2.845E-05	1.547E-05	1.004E-05	6.730E-06	4.784E-06	4.733E-06

FLIGHT NO. 86 FILTER NO. 5

PATH RADIANCE FROM GROUND TO ALTITUDE (WATTS/STER.SQ.M MICRO M.)

ALTITUDE METERS ZENITH ANGLE OF PATH OF SIGHT (DEGREES)

	93	95	100	105	120	150	180
305	2.160E-05	1.259E-05	6.552E-06	4.473E-06	2.452E-06	1.666E-06	1.325E-06
610	4.611E-05	2.214E-05	1.183E-05	8.122E-06	4.437E-06	2.977E-06	2.445E-06
914	6.619E-05	3.076E-05	1.677E-05	1.150E-05	6.322E-06	4.260E-06	3.726E-06
1219	8.749E-05	3.813E-05	2.121E-05	1.474E-05	8.045E-06	5.443E-06	4.770E-06
1524	6.374E-05	4.407E-05	2.510E-05	1.757E-05	9.578E-06	6.579E-06	6.186E-06

AZIMUTH OF PATH OF SIGHT = 270

FLIGHT NO. 86		FILTER NO. 1						
PATH RADIANCE FROM GROUND TO ALTITUDE (WATTS/STER.SQ.M MICRO M.)		ZENITH ANGLE OF PATH OF SIGHT (DEGREES)						
ALTITUDE		93	95	100	105	120	150	180
METERS								
305	3.049E-05	1.755E-05	8.895E-06	5.925E-06	3.042E-06	1.983E-06	1.988E-06	
610	4.473E-05	2.716E-05	1.420E-05	9.545E-06	4.919E-06	3.147E-06	3.119E-06	
914	6.337E-05	3.984E-05	2.125E-05	1.442E-05	7.574E-06	5.005E-06	5.080E-06	
1219	8.150E-05	5.327E-05	2.917E-05	2.006E-05	1.083E-05	7.482E-06	7.589E-06	
1524	8.908E-05	6.111E-05	3.452E-05	2.397E-05	1.302E-05	9.347E-06	9.779E-06	

FLIGHT NO. 86		FILTER NO. 2						
PATH RADIANCE FROM GROUND TO ALTITUDE (WATTS/STER.SQ.M MICRO M.)		ZENITH ANGLE OF PATH OF SIGHT (DEGREES)						
ALTITUDE		93	95	100	105	120	150	180
METERS								
305	2.631E-05	1.501E-05	7.647E-06	5.122E-06	2.712E-06	1.851E-06	1.905E-06	
610	3.792E-05	2.257E-05	1.175E-05	7.920E-06	4.186E-06	2.805E-06	2.859E-06	
914	5.190E-05	3.189E-05	1.686E-05	1.143E-05	6.090E-06	4.147E-06	4.296E-06	
1219	6.380E-05	4.063E-05	2.194E-05	1.502E-05	8.137E-06	5.687E-06	5.857E-06	
1524	6.845E-05	4.526E-05	2.500E-05	1.723E-05	9.360E-06	6.675E-06	6.958E-06	

FLIGHT NO. 86		FILTER NO. 3						
PATH RADIANCE FROM GROUND TO ALTITUDE (WATTS/STER.SQ.M MICRO M.)		ZENITH ANGLE OF PATH OF SIGHT (DEGREES)						
ALTITUDE		93	95	100	105	120	150	180
METERS								
305	8.799E-06	4.894E-06	2.418E-06	1.585E-06	7.853E-07	4.918E-07	4.987E-07	
610	1.638E-05	9.382E-06	4.705E-06	3.105E-06	1.566E-06	1.031E-06	1.112E-06	
914	2.434E-05	1.431E-05	7.276E-06	4.836E-06	2.487E-06	1.713E-06	1.922E-06	
1219	3.038E-05	1.841E-05	9.540E-06	6.410E-06	3.377E-06	2.445E-06	2.739E-06	
1524	3.558E-05	2.215E-05	1.166E-05	7.898E-06	4.236E-06	3.375E-06	3.827E-06	

FLIGHT NO. 86		FILTER NO. 4						
PATH RADIANCE FROM GROUND TO ALTITUDE (WATTS/STER.SQ.M MICRO M.)		ZENITH ANGLE OF PATH OF SIGHT (DEGREES)						
ALTITUDE		93	95	100	105	120	150	180
METERS								
305	1.258E-05	7.065E-06	3.611E-06	2.458E-06	1.336E-06	9.035E-07	9.133E-07	
610	2.306E-05	1.331E-05	6.881E-06	4.696E-06	2.564E-06	1.757E-06	1.822E-06	
914	3.207E-05	1.900E-05	9.939E-06	6.810E-06	3.745E-06	2.613E-06	2.772E-06	
1219	4.027E-05	2.452E-05	1.300E-05	8.960E-06	4.991E-06	3.619E-06	3.842E-06	
1524	4.583E-05	2.864E-05	1.538E-05	1.062E-05	5.903E-06	4.437E-06	4.733E-06	

FLIGHT NO. 86		FILTER NO. 5						
PATH RADIANCE FROM GROUND TO ALTITUDE (WATTS/STER.SQ.M MICRO M.)		ZENITH ANGLE OF PATH OF SIGHT (DEGREES)						
ALTITUDE		93	95	100	105	120	150	180
METERS								
305	2.146E-05	1.234E-05	6.260E-06	4.168E-06	2.122E-06	1.349E-06	1.325E-06	
610	3.592E-05	2.178E-05	1.138E-05	7.649E-06	3.924E-06	2.481E-06	2.445E-06	
914	4.805E-05	3.041E-05	1.624E-05	1.105E-05	5.744E-06	3.696E-06	3.726E-06	
1219	5.706E-05	3.763E-05	2.077E-05	1.420E-05	7.500E-06	4.938E-06	4.970E-06	
1524	6.336E-05	4.350E-05	2.459E-05	1.705E-05	9.132E-06	6.158E-06	6.186E-06	

AZIMUTH OF PATH OF SIGHT =		FLIGHT NO. 86		FILTER NO. 1					
		DIRECTIONAL PATH REFLECTANCE FROM GROUND TO ALTITUDE		ZENITH ANGLE OF PATH OF SIGHT (DEGREES)					
ALTITUDE	METERS	93	95	100	105	120	150	180	
305		8.558E-02	4.426E-02	2.012E-02	1.262E-02	5.827E-03	3.491E-03	3.830E-03	
610		1.481E-01	7.479E-02	3.338E-02	2.088E-02	9.622E-03	5.680E-03	6.069E-03	
914		2.440E-01	1.183E-01	5.147E-02	3.212E-02	1.501E-02	9.210E-03	9.976E-03	
1219		3.727E-01	1.723E-01	7.301E-02	4.540E-02	2.146E-02	1.370E-02	1.504E-02	
1524		4.987E-01	2.198E-01	9.081E-02	5.605E-02	2.629E-02	1.741E-02	1.959E-02	

		FLIGHT NO. 86		FILTER NO. 2					
		DIRECTIONAL PATH REFLECTANCE FROM GROUND TO ALTITUDE		ZENITH ANGLE OF PATH OF SIGHT (DEGREES)					
ALTITUDE	METERS	93	95	100	105	120	150	180	
305		5.887E-02	3.070E-02	1.424E-02	9.096E-03	4.399E-03	2.844E-03	3.204E-03	
610		9.691E-02	4.977E-02	2.273E-02	1.446E-02	6.936E-03	4.387E-03	4.845E-03	
914		1.500E-01	7.510E-02	3.365E-02	2.132E-02	1.027E-02	6.594E-03	7.392E-03	
1219		2.110E-01	1.026E-01	4.513E-02	2.850E-02	1.370E-02	8.992E-03	1.007E-02	
1524		2.609E-01	1.232E-01	5.341E-02	3.357E-02	1.610E-02	1.060E-02	1.205E-02	

		FLIGHT NO. 86		FILTER NO. 3					
		DIRECTIONAL PATH REFLECTANCE FROM GROUND TO ALTITUDE		ZENITH ANGLE OF PATH OF SIGHT (DEGREES)					
ALTITUDE	METERS	93	95	100	105	120	150	180	
305		4.008E-02	2.116E-02	9.835E-03	6.220E-03	2.869E-03	1.658E-03	1.796E-03	
610		8.083E-02	4.232E-02	1.943E-02	1.227E-02	5.724E-03	3.484E-03	4.022E-03	
914		1.292E-01	6.697E-02	3.045E-02	1.924E-02	9.103E-03	5.824E-03	6.987E-03	
1219		1.749E-01	8.957E-02	4.050E-02	2.567E-02	1.214E-02	8.229E-03	1.000E-02	
1524		2.214E-01	1.118E-01	5.020E-02	3.183E-02	1.539E-02	1.090E-02	1.404E-02	

		FLIGHT NO. 86		FILTER NO. 4					
		DIRECTIONAL PATH REFLECTANCE FROM GROUND TO ALTITUDE		ZENITH ANGLE OF PATH OF SIGHT (DEGREES)					
ALTITUDE	METERS	93	95	100	105	120	150	180	
305		3.106E-02	1.655E-02	7.828E-03	5.061E-03	2.533E-03	1.600E-03	1.801E-03	
610		6.001E-02	3.180E-02	1.494E-02	9.674E-03	4.867E-03	3.136E-03	3.607E-03	
914		8.826E-02	4.657E-02	2.181E-02	1.416E-02	7.200E-03	4.741E-03	5.512E-03	
1219		1.187E-01	6.205E-02	2.891E-02	1.880E-02	9.619E-03	6.482E-03	7.669E-03	
1524		1.428E-01	7.391E-02	3.428E-02	2.230E-02	1.141E-02	7.811E-03	9.468E-03	

		FLIGHT NO. 86		FILTER NO. 5					
		DIRECTIONAL PATH REFLECTANCE FROM GROUND TO ALTITUDE		ZENITH ANGLE OF PATH OF SIGHT (DEGREES)					
ALTITUDE	METERS	93	95	100	105	120	150	180	
305		9.501E-02	4.913E-02	2.237E-02	1.404E-02	6.466E-03	3.795E-03	4.093E-03	
610		1.912E-01	9.583E-02	4.261E-02	2.665E-02	1.227E-02	7.176E-03	7.636E-03	
914		3.029E-01	1.462E-01	6.380E-02	3.958E-02	1.835E-02	1.096E-02	1.175E-02	
1219		4.290E-01	1.984E-01	8.417E-02	5.224E-02	2.429E-02	1.470E-02	1.582E-02	
1524		5.746E-01	2.531E-01	1.048E-01	6.467E-02	3.001E-02	1.831E-02	1.988E-02	

AZIMUTH OF PATH OF SIGHT = 90

FLIGHT NO. 86		FILTER NO. 1						
DIRECTIONAL PATH REFLECTANCE FROM GROUND TO ALTITUDE								
ALTITUDE	ZENITH ANGLE OF PATH OF SIGHT (DEGREES)							
METERS	93	95	100	105	120	150	180	
305	7.523E-02	3.984E-02	1.927E-02	1.282E-02	6.858E-03	4.646E-03	3.890E-03	
610	1.334E-01	6.861E-02	3.219E-02	2.113E-02	1.102E-02	7.240E-03	6.089E-03	
914	2.258E-01	1.110E-01	5.041E-02	3.282E-02	1.706E-02	1.143E-02	9.976E-03	
1219	3.320E-01	1.645E-01	7.202E-02	4.638E-02	2.385E-02	1.622E-02	1.504E-02	
1524	4.792E-01	2.127E-01	9.014E-02	5.727E-02	2.878E-02	1.977E-02	1.954E-02	

FLIGHT NO. 86			FILTER NO. 2				
DIRECTIONAL PATH REFLECTANCE FROM GROUND TO ALTITUDE							
ALTITUDE	ZENITH ANGLE OF PATH OF SIGHT (DEGREES)						
METERS	93	95	100	105	120	150	180
305	5.448E-02	2.906E-02	1.422E-02	9.498E-03	5.173E-03	3.642E-03	3.204E-03
610	9.002E-02	4.715E-02	2.260E-02	1.498E-02	8.015E-03	5.537E-03	4.845E-03
914	1.407E-01	7.169E-02	3.355E-02	2.210E-02	1.177E-02	6.192E-03	7.332E-03
1219	2.002E-01	9.873E-02	4.502E-02	2.941E-02	1.547E-02	1.080E-02	1.007E-02
1524	2.497E-01	1.193E-01	5.330E-02	3.452E-02	1.785E-02	1.247E-02	1.205E-02

FLIGHT NO. 86			FILTER NO. 3				
DIRECTIONAL PATH REFLECTANCE FROM GROUND TO ALTITUDE							
ALTITUDE	ZENITH ANGLE OF PATH OF SIGHT (DEGREES)						
METERS	93	95	100	105	120	150	180
305	4.158E-02	2.243E-02	1.092E-02	7.146E-03	3.522E-03	2.149E-03	1.796E-03
610	7.908E-02	4.232E-02	2.042E-02	1.341E-02	6.837E-03	4.589E-03	4.022E-03
914	1.230E-01	6.507E-02	3.103E-02	2.041E-02	1.062E-02	7.585E-03	6.987E-03
1219	1.665E-01	8.679E-02	4.083E-02	2.679E-02	1.394E-02	1.018E-02	1.000E-02
1524	2.120E-01	1.085E-01	5.033E-02	3.286E-02	1.699E-02	1.307E-02	1.404E-02

FLIGHT NO. 86			FILTER NO. 4					
DIRECTIONAL PATH REFLECTANCE FROM GROUND TO ALTITUDE								
ALTITUDE	ZENITH ANGLE OF PATH OF SIGHT (DEGREES)							
METERS	93	95	100	105	120	150	180	
305	2.583E-02	1.416E-02	7.172E-03	4.923E-03	2.816E-03	2.086E-03	1.801E-03	
610	5.111E-02	2.784E-02	1.395E-02	9.529E-03	5.445E-03	4.099E-03	3.607E-03	
914	7.741E-02	4.180E-02	2.068E-02	1.407E-02	7.986E-03	6.050E-03	5.512E-03	
1219	1.084E-01	5.773E-02	2.806E-02	1.894E-02	1.056E-02	7.963E-03	7.669E-03	
1524	1.444E-01	7.557E-02	3.603E-02	2.398E-02	1.281E-02	9.474E-03	9.488E-03	

FLIGHT NO. 86			FILTER NO. 5				
DIRECTIONAL PATH REFLECTANCE FROM GROUND TO ALTITUDE							
ALTITUDE	ZENITH ANGLE OF PATH OF SIGHT (DEGREES)						
METERS	93	95	100	105	120	150	180
305	8.424E-02	4.444E-02	2.127E-02	1.401E-02	7.260E-03	4.801E-03	4.093E-03
610	1.726E-01	8.796E-02	4.085E-02	2.660E-02	1.360E-02	8.878E-03	7.636E-03
914	2.800E-01	1.369E-01	6.165E-02	3.979E-02	2.019E-02	1.328E-02	1.175E-02
1219	4.033E-01	1.883E-01	8.220E-02	5.253E-02	2.632E-02	1.727E-02	1.582E-02
1524	5.470E-01	2.426E-01	1.028E-01	6.505E-02	3.218E-02	2.110E-02	1.988E-02



AZIMUTH OF PATH OF SIGHT = 180

FLIGHT NO. 86 FILTER NO. 1

DIRECTIONAL PATH REFLECTANCE FROM GROUND TO ALTITUDE		ZENITH ANGLE OF PATH OF SIGHT (DEGREES)							
ALTITUDE METERS		93	95	100	105	120	150	180	
305		7.466E-02	3.969E-02	1.935E-02	1.297E-02	7.034E-03	4.746E-03	3.830E-03	
610		1.321E-01	6.814E-02	3.221E-02	2.128E-02	1.122E-02	7.330E-03	6.069E-03	
914		2.230E-01	1.098E-01	4.994E-02	3.260E-02	1.695E-02	1.121E-02	9.977E-03	
1219		3.479E-01	1.627E-01	7.137E-02	4.607E-02	2.371E-02	1.599E-02	1.504E-02	
1524		4.734E-01	2.103E-01	8.937E-02	5.696E-02	2.872E-02	1.982E-02	1.950E-02	

FLIGHT NO. 86 FILTER NO. 2

DIRECTIONAL PATH REFLECTANCE FROM GROUND TO ALTITUDE		ZENITH ANGLE OF PATH OF SIGHT (DEGREES)							
ALTITUDE METERS		93	95	100	105	120	150	180	
305		5.343E-02	2.863E-02	1.416E-02	9.546E-03	5.291E-03	3.741E-03	3.204E-03	
610		8.856E-02	4.657E-02	2.252E-02	1.504E-02	8.168E-03	5.623E-03	4.845E-03	
914		1.386E-01	7.073E-02	3.321E-02	2.196E-02	1.173E-02	8.077E-03	7.332E-03	
1219		1.976E-01	9.752E-02	4.457E-02	2.920E-02	1.539E-02	1.065E-02	1.007E-02	
1524		2.465E-01	1.179E-01	5.279E-02	3.427E-02	1.777E-02	1.238E-02	1.205E-02	

FLIGHT NO. 86 FILTER NO. 3

DIRECTIONAL PATH REFLECTANCE FROM GROUND TO ALTITUDE		ZENITH ANGLE OF PATH OF SIGHT (DEGREES)							
ALTITUDE METERS		93	95	100	105	120	150	180	
305		3.251E-02	1.761E-02	8.717E-03	5.839E-03	3.138E-03	2.164E-03	1.796E-03	
610		6.761E-02	3.622E-02	1.761E-02	1.172E-02	6.269E-03	4.455E-03	4.022E-03	
914		1.113E-01	5.877E-02	2.801E-02	1.853E-02	9.826E-03	7.122E-03	6.987E-03	
1219		1.547E-01	8.047E-02	3.780E-02	2.491E-02	1.315E-02	9.694E-03	1.000E-02	
1524		2.007E-01	1.026E-01	4.755E-02	3.119E-02	1.635E-02	1.274E-02	1.404E-02	

FLIGHT NO. 86 FILTER NO. 4

DIRECTIONAL PATH REFLECTANCE FROM GROUND TO ALTITUDE		ZENITH ANGLE OF PATH OF SIGHT (DEGREES)							
ALTITUDE METERS		93	95	100	105	120	150	180	
305		2.679E-02	1.477E-02	7.574E-03	5.247E-03	3.063E-03	2.280E-03	1.801E-03	
610		5.317E-02	2.908E-02	1.471E-02	1.012E-02	5.853E-03	4.378E-03	3.607E-03	
914		8.064E-02	4.363E-02	2.167E-02	1.479E-02	8.397E-03	6.225E-03	5.512E-03	
1219		1.108E-01	5.913E-02	2.886E-02	1.955E-02	1.094E-02	8.127E-03	7.669E-03	
1524		1.349E-01	7.100E-02	3.426E-02	2.308E-02	1.277E-02	9.622E-03	9.488E-03	

FLIGHT NO. 86 FILTER NO. 5

DIRECTIONAL PATH REFLECTANCE FROM GROUND TO ALTITUDE		ZENITH ANGLE OF PATH OF SIGHT (DEGREES)							
ALTITUDE METERS		93	95	100	105	120	150	180	
305		8.302E-02	4.407E-02	2.143E-02	1.430E-02	7.669E-03	5.158E-03	4.093E-03	
610		1.710E-01	8.756E-02	4.112E-02	2.706E-02	1.417E-02	9.330E-03	7.636E-03	
914		2.776E-01	1.361E-01	6.166E-02	4.006E-02	2.059E-02	1.359E-02	1.175E-02	
1219		4.017E-01	1.878E-01	8.233E-02	5.285E-02	2.670E-02	1.744E-02	1.582E-02	
1524		5.450E-01	2.420E-01	1.029E-01	6.538E-02	3.256E-02	2.123E-02	1.980E-02	

AZIMUTH OF PATH OF SIGHT = 270								
FLIGHT NO. 86			FILTER NO. 1					
DIRECTIONAL PATH REFLECTANCE FROM GROUND TO ALTITUDE								
ZENITH ANGLE OF PATH OF SIGHT (DEGREES)								
ALTITUDE	93		95	100	105	120	150	180
METERS								
305	7.340E-02	3.841E-02	1.816E-02	1.182E-02	5.933E-03	3.827E-03	3.850E-03	
610	1.307E-01	6.653E-02	3.067E-02	1.978E-02	9.784E-03	6.144E-03	6.069E-03	
914	2.227E-01	1.084E-01	4.841E-02	3.096E-02	1.534E-02	9.876E-03	9.976E-03	
1219	3.478E-01	1.616E-01	7.016E-02	4.467E-02	2.237E-02	1.493E-02	1.504E-02	
1524	4.730E-01	2.092E-01	8.822E-02	5.560E-02	2.746E-02	1.887E-02	1.969E-02	

FLIGHT NO. 86			FILTER NO. 2				
DIRECTIONAL PATH REFLECTANCE FROM GROUND TO ALTITUDE							
ALTITUDE	ZENITH ANGLE OF PATH OF SIGHT (DEGREES)						
METERS	93	95	100	105	120	150	180
305	5.283E-02	2.794E-02	1.347E-02	8.858E-03	4.607E-03	3.119E-03	3.204E-03
610	8.794E-02	4.569E-02	2.159E-02	1.409E-02	7.215E-03	4.767E-03	4.845E-03
914	1.386E-01	6.997E-02	3.225E-02	2.089E-02	1.064E-02	7.103E-03	7.332E-03
1219	1.975E-01	9.680E-02	4.374E-02	2.823E-02	1.443E-02	9.822E-03	1.007E-02
1524	2.462E-01	1.171E-01	5.194E-02	3.329E-02	1.684E-02	1.163E-02	1.205E-02

FLIGHT NO. 86			FILTER NO. 3					
DIRECTIONAL PATH REFLECTANCE FROM GROUND TO ALTITUDE								
ALTITUDE		ZENITH ANGLE OF PATH OF SIGHT (DEGREES)						
METERS	93	95	100	105	120	150	180	
305	3.487E-02	1.862E-02	8.928E-03	5.796E-03	2.843E-03	1.773E-03	1.796E-03	
610	7.136E-02	3.771E-02	1.786E-02	1.156E-02	5.724E-03	3.736E-03	4.022E-03	
914	1.163E-01	6.066E-02	2.836E-02	1.833E-02	9.173E-03	6.241E-03	6.987E-03	
1219	1.594E-01	8.224E-02	3.818E-02	2.473E-02	1.257E-02	8.956E-03	1.000E-02	
1524	2.047E-01	1.041E-01	4.787E-02	3.100E-02	1.591E-02	1.243E-02	1.404E-02	

FLIGHT NO. 86				FILTER NO. 4				
DIRECTIONAL PATH REFLECTANCE FROM GROUND TO ALTITUDE								
ALTITUDE		ZENITH ANGLE OF PATH OF SIGHT (DEGREES)						
METERS	23	95	100	105	120	150	180	
305	2.684E-02	1.458E-02	7.268E-03	4.907E-03	2.646E-03	1.783E-03	1.801E-03	
610	5.332E-02	2.879E-02	1.419E-02	9.526E-03	5.119E-03	3.484E-03	3.607E-03	
914	8.059E-02	4.309E-02	2.098E-02	1.403E-02	7.539E-03	5.205E-03	5.512E-03	
1219	1.101E-01	5.829E-02	2.810E-02	1.876E-02	1.013E-02	7.244E-03	7.669E-03	
1524	1.367E-01	7.146E-02	3.405E-02	2.261E-02	1.208E-02	8.923E-03	9.488E-03	

FLIGHT NO. 86			FILTER NO. 5					
DIRECTIONAL PATH REFLECTANCE FROM GROUND TO ALTITUDE								
		ZENITH ANGLE OF PATH OF SIGHT (DEGREES)						
ALTITUDE		93	95	100	105	120	150	180
METERS								
305		8.248E-02	4.323E-02	2.047E-02	1.333E-02	6.635E-03	4.176E-03	4.093E-03
610		1.701E-01	8.616E-02	3.957E-02	2.548E-02	1.253E-02	7.776E-03	7.636E-03
914		1.770E-01	1.346E-01	5.994E-02	3.824E-02	1.871E-02	1.172E-02	1.175E-02
1219		3.976E-01	1.853E-01	8.035E-02	5.091E-02	2.489E-02	1.582E-02	1.582E-02
1524		5.401E-01	2.389E-01	1.008E-01	6.342E-02	3.089E-02	1.995E-02	1.988E-02

#### FLIGHT 87

Starlight before moonrise. Data were recorded over the Gulf of Siam approximately 8 km south of Rayong. The water depth was approximately 20 m (10 fm). Data-taking started at 1926 local time and was completed at 2037, before moonrise. At the beginning of the flight there were high cirrus clouds to the north. Near the end of the flight some stratus was seen along the beach line at an estimated altitude of 1000 to 1200 m.

FLIGHT NO. 67 FILTER NO. 1  
 INRADIANCE (WATTS/SQ. M. MICRO M.)

ALTITUDE (METERS)	DOWN- WELLING	UP- WELLING	ALBEDO	SCALAR DOWNWELLING	SCALAR UPWELLING	SCALAR TOTAL	SCALAR ALBEDO
191	8.752E-06	1.395E-06	.159	1.708E-05	5.788E-06	2.287E-05	.339
481	8.237E-06	1.345E-06	.163	1.572E-05	6.523E-06	2.225E-05	.415
790	8.105E-06	1.250E-06	.154	1.581E-05	6.755E-06	2.256E-05	.427
1081	8.205E-06	1.808E-06	.220	1.604E-05	1.035E-05	2.639E-05	.645
1398	8.882E-06	1.499E-06	.169	1.726E-05	7.758E-06	2.502E-05	.450
1706	8.389E-06	2.081E-06	.248	1.617E-05	1.045E-05	2.661E-05	.643

FLIGHT NO. 67 FILTER NO. 2  
 INRADIANCE (WATTS/SQ. M. MICRO M.)

ALTITUDE (METERS)	DOWN- WELLING	UP- WELLING	ALBEDO	SCALAR DOWNWELLING	SCALAR UPWELLING	SCALAR TOTAL	SCALAR ALBEDO
192	9.390E-06	1.477E-06	.157	1.860E-05	7.679E-06	2.627E-05	.413
482	9.191E-06	2.425E-06	.264	1.802E-05	1.089E-05	2.891E-05	.604
790	9.214E-06	1.662E-06	.180	1.820E-05	9.771E-06	2.798E-05	.537
1081	9.663E-06	3.286E-06	.340	1.916E-05	1.791E-05	3.707E-05	.935
1397	1.001E-05	2.237E-06	.223	1.986E-05	1.152E-05	3.138E-05	.580
1701	9.748E-06	3.167E-06	.325	1.904E-05	2.400E-05	4.304E-05	1.260

FLIGHT NO. 67 FILTER NO. 3  
 INRADIANCE (WATTS/SQ. M. MICRO M.)

ALTITUDE (METERS)	DOWN- WELLING	UP- WELLING	ALBEDO	SCALAR DOWNWELLING	SCALAR UPWELLING	SCALAR TOTAL	SCALAR ALBEDO
190	1.572E-05	3.765E-06	.240	4.164E-05	2.033E-05	6.197E-05	.488
482	1.577E-05	3.352E-06	.213	3.293E-05	1.749E-05	5.042E-05	.531
792	1.529E-05	3.523E-06	.231	3.192E-05	1.934E-05	5.126E-05	.606
1081	1.754E-05	4.829E-06	.275	3.644E-05	3.024E-05	6.668E-05	.830
1396	1.696E-05	3.594E-06	.212	3.524E-05	2.199E-05	5.723E-05	.624
1701	1.769E-05	4.649E-06	.263	3.569E-05	3.058E-05	6.627E-05	.857

FLIGHT NO. 67 FILTER NO. 4  
 INRADIANCE (WATTS/SQ. M. MICRO M.)

ALTITUDE (METERS)	DOWN- WELLING	UP- WELLING	ALBEDO	SCALAR DOWNWELLING	SCALAR UPWELLING	SCALAR TOTAL	SCALAR ALBEDO
----------------------	------------------	----------------	--------	-----------------------	---------------------	-----------------	------------------

FLIGHT NO. 67 FILTER NO. 5  
 INRADIANCE (WATTS/SQ. M. MICRO M.)

ALTITUDE (METERS)	DOWN- WELLING	UP- WELLING	ALBEDO	SCALAR DOWNWELLING	SCALAR UPWELLING	SCALAR TOTAL	SCALAR ALBEDO
192	1.328E-05	2.830E-06	.213	2.609E-05	1.035E-05	3.645E-05	.397
482	1.322E-05	2.279E-06	.172	2.682E-05	1.253E-05	3.935E-05	.467
791	1.327E-05	4.117E-06	.310	2.612E-05	1.399E-05	4.011E-05	.536
1081	1.590E-05	3.483E-06	.219	3.213E-05	1.963E-05	5.175E-05	.611
1397	1.404E-05	2.528E-06	.180	2.779E-05	1.228E-05	4.007E-05	.442
1701	1.647E-05	5.962E-06	.362	3.238E-05	2.973E-05	6.212E-05	.918

FLIGHT NO. 87  
 DIRECTIONAL REFLECTANCE CO. BACKGROUND  
 FILTERS

ZENITH ANGLE	1	2	5	3	4
93	1.61704	1.51482	1.57108	3.92748	
95	.72787	1.44968	.98526	2.04687	
100	.57560	.46131	.47340	.58219	
105	.20323	.37180	1.04620	.26428	
120	.18675	.13455	.18714	.22138	
150	.08641	.08964	.10805	.13462	
180	.07900	.08699	.10338	.12741	

DATE 101200 FLIGHT NO. 47 GROUND LEVEL ALTITUDE (M.)= 34 ILP#1

ALTITUDE (METERS)	TOTAL FILTERS	SCATTERING COEFFICIENT (PER METER)	1	2	3	4	5
0	1.230E-04	1.071E-04	9.445E-05	6.653E-05	1.095E-04		
30	1.226E-04	1.067E-04	9.414E-05	6.631E-05	1.091E-04		
61	1.222E-04	1.064E-04	9.383E-05	6.609E-05	1.087E-04		
91	1.218E-04	1.060E-04	9.351E-05	6.587E-05	1.083E-04		
122	1.213E-04	1.057E-04	9.320E-05	6.565E-05	1.079E-04		
152	1.209E-04	1.053E-04	9.289E-05	6.543E-05	1.075E-04		
183	1.205E-04	1.050E-04	9.258E-05	6.521E-05	1.071E-04		
213	1.202E-04	1.121E-04	9.228E-05	6.528E-05	1.065E-04		
244	1.442E-04	1.046E-04	9.197E-05	6.569E-05	1.066E-04		
274	1.539E-04	9.841E-05	8.928E-05	6.320E-05	1.044E-04		
305	1.556E-04	9.646E-05	8.457E-05	5.959E-05	1.051E-04		
335	1.531E-04	9.623E-05	8.296E-05	5.679E-05	1.095E-04		
366	1.481E-04	9.594E-05	8.649E-05	5.565E-05	1.087E-04		
396	1.344E-04	9.805E-05	8.680E-05	5.504E-05	1.097E-04		
427	1.247E-04	9.875E-05	8.833E-05	5.599E-05	1.102E-04		
457	1.142E-04	9.893E-05	8.885E-05	5.548E-05	1.074E-04		
488	1.127E-04	9.974E-05	8.878E-05	5.471E-05	1.067E-04		
518	1.123E-04	9.979E-05	8.834E-05	5.238E-05	1.062E-04		
549	1.125E-04	1.001E-04	8.567E-05	5.076E-05	1.064E-04		
579	1.125E-04	9.824E-05	8.266E-05	4.923E-05	1.065E-04		
610	1.126E-04	9.207E-05	8.138E-05	4.780E-05	1.035E-04		
640	1.078E-04	8.347E-05	7.647E-05	4.583E-05	1.011E-04		
671	9.533E-05	7.633E-05	6.244E-05	4.337E-05	9.714E-05		
701	8.401E-05	6.918E-05	5.404E-05	4.268E-05	9.227E-05		
732	9.608E-05	7.246E-05	5.672E-05	4.222E-05	8.907E-05		
762	9.404E-05	7.178E-05	5.727E-05	4.184E-05	8.645E-05		
792	9.013E-05	7.178E-05	5.837E-05	4.197E-05	9.567E-05		
823	9.608E-05	7.007E-05	5.871E-05	4.249E-05	9.342E-05		
853	9.608E-05	7.193E-05	5.918E-05	4.283E-05	9.443E-05		
884	9.626E-05	7.388E-05	5.887E-05	4.322E-05	9.495E-05		
914	9.536E-05	7.366E-05	5.889E-05	4.291E-05	9.536E-05		
945	9.542E-05	7.240E-05	5.930E-05	4.248E-05	9.535E-05		
975	9.248E-05	7.121E-05	5.821E-05	4.203E-05	9.435E-05		
1006	9.244E-05	7.713E-05	5.823E-05	4.205E-05	9.471E-05		
1036	9.342E-05	5.541E-05	5.455E-05	4.284E-05	9.455E-05		
1067	9.423E-05	5.417E-05	5.325E-05	4.283E-05	9.597E-05		
1097	9.473E-05	5.227E-05	5.127E-05	4.297E-05	1.000E-04		
1128	9.101E-05	5.185E-05	5.649E-05	4.317E-05	1.017E-04		
1158	8.500E-05	5.068E-05	4.977E-05	4.328E-05	1.012E-04		
1189	8.072E-05	5.944E-05	4.864E-05	4.293E-05	1.017E-04		
1219	8.070E-05	5.988E-05	4.854E-05	4.223E-05	9.745E-05		
1250	8.835E-05	5.846E-05	4.728E-05	4.171E-05	9.133E-05		
1280	8.748E-05	5.846E-05	4.648E-05	4.641E-05	9.157E-05		
1311	8.632E-05	5.774E-05	4.649E-05	4.632E-05	9.027E-05		
1341	8.414E-05	5.768E-05	4.649E-05	4.557E-05	9.055E-05		
1372	8.208E-05	5.720E-05	4.647E-05	4.508E-05	8.955E-05		
1402	7.885E-05	5.640E-05	4.600E-05	4.527E-05	8.771E-05		
1433	7.837E-05	5.575E-05	4.555E-05	4.509E-05	8.445E-05		
1463	7.747E-05	5.561E-05	4.569E-05	4.510E-05	8.364E-05		
1494	7.661E-05	5.506E-05	4.559E-05	4.543E-05	8.515E-05		
1524	7.608E-05	5.476E-05	4.514E-05	4.544E-05	8.335E-05		
1554	7.779E-05	5.424E-05	4.210E-05	4.787E-05	8.186E-05		
1585	7.604E-05	5.443E-05	4.104E-05	5.765E-05	8.115E-05		
1615	7.606E-05	5.477E-05	4.173E-05	5.765E-05	8.247E-05		
1646	7.509E-05	5.376E-05	4.202E-05	5.726E-05	8.075E-05		
1676	7.444E-05	5.381E-05	4.246E-05	5.717E-05	8.034E-05		
1707	7.333E-05	5.361E-05	4.243E-05	5.717E-05	7.865E-05		
1737	7.369E-05	5.345E-05	4.127E-05	5.705E-05	7.845E-05		
1768	7.244E-05	5.274E-05	4.114E-05	5.692E-05	7.813E-05		
1798	7.201E-05	5.310E-05	4.200E-05	5.680E-05	7.785E-05		
1829	7.200E-05	5.272E-05	4.040E-05	5.668E-05	7.761E-05		

FIRST DATA ALT. 7 7 0 7 6  
LAST DATA ALT. 27 26 57 57 57

FLIGHT NO. 87		FILTER NO. 1						
NEAR TRANS ILLUMINANCE FROM GROUND TO ALTITUDE		ZENITH ANGLE OF PATH OF SIG T (DEGREES)						
ALTITUDE METERS	93	95	100	105	120	150	180	
300	.4677472	.6358021	.7960431	.9585588	.9240355	.9554470	.9612448	
610	.7177050	.4086935	.6482001	.7308440	.7555932	.9138851	.9249774	
914	.1211140	.2418917	.5389982	.6605644	.6068255	.8824462	.8982363	
1217	.0675730	.2112313	.4542363	.5924017	.7624014	.8551543	.8732705	
1524	.0394541	.1042104	.3463590	.5374619	.7251320	.8306386	.8517474	

FLIGHT NO. 87		FILTER NO. 2						
NEAR TRANSMITTANCE FROM GROUND TO ALTITUDE		ZENITH ANGLE OF PATH OF SIG T (DEGREES)						
ALTITUDE METERS	93	95	100	105	120	150	180	
300	.5370350	.6911904	.4307923	.4830504	.9376454	.9655124	.9683225	
610	.7988011	.4416176	.6994490	.7867914	.6832650	.9308437	.9398239	
914	.1896310	.3745110	.6149657	.7216163	.7446056	.9070968	.9190743	
1217	.1254124	.3021711	.5484459	.6683106	.6117123	.8865297	.9009508	
1524	.0661510	.2476235	.4462934	.6249760	.7840271	.8669445	.8854530	

FLIGHT NO. 87		FILTER NO. 3						
NEAR TRANSMITTANCE FROM GROUND TO ALTITUDE		ZENITH ANGLE OF PATH OF SIG T (DEGREES)						
ALTITUDE METERS	93	95	100	105	120	150	180	
300	.5812991	.7240776	.6504130	.8969815	.9452767	.9660303	.9722534	
610	.4365959	.5353926	.7308328	.6102744	.9681154	.9350613	.9470050	
914	.2368573	.4319020	.6561396	.7537343	.6638673	.9169791	.9294408	
1217	.1679009	.3577332	.5769324	.7073959	.6355457	.9017173	.9143023	
1524	.1242203	.3052611	.5512537	.6706642	.6131531	.8874379	.9017590	

FLIGHT NO. 87		FILTER NO. 4					
NEAR TRANSMITTANCE FROM GROUND TO ALTITUDE		ZENITH ANGLE OF PATH OF SIG T (DEGREES)					
ALTITUDE METERS	93	95	100	105	120	150	180
300	.6826117	.7967293	.8922096	.9263327	.9611636	.9773903	.9803425
610	.4935207	.6594697	.8114312	.6691905	.9300014	.9569677	.9643658
914	.3777857	.5570317	.7521995	.6260926	.9058358	.9445030	.9517556
1217	.2661466	.4479563	.6975620	.7853517	.6624319	.9303343	.9393735
1524	.2236097	.4450207	.6506715	.7496686	.6614451	.9174949	.9281407

FLIGHT NO. 87		FILTER NO. 5						
NEAR TRANSMITTANCE FROM GROUND TO ALTITUDE		ZENITH ANGLE OF PATH OF SIG T (DEGREES)						
ALTITUDE METERS	93	95	100	105	120	150	180	
300	.5319274	.6368136	.8281478	.4811635	.9366108	.9628966	.9677545	
610	.7794736	.4714665	.6856491	.7761226	.9771559	.9271212	.9365542	
914	.1569771	.3591754	.5811662	.6944215	.6282235	.8968966	.9100679	
1217	.0643714	.2792765	.4878247	.6178006	.7793547	.8659509	.8826107	
1524	.0472202	.1757316	.4178129	.5566103	.7385314	.8354647	.8523779	

FLIGHT NO. 87		FILTER NO. 1						
PATH RADIANCE FROM GROUND TO ALTITUDE (WATTS/STER.SQ.M MICRO P.)		ZENITH ANGLE OF PATH OF SIGHT (DEGREES)						
ALTITUDE METERS	93	95	100	105	120	150	180	
300	1.011E-06	6.77E-07	3.620E-07	2.390E-07	1.092E-07	5.12E-08	4.139E-08	
610	1.477E-06	1.103E-06	6.426E-07	4.381E-07	2.060E-07	9.75E-08	7.881E-08	
914	1.701E-06	1.342E-06	8.311E-07	5.794E-07	2.779E-07	1.32E-07	1.067E-07	
1214	1.950E-06	1.545E-06	1.032E-06	7.325E-07	3.566E-07	1.68E-07	1.361E-07	
1524	2.059E-06	1.742E-06	1.175E-06	8.486E-07	4.208E-07	2.00E-07	1.619E-07	

FLIGHT NO. 87		FILTER NO. 2						
PATH RADIANCE FROM GROUND TO ALTITUDE (WATTS/STER.SQ.M MICRO P.)		ZENITH ANGLE OF PATH OF SIGHT (DEGREES)						
ALTITUDE METERS	93	95	100	105	120	150	180	
300	1.050E-06	6.440E-07	3.622E-07	2.366E-07	1.053E-07	4.757E-08	3.806E-08	
610	1.690E-06	1.206E-06	6.774E-07	4.552E-07	2.090E-07	9.49E-08	7.548E-08	
914	2.021E-06	1.522E-06	8.918E-07	6.102E-07	2.844E-07	1.29E-07	1.026E-07	
1214	2.427E-06	1.842E-06	1.134E-06	7.860E-07	3.702E-07	1.66E-07	1.314E-07	
1524	2.612E-06	2.057E-06	1.301E-06	8.137E-07	4.360E-07	1.96E-07	1.553E-07	

FLIGHT NO. 87		FILTER NO. 3						
PATH RADIANCE FROM GROUND TO ALTITUDE (WATTS/STER.SQ.M MICRO P.)		ZENITH ANGLE OF PATH OF SIGHT (DEGREES)						
ALTITUDE METERS	93	95	100	105	120	150	180	
300	2.470E-06	1.634E-06	8.292E-07	5.338E-07	2.243E-07	9.081E-08	6.973E-08	
610	3.427E-06	2.426E-06	1.347E-06	8.919E-07	3.876E-07	1.61E-07	1.252E-07	
914	3.865E-06	2.892E-06	1.675E-06	1.129E-06	5.004E-07	2.10E-07	1.634E-07	
1214	4.490E-06	3.411E-06	2.039E-06	1.391E-06	6.233E-07	2.61E-07	2.027E-07	
1524	4.760E-06	3.719E-06	2.286E-06	1.576E-06	7.144E-07	3.01E-07	2.332E-07	

FLIGHT NO. 87		FILTER NO. 4						
PATH RADIANCE FROM GROUND TO ALTITUDE (WATTS/STER.SQ.M MICRO P.)		ZENITH ANGLE OF PATH OF SIGHT (DEGREES)						
ALTITUDE METERS	93	95	100	105	120	150	180	
300								
610								
914								
1214								
1524								

FLIGHT NO. 87		FILTER NO. 5						
PATH RADIANCE FROM GROUND TO ALTITUDE (WATTS/STER.SQ.M MICRO P.)		ZENITH ANGLE OF PATH OF SIGHT (DEGREES)						
ALTITUDE METERS	93	95	100	105	120	150	180	
300	1.453E-06	9.561E-07	5.017E-07	3.297E-07	1.480E-07	6.49E-08	5.233E-08	
610	2.462E-06	1.707E-06	9.549E-07	6.496E-07	2.973E-07	1.32E-07	1.052E-07	
914	2.899E-06	2.216E-06	1.336E-06	8.239E-07	4.370E-07	1.96E-07	1.551E-07	
1214	3.573E-06	2.834E-06	1.787E-06	1.257E-06	6.028E-07	2.71E-07	2.140E-07	
1524	3.711E-06	3.030E-06	2.056E-06	1.475E-06	7.217E-07	3.20E-07	2.542E-07	

FLIGHT NO. 87		FILTER NO. 1						
ALTIMETER		DIRECTIONAL PATH REFLECTANCE FROM GROUND TO ALTITUDE						
METERS		ZENITH ANGLE OF PATH OF SIGHT (DEGREES)						
		93	95	100	105	120	150	180
300	7.7001E-01	5.037E-01	1.631E-01	5.993E-02	4.242E-02	1.926E-02	1.546E-02	
610	2.418E-00	9.606E-01	3.614E-01	2.126E-01	8.644E-02	3.43E-02	3.059E-02	
914	5.049E-00	1.023E-00	5.535E-01	3.149E-01	1.237E-01	5.353E-02	4.26E-02	
1214	1.034E-01	2.713E-00	9.044E-01	4.438E-01	1.079E-01	7.984E-02	5.593E-02	
1524	1.873E-01	5.023E-00	1.004E-00	5.668E-01	2.083E-01	8.66E-02	6.823E-02	

FLIGHT NO. 87		FILTER NO. 2						
ALTIMETER		DIRECTIONAL PATH REFLECTANCE FROM GROUND TO ALTITUDE						
METERS		ZENITH ANGLE OF PATH OF SIGHT (DEGREES)						
		93	95	100	105	120	150	180
300	6.582E-01	3.324E-01	1.459E-01	5.966E-02	3.756E-02	1.652E-02	1.315E-02	
610	1.897E-00	5.223E-01	3.240E-01	2.936E-01	7.716E-02	3.414E-02	2.687E-02	
914	3.563E-00	1.533E-00	4.822E-01	2.829E-01	1.127E-01	4.767E-02	3.735E-02	
1214	6.478E-00	2.007E-00	6.915E-01	5.935E-01	1.226E-01	6.283E-02	4.860E-02	
1524	1.014E-01	2.723E-00	8.708E-01	4.491E-01	1.861E-01	7.57E-02	5.86E-02	

FLIGHT NO. 87		FILTER NO. 3						
ALTIMETER		DIRECTIONAL PATH REFLECTANCE FROM GROUND TO ALTITUDE						
METERS		ZENITH ANGLE OF PATH OF SIGHT (DEGREES)						
		93	95	100	105	120	150	180
300	8.521E-01	4.443E-01	1.999E-01	2.189E-01	4.743E-02	1.875E-02	1.434E-02	
610	1.976E-00	9.027E-01	3.655E-01	2.200E-01	8.639E-02	3.43E-02	2.643E-02	
914	3.279E-00	1.554E-00	5.104E-01	2.793E-01	1.158E-01	4.57E-02	3.514E-02	
1214	5.350E-00	1.906E-00	6.829E-01	3.929E-01	1.490E-01	5.80E-02	4.431E-02	
1524	7.063E-00	2.435E-00	9.290E-01	4.597E-01	1.756E-01	6.783E-02	5.159E-02	

FLIGHT NO. 87		FILTER NO. 4						
ALTIMETER		DIRECTIONAL PATH REFLECTANCE FROM GROUND TO ALTITUDE						
METERS		ZENITH ANGLE OF PATH OF SIGHT (DEGREES)						
		93	95	100	105	120	150	180
300								
610								
914								
1214								
1524								

FLIGHT NO. 87		FILTER NO. 5						
ALTIMETER		DIRECTIONAL PATH REFLECTANCE FROM GROUND TO ALTITUDE						
METERS		ZENITH ANGLE OF PATH OF SIGHT (DEGREES)						
		93	95	100	105	120	150	180
300	6.461E-01	3.272E-01	1.433E-01	5.849E-02	3.736E-02	1.621E-02	1.279E-02	
610	2.019E-00	8.554E-01	3.324E-01	1.979E-01	8.414E-02	3.38E-02	2.656E-02	
914	4.369E-00	1.545E-00	5.435E-01	2.144E-01	1.248E-01	5.175E-02	4.030E-02	
1214	1.002E-01	2.405E-00	6.464E-01	4.812E-01	1.429E-01	7.41E-02	5.772E-02	
1524	1.834E-01	4.172E-00	1.164E-00	5.267E-01	2.311E-01	9.243E-02	7.103E-02	



#### FLIGHT 88I

Starlight before moonrise with a cloud overcast. Data were gathered over the Gulf of Siam approximately 8 km south of Rayong. Depth of water was approximately 20 m (10 fm). Weather was described as clear with some clouds at 600 m. A thick overcast was seen approximately 30 km south of the flight area. A thunderstorm with bright lightning flashes was in the northwest direction. Data-taking started at 2111 local time and ended at 2226.

FLIGHT NO. 88 I				FILTER NO. 1			
IRRADIANCE (WATTS/SQ.M. MICRO M.)							
ALTITUDE (METERS)	DOWN- WELLING	UP- WELLING	ALBEDO	SCALAR DOWNWELLING	SCALAR UPWELLING	SCALAR TOTAL	SCALAR ALBEDO
502	9.083E-06	1.689E-06	.186	1.812E-05	1.469E-05	3.281E-05	.811
810	1.177E-05	3.228E-06	.274	2.842E-05	1.690E-05	4.532E-05	.640
1116	8.838E-06	1.567E-06	.177	1.757E-05	1.019E-05	2.776E-05	.580
1416	9.435E-06	1.856E-06	.197	1.903E-05	8.854E-06	2.789E-05	.465
1707	1.053E-05	1.216E-06	.115	2.088E-05	6.884E-06	2.776E-05	.330

FLIGHT NO. 88 I				FILTER NO. 2			
IRRADIANCE(WATTS/SQ.M.MICRO M.)							
ALTITUDE (METERS)	DOWN- WELLING	UP- WELLING	ALBEDO	SCALAR DOWNWELLING	SCALAR UPWELLING	SCALAR TOTAL	SCALAR ALBEDO
196	1.109E-05	3.111E-06	.281	2.899E-05	1.729E-05	4.628E-05	.597
501	1.018E-05	3.424E-06	.337	2.465E-05	2.233E-05	4.698E-05	.906
809	1.216E-05	4.288E-06	.353	2.818E-05	2.429E-05	5.248E-05	.862
1116	1.352E-05	2.898E-06	.214	2.498E-05	1.911E-05	4.409E-05	.765
1417	1.018E-05	2.569E-06	.252	2.679E-05	1.178E-05	3.857E-05	.440
1707	9.523E-06	2.310E-06	.243	1.905E-05	1.171E-05	3.077E-05	.615

FLIGHT NO. 88 I				FILTER NO. 3			
IRRADIANCE (WATTS/SQ.M. MICRO M.)							
ALTITUDE (METERS)	DOWN- WELLING	UP- WELLING	ALBEDO	SCALAR DOWNWELLING	SCALAR UPWELLING	SCALAR TOTAL	SCALAR ALBEDO
195	1.537E-05	4.325E-06	.281	3.752E-05	2.476E-05	6.228E-05	.660
503	1.565E-05	4.221E-06	.270	3.453E-05	2.933E-05	6.386E-05	.849
810	1.675E-05	4.451E-06	.266	4.123E-05	2.718E-05	6.841E-05	.659
1118	1.614E-05	4.312E-06	.267	3.777E-05	2.717E-05	6.494E-05	.712
1416	1.475E-05	3.881E-06	.263	3.145E-05	2.155E-05	5.300E-05	.685
1706	1.427E-05	3.628E-06	.254	3.121E-05	2.328E-05	5.449E-05	.746

FLIGHT NO. 88 I				FILTER NO. 4			
IRRADIANCE(WATTS/SQ.M.MICRO M.)							
ALTITUDE	DOWN-	UP-		SCALAR	SCALAR	SCALAR	SCALAR
(METERS)	WELLING	WELLING	ALBEDO	DOWNWELLING	UPWELLING	TOTAL	ALBEDO
195							
500							
808							
1116							
1415							
1706							

FLIGHT NO. 88 I				FILTER NO. 5			
IRRADIANCE (WATTS/SQ.M. MICRO M.)							
ALTITUDE (METERS)	UP-		ALBEDO	SCALAR		SCALAR TOTAL	SCALAR ALBEDO
	DOWN- WELLING	WELLING		DOWNWELLING	UPWELLING		
197	1.162E-05	2.170E-06	.187	2.541E-05	1.190E-05	3.731E-05	.468
502	1.407E-05	2.991E-06	.213	3.143E-05	1.543E-05	4.686E-05	.491
809	1.293E-05	2.429E-06	.188	2.825E-05	1.148E-05	3.973E-05	.406
1116	1.280E-05	2.882E-06	.225	2.752E-05	1.367E-05	4.119E-05	.497
1417	1.209E-05	2.415E-06	.200	2.491E-05	1.007E-05	3.497E-05	.404
1707	1.218E-05	2.623E-06	.215	2.546E-05	1.278E-05	3.824E-05	.502

FLIGHT NO. 88 I				
DIRECTIONAL REFLECTANCE OF BACKGROUND				
ZENITH ANGLE	FILTERS			
	1	2	3	4
95	5.93176	4.79026	3.76619	5.05326
95	1.58513	1.80693	1.58344	3.05918
100	.45891	.77244	.47718	.72591
105	.27270	.64826	.34030	.49964
120	.12811	.30431	.17591	.27824
150	.04009	.08886	.09692	.13313
180	.07565	.07814	.09482	.12929

DATE 101968 FLIGHT NO. 88 I GROUND LEVEL ALTITUDE (M.)= 28 IUP=1

ALTITUDE (METERS)	FILTERS	TOTAL SCATTERING COEFFICIENT (PER METER)				
	1	2	3	4	5	
0	1.075E-04	8.003E-05	5.588E-05	4.678E-05	9.865E-05	
30	1.072E-04	7.976E-05	5.569E-05	4.662E-05	9.832E-05	
61	1.068E-04	7.950E-05	5.551E-05	4.647E-05	9.799E-05	
91	1.064E-04	7.923E-05	5.532E-05	4.631E-05	9.766E-05	
122	1.061E-04	7.897E-05	5.514E-05	4.616E-05	9.734E-05	
152	1.057E-04	7.871E-05	5.495E-05	4.601E-05	9.702E-05	
183	1.054E-04	7.844E-05	5.431E-05	4.585E-05	9.669E-05	
213	1.050E-04	7.860E-05	5.423E-05	4.478E-05	9.642E-05	
244	1.001E-04	7.763E-05	5.246E-05	4.310E-05	9.634E-05	
274	1.028E-04	7.625E-05	5.146E-05	4.324E-05	9.382E-05	
305	1.055E-04	7.555E-05	5.120E-05	4.334E-05	9.353E-05	
335	1.061E-04	7.557E-05	5.075E-05	4.406E-05	9.133E-05	
366	1.052E-04	7.453E-05	5.098E-05	4.317E-05	8.991E-05	
396	9.975E-05	7.394E-05	5.092E-05	4.290E-05	8.962E-05	
427	9.771E-05	7.309E-05	5.094E-05	4.181E-05	8.933E-05	
457	9.654E-05	7.392E-05	4.999E-05	4.152E-05	8.941E-05	
488	9.510E-05	7.566E-05	5.028E-05	4.091E-05	8.955E-05	
518	9.235E-05	7.382E-05	4.988E-05	4.063E-05	8.905E-05	
549	9.007E-05	7.209E-05	4.958E-05	4.061E-05	8.901E-05	
579	9.065E-05	7.316E-05	4.949E-05	4.045E-05	8.844E-05	
610	9.045E-05	7.334E-05	4.988E-05	4.037E-05	8.850E-05	
640	8.997E-05	7.273E-05	4.993E-05	4.024E-05	8.831E-05	
671	8.911E-05	7.264E-05	4.925E-05	4.038E-05	8.831E-05	
701	8.845E-05	7.191E-05	4.844E-05	4.051E-05	8.823E-05	
732	8.803E-05	7.142E-05	4.827E-05	4.057E-05	8.882E-05	
762	8.758E-05	7.116E-05	4.823E-05	4.077E-05	8.825E-05	
792	8.837E-05	7.043E-05	4.805E-05	4.087E-05	8.678E-05	
823	8.719E-05	6.985E-05	4.838E-05	4.043E-05	8.568E-05	
853	8.696E-05	6.927E-05	4.813E-05	4.028E-05	8.527E-05	
884	8.696E-05	6.861E-05	4.833E-05	4.038E-05	8.474E-05	
914	8.646E-05	6.753E-05	4.802E-05	3.998E-05	8.409E-05	
945	8.663E-05	6.683E-05	4.826E-05	3.984E-05	8.418E-05	
975	8.645E-05	6.739E-05	4.761E-05	3.993E-05	8.368E-05	
1006	8.702E-05	6.839E-05	4.764E-05	3.963E-05	8.343E-05	
1036	8.665E-05	6.861E-05	4.777E-05	3.942E-05	8.365E-05	
1067	8.885E-05	6.781E-05	4.746E-05	3.935E-05	8.337E-05	
1097	8.405E-05	6.703E-05	4.664E-05	3.892E-05	8.211E-05	
1128	8.344E-05	6.707E-05	4.634E-05	3.874E-05	8.194E-05	
1158	8.349E-05	6.521E-05	4.636E-05	3.876E-05	8.052E-05	
1189	8.271E-05	6.452E-05	4.637E-05	3.871E-05	7.833E-05	
1219	8.396E-05	6.395E-05	4.602E-05	3.897E-05	7.760E-05	
1250	8.405E-05	6.425E-05	4.552E-05	3.879E-05	7.775E-05	
1280	8.200E-05	6.408E-05	4.507E-05	3.867E-05	7.803E-05	
1311	8.087E-05	6.374E-05	4.475E-05	3.863E-05	7.792E-05	
1341	7.929E-05	6.415E-05	4.447E-05	3.867E-05	7.736E-05	
1372	7.956E-05	6.795E-05	4.446E-05	3.841E-05	7.736E-05	
1402	7.843E-05	6.229E-05	4.450E-05	3.839E-05	7.593E-05	
1433	7.717E-05	6.187E-05	4.345E-05	3.811E-05	7.528E-05	
1463	7.648E-05	6.211E-05	4.350E-05	3.801E-05	7.490E-05	
1494	7.610E-05	6.202E-05	4.323E-05	3.801E-05	7.470E-05	
1524	7.654E-05	6.177E-05	4.352E-05	3.771E-05	7.321E-05	
1554	7.636E-05	6.170E-05	4.306E-05	3.748E-05	7.106E-05	
1585	7.671E-05	6.206E-05	4.337E-05	3.724E-05	6.943E-05	
1615	7.619E-05	6.136E-05	4.325E-05	3.705E-05	6.909E-05	
1646	7.619E-05	6.122E-05	4.332E-05	3.685E-05	6.867E-05	
1676	7.624E-05	6.099E-05	4.333E-05	3.661E-05	6.874E-05	
1707	7.563E-05	6.078E-05	4.252E-05	3.649E-05	7.013E-05	
1737	7.538E-05	6.047E-05	4.249E-05	3.637E-05	6.990E-05	
1768	7.513E-05	6.071E-05	4.234E-05	3.625E-05	6.966E-05	
1798	7.480E-05	6.051E-05	4.226E-05	3.613E-05	6.943E-05	
1829	7.463E-05	6.031E-05	4.206E-05	3.601E-05	6.920E-05	

FIRST DATA ALT.

LAST DATA ALT.

57

59

58

56

57

FLIGHT NO. 88 I		FILTER NO. 1						
BEAM TRANSMITTANCE FROM GROUND TO ALTITUDE		ZENITH ANGLE OF PATH OF SIGHT (DEGREES)						
ALTITUDE METERS	93	95	100	105	120	150	180	
305	.5388744	.6921407	.8313654	.8834590	.9378730	.9636456	.9684384	
610	.3010449	.4927715	.7010286	.7879529	.8839437	.9312541	.9401828	
914	.1754306	.3620991	.6005804	.7102935	.8377194	.9028195	.9152701	
1219	.1028332	.2687224	.5170850	.6424237	.7952819	.8761245	.8917858	
1524	.0616748	.2035043	.4497449	.5850141	.7576636	.8519531	.8704388	

FLIGHT NO. 83 I		FILTER NO. 2						
BEAM TRANSMITTANCE FROM GROUND TO ALTITUDE		ZENITH ANGLE OF PATH OF SIGHT (DEGREES)						
ALTITUDE METERS	93	95	100	105	120	150	180	
305	.6305069	.7599491	.8712937	.9117062	.9532776	.9727524	.9763593	
610	.4047154	.5866233	.7651335	.8355961	.9112182	.9477373	.9545775	
914	.2624667	.4578991	.6756737	.7687167	.8727066	.9244007	.9341877	
1219	.1727540	.3624224	.6008494	.7105069	.8378497	.9029006	.9153413	
1524	.1152940	.2907243	.5379178	.6596759	.8062665	.8830909	.8979235	

FLIGHT NO. 88 I		FILTER NO. 3						
BEAM TRANSMITTANCE FROM GROUND TO ALTITUDE		ZENITH ANGLE OF PATH OF SIGHT (DEGREES)						
ALTITUDE METERS	93	95	100	105	120	150	180	
305	.7269810	.8271603	.9091540	.9380993	.9674643	.9810843	.9835976	
610	.5377186	.6936518	.8322760	.8841081	.9382296	.9638572	.9686225	
914	.3995208	.5852389	.7642267	.8349315	.9108430	.9475120	.9543809	
1219	.2976237	.4962772	.7035274	.7898361	.8850366	.9319188	.9407639	
1524	.2239461	.4248873	.6507691	.7495894	.8613980	.9174659	.9281153	

FLIGHT NO. 88 I		FILTER NO. 4						
BEAM TRANSMITTANCE FROM GROUND TO ALTITUDE		ZENITH ANGLE OF PATH OF SIGHT (DEGREES)						
ALTITUDE METERS	93	95	100	105	120	150	180	
305	.7660121	.8533100	.9234680	.9479832	.9727274	.9841622	.9862694	
610	.5763089	.7372818	.8581515	.9024567	.9482591	.9697924	.9737859	
914	.4474439	.6400011	.7993191	.8604637	.9251562	.9560801	.9618504	
1219	.3643564	.5578589	.7460674	.8215682	.9032673	.9429540	.9504038	
1524	.2851240	.4877477	.6974324	.7852386	.8823662	.9302943	.9393435	

FLIGHT NO. 88 I		FILTER NO. 5						
BEAM TRANSMITTANCE FROM GROUND TO ALTITUDE		ZENITH ANGLE OF PATH OF SIGHT (DEGREES)						
ALTITUDE METERS	93	95	100	105	120	150	180	
305	.5663051	.7128567	.8437865	.8772932	.9427159	.9665154	.9709356	
610	.3309311	.5210033	.7209073	.8028747	.8925695	.9364901	.9447590	
914	.1943683	.3842387	.6187385	.7246310	.8464303	.9082277	.9200165	
1219	.1162377	.2882340	.5356002	.6577676	.8050584	.8823267	.8972505	
1524	.0711403	.2206037	.4683308	.6011261	.7683943	.8588988	.8765811	

FLIGHT NO. 88 1		FILTER NO. 1						
PATH RADIANCE FROM GROUND TO ALTITUDE (WATTS/STER.SQ.M MICRO M.)		ZENITH ANGLE OF PATH OF SIGHT (DEGREES)						
ALTITUDE METERS	95	95	100	105	120	150	180	
305	1.431E-06	9.417E-07	4.930E-07	3.209E-07	1.380E-07	5.771E-08	4.478E-08	
610	2.199E-06	1.570E-06	8.133E-07	5.900E-07	2.605E-07	1.103E-07	8.577E-08	
914	2.647E-06	2.140E-06	1.268E-06	8.655E-07	3.920E-07	1.680E-07	1.308E-07	
1219	2.639E-06	2.303E-06	1.463E-06	1.024E-06	4.777E-07	2.087E-07	1.633E-07	
1524	2.697E-06	2.327E-06	1.572E-06	1.128E-06	5.434E-07	2.413E-07	1.897E-07	

FLIGHT NO. 94 1		FILTER NO. 2						
PATH RADIANCE FROM GROUND TO ALTITUDE (WATTS/STER.SQ.M MICRO M.)		ZENITH ANGLE OF PATH OF SIGHT (DEGREES)						
ALTITUDE METERS	95	95	100	105	120	150	180	
305	1.665E-06	1.067E-06	5.474E-07	3.544E-07	1.526E-07	6.261E-08	4.751E-08	
610	2.749E-06	1.876E-06	1.020E-06	6.748E-07	2.959E-07	1.217E-07	9.233E-08	
914	2.510E-06	2.507E-06	1.453E-06	9.795E-07	4.385E-07	1.821E-07	1.384E-07	
1219	3.752E-06	2.873E-06	1.734E-06	1.193E-06	5.459E-07	2.307E-07	1.763E-07	
1524	3.736E-06	3.017E-06	1.914E-06	1.341E-06	6.267E-07	2.686E-07	2.061E-07	

FLIGHT NO. 86 1		FILTER NO. 3						
PATH RADIANCE FROM GROUND TO ALTITUDE (WATTS/STER.SQ.M MICRO M.)		ZENITH ANGLE OF PATH OF SIGHT (DEGREES)						
ALTITUDE METERS	95	95	100	105	120	150	180	
305	1.664E-06	1.038E-06	5.199E-07	3.326E-07	1.393E-07	5.554E-08	4.222E-08	
610	2.664E-06	1.848E-06	9.744E-07	6.318E-07	2.674E-07	1.069E-07	8.132E-08	
914	3.875E-06	2.595E-06	1.402E-06	9.206E-07	3.941E-07	1.579E-07	1.201E-07	
1219	4.473E-06	3.154E-06	1.766E-06	1.174E-06	5.007E-07	2.046E-07	1.557E-07	
1524	4.695E-06	3.451E-06	2.008E-06	1.354E-06	5.958E-07	2.419E-07	1.844E-07	

FLIGHT NO. 80 1		FILTER NO. 4						
PATH RADIANCE FROM GROUND TO ALTITUDE (WATTS/STER.SQ.M MICRO M.)		ZENITH ANGLE OF PATH OF SIGHT (DEGREES)						
ALTITUDE METERS	95	95	100	105	120	150	180	
305								
610								
914								
1219								
1524								

FLIGHT NO. 83 1		FILTER NO. 5						
PATH RADIANCE FROM GROUND TO ALTITUDE (WATTS/STER.SQ.M MICRO M.)		ZENITH ANGLE OF PATH OF SIGHT (DEGREES)						
ALTITUDE METERS	95	95	100	105	120	150	180	
305	1.499E-06	7.738E-07	5.026E-07	3.259E-07	1.412E-07	6.038E-08	4.722E-08	
610	2.565E-06	1.788E-06	9.833E-07	6.522E-07	2.892E-07	1.242E-07	9.696E-08	
914	3.333E-06	2.274E-06	1.335E-06	9.673E-07	4.130E-07	1.802E-07	1.411E-07	
1219	3.279E-06	2.609E-06	1.615E-06	1.121E-06	5.228E-07	2.308E-07	1.810E-07	
1524	3.257E-06	2.727E-06	1.789E-06	1.270E-06	6.067E-07	2.718E-07	2.139E-07	

FLIGHT NO. 88 I		FILTER NO. 1						
DIRECTIONAL PATH REFLECTANCE FROM GROUND TO ALTITUDE		ZENITH ANGLE OF PATH OF SIGHT (DEGREES)						
ALTITUDE		93	95	100	105	120	150	180
METERS								
305	9.183E-01	4.705E-01	2.051E-01	1.256E-01	5.089E-02	2.071E-02	1.599E-02	
610	2.526E 00	1.102E 00	4.358E-01	2.590E-01	1.019E-01	4.097E-02	3.155E-02	
914	5.612E 00	2.044E 00	7.305E-01	4.214E-01	1.618E-01	6.435E-02	4.943E-02	
1219	9.547E 00	2.964E 00	9.783E-01	5.514E-01	2.078E-01	8.239E-02	6.333E-02	
1524	1.513E 01	3.955E 00	1.209E 00	6.666E-01	2.472E-01	9.795E-02	7.539E-02	

FLIGHT NO. 88 I		FILTER NO. 2						
DIRECTIONAL PATH REFLECTANCE FROM GROUND TO ALTITUDE		ZENITH ANGLE OF PATH OF SIGHT (DEGREES)						
ALTITUDE		93	95	100	105	120	150	180
METERS								
305	7.483E-01	7.979E-01	1.780E-01	1.102E-01	4.537E-02	1.824E-02	1.379E-02	
610	1.918E 00	9.000E-01	3.779E-01	2.288E-01	9.200E-02	3.639E-02	2.741E-02	
914	3.789E 00	1.570E 00	6.092E-01	3.611E-01	1.424E-01	5.582E-02	4.198E-02	
1219	6.154E 00	2.246E 00	8.179E-01	4.756E-01	1.946E-01	7.241E-02	5.457E-02	
1524	9.183E 00	2.941E 00	1.008E 00	5.760E-01	2.202E-01	8.619E-02	6.503E-02	

FLIGHT NO. 88 I		FILTER NO. 3						
DIRECTIONAL PATH REFLECTANCE FROM GROUND TO ALTITUDE		ZENITH ANGLE OF PATH OF SIGHT (DEGREES)						
ALTITUDE		93	95	100	105	120	150	180
METERS								
305	4.679E-01	2.554E-01	1.169E-01	7.246E-02	2.943E-02	1.157E-02	8.772E-03	
610	1.088E 00	5.504E-01	2.393E-01	1.461E-01	5.826E-02	2.266E-02	1.716E-02	
914	1.957E 00	9.062E-01	3.751E-01	2.254E-01	8.843E-02	3.406E-02	2.572E-02	
1219	3.072E 00	1.299E 00	5.131E-01	3.038E-01	1.175E-01	4.487E-02	3.382E-02	
1524	4.235E 00	1.660E 00	6.306E-01	3.691E-01	1.414E-01	5.388E-02	4.000E-02	

FLIGHT NO. 88 I		FILTER NO. 4						
DIRECTIONAL PATH REFLECTANCE FROM GROUND TO ALTITUDE		ZENITH ANGLE OF PATH OF SIGHT (DEGREES)						
ALTITUDE		93	95	100	105	120	150	180
METERS								
305								
610								
914								
1219								
1524								

FLIGHT NO. 88 I		FILTER NO. 5						
DIRECTIONAL PATH REFLECTANCE FROM GROUND TO ALTITUDE		ZENITH ANGLE OF PATH OF SIGHT (DEGREES)						
ALTITUDE		93	95	100	105	120	150	180
METERS								
305	7.159E-01	3.694E-01	1.612E-01	9.877E-02	4.050E-02	1.689E-02	1.315E-02	
610	2.096E 00	9.280E-01	3.688E-01	2.197E-01	8.761E-02	3.588E-02	2.775E-02	
914	4.220E 00	1.600E 00	5.876E-01	3.386E-01	1.320E-01	5.364E-02	4.146E-02	
1219	7.627E 00	2.439E 00	8.153E-01	4.610E-01	1.756E-01	7.073E-02	5.456E-02	
1524	1.238E 01	3.343E 00	1.033E 00	5.712E-01	2.135E-01	8.556E-02	6.598E-02	

#### FLIGHT 88 II

Starlight before moonrise with scattered clouds. The location for this flight was a valley about 40 km east of Rayong. The terrain was relatively flat, cultivated (but not with rice paddies), and interspersed with small tree-covered knolls. In addition to the scattered clouds at 600 m, there was an overcast, 140 km to the south and thunderstorms were seen in the northwest direction. Data-taking started at 2242 local time and ended at 2332.

FLIGHT NO. 88 II      FILTER NO. 3  
 IRRADIANCE (WATTS/SQ. M. MICRO M.)

ALTITUDE (METERS)	DOWN- WELLING	UP- WELLING	ALBEDO	SCALAR DOWNWELLING	SCALAR UPWELLING	SCALAR TOTAL	SCALAR ALBEDO
779	9.351E-06	9.463E-07	.113	1.674E-05	5.785E-06	2.253E-05	.345
1072	7.287E-06	1.040E-06	.143	1.458E-05	5.463E-06	2.004E-05	.375
1388	9.381E-06	1.713E-06	.103	1.897E-05	1.043E-05	2.900E-05	.561
1707	9.694E-06	1.125E-06	.103	1.383E-05	6.586E-06	2.041E-05	.476

FLIGHT NO. 88 II      FILTER NO. 3  
 IRRADIANCE (WATTS/SQ. M. MICRO M.)

ALTITUDE (METERS)	DOWN- WELLING	UP- WELLING	ALBEDO	SCALAR DOWNWELLING	SCALAR UPWELLING	SCALAR TOTAL	SCALAR ALBEDO
780	9.054E-06	1.090E-06	.175	1.935E-05	9.431E-06	2.878E-05	.487
1072	9.973E-06	4.310E-06	.503	1.748E-05	1.535E-05	3.283E-05	.878
1387	9.003E-06	2.246E-06	.229	1.977E-05	1.233E-05	3.210E-05	.624
1706	9.030E-06	1.969E-06	.245	1.682E-05	9.786E-06	2.661E-05	.582

FLIGHT NO. 88 II      FILTER NO. 3  
 IRRADIANCE (WATTS/SQ. M. MICRO M.)

ALTITUDE (METERS)	DOWN- WELLING	UP- WELLING	ALBEDO	SCALAR DOWNWELLING	SCALAR UPWELLING	SCALAR TOTAL	SCALAR ALBEDO
779	1.470E-05	3.005E-06	.203	3.136E-05	2.150E-05	5.286E-05	.686
1071	1.475E-05	4.351E-06	.295	3.041E-05	2.210E-05	5.251E-05	.727
1388	1.627E-05	4.004E-06	.246	4.607E-05	2.645E-05	7.252E-05	.574
1706	1.578E-05	3.281E-06	.238	2.912E-05	1.935E-05	4.847E-05	.664

FLIGHT NO. 88 II      FILTER NO. 3  
 IRRADIANCE (WATTS/SQ. M. MICRO M.)

ALTITUDE (METERS)	DOWN- WELLING	UP- WELLING	ALBEDO	SCALAR DOWNWELLING	SCALAR UPWELLING	SCALAR TOTAL	SCALAR ALBEDO
779							
1071							
1388							
1707							

FLIGHT NO. 88 II      FILTER NO. 3  
 IRRADIANCE (WATTS/SQ. M. MICRO M.)

ALTITUDE (METERS)	DOWN- WELLING	UP- WELLING	ALBEDO	SCALAR DOWNWELLING	SCALAR UPWELLING	SCALAR TOTAL	SCALAR ALBEDO
779	1.121E-05	2.047E-06	.146	2.287E-05	1.089E-05	3.375E-05	.476
1072	1.174E-05	2.040E-06	.174	2.405E-05	1.125E-05	3.530E-05	.468
1388	1.169E-05	2.142E-06	.183	2.378E-05	1.128E-05	3.506E-05	.474
1706	1.180E-05	2.063E-06	.158	2.245E-05	1.060E-05	3.305E-05	.472

FLIGHT NO. 88 II  
 IRRADIANCE (WATTS/SQ. M. MICRO M.)

ANGLE	1	2	5	3	4
90	1.188E-05	3.850E-06	3.47437	6.00634	
90	1.05935	2.31355	2.35217	3.42457	
100	1.17023	.41524	.34201	.36297	
100	1.1734	.28015	.21322	.21615	
100	1.06916	.15831	.15306	.15783	
100	1.1712	.16715	.12779	.12986	
100	1.1712	.08448	.11660	.11631	



DATE 101908 FLIGHT NO. 88 II GROUND LEVEL ALTITUDE (M.)= 44 ILP=1

ALTITUDE (METERS)	TOTAL SCATTERING COEFFICIENT (FE. METER)				
	FILICERS	1	2	3	4
0	8.547E-05	6.798E-05	5.304E-05	4.110E-05	9.110E-05
30	8.519E-05	6.776E-05	5.287E-05	4.097E-05	9.088E-05
61	8.490E-05	6.753E-05	5.269E-05	4.083E-05	9.045E-05
91	8.462E-05	6.731E-05	5.252E-05	4.069E-05	9.015E-05
122	8.434E-05	6.708E-05	5.234E-05	4.056E-05	8.985E-05
152	8.406E-05	6.686E-05	5.217E-05	4.042E-05	8.955E-05
183	8.378E-05	6.664E-05	5.199E-05	4.029E-05	8.925E-05
213	8.350E-05	6.641E-05	5.182E-05	4.016E-05	8.895E-05
244	8.322E-05	6.619E-05	5.165E-05	4.002E-05	8.865E-05
274	8.294E-05	6.597E-05	5.148E-05	3.989E-05	8.835E-05
305	8.267E-05	6.575E-05	5.130E-05	3.976E-05	8.805E-05
335	8.239E-05	6.554E-05	5.113E-05	3.962E-05	8.775E-05
366	8.212E-05	6.532E-05	5.096E-05	3.949E-05	8.745E-05
396	8.184E-05	6.510E-05	5.079E-05	3.936E-05	8.715E-05
427	8.157E-05	6.488E-05	5.063E-05	3.923E-05	8.685E-05
457	8.130E-05	6.467E-05	5.046E-05	3.910E-05	8.655E-05
488	8.103E-05	6.445E-05	5.029E-05	3.897E-05	8.625E-05
518	8.076E-05	6.424E-05	5.012E-05	3.884E-05	8.595E-05
549	8.049E-05	6.402E-05	4.995E-05	3.871E-05	8.565E-05
579	8.022E-05	6.381E-05	4.979E-05	3.858E-05	8.535E-05
610	7.995E-05	6.360E-05	4.962E-05	3.845E-05	8.505E-05
640	7.968E-05	6.339E-05	4.946E-05	3.832E-05	8.475E-05
671	7.941E-05	6.318E-05	4.929E-05	3.820E-05	8.445E-05
701	7.914E-05	6.297E-05	4.913E-05	3.807E-05	8.415E-05
732	7.887E-05	6.276E-05	4.897E-05	3.794E-05	8.385E-05
762	7.860E-05	6.255E-05	4.880E-05	3.782E-05	8.355E-05
792	7.833E-05	6.234E-05	4.864E-05	3.769E-05	8.325E-05
823	7.806E-05	6.213E-05	4.848E-05	3.756E-05	8.295E-05
853	7.779E-05	6.192E-05	4.832E-05	3.744E-05	8.265E-05
884	7.752E-05	6.171E-05	4.816E-05	3.731E-05	8.235E-05
914	7.725E-05	6.150E-05	4.800E-05	3.719E-05	8.205E-05
945	7.698E-05	6.129E-05	4.784E-05	3.706E-05	8.175E-05
975	7.671E-05	6.108E-05	4.768E-05	3.694E-05	8.145E-05
1006	7.644E-05	6.087E-05	4.752E-05	3.681E-05	8.115E-05
1036	7.617E-05	6.066E-05	4.736E-05	3.669E-05	8.085E-05
1067	7.590E-05	6.045E-05	4.720E-05	3.656E-05	8.055E-05
1097	7.563E-05	6.024E-05	4.704E-05	3.644E-05	8.025E-05
1128	7.536E-05	6.003E-05	4.688E-05	3.632E-05	7.995E-05
1158	7.509E-05	5.982E-05	4.672E-05	3.620E-05	7.965E-05
1189	7.482E-05	5.961E-05	4.656E-05	3.608E-05	7.935E-05
1219	7.455E-05	5.940E-05	4.640E-05	3.596E-05	7.905E-05
1250	7.428E-05	5.919E-05	4.624E-05	3.584E-05	7.875E-05
1280	7.401E-05	5.898E-05	4.608E-05	3.572E-05	7.845E-05
1311	7.374E-05	5.877E-05	4.592E-05	3.560E-05	7.815E-05
1341	7.347E-05	5.856E-05	4.576E-05	3.548E-05	7.785E-05
1372	7.320E-05	5.835E-05	4.560E-05	3.536E-05	7.755E-05
1402	7.293E-05	5.814E-05	4.544E-05	3.524E-05	7.725E-05
1433	7.266E-05	5.793E-05	4.528E-05	3.512E-05	7.695E-05
1463	7.239E-05	5.772E-05	4.512E-05	3.500E-05	7.665E-05
1494	7.212E-05	5.751E-05	4.496E-05	3.488E-05	7.635E-05
1524	7.185E-05	5.730E-05	4.480E-05	3.476E-05	7.605E-05
1554	7.158E-05	5.709E-05	4.464E-05	3.464E-05	7.575E-05
1585	7.131E-05	5.688E-05	4.448E-05	3.452E-05	7.545E-05
1615	7.104E-05	5.667E-05	4.432E-05	3.440E-05	7.515E-05
1646	7.077E-05	5.646E-05	4.416E-05	3.428E-05	7.485E-05
1676	7.050E-05	5.625E-05	4.400E-05	3.416E-05	7.455E-05
1707	7.023E-05	5.604E-05	4.384E-05	3.404E-05	7.425E-05
1737	6.996E-05	5.583E-05	4.368E-05	3.392E-05	7.395E-05
1768	6.969E-05	5.562E-05	4.352E-05	3.380E-05	7.365E-05
1798	6.942E-05	5.541E-05	4.336E-05	3.368E-05	7.335E-05
1829	6.915E-05	5.520E-05	4.320E-05	3.356E-05	7.305E-05

FIRST DATA ALT. 27 21 25 26 27  
LAST DATA ALT. 27 57 57 59 59

FLIGHT NO. 88 II		FILTER NO. 1						
ALTIMETER		BEAM TRANSMITTANCE FROM GROUND TO ALTITUDE						
METERS		ZENITH ANGLE OF PATH OF SIGHT (DEGREES)						
		93	95	100	105	120	150	180
300	.6162093	.7452875	.8026160	.9057449	.9500460	.9708471	.9747030	
610	.5750500	.5508334	.7480614	.5230407	.9041050	.9434588	.9508444	
914	.2316244	.4255637	.6512880	.7499911	.8616349	.9176128	.9282440	
1214	.1454674	.3279409	.5714431	.6869848	.8237749	.8928616	.9074001	
1524	.0924661	.2261082	.5047564	.6321064	.7884447	.8718955	.8880567	

FLIGHT NO. 88 II		FILTER NO. 2						
ALTIMETER		BEAM TRANSMITTANCE FROM GROUND TO ALTITUDE						
METERS		ZENITH ANGLE OF PATH OF SIGHT (DEGREES)						
		93	95	100	105	120	150	180
300	.6751102	.7714970	.8092639	.9242797	.9600674	.9767424	.9798767	
610	.4583946	.6312584	.7938388	.8565011	.9226484	.9547621	.9617020	
914	.3133104	.5077045	.7116123	.7959145	.8885557	.9340564	.9426524	
1214	.2176613	.4141407	.6424550	.7431507	.8576559	.9151535	.9260453	
1524	.1501695	.3418672	.5834453	.6966324	.8293402	.8975948	.9176412	

FLIGHT NO. 88 II		FILTER NO. 3						
ALTIMETER		BEAM TRANSMITTANCE FROM GROUND TO ALTITUDE						
METERS		ZENITH ANGLE OF PATH OF SIGHT (DEGREES)						
		93	95	100	105	120	150	180
300	.7054050	.8032296	.9124961	.9404116	.9684979	.9818064	.9842245	
610	.5443127	.6964366	.8351525	.8861571	.9393545	.9645242	.9692030	
914	.4060667	.5932897	.7894795	.8387775	.9130123	.9468142	.9555168	
1214	.3142262	.5124075	.7144132	.7983896	.8896850	.9340235	.9433902	
1524	.2437282	.4463374	.6676565	.7621251	.8688250	.9220247	.9321678	

FLIGHT NO. 88 II		FILTER NO. 4						
ALTIMETER		BEAM TRANSMITTANCE FROM GROUND TO ALTITUDE						
METERS		ZENITH ANGLE OF PATH OF SIGHT (DEGREES)						
		93	95	100	105	120	150	180
300	.7864633	.8561613	.9315002	.9535074	.9756574	.9858727	.9877537	
610	.6230910	.7272055	.8697135	.9105065	.9526768	.9723984	.9780516	
914	.4948965	.6530757	.8136559	.8707881	.9308858	.9554941	.9648242	
1214	.3948172	.5942665	.7635891	.8344641	.9105750	.9473534	.9542426	
1524	.3123303	.5165975	.7178410	.8005819	.8912452	.9356900	.9447049	

FLIGHT NO. 88 II		FILTER NO. 5						
ALTIMETER		BEAM TRANSMITTANCE FROM GROUND TO ALTITUDE						
METERS		ZENITH ANGLE OF PATH OF SIGHT (DEGREES)						
		93	95	100	105	120	150	180
300	.5906811	.7309082	.8544732	.9998596	.9468485	.9689575	.9770239	
610	.3515053	.5708765	.7338986	.8125533	.8981232	.9358498	.9476236	
914	.2107380	.4027145	.6335004	.7361851	.8533858	.9125317	.9247410	
1214	.1302632	.3078216	.5535696	.6724932	.8143360	.8861842	.9024166	
1524	.0820213	.2399930	.4685573	.6184230	.7797610	.8662115	.8847407	

FLIGHT NO. 88 II      FILTER NO. 1

PATH RADIANCE FROM GROUND TO ALTITUDE (WATT/STER.SQ.M MICRO M.)

ALTITUDE      ZENITH ANGLE OF PATH OF SIGHT (DEGREES)

METERS	93	95	100	105	120	150	180
300	7.511E-07	4.813E-07	2.455E-07	1.586E-07	6.972E-08	3.194E-08	2.577E-08
610	1.204E-06	8.249E-07	4.504E-07	2.978E-07	1.338E-07	6.194E-08	5.008E-08
914	1.471E-06	1.040E-06	6.214E-07	4.191E-07	1.925E-07	8.995E-08	7.290E-08
1219	1.614E-06	1.249E-06	7.566E-07	5.206E-07	2.441E-07	1.152E-07	9.341E-08
1524	1.666E-06	1.472E-06	9.317E-07	6.497E-07	3.082E-07	1.445E-07	1.172E-07

FLIGHT NO. 88 II      FILTER NO. 2

PATH RADIANCE FROM GROUND TO ALTITUDE (WATT/STER.SQ.M MICRO M.)

ALTITUDE      ZENITH ANGLE OF PATH OF SIGHT (DEGREES)

METERS	93	95	100	105	120	150	180
300	6.231E-07	5.195E-07	2.630E-07	1.698E-07	7.435E-08	3.511E-08	2.628E-08
610	1.372E-06	9.146E-07	4.896E-07	3.218E-07	1.434E-07	6.445E-08	5.119E-08
914	1.754E-06	1.246E-06	6.903E-07	4.619E-07	2.100E-07	9.487E-08	7.540E-08
1219	2.194E-06	1.535E-06	8.950E-07	5.110E-07	2.357E-07	1.290E-07	1.019E-07
1524	2.417E-06	1.750E-06	1.003E-06	7.351E-07	3.480E-07	1.572E-07	1.246E-07

FLIGHT NO. 88 II      FILTER NO. 3

PATH RADIANCE FROM GROUND TO ALTITUDE (WATT/STER.SQ.M MICRO M.)

ALTITUDE      ZENITH ANGLE OF PATH OF SIGHT (DEGREES)

METERS	93	95	100	105	120	150	180
300	1.422E-06	8.224E-07	4.090E-07	2.602E-07	1.082E-07	4.420E-08	3.421E-08
610	2.284E-06	1.437E-06	7.706E-07	4.972E-07	2.095E-07	8.618E-08	6.674E-08
914	2.462E-06	2.004E-06	1.077E-06	7.040E-07	3.008E-07	1.247E-07	9.677E-08
1219	3.475E-06	2.426E-06	1.346E-06	8.905E-07	3.864E-07	1.620E-07	1.263E-07
1524	4.171E-06	2.944E-06	1.674E-06	1.115E-06	4.857E-07	2.030E-07	1.580E-07

FLIGHT NO. 88 II      FILTER NO. 4

PATH RADIANCE FROM GROUND TO ALTITUDE (WATT/STER.SQ.M MICRO M.)

ALTITUDE      ZENITH ANGLE OF PATH OF SIGHT (DEGREES)

METERS	93	95	100	105	120	150	180
300							
610							
914							
1219							
1524							

FLIGHT NO. 88 II      FILTER NO. 5

PATH RADIANCE FROM GROUND TO ALTITUDE (WATT/STER.SQ.M MICRO M.)

ALTITUDE      ZENITH ANGLE OF PATH OF SIGHT (DEGREES)

METERS	93	95	100	105	120	150	180
300	1.222E-06	7.638E-07	4.055E-07	2.628E-07	1.166E-07	5.176E-08	4.123E-08
610	1.433E-06	1.344E-06	7.415E-07	4.918E-07	2.234E-07	1.003E-07	8.006E-08
914	2.362E-06	1.736E-06	1.023E-06	6.433E-07	3.215E-07	1.458E-07	1.166E-07
1219	2.642E-06	2.051E-06	1.259E-06	7.688E-07	4.072E-07	1.864E-07	1.494E-07
1524	2.805E-06	2.225E-06	1.450E-06	8.117E-07	4.340E-07	2.231E-07	1.790E-07

FLIGHT NO. 88 II      FILTER NO. 1

ALTITUDE METERS	DIRECTIONAL PATH REFLECTANCE FROM GROUND TO ALTITUDE ZENITH ANGLE OF PATH OF SIGHT (DEGREES)						
	93	95	100	105	120	150	180
305	4.631E-01	2.436E-01	1.070E-01	5.88E-02	2.761E-02	1.237E-02	9.947E-03
610	1.268E-00	5.557E-01	2.267E-01	1.361E-01	5.569E-02	2.470E-02	1.981E-02
914	2.398E-00	9.546E-01	3.589E-01	1.102E-01	8.103E-02	3.685E-02	2.954E-02
1219	4.176E-00	1.652E-00	4.980E-01	1.451E-01	1.115E-01	4.847E-02	3.872E-02
1524	7.674E-00	2.192E-00	6.944E-01	1.906E-01	1.470E-01	6.252E-02	4.964E-02

FLIGHT NO. 88 II      FILTER NO. 2

ALTITUDE METERS	DIRECTIONAL PATH REFLECTANCE FROM GROUND TO ALTITUDE ZENITH ANGLE OF PATH OF SIGHT (DEGREES)						
	93	95	100	105	120	150	180
305	3.966E-01	2.135E-01	9.619E-02	5.977E-02	2.519E-02	1.105E-02	8.723E-03
610	9.737E-01	4.733E-01	2.006E-01	1.222E-01	5.055E-02	2.194E-02	1.733E-02
914	1.621E-00	7.914E-01	3.156E-01	1.088E-01	7.686E-02	3.304E-02	2.602E-02
1219	3.129E-00	1.206E-00	4.532E-01	1.675E-01	1.084E-01	4.586E-02	3.580E-02
1524	4.923E-00	1.675E-00	5.924E-01	1.432E-01	1.365E-01	5.716E-02	4.452E-02

FLIGHT NO. 88 II      FILTER NO. 3

ALTITUDE METERS	DIRECTIONAL PATH REFLECTANCE FROM GROUND TO ALTITUDE ZENITH ANGLE OF PATH OF SIGHT (DEGREES)						
	93	95	100	105	120	150	180
305	3.827E-01	2.098E-01	9.530E-02	5.884E-02	2.374E-02	9.571E-03	7.389E-03
610	8.940E-01	4.527E-01	1.962E-01	1.193E-01	4.743E-02	1.905E-02	1.465E-02
914	1.540E-00	7.190E-01	2.976E-01	1.784E-01	7.005E-02	2.793E-02	2.153E-02
1219	2.350E-00	1.017E-00	4.002E-01	1.371E-01	9.230E-02	3.684E-02	2.847E-02
1524	3.638E-00	1.412E-00	5.336E-01	1.110E-01	1.189E-01	4.680E-02	3.603E-02

FLIGHT NO. 88 II      FILTER NO. 4

ALTITUDE METERS	DIRECTIONAL PATH REFLECTANCE FROM GROUND TO ALTITUDE ZENITH ANGLE OF PATH OF SIGHT (DEGREES)						
	93	95	100	105	120	150	180
305							
610							
914							
1219							
1524							

FLIGHT NO. 88 II      FILTER NO. 5

ALTITUDE METERS	DIRECTIONAL PATH REFLECTANCE FROM GROUND TO ALTITUDE ZENITH ANGLE OF PATH OF SIGHT (DEGREES)						
	93	95	100	105	120	150	180
305	5.801E-01	3.027E-01	1.331E-01	1.190E-02	3.453E-02	1.496E-02	1.188E-02
610	1.544E-00	7.016E-01	2.834E-01	1.598E-01	6.977E-02	2.993E-02	2.369E-02
914	3.144E-00	1.223E-00	4.530E-01	1.541E-01	1.057E-01	4.482E-02	3.541E-02
1219	5.094E-00	1.677E-00	6.388E-01	1.623E-01	1.402E-01	5.887E-02	4.643E-02
1524	9.546E-00	2.658E-00	8.324E-01	4.614E-01	1.737E-01	7.222E-02	5.686E-02

#### FLIGHT 89

Starlight before moonrise with thick overcast at 1500 m. The flight pattern was from Lop Buri to approximately 40 km west of Sing Buri. The terrain was flat (river delta country) and cultivated with rice paddies and other crops; there were also small scattered settlements. The illumination from ground lights on the surface of the overcast was readily discernible. Data-taking started at 2020 local time and ended at 2110.

FLIGHT NO. 89				FILTER NO. 1			
IRRADIANCE (WATTS/SQ.M. MICRO M.)							
ALTITUDE	DOWN-	UP-		SCALAR	SCALAR	SCALAR	SCALAR
(METERS)	WELLING	WELLING	ALBEDO	DOWNWELLING	UPWELLING	TOTAL	ALBEDO
362	6.204E-06	9.175E-07	.148	1.280E-05	4.979E-06	1.778E-05	.389
642	4.784E-06	1.661E-06	.347	9.464E-06	7.604E-06	1.707E-05	.804
943	6.569E-06	1.595E-06	.243	1.177E-05	7.354E-06	1.912E-05	.625
1236	5.543E-06	1.484E-06	.268	1.027E-05	6.329E-06	1.660E-05	.616

FLIGHT NO. 89				FILTER NO. 2			
IRRADIANCE (WATTS/SQ.M. MICRO M.)							
ALTITUDE	DOWN-	UP-		SCALAR	SCALAR	SCALAR	SCALAR
(METERS)	WELLING	WELLING	ALBEDO	DOWNWELLING	UPWELLING	TOTAL	ALBEDO
363	5.577E-06	2.658E-06	.477	1.175E-05	1.024E-05	2.199E-05	.871
642	5.117E-06	2.923E-06	.571	1.011E-05	1.210E-05	2.220E-05	1.197
943	6.537E-06	5.476E-06	.838	1.251E-05	1.670E-05	2.922E-05	1.335
1235	4.821E-06	2.429E-06	.504	9.707E-06	1.016E-05	1.987E-05	1.047

FLIGHT NO. 89				FILTER NO. 3			
IRRADIANCE (WATTS/SQ.M. MICRO M.)							
ALTITUDE	DOWN-	UP-		SCALAR	SCALAR	SCALAR	SCALAR
(METERS)	WELLING	WELLING	ALBEDO	DOWNWELLING	UPWELLING	TOTAL	ALBEDO
361	9.706E-06	3.367E-06	.347	1.987E-05	1.687E-05	3.674E-05	.849
642	1.024E-05	4.964E-06	.485	1.986E-05	2.381E-05	4.367E-05	1.199
942	1.103E-05	6.713E-06	.609	2.135E-05	2.324E-05	4.459E-05	1.089
1237	1.065E-05	4.189E-06	.393	1.990E-05	1.958E-05	3.948E-05	.984

FLIGHT NO. 89				FILTER NO. 4			
IRRADIANCE (WATTS/SQ.M. MICRO M.)							
ALTITUDE	DOWN-	UP-		SCALAR	SCALAR	SCALAR	SCALAR
(METERS)	WELLING	WELLING	ALBEDO	DOWNWELLING	UPWELLING	TOTAL	ALBEDO
360							
641							
941							
1236							

FLIGHT NO. 89				FILTER NO. 5			
IRRADIANCE (WATTS/SQ.M. MICRO M.)							
ALTITUDE	DOWN-	UP-		SCALAR	SCALAR	SCALAR	SCALAR
(METERS)	WELLING	WELLING	ALBEDO	DOWNWELLING	UPWELLING	TOTAL	ALBEDO
360	6.190E-06	4.105E-06	.663	1.222E-05	1.461E-05	2.683E-05	1.195
641	9.214E-06	2.970E-06	.317	1.774E-05	1.382E-05	3.156E-05	.779
942	5.114E-06	1.984E-06	.388	1.003E-05	7.609E-06	1.764E-05	.759
1236	8.397E-06	3.500E-06	.417	1.617E-05	1.272E-05	2.889E-05	.787

FLIGHT NO. 89					
DIRECTIONAL REFLECTANCE OF BACKGROUND					
ZENITH	FILTERS				
ANGLE	1	2	5	3	4
93	2.92435	4.05109	3.61836	5.80155	
95	1.75028	2.30967	3.69624	2.43506	
100	.46289	2.54312	2.39443	.94012	
105	.24575	1.60970	1.25284	.47145	
120	.10396	.44427	.32637	.31129	
150	.08483	.23793	.21612	.22992	
180	.08101	.17074	.19414	.21369	

DATE 102168 FLIGHT NO. 89 GROUND LEVEL ALTITUDE ( M.)= 44 IUP=1

ALTITUDE (METERS)	TOTAL SCATTERING COEFFICIENT (PER METER)				
	FILTERS	1	2	3	4
0		1.961E-04	1.403E-04	8.712E-05	6.569E-05
30		1.954E-04	1.398E-04	8.683E-05	6.547E-05
61		1.948E-04	1.393E-04	8.654E-05	6.525E-05
91		1.941E-04	1.389E-04	8.625E-05	6.504E-05
122		1.935E-04	1.384E-04	8.597E-05	6.482E-05
152		1.928E-04	1.380E-04	8.568E-05	6.460E-05
183		1.922E-04	1.375E-04	8.540E-05	6.439E-05
213		1.916E-04	1.370E-04	8.511E-05	6.417E-05
244		1.909E-04	1.366E-04	8.483E-05	6.396E-05
274		1.903E-04	1.361E-04	8.455E-05	6.375E-05
305		1.897E-04	1.357E-04	8.426E-05	6.354E-05
335		1.890E-04	1.352E-04	8.398E-05	6.333E-05
366		1.884E-04	1.348E-04	8.370E-05	6.248E-05
396		1.878E-04	1.325E-04	8.389E-05	6.291E-05
427		1.859E-04	1.303E-04	8.349E-05	6.123E-05
457		1.835E-04	1.300E-04	8.324E-05	6.131E-05
488		1.831E-04	1.297E-04	8.291E-05	6.044E-05
518		1.813E-04	1.293E-04	8.216E-05	6.007E-05
549		1.810E-04	1.296E-04	8.226E-05	5.977E-05
579		1.791E-04	1.297E-04	8.210E-05	5.947E-05
610		1.798E-04	1.288E-04	8.181E-05	5.927E-05
640		1.779E-04	1.271E-04	8.156E-05	5.907E-05
671		1.763E-04	1.271E-04	8.121E-05	5.867E-05
701		1.759E-04	1.260E-04	8.080E-05	5.806E-05
732		1.723E-04	1.243E-04	8.046E-05	5.788E-05
762		1.700E-04	1.236E-04	8.002E-05	5.768E-05
792		1.675E-04	1.233E-04	8.006E-05	5.741E-05
823		1.652E-04	1.230E-04	8.011E-05	5.739E-05
853		1.634E-04	1.229E-04	7.950E-05	5.599E-05
884		1.640E-04	1.209E-04	7.976E-05	5.559E-05
914		1.630E-04	1.211E-04	7.891E-05	5.559E-05
945		1.603E-04	1.189E-04	7.839E-05	5.507E-05
975		1.577E-04	1.162E-04	7.714E-05	5.417E-05
1006		1.560E-04	1.144E-04	7.595E-05	5.417E-05
1036		1.557E-04	1.134E-04	7.495E-05	5.354E-05
1067		1.564E-04	1.123E-04	7.354E-05	5.213E-05
1097		1.559E-04	1.116E-04	7.149E-05	5.165E-05
1128		1.574E-04	1.099E-04	7.203E-05	5.169E-05
1158		1.595E-04	1.081E-04	7.052E-05	5.137E-05
1189		1.673E-04	1.063E-04	6.975E-05	5.099E-05
1219		1.641E-04	1.040E-04	6.854E-05	5.101E-05
1250		1.625E-04	1.032E-04	6.724E-05	5.044E-05
1280		1.590E-04	1.011E-04	6.622E-05	5.048E-05
1311		1.538E-04	1.004E-04	6.518E-05	5.018E-05
1341		1.500E-04	9.959E-05	6.442E-05	4.995E-05
1372		1.495E-04	9.925E-05	6.421E-05	4.978E-05

FIRST DATA ALT. 14 13 13 12 14  
LAST DATA ALT. 45 45 45 45 46

		FLIGHT NO. 39		FILTER NO. 1				
		BEAM TRANSMITTANCE FROM GROUND TO ALTITUDE		ZENITH ANGLE OF PATH OF SIGHT (DEGREES)				
ALTITUDE METERS		93	95	100	105	120	150	180
305		.3220060	.5094440	.7128346	.7968315	.8890855	.9343779	.9429133
610		.1067433	.2673257	.5157343	.6412973	.7945598	.8756652	.8913809
914		.0376170	.1473058	.3824030	.5246903	.7161618	.8246899	.8462634
1219		.0138910	.0844833	.2892915	.4351076	.6500157	.7798149	.8062355

		FLIGHT NO. 89		FILTER NO. 2				
		BEAM TRANSMITTANCE FROM GROUND TO ALTITUDE		ZENITH ANGLE OF PATH OF SIGHT (DEGREES)				
ALTITUDE METERS		93	95	100	105	120	150	180
305		.4445543	.6172429	.7849244	.8500361	.9193356	.9526026	.9588199
610		.2024735	.3899337	.6233245	.7282301	.8486038	.9095735	.9211970
914		.0946784	.2524560	.5011308	.6290565	.7866727	.8706361	.8869437
1219		.0467847	.1704314	.4114406	.5510982	.7345989	.8368817	.8570874

		FLIGHT NO. 89		FILTER NO. 3				
		BEAM TRANSMITTANCE FROM GROUND TO ALTITUDE		ZENITH ANGLE OF PATH OF SIGHT (DEGREES)				
ALTITUDE METERS		93	95	100	105	120	150	180
305		.6044247	.7410746	.8603643	.9040174	.9491076	.9702934	.9742215
610		.3675871	.5542212	.7436217	.8107403	.9022378	.9423334	.9498620
914		.2249910	.4184043	.6457662	.7457153	.8590924	.9160473	.9268724
1219		.1417959	.3232854	.5673570	.6836851	.8213254	.8925763	.9062700

		FLIGHT NO. 89		FILTER NO. 4				
		BEAM TRANSMITTANCE FROM GROUND TO ALTITUDE		ZENITH ANGLE OF PATH OF SIGHT (DEGREES)				
ALTITUDE METERS		93	95	100	105	120	150	180
305		.6841142	.7977629	.8927904	.9267372	.9613809	.9775179	.9805003
610		.4740657	.6439625	.8017985	.8622535	.9261519	.9566740	.9623678
914		.3334553	.5266281	.7248032	.8057832	.8942418	.9375027	.9456436
1219		.2394530	.4378215	.6606378	.7571971	.8659124	.9202389	.9305441
1524		.1737932	.3678043	.6053113	.7140426	.8400053	.9042410	.9165180

		FLIGHT NO. 89		FILTER NO. 5				
		BEAM TRANSMITTANCE FROM GROUND TO ALTITUDE		ZENITH ANGLE OF PATH OF SIGHT (DEGREES)				
ALTITUDE METERS		93	95	100	105	120	150	180
305		.3698340	.5532119	.7429417	.8192577	.9019512	.9421606	.9497111
610		.1401428	.3138735	.5590056	.6769166	.8171063	.8899262	.9039393
914		.0560898	.1860073	.4299024	.5675690	.7458830	.8442793	.8636432
1219		.0243491	.1169454	.3405741	.4354551	.6879213	.8057549	.8294102



FLIGHT NO. 89		FILTER NO. 1						
PATH RADIANCE FROM GROUND TO ALTITUDE (WATTS/STER.SQ.M MICRO M.)		ZENITH ANGLE OF PATH OF SIGHT (DEGREES)						
ALTITUDE METERS	93	95	100	105	120	150	180	
305	1.060E-06	7.516E-07	4.153E-07	2.747E-07	1.204E-07	5.195E-08	4.094E-08	
610	1.397E-06	1.126E-06	7.058E-07	4.906E-07	2.274E-07	1.003E-07	7.906E-08	
914	1.531E-06	1.332E-06	9.181E-07	6.661E-07	3.252E-07	1.472E-07	1.162E-07	
1219	1.536E-06	1.414E-06	1.053E-06	7.919E-07	4.045E-07	1.889E-07	1.502E-07	

FLIGHT NO. 89		FILTER NO. 2						
PATH RADIANCE FROM GROUND TO ALTITUDE (WATTS/STER.SQ.M MICRO M.)		ZENITH ANGLE OF PATH OF SIGHT (DEGREES)						
ALTITUDE METERS	93	95	100	105	120	150	180	
305	1.132E-06	7.747E-07	4.244E-07	2.850E-07	1.308E-07	5.662E-08	4.388E-08	
610	1.638E-06	1.244E-06	7.491E-07	5.208E-07	2.477E-07	1.089E-07	8.369E-08	
914	2.003E-06	1.622E-06	1.049E-06	7.526E-07	3.737E-07	1.689E-07	1.303E-07	
1219	2.129E-06	1.830E-06	1.263E-06	9.322E-07	4.906E-07	2.232E-07	1.729E-07	

FLIGHT NO. 89		FILTER NO. 3						
PATH RADIANCE FROM GROUND TO ALTITUDE (WATTS/STER.SQ.M MICRO M.)		ZENITH ANGLE OF PATH OF SIGHT (DEGREES)						
ALTITUDE METERS	93	95	100	105	120	150	180	
305	1.370E-06	8.856E-07	4.582E-07	2.980E-07	1.290E-07	5.478E-08	4.285E-08	
610	2.303E-06	1.597E-06	8.805E-07	5.864E-07	2.605E-07	1.110E-07	8.638E-08	
914	3.003E-06	2.210E-06	1.292E-06	8.825E-07	4.062E-07	1.734E-07	1.355E-07	
1219	3.323E-06	2.583E-06	1.592E-06	1.111E-06	5.268E-07	2.319E-07	1.794E-07	

FLIGHT NO. 89		FILTER NO. 4						
PATH RADIANCE FROM GROUND TO ALTITUDE (WATTS/STER.SQ.M MICRO M.)		ZENITH ANGLE OF PATH OF SIGHT (DEGREES)						
ALTITUDE METERS	93	95	100	105	120	150	180	
305								
610								
914								
1219								

FLIGHT NO. 89		FILTER NO. 5						
PATH RADIANCE FROM GROUND TO ALTITUDE (WATTS/STER.SQ.M MICRO M.)		ZENITH ANGLE OF PATH OF SIGHT (DEGREES)						
ALTITUDE METERS	93	95	100	105	120	150	180	
305	1.570E-06	1.115E-06	6.397E-07	4.425E-07	2.122E-07	8.730E-08	6.547E-08	
610	2.247E-06	1.775E-06	1.123E-06	6.023E-07	3.958E-07	1.677E-07	1.272E-07	
914	2.269E-06	1.984E-06	1.380E-06	1.019E-06	5.177E-07	2.274E-07	1.751E-07	
1219	2.155E-06	1.995E-06	1.495E-06	1.139E-06	6.003E-07	2.732E-07	2.129E-07	

FLIGHT NO. 89			FILTER NO. 1				
DIRECTIONAL PATH REFLECTANCE FROM GROUND TO ALTITUDE							
ALTITUDE	ZENITH ANGLE OF PATH OF SIGHT (DEGREES)						
METERS	93	95	100	105	120	150	180
305	1.667E 00	7.471E-01	2.950E-01	1.746E-01	6.859E-02	2.815E-02	2.199E-02
610	6.627E 00	2.133E 00	6.931E-01	3.874E-01	1.449E-01	5.803E-02	4.491E-02
914	2.061E 01	4.578E 00	1.216E 00	6.429E-01	2.300E-01	9.042E-02	6.952E-02
1219	5.601E 01	8.476E 00	1.843E 00	9.217E-01	3.151E-01	1.227E-01	9.436E-02

FLIGHT NO. 89			FILTER NO. 2				
DIRECTIONAL PATH REFLECTANCE FROM GROUND TO ALTITUDE							
ALTITUDE	ZENITH ANGLE OF PATH OF SIGHT (DEGREES)						
METERS	93	95	100	105	120	150	180
305	1.434E 00	7.070E-01	3.046E-01	1.889E-01	8.018E-02	3.348E-02	2.560E-02
610	4.558E 00	1.797E 00	6.770E-01	4.029E-01	1.644E-01	6.743E-02	5.130E-02
914	1.192E 01	3.619E 00	1.179E 00	6.739E-01	2.676E-01	1.093E-01	8.273E-02
1219	2.563E 01	6.048E 00	1.730E 00	9.529E-01	3.685E-01	1.502E-01	1.136E-01

FLIGHT NO. 89			FILTER NO. 3					
DIRECTIONAL PATH REFLECTANCE FROM GROUND TO ALTITUDE								
ALTITUDE	ZENITH ANGLE OF PATH OF SIGHT (DEGREES)							
METERS	93	95	100	105	120	150	180	
305	7.337E-01	3.868E-01	1.724E-01	1.067E-01	4.399E-02	1.827E-02	1.424E-02	
610	2.028E 00	9.327E-01	3.832E-01	2.315E-01	9.345E-02	3.813E-02	2.943E-02	
914	4.320E 00	1.710E 00	6.476E-01	3.830E-01	1.530E-01	6.198E-02	4.732E-02	
1219	7.586E 00	2.586E 00	9.082E-01	5.262E-01	2.076E-01	8.411E-02	6.407E-02	

FLIGHT NO. 89		FILTER NO. 4						
DIRECTIONAL PATH REFLECTANCE FROM GROUND TO ALTITUDE								
ALTITUDE	ZENITH ANGLE OF PATH OF SIGHT (DEGREES)							
METERS	93	95	100	105	120	150	180	
305								
610								
914								
1219								

FLIGHT NO. 89			FILTER NO. 5					
DIRECTIONAL PATH REFLECTANCE FROM GROUND TO ALTITUDE								
ALTITUDE	ZENITH ANGLE OF PATH OF SIGHT (DEGREES)							
METERS	93	95	100	105	120	150	180	
305	2.154E 00	1.023E 00	4.370E-01	2.742E-01	1.194E-01	4.703E-02	3.499E-02	
610	8.138E 00	2.871E 00	1.019E 00	6.016E-01	2.459E-01	9.562E-02	7.142E-02	
914	2.053E 01	5.414E 00	1.629E 00	9.111E-01	3.523E-01	1.367E-01	1.029E-01	
1219	4.492E 01	8.657E 00	2.229E 00	1.191E 00	4.429E-01	1.721E-01	1.303E-01	

#### FLIGHT 91

Moonlight. The flight pattern was from Lop Buri to approximately 40 km west of Sing Buri. The terrain was flat (river delta country) and cultivated with rice paddies and other crops; there were also small scattered settlements. This was the dry season (March) when crops had been harvested, ground cover had yellowed, rice paddies were dry, and the stubble was being burned off. Water was still present in some of the fields however and reflected moonlight was observed at the beginning of the flight. The atmosphere was free of clouds but quite hazy, especially near the ground, and there was very little wind. Data were recorded from 2052 local time to 2321. The moon phase angle was  $40^\circ$ ; the moon zenith angle was  $15^\circ$  at the start of sky radiance data-taking,  $11^\circ$  at transit, and  $18^\circ$  when sky radiance data-taking ended.

FLIGHT NO. 01				FILTER NO. 1			
IRRADIANCE (WATTS/SQ.M. MICRO M.)							
ALTITUDE (METERS)	DOWN- WELLING	UP- WELLING	ALBEDO	SCALAR DOWNWELLING	SCALAR UPWELLING	SCALAR TOTAL	SCALAR ALBEDO
131	8.776E-04	2.172E-05	.059	1.265E-03	1.351E-04	1.400E-03	.107
440	1.246E-03	3.628E-05	.057	1.249E-03	1.653E-04	1.815E-03	.101
764	1.093E-03	3.177E-05	.074	1.482E-03	2.059E-04	1.688E-03	.139
1086	8.891E-04	2.679E-05	.098	1.294E-03	2.271E-04	1.521E-03	.176
1381	1.274E-03	2.437E-05	.074	1.648E-03	2.459E-04	1.893E-03	.149
1688	1.163E-03	1.086E-04	.053	1.562E-03	2.612E-04	1.843E-03	.180

FLIGHT NO. 01				FILTER NO. 2			
IRRADIANCE (WATTS/SQ.M. MICRO M.)							
ALTITUDE (METERS)	DOWN- WELLING	UP- WELLING	ALBEDO	SCALAR DOWNWELLING	SCALAR UPWELLING	SCALAR TOTAL	SCALAR ALBEDO
131	7.461E-04	6.513E-05	.069	1.323E-03	1.604E-04	1.483E-03	.121
445	9.682E-04	3.396E-05	.054	1.337E-03	1.980E-04	1.535E-03	.145
764	1.023E-03	3.11E-05	.079	1.410E-03	2.083E-04	1.618E-03	.148
1080	1.319E-03	2.354E-05	.071	1.701E-03	2.377E-04	1.939E-03	.140
1379	1.247E-03	2.847E-05	.073	1.597E-03	2.473E-04	1.835E-03	.156
1686	9.091E-04	1.172E-04	.129	1.294E-03	2.893E-04	1.584E-03	.223

FLIGHT NO. 01				FILTER NO. 3			
IRRADIANCE (WATTS/SQ.M. MICRO M.)							
ALTITUDE (METERS)	DOWN- WELLING	UP- WELLING	ALBEDO	SCALAR DOWNWELLING	SCALAR UPWELLING	SCALAR TOTAL	SCALAR ALBEDO
179	1.276E-03	1.731E-05	.076	1.627E-03	2.121E-04	1.839E-03	.130
449	1.121E-03	1.131E-04	.101	1.458E-03	2.549E-04	1.713E-03	.175
767	1.681E-03	1.179E-04	.070	2.539E-03	2.664E-04	2.306E-03	.131
1079	1.533E-03	1.514E-04	.099	1.874E-03	3.295E-04	2.204E-03	.176
1379	1.313E-03	1.650E-04	.126	1.392E-03	3.554E-04	1.947E-03	.223
1684	1.308E-02	1.545E-04	.118	1.613E-03	3.461E-04	1.959E-03	.215

FLIGHT NO. 01				FILTER NO. 4			
IRRADIANCE (WATTS/SQ.M. MICRO M.)							
ALTITUDE (METERS)	DOWN- WELLING	UP- WELLING	ALBEDO	SCALAR DOWNWELLING	SCALAR UPWELLING	SCALAR TOTAL	SCALAR ALBEDO
176	9.407E-04	1.068E-04	.114	1.176E-03	2.268E-04	1.403E-03	.193
441	9.029E-04	1.389E-04	.154	1.130E-03	2.865E-04	1.417E-03	.253
755	1.206E-03	1.497E-04	.124	1.446E-03	3.100E-04	1.756E-03	.214
1079	1.500E-03	1.446E-04	.096	1.758E-03	3.024E-04	2.060E-03	.172
1373	2.668E-04	1.453E-04	.399	5.464E-04	2.120E-04	8.584E-04	.71
1684	1.033E-03	1.425E-04	.128	1.238E-03	3.63E-04	1.545E-03	.247

FLIGHT NO. 01				FILTER NO. 5			
IRRADIANCE (WATTS/SQ.M. MICRO M.)							
ALTITUDE (METERS)	DOWN- WELLING	UP- WELLING	ALBEDO	SCALAR DOWNWELLING	SCALAR UPWELLING	SCALAR TOTAL	SCALAR ALBEDO
172	1.001E-03	7.162E-05	.072	1.376E-03	1.668E-04	1.543E-03	.121
443	1.014E-03	9.221E-05	.091	1.403E-03	2.176E-04	1.620E-03	.155
759	7.77E-04	1.071E-04	.131	1.167E-03	2.562E-04	1.423E-03	.215
1036	9.703E-04	1.277E-04	.111	1.354E-03	2.643E-04	1.618E-03	.195
1371	3.316E-04	1.169E-04	.141	1.178E-03	2.815E-04	1.459E-03	.239
1596	9.604E-04	1.355E-04	.141	1.297E-03	3.196E-04	1.611E-03	.247

FLIGHT NO. 91					
AZIMUTH OF PATH OF SIGHT = 0					
DIRECTIONAL REFLECTANCE OF BACKGROUND					
ZENITH ANGLE	FILTERS				
	1	2	5	3	4
93	.26938	.22511	.21475	.15894	.16193
95	.14350	.16303	.14116	.11610	.13559
100	.09147	.09440	.08918	.08500	.23354
105	.06731	.08329	.07365	.08023	.11102
120	.04936	.06021	.05937	.08059	.08460
150	.04899	.05963	.10372	.07300	.16352
180	.06250	.07230	.06130	.12074	.07355

FLIGHT NO. 91					
AZIMUTH OF PATH OF SIGHT = 90					
DIRECTIONAL REFLECTANCE OF BACKGROUND					
ZENITH ANGLE	FILTERS				
	1	2	5	3	4
93	.25520	.19697	.14668	.15647	.15339
95	.20601	.15933	.13232	.13450	.14041
100	.09427	.10023	.08013	.07772	.12817
105	.07215	.08211	.06317	.07327	.09120
120	.05250	.05407	.05513	.09730	.07123
150	.03677	.06161	.07696	.06277	.18121
180	.06250	.07230	.06130	.12074	.07355

FLIGHT NO. 91					
AZIMUTH OF PATH OF SIGHT = 180					
DIRECTIONAL REFLECTANCE OF BACKGROUND					
ZENITH ANGLE	FILTERS				
	1	2	5	3	4
93	.12938	.13437	.14535	.13452	.24979
95	.10246	.09920	.11435	.09043	.16720
100	.07642	.07763	.08999	.07988	.11737
105	.07677	.06266	.06518	.09528	.08839
120	.04901	.05706	.04610	.06035	.09658
150	.07786	.06105	.06899	.03672	.20696
180	.06250	.07230	.06130	.12074	.07355

FLIGHT NO. 91					
AZIMUTH OF PATH OF SIGHT = 270					
DIRECTIONAL REFLECTANCE OF BACKGROUND					
ZENITH ANGLE	FILTERS				
	1	2	5	3	4
93	.11977	.14966	.19981	.13181	.17043
95	.10129	.10825	.12616	.09766	.15506
100	.05003	.08767	.06144	.07366	.14869
105	.07603	.07490	.06545	.08934	.14460
120	.05655	.06413	.04374	.05685	.06618
150	.07170	.06077	.04120	.06421	.22009
180	.06250	.07230	.06130	.12074	.07355

DATE 22869 FLIGHT NO. 91 GROUND LEVEL ALTITUDE (M.)= 24 TOP=1

ALTITUDE (METERS)	TOTAL SCATTERING COEFFICIENT (PER METER)				
FILTERS	1	2	3	4	5
0	1.228E-04	1.038E-04	6.452E-05	4.123E-05	9.012E-05
30	1.224E-04	1.026E-04	6.437E-05	4.109E-05	8.982E-05
61	1.220E-04	1.023E-04	6.415E-05	4.096E-05	8.952E-05
91	1.216E-04	1.020E-04	6.394E-05	4.082E-05	8.922E-05
122	1.212E-04	1.016E-04	6.373E-05	4.068E-05	8.893E-05
152	1.208E-04	1.013E-04	6.352E-05	4.055E-05	8.863E-05
183	1.204E-04	9.93E-05	6.269E-05	4.018E-05	8.833E-05
213	1.174E-04	9.963E-05	6.099E-05	3.948E-05	8.715E-05
244	1.158E-04	9.800E-05	6.005E-05	3.894E-05	8.623E-05
274	1.147E-04	9.719E-05	5.909E-05	3.854E-05	8.552E-05
305	1.138E-04	9.628E-05	5.859E-05	3.804E-05	8.501E-05
335	1.162E-04	9.844E-05	5.777E-05	3.800E-05	8.452E-05
365	1.139E-04	9.701E-05	5.682E-05	3.701E-05	8.715E-05
396	1.143E-04	9.052E-05	5.686E-05	3.619E-05	8.701E-05
427	1.063E-04	9.402E-05	5.366E-05	3.639E-05	8.608E-05
457	1.064E-04	9.719E-05	5.395E-05	3.765E-05	8.428E-05
488	1.103E-04	1.006E-04	5.619E-05	3.850E-05	8.253E-05
518	1.187E-04	1.027E-04	5.859E-05	3.877E-05	8.508E-05
549	1.204E-04	1.032E-04	5.918E-05	3.957E-05	8.966E-05
579	1.261E-04	1.042E-04	5.958E-05	3.907E-05	9.054E-05
610	1.266E-04	1.116E-04	5.965E-05	3.945E-05	9.105E-05
640	1.269E-04	1.145E-04	5.253E-05	4.024E-05	9.014E-05
671	1.300E-04	1.186E-04	6.633E-05	4.129E-05	8.640E-05
701	1.384E-04	1.151E-04	7.765E-05	4.190E-05	8.905E-05
732	1.473E-04	1.075E-04	8.625E-05	4.259E-05	8.959E-05
762	1.512E-04	1.006E-04	5.325E-05	4.275E-05	9.448E-05
792	1.503E-04	1.020E-04	6.073E-05	4.214E-05	1.007E-04
823	1.514E-04	1.025E-04	6.047E-05	4.183E-05	1.006E-04
854	1.427E-04	1.017E-04	6.356E-05	4.152E-05	1.104E-04
884	1.417E-04	1.041E-04	5.555E-05	4.165E-05	1.122E-04
914	1.512E-04	1.035E-04	6.531E-05	4.205E-05	1.080E-04
945	1.554E-04	1.041E-04	6.720E-05	4.183E-05	1.040E-04
975	1.503E-04	1.147E-04	6.522E-05	4.054E-05	9.977E-05
1006	1.499E-04	1.179E-04	6.510E-05	3.998E-05	8.916E-05
1036	1.423E-04	1.109E-04	6.368E-05	4.068E-05	9.039E-05
1067	1.438E-04	1.064E-04	6.343E-05	4.024E-05	9.315E-05
1097	1.427E-04	1.048E-04	6.267E-05	4.108E-05	9.698E-05
1128	1.377E-04	1.066E-04	6.360E-05	4.089E-05	9.790E-05
1158	1.372E-04	1.074E-04	6.389E-05	4.055E-05	9.604E-05
1189	1.402E-04	1.071E-04	6.533E-05	4.056E-05	9.313E-05
1219	1.415E-04	1.063E-04	6.343E-05	4.008E-05	9.454E-05
1250	1.423E-04	1.080E-04	6.313E-05	3.991E-05	9.399E-05
1280	1.422E-04	1.087E-04	6.421E-05	3.991E-05	9.758E-05
1311	1.409E-04	1.082E-04	6.364E-05	4.174E-05	1.001E-04
1341	1.408E-04	1.097E-04	6.374E-05	4.131E-05	9.961E-05
1371	1.414E-04	1.099E-04	6.384E-05	4.159E-05	1.017E-04
1402	1.414E-04	1.086E-04	6.332E-05	4.082E-05	1.019E-04
1433	1.423E-04	1.051E-04	6.362E-05	4.084E-05	9.765E-05
1463	1.424E-04	1.036E-04	6.346E-05	4.144E-05	9.627E-05
1494	1.436E-04	1.030E-04	6.310E-05	4.073E-05	9.498E-05
1524	1.423E-04	1.031E-04	6.282E-05	4.074E-05	9.616E-05
1554	1.403E-04	1.041E-04	6.351E-05	4.094E-05	9.604E-05
1585	1.330E-04	1.040E-04	6.359E-05	4.125E-05	9.753E-05
1615	1.305E-04	1.044E-04	6.372E-05	4.034E-05	9.721E-05
1646	1.317E-04	1.042E-04	6.223E-05	4.030E-05	9.617E-05
1676	1.302E-04	1.043E-04	6.265E-05	3.965E-05	9.485E-05
1707	1.297E-04	1.040E-04	6.180E-05	3.957E-05	9.554E-05
1737	1.293E-04	1.036E-04	6.168E-05	3.939E-05	9.422E-05
1768	1.289E-04	1.033E-04	6.144E-05	3.926E-05	9.470E-05
1798	1.284E-04	1.029E-04	6.124E-05	3.913E-05	9.458E-05
1829	1.280E-04	1.025E-04	6.103E-05	3.900E-05	9.427E-05

FIRST DATA ALT. 7 6 6 6 7  
 LAST DATA ALT. 56 56 56 56 56

FLIGHT NO. 91		FILTER NO. 1						
ALTIITUDE		BEAM TRANSMITTANCE FROM GROUND TO ALTIITUDE						
METERS		ZENITH ANGLE OF PATH OF SIGHT (DEGREES)						
		93	95	100	105	120	150	180
305		.4956753	.6585357	.8198552	.8687758	.9297716	.9588310	.9642467
610		.2469233	.4382783	.6609841	.7574634	.8660700	.9203356	.9306788
914		.1045473	.2608397	.5152635	.6409045	.7943078	.9755048	.8912395
1219		.0426540	.1605356	.3392716	.5401057	.7269793	.8318590	.526308
1524		.0174361	.0977273	.3112257	.4569766	.6667272	.7913278	.8165336

FLIGHT NO. 91		FILTER NO. 2						
ALTIITUDE		BEAM TRANSMITTANCE FROM GROUND TO ALTIITUDE						
METERS		ZENITH ANGLE OF PATH OF SIGHT (DEGREES)						
		93	95	100	105	120	150	180
305		.5544726	.7040015	.8384857	.8885284	.9406549	.9652949	.9698737
610		.3063153	.4976554	.7045073	.7905741	.8854646	.9321789	.9409913
914		.1594666	.3413253	.5934609	.6966448	.8293479	.8975996	.9176854
1219		.0811354	.2334661	.4818427	.6127075	.7760222	.8638112	.8809212
1524		.0412009	.1605417	.3992792	.5401154	.7269840	.8318621	.8526336

FLIGHT NO. 91		FILTER NO. 3						
ALTIITUDE		BEAM TRANSMITTANCE FROM GROUND TO ALTIITUDE						
METERS		ZENITH ANGLE OF PATH OF SIGHT (DEGREES)						
		93	95	100	105	120	150	180
305		.5929933	.8039278	.9320552	.9291477	.9676718	.9782755	.9811584
610		.4919715	.6582449	.8106757	.8686465	.9297000	.9587883	.9642095
914		.3332094	.5200913	.7244323	.8055065	.8940828	.9374064	.9455595
1219		.2233258	.4197680	.6468278	.7465358	.8595798	.9163473	.9271353
1524		.1493843	.3361591	.5785264	.6927346	.8269349	.8960909	.9093596

FLIGHT NO. 91		FILTER NO. 4						
ALTIITUDE		BEAM TRANSMITTANCE FROM GROUND TO ALTIITUDE						
METERS		ZENITH ANGLE OF PATH OF SIGHT (DEGREES)						
		93	95	100	105	120	150	180
305		.7921244	.8591923	.9320552	.9538886	.9758593	.9859904	.9878559
610		.6297463	.7613314	.8720887	.9122643	.9535796	.9729303	.9765140
914		.4887900	.6580996	.8105855	.8685621	.9296643	.9587671	.9641910
1219		.3795539	.5707065	.7546423	.8278916	.9068594	.9451172	.9522916
1524		.2928727	.4945675	.7023099	.7889188	.8845044	.9315952	.9404809

FLIGHT NO. 91		FILTER NO. 5						
ALTIITUDE		BEAM TRANSMITTANCE FROM GROUND TO ALTIITUDE						
METERS		ZENITH ANGLE OF PATH OF SIGHT (DEGREES)						
		93	95	100	105	120	150	180
305		.7957277	.7343646	.8567387	.9014593	.9477164	.9694720	.9735073
610		.3551575	.5437594	.7360668	.8141632	.8990438	.9404059	.9481797
914		.1954157	.3848691	.6192478	.7250311	.8466722	.9083776	.9201479
1219		.1074582	.2749152	.5230321	.6473715	.7984467	.8781357	.8935584
1524		.0579934	.1951890	.4404029	.5768331	.75271604	.8483749	.8672718

AZIMUTH OF PATH OF SIGHT =		FLIGHT NO. 91		FILTER NO. 1			
PATH RADIANCE FROM GROUND TO ALTITUDE (WATTS/STER. SQ. CM MICRO W.)		ZENITH ANGLE OF PATH OF SIGHT (DEGREES)					
ALTITUDE METERS	93	95	100	105	120	150	180
55	5.4071-05	3.3511-05	1.7091-05	1.1001-05	4.9621-06	7.6821-06	2.6261-06
910	9.4741-05	5.9061-05	3.2831-05	2.1831-05	1.0301-05	5.7891-06	2.7981-06
914	9.9041-05	7.7721-05	4.7691-05	3.3051-05	1.6351-05	9.4041-06	9.4111-06
1219	1.0481-04	8.9071-05	5.9451-05	4.2711-05	2.1961-05	1.2791-05	1.2671-05
1524	1.1391-04	1.0031-04	7.0771-05	5.2231-05	2.7821-05	1.6481-05	1.6461-05

FLIGHT NO. 91		FILTER NO. 2					
PATH RADIANCE FROM GROUND TO ALTITUDE (WATTS/STER. SQ. CM MICRO W.)		ZENITH ANGLE OF PATH OF SIGHT (DEGREES)					
ALTITUDE METERS	93	95	100	105	120	150	180
55	4.6071-05	2.7421-05	1.4821-05	9.1061-06	4.2041-06	2.3191-06	2.2931-06
910	7.3971-05	5.0371-05	2.7521-05	1.8231-05	8.5571-06	4.7751-06	4.7191-06
914	9.1111-05	6.7461-05	4.9721-05	2.7111-05	1.3191-05	7.4841-06	7.3851-06
1219	1.0371-04	3.2051-05	5.1771-05	3.6181-05	1.8161-05	1.0521-05	1.0521-05
1524	1.1011-04	5.2541-05	6.1331-05	4.4071-05	2.2721-05	1.3361-05	1.3471-05

FLIGHT NO. 91		FILTER NO. 3					
PATH RADIANCE FROM GROUND TO ALTITUDE (WATTS/STER. SQ. CM MICRO W.)		ZENITH ANGLE OF PATH OF SIGHT (DEGREES)					
ALTITUDE METERS	93	95	100	105	120	150	180
55	3.7401-05	2.1661-05	1.0301-05	6.7411-06	3.0621-06	1.7371-06	1.8521-06
910	5.9391-05	3.7521-05	1.9361-05	1.2591-05	5.8031-06	3.3911-06	3.5951-06
914	8.1591-05	5.4681-05	2.2531-05	1.9621-05	9.3801-06	5.5501-06	5.9541-06
1219	9.5131-05	5.8921-05	3.9051-05	2.6271-05	1.2931-05	7.7441-06	8.3141-06
1524	1.0361-04	7.8541-05	4.6731-05	3.2181-05	1.6161-05	9.7861-06	1.0471-05

FLIGHT NO. 91		FILTER NO. 4					
PATH RADIANCE FROM GROUND TO ALTITUDE (WATTS/STER. SQ. CM MICRO W.)		ZENITH ANGLE OF PATH OF SIGHT (DEGREES)					
ALTITUDE METERS	93	95	100	105	120	150	180
55	1.7421-05	1.0971-05	5.3331-06	3.4221-06	1.6051-06	9.4991-07	9.9661-07
910	2.1871-05	2.0351-05	1.0231-05	6.7111-06	3.2331-06	1.9521-06	2.0491-06
914	4.9911-05	3.1051-05	1.0221-05	1.0731-05	5.2711-06	3.2251-06	3.4071-06
1219	6.1111-05	3.0631-05	2.1351-05	1.4021-05	7.7691-06	4.4901-06	4.7931-06
1524	6.4071-05	4.5031-05	2.5261-05	1.7151-05	8.6511-06	5.3281-06	5.0281-06

FLIGHT NO. 91		FILTER NO. 5					
PATH RADIANCE FROM GROUND TO ALTITUDE (WATTS/STER. SQ. CM MICRO W.)		ZENITH ANGLE OF PATH OF SIGHT (DEGREES)					
ALTITUDE METERS	93	95	100	105	120	150	180
55	4.4101-05	2.6451-05	1.3251-05	8.5221-06	3.9111-06	2.2051-06	2.2001-06
910	6.9921-05	4.6571-05	2.5101-05	1.6011-05	7.8871-06	4.5011-06	4.4501-06
914	8.4821-05	6.2311-05	3.6221-05	2.4691-05	1.7091-05	6.9251-06	6.7271-06
1219	9.5191-05	7.4511-05	4.6171-05	3.2231-05	1.0191-05	9.3291-06	9.0441-06
1524	1.0031-04	8.3361-05	5.4411-05	3.3961-05	2.0701-05	1.1591-05	1.1271-05



AZIMUTH OF PATH OF SIGHT 4 90		FLIGHT NO. 91		FILTER NO. 1					
PATH RADIANCE FROM GROUND TO ALTITUDE (WATTS/STER.SQ.M MICRO M.)		ZENITH ANGLE OF PATH OF SIGHT (DEGREES)							
ALTITUDE METERS	93	95	100	105	120	150	180		
305	4.613E-05	2.907E-05	1.511E-05	1.017E-05	5.011E-06	3.014E-06	2.626E-06		
610	7.330E-05	5.179E-05	2.773E-05	2.040E-05	1.050E-05	6.563E-06	5.798E-06		
914	8.825E-05	6.961E-05	4.370E-05	3.105E-05	1.650E-05	1.043E-05	9.411E-06		
1219	9.383E-05	7.015E-05	5.456E-05	4.009E-05	2.199E-05	1.392E-05	1.267E-05		
1524	1.003E-04	8.972E-05	6.482E-05	4.904E-05	2.788E-05	1.804E-05	1.646E-05		

FLIGHT NO. 91		FILTER NO. 2							
PATH RADIANCE FROM GROUND TO ALTITUDE (WATTS/STER.SQ.M MICRO M.)		ZENITH ANGLE OF PATH OF SIGHT (DEGREES)							
ALTITUDE METERS	93	95	100	105	120	150	180		
305	4.011E-05	2.476E-05	1.298E-05	8.643E-06	4.316E-06	2.641E-06	2.293E-06		
610	6.390E-05	4.392E-05	2.471E-05	1.687E-05	8.607E-06	5.313E-06	4.719E-06		
914	3.057E-05	6.042E-05	3.631E-05	2.439E-05	1.323E-05	8.202E-06	7.385E-06		
1219	9.212E-05	7.398E-05	4.738E-05	3.402E-05	1.830E-05	1.161E-05	1.052E-05		
1524	9.637E-05	8.212E-05	5.590E-05	4.122E-05	2.289E-05	1.482E-05	1.347E-05		

FLIGHT NO. 91		FILTER NO. 3							
PATH RADIANCE FROM GROUND TO ALTITUDE (WATTS/STER.SQ.M MICRO M.)		ZENITH ANGLE OF PATH OF SIGHT (DEGREES)							
ALTITUDE METERS	93	95	100	105	120	150	180		
305	3.013E-05	1.785E-05	9.158E-06	6.088E-06	3.117E-06	2.082E-06	1.852E-06		
610	5.017E-05	3.191E-05	1.798E-05	1.152E-05	5.942E-06	3.954E-06	3.595E-06		
914	6.964E-05	4.747E-05	2.653E-05	1.819E-05	9.550E-06	6.448E-06	5.954E-06		
1219	8.257E-05	5.983E-05	3.508E-05	2.453E-05	1.317E-05	8.970E-06	8.314E-06		
1524	8.854E-05	6.813E-05	4.172E-05	2.989E-05	1.642E-05	1.130E-05	1.047E-05		

FLIGHT NO. 91		FILTER NO. 4							
PATH RADIANCE FROM GROUND TO ALTITUDE (WATTS/STER.SQ.M MICRO M.)		ZENITH ANGLE OF PATH OF SIGHT (DEGREES)							
ALTITUDE METERS	93	95	100	105	120	150	180		
305	1.003E-05	9.24E-06	4.709E-06	3.142E-06	1.642E-06	1.127E-06	9.966E-07		
610	2.906E-05	1.773E-05	9.421E-06	6.304E-06	3.325E-06	2.269E-06	2.049E-06		
914	4.235E-05	2.721E-05	1.475E-05	1.013E-05	5.397E-06	3.721E-06	3.407E-06		
1219	5.290E-05	3.563E-05	1.949E-05	1.377E-05	7.456E-06	5.199E-06	4.793E-06		
1524	5.555E-05	3.957E-05	2.332E-05	1.617E-05	8.877E-06	6.131E-06	5.628E-06		

FLIGHT NO. 91		FILTER NO. 5							
PATH RADIANCE FROM GROUND TO ALTITUDE (WATTS/STER.SQ.M MICRO M.)		ZENITH ANGLE OF PATH OF SIGHT (DEGREES)							
ALTITUDE METERS	93	95	100	105	120	150	180		
305	3.076E-05	2.359E-05	1.223E-05	8.109E-06	4.040E-06	2.502E-06	2.200E-06		
610	6.255E-05	4.205E-05	2.327E-05	1.580E-05	8.045E-06	4.990E-06	4.450E-06		
914	7.49E-05	5.687E-05	3.373E-05	2.349E-05	1.221E-05	7.495E-06	6.727E-06		
1219	1.037E-04	6.733E-05	4.362E-05	3.088E-05	1.634E-05	1.006E-05	9.044E-06		
1524	9.723E-05	7.518E-05	5.034E-05	3.682E-05	2.017E-05	1.259E-05	1.127E-05		

AZIMUTH OF PATH OF SIGHT = 100		FLIGHT NO. 91		FILTER NO. 1		ALTIMETER (WATTS/STER. SQ. M. MICRO M.)	
ALTITUDE	PATH DISTANCE FROM GROUND TO	ALTITUDE	ZENITH ANGLE OF PATH OF SIGHT (DEGREES)	ALTITUDE	ZENITH ANGLE OF PATH OF SIGHT (DEGREES)	ALTITUDE	ZENITH ANGLE OF PATH OF SIGHT (DEGREES)
METERS	93	95	100	105	120	150	100
305	4.238E-05	2.08E-05	1.437E-05	9.695E-06	4.935E-06	2.090E-06	2.620E-06
610	6.841E-05	4.04E-05	2.811E-05	1.962E-05	1.047E-05	6.727E-06	2.798E-06
914	8.278E-05	6.550E-05	4.157E-05	2.990E-05	1.639E-05	1.057E-05	9.411E-06
1219	8.510E-05	7.511E-05	5.192E-05	3.857E-05	2.178E-05	1.406E-05	1.267E-05
1524	9.477E-05	8.452E-05	6.158E-05	4.705E-05	2.743E-05	1.800E-05	1.646E-05

FLIGHT NO. 91		FILTER NO. 2		ALTIMETER (WATTS/STER. SQ. M. MICRO M.)	
ALTITUDE	PATH DISTANCE FROM GROUND TO	ALTITUDE	ZENITH ANGLE OF PATH OF SIGHT (DEGREES)	ALTITUDE	ZENITH ANGLE OF PATH OF SIGHT (DEGREES)
METERS	93	95	100	105	120
305	3.304E-05	2.353E-05	1.250E-05	8.406E-06	4.309E-06
610	6.051E-05	4.176E-05	2.372E-05	1.635E-05	8.543E-06
914	7.585E-05	5.715E-05	3.468E-05	2.449E-05	1.306E-05
1219	8.757E-05	7.044E-05	4.534E-05	3.241E-05	1.795E-05
1524	9.171E-05	7.822E-05	5.450E-05	3.972E-05	2.237E-05

FLIGHT NO. 91		FILTER NO. 3		ALTIMETER (WATTS/STER. SQ. M. MICRO M.)	
ALTITUDE	PATH DISTANCE FROM GROUND TO	ALTITUDE	ZENITH ANGLE OF PATH OF SIGHT (DEGREES)	ALTITUDE	ZENITH ANGLE OF PATH OF SIGHT (DEGREES)
METERS	93	95	100	105	120
305	2.670E-05	1.704E-05	8.315E-06	5.945E-06	3.130E-06
610	4.792E-05	3.05E-05	1.620E-05	1.123E-05	5.910E-06
914	6.741E-05	4.587E-05	2.575E-05	1.777E-05	9.431E-06
1219	8.001E-05	5.790E-05	3.402E-05	2.383E-05	1.289E-05
1524	8.564E-05	6.582E-05	4.022E-05	2.588E-05	1.596E-05

FLIGHT NO. 91		FILTER NO. 4		ALTIMETER (WATTS/STER. SQ. M. MICRO M.)	
ALTITUDE	PATH DISTANCE FROM GROUND TO	ALTITUDE	ZENITH ANGLE OF PATH OF SIGHT (DEGREES)	ALTITUDE	ZENITH ANGLE OF PATH OF SIGHT (DEGREES)
METERS	93	95	100	105	120
305	1.575E-05	9.122E-06	4.691E-06	3.159E-06	1.682E-06
610	2.849E-05	1.741E-05	9.187E-06	6.245E-06	3.328E-06
914	4.15E-05	2.672E-05	1.450E-05	9.953E-06	5.330E-06
1219	5.224E-05	3.513E-05	1.963E-05	1.361E-05	7.346E-06
1524	5.459E-05	3.893E-05	2.267E-05	1.597E-05	8.757E-06

FLIGHT NO. 91		FILTER NO. 5		ALTIMETER (WATTS/STER. SQ. M. MICRO M.)	
ALTITUDE	PATH DISTANCE FROM GROUND TO	ALTITUDE	ZENITH ANGLE OF PATH OF SIGHT (DEGREES)	ALTITUDE	ZENITH ANGLE OF PATH OF SIGHT (DEGREES)
METERS	93	95	100	105	120
305	3.475E-05	2.184E-05	1.147E-05	7.702E-06	3.980E-06
610	5.887E-05	3.986E-05	2.214E-05	1.519E-05	7.958E-06
914	7.268E-05	5.342E-05	3.214E-05	2.263E-05	1.205E-05
1219	8.113E-05	6.440E-05	4.087E-05	2.939E-05	1.598E-05
1524	8.362E-05	7.073E-05	4.78E-05	3.529E-05	1.978E-05

AZIMUTH OF PATH OF SIGHT = 270  
 FLIGHT NO. 91      FILTER NO. 1  
 PATH RADIANCE FROM GROUND TO ALTITUDE (WATTS/STER.SQ.M MICRO M.)  
 ALTITUDE      ZENITH ANGLE OF PATH OF SIGHT (DEGREES)  
 METERS      93      95      100      105      120      150      180

305	4.79E-05	2.867E-05	1.504E-05	9.923E-06	4.797E-06	2.793E-06	2.626E-06
610	7.352E-05	5.185E-05	2.943E-05	2.007E-05	1.011E-05	6.089E-06	5.798E-06
914	8.833E-05	6.951E-05	4.350E-05	3.078E-05	1.613E-05	9.893E-06	9.411E-06
1219	9.551E-05	8.114E-05	5.494E-05	4.016E-05	2.176E-05	1.344E-05	1.267E-05
1524	1.073E-04	9.55E-05	6.512E-05	4.897E-05	2.742E-05	1.722E-05	1.646E-05

FLIGHT NO. 91      FILTER NO. 2  
 PATH RADIANCE FROM GROUND TO ALTITUDE (WATTS/STER.SQ.M MICRO M.)  
 ALTITUDE      ZENITH ANGLE OF PATH OF SIGHT (DEGREES)  
 METERS      93      95      100      105      120      150      180

305	4.193E-05	2.568E-05	1.325E-05	8.679E-06	4.148E-06	2.405E-06	2.293E-06
610	6.137E-05	4.478E-05	2.496E-05	1.605E-05	8.345E-06	4.934E-06	4.719E-06
914	8.101E-05	6.079E-05	3.643E-05	2.531E-05	1.295E-05	7.763E-06	7.385E-06
1219	9.449E-05	7.536E-05	4.781E-05	3.401E-05	1.787E-05	1.089E-05	1.052E-05
1524	9.88E-05	8.363E-05	5.638E-05	4.114E-05	2.226E-05	1.380E-05	1.347E-05

FLIGHT NO. 91      FILTER NO. 3  
 PATH RADIANCE FROM GROUND TO ALTITUDE (WATTS/STER.SQ.M MICRO M.)  
 ALTITUDE      ZENITH ANGLE OF PATH OF SIGHT (DEGREES)  
 METERS      93      95      100      105      120      150      180

305	3.149E-05	1.845E-05	9.31E-06	6.015E-06	2.962E-06	1.826E-06	1.852E-06
610	5.249E-05	3.313E-05	1.75E-05	1.164E-05	5.766E-06	3.549E-06	3.595E-06
914	7.331E-05	4.942E-05	2.725E-05	1.642E-05	9.290E-06	5.800E-06	5.954E-06
1219	8.751E-05	6.273E-05	3.616E-05	2.485E-05	1.276E-05	8.046E-06	8.314E-06
1524	9.364E-05	7.126E-05	4.315E-05	3.025E-05	1.590E-05	1.013E-05	1.047E-05

FLIGHT NO. 91      FILTER NO. 4  
 PATH RADIANCE FROM GROUND TO ALTITUDE (WATTS/STER.SQ.M MICRO M.)  
 ALTITUDE      ZENITH ANGLE OF PATH OF SIGHT (DEGREES)  
 METERS      93      95      100      105      120      150      180

305	1.710E-05	9.793E-06	4.929E-06	3.247E-06	1.617E-06	1.009E-06	9.966E-07
610	3.077E-05	1.861E-05	9.651E-06	6.433E-06	3.250E-06	2.043E-06	2.049E-06
914	4.513E-05	2.872E-05	1.533E-05	1.033E-05	5.283E-06	3.348E-06	3.407E-06
1219	5.700E-05	3.79E-05	2.055E-05	1.419E-05	7.343E-06	4.670E-06	4.793E-06
1524	6.953E-05	4.203E-05	2.407E-05	1.654E-05	8.748E-06	5.549E-06	5.628E-06

FLIGHT NO. 91      FILTER NO. 5  
 PATH RADIANCE FROM GROUND TO ALTITUDE (WATTS/STER.SQ.M MICRO M.)  
 ALTITUDE      ZENITH ANGLE OF PATH OF SIGHT (DEGREES)  
 METERS      93      95      100      105      120      150      180

305	3.891E-05	2.355E-05	1.211E-05	7.959E-06	3.859E-06	2.283E-06	2.200E-06
610	6.213E-05	4.226E-05	2.325E-05	1.567E-05	7.809E-06	4.654E-06	4.450E-06
914	7.963E-05	5.79C-05	3.417E-05	2.3.6E-05	1.206E-05	7.177E-06	6.727E-06
1219	8.750E-05	6.911E-05	4.338E-05	3.077E-05	1.612E-05	9.653E-06	9.044E-06
1524	9.021E-05	7.582E-05	5.060E-05	3.68CE-05	1.983E-05	1.201E-05	1.127E-05

AZIMUTH OF PATH OF SIGHT =								
FLIGHT NO. 01			FILTER NO. 1					
DIRECTIONAL PATH REFLECTANCE FROM GROUND TO ALTITUDE								
ZENITH ANGLE OF PATH OF SIGHT (DEGREES)								
ALTITUDE	93	95	100	105	120	150	180	
METERS								
305	3.905E-01	1.872E-01	7.546E-02	4.533E-02	1.911E-02	1.001E-02	9.749E-03	
910	1.227E-00	4.825E-01	1.776E-01	1.032E-01	4.258E-02	2.252E-02	2.230E-02	
914	3.391E-00	1.043E-00	3.314E-01	1.846E-01	7.367E-02	3.845E-02	1.780E-02	
1219	3.797E-00	1.980E-00	5.334E-01	2.831E-01	1.082E-01	5.504E-02	5.321E-02	
1524	2.339E-01	3.674E-01	6.141E-01	4.095E-01	1.494E-01	7.456E-02	7.161E-02	

FLIGHT NO. 01								
FILTER NO. 2								
DIRECTIONAL PATH REFLECTANCE FROM GROUND TO ALTITUDE								
ALTITUDE	ZENITH ANGLE OF PATH OF SIGHT (DEGREES)							
METERS	93	95	100	105	120	150	180	
305	2.899E-01	1.388E-01	5.858E-02	3.553E-02	1.512E-02	7.977E-03	7.849E-03	
910	4.008E-01	3.361E-01	1.297E-01	7.655E-02	3.209E-02	1.701E-02	1.665E-02	
914	1.872E-00	6.553E-01	2.260E-01	1.292E-01	5.281E-02	2.769E-02	2.693E-02	
1219	4.243E-00	1.175E-00	3.561E-01	1.961E-01	7.770E-02	4.043E-02	3.964E-02	
1524	8.871E-01	1.916E-00	5.106E-01	2.705E-01	1.038E-01	5.333E-02	5.247E-02	

FLIGHT NO. 01								
FILTER NO. 3								
DIRECTIONAL PATH REFLECTANCE FROM GROUND TO ALTITUDE								
ALTITUDE	ZENITH ANGLE OF PATH OF SIGHT (DEGREES)							
METERS	93	95	100	105	120	150	180	
305	1.331E-01	6.640E-02	2.909E-02	1.785E-02	7.832E-03	4.371E-03	4.648E-03	
910	2.597E-01	1.406E-01	5.879E-02	3.567E-02	1.554E-02	8.706E-03	9.17E-03	
914	2.228E-01	2.568E-01	1.007E-01	5.997E-02	2.563E-02	1.458E-02	1.550E-02	
1219	1.060E-00	4.042E-01	1.436E-01	8.694E-02	3.703E-02	2.080E-02	2.208E-02	
1524	1.703E-00	5.759E-01	1.988E-01	1.144E-01	4.812E-02	2.689E-02	2.835E-02	

FLIGHT NO. 01								
FILTER NO. 4								
DIRECTIONAL PATH REFLECTANCE FROM GROUND TO ALTITUDE								
ALTITUDE	ZENITH ANGLE OF PATH OF SIGHT (DEGREES)							
METERS	93	95	100	105	120	150	180	
305	8.209E-02	4.219E-02	1.911E-02	1.198E-02	5.494E-03	3.217E-03	3.369E-03	
910	1.791E-01	3.923E-01	3.938E-02	1.457E-02	1.132E-02	6.701E-03	7.006E-03	
914	3.246E-01	1.576E-01	6.683E-02	4.126E-02	1.894E-02	1.123E-02	1.180E-02	
1219	5.877E-01	2.376E-01	9.872E-02	5.596E-02	2.677E-02	1.587E-02	1.681E-02	
1524	7.306E-01	3.041E-01	1.201E-01	7.209E-02	3.266E-02	1.910E-02	1.998E-02	

FLIGHT NO. 01								
FILTER NO. 5								
DIRECTIONAL PATH REFLECTANCE FROM GROUND TO ALTITUDE								
ALTITUDE	ZENITH ANGLE OF PATH OF SIGHT (DEGREES)							
METERS	93	95	100	105	120	150	180	
305	2.324E-01	1.137E-01	4.333E-02	2.966E-02	1.294E-02	7.135E-03	7.091E-03	
910	6.176E-01	2.690E-01	1.070E-01	6.798E-02	2.752E-02	1.502E-02	1.472E-02	
914	1.362E-00	5.079E-01	1.831E-01	1.068E-01	4.481E-02	2.392E-02	2.293E-02	
1219	2.774E-00	8.537E-01	2.779E-01	1.562E-01	6.362E-02	3.333E-02	3.175E-02	
1524	5.428E-00	1.341E-00	3.870E-01	2.113E-01	9.340E-02	4.287E-02	4.077E-02	

AZIMUTH OF PATH OF SIGHT = 90

FLIGHT NO. 91		FILTER NO. 1						
DIRECTIONAL PATH REFLECTANCE FROM GROUND TO ALTITUDE		ZENITH ANGLE OF PATH OF SIGHT (DEGREES)						
ALTITUDE		93	95	100	105	120	150	180
METERS								
505		4.332E-01	1.576E-01	6.761E-02	4.192E-02	1.929E-02	1.125E-02	9.749E-03
610		1.764E-00	4.230E-01	1.810E-01	9.643E-02	4.339E-02	2.553E-02	2.230E-02
914		3.022E-00	9.334E-01	3.036E-01	1.735E-01	7.436E-02	4.263E-02	3.780E-02
1219		7.875E-00	1.787E-00	4.892E-01	2.657E-01	1.043E-01	5.990E-02	5.321E-02
1524		2.070E-01	3.286E-00	7.456E-01	3.842E-01	1.497E-01	8.162E-02	7.216E-02

FLIGHT NO. 91		FILTER NO. 2						
DIRECTIONAL PATH REFLECTANCE FROM GROUND TO ALTITUDE		ZENITH ANGLE OF PATH OF SIGHT (DEGREES)						
ALTITUDE		93	95	100	105	120	150	180
METERS								
505		2.402E-01	1.168E-01	5.142E-02	3.230E-02	1.524E-02	9.084E-03	7.849E-03
610		6.927E-01	2.930E-01	1.165E-01	7.086E-02	3.228E-02	1.893E-02	1.665E-02
914		1.678E-00	5.869E-01	2.060E-01	1.210E-01	5.297E-02	3.034E-02	2.693E-02
1219		3.770E-00	1.052E-00	3.264E-01	1.343E-01	7.830E-02	4.464E-02	3.964E-02
1524		7.700E-00	1.699E-00	4.849E-01	2.534E-01	1.045E-01	5.917E-02	5.247E-02

FLIGHT NO. 91		FILTER NO. 3						
DIRECTIONAL PATH REFLECTANCE FROM GROUND TO ALTITUDE		ZENITH ANGLE OF PATH OF SIGHT (DEGREES)						
ALTITUDE		93	95	100	105	120	150	180
METERS								
505		1.072E-01	5.465E-02	2.515E-02	1.512E-02	7.911E-03	5.239E-03	4.648E-03
610		2.511E-01	1.193E-01	5.186E-02	3.264E-02	1.573E-02	1.015E-02	9.178E-03
914		5.160E-01	2.221E-01	9.015E-02	5.560E-02	2.630E-02	1.694E-02	1.550E-02
1219		9.107E-01	4.309E-01	1.335E-01	8.068E-02	3.771E-02	2.410E-02	2.208E-02
1524		1.461E-00	4.989E-01	1.754E-01	1.062E-01	4.885E-02	3.104E-02	2.835E-02

FLIGHT NO. 91		FILTER NO. 4						
DIRECTIONAL PATH REFLECTANCE FROM GROUND TO ALTITUDE		ZENITH ANGLE OF PATH OF SIGHT (DEGREES)						
ALTITUDE		93	95	100	105	120	150	180
METERS								
505		6.777E-02	3.553E-02	1.607E-02	1.100E-02	5.619E-03	3.818E-03	3.369E-03
610		1.541E-01	7.775E-02	3.569E-02	2.398E-02	1.164E-02	7.789E-03	7.006E-03
914		2.394E-01	1.351E-01	6.070E-02	3.882E-02	1.939E-02	1.296E-02	1.180E-02
1219		4.054E-01	2.055E-01	3.003E-02	5.555E-02	2.746E-02	1.837E-02	1.681E-02
1524		6.334E-01	2.572E-01	1.095E-01	6.646E-02	3.352E-02	2.198E-02	1.998E-02

FLIGHT NO. 91		FILTER NO. 5						
DIRECTIONAL PATH REFLECTANCE FROM GROUND TO ALTITUDE		ZENITH ANGLE OF PATH OF SIGHT (DEGREES)						
ALTITUDE		93	95	100	105	120	150	180
METERS								
505		7.041E-01	1.070E-01	4.477E-02	2.822E-02	1.337E-02	8.098E-03	7.091E-03
610		5.525E-01	2.428E-01	2.917E-02	6.089E-02	2.807E-02	1.665E-02	1.472E-02
914		1.236E-00	4.635E-01	1.709E-02	1.016E-01	4.525E-02	2.588E-02	2.293E-02
1219		5.517E-00	7.797E-01	2.580E-01	1.467E-01	6.419E-02	3.595E-02	3.175E-02
1524		4.327E-00	1.220E-00	3.586E-01	2.002E-01	8.414E-02	4.655E-02	4.077E-02

AZIMUTH OF PATH OF SIGHT = 180  
FLIGHT NO. 91      FILTER NO. 1  
DIRECTIONAL PATH REFLECTANCE FROM GROUND TO ALTITUDE  
ZENITH ANGLE OF PATH OF SIGHT (DEGREES)

ALTITUDE METERS	93	95	100	105	120	150	180
305	3.061E-01	1.457E-01	6.345E-01	3.996E-02	1.919E-02	1.153E-02	9.749E-03
510	9.118E-01	3.960E-01	1.526E-01	9.270E-02	4.329E-02	2.617E-02	2.230E-02
914	2.835E-00	8.788E-01	1.888E-01	1.670E-01	7.388E-02	4.320E-02	3.780E-02
1219	7.394E-00	1.674E-00	4.655E-01	2.557E-01	1.073E-01	6.051E-02	3.321E-02
1524	1.945E-01	6.09E-01	7.033E-01	3.686E-01	1.473E-01	8.141E-02	7.216E-02

FLIGHT NO. 91      FILTER NO. 2  
DIRECTIONAL PATH REFLECTANCE FROM GROUND TO ALTITUDE  
ZENITH ANGLE OF PATH OF SIGHT (DEGREES)

ALTITUDE METERS	93	95	100	105	120	150	180
305	2.278E-01	1.112E-01	4.950E-02	3.142E-02	1.521E-02	9.225E-03	7.849E-03
510	6.560E-01	2.795E-01	1.118E-01	6.366E-02	3.204E-02	1.895E-02	1.665E-02
914	1.580E-00	5.551E-01	1.974E-01	1.167E-01	5.229E-02	3.072E-02	2.693E-02
1219	5.586E-00	1.002E-00	3.124E-01	1.778E-01	7.682E-02	4.385E-02	3.964E-02
1524	7.391E-00	1.619E-00	4.450E-01	2.442E-01	1.022E-01	5.769E-02	5.247E-02

FLIGHT NO. 91      FILTER NO. 3  
DIRECTIONAL PATH REFLECTANCE FROM GROUND TO ALTITUDE  
ZENITH ANGLE OF PATH OF SIGHT (DEGREES)

ALTITUDE METERS	93	95	100	105	120	150	180
305	1.019E-01	5.218E-02	2.430E-02	1.575E-02	9.006E-03	5.315E-03	4.648E-03
510	2.398E-01	1.144E-01	5.012E-02	3.183E-02	1.565E-02	1.004E-02	9.178E-03
914	4.981E-01	2.147E-01	3.749E-02	5.431E-02	2.597E-02	1.642E-02	1.550E-02
1219	7.205E-01	3.399E-01	1.295E-01	7.875E-02	3.693E-02	2.318E-02	2.208E-02
1524	1.411E-00	4.821E-01	1.724E-01	1.030E-01	4.752E-02	2.962E-02	2.835E-02

FLIGHT NO. 91      FILTER NO. 4  
DIRECTIONAL PATH REFLECTANCE FROM GROUND TO ALTITUDE  
ZENITH ANGLE OF PATH OF SIGHT (DEGREES)

ALTITUDE METERS	93	95	100	105	120	150	180
305	6.656E-02	3.50E-02	1.681E-02	1.106E-02	5.756E-03	3.897E-03	3.369E-03
510	1.511E-01	7.637E-02	3.513E-02	2.286E-02	1.166E-02	7.688E-03	7.009E-03
914	2.840E-01	1.356E-01	5.972E-02	3.827E-02	1.915E-02	1.248E-02	1.180E-02
1219	4.597E-01	2.053E-01	3.685E-02	5.491E-02	2.705E-02	1.749E-02	1.681E-02
1524	6.225E-01	2.629E-01	1.073E-01	6.760E-02	3.306E-02	2.106E-02	1.998E-02

FLIGHT NO. 91      FILTER NO. 5  
DIRECTIONAL PATH REFLECTANCE FROM GROUND TO ALTITUDE  
ZENITH ANGLE OF PATH OF SIGHT (DEGREES)

ALTITUDE METERS	93	95	100	105	120	150	180
305	1.882E-01	9.323E-02	4.197E-02	2.680E-02	1.317E-02	8.228E-03	7.091E-03
510	5.201E-01	2.291E-01	9.446E-02	5.852E-02	2.770E-02	1.668E-02	1.472E-02
914	1.167E-00	4.387E-01	1.631E-01	9.790E-02	4.465E-02	2.597E-02	2.293E-02
1219	2.364E-00	7.349E-01	2.451E-01	1.424E-01	6.280E-02	3.579E-02	3.175E-02
1524	4.523E-00	1.137E-00	3.408E-01	1.719E-01	8.250E-02	4.649E-02	4.077E-02

AZIMUTH OF PATH OF SIGHT = 270								
FLIGHT NO. 71      FILTER NO. 1								
DIRECTIONAL PATH REFLECTANCE FROM GROUND TO ALTITUDE								
ALTITUDE	ZENITH ANGLE OF PATH OF SIGHT (DEGREES)							
METERS	93	95	100	105	120	150	180	
305	3.308E-01	1.553E-01	6.638E-02	4.089E-02	1.847E-02	1.043E-02	9.749E-03	
610	1.066E-00	4.219E-01	1.594E-01	9.485E-02	4.178E-02	2.368E-02	2.230E-02	
914	3.025E-00	7.326E-01	3.027E-01	1.719E-01	7.770E-02	4.045E-02	3.780E-02	
1219	8.010E-00	1.809E-00	4.926E-01	2.667E-01	1.071E-01	5.782E-02	5.321E-02	
1524	2.101E-01	3.321E-00	7.491E-01	3.836E-01	1.472E-01	7.791E-02	7.216E-02	

FLIGHT NO. 91      FILTER NO. 2								
DIRECTIONAL PATH REFLECTANCE FROM GROUND TO ALTITUDE								
ALTITUDE	ZENITH ANGLE OF PATH OF SIGHT (DEGREES)							
METERS	93	95	100	105	120	150	180	
305	2.511E-01	1.211E-01	5.247E-02	3.243E-02	1.464E-02	8.272E-03	7.849E-03	
610	7.037E-01	1.963E-01	1.176E-01	7.076E-02	3.129E-02	1.757E-02	1.665E-02	
914	1.687E-00	5.905E-01	2.073E-01	1.207E-01	5.187E-02	2.872E-02	2.693E-02	
1219	3.867E-00	1.072E-00	3.294E-01	1.843E-01	7.645E-02	4.135E-02	3.964E-02	
1524	7.932E-00	1.730E-00	4.688E-01	2.529E-01	1.017E-01	5.509E-02	5.247E-02	

FLIGHT NO. 91      FILTER NO. 3								
DIRECTIONAL PATH REFLECTANCE FROM GROUND TO ALTITUDE								
ALTITUDE	ZENITH ANGLE OF PATH OF SIGHT (DEGREES)							
METERS	93	95	100	105	120	150	180	
305	1.119E-01	5.649E-02	2.557E-02	1.612E-02	7.575E-03	4.596E-03	4.648E-03	
610	2.626E-01	1.239E-01	5.315E-02	3.299E-02	1.527E-02	9.113E-03	9.178E-03	
914	5.416E-01	2.313E-01	9.261E-02	5.630E-02	2.558E-02	1.523E-02	1.550E-02	
1219	9.047E-01	3.679E-01	1.376E-01	8.136E-02	3.654E-02	2.162E-02	2.203E-02	
1524	1.543E-00	5.219E-01	1.836E-01	1.075E-01	4.733E-02	2.782E-02	2.835E-02	

FLIGHT NO. 91      FILTER NO. 4								
DIRECTIONAL PATH REFLECTANCE FROM GROUND TO ALTITUDE								
ALTITUDE	ZENITH ANGLE OF PATH OF SIGHT (DEGREES)							
METERS	93	95	100	105	120	150	180	
305	7.277E-02	3.763E-02	1.766E-02	1.137E-02	5.534E-03	3.416E-03	3.369E-03	
610	1.630E-01	7.165E-02	3.696E-02	2.355E-02	1.138E-02	7.014E-03	7.006E-03	
914	3.083E-01	1.454E-01	6.316E-02	3.971E-02	1.896E-02	1.166E-02	1.180E-02	
1219	5.615E-01	2.727E-01	9.227E-02	5.724E-02	2.704E-02	1.650E-02	1.681E-02	
1524	6.784E-01	2.938E-01	1.144E-01	7.044E-02	3.303E-02	1.989E-02	1.999E-02	

FLIGHT NO. 91      FILTER NO. 5								
DIRECTIONAL PATH REFLECTANCE FROM GROUND TO ALTITUDE								
ALTITUDE	ZENITH ANGLE OF PATH OF SIGHT (DEGREES)							
METERS	93	95	100	105	120	150	180	
305	2.048E-01	1.005E-01	4.433E-02	2.770E-02	1.277E-02	7.387E-03	7.091E-03	
610	5.575E-01	2.441E-01	9.907E-02	6.040E-02	2.725E-02	1.553E-02	1.472E-02	
914	1.263E-00	5.719E-01	1.731E-01	1.024E-01	4.476E-02	2.478E-02	2.293E-02	
1219	2.550E-00	7.867E-01	2.602E-01	1.491E-01	6.334E-02	3.449E-02	3.175E-02	
1524	4.879E-00	1.219E-00	3.604E-01	2.001E-01	8.769E-02	4.440E-02	4.077E-02	

#### FLIGHT 92

Moonlight (approximately one and one-half days before the quarter moon). The flight pattern was from Lop Buri to approximately 40 km west of Sing Buri. The terrain was flat (river delta country) and cultivated with rice paddies; and there were also small scattered settlements. This was the dry season (March) when crops had been harvested, ground cover had yellowed, rice paddies were dry, and the stubble was being burned off. The atmosphere was free of clouds but hazy at the lower altitudes. Data were recorded from just after midnight, 0031 local time, until 0253. The moon phase angle was  $70^\circ$ ; the moon zenith angle during sky radiance data-taking ranged from  $74^\circ$  to  $54^\circ$ .



FLIGHT NO. 92				FILTER NO. 1			
IRRADIANCE (WATTS/SG.M. MICRO M.)							
ALTITUDE (METERS)	DOWN- WELLING	UP- WELLING	ALBEDO	SCALAR DOWNWELLING	SCALAR UPWELLING	SCALAR TOTAL	SCALAR ALBEDO
164	7.947E-05	6.766E-06	.085	1.841E-04	2.271E-05	2.068E-04	.122
472	1.117E-04	1.214E-05	.109	2.814E-04	4.052E-05	3.219E-04	.144
771	1.351E-04	1.774E-05	.131	3.222E-04	6.042E-05	3.827E-04	.187
1066	1.133E-04	7.675E-05	.236	2.740E-04	8.371E-05	3.577E-04	.305
1376	2.175E-04	3.528E-05	.162	4.634E-04	1.058E-04	5.732E-04	.237
1767	1.074E-04	4.464E-05	.147	6.261E-04	1.320E-04	7.551E-04	.212

FL' . NC.92				FILTER NO. 2			
IRRADIANCE(WATTS/SG.M. MICRO M.)							
ALTITUDE (METERS)	DOWN- WELLING	UP- WELLING	ALBECC	SCALAR		SCALAF	SCALAF
				DOWNWELLING	UPWELLING	TOTAL	ALBECC
170	2.635E-05	9.074E-06	.105	2.085E-04	2.727E-05	2.358E-04	.121
472	1.220E-04	1.719E-05	.141	2.245E-04	5.446E-05	2.789E-04	.168
778	1.468E-04	2.264E-05	.154	3.615E-04	7.323E-05	4.347E-04	.202
1065	1.048E-04	3.140E-05	.200	2.629E-04	9.764E-05	3.617E-04	.271
1381	1.959E-04	4.080E-05	.204	4.806E-04	1.225E-04	5.831E-04	.266
1706	1.693E-04	4.855E-05	.287	3.768E-04	1.422E-04	5.190E-04	.278

FLIGHT NO. 92				FILTER NO. 3			
IRRADIANCE (WATTS/SG.M. MICRO M.)							
ALTITUDE (METERS)	DOWN- WELLING	UP- WELLING	ALBEDO	SCALAR DOWNWELLING	SCALAR UPWELLING	SCALAR TOTAL	SCALAR ALBEDO
167	1.083E-04	2.291E-05	.221	3.071E-04	6.361E-05	3.707E-04	.207
472	1.380E-04	2.022E-05	.209	4.051E-04	7.756E-05	4.831E-04	.192
779	2.025E-04	3.719E-05	.164	5.268E-04	1.069E-04	6.337E-04	.202
1064	1.996E-04	3.904E-05	.156	4.667E-04	1.145E-04	5.816E-04	.246
1377	2.556E-04	5.054E-05	.155	5.986E-04	1.464E-04	7.450E-04	.245

FLIGHT NO. 92				FILTER NO. 4			
IRRADIANCE (WATTS/SG.M. MICRO M.)							
ALTITUDE (METERS)	DOWN- WELLING	UP- WELLING	ALBEDO	SCALAR DOWNWELLING	SCALAR UPWELLING	SCALAR TOTAL	SCALAR ALBEDO
168							
467							
779							
1065							
1320							
1704							

FLIGHT NO. 92				FILTER NO. 5			
IRRADIANCE (WATTS/SG.M. MICRO M.)							
ALTITUDE	DOWN-	UP-		SCALAR	SCALAR	SCALAR	SCALAR
(METERS)	WELLING	WELLING	ALBEDO	DOWNWELLING	UPWELLING	TOTAL	ALBEDO
170	1.207E-04	1.237E-05	.111	3.110E-04	4.069E-05	3.517E-04	.131
466	1.278E-04	1.958E-05	.141	2.460E-04	5.502E-05	4.051E-04	.171
778	1.477E-04	7.575E-05	.174	2.672E-04	7.934E-05	4.468E-04	.217
1063	1.494E-04	3.459E-05	.222	3.452E-04	1.050E-04	4.543E-04	.301
1376	2.265E-04	4.089E-05	.173	5.450E-04	1.243E-04	6.694E-04	.228
1657	2.393E-04	5.070E-05	.212	5.077E-04	1.457E-04	6.534E-04	.287

FLIGHT NO. 92				
AZIMUTH OF PATH OF SIGHT = 0				
DIRECTIONAL REFLECTANCE OF BACKGROUND				
ZENITH	FILTERS			
ANGLE	1	2	5	3
93	.79615	.80305	.56556	1.57400
95	.64310	.62787	.62903	.52559
100	.45085	.35732	.30964	.43106
105	.21840	.22517	.22873	.29805
120	.10257	.12463	.17655	.20064
150	.05926	.07302	.04753	.05357
180	.04821	.07767	.05582	.10235

FLIGHT NO. 92				
AZIMUTH OF PATH OF SIGHT = 90				
DIRECTIONAL REFLECTANCE OF BACKGROUND				
ZENITH	FILTERS			
ANGLE	1	2	5	3
93	.44987	.43872	1.12151	.54671
95	.29600	.20402	.44551	.31027
100	.16568	.15556	.10121	.21584
105	.12146	.14300	.13268	.18137
120	.08226	.05660	.06055	.12750
150	.05512	.06185	.05064	.05165
180	.04521	.07767	.05582	.10235

FLIGHT NO. 92				
AZIMUTH OF PATH OF SIGHT = 180				
DIRECTIONAL REFLECTANCE OF BACKGROUND				
ZENITH	FILTERS			
ANGLE	1	2	5	3
93	.27222	.25295	.25547	.65613
95	.28611	.4710	.20484	.58082
100	.16877	.21544	.15431	.27427
105	.15205	.15652	.15730	.25156
120	.11599	.11618	.11625	.20925
150	.05975	.08502	.08857	.12717
180	.04821	.07767	.05582	.10235

FLIGHT NO. 92				
AZIMUTH OF PATH OF SIGHT = 270				
DIRECTIONAL REFLECTANCE OF BACKGROUND				
ZENITH	FILTERS			
ANGLE	1	2	5	3
93	.29741	.30135	.27829	.30451
95	.16897	.21509	.20868	.24505
100	.11632	.13950	.15217	.22417
105	.09747	.11454	.22402	.15420
120	.06980	.11022	.05062	.14170
150	.06361	.05805	.06508	.08642
180	.04821	.07767	.05582	.10235

DATE 30965 FLIGHT NO. 52 CIRCLE LEVEL ALTITUDE (M.)= 24 ILP=1

ALTITUDE (METERS)	TOTAL SCATTERING COEFFICIENT (PER METER)				
	FILTER 1	2	3	4	5
0	2.223E-04	1.769E-04	1.120E-04	6.978E-05	1.875E-04
30	2.215E-04	1.783E-04	1.126E-04	6.955E-05	1.865E-04
61	2.208E-04	1.777E-04	1.122E-04	6.931E-05	1.863E-04
91	2.200E-04	1.771E-04	1.115E-04	6.908E-05	1.856E-04
122	2.193E-04	1.765E-04	1.115E-04	6.885E-05	1.850E-04
152	2.186E-04	1.759E-04	1.111E-04	6.862E-05	1.844E-04
183	2.178E-04	1.772E-04	1.107E-04	6.848E-05	1.838E-04
213	2.143E-04	1.767E-04	1.104E-04	6.848E-05	1.804E-04
244	2.108E-04	1.692E-04	1.085E-04	6.734E-05	1.776E-04
274	2.042E-04	1.547E-04	1.045E-04	6.309E-05	1.732E-04
305	1.920E-04	1.413E-04	1.006E-04	5.800E-05	1.693E-04
335	1.690E-04	1.368E-04	8.914E-05	5.492E-05	1.585E-04
366	1.546E-04	1.432E-04	8.619E-05	5.482E-05	1.356E-04
396	1.518E-04	1.487E-04	8.694E-05	5.730E-05	1.315E-04
427	1.605E-04	1.525E-04	9.047E-05	5.883E-05	1.255E-04
457	1.671E-04	1.523E-04	9.227E-05	5.871E-05	1.415E-04
488	1.707E-04	1.542E-04	9.309E-05	5.919E-05	1.446E-04
518	1.673E-04	1.568E-04	9.394E-05	5.828E-05	1.404E-04
549	1.644E-04	1.528E-04	9.435E-05	5.896E-05	1.375E-04
579	1.579E-04	1.449E-04	9.448E-05	5.617E-05	1.373E-04
610	1.578E-04	1.408E-04	9.309E-05	5.611E-05	1.392E-04
640	1.555E-04	1.394E-04	9.055E-05	5.573E-05	1.383E-04
671	1.556E-04	1.385E-04	8.961E-05	5.464E-05	1.410E-04
701	1.566E-04	1.372E-04	8.851E-05	5.475E-05	1.442E-04
732	1.590E-04	1.360E-04	8.917E-05	5.579E-05	1.475E-04
762	1.707E-04	1.351E-04	8.848E-05	5.887E-05	1.457E-04
792	1.736E-04	1.337E-04	8.765E-05	5.868E-05	1.358E-04
823	1.667E-04	1.344E-04	8.830E-05	5.651E-05	1.284E-04
853	1.636E-04	1.372E-04	8.858E-05	5.622E-05	1.437E-04
884	1.617E-04	1.413E-04	8.855E-05	5.648E-05	1.421E-04
914	1.615E-04	1.510E-04	8.807E-05	5.640E-05	1.405E-04
945	1.610E-04	1.481E-04	8.914E-05	5.680E-05	1.354E-04
975	1.594E-04	1.432E-04	9.211E-05	5.748E-05	1.381E-04
1006	1.572E-04	1.357E-04	9.325E-05	5.833E-05	1.352E-04
1036	1.565E-04	1.380E-04	9.051E-05	5.810E-05	1.361E-04
1067	1.571E-04	1.370E-04	9.112E-05	5.857E-05	1.347E-04
1097	1.562E-04	1.365E-04	9.237E-05	5.844E-05	1.350E-04
1128	1.557E-04	1.359E-04	9.307E-05	5.895E-05	1.337E-04
1158	1.521E-04	1.364E-04	9.527E-05	5.882E-05	1.345E-04
1189	1.510E-04	1.392E-04	9.145E-05	5.847E-05	1.341E-04
1219	1.506E-04	1.455E-04	9.542E-05	5.871E-05	1.362E-04
1250	1.462E-04	1.471E-04	8.424E-05	5.453E-05	1.392E-04
1280	1.458E-04	1.261E-04	8.407E-05	5.455E-05	1.446E-04
1311	1.535E-04	1.264E-04	8.415E-05	5.810E-05	1.492E-04
1341	1.688E-04	1.257E-04	8.921E-05	5.847E-05	1.485E-04
1372	1.720E-04	1.285E-04	8.877E-05	6.042E-05	1.527E-04
1402	1.697E-04	1.338E-04	9.127E-05	6.246E-05	1.631E-04
1433	1.877E-04	1.400E-04	9.512E-05	6.546E-05	1.542E-04
1463	1.962E-04	1.462E-04	9.492E-05	6.785E-05	1.642E-04
1494	1.916E-04	1.510E-04	9.422E-05	6.720E-05	1.677E-04
1524	1.907E-04	1.546E-04	9.689E-05	6.497E-05	1.782E-04
1554	1.913E-04	1.531E-04	9.744E-05	6.782E-05	1.857E-04
1585	2.072E-04	1.526E-04	9.948E-05	7.019E-05	1.737E-04
1615	1.975E-04	1.528E-04	9.805E-05	7.284E-05	1.625E-04
1646	1.952E-04	1.569E-04	1.022E-04	6.717E-05	1.870E-04
1676	2.002E-04	1.513E-04	1.120E-04	6.303E-05	1.524E-04
1707	1.868E-04	1.500E-04	1.120E-04	6.282E-05	1.510E-04
1737	1.862E-04	1.503E-04	1.120E-04	6.261E-05	1.514E-04
1768	1.856E-04	1.498E-04	1.118E-04	6.240E-05	1.505E-04
1798	1.849E-04	1.493E-04	1.115E-04	6.215E-05	1.504E-04
1829	1.843E-04	1.488E-04	1.111E-04	6.198E-05	1.495E-04

FIRST DATA ALT. 6 6 6 6 7  
LAST DATA ALT. 57 56 56 56 56

		FLIGHT NO. 92		FILTER NO. 1			
		BEAM TRANSMITTANCE FROM GROUND TO ALTITUDE					
ALTITUDE		ZENITH ANGLE OF PATH OF SIGHT (DEGREES)					
METERS		93	95	100	105	120	150
305		.2819373	.4707406	.6851188	.7759058	.8765242	.9269714
610		.1092256	.2654542	.5135195	.6597819	.7535874	.8750462
914		.0389509	.1504887	.2865481	.4384811	.57188255	.6826460
1219		.0145880	.0770578	.1537108	.2435553	.3424787	.4422714
1524		.0045041	.0277878	.0519727	.0851385	.1285545	.17262524

		FLIGHT NO. 92		FILTER NO. 2			
		BEAM TRANSMITTANCE FROM GROUND TO ALTITUDE					
ALTITUDE		ZENITH ANGLE OF PATH OF SIGHT (DEGREES)					
METERS		93	95	100	105	120	150
305		.3631207	.5472674	.7289240	.8162821	.9002547	.9411267
610		.1491437	.3257858	.5095552	.6654812	.8224291	.9327686
914		.0640417	.2011609	.4471380	.5827365	.7561355	.8504606
1219		.0266506	.1121465	.2495225	.4025757	.5641452	.6854558
1524		.0110064	.078515	.1740563	.3155593	.4779181	.6771024

		FLIGHT NO. 92		FILTER NO. 3			
		BEAM TRANSMITTANCE FROM GROUND TO ALTITUDE					
ALTITUDE		ZENITH ANGLE OF PATH OF SIGHT (DEGREES)					
METERS		93	95	100	105	120	150
305		.5238670	.6700152	.8242880	.8747775	.9351218	.9620115
610		.3019244	.4537261	.7017095	.7884668	.8842419	.9314256
914		.1749298	.3615462	.6001195	.7059280	.8374962	.9028807
1219		.0988537	.2225306	.4100703	.6214004	.7920565	.8740715
1524		.0560027	.1422470	.2737557	.4575078	.7501820	.8470558

		FLIGHT NO. 92		FILTER NO. 4			
		BEAM TRANSMITTANCE FROM GROUND TO ALTITUDE					
ALTITUDE		ZENITH ANGLE OF PATH OF SIGHT (DEGREES)					
METERS		93	95	100	105	120	150
305		.6714840	.7889854	.8576465	.9237910	.9595286	.9764201
610		.4765666	.6481100	.8031254	.8622287	.9266855	.9565546
914		.3374108	.5104003	.7274043	.8177221	.8552550	.9281763
1219		.2376848	.4258847	.6591691	.7560677	.8652434	.9198253
1524		.1617400	.3222507	.5224427	.7226726	.8327607	.9003536

		FLIGHT NO. 92		FILTER NO. 5			
		BEAM TRANSMITTANCE FROM GROUND TO ALTITUDE					
ALTITUDE		ZENITH ANGLE OF PATH OF SIGHT (DEGREES)					
METERS		93	95	100	105	120	150
305		.3428442	.5288484	.7202352	.8089277	.8548571	.9278957
610		.1465566	.3226849	.5668278	.6822570	.7710552	.8524073
914		.0613220	.1863244	.4417095	.5775883	.7125247	.8488750
1219		.0281915	.1222452	.2475554	.4024852	.5830037	.6800776
1524		.0198763	.0712276	.1525578	.2710755	.4105147	.5681555

AZIMUTH OF PATH OF SIGHT =		FLIGHT NO. 92		FILTER NO. 1			
ALTITUDE		PATH RADIANCE FROM GROUND TO ALTITUDE (WATTS/STER. SC. MICR M.)		ZENITH ANGLE OF PATH OF SIGHT (DEGREES)			
METERS		93	95	100	105	120	150
305		2.671E-05	1.772E-05	9.660E-06	5.575E-06	1.582E-06	6.363E-07
610		4.559E-05	3.325E-05	1.627E-05	1.157E-05	4.235E-06	1.377E-06
914		5.570E-05	4.427E-05	2.655E-05	1.743E-05	6.725E-06	2.253E-06
1219		5.751E-05	4.936E-05	3.223E-05	2.200E-05	9.023E-06	3.153E-06
1524		8.205E-05	6.755E-05	4.428E-05	2.050E-05	1.271E-05	4.470E-06

FLIGHT NO. 92		FILTER NO. 2					
ALTITUDE		PATH RADIANCE FROM GROUND TO ALTITUDE (WATTS/STER. SC. MICR M.)		ZENITH ANGLE OF PATH OF SIGHT (DEGREES)			
METERS		93	95	100	105	120	150
305		2.953E-05	1.880E-05	5.278E-06	5.624E-06	1.925E-06	6.015E-07
610		5.522E-05	3.600E-05	2.040E-05	1.276E-05	4.539E-06	1.421E-06
914		7.642E-05	5.112E-05	2.557E-05	1.501E-05	7.092E-06	2.282E-06
1219		6.457E-05	5.492E-05	3.517E-05	2.253E-05	9.346E-06	3.149E-06
1524		8.249E-05	6.894E-05	4.460E-05	2.042E-05	1.238E-05	4.224E-06

FLIGHT NO. 92		FILTER NO. 3					
ALTITUDE		PATH RADIANCE FROM GROUND TO ALTITUDE (WATTS/STER. SC. MICR M.)		ZENITH ANGLE OF PATH OF SIGHT (DEGREES)			
METERS		93	95	100	105	120	150
305		4.523E-05	2.712E-05	1.284E-05	7.655E-06	2.663E-06	7.373E-07
610		7.456E-05	4.895E-05	2.437E-05	1.480E-05	5.057E-06	1.448E-06
914		9.890E-05	6.895E-05	3.615E-05	2.222E-05	7.770E-06	2.266E-06
1219		1.072E-04	8.065E-05	4.492E-05	2.834E-05	1.021E-05	3.085E-06
1524		1.247E-04	9.685E-05	5.556E-05	3.559E-05	1.300E-05	3.972E-06

FLIGHT NO. 92		FILTER NO. 4					
ALTITUDE		PATH RADIANCE FROM GROUND TO ALTITUDE (WATTS/STER. SC. MICR M.)		ZENITH ANGLE OF PATH OF SIGHT (DEGREES)			
METERS		93	95	100	105	120	150
305							
610							
914							
1219							
1524							

FLIGHT NO. 92		FILTER NO. 5					
ALTITUDE		PATH RADIANCE FROM GROUND TO ALTITUDE (WATTS/STER. SC. MICR M.)		ZENITH ANGLE OF PATH OF SIGHT (DEGREES)			
METERS		93	95	100	105	120	150
305		5.099E-05	3.307E-05	1.639E-05	5.875E-06	3.212E-06	9.265E-07
610		6.436E-05	4.734E-05	2.610E-05	1.634E-05	5.758E-06	1.769E-06
914		7.553E-05	5.842E-05	3.455E-05	2.266E-05	8.514E-06	2.724E-06
1219		9.700E-05	7.124E-05	4.452E-05	2.967E-05	1.154E-05	3.606E-06
1524		1.066E-04	8.875E-05	5.702E-05	2.865E-05	1.541E-05	5.150E-06

FLIGHT NO. 92      FILTER NO. 1

PATH RADIANCE FROM ORIGIN TO ALTITUDE (WATTS/STER. SEC. MICRO M.)

ALTITUDE      ZENITH ANGLE OF PATH OF SIGHT (DEGREES)

METERS	92	95	100	105	120	150	180
305	1.112E-05	7.615E-06	4.214E-06	2.781E-06	1.279E-06	5.740E-07	4.606E-07
610	1.735E-05	1.214E-05	7.931E-06	5.400E-06	2.852E-06	1.234E-06	8.77E-07
914	2.319E-05	1.809E-05	1.17E-05	8.378E-06	4.155E-06	2.076E-06	1.442E-06
1219	2.774E-05	2.204E-05	1.525E-05	1.120E-05	5.761E-06	2.845E-06	2.007E-06
1524	3.22E-05	2.522E-05	2.017E-05	1.515E-05	8.033E-06	4.037E-06	2.275E-06

FLIGHT NO. 92      FILTER NO. 2

PATH RADIANCE FROM ORIGIN TO ALTITUDE (WATTS/STER. SEC. MICRO M.)

ALTITUDE      ZENITH ANGLE OF PATH OF SIGHT (DEGREES)

METERS	92	95	100	105	120	150	180
305	1.066E-05	7.159E-06	3.812E-06	2.523E-06	1.143E-06	5.12E-07	4.03E-07
610	1.847E-05	1.353E-05	7.945E-06	5.400E-06	2.852E-06	1.234E-06	8.77E-07
914	2.326E-05	1.854E-05	1.172E-05	8.378E-06	4.155E-06	2.076E-06	1.442E-06
1219	2.656E-05	2.241E-05	1.515E-05	1.120E-05	5.761E-06	2.845E-06	2.007E-06
1524	3.179E-05	2.714E-05	1.911E-05	1.421E-05	7.475E-06	3.745E-06	1.645E-06

FLIGHT NO. 92      FILTER NO. 3

PATH RADIANCE FROM ORIGIN TO ALTITUDE (WATTS/STER. SEC. MICRO M.)

ALTITUDE      ZENITH ANGLE OF PATH OF SIGHT (DEGREES)

METERS	92	95	100	105	120	150	180
305	1.147E-05	7.130E-06	3.715E-06	2.423E-06	1.107E-06	5.304E-07	4.427E-07
610	1.859E-05	1.293E-05	7.191E-06	4.823E-06	2.781E-06	1.125E-06	8.426E-07
914	2.535E-05	1.849E-05	1.088E-05	7.415E-06	3.857E-06	1.841E-06	1.540E-06
1219	2.924E-05	2.285E-05	1.419E-05	1.000E-05	5.031E-06	2.61E-06	2.147E-06
1524	3.353E-05	2.722E-05	1.762E-05	1.285E-05	6.419E-06	3.332E-06	2.188E-06

FLIGHT NO. 92      FILTER NO. 4

PATH RADIANCE FROM ORIGIN TO ALTITUDE (WATTS/STER. SEC. MICRO M.)

ALTITUDE      ZENITH ANGLE OF PATH OF SIGHT (DEGREES)

METERS	92	95	100	105	120	150	180
305							
610							
914							
1219							
1524							

FLIGHT NO. 92      FILTER NO. 5

PATH RADIANCE FROM ORIGIN TO ALTITUDE (WATTS/STER. SEC. MICRO M.)

ALTITUDE      ZENITH ANGLE OF PATH OF SIGHT (DEGREES)

METERS	92	95	100	105	120	150	180
305	1.508E-05	1.008E-05	5.474E-06	3.605E-06	1.625E-06	7.761E-07	6.360E-07
610	2.183E-05	1.428E-05	9.677E-06	6.621E-06	3.145E-06	1.524E-06	1.252E-06
914	2.658E-05	2.143E-05	1.374E-05	9.725E-06	4.812E-06	2.378E-06	1.951E-06
1219	3.164E-05	2.61E-05	1.794E-05	1.203E-05	6.662E-06	3.248E-06	2.715E-06
1524	3.687E-05	3.07E-05	2.270E-05	1.602E-05	8.907E-06	4.531E-06	3.705E-06

AZIMUTH OF PATH OF SIGHT = 100  
 FLIGHT NO. 92 FILTER NO. 1  
 PATH RADIANCE FROM GROUND TO ALTITUDE (WATTS/STER. SEC. MICRO M.)  
 ZENITH ANGLE OF PATH OF SIGHT (DEGREES)

ALTITUDE METERS	92	95	100	105	120	150	180
305	1.0211-C5	7.1151-C6	4.0101-C6	2.7161-C6	1.2751-C6	5.8891-C7	4.6061-C7
610	1.6441-C5	1.2561-C5	7.7811-C6	5.4971-C6	2.7321-C6	1.2751-C6	9.9731-C7
914	2.0771-C5	1.7181-C5	1.1111-C5	6.4241-C6	4.7931-C6	2.0971-C6	1.6421-C6
1219	2.2351-C5	2.0351-C5	1.4551-C5	1.0981-C5	5.9591-C6	2.9231-C6	2.3071-C6
1524	2.9011-C5	2.5951-C5	1.8591-C5	1.4701-C5	6.2491-C6	4.1781-C6	3.2751-C6

FLIGHT NO. 92 FILTER NO. 2  
 PATH RADIANCE FROM GROUND TO ALTITUDE (WATTS/STER. SEC. MICRO M.)  
 ZENITH ANGLE OF PATH OF SIGHT (DEGREES)

ALTITUDE METERS	92	95	100	105	120	150	180
305	1.0141-C5	6.7541-C6	2.7371-C6	2.5221-C6	1.1531-C6	5.5041-C7	4.3121-C7
610	1.7621-C5	1.3061-C5	7.5171-C6	5.5721-C6	2.7761-C6	1.2941-C6	1.0141-C6
914	2.0191-C5	1.7771-C5	1.3151-C5	6.5121-C6	4.4261-C6	2.1011-C6	1.6401-C6
1219	2.4231-C5	2.0871-C5	1.4271-C5	1.0951-C5	5.9441-C6	2.8661-C6	2.2721-C6
1524	2.7771-C5	2.4511-C5	1.8541-C5	1.3681-C5	7.0001-C6	3.8721-C6	3.0491-C6

FLIGHT NO. 92 FILTER NO. 3  
 PATH RADIANCE FROM GROUND TO ALTITUDE (WATTS/STER. SEC. MICRO M.)  
 ZENITH ANGLE OF PATH OF SIGHT (DEGREES)

ALTITUDE METERS	92	95	100	105	120	150	180
305	1.0431-C5	6.5941-C6	2.4171-C6	2.4171-C6	1.1121-C6	5.4791-C7	4.4271-C7
610	1.1241-C5	1.1751-C5	7.2411-C6	5.1891-C6	2.1781-C6	1.1931-C6	9.4261-C7
914	2.5331-C5	1.7141-C5	1.1531-C5	6.2621-C6	4.3171-C6	1.9951-C6	1.5401-C6
1219	2.9041-C5	2.3151-C5	1.5111-C5	1.1111-C5	6.8841-C6	2.8021-C6	2.1471-C6
1524	3.1601-C5	2.4421-C5	1.8121-C5	1.3671-C5	7.6301-C6	3.8771-C6	2.7861-C6

FLIGHT NO. 92 FILTER NO. 4  
 PATH RADIANCE FROM GROUND TO ALTITUDE (WATTS/STER. SEC. MICRO M.)  
 ZENITH ANGLE OF PATH OF SIGHT (DEGREES)

ALTITUDE METERS	92	95	100	105	120	150	180
305							
610							
914							
1219							
1524							

FLIGHT NO. 92 FILTER NO. 5  
 PATH RADIANCE FROM GROUND TO ALTITUDE (WATTS/STER. SEC. MICRO M.)  
 ZENITH ANGLE OF PATH OF SIGHT (DEGREES)

ALTITUDE METERS	92	95	100	105	120	150	180
305	1.0111-C5	6.7111-C6	2.2111-C6	2.4151-C6	1.7411-C6	5.1141-C7	6.3801-C7
610	2.2111-C5	1.2211-C5	7.4111-C6	5.1571-C6	2.4151-C6	1.1511-C6	1.2211-C6
914	2.4741-C5	2.1211-C5	1.3611-C5	5.5171-C6	5.2621-C6	2.5141-C6	1.5511-C6
1219	2.5191-C5	2.4111-C5	1.7541-C5	1.1511-C5	7.3251-C6	1.1511-C6	2.7571-C6
1524	2.2911-C5	2.4121-C5	2.1111-C5	1.1511-C5	6.7551-C6	4.1111-C6	3.7791-C6

AZIMUTH OF PATH OF SIGHT = 270								
FLIGHT NO. 92			FILTER NO. 1					
PATH RADIANCE FROM GROUND TO ALTITUDE (WATTS/STER. SQ. M. MICRO M.)								
ALTITUDE	ZENITH ANGLE OF PATH OF SIGHT (DEGREES)							
METERS	93	95	100	105	120	150	180	
305	1.136E-05	7.769E-06	4.259E-06	2.755E-06	1.240E-06	5.688E-07	4.608E-07	
610	1.718E-05	1.304E-05	7.852E-06	5.264E-06	2.536E-06	1.28E-06	9.972E-07	
914	2.197E-05	1.788E-05	1.159E-05	8.213E-06	4.041E-06	1.993E-06	1.642E-06	
1219	2.556E-05	2.182E-05	1.510E-05	1.055E-05	5.573E-06	2.791E-06	2.307E-06	
1524	3.105E-05	2.709E-05	1.944E-05	1.452E-05	7.677E-06	3.942E-06	3.275E-06	

FLIGHT NO. 92			FILTER NO. 2					
PATH RADIANCE FROM GROUND TO ALTITUDE (WATTS/STER. SQ. M. MICRO M.)								
ALTITUDE	ZENITH ANGLE OF PATH OF SIGHT (DEGREES)							
METERS	93	95	100	105	120	150	180	
305	1.121E-05	7.417E-06	3.508E-06	2.505E-06	1.154E-06	5.220E-07	4.312E-07	
610	1.870E-05	1.372E-05	6.077E-06	5.454E-06	2.597E-06	1.244E-06	1.014E-06	
914	2.343E-05	1.662E-05	1.176E-05	8.274E-06	4.069E-06	2.001E-06	1.640E-06	
1219	2.659E-05	2.241E-05	1.510E-05	1.054E-05	5.565E-06	2.782E-06	2.272E-06	
1524	3.117E-05	2.655E-05	1.892E-05	1.402E-05	7.325E-06	3.715E-06	3.049E-06	

FLIGHT NO. 92			FILTER NO. 3					
PATH RADIANCE FROM GROUND TO ALTITUDE (WATTS/STER. SQ. M. MICRO M.)								
ALTITUDE	ZENITH ANGLE OF PATH OF SIGHT (DEGREES)							
METERS	93	95	100	105	120	150	180	
305	1.122E-05	6.983E-06	3.651E-06	2.402E-06	1.115E-06	5.455E-07	4.427E-07	
610	1.820E-05	1.261E-05	7.027E-06	4.741E-06	2.272E-06	1.145E-06	9.47E-07	
914	2.469E-05	1.801E-05	1.059E-05	7.215E-06	3.615E-06	1.87E-06	1.540E-06	
1219	2.886E-05	2.243E-05	1.392E-05	9.629E-06	4.580E-06	2.5E-06	2.147E-06	
1524	3.306E-05	2.661E-05	1.737E-05	1.251E-05	6.467E-06	3.37E-06	2.786E-06	

FLIGHT NO. 2		FILTER NO. 4						
PATH RADIANCE FROM GROUND TO ALTITUDE (WATTS/STER. SQ. M. MICRO M.)								
ALTITUDE	ZENITH ANGLE OF PATH OF SIGHT (DEGREES)							
METERS	95	100	105	120	150	180		
305								
610								
914								
1219								
1524								

FLIGHT NO. 92			FILTER NO. 5					
PATH RADIANCE FROM GROUND TO ALTITUDE (WATTS/STER. SQ. M. MICRO M.)								
ZENITH ANGLE OF PATH OF SIGHT (DEGREES)								
ALTITUDE	93	95	100	105	120	150	180	
METERS								
305	1.418E-05	9.520E-06	5.230E-06	3.452E-06	1.629E-06	7.520E-07	6.280E-07	
610	2.036E-05	1.524E-05	9.127E-06	6.217E-06	3.084E-06	1.524E-06	1.253E-06	
914	2.532E-05	2.037E-05	1.210E-05	8.27E-06	4.704E-06	2.300E-06	1.957E-06	
1219	2.976E-05	2.504E-05	1.700E-05	1.241E-05	6.464E-06	3.237E-06	2.757E-06	
1524	3.460E-05	3.016E-05	2.147E-05	1.608E-05	8.619E-06	4.514E-06	3.735E-06	



AZIMUTH OF PATH OF SIGHT :		FLIGHT NO. 92		FILTER NO. 1					
		DIRECTIONAL PATH REFLECTANCE FROM GROUND TO ALTITUDE		Z-NITH ANGLE OF PATH OF SIGHT (DEGREES)					
ALTITUDE	METERS	92	95	100	105	120	150	180	
305		3.748E-02	1.489E-02	5.721E-01	2.844E-01	8.935E-02	2.715E-02	1.546E-02	
610		1.729E-01	4.900E-01	1.406E-01	7.152E-01	2.113E-01	6.222E-02	4.428E-02	
914		5.665E-01	1.162E-01	2.720E-01	1.305E-01	3.700E-01	1.078E-01	7.661E-02	
1219		1.570E-02	2.242E-01	4.354E-01	1.587E-01	5.468E-01	1.554E-01	1.129E-01	
1524		6.618E-02	5.551E-01	8.095E-01	3.360E-01	8.542E-01	2.401E-01	1.689E-01	

		FLIGHT NO. 92		FILTER NO. 2					
		DIRECTIONAL PATH REFLECTANCE FROM GROUND TO ALTITUDE		Z-NITH ANGLE OF PATH OF SIGHT (DEGREES)					
ALTITUDE	METERS	92	95	100	105	120	150	180	
305		2.559E-02	1.200E-02	4.568E-01	2.507E-01	7.835E-02	2.325E-02	1.654E-02	
610		1.349E-01	4.320E-01	1.308E-01	6.774E-01	2.008E-01	5.787E-02	4.068E-02	
914		3.773E-01	5.246E-01	2.406E-01	1.187E-01	3.412E-01	9.757E-02	6.861E-02	
1219		8.889E-01	1.623E-01	3.646E-01	1.733E-01	4.858E-01	1.414E-01	9.519E-02	
1524		2.727E-02	3.307E-01	5.921E-01	2.643E-01	7.062E-01	1.952E-01	1.389E-01	

		FLIGHT NO. 92		FILTER NO. 3					
		DIRECTIONAL PATH REFLECTANCE FROM GROUND TO ALTITUDE		Z-NITH ANGLE OF PATH OF SIGHT (DEGREES)					
ALTITUDE	METERS	92	95	100	105	120	150	180	
305		2.504E-02	1.158E-02	4.519E-01	2.541E-01	8.259E-02	2.223E-02	1.328E-02	
610		7.201E-02	2.878E-01	1.007E-01	5.445E-01	1.672E-01	4.508E-02	2.908E-02	
914		1.401E-01	5.522E-01	1.748E-01	9.081E-01	2.651E-01	7.281E-02	4.881E-02	
1219		2.145E-01	8.911E-01	2.550E-01	1.285E-01	3.728E-01	1.024E-01	6.957E-02	
1524		6.421E-01	1.461E-01	3.687E-01	1.759E-01	5.025E-01	1.300E-01	5.231E-02	

		FLIGHT NO. 92		FILTER NO. 4					
		DIRECTIONAL PATH REFLECTANCE FROM GROUND TO ALTITUDE		Z-NITH ANGLE OF PATH OF SIGHT (DEGREES)					
ALTITUDE	METERS	92	95	100	105	120	150	180	
305									
610									
914									
1219									
1524									

		FLIGHT NO. 92		FILTER NO. 5					
		DIRECTIONAL PATH REFLECTANCE FROM GROUND TO ALTITUDE		Z-NITH ANGLE OF PATH OF SIGHT (DEGREES)					
ALTITUDE	METERS	92	95	100	105	120	150	180	
305		3.664E-02	1.628E-02	5.878E-01	3.166E-01	9.518E-02	2.572E-02	1.756E-02	
610		1.143E-01	3.815E-01	1.159E-01	6.226E-01	1.835E-01	5.162E-02	2.601E-02	
914		3.120E-01	7.748E-01	2.072E-01	1.022E-01	2.944E-01	8.356E-02	5.870E-02	
1219		1.654E-01	1.570E-01	2.221E-01	1.587E-01	4.325E-01	1.225E-01	8.622E-02	
1524		1.110E-02	3.246E-01	5.550E-01	2.407E-01	6.781E-01	1.749E-01	1.225E-01	

FLIGHT NO. 92      FILTER NO. 1

DIRECTIONAL PATH REFLECTANCE FROM GROUND TO ALTITUDE

ALTITUDE      ZENITH ANGLE OF PATH OF SIGHT (DEGREES)

ALTITUDE METERS	93	95	100	105	120	150	180
305	1.460E-02	6.395E-01	4.427E-01	1.417E-01	5.625E-02	2.445E-02	1.546E-02
610	6.521E-02	1.957E-01	6.104E-01	3.376E-01	1.792E-01	5.178E-02	4.428E-02
914	2.257E-01	4.751E-01	1.203E-01	6.771E-01	2.786E-01	9.694E-02	7.661E-02
1219	6.978E-01	1.001E-01	2.054E-01	1.009E-01	3.487E-01	1.441E-01	1.129E-01
1524	2.629E-02	2.326E-01	3.671E-01	1.668E-01	5.355E-01	2.168E-01	1.685E-01

FLIGHT NO. 92      FILTER NO. 2

DIRECTIONAL PATH REFLECTANCE FROM GROUND TO ALTITUDE

ALTITUDE      ZENITH ANGLE OF PATH OF SIGHT (DEGREES)

ALTITUDE METERS	93	95	100	105	120	150	180
305	1.089E-02	4.740E-01	1.897E-01	1.125E-01	4.620E-02	2.060E-02	1.654E-02
610	4.105E-02	1.510E-01	5.075E-01	2.880E-01	1.140E-01	5.063E-02	4.068E-02
914	1.327E-01	2.352E-01	8.550E-01	5.162E-01	1.967E-01	8.459E-02	6.861E-02
1219	3.444E-01	6.057E-01	1.177E-01	3.114E-01	2.551E-01	1.252E-01	9.515E-02
1524	1.074E-02	1.307E-01	2.527E-01	1.232E-01	4.262E-01	1.766E-01	1.385E-01

FLIGHT NO. 92      FILTER NO. 3

DIRECTIONAL PATH REFLECTANCE FROM GROUND TO ALTITUDE

ALTITUDE      ZENITH ANGLE OF PATH OF SIGHT (DEGREES)

ALTITUDE METERS	93	95	100	105	120	150	180
305	6.348E-01	3.039E-01	1.307E-01	8.020E-02	3.424E-02	1.559E-02	1.228E-02
610	1.174E-02	7.554E-01	2.932E-01	1.778E-01	7.564E-02	3.505E-02	2.900E-02
914	4.064E-02	1.484E-01	2.721E-01	2.054E-01	1.207E-01	5.916E-02	4.881E-02
1219	9.009E-02	2.324E-01	1.075E-01	4.552E-01	1.842E-01	8.521E-02	6.557E-02
1524	1.721E-01	4.107E-01	1.109E-01	6.533E-01	2.509E-01	1.141E-01	9.321E-02

FLIGHT NO. 92      FILTER NO. 4

DIRECTIONAL PATH REFLECTANCE FROM GROUND TO ALTITUDE

ALTITUDE      ZENITH ANGLE OF PATH OF SIGHT (DEGREES)

ALTITUDE METERS	93	95	100	105	120	150	180
305							
610							
914							
1219							
1524							

FLIGHT NO. 92      FILTER NO. 5

DIRECTIONAL PATH REFLECTANCE FROM GROUND TO ALTITUDE

ALTITUDE      ZENITH ANGLE OF PATH OF SIGHT (DEGREES)

ALTITUDE METERS	93	95	100	105	120	150	180
305	1.147E-02	4.961E-01	1.952E-01	1.164E-01	4.705E-02	2.154E-02	1.756E-02
610	3.877E-02	1.314E-01	4.445E-01	2.523E-01	9.574E-02	4.446E-02	3.601E-02
914	1.128E-01	2.042E-01	8.100E-01	4.711E-01	1.674E-01	7.294E-02	5.870E-02
1219	2.145E-01	5.607E-01	1.342E-01	6.855E-01	2.657E-01	1.077E-01	8.223E-02
1524	5.71E-01	1.172E-01	1.276E-01	1.172E-01	4.15E-01	1.525E-01	1.225E-01

AZIMUTH OF PATH OF SIGHT = 180														
FLIGHT NO. 92			FILTER NO. 1											
DIRECTIONAL PATH REFLECTANCE FROM GROUND TO ALTITUDE														
ZENITH ANGLE OF PATH OF SIGHT (DEGREES)														
ALTITUDE	93		95		100		105		120		150		180	
METERS														
305	1.446E	CO	5.48E	01	2.318E	01	1.385E	01	5.769E	02	2.513E	02	1.946E	02
610	6.179E	00	1.811E	00	5.988E	01	3.398E	01	1.362E	01	5.765E	02	4.428E	02
914	2.113E	C1	4.509E	00	1.177E	00	6.305E	01	2.417E	01	1.004E	01	7.661E	02
1219	6.330E	C1	9.241E	00	1.959E	00	9.683E	01	3.607E	01	1.478E	01	1.129E	01
1524	2.340E	C2	2.118E	C1	3.456E	00	1.619E	00	5.611E	01	2.244E	01	1.689E	01

FLIGHT NO. 92			FILTER NO. 2					
DIRECTIONAL PATH REFLECTANCE FROM GROUND TO ALTITUDE								
ZENITH ANGLE OF PATH OF SIGHT (DEGREES)								
ALTITUDE METERS	93	95	100	105	120	150	180	
305	1.016E-00	4.490E-01	1.840E-01	1.124E-01	4.823E-02	2.128E-02	1.654E-02	
610	4.459E-00	1.458E-00	5.057E-01	2.958E-01	1.228E-01	5.269E-02	4.068E-02	
914	1.260E-01	3.230E-00	9.511E-01	5.215E-01	2.124E-01	8.984E-02	6.661E-02	
1219	3.307E-01	6.165E-00	1.525E-00	8.097E-01	3.115E-01	1.296E-01	9.519E-02	
1524	9.179E-01	1.178E-01	2.395E-00	1.204E-00	4.449E-01	1.827E-01	1.389E-01	

FLIGHT NO. 92			FILTER NO. 3					
DIRECTIONAL PATH REFLECTANCE FROM GROUND TO ALTITUDE								
ZENITH ANGLE OF PATH OF SIGHT (DEGREES)								
ALTITUDE	93		95	100	105	120	150	180
METERS								
305	5.778E-01	7.010E-01	1.261E-01	6.046E-02	3.667E-02	1.652E-02	1.228E-02	
610	1.762E-00	7.432E-01	3.037E-01	1.852E-01	8.445E-02	3.714E-02	2.908E-02	
914	4.201E-00	1.503E-00	5.572E-01	3.288E-01	1.455E-01	6.411E-02	4.881E-02	
1219	8.520E-00	2.547E-00	6.540E-01	5.054E-01	2.199E-01	9.304E-02	6.597E-02	
1524	1.637E-01	3.586E-00	1.203E-00	6.910E-01	2.950E-01	1.246E-01	9.231E-02	

FLIGHT NO. 92				FILTER NO. 4			
DIRECTIONAL PATH REFLECTANCE FROM GROUND TO ALTITUDE							
ZENITH ANGLE OF PATH OF SIGHT (DEGREES)							
ALTITUDE	92	95	100	105	120	150	180
METERS							
305							
610							
914							
1219							
1524							

FLIGHT NO. 92			FILTER NO. 5					
DIRECTIONAL PATH REFLECTANCE FROM GROUND TO ALTITUDE								
ZENITH ANGLE OF PATH OF SIGHT (DEGREES)								
ALTITUDE METERS	93	95	100	105	120	150	180	
305	1.030E-00	4.532E-01	1.868E-01	1.153E-01	5.066E-02	2.266E-02	1.756E-02	
610	3.974E-00	1.227E-00	4.220E-01	2.552E-01	1.082E-01	4.693E-02	3.601E-02	
914	1.049E-01	2.690E-00	7.938E-01	4.464E-01	1.819E-01	7.705E-02	5.870E-02	
1219	2.898E-01	5.214E-00	1.212E-00	7.015E-01	2.755E-01	1.143E-01	8.623E-02	
1524	8.679E-01	1.072E-01	2.123E-00	1.075E-00	4.025E-01	1.628E-01	1.225E-01	

AZIMUTH OF PATH OF SIGHT = 270

		FLIGHT NO. 92		FILTER NO. 1					
		DIRECTIONAL PATH REFLECTANCE FROM GROUND TO ALTITUDE		ZENITH ANGLE OF PATH OF SIGHT (DEGREES)					
ALTITUDE	METERS	93	95	100	105	120	150	180	
305		1.554E C0	6.528E-01	2.459E-01	1.427E-01	5.551E-C2	2.427E-C2	1.546E-C2	
610		6.459E C0	1.943E C0	6.044E-01	3.328E-01	1.264E-01	5.504E-C2	4.428E-C2	
914		2.235E C1	4.700E C0	1.185E C0	6.147E-01	2.224E-01	9.538E-C2	7.661E-C2	
1219		6.929E C1	9.908E C0	2.019E C0	9.849E-01	3.373E-01	1.411E-C1	1.125E-C1	
1524		2.504E C2	2.241E C1	3.530E C0	1.000E C0	5.155E-C3	2.118E-C1	1.689E-C1	

		FLIGHT NO. 92		FILTER NO. 2					
		DIRECTIONAL PATH REFLECTANCE FROM GROUND TO ALTITUDE		ZENITH ANGLE OF PATH OF SIGHT (DEGREES)					
ALTITUDE	METERS	93	95	100	105	120	150	180	
305		1.130E C0	4.921E-C1	1.904E-C1	1.156E-C1	4.645E-C2	2.057E-C2	1.654E-C2	
610		4.562E C0	1.533E C0	5.147E-C1	2.516E-C1	1.149E-C1	5.067E-C2	4.068E-C2	
914		1.232E C1	3.366E C0	5.566E-C1	5.166E-C1	1.958E-C1	6.554E-C2	6.861E-C2	
1219		3.630E C1	6.621E C0	1.577E C0	6.055E-C1	2.917E-C1	1.250E-C1	9.519E-C2	
1524		1.030E C2	1.293E C1	2.517E C0	1.215E C0	4.176E-C1	1.754E-C1	1.389E-C1	

		FLIGHT NO. 92		FILTER NO. 3					
		DIRECTIONAL PATH REFLECTANCE FROM GROUND TO ALTITUDE		ZENITH ANGLE OF PATH OF SIGHT (DEGREES)					
ALTITUDE	METERS	93	95	100	105	120	150	180	
305		6.212E-01	2.976E-C1	1.285E-C1	7.931E-C2	3.458E-C2	1.654E-C2	1.328E-C2	
610		1.778E C0	7.407E-C1	2.905E-C1	1.744E-C1	7.455E-C2	3.564E-C2	2.508E-C2	
914		4.053E C0	1.445E C0	5.121E-C1	2.585E-C1	1.252E-C1	5.570E-C2	4.881E-C2	
1219		8.469E C0	2.478E C0	7.902E-C1	4.473E-C1	1.824E-C1	1.582E-C2	6.597E-C2	
1524		1.712E C1	4.045E C0	1.152E C0	6.222E-C1	2.508E-C1	1.156E-C1	9.231E-C2	

		FLIGHT NO. 92		FILTER NO. 4					
		DIRECTIONAL PATH REFLECTANCE FROM GROUND TO ALTITUDE		ZENITH ANGLE OF PATH OF SIGHT (DEGREES)					
ALTITUDE	METERS	93	95	100	105	120	150	180	
305									
610									
914									
1219									
1524									

		FLIGHT NO. 92		FILTER NO. 5					
		DIRECTIONAL PATH REFLECTANCE FROM GROUND TO ALTITUDE		ZENITH ANGLE OF PATH OF SIGHT (DEGREES)					
ALTITUDE	METERS	93	95	100	105	120	150	180	
305		1.077E C0	4.687E-C1	1.875E-C1	1.127E-C1	4.765E-C2	2.154E-C2	1.066E-C2	
610		5.816E C0	1.230E C0	4.157E-C1	2.407E-C1	9.778E-C2	4.474E-C2	3.601E-C2	
914		1.074E C1	2.702E C0	7.719E-C1	4.201E-C1	1.624E-C1	7.301E-C2	5.840E-C2	
1219		7.956E C1	5.341E C0	1.271E C0	6.561E-C1	2.428E-C1	1.074E-C1	6.623E-C2	
1524		9.122E C1	1.102E C1	2.105E C0	1.015E C0	3.506E-C1	1.523E-C1	1.225E-C1	

#### FLIGHT 93

Quarter moon. Data were gathered over the wooded terrain of the Khorat Plateau some 60 km east of Khorat. There were very few artificial lights under the flight pattern. The terrain consisted primarily of dry rice paddies and deciduous trees. This was the dry season (March) and the vegetation (tree leaves and ground cover) had lost the green color of the wet season. The atmosphere was very hazy at low altitudes. Some clouds at an undetermined altitude occasionally obscured the moon. Data-taking started at 0111 local time and ended at 0334. The moon phase angle was  $83^\circ$ ; the moon zenith angle ranged from  $77^\circ$  at the start of sky radiance data-taking to  $58^\circ$  at the end.

FLIGHT NO. 1      FILTER NO. 1  
 IRRADIANCE (WATTS/SQ.M. MICRO P.)

ALTITUDE (METERS)	DOWN- WELLING	UP- WELLING	ALBEDO	SCALAR DOWNWELLING	SCALAR UPWELLING	SCALAR TOTAL	SCALAR ALBEDO
297	5.536E-05	4.534E-06	.114	7.436E-05	1.092E-05	8.528E-05	.147
600	5.169E-05	5.793E-06	.112	1.157E-04	1.936E-05	1.360E-04	.166
894	7.647E-05	1.308E-05	.171	1.944E-04	4.180E-05	2.362E-04	.215
1210	8.670E-05	1.047E-05	.190	2.070E-04	5.032E-05	2.573E-04	.243
1535	1.116E-04	2.579E-05	.236	2.707E-04	5.027E-05	3.210E-04	.296
1836	1.192E-04	5.121E-05	.275	2.796E-04	9.551E-05	3.783E-04	.352

FLIGHT NO. 2      FILTER NO. 2  
 IRRADIANCE (WATTS/SQ.M. MICRO P.)

ALTITUDE (METERS)	DOWN- WELLING	UP- WELLING	ALBEDO	SCALAR DOWNWELLING	SCALAR UPWELLING	SCALAR TOTAL	SCALAR ALBEDO
294	4.001E-05	5.031E-05	.126	1.672E-05	1.396E-05	1.007E-04	.161
606	5.503E-05	7.584E-05	.143	1.780E-04	2.338E-05	1.520E-04	.182
899	3.719E-05	1.593E-05	.194	2.383E-04	5.163E-05	2.600E-04	.244
1213	1.169E-04	2.143E-05	.143	2.933E-04	6.349E-05	3.567E-04	.217
1533	1.165E-04	5.909E-05	.250	2.811E-04	8.608E-05	3.672E-04	.306
1828	2.739E-05	3.622E-05	.412	2.117E-04	1.052E-04	3.169E-04	.497

FLIGHT NO. 3      FILTER NO. 3  
 IRRADIANCE (WATTS/SQ.M. MICRO P.)

ALTITUDE (METERS)	DOWN- WELLING	UP- WELLING	ALBEDO	SCALAR DOWNWELLING	SCALAR UPWELLING	SCALAR TOTAL	SCALAR ALBEDO
291	4.063E-05	1.044E-05	.214	1.305E-04	2.920E-05	1.597E-04	.224
598	4.767E-05	1.094E-05	.223	1.176E-04	2.944E-05	1.471E-04	.250
893	6.465E-05	1.046E-05	.242	2.422E-04	6.508E-05	3.073E-04	.264
1212	1.283E-04	1.502E-05	.231	3.389E-04	8.770E-05	4.266E-04	.259
1534	7.029E-05	3.382E-05	.421	1.311E-04	9.742E-05	2.805E-04	.432
1839	1.307E-04	1.923E-05	.300	3.114E-04	1.130E-04	4.244E-04	.363

FLIGHT NO. 4      FILTER NO. 4  
 IRRADIANCE (WATTS/SQ.M. MICRO P.)

ALTITUDE (METERS)	DOWN- WELLING	UP- WELLING	ALBEDO	SCALAR DOWNWELLING	SCALAR UPWELLING	SCALAR TOTAL	SCALAR ALBEDO
299							
597							
901							
1212							
1534							
1839							

FLIGHT NO. 5      FILTER NO. 5  
 IRRADIANCE (WATTS/SQ.M. MICRO P.)

ALTITUDE (METERS)	DOWN- WELLING	UP- WELLING	ALBEDO	SCALAR DOWNWELLING	SCALAR UPWELLING	SCALAR TOTAL	SCALAR ALBEDO
286	5.927E-05	2.563E-06	.106	1.309E-04	1.949E-05	1.504E-04	.149
597	1.000E-05	1.040E-05	.137	1.911E-04	2.130E-05	2.224E-04	.164
897	6.793E-05	9.597E-06	.152	1.371E-04	2.713E-05	1.572E-04	.09
1213	1.735E-04	2.482E-05	.143	4.123E-04	7.775E-05	4.901E-04	.189
1534	1.704E-04	3.276E-05	.272	2.557E-04	9.515E-05	3.809E-04	.333
1837	1.316E-04	3.814E-05	.275	3.714E-04	1.060E-04	4.294E-04	.336

FLIGHT NO. 93  
 AZIMUTH OF PATH OF SIGHT = 0  
 DIRECTIONAL REFLECTANCE OF BACKGROUND  
 FILTERS

ZENITH ANGLE	1	2	3	4
93		1.18590		
95		.91263		
100		.45401		
105		.34673		
120		.12406		
150		.05904		
180		.05777		

FLIGHT NO. 93  
 AZIMUTH OF PATH OF SIGHT = 90  
 DIRECTIONAL REFLECTANCE OF BACKGROUND  
 FILTERS

ZENITH ANGLE	1	2	3	4
93		.41719		
95		.36041		
100		.27722		
105		.15879		
120		.09237		
150		.06542		
180		.06777		

FLIGHT NO. 93  
 AZIMUTH OF PATH OF SIGHT = 180  
 DIRECTIONAL REFLECTANCE OF BACKGROUND  
 FILTERS

ZENITH ANGLE	1	2	3	4
93		.32751		
95		.30095		
100		.22899		
105		.18524		
120		.12433		
150		.06590		
180		.06777		

FLIGHT NO. 93  
 AZIMUTH OF PATH OF SIGHT = 270  
 DIRECTIONAL REFLECTANCE OF BACKGROUND  
 FILTERS

ZENITH ANGLE	1	2	3	4
93		.38397		
95		.30207		
100		.19614		
105		.15400		
120		.10154		
150		.07225		
180		.06777		

DATE 31069 FLIGHT NO. 13 GROUND LEVEL ALTITUDE (M.)= 226 IUP=1

ALTITUDE (METERS)	TOTAL SCATTERING COEFFICIENT (PER METER)	1	2	3	4	5
0	2.534E-04	1.000E-04	1.325E-04	3.001E-05	2.190E-04	
30	2.440E-04	2.085E-04	1.327E-04	3.637E-05	2.132E-04	
61	2.440E-04	2.072E-04	1.316E-04	3.604E-05	2.175E-04	
91	2.470E-04	2.072E-04	1.311E-04	3.575E-05	2.168E-04	
121	2.471E-04	2.055E-04	1.307E-04	3.546E-05	2.161E-04	
152	2.461E-04	2.052E-04	1.303E-04	3.518E-05	2.153E-04	
183	2.455E-04	2.051E-04	1.295E-04	3.490E-05	2.146E-04	
213	2.447E-04	2.044E-04	1.294E-04	3.461E-05	2.139E-04	
244	2.437E-04	2.037E-04	1.290E-04	3.433E-05	2.132E-04	
274	2.43E-04	2.031E-04	1.275E-04	3.405E-05	2.125E-04	
305	2.42E-04	2.024E-04	1.271E-04	3.377E-05	2.118E-04	
335	2.392E-04	1.960E-04	1.277E-04	3.349E-05	2.091E-04	
366	2.381E-04	1.912E-04	1.256E-04	3.230E-05	2.017E-04	
396	2.265E-04	1.907E-04	1.234E-04	3.091E-05	2.012E-04	
427	2.310E-04	1.755E-04	1.232E-04	7.593E-05	1.996E-04	
457	2.375E-04	1.725E-04	1.255E-04	7.584E-05	2.024E-04	
488	2.425E-04	2.052E-04	1.274E-04	7.785E-05	2.040E-04	
518	2.459E-04	2.079E-04	1.313E-04	7.833E-05	2.067E-04	
549	2.465E-04	2.111E-04	1.339E-04	8.010E-05	2.113E-04	
579	2.462E-04	2.136E-04	1.340E-04	8.134E-05	2.132E-04	
610	2.501E-04	2.177E-04	1.364E-04	8.328E-05	2.167E-04	
640	2.500E-04	2.197E-04	1.367E-04	8.434E-05	2.185E-04	
671	2.529E-04	2.214E-04	1.370E-04	8.442E-05	2.201E-04	
701	2.567E-04	2.27E-04	1.375E-04	8.455E-05	2.252E-04	
732	2.553E-04	2.251E-04	1.376E-04	8.443E-05	2.267E-04	
762	2.426E-04	2.213E-04	1.377E-04	8.437E-05	2.169E-04	
792	2.371E-04	2.211E-04	1.365E-04	8.687E-05	2.075E-04	
823	2.317E-04	2.13E-04	1.321E-04	8.741E-05	2.044E-04	
853	2.258E-04	2.132E-04	1.357E-04	8.465E-05	2.006E-04	
884	2.236E-04	2.119E-04	1.252E-04	8.660E-05	2.011E-04	
914	2.277E-04	2.231E-04	1.260E-04	8.710E-05	2.054E-04	
945	2.301E-04	2.217E-04	1.255E-04	8.653E-05	2.095E-04	
975	2.374E-04	2.132E-04	1.355E-04	8.494E-05	2.110E-04	
1006	2.373E-04	2.141E-04	1.332E-04	8.402E-05	2.126E-04	
1036	2.391E-04	2.157E-04	1.326E-04	8.479E-05	2.181E-04	
1067	2.460E-04	2.13E-04	1.332E-04	8.393E-05	2.165E-04	
1097	2.519E-04	2.072E-04	1.315E-04	8.538E-05	2.223E-04	
1128	2.517E-04	2.094E-04	1.355E-04	8.412E-05	2.208E-04	
1158	2.516E-04	2.130E-04	1.383E-04	8.426E-05	2.218E-04	
1189	2.558E-04	2.156E-04	1.412E-04	8.126E-05	2.214E-04	
1219	2.455E-04	2.132E-04	1.390E-04	8.734E-05	2.254E-04	
1250	2.479E-04	2.14E-04	1.342E-04	8.429E-05	2.199E-04	
1280	2.504E-04	2.204E-04	1.416E-04	8.447E-05	2.177E-04	
1311	2.505E-04	2.265E-04	1.421E-04	8.211E-05	2.137E-04	
1341	2.506E-04	1.979E-04	1.414E-04	8.032E-05	2.135E-04	
1372	2.415E-04	1.945E-04	1.455E-04	7.977E-05	2.055E-04	
1402	2.342E-04	1.924E-04	1.384E-04	8.005E-05	2.036E-04	
1433	2.271E-04	1.943E-04	1.320E-04	7.705E-05	2.013E-04	
1463	2.133E-04	1.952E-04	1.326E-04	8.106E-05	2.002E-04	
1494	2.062E-04	1.970E-04	1.324E-04	7.555E-05	2.006E-04	
1524	1.957E-04	1.963E-04	1.322E-04	7.927E-05	1.985E-04	
1554	2.032E-04	2.000E-04	1.407E-04	7.903E-05	1.995E-04	
1585	2.111E-04	1.997E-04	1.314E-04	7.705E-05	1.997E-04	
1615	2.111E-04	1.992E-04	1.317E-04	7.550E-05	2.005E-04	
1646	2.11E-04	1.992E-04	1.744E-04	7.24E-05	1.982E-04	
1676	2.002E-04	2.032E-04	1.309E-04	7.793E-05	1.988E-04	
1707	2.223E-04	2.033E-04	1.306E-04	7.772E-05	1.962E-04	
1737	2.005E-04	2.045E-04	1.317E-04	7.746E-05	1.999E-04	
1768	2.077E-04	1.758E-04	1.343E-04	7.720E-05	2.009E-04	
1798	2.079E-04	1.369E-04	1.350E-04	7.695E-05	2.011E-04	
1829	2.167E-04	1.753E-04	1.345E-04	7.669E-05	2.016E-04	

FIRST DATA ALT. 11 11 12 12 11  
LAST DATA ALT. 61 61 61 60 61



FLIGHT NO. 93		FILTER NO. 1					
BEAM TRANSMITTANCE FROM GROUND TO ALTITUDE		ZENITH ANGLE OF PATH OF SIGHT (DEGREES)					
ALTITUDE METERS	93	95	100	105	120	150	180
305	.2352133	.4225852	.6489970	.7412173	.8605826	.9169544	.9276759
610	.0562550	.1931840	.4266144	.5646532	.7438971	.8429812	.8624947
914	.0125057	.0785978	.2789944	.4246549	.6418851	.7741684	.8011773
1219	.0021145	.0334748	.1317779	.3185770	.5531479	.7104432	.7437391
1524	.0016371	.0147759	.1265735	.4101738	.4795474	.6543050	.6925658

FLIGHT NO. 93		FILTER NO. 2					
BEAM TRANSMITTANCE FROM GROUND TO ALTITUDE		ZENITH ANGLE OF PATH OF SIGHT (DEGREES)					
ALTITUDE METERS	93	95	100	105	120	150	180
305	.2743323	.4669059	.6768280	.7647870	.8821005	.9301326	.9392021
610	.0890298	.2400910	.4486514	.6185149	.7798209	.8662499	.8830747
914	.0237706	.1122257	.3336145	.4787671	.6829991	.8024213	.8264376
1219	.0052547	.0529454	.2180109	.3717551	.5991680	.7439909	.7740594
1524	.001744	.0252467	.1018106	.2435167	.5301838	.6932623	.7281371

FLIGHT NO. 93		FILTER NO. 3					
BEAM TRANSMITTANCE FROM GROUND TO ALTITUDE		ZENITH ANGLE OF PATH OF SIGHT (DEGREES)					
ALTITUDE METERS	93	95	100	105	120	150	180
305	.4650977	.6340592	.7755861	.8577654	.9236534	.9551831	.9610089
610	.2156231	.4065770	.5749653	.7373263	.8540745	.9129544	.9241616
914	.0950133	.2526647	.4513326	.6292316	.7867860	.8707086	.8870096
1219	.0414295	.1582962	.3464663	.5375595	.7252012	.8306837	.8515874
1524	.0173945	.0775595	.3115992	.4573820	.6370031	.7915168	.8117026

FLIGHT NO. 93		FILTER NO. 4					
BEAM TRANSMITTANCE FROM GROUND TO ALTITUDE		ZENITH ANGLE OF PATH OF SIGHT (DEGREES)					
ALTITUDE METERS	93	95	100	105	120	150	180
305	.6062051	.7423719	.8611206	.9345884	.9493972	.9704643	.9743707
610	.3741501	.5601980	.7475756	.8226871	.9030010	.9433359	.9507371
914	.2222763	.4152812	.6433424	.7438392	.8579711	.9153568	.9262673
1219	.1306216	.3078045	.5535541	.6724805	.8143300	.8881792	.9024024
1524	.0779971	.2315776	.4798724	.6110340	.7749243	.8631054	.8802979

FLIGHT NO. 93		FILTER NO. 5					
BEAM TRANSMITTANCE FROM GROUND TO ALTITUDE		ZENITH ANGLE OF PATH OF SIGHT (DEGREES)					
ALTITUDE METERS	93	95	100	105	120	150	180
305	.2821341	.4709001	.6252353	.7759783	.8769760	.9270090	.9364700
610	.0819790	.2787629	.4769461	.6085230	.7732743	.8620438	.8793602
914	.0223173	.1085378	.3190564	.4734103	.6790327	.7997275	.8240344
1219	.0059171	.0508295	.2241748	.3666344	.5949235	.7409435	.7713129
1524	.0015467	.0245164	.1554720	.2568529	.5239185	.6885205	.7233721

AZIMUTH OF PATH OF SIGHT =		FLIGHT NO. 93		FILTER NO. 1		PATH RADIANCE FROM GROUND TO ALTITUDE (WATTS/STER.SQ.M MICRO M.)	
ALTITUDE		ZENITH ANGLE OF PATH OF SIGHT (DEGREES)					
METERS		75	95	100	105	120	150
305	8.404E-06	5.859E-06	3.153E-06	1.91E-06	7.673E-07	2.905E-07	2.259E-07
610	1.312E-05	1.151E-05	6.75E-06	4.42E-06	1.746E-06	6.392E-07	4.868E-07
914	3.207E-05	2.445E-05	1.449E-05	9.555E-06	3.728E-06	1.265E-06	9.129E-07
1219	4.132E-05	3.457E-05	2.234E-05	1.523E-05	6.169E-06	2.084E-06	1.472E-06
1524	5.227E-05	4.454E-05	3.024E-05	2.116E-05	8.923E-06	3.049E-06	2.134E-06

FLIGHT NO. 93		FILTER NO. 2		PATH RADIANCE FROM GROUND TO ALTITUDE (WATTS/STER.SQ.M MICRO M.)	
ALTITUDE		ZENITH ANGLE OF PATH OF SIGHT (DEGREES)			
METERS		75	95	100	105
305	9.934E-06	6.665E-06	3.475E-06	2.158E-06	8.081E-07
610	1.757E-05	1.311E-05	7.335E-06	4.749E-06	1.817E-06
914	3.614E-05	2.72E-05	1.589E-05	1.029E-05	3.931E-06
1219	5.796E-05	4.54E-05	2.751E-05	1.815E-05	7.003E-06
1524	6.675E-05	5.638E-05	3.678E-05	2.501E-05	1.003E-05

FLIGHT NO. 93		FILTER NO. 3		PATH RADIANCE FROM GROUND TO ALTITUDE (WATTS/STER.SQ.M MICRO M.)	
ALTITUDE		ZENITH ANGLE OF PATH OF SIGHT (DEGREES)			
METERS		75	95	100	105
305	1.663E-05	1.031E-05	5.054E-06	3.029E-06	1.050E-06
610	2.122E-05	1.526E-05	7.315E-06	5.196E-06	1.897E-06
914	3.864E-05	2.712E-05	1.524E-05	9.649E-06	3.516E-06
1219	6.556E-05	4.793E-05	2.677E-05	1.697E-05	6.176E-06
1524	6.743E-05	5.507E-05	3.379E-05	2.218E-05	8.469E-06

FLIGHT NO. 93		FILTER NO. 4		PATH RADIANCE FROM GROUND TO ALTITUDE (WATTS/STER.SQ.M MICRO M.)	
ALTITUDE		ZENITH ANGLE OF PATH OF SIGHT (DEGREES)			
METERS		75	95	100	105
305					
610					
914					
1219					
1524					

FLIGHT NO. 93		FILTER NO. 5		PATH RADIANCE FROM GROUND TO ALTITUDE (WATTS/STER.SQ.M MICRO M.)	
ALTITUDE		ZENITH ANGLE OF PATH OF SIGHT (DEGREES)			
METERS		75	95	100	105
305	1.396E-05	1.233E-05	6.775E-06	4.120E-06	1.461E-06
610	2.266E-05	2.434E-05	1.376E-05	8.759E-06	3.180E-06
914	2.902E-05	2.539E-05	1.705E-05	1.194E-05	4.498E-06
1219	6.064E-05	4.671E-05	2.967E-05	1.914E-05	7.434E-06
1524	7.737E-05	6.451E-05	4.162E-05	2.832E-05	1.129E-05

AZIMUTH OF PATH OF SIGHT = 0		FLIGHT NO. 22		FILE NO. 1				
ALTIITUDE		PATH RADIANCE FROM GROUND TO ALTITUDE (WATTS/STER. RAD. MICRO M.)		ZENITH ANGLE OF PATH OF SIGHT (DEGREES)				
METERS		73	95	105	125	15	170	
305		4.6004E-06	5.272E-06	1.322E-06	1.733E-06	5.675E-07	2.746E-07	2.259E-07
310		7.904E-06	9.924E-06	3.72E-06	2.999E-06	1.241E-06	5.969E-07	4.868E-07
314		1.231E-05	1.007E-05	6.690E-06	4.615E-06	2.485E-06	1.138E-06	9.128E-07
1219		1.490E-05	1.385E-05	9.887E-06	7.377E-06	3.827E-06	1.847E-06	1.472E-06
1224		1.947E-05	1.74E-05	1.33E-05	1.005E-05	5.453E-06	2.684E-06	2.134E-06

FLIGHT NO. 23		FILE NO. 2					
PATH RADIANCE FROM GROUND TO ALTITUDE (WATTS/STER. RAD. MICRO M.)		ZENITH ANGLE OF PATH OF SIGHT (DEGREES)					
ALTITUDE METERS	73	95	105	125	15	17	19
305	5.193E-06	5.537E-06	1.702E-06	1.277E-06	5.846E-07	2.755E-07	2.247E-07
310	8.147E-06	8.726E-06	3.832E-06	2.604E-06	1.258E-06	5.995E-07	4.865E-07
314	1.302E-05	1.053E-05	6.833E-06	4.916E-06	2.426E-06	1.158E-06	9.278E-07
1219	1.409E-05	1.531E-05	1.059E-05	7.798E-06	4.015E-06	1.945E-06	1.551E-06
1224	2.132E-05	1.891E-05	1.327E-05	1.054E-05	5.654E-06	2.603E-06	2.238E-06

FLIGHT NO. 24		FILE NO. 3						
ALTIITUDE		PATH RADIANCE FROM GROUND TO ALTITUDE (WATTS/STER. RAD. MICRO M.)		ZENITH ANGLE OF PATH OF SIGHT (DEGREES)				
METERS		73	95	105	125	150	170	
305		5.513E-06	5.734E-06	1.966E-06	1.282E-06	5.872E-07	2.632E-07	2.338E-07
310		3.349E-05	6.079E-06	5.513E-06	2.305E-06	1.125E-06	5.459E-07	4.510E-07
314		1.256E-05	9.573E-06	5.770E-06	4.081E-06	1.979E-06	9.553E-07	7.754E-07
1219		1.238E-05	1.443E-05	9.189E-06	6.533E-06	3.200E-06	1.576E-06	1.260E-06
1224		2.102E-05	1.773E-05	1.257E-05	3.927E-06	4.553E-06	2.220E-06	1.777E-06

FLIGHT NO. 25		FILE NO. 4					
ALTIITUDE		PATH RADIANCE FROM GROUND TO ALTITUDE (WATTS/STER. RAD. MICRO M.)		ZENITH ANGLE OF PATH OF SIGHT (DEGREES)			
METERS		73	95	105	125	150	170
305							
310							
314							
1219							
1224							

FLIGHT NO. 26		FILE NO. 5					
ALTIITUDE		PATH RADIANCE FROM GROUND TO ALTITUDE (WATTS/STER. RAD. MICRO M.)					
METERS		ZENITH ANGLE OF PATH OF SIGHT (DEGREES)					
	73	75	100	125	150	180	
305	7.430E-06	5.175E-06	2.733E-06	1.405E-06	5.561E-07	3.909E-07	3.125E-07
310	1.135E-05	8.977E-06	5.502E-06	3.817E-06	1.807E-06	8.442E-07	6.764E-07
314	1.201E-05	1.073E-05	7.569E-06	5.493E-06	2.731E-06	1.302E-06	1.047E-06
1219	1.919E-05	1.609E-05	1.126E-05	8.344E-06	4.468E-06	1.699E-06	1.490E-06
1224	2.433E-05	2.132E-05	1.555E-05	1.180E-05	6.325E-06	3.143E-06	2.530E-06

		FLIGHT NO. 93		FILTER NO. 1					
		PATH RADIANCE FROM GROUND TO ALTITUDE (WATTS/STER. SQ. CM MICRO V.)		ZENITH ANGLE OF PATH OF SIGHT (DEGREES)					
ALTITUDE	METERS	93	95	100	105	120	150	180	
305		4.230E-06	3.061E-06	1.755E-06	1.189E-06	5.628E-07	2.770E-07	2.259E-07	
610		6.706E-05	5.352E-06	3.438E-06	2.439E-06	1.211E-06	5.989E-07	4.868E-07	
914		1.057E-05	1.773E-06	5.958E-06	4.401E-06	2.281E-06	1.125E-06	9.128E-07	
1219		1.362E-05	1.193E-05	5.705E-06	6.684E-06	3.635E-06	1.815E-06	1.472E-06	
1524		1.655E-05	1.531E-05	1.153E-05	9.067E-06	5.159E-06	2.627E-06	2.134E-06	

		FLIGHT NO. 93		FILTER NO. 2					
		PATH RADIANCE FROM GROUND TO ALTITUDE (WATTS/STER. SQ. CM MICRO V.)		ZENITH ANGLE OF PATH OF SIGHT (DEGREES)					
ALTITUDE	METERS	93	95	100	105	120	150	180	
305		4.563E-06	3.151E-06	1.771E-06	1.195E-06	5.671E-07	2.770E-07	2.246E-07	
610		7.181E-06	5.592E-06	3.427E-06	2.463E-06	1.223E-06	6.030E-07	4.865E-07	
914		1.112E-05	9.126E-06	5.119E-06	4.472E-06	2.370E-06	1.148E-06	9.278E-07	
1219		1.547E-05	1.323E-05	7.428E-06	7.102E-06	3.852E-06	1.918E-06	1.551E-06	
1524		1.826E-05	1.636E-05	1.233E-05	9.609E-06	5.446E-06	2.762E-06	2.238E-06	

		FLIGHT NO. 93		FILTER NO. 3					
		PATH RADIANCE FROM GROUND TO ALTITUDE (WATTS/STER. SQ. CM MICRO V.)		ZENITH ANGLE OF PATH OF SIGHT (DEGREES)					
ALTITUDE	METERS	93	95	100	105	120	150	180	
305		5.214E-06	3.357E-06	1.819E-06	1.223E-06	5.835E-07	2.838E-07	2.338E-07	
610		7.553E-06	5.556E-06	3.297E-06	2.285E-06	1.124E-06	5.497E-07	4.510E-07	
914		1.106E-05	8.554E-06	5.363E-06	3.839E-06	1.944E-06	9.497E-07	7.754E-07	
1219		1.561E-05	1.253E-05	8.294E-06	6.071E-06	3.187E-06	1.559E-06	1.266E-06	
1524		1.754E-05	1.510E-05	1.065E-05	8.040E-06	4.390E-06	2.133E-06	1.777E-06	

		FLIGHT NO. 93		FILTER NO. 4					
		PATH RADIANCE FROM GROUND TO ALTITUDE (WATTS/STER. SQ. CM MICRO V.)		ZENITH ANGLE OF PATH OF SIGHT (DEGREES)					
ALTITUDE	METERS	93	95	100	105	120	150	180	
305									
610									
914									
1219									
1524									

		FLIGHT NO. 93		FILTER NO. 5					
		PATH RADIANCE FROM GROUND TO ALTITUDE (WATTS/STER. SQ. CM MICRO V.)		ZENITH ANGLE OF PATH OF SIGHT (DEGREES)					
ALTITUDE	METERS	93	95	100	105	120	150	180	
305		6.611E-06	4.619E-06	2.679E-06	1.784E-06	8.458E-07	3.957E-07	3.125E-07	
610		9.197E-06	7.846E-06	5.010E-06	3.571E-06	1.789E-06	8.539E-07	6.754E-07	
914		1.091E-05	9.021E-06	6.333E-06	5.118E-06	2.706E-06	1.324E-06	1.047E-06	
1219		1.605E-05	1.421E-05	1.028E-05	7.864E-06	4.344E-06	2.148E-06	1.690E-06	
1524		2.067E-05	1.847E-05	1.401E-05	1.101E-05	6.346E-06	3.195E-06	2.530E-06	

AZIMUTH OF PATH OF SIGHT = 276		FLIGHT NO. 14		FILM NO. 1		
PATH DISTANCE FROM GROUND TO ALTITUDE (WATTS/STER. SEC. MICRO M.)		ZENITH ANGLE OF PATH OF SIGHT (DEGREES)				
ALTITUDE METERS	3	65	100	135	170	190
5	6.7307-06	3.3231-06	1.6677-06	1.2658-06	5.7031-07	2.7307-07
10	7.3119-06	3.3231-06	3.6677-06	2.5531-06	1.2121-06	5.8805-07
14	1.1749-05	9.374-06	1.3667-05	4.5941-06	2.2701-06	1.1071-06
1219	1.5577-05	1.347-05	9.571-06	7.0591-06	1.6311-06	1.7891-06
1224	1.5577-05	1.347-05	1.2241-05	9.571-06	5.1341-06	2.556-06

FLIGHT NO. 3		FILM NO. 2				
PATH DISTANCE FROM GROUND TO ALTITUDE (WATTS/STER. SEC. MICRO M.)		ZENITH ANGLE OF PATH OF SIGHT (DEGREES)				
ALTITUDE METERS	33	65	100	135	170	190
5	9.0501-06	3.4561-06	1.6221-06	1.2541-06	5.671-07	2.717-07
10	7.3211-06	6.0471-06	3.711-06	2.5571-06	1.211-06	5.8891-07
14	1.2401-05	1.0151-05	1.341-06	4.6411-06	2.224-06	1.1251-06
1219	1.7451-05	1.451-05	1.0761-05	7.3621-06	4.759-06	1.8771-06
1224	1.6821-05	1.551-05	1.2261-05	9.977-06	5.309-06	2.699-06

FLIGHT NO. 3		FILM NO. 3				
PATH DISTANCE FROM GROUND TO ALTITUDE (WATTS/STER. SEC. MICRO M.)		ZENITH ANGLE OF PATH OF SIGHT (DEGREES)				
ALTITUDE METERS	33	65	100	135	170	190
5	7.1307-06	4.556-06	2.401-06	1.566-06	6.754-07	2.939-07
10	9.7021-06	7.791-06	3.1291-06	2.7811-06	1.253-06	5.619-07
14	1.3171-05	1.0171-05	1.2771-06	4.3541-06	2.0511-06	9.5491-07
1219	1.774-05	1.444-05	3.2751-06	6.3211-06	3.231-06	1.548-06
1224	1.6921-05	1.7591-05	1.2741-05	6.7761-06	4.4541-06	2.1711-06

FLIGHT NO. 33		FILM NO. 4				
PATH DISTANCE FROM GROUND TO ALTITUDE (WATTS/STER. SEC. MICRO M.)		ZENITH ANGLE OF PATH OF SIGHT (DEGREES)				
ALTITUDE METERS	33	65	100	135	170	190
5						
10						
14						
1219						
1224						

FLIGHT NO. 5		FILM NO. 5				
PATH DISTANCE FROM GROUND TO ALTITUDE (WATTS/STER. SEC. MICRO M.)		ZENITH ANGLE OF PATH OF SIGHT (DEGREES)				
ALTITUDE METERS	15	30	45	60	75	90
5	7.5307-06	3.0721-06	2.0111-06	1.622-06	8.3781-07	3.1251-07
10	1.0631-05	3.376-06	2.2191-06	3.2291-06	1.7341-06	8.303-07
14	1.1241-05	4.9331-06	1.9491-06	5.0731-06	2.5721-06	1.2741-06
1219	1.754-05	1.451-05	1.0781-05	7.715-06	4.036-06	1.7451-06
1224	2.2551-06	1.942-05	1.4471-05	1.654-05	2.915-06	3.052-06

AZIMUTH OF PATH OF SIGHT = 0		FLIGHT NO. 93		FILTER NO. 1					
		DIRECTIONAL PATH REFLECTANCE FROM GROUND TO ALTITUDE		ZENITH ANGLE OF PATH OF SIGHT (DEGREES)					
ALTITUDE	METERS	93	95	100	105	120	150	180	
305	3.177E-00	1.231E-01	4.313E-01	2.363E-01	7.917E-02	2.812E-02	2.162E-02		
610	2.387E-01	5.679E-00	1.408E-00	6.944E-01	2.084E-01	6.732E-02	5.012E-02		
914	2.215E-02	2.752E-01	4.612E-00	1.998E-00	5.156E-01	1.451E-01	1.012E-01		
1219	1.299E-03	9.100E-01	1.091E-01	4.245E-00	9.902E-01	2.604E-01	1.757E-01		
1524	7.270E-03	2.677E-01	2.227E-01	7.708E-00	1.652E-00	4.138E-01	2.736E-01		

		FLIGHT NO. 94		FILTER NO. 2					
		DIRECTIONAL PATH REFLECTANCE FROM GROUND TO ALTITUDE		ZENITH ANGLE OF PATH OF SIGHT (DEGREES)					
ALTITUDE	METERS	93	95	100	105	120	150	180	
305	2.614E-00	1.075E-00	3.916E-01	2.159E-01	7.193E-02	2.472E-02	1.879E-02		
610	1.550E-01	4.236E-00	1.108E-00	6.018E-01	1.430E-01	5.400E-02	4.320E-02		
914	1.191E-02	1.903E-01	3.719E-00	1.688E-00	4.519E-01	1.270E-01	8.810E-02		
1219	7.277E-03	6.746E-01	9.443E-00	3.634E-00	9.178E-01	2.366E-01	1.673E-01		
1524	3.006E-03	1.687E-02	1.795E-01	6.691E-00	1.485E-00	3.685E-01	2.414E-01		

		FLIGHT NO. 95		FILTER NO. 3					
		DIRECTIONAL PATH REFLECTANCE FROM GROUND TO ALTITUDE		ZENITH ANGLE OF PATH OF SIGHT (DEGREES)					
ALTITUDE	METERS	93	95	100	105	120	150	180	
305	2.308E-00	1.050E-00	4.100E-01	2.279E-01	7.334E-02	2.215E-02	1.570E-02		
610	6.353E-01	2.434E-00	8.450E-01	4.548E-01	1.433E-01	4.394E-02	1.149E-02		
914	2.524E-01	7.021E-00	1.961E-00	9.296E-01	2.884E-01	8.191E-02	5.641E-02		
1219	1.021E-02	1.954E-01	4.357E-00	2.037E-00	5.496E-01	1.450E-01	9.593E-02		
1524	2.504E-02	3.628E-01	6.998E-00	3.129E-00	8.194E-01	2.144E-01	1.404E-01		

		FLIGHT NO. 96		FILTER NO. 4					
		DIRECTIONAL PATH REFLECTANCE FROM GROUND TO ALTITUDE		ZENITH ANGLE OF PATH OF SIGHT (DEGREES)					
ALTITUDE	METERS	93	95	100	105	120	150	180	
305									
610									
914									
1219									
1524									

		FLIGHT NO. 97		FILTER NO. 5					
		DIRECTIONAL PATH REFLECTANCE FROM GROUND TO ALTITUDE		ZENITH ANGLE OF PATH OF SIGHT (DEGREES)					
ALTITUDE	METERS	93	95	100	105	120	150	180	
305	3.021E-00	1.549E-01	5.563E-01	3.018E-01	9.471E-02	2.728E-02	1.897E-02		
610	2.265E-01	6.047E-00	1.641E-00	8.183E-01	2.338E-01	6.402E-02	4.372E-02		
914	7.378E-01	1.356E-01	2.955E-00	1.386E-00	3.765E-01	1.040E-01	7.220E-02		
1219	5.925E-02	5.224E-01	7.271E-00	2.967E-00	7.104E-01	1.828E-01	1.246E-01		
1524	2.843E-02	1.496E-02	1.522E-01	5.613E-00	1.225E-00	2.993E-01	1.987E-01		

AZIMUTH OF PATH OF SIGHT = 90  
 FLIGHT NO. 93      FILM NO. 1  
 DIRECTIONAL PATH REFLECTANCE FROM GROUND TO ALTITUDE  
 ALTITUDE      ZENITH ANGLE OF PATH OF SIGHT (DEGREES)  
 METERS      93      95      100      105      120      150      180

305	1.734E-00	6.874E-01	2.534E-01	1.469E-01	5.855E-02	2.658E-02	2.162E-00
310	1.184E-01	2.872E-00	7.751E-01	4.080E-01	1.481E-01	6.287E-02	5.012E-00
314	8.493E-01	1.137E-01	2.179E-00	1.007E-00	3.295E-01	1.305E-01	1.012E-01
1219	4.299E-02	4.672E-01	4.829E-00	2.056E-00	6.143E-01	2.308E-01	1.757E-01
1524	2.710E-03	1.046E-02	9.521E-00	3.690E-00	1.009E-00	3.642E-01	2.736E-01

FLIGHT NO. 93      FILM NO. 2  
 DIRECTIONAL PATH REFLECTANCE FROM GROUND TO ALTITUDE  
 ALTITUDE      ZENITH ANGLE OF PATH OF SIGHT (DEGREES)  
 METERS      93      95      100      105      120      150      180

305	1.367E-00	5.74E-01	2.211E-01	1.298E-01	5.205E-02	2.326E-02	1.878E-00
310	7.185E-00	2.059E-00	5.201E-01	3.582E-01	1.266E-01	5.434E-02	4.326E-00
314	4.41E-01	7.371E-00	1.620E-00	3.666E-01	2.789E-01	1.134E-01	8.816E-00
1219	2.772E-02	2.270E-01	3.633E-00	1.647E-00	5.263E-01	2.052E-01	1.773E-01
1524	9.601E-02	5.676E-01	6.771E-00	2.820E-00	8.339E-01	3.175E-01	2.414E-01

FLIGHT NO. 93      FILM NO. 3  
 DIRECTIONAL PATH REFLECTANCE FROM GROUND TO ALTITUDE  
 ALTITUDE      ZENITH ANGLE OF PATH OF SIGHT (DEGREES)  
 METERS      93      95      100      105      120      150      180

305	8.061E-01	5.773E-01	1.950E-01	9.688E-02	4.107E-02	1.913E-02	1.570E-00
310	2.499E-00	9.705E-01	3.574E-01	2.490E-01	8.502E-02	4.866E-02	3.149E-00
314	8.531E-00	2.445E-00	7.543E-01	4.189E-01	1.623E-01	7.081E-02	5.641E-00
1219	2.347E-01	5.332E-00	1.456E-00	7.843E-01	2.901E-01	1.224E-01	9.793E-00
1524	7.799E-01	1.189E-01	2.499E-00	1.246E-00	4.456E-01	1.810E-01	1.404E-01

FLIGHT NO. 93      FILM NO. 4  
 DIRECTIONAL PATH REFLECTANCE FROM GROUND TO ALTITUDE  
 ALTITUDE      ZENITH ANGLE OF PATH OF SIGHT (DEGREES)  
 METERS      93      95      100      105      120      150      180

305							
310							
314							
1219							
1524							

FLIGHT NO. 93      FILM NO. 5  
 DIRECTIONAL PATH REFLECTANCE FROM GROUND TO ALTITUDE  
 ALTITUDE      ZENITH ANGLE OF PATH OF SIGHT (DEGREES)  
 METERS      93      95      100      105      120      150      180

305	1.607E-00	5.247E-01	2.364E-01	1.386E-01	5.550E-02	2.397E-02	1.897E-00
310	7.873E-00	2.206E-00	6.558E-01	3.565E-01	1.328E-01	5.567E-02	4.372E-00
314	3.705E-01	5.743E-00	1.312E-00	6.596E-01	2.216E-01	9.254E-02	7.220E-00
1219	1.857E-00	1.300E-01	2.855E-00	1.293E-00	4.118E-01	1.611E-01	1.246E-01
1524	8.941E-00	4.944E-01	5.664E-00	2.339E-00	6.354E-01	2.995E-01	1.987E-01

AZIMUTH OF PATH OF SIGHT = 150  
 FLIGHT NO. 93      FILTER NO. 1  
 DIRECTIONAL PATH REFLECTANCE FROM GROUND TO ALTITUDE  
 ALTITUDE      ZENITH ANGLE OF PATH OF SIGHT (DEGREES)  
 METERS      93      95      100      105      120      150      180

305	1.51E-01	6.47E-01	2.40E-01	1.41E-01	5.20E-02	1.68E-02	2.16E-02
610	1.65E-01	2.59E-01	7.15E-01	3.83E-01	1.44E-01	6.10E-02	5.01E-02
914	7.29E-01	9.91E-01	1.97E-01	9.20E-01	3.15E-01	1.29E-01	1.01E-01
1219	4.28E-01	3.17E-01	4.28E-01	1.80E-01	3.03E-01	2.26E-01	1.75E-01
1524	2.51E-01	9.02E-01	8.49E-01	3.32E-01	9.55E-01	3.56E-01	2.73E-01

FLIGHT NO. 93      FILTER NO. 2  
 DIRECTIONAL PATH REFLECTANCE FROM GROUND TO ALTITUDE  
 ALTITUDE      ZENITH ANGLE OF PATH OF SIGHT (DEGREES)  
 METERS      93      95      100      105      120      150      180

305	1.20E-01	4.01E-01	1.99E-01	1.19E-01	2.04E-02	2.33E-02	1.87E-02
610	6.33E-01	1.82E-01	3.01E-01	3.12E-01	1.23E-01	5.46E-02	4.32E-02
914	3.68E-01	8.38E-01	1.44E-01	7.33E-01	2.66E-01	1.12E-01	8.81E-02
1219	1.94E-01	1.96E-01	4.22E-01	1.59E-01	2.04E-01	2.92E-01	1.77E-01
1524	8.22E-01	4.49E-01	8.71E-01	2.57E-01	8.06E-01	3.12E-01	2.41E-01

FLIGHT NO. 93      FILTER NO. 3  
 DIRECTIONAL PATH REFLECTANCE FROM GROUND TO ALTITUDE  
 ALTITUDE      ZENITH ANGLE OF PATH OF SIGHT (DEGREES)  
 METERS      93      95      100      105      120      150      180

305	7.23E-01	3.41E-01	1.47E-01	9.20E-02	4.07E-02	1.91E-02	1.57E-02
610	2.27E-01	8.45E-01	3.39E-01	2.00E-01	8.49E-02	3.88E-02	3.14E-02
914	7.51E-01	2.16E-01	6.92E-01	3.93E-01	1.59E-01	7.03E-02	5.64E-02
1219	2.44E-01	5.13E-01	1.39E-01	7.28E-01	1.83E-01	1.21E-01	9.59E-02
1524	6.50E-01	9.95E-01	2.20E-01	1.13E-01	4.24E-01	1.78E-01	1.40E-01

FLIGHT NO. 93      FILTER NO. 4  
 DIRECTIONAL PATH REFLECTANCE FROM GROUND TO ALTITUDE  
 ALTITUDE      ZENITH ANGLE OF PATH OF SIGHT (DEGREES)  
 METERS      93      95      100      105      120      150      180

305							
610							
914							
1219							
1524							

FLIGHT NO. 93      FILTER NO. 5  
 DIRECTIONAL PATH REFLECTANCE FROM GROUND TO ALTITUDE  
 ALTITUDE      ZENITH ANGLE OF PATH OF SIGHT (DEGREES)  
 METERS      93      95      100      105      120      150      180

305	1.33E-01	5.57E-01	2.10E-01	1.36E-01	5.48E-02	2.42E-02	1.89E-02
610	6.96E-01	1.95E-01	3.97E-01	1.35E-01	1.31E-01	5.63E-02	4.37E-02
914	2.77E-01	5.03E-01	1.17E-01	6.14E-01	2.26E-01	9.40E-02	7.22E-02
1219	1.62E-01	1.58E-01	2.67E-01	1.21E-01	4.15E-01	1.64E-01	1.24E-01
1524	7.59E-01	4.28E-01	5.12E-01	2.18E-01	6.88E-01	2.63E-01	1.98E-01



AZIMUTH OF PATH OF SIGHT = 270

FLIGHT NO. 93

FILM NO. 1

DIRECTIONAL PATH REFLECTANCE FROM GROUND TO ALTITUDE

ALTITUDE METERS	93	95	100	105	120	150	180
305	1.807E-00	7.123E-01	2.608E-01	1.501E-01	5.884E-02	2.643E-02	2.162E-02
610	1.154E-01	2.822E-00	7.623E-01	4.014E-01	1.447E-01	6.194E-02	5.012E-02
914	8.104E-01	1.087E-01	2.035E-00	9.603E-01	3.140E-01	1.270E-01	1.012E-01
1219	4.905E-02	5.573E-01	4.651E-00	1.967E-00	5.826E-01	2.236E-01	1.757E-01
1524	2.639E-03	1.014E-02	9.247E-00	3.515E-00	9.503E-01	3.508E-01	2.736E-01

FLIGHT NO. 93

FILM NO. 2

DIRECTIONAL PATH REFLECTANCE FROM GROUND TO ALTITUDE

ALTITUDE METERS	93	95	100	105	120	150	180
305	1.329E-00	5.573E-01	2.140E-01	1.255E-01	5.049E-02	2.293E-02	1.878E-02
610	6.894E-00	1.970E-00	5.947E-01	3.241E-01	1.219E-01	5.338E-02	4.326E-02
914	4.125E-01	7.034E-00	1.533E-00	7.628E-01	2.637E-01	1.101E-01	8.216E-02
1219	2.191E-02	2.177E-01	3.451E-00	1.555E-00	4.939E-01	1.981E-01	1.573E-01
1524	9.379E-02	5.479E-01	4.471E-00	2.672E-00	7.864E-01	3.057E-01	2.414E-01

FLIGHT NO. 93

FILM NO. 3

DIRECTIONAL PATH REFLECTANCE FROM GROUND TO ALTITUDE

ALTITUDE METERS	93	95	100	105	120	150	180
305	9.905E-01	4.637E-01	1.951E-01	1.178E-01	4.726E-02	1.986E-02	1.370E-02
610	2.104E-00	1.132E-00	4.193E-01	2.434E-01	9.466E-02	3.972E-02	3.149E-02
914	8.901E-00	2.597E-00	8.080E-01	4.466E-01	1.684E-01	7.077E-02	5.641E-02
1219	2.309E-01	5.994E-00	1.511E-00	7.914E-01	2.875E-01	1.202E-01	9.593E-02
1524	7.754E-01	1.105E-01	2.494E-00	1.239E-00	4.309E-01	1.770E-01	1.404E-01

FLIGHT NO. 93

FILM NO. 4

DIRECTIONAL PATH REFLECTANCE FROM GROUND TO ALTITUDE

ALTITUDE METERS	93	95	100	105	120	150	180
305							
610							
914							
1219							
1524							

FLIGHT NO. 93

FILM NO. 5

DIRECTIONAL PATH REFLECTANCE FROM GROUND TO ALTITUDE

ALTITUDE METERS	93	95	100	105	120	150	180
305	1.478E-00	6.122E-01	2.332E-01	1.364E-01	5.431E-02	2.374E-02	1.897E-02
610	7.374E-00	2.081E-00	6.220E-01	3.390E-01	1.174E-01	5.475E-02	4.372E-02
914	2.868E-01	5.205E-00	1.204E-00	6.097E-01	2.153E-01	9.056E-02	7.220E-02
1219	1.724E-02	1.656E-01	2.631E-00	1.195E-00	3.257E-01	1.569E-01	1.246E-01
1524	8.315E-02	4.587E-01	5.266E-00	2.169E-00	3.418E-01	2.520E-01	1.987E-01

#### FLIGHT 96

Quarter moon. Data were gathered over the wooded terrain about 60 km east of Khorat. There were very few artificial lights under the flight pattern. The terrain consisted primarily of dry rice paddies and deciduous trees. This was the dry season (although it had rained in this area during the afternoon) and the vegetation (leaves on trees and ground cover) had lost the green color of the wet season. The atmosphere was very hazy at low altitudes. There was considerable thin cirrus estimated at 6000 m. The data-taking started at 2047 local time and ended at 2314. The moon phase angle was  $95^\circ$ ; the moon zenith angle was  $42^\circ$  at the start of sky radiance data-taking and was  $65^\circ$  at the end.

FLIGHT NO. 96				FILTER NO. 1			
IRRADIANCE(WATTS/SQ.M.MICRO M.)							
ALTITUDE (METERS)	DOWN- WELLING	UP- WELLING	ALBEDO	SCALAR DOWNWELLING	SCALAR UPWELLING	SCALAR TOTAL	SCALAR ALBEDO
244	1.041E-04	7.567E-06	.073	1.899E-04	2.006E-05	2.089E-04	.106
564	1.160E-04	1.048E-05	.080	2.096E-04	2.844E-05	2.381E-04	.136
851	1.121E-04	1.371E-05	.122	2.194E-04	4.124E-05	2.606E-04	.189
1143	9.136E-05	1.486E-05	.163	1.837E-04	4.795E-05	2.316E-04	.261
1469	8.203E-05	1.737E-05	.212	1.918E-04	5.285E-05	2.457E-04	.281

FLIGHT NO. 96				FILTER NO. 2			
IRRADIANCE(WATTS/SQ.M.MICRO M.)							
ALTITUDE (METERS)	DOWN- WELLING	UP- WELLING	ALBEDO	SCALAR DOWNWELLING	SCALAR UPWELLING	SCALAR TOTAL	SCALAR ALBEDO
245	1.319E-04	1.127E-05	.085	2.288E-04	2.754E-05	2.563E-04	.120
572	1.096E-04	1.367E-05	.125	2.011E-04	3.480E-05	2.359E-04	.173
854	9.659E-05	1.504E-05	.156	1.930E-04	4.135E-05	2.344E-04	.214
1144	8.832E-05	1.718E-05	.194	1.847E-04	4.691E-05	2.315E-04	.254
1477	7.570E-05	2.110E-05	.279	1.742E-04	5.998E-05	2.342E-04	.344
1796	8.394E-05	2.300E-05	.274	2.129E-04	6.862E-05	2.815E-04	.322

FLIGHT NO. 96				FILTER NO. 3			
IRRADIANCE(WATTS/SQ.M.MICRO M.)							
ALTITUDE (METERS)	DOWN- WELLING	UP- WELLING	ALBEDO	SCALAR DOWNWELLING	SCALAR UPWELLING	SCALAR TOTAL	SCALAR ALBEDO
244	1.394E-04	2.612E-05	.167	2.466E-04	5.425E-05	3.008E-04	.120
572	1.242E-04	2.911E-05	.234	2.391E-04	6.852E-05	3.076E-04	.286
843	1.187E-04	2.758E-05	.232	2.358E-04	6.514E-05	3.010E-04	.276
1144	1.197E-04	2.508E-05	.209	2.343E-04	5.727E-05	2.916E-04	.244
1478	8.868E-05	2.402E-05	.350	1.636E-04	6.027E-05	2.238E-04	.368
1796	1.037E-04	2.676E-05	.258	2.697E-04	7.873E-05	3.484E-04	.292

FLIGHT NO. 96				FILTER NO. 4			
IRRADIANCE(WATTS/SQ.M.MICRO M.)							
ALTITUDE (METERS)	DOWN- WELLING	UP- WELLING	ALBEDO	SCALAR DOWNWELLING	SCALAR UPWELLING	SCALAR TOTAL	SCALAR ALBEDO
251							
572							
842							
1144							
1478							
1794							

FLIGHT NO. 96				FILTER NO. 5			
IRRADIANCE(WATTS/SQ.M.MICRO M.)							
ALTITUDE (METERS)	DOWN- WELLING	UP- WELLING	ALBEDO	SCALAR DOWNWELLING	SCALAR UPWELLING	SCALAR TOTAL	SCALAR ALBEDO
249	1.248E-04	1.151E-05	.092	2.283E-04	2.764E-05	2.562E-04	.122
571	8.696E-05	1.571E-05	.161	1.774E-04	4.589E-05	2.233E-04	.259
1143	9.610E-05	2.271E-05	.226	2.025E-04	5.696E-05	2.594E-04	.281
1477	6.061E-05	1.454E-05	.240	1.437E-04	4.258E-05	1.863E-04	.296
1792	7.421E-05	2.164E-05	.252	1.943E-04	6.972E-05	2.640E-04	.359

FLIGHT NO. 96					
AZIMUTH OF PATH OF SIGHT = 0					
DIRECTIONAL REFLECTANCE OF BACKGROUND					
ZENITH	FILTERS				
ANGLE	1	2	5	3	4
93	.28382	.30472	.29159	.41293	
95	.22595	.21087	.22388	.28139	
100	.11378	.13140	.12849	.17256	
105	.08293	.10193	.09689	.15961	
120	.08287	.07757	.07413	.17807	
150	.05731	.06146	.07685	.15755	
180	.09103	.08892	.12904	.20512	

FLIGHT NO. 96					
AZIMUTH OF PATH OF SIGHT = 90					
DIRECTIONAL REFLECTANCE OF BACKGROUND					
ZENITH	FILTERS				
ANGLE	1	2	5	3	4
93	.29611	.24283	.22184	.31216	
95	.19010	.18626	.16618	.22684	
100	.10465	.10825	.11101	.18378	
105	.07880	.08960	.09103	.15513	
120	.07582	.07945	.07427	.16143	
150	.07644	.07714	.06019	.18610	
180	.09103	.08292	.12904	.20512	

FLIGHT NO. 96					
AZIMUTH OF PATH OF SIGHT = 180					
DIRECTIONAL REFLECTANCE OF BACKGROUND					
ZENITH	FILTERS				
ANGLE	1	2	5	3	4
93	.24017	.18556	.20147	.22844	
95	.16920	.14448	.17782	.27083	
100	.08487	.10874	.12439	.27975	
105	.07897	.09449	.11700	.33570	
120	.09205	.09154	.05656	.19451	
150	.08119	.08859	.05316	.26564	
180	.09103	.08892	.12904	.20512	

FLIGHT NO. 96					
AZIMUTH OF PATH OF SIGHT = 270					
DIRECTIONAL REFLECTANCE OF BACKGROUND					
ZENITH	FILTERS				
ANGLE	1	2	5	3	4
93	.19571	.20467	.22252	.22140	
95	.15638	.15170	.15007	.20148	
100	.08722	.11331	.10769	.18396	
105	.07188	.09480	.09892	.17358	
120	.07836	.08199	.07402	.19023	
150	.05795	.07380	.06245	.20448	
180	.09103	.08892	.12904	.20512	

DATE 32569 FLIGHT NO. 92 OBLONG LEVEL ALTITUDE (M.)= 202 IUP=1

ALTITUDE (METERS)	TOTAL SCATTERING COEFFICIENT (PER METRE)				
FILTERS	1	2	3	4	5
0	9.809E-05	7.778E-05	4.841E-05		1.066E-04
30	9.777E-05	7.752E-05	4.825E-05		1.062E-04
61	9.744E-05	7.726E-05	4.809E-05		1.058E-04
91	9.712E-05	7.701E-05	4.793E-05		1.055E-04
122	9.680E-05	7.675E-05	4.777E-05		1.051E-04
152	9.647E-05	7.650E-05	4.761E-05		1.048E-04
183	9.615E-05	7.624E-05	4.745E-05		1.044E-04
213	9.583E-05	7.599E-05	4.729E-05		1.041E-04
244	9.551E-05	7.573E-05	4.714E-05		1.038E-04
274	9.522E-05	7.532E-05	4.691E-05		1.037E-04
305	9.583E-05	7.541E-05	4.717E-05		1.043E-04
335	9.334E-05	7.082E-05	4.698E-05		9.846E-05
366	9.229E-05	6.753E-05	4.750E-05		9.380E-05
396	9.227E-05	6.674E-05	4.741E-05		9.211E-05
427	8.784E-05	6.612E-05	4.617E-05		9.215E-05
457	8.354E-05	6.692E-05	4.618E-05		8.936E-05
488	8.030E-05	6.503E-05	4.371E-05		8.745E-05
518	7.980E-05	6.497E-05	4.350E-05		8.624E-05
549	8.220E-05	6.624E-05	4.196E-05		8.612E-05
579	8.164E-05	6.836E-05	4.066E-05		8.402E-05
610	8.157E-05	6.723E-05	4.073E-05		8.565E-05
640	8.260E-05	6.415E-05	4.077E-05		8.892E-05
671	8.305E-05	6.047E-05	3.905E-05		8.633E-05
701	8.011E-05	5.915E-05	3.957E-05		8.829E-05
732	7.285E-05	6.013E-05	4.185E-05		8.216E-05
762	8.855E-05	6.043E-05	4.437E-05		8.461E-05
792	7.281E-05	6.028E-05	4.175E-05		8.556E-05
823	7.860E-05	5.847E-05	4.063E-05		7.302E-05
853	7.915E-05	5.091E-05	3.771E-05		7.029E-05
884	8.055E-05	4.494E-05	3.816E-05		7.064E-05
914	8.225E-05	4.688E-05	3.962E-05		6.878E-05
945	8.235E-05	4.660E-05	4.167E-05		7.003E-05
975	9.380E-05	5.114E-05	4.322E-05		7.013E-05
1006	1.006E-04	5.064E-05	4.461E-05		7.045E-05
1036	1.058E-04	6.383E-05	4.517E-05		6.762E-05
1067	1.067E-04	6.445E-05	4.555E-05		6.555E-05
1097	1.054E-04	6.405E-05	4.537E-05		6.558E-05
1128	1.037E-04	6.318E-05	4.561E-05		6.570E-05
1158	1.052E-04	6.015E-05	4.444E-05		6.444E-05
1189	1.067E-04	5.313E-05	4.350E-05		6.463E-05
1219	1.043E-04	5.490E-05	4.205E-05		6.496E-05
1250	1.042E-04	5.404E-05	3.859E-05		6.682E-05
1280	1.026E-04	5.326E-05	3.851E-05		6.718E-05
1311	1.012E-04	5.528E-05	4.226E-05		6.648E-05
1341	9.489E-05	5.707E-05	4.507E-05		6.527E-05
1372	9.241E-05	6.602E-05	4.516E-05		6.644E-05
1402	9.528E-05	7.103E-05	4.565E-05		6.653E-05
1433	9.522E-05	7.087E-05	4.623E-05		6.782E-05
1463	9.480E-05	6.941E-05	4.859E-05		6.615E-05
1494	9.423E-05	7.721E-05	5.340E-05		6.813E-05
1524	9.232E-05	8.497E-05	5.616E-05		6.747E-05
1554	8.808E-05	9.026E-05	5.649E-05		7.370E-05
1585	7.552E-05	9.768E-05	5.747E-05		7.443E-05
1615	7.559E-05	1.042E-04	6.156E-05		6.696E-05
1646	7.428E-05	1.142E-04	6.484E-05		6.673E-05
1676	7.575E-05	1.203E-04	1.240E-05		6.651E-05
1707	7.469E-05	1.123E-04	7.651E-05		6.629E-05
1737	7.476E-05	8.335E-05	7.528E-05		6.607E-05
1768	7.715E-05	8.079E-05	6.146E-05		6.585E-05
1798	7.979E-05	8.052E-05	8.119E-05		6.563E-05
1829	7.952E-05	8.025E-05	8.052E-05		6.541E-05

FIRST DATA ALT. 9 9 9 9 9  
LAST DATA ALT. 60 55 59 57 54

		FLIGHT NO. 96		FILTER NO. 1				
		BEAM TRANSMITTANCE FROM GROUND TO ALTITUDE		ZENITH ANGLE OF PATH OF SIGHT (DEGREES)				
ALTITUDE								
METERS		93	95	100	105	120	150	180
305		.5667653	.7132486	.8435556	.8924415	.9427970	.9665634	.9709774
610		.3279649	.5275934	.7254697	.8062802	.8545272	.9276754	.9457945
914		.2093929	.4015756	.6225966	.7354803	.8529667	.9122705	.9235620
1219		.1124088	.2822230	.5299646	.6531160	.8021067	.8804573	.8956029
1524		.0607768	.2007281	.4466549	.5823144	.7558517	.8507762	.8693973

		FLIGHT NO. 96		FILTER NO. 2				
		BEAM TRANSMITTANCE FROM GROUND TO ALTITUDE		ZENITH ANGLE OF PATH OF SIGHT (DEGREES)				
ALTITUDE	METERS	93	95	100	105	120	150	180
305		.6375982	.7650180	.8742057	.9137495	.9543825	.9734034	.9769252
610		.4255737	.6042632	.7766606	.8440213	.9159626	.9505831	.9570593
914		.2982132	.4937564	.7017015	.7884829	.8842514	.9314413	.9402464
1219		.2075267	.4033832	.6340742	.7365935	.8536348	.9126829	.9239236
1524		.1379001	.3220219	.5662429	.6827841	.8207649	.8922246	.9059608

		FLIGHT NO. 96		FILTER NO. 3				
		BEAM TRANSMITTANCE FROM GROUND TO ALTITUDE		ZENITH ANGLE OF PATH OF SIGHT (DEGREES)				
ALTITUDE	METERS	93	95	100	105	120	150	180
305		.7559045	.8465786	.9198044	.9454583	.9713894	.9833781	.9855889
610		.5787694	.7244045	.8505956	.8971178	.9453510	.9680743	.9722916
914		.4518418	.6289478	.7923602	.8554304	.9223510	.9544053	.9603911
1219		.3436368	.5391914	.7334308	.8122058	.8979243	.9397297	.9475887
1524		.2577716	.4599724	.6772075	.7698870	.8733941	.9248211	.9345556

		FLIGHT NO. 96		FILTER NO. 4				
		BEAM TRANSMITTANCE FROM GROUND TO ALTITUDE		ZENITH ANGLE OF PATH OF SIGHT (DEGREES)				
ALTITUDE	METERS	93	95	100	105	120	150	180
	305							
	610							
	914							
	1219							
	1524							

		FLIGHT NO. 96		FILTER NO. 5				
		BEAM TRANSMITTANCE FROM GROUND TO ALTITUDE		ZENITH ANGLE OF PATH OF SIGHT (DEGREES)				
ALTITUDE	METERS	93	95	100	105	120	150	180
305		.5389601	.6922076	.8314058	.8834878	.9378888	.9636550	.9684466
610		.3149739	.5062151	.7105634	.7951273	.8681007	.9337802	.9423910
914		.2102834	.4030987	.6337997	.7364185	.8525758	.9126181	.9288667
1219		.1373737	.3184524	.5630839	.6802260	.8191717	.8912243	.9050810
1524		.0842597	.2521069	.5007828	.6287634	.7844830	.8705149	.8868388

AZIMUTH OF PATH OF SIGHT = C								
FLIGHT NO. 96 FILTER NO. 1								
PATH RADIANCE FROM GROUND TO ALTITUDE (WATTS/STER.SQ.M MICR M.)								
ALTITUDE	ZENITH ANGLE OF PATH OF SIGHT (DEGREES)							
METERS	93	95	100	105	120	150	180	
305	8.342E-06	5.065E-06	2.560E-06	1.645E-06	7.950E-07	3.696E-07	3.278E-07	
610	1.379E-05	9.107E-06	4.823E-06	3.141E-06	1.359E-06	6.916E-07	6.105E-07	
914	1.952E-05	1.352E-05	7.362E-06	4.804E-06	2.100E-06	9.642E-07	8.668E-07	
1219	2.454E-05	1.824E-05	1.048E-05	6.941E-06	3.032E-06	1.373E-06	1.168E-06	
1524	2.943E-05	2.283E-05	1.361E-05	9.145E-06	3.989E-06	1.743E-06	1.450E-06	

FLIGHT NO. 96 FILTER NO. 2								
PATH RADIANCE FROM GROUND TO ALTITUDE (WATTS/STER.SQ.M MICR M.)								
ALTITUDE	ZENITH ANGLE OF PATH OF SIGHT (DEGREES)							
METERS	93	95	100	105	120	150	180	
305	8.786E-06	5.188E-06	2.551E-06	1.615E-06	7.037E-07	3.522E-07	3.200E-07	
610	1.382E-05	8.839E-06	4.557E-06	2.922E-06	1.275E-06	6.275E-07	5.64E-07	
914	1.764E-05	1.189E-05	6.324E-06	4.065E-06	1.768E-06	8.438E-07	7.480E-07	
1219	2.116E-05	1.490E-05	8.166E-06	5.312E-06	2.288E-06	1.056E-06	9.199E-07	
1524	2.454E-05	1.806E-05	1.025E-05	6.749E-06	2.921E-06	1.310E-06	1.116E-06	

FLIGHT NO. 96 FILTER NO. 3								
PATH RADIANCE FROM GROUND TO ALTITUDE (WATTS/STER.SQ.M MICR M.)								
ALTITUDE	ZENITH ANGLE OF PATH OF SIGHT (DEGREES)							
METERS	93	95	100	105	120	150	180	
305	7.411E-06	4.205E-06	2.005E-06	1.251E-06	5.330E-07	2.632E-07	2.422E-07	
610	1.345E-05	2.060E-06	3.555E-06	2.479E-06	1.043E-06	4.597E-07	4.541E-07	
914	1.842E-05	1.156E-05	5.781E-06	3.623E-06	1.508E-06	7.008E-07	6.274E-07	
1219	2.247E-05	1.420E-05	7.622E-06	4.825E-06	2.001E-06	9.161E-07	8.098E-07	
1524	2.527E-05	1.747E-05	9.293E-06	5.945E-06	2.472E-06	1.110E-06	9.651E-07	

FLIGHT NO. 96 FILTER NO. 4								
PATH RADIANCE FROM GROUND TO ALTITUDE (WATTS/STER.SQ.M MICR M.)								
ALTITUDE	ZENITH ANGLE OF PATH OF SIGHT (DEGREES)							
METERS	93	95	100	105	120	150	180	
305								
610								
914								
1219								
1524								

FLIGHT NO. 96 FILTER NO. 5								
PATH RADIANCE FROM GROUND TO ALTITUDE (WATTS/STER.SQ.M MICR M.)								
ALTITUDE	ZENITH ANGLE OF PATH OF SIGHT (DEGREES)							
METERS	93	95	100	105	120	150	180	
305	1.248E-05	7.576E-06	3.770E-06	2.371E-06	9.925E-07	4.635E-07	4.167E-07	
610	1.817E-05	1.223E-05	6.514E-06	4.195E-06	1.784E-06	8.156E-07	7.182E-07	
914	2.172E-05	1.541E-05	8.536E-06	5.569E-06	2.263E-06	1.072E-06	9.325E-07	
1219	2.550E-05	1.882E-05	1.077E-05	7.102E-06	3.055E-06	1.358E-06	1.176E-06	
1524	2.692E-05	2.088E-05	1.244E-05	8.224E-06	3.616E-06	1.585E-06	1.357E-06	

-----  
 AZIMUTH OF PATH OF SIGHT = 90

		FLIGHT NO. 96		FILTER NO. 1				
		PATH RADIANCE FROM GROUND TO ALTITUDE(WATTS/STER.SC.M MICRO M.)						
ALTITUDE		ZENITH ANGLE OF PATH OF SIGHT (DEGREES)						
METERS		93	95	100	105	120	150	180
305		6.762E-06	4.162E-06	2.176E-06	1.445E-06	7.034E-07	3.842E-07	3.278E-07
610		1.052E-05	7.106E-06	3.937E-06	2.662E-06	1.310E-06	7.146E-07	6.105E-07
914		1.296E-05	9.390E-06	5.475E-06	3.768E-06	1.878E-06	1.017E-06	8.668E-07
1219		1.462E-05	1.142E-05	7.159E-06	5.057E-06	2.574E-06	1.383E-06	1.168E-06
1524		1.565E-05	1.301E-05	8.589E-06	6.209E-06	3.225E-06	1.727E-06	1.430E-06

		FLIGHT NO. 96		FILTER NO. 2				
		PATH RADIANCE FROM GROUND TO ALTITUDE (WATTS/STER.SC.M MICRO M.)						
ALTITUDE		ZENITH ANGLE OF PATH OF SIGHT (DEGREES)						
METERS		93	95	100	105	120	150	180
305		6.582E-06	3.954E-06	2.037E-06	1.347E-06	6.577E-07	3.661E-07	3.260E-07
610		9.935E-06	6.502E-06	3.526E-06	2.369E-06	1.166E-06	6.458E-07	5.642E-07
914		1.166E-05	8.146E-06	4.618E-06	3.150E-06	1.567E-06	8.613E-07	7.480E-07
1219		1.279E-05	9.459E-06	5.603E-06	3.886E-06	1.959E-06	1.069E-06	9.199E-07
1524		1.365E-05	1.078E-05	6.676E-06	4.714E-06	2.417E-06	1.309E-06	1.116E-06

		FLIGHT NO. 96		FILTER NO. 3			
		PATH RADIANCE FROM GROUND TO ALTITUDE (WATTS/STER.SC.M MICRO M.)					
ALTITUDE		ZENITH ANGLE OF PATH OF SIGHT (DEGREES)					
METERS		93	95	100	105	120	150
305	5.289E-06	3.055E-06	1.536E-06	1.006E-06	4.842E-07	2.703E-07	2.422E-07
610	8.986E-06	5.534E-06	2.880E-06	1.907E-06	9.241E-07	5.108E-07	4.541E-07
914	1.140E-05	7.407E-06	3.982E-06	2.667E-06	1.303E-06	7.129E-07	6.274E-07
1219	1.324E-05	9.070E-06	5.053E-06	3.429E-06	1.696E-06	9.278E-07	8.098E-07
1524	1.402E-05	1.015E-05	5.894E-06	4.061E-06	2.039E-06	1.113E-06	9.651E-07

		FLIGHT NO. 96		FILTER NO. 4			
		PATH RADIANCE FROM GROUND TO ALTITUDE (WATTS/STER.SC.M MICRO M.)					
ALTITUDE		ZENITH ANGLE OF PATH OF SIGHT (DEGREES)					
METERS		93	95	100	105	120	150
305							
610							
914							
1219							
1524							

		FLIGHT NO. 96		FILTER NO. 5			
		PATH RADIANCE FROM GROUND TO ALTITUDE (WATTS/STER.SC.M MICRO M.)					
		ZENITH ANGLE OF PATH OF SIGHT (DEGREES)					
ALTITUDE		93	95	100	105	120	150
METERS							180
305		8.497E-06	5.273E-06	2.762E-06	1.829E-06	8.792E-07	4.784E-07
610		1.207E-05	8.313E-06	4.667E-06	3.163E-06	1.546E-06	8.329E-07
914		1.360E-05	9.978E-06	5.871E-06	4.049E-06	2.009E-06	1.060E-06
1219		1.470E-05	1.131E-05	7.011E-06	4.904E-06	2.493E-06	1.249E-06
1524		1.457E-05	1.196E-05	7.753E-06	5.554E-06	2.868E-06	1.557E-06
							1.257E-06



AZIMUTH OF PATH OF SIGHT = 180  
 FLIGHT NO. 96      FILTER NO. 1  
 PATH RADIANCE FROM GROUND TO ALTITUDE (WATTS/STER.SQ.M MICRON M.)  
 ALTITUDE      ZENITH ANGLE OF PATH OF SIGHT (DEGREES)  
 METERS      93      95      100      105      120      150      180

305	6.698E-06	4.149E-06	2.204E-06	1.488E-06	7.573E-07	4.132E-07	3.278E-07
610	1.018E-05	6.952E-06	3.936E-06	2.715E-06	1.410E-06	7.709E-07	6.105E-07
914	1.239E-05	9.101E-06	5.450E-06	3.847E-06	2.049E-06	1.109E-06	8.668E-07
1219	1.354E-05	1.083E-05	6.963E-06	5.053E-06	2.766E-06	1.494E-06	1.168E-06
1524	1.446E-05	1.220E-05	8.303E-06	6.169E-06	3.450E-06	1.852E-06	1.450E-06

FLIGHT NO. 96      FILTER NO. 2  
 PATH RADIANCE FROM GROUND TO ALTITUDE (WATTS/STER.SQ.M MICRON M.)  
 ALTITUDE      ZENITH ANGLE OF PATH OF SIGHT (DEGREES)  
 METERS      93      95      100      105      120      150      180

305	6.587E-06	4.001E-06	2.115E-06	1.426E-06	7.555E-07	4.241E-07	3.200E-07
610	9.783E-06	6.485E-06	3.616E-06	2.456E-06	1.327E-06	7.412E-07	5.642E-07
914	1.139E-05	8.067E-06	4.711E-06	3.307E-06	1.779E-06	9.615E-07	7.480E-07
1219	1.239E-05	9.296E-06	5.679E-06	4.054E-06	2.212E-06	1.207E-06	9.199E-07
1524	1.353E-05	1.064E-05	6.769E-06	4.908E-06	2.706E-06	1.455E-06	1.116E-06

FLIGHT NO. 96      FILTER NO. 3  
 PATH RADIANCE FROM GROUND TO ALTITUDE (WATTS/STER.SQ.M MICRON M.)  
 ALTITUDE      ZENITH ANGLE OF PATH OF SIGHT (DEGREES)  
 METERS      93      95      100      105      120      150      180

305	5.125E-06	3.015E-06	1.577E-06	1.075E-06	5.811E-07	3.325E-07	2.422E-07
610	8.647E-06	5.422E-06	2.942E-06	2.030E-06	1.105E-06	6.203E-07	4.541E-07
914	1.083E-05	7.206E-06	4.050E-06	2.832E-06	1.557E-06	8.577E-07	6.274E-07
1219	1.239E-05	8.666E-06	5.031E-06	3.578E-06	1.984E-06	1.091E-06	8.098E-07
1524	1.310E-05	9.662E-06	5.854E-06	4.200E-06	2.347E-06	1.286E-06	9.651E-07

FLIGHT NO. 96      FILTER NO. 4  
 PATH RADIANCE FROM GROUND TO ALTITUDE (WATTS/STER.SQ.M MICRON M.)  
 ALTITUDE      ZENITH ANGLE OF PATH OF SIGHT (DEGREES)  
 METERS      93      95      100      105      120      150      180

305							
610							
914							
1219							
1524							

FLIGHT NO. 96      FILTER NO. 5  
 PATH RADIANCE FROM GROUND TO ALTITUDE (WATTS/STER.SQ.M MICRON M.)  
 ALTITUDE      ZENITH ANGLE OF PATH OF SIGHT (DEGREES)  
 METERS      93      95      100      105      120      150      180

305	8.201E-06	5.172E-06	2.819E-06	1.942E-06	1.046E-06	5.614E-07	4.167E-07
610	1.125E-05	7.960E-06	4.645E-06	3.270E-06	1.776E-06	9.543E-07	7.182E-07
914	1.271E-05	9.484E-06	5.754E-06	4.143E-06	2.270E-06	1.220E-06	9.325E-07
1219	1.362E-05	1.050E-05	6.952E-06	5.055E-06	2.811E-06	1.514E-06	1.176E-06
1524	1.366E-05	1.151E-05	7.707E-06	5.704E-06	3.215E-06	1.732E-06	1.357E-06

AZIMUTH OF PATH OF SIGHT = 270

FLIGHT NO. 96

FILTER NO. 1

PATH RADIANCE FROM GROUND TO ALTITUDE (WATTS/STER.SQ.M MICR M.)

ALTITUDE METERS	93	95	100	105	120	150	180
305	6.873E-06	4.221E-06	2.195E-06	1.450E-06	6.976E-07	3.776E-07	3.278E-07
610	1.047E-05	7.082E-06	3.922E-06	2.646E-06	1.296E-06	7.043E-07	6.185E-07
914	1.284E-05	9.312E-06	5.424E-06	3.728E-06	1.853E-06	1.005E-06	8.668E-07
1219	1.425E-05	1.121E-05	6.983E-06	4.921E-06	2.503E-06	1.357E-06	1.168E-06
1524	1.493E-05	1.247E-05	8.244E-06	5.954E-06	3.105E-06	1.690E-06	1.450E-06

FLIGHT NO. 96

FILTER NO. 2

PATH RADIANCE FROM GROUND TO ALTITUDE (WATTS/STER.SQ.M MICR M.)

ALTITUDE METERS	93	95	100	105	120	150	180
305	6.590E-06	3.961E-06	2.039E-06	1.345E-06	6.566E-07	3.689E-07	3.200E-07
610	9.838E-06	6.457E-06	3.506E-06	2.362E-06	1.170E-06	6.529E-07	5.642E-07
914	1.160E-05	8.109E-06	4.600E-06	3.142E-06	1.570E-06	8.686E-07	7.480E-07
1219	1.288E-05	9.499E-06	5.604E-06	3.879E-06	1.954E-06	1.072E-06	9.199E-07
1524	1.404E-05	1.088E-05	6.655E-06	4.700E-06	2.397E-06	1.305E-06	1.116E-06

FLIGHT NO. 96

FILTER NO. 3

PATH RADIANCE FROM GROUND TO ALTITUDE (WATTS/STER.SQ.M MICR M.)

ALTITUDE METERS	93	95	100	105	120	150	180
305	5.081E-06	2.956E-06	1.504E-06	9.964E-07	4.971E-07	2.823E-07	2.422E-07
610	8.748E-06	5.414E-06	2.850E-06	1.912E-06	9.536E-07	5.322E-07	4.541E-07
914	1.116E-05	7.277E-06	3.956E-06	2.681E-06	1.347E-06	7.418E-07	6.274E-07
1219	1.296E-05	8.902E-06	4.958E-06	3.422E-06	1.731E-06	9.548E-07	8.098E-07
1524	1.389E-05	1.004E-05	5.846E-06	4.050E-06	2.068E-06	1.139E-06	9.651E-07

FLIGHT NO. 96

FILTER NO. 4

PATH RADIANCE FROM GROUND TO ALTITUDE (WATTS/STER.SQ.M MICR M.)

ALTITUDE METERS	93	95	100	105	120	150	180
305							
610							
914							
1219							
1524							

FLIGHT NO. 96

FILTER NO. 5

PATH RADIANCE FROM GROUND TO ALTITUDE (WATTS/STER.SQ.M MICR M.)

ALTITUDE METERS	93	95	100	105	120	150	180
305	8.167E-06	5.082E-06	2.679E-06	1.786E-06	8.748E-07	4.816E-07	4.167E-07
610	1.156E-05	7.985E-06	4.507E-06	2.974E-06	1.530E-06	8.357E-07	7.182E-07
914	1.312E-05	9.630E-06	5.687E-06	3.942E-06	1.990E-06	1.088E-06	9.325E-07
1219	1.479E-05	1.112E-05	6.851E-06	4.828E-06	2.479E-06	1.372E-06	1.176E-06
1524	1.447E-05	1.181E-05	7.634E-06	5.476E-06	2.855E-06	1.583E-06	1.357E-06

AZIMUTH OF PATH OF SIGHT = 0  
 FLIGHT NO. 96 FILTER NO. 1  
 DIRECTIONAL PATH REFLECTANCE FROM GROUND TO ALTITUDE  
 ZENITH ANGLE OF PATH OF SIGHT (DEGREES)

ALTITUDE METERS	93	95	100	105	120	150	180
305	4.442E-01	2.143E-01	9.156E-02	5.564E-02	2.353E-02	1.154E-02	1.019E-02
610	1.232E 00	5.210E-01	2.011E-01	1.176E-01	4.720E-02	2.226E-02	1.948E-02
914	2.813E 00	1.016E 00	3.512E-01	1.971E-01	7.429E-02	3.289E-02	2.833E-02
1219	6.589E 00	1.951E 00	5.947E-01	3.210E-01	1.141E-01	4.705E-02	3.934E-02
1524	1.461E 01	3.433E 00	9.159E-01	4.740E-01	1.593E-01	6.182E-02	5.033E-02

FLIGHT NO. 96 FILTER NO. 2  
 DIRECTIONAL PATH REFLECTANCE FROM GROUND TO ALTITUDE  
 ZENITH ANGLE OF PATH OF SIGHT (DEGREES)

ALTITUDE METERS	93	95	100	105	120	150	180
305	7.282E-01	1.615E-01	6.948E-02	4.209E-02	1.755E-02	8.616E-03	7.800E-03
610	7.732E-01	3.483E-01	1.397E-01	8.244E-02	3.315E-02	1.572E-02	1.404E-02
914	1.409E 00	5.736E-01	2.146E-01	1.234E-01	4.762E-02	2.157E-02	1.894E-02
1219	2.428E 00	8.798E-01	3.067E-01	1.718E-01	6.384E-02	2.755E-02	2.371E-02
1524	4.238E 00	1.336E 00	4.217E-01	2.354E-01	8.476E-02	3.497E-02	2.934E-02

FLIGHT NO. 96 FILTER NO. 3  
 DIRECTIONAL PATH REFLECTANCE FROM GROUND TO ALTITUDE  
 ZENITH ANGLE OF PATH OF SIGHT (DEGREES)

ALTITUDE METERS	93	95	100	105	120	150	180
305	2.210E-01	1.120E-01	4.913E-02	2.984E-02	1.237E-02	6.033E-03	5.541E-03
610	5.239E-01	2.511E-01	1.048E-01	6.226E-02	2.466E-02	1.164E-02	1.053E-02
914	9.188E-01	4.142E-01	1.645E-01	9.574E-02	3.666E-02	1.655E-02	1.473E-02
1219	1.474E 00	6.187E-01	2.342E-01	1.329E-01	5.022E-02	2.198E-02	1.926E-02
1524	2.210E 00	8.559E-01	3.092E-01	1.741E-01	6.381E-02	2.704E-02	2.328E-02

FLIGHT NO. 96 FILTER NO. 4  
 DIRECTIONAL PATH REFLECTANCE FROM GROUND TO ALTITUDE  
 ZENITH ANGLE OF PATH OF SIGHT (DEGREES)

ALTITUDE METERS	93	95	100	105	120	150	180
305							
610							
914							
1219							
1524							

FLIGHT NO. 96 FILTER NO. 5  
 DIRECTIONAL PATH REFLECTANCE FROM GROUND TO ALTITUDE  
 ZENITH ANGLE OF PATH OF SIGHT (DEGREES)

ALTITUDE METERS	93	95	100	105	120	150	180
305	5.828E-01	2.756E-01	1.141E-01	6.755E-02	3.647E-02	1.711E-02	1.623E-02
610	1.452E 00	6.080E-01	2.308E-01	1.328E-01	5.016E-02	2.199E-02	1.919E-02
914	2.600E 00	9.621E-01	3.390E-01	1.904E-01	7.028E-02	2.956E-02	2.541E-02
1219	4.673E 00	1.488E 00	4.815E-01	2.628E-01	9.389E-02	3.825E-02	3.272E-02
1524	7.592E 00	2.085E 00	6.254E-01	3.333E-01	1.157E-01	4.584E-02	3.850E-02

AZIMUTH OF PATH OF SIGHT = °C

FLIGHT NO. 96

FILTER NO. 1

ALTITUDE	DIRECTIONAL PATH REFLECTANCE FROM GROUND TO ALTITUDE						
METERS	ZENITH ANGLE OF PATH OF SIGHT (DEGREES)						
	93	95	100	105	120	150	180
305	3.600E-01	1.761E-01	7.779E-02	4.886E-02	2.252E-02	1.200E-02	1.019E-02
610	9.393E-01	4.065E-01	1.638E-01	9.963E-02	4.418E-02	2.300E-02	1.948E-02
914	1.868E-00	7.057E-01	2.612E-01	1.546E-01	6.644E-02	3.366E-02	2.833E-02
1219	3.924E-00	1.227E-00	4.077E-01	2.237E-01	9.667E-02	4.739E-02	3.924E-02
1524	7.772E-00	1.956E-00	5.803E-01	3.218E-01	1.289E-01	6.125E-02	5.033E-02

FLIGHT NO. 96

FILTER NO. 2

ALTITUDE	DIRECTIONAL PATH REFLECTANCE FROM GROUND TO ALTITUDE						
METERS	ZENITH ANGLE OF PATH OF SIGHT (DEGREES)						
	93	95	100	105	120	150	180
305	2.458E-01	1.231E-01	5.548E-02	3.511E-02	1.641E-02	8.956E-03	7.800E-03
610	5.560E-01	2.562E-01	1.081E-01	6.683E-02	3.022E-02	1.618E-02	1.404E-02
914	9.311E-01	3.929E-01	1.567E-01	9.515E-02	4.221E-02	2.202E-02	1.894E-02
1219	1.467E-00	5.584E-01	2.105E-01	1.256E-01	5.466E-02	2.788E-02	2.371E-02
1524	2.392E-00	7.975E-01	2.808E-01	1.444E-01	7.013E-02	3.493E-02	2.934E-02

FLIGHT NO. 96

FILTER NO. 3

ALTITUDE	DIRECTIONAL PATH REFLECTANCE FROM GROUND TO ALTITUDE						
METERS	ZENITH ANGLE OF PATH OF SIGHT (DEGREES)						
	93	95	100	105	120	150	180
305	1.577E-01	8.144E-02	3.764E-02	2.357E-02	1.124E-02	6.196E-03	5.541E-03
610	3.500E-01	1.722E-01	7.632E-02	4.792E-02	2.203E-02	1.189E-02	1.053E-02
914	5.688E-01	2.655E-01	1.133E-01	7.028E-02	3.183E-02	1.684E-02	1.473E-02
1219	8.685E-01	3.782E-01	1.553E-01	9.517E-02	4.259E-02	2.226E-02	1.926E-02
1524	1.226E-00	4.976E-01	1.962E-01	1.169E-01	5.262E-02	2.712E-02	2.328E-02

FLIGHT NO. 96

FILTER NO. 4

ALTITUDE	DIRECTIONAL PATH REFLECTANCE FROM GROUND TO ALTITUDE						
METERS	ZENITH ANGLE OF PATH OF SIGHT (DEGREES)						
	93	95	100	105	120	150	180
305							
610							
914							
1219							
1524							

FLIGHT NO. 96

FILTER NO. 5

ALTITUDE	DIRECTIONAL PATH REFLECTANCE FROM GROUND TO ALTITUDE						
METERS	ZENITH ANGLE OF PATH OF SIGHT (DEGREES)						
	93	95	100	105	120	150	180
305	3.969E-01	1.918E-01	8.363E-02	5.212E-02	2.360E-02	1.250E-02	1.082E-02
610	9.646E-01	4.134E-01	1.653E-01	1.001E-01	4.362E-02	2.245E-02	1.919E-02
914	1.628E-00	6.231E-01	2.332E-01	1.384E-01	5.926E-02	2.980E-02	2.541E-02
1219	2.693E-00	8.998E-01	3.134E-01	1.622E-01	7.660E-02	3.811E-02	3.272E-02
1524	4.108E-00	1.194E-00	3.897E-01	2.224E-01	9.175E-02	4.502E-02	3.850E-02

AZIMUTH OF PATH OF SIGHT = 110		FLIGHT NO. 96		FILTER NO. 1					
DIRECTIONAL PATH REFLECTANCE FROM GROUND TO ALTITUDE		ZENITH ANGLE OF PATH OF SIGHT (DEGREES)							
ALTITUDE		93	95	100	105	120	150	180	
METERS									
305		3.566E-01	1.756E-01	7.882E-02	5.032E-02	2.424E-02	1.290E-02	1.019E-02	
610		9.092E-01	3.977E-01	1.637E-01	1.016E-01	4.757E-02	2.481E-02	1.948E-02	
914		1.786E 00	6.840E-01	2.600E-01	1.578E-01	7.251E-02	3.670E-02	2.833E-02	
1219		3.636E 00	1.158E 00	3.965E-01	2.335E-01	1.041E-01	5.120E-02	3.934E-02	
1524		7.178E 00	1.835E 00	5.610E-01	3.197E-01	1.378E-01	6.568E-02	5.033E-02	

FLIGHT NO. 96		FILTER NO. 2							
DIRECTIONAL PATH REFLECTANCE FROM GROUND TO ALTITUDE		ZENITH ANGLE OF PATH OF SIGHT (DEGREES)							
ALTITUDE		93	95	100	105	120	150	180	
METERS									
305		2.460E-01	1.245E-01	5.762E-02	3.743E-02	1.865E-02	1.038E-02	7.800E-03	
610		5.475E-01	2.555E-01	1.109E-01	7.043E-02	3.450E-02	1.857E-02	1.404E-02	
914		9.094E-01	3.891E-01	1.599E-01	9.688E-02	4.792E-02	2.510E-02	1.894E-02	
1219		1.421E 00	5.484E-01	2.133E-01	1.311E-01	6.170E-02	3.149E-02	2.371E-02	
1524		2.336E 00	7.871E-01	2.847E-01	1.712E-01	7.851E-02	3.893E-02	2.934E-02	

FLIGHT NO. 96		FILTER NO. 3							
DIRECTIONAL PATH REFLECTANCE FROM GROUND TO ALTITUDE		ZENITH ANGLE OF PATH OF SIGHT (DEGREES)							
ALTITUDE		93	95	100	105	120	150	180	
METERS									
305		1.528E-01	8.028E-02	3.664E-02	2.562E-02	1.348E-02	7.622E-03	5.541E-03	
610		3.368E-01	1.687E-01	7.797E-02	5.101E-02	2.634E-02	1.444E-02	1.053E-02	
914		5.429E-01	2.583E-01	1.152E-01	7.464E-02	3.804E-02	2.026E-02	1.477E-02	
1219		8.129E-01	3.623E-01	1.552E-01	9.921E-02	4.982E-02	2.618E-02	1.926E-02	
1524		1.146E 00	4.736E-01	1.948E-01	1.230E-01	6.056E-02	3.133E-02	2.328E-02	

FLIGHT NO. 96		FILTER NO. 4							
DIRECTIONAL PATH REFLECTANCE FROM GROUND TO ALTITUDE		ZENITH ANGLE OF PATH OF SIGHT (DEGREES)							
ALTITUDE		93	95	100	105	120	150	180	
METERS									
305									
610									
914									
1219									
1524									

FLIGHT NO. 96		FILTER NO. 5							
DIRECTIONAL PATH REFLECTANCE FROM GROUND TO ALTITUDE		ZENITH ANGLE OF PATH OF SIGHT (DEGREES)							
ALTITUDE		93	95	100	105	120	150	180	
METERS									
305		3.830E-01	1.881E-01	8.533E-02	5.533E-02	2.807E-02	1.466E-02	1.083E-02	
610		9.071E-01	3.958E-01	1.646E-01	1.035E-01	5.035E-02	2.573E-02	1.919E-02	
914		1.522E 00	5.923E-01	2.301E-01	1.416E-01	6.696E-02	3.365E-02	2.541E-02	
1219		2.543E 00	8.613E-01	3.108E-01	1.871E-01	8.637E-02	4.277E-02	3.272E-02	
1524		3.910E 00	1.149E 00	3.874E-01	2.284E-01	1.029E-01	5.009E-02	3.850E-02	

AZIMUTH OF PATH OF SIGHT = 270

		FLIGHT NO. 96		FILTER NO. 1			
		DIRECTIONAL PATH REFLECTANCE FROM GROUND TO ALTITUDE		ZENITH ANGLE OF PATH OF SIGHT (DEGREES)			
ALTITUDE	METERS	93	95	100	105	120	150
305		3.660E-01	1.786E-01	7.848E-02	4.904E-02	2.293E-02	1.176E-02
610		2.352E-01	4.053E-01	1.631E-01	9.905E-02	4.372E-02	2.267E-02
914		1.850E 00	6.998E-01	2.588E-01	1.530E-01	6.558E-02	3.324E-02
1219		3.827E 00	1.199E 00	3.977E-01	2.274E-01	9.417E-02	4.652E-02
1524		7.412E 00	1.875E 00	5.570E-01	3.086E-01	1.240E-01	5.997E-02

		FLIGHT NO. 96		FILTER NO. 2			
		DIRECTIONAL PATH REFLECTANCE FROM GROUND TO ALTITUDE		ZENITH ANGLE OF PATH OF SIGHT (DEGREES)			
ALTITUDE	METERS	93	95	100	105	120	150
305		2.461E-01	1.233E-01	5.554E-02	3.517E-02	1.646E-02	9.026E-03
610		5.505E-01	2.542E-01	1.075E-01	6.663E-02	3.042E-02	1.636E-02
914		9.266E-01	3.911E-01	1.561E-01	9.489E-02	4.227E-02	2.221E-02
1219		1.478E 00	5.608E-01	2.105E-01	1.254E-01	5.450E-02	2.796E-02
1524		2.425E 00	8.043E-01	2.812E-01	1.639E-01	6.954E-02	3.484E-02

		FLIGHT NO. 96		FILTER NO. 3			
		DIRECTIONAL PATH REFLECTANCE FROM GROUND TO ALTITUDE		ZENITH ANGLE OF PATH OF SIGHT (DEGREES)			
ALTITUDE	METERS	93	95	100	105	120	150
305		1.515E-01	7.871E-02	3.485E-02	2.386E-02	1.154E-02	6.470E-03
610		3.407E-01	1.685E-01	7.354E-02	4.803E-02	2.274E-02	1.239E-02
914		5.566E-01	2.608E-01	1.125E-01	7.065E-02	3.252E-02	1.752E-02
1219		8.501E-01	3.721E-01	1.536E-01	9.496E-02	4.345E-02	2.290E-02
1524		1.214E 00	4.921E-01	1.946E-01	1.166E-01	5.337E-02	2.776E-02

		FLIGHT NO. 96		FILTER NO. 4			
		DIRECTIONAL PATH REFLECTANCE FROM GROUND TO ALTITUDE		ZENITH ANGLE OF PATH OF SIGHT (DEGREES)			
ALTITUDE	METERS	93	95	100	105	120	150
305							
610							
914							
1219							
1524							

		FLIGHT NO. 96		FILTER NO. 5			
		DIRECTIONAL PATH REFLECTANCE FROM GROUND TO ALTITUDE		ZENITH ANGLE OF PATH OF SIGHT (DEGREES)			
ALTITUDE	METERS	93	95	100	105	120	150
305		3.814E-01	1.848E-01	8.111E-02	5.090E-02	2.348E-02	1.258E-02
610		9.241E-01	3.971E-01	1.597E-01	9.733E-02	4.338E-02	2.253E-02
914		1.571E 00	6.014E-01	2.259E-01	1.347E-01	5.868E-02	3.001E-02
1219		2.638E 00	8.786E-01	3.043E-01	1.787E-01	7.617E-02	3.875E-02
1524		4.080E 00	1.179E 00	3.827E-01	2.192E-01	5.139E-02	4.578E-02

#### FLIGHT 97

Moonlight. The flight was made over the Gulf of Siam, approximately 130 km south of Rayong, where water depth was about 55 m (30 fm). The atmosphere was essentially clear except for small scattered clouds at about a 450-meter altitude. Data-gathering started at 2132 local time and ended at 2400. The moon phase angle was  $71^\circ$ ; the moon zenith angle was  $29^\circ$  when sky radiance data-taking started and  $54^\circ$  when data-taking ended.

FLIGHT NO. 97				FILTER NO. 1			
IRRADIANCE (WATTS/SQ.M. MICRO M.)							
ALTITUDE (METERS)	DOWN- WELLING	UP- WELLING	ALBEDO	SCALAR DOWNWELLING	SCALAR UPWELLING	SCALAR TOTAL	SCALAR ALBEDO
176	4.212E-04	2.395E-05	.057	5.923E-04	6.622E-05	6.585E-04	.112
487	3.442E-04	2.994E-05	.067	5.248E-04	8.563E-05	6.104E-04	.163
773	2.332E-04	3.122E-05	.134	4.069E-04	9.167E-05	4.988E-04	.226
1072	2.524E-04	3.241E-05	.128	4.395E-04	9.717E-05	5.367E-04	.221
1387	3.335E-04	3.814E-05	.114	5.796E-04	1.141E-04	6.938E-04	.197
1692	2.630E-04	3.907E-05	.149	5.065E-04	1.206E-04	6.271E-04	.30

FLIGHT NO. 97				FILTER NO. 2			
IRRADIANCE (WATTS/SQ.M. MICRO M.)							
ALTITUDE (METERS)	DOWN- WELLING	UP- WELLING	ALBEDO	SCALAR DOWNWELLING	SCALAR UPWELLING	SCALAR TOTAL	SCALAR ALBEDO
177	3.340E-04	2.199E-05	.066	4.973E-04	6.026E-05	5.575E-04	.121
473	3.446E-04	2.589E-05	.075	5.198E-04	7.634E-05	5.961E-04	.147
773	1.532E-04	2.961E-05	.193	2.941E-04	8.957E-05	3.837E-04	.305
1071	2.648E-04	3.164E-05	.120	4.526E-04	9.634E-05	5.489E-04	.213
1343	3.462E-04	3.334E-05	.096	5.940E-04	1.015E-04	6.955E-04	.171
1693	4.15E-04	3.650E-05	.151	4.691E-04	1.143E-04	5.833E-04	.44

FLIGHT NO. 97				FILTER NO. 3			
IRRADIANCE (WATTS/SQ.M. MICRO M.)							
ALTITUDE (METERS)	DOWN- WELLING	UP- WELLING	ALBEDO	SCALAR DOWNWELLING	SCALAR UPWELLING	SCALAR TOTAL	SCALAR ALBEDO
149	4.136E-04	2.025E-05	.049	5.765E-04	5.580E-05	6.323E-04	.097
467	3.034E-04	2.361E-05	.077	4.532E-04	6.557E-05	5.188E-04	.145
779	1.728E-04	2.450E-05	.142	2.971E-04	7.563E-05	3.727E-04	.255
1072	2.167E-04	2.554E-05	.110	3.897E-04	9.460E-05	4.743E-04	.217
1381	3.847E-04	3.027E-05	.079	6.432E-04	9.558E-05	7.387E-04	.149
1694	2.113E-04	1.762E-05	.178	4.124E-04	1.219E-04	5.343E-04	.296

FLIGHT NO. 97				FILTER NO. 5			
IRRADIANCE (WATTS/SQ.M. MICRO M.)							
ALTITUDE (METERS)	DOWN- WELLING	UP- WELLING	ALBEDO	SCALAR DOWNWELLING	SCALAR UPWELLING	SCALAR TOTAL	SCALAR ALBEDO
155	2.626E-04	2.181E-05	.053	4.200E-04	5.952E-05	4.799E-04	.142
478	3.683E-04	2.558E-05	.069	5.759E-04	7.871E-05	6.546E-04	.107
779	2.297E-04	2.879E-05	.125	4.060E-04	8.935E-05	4.954E-04	.220
1072	2.435E-04	3.036E-05	.125	4.397E-04	9.514E-05	5.344E-04	.217
1336	2.786E-04	3.650E-05	.131	5.301E-04	1.157E-04	6.458E-04	.216
1695	2.864E-04	3.873E-05	.135	5.494E-04	1.278E-04	6.772E-04	.224



FLIGHT NO. 97					
AZIMUTH OF PATH OF SIGHT = 0					
DIRECTIONAL REFLECTANCE OF BACKGROUND					
ZENITH	FILTERS				
ANGLE	1	2	5	3	4
93	.30497	.37661	.36446	.23943	
95	.23970	.29368	.28890	.17741	
100	.18082	.21111	.19020	.13459	
105	.14098	.16399	.14670	.11033	
120	.08337	.08953	.07144	.07261	
150	.15200	.19611	.06097	.16858	
180	.03859	.04325	.05597	.02948	

FLIGHT NO. 97					
AZIMUTH OF PATH OF SIGHT = 90					
DIRECTIONAL REFLECTANCE OF BACKGROUND					
ZENITH	FILTERS				
ANGLE	1	2	5	3	4
93	.16190	.19140	.19985	.18420	
95	.14258	.15891	.17487	.12645	
100	.10467	.13312	.12083	.07929	
105	.08333	.09267	.09514	.05870	
120	.04265	.04343	.05032	.02517	
150	.03224	.03600	.03015	.02275	
180	.03859	.04325	.05597	.02948	

FLIGHT NO. 97					
AZIMUTH OF PATH OF SIGHT = 180					
DIRECTIONAL REFLECTANCE OF BACKGROUND					
ZENITH	FILTERS				
ANGLE	1	2	5	3	4
93	.15319	.15707	.16607	.13457	
95	.11541	.13479	.14273	.09881	
100	.08878	.10744	.11090	.06257	
105	.07165	.08053	.08402	.05323	
120	.04212	.04129	.05070	.02278	
150	.02344	.02377	.03060	.02232	
180	.03859	.04325	.05597	.02948	

FLIGHT NO. 97					
AZIMUTH OF PATH OF SIGHT = 270					
DIRECTIONAL REFLECTANCE OF BACKGROUND					
ZENITH	FILTERS				
ANGLE	1	2	5	3	4
93	.16584	.18728	.35180	.10907	
95	.12893	.14145	.31738	.07713	
100	.09211	.10836	.22550	.06019	
105	.07310	.08650	.16745	.04284	
120	.04152	.04121	.08747	.02256	
150	.02488	.02641	.12581	.02235	
180	.03859	.04325	.05597	.02948	

DATE 32769 FLIGHT NO. 97 GROUND LEVEL ALTITUDE ( M.)= 42 IUP=1

ALTITUDE (METERS)	TOTAL SCATTERING COEFFICIENT (PER METER)				
FILTERS	1	2	3	4	5
0	5.001E-05	4.476E-05	2.535E-05		4.708E-05
30	4.984E-05	4.461E-05	2.527E-05		4.693E-05
61	4.968E-05	4.446E-05	2.518E-05		4.677E-05
91	4.951E-05	4.431E-05	2.510E-05		4.662E-05
122	4.935E-05	4.416E-05	2.501E-05		4.646E-05
152	4.918E-05	4.402E-05	2.493E-05		4.631E-05
183	4.900E-05	4.432E-05	2.486E-05		4.615E-05
213	4.979E-05	4.493E-05	2.482E-05		4.567E-05
244	5.117E-05	4.649E-05	2.528E-05		4.588E-05
274	5.208E-05	4.747E-05	2.564E-05		4.643E-05
305	5.299E-05	4.860E-05	2.556E-05		4.687E-05
335	5.285E-05	4.928E-05	2.610E-05		4.728E-05
366	5.349E-05	5.041E-05	2.600E-05		4.781E-05
396	5.503E-05	5.226E-05	2.631E-05		4.814E-05
427	5.601E-05	5.702E-05	2.569E-05		4.827E-05
457	5.617E-05	6.879E-05	2.704E-05		4.764E-05
488	6.520E-05	7.346E-05	2.641E-05		4.903E-05
518	7.986E-05	5.969E-05	2.593E-05		4.807E-05
549	5.706E-05	5.067E-05	2.601E-05		4.888E-05
579	5.912E-05	5.355E-05	2.603E-05		4.973E-05
610	6.243E-05	5.307E-05	2.724E-05		4.925E-05
640	6.204E-05	5.597E-05	2.793E-05		4.977E-05
671	6.245E-05	5.372E-05	2.850E-05		5.114E-05
701	6.613E-05	5.249E-05	2.910E-05		4.774E-05
732	6.758E-05	5.812E-05	3.344E-05		4.352E-05
762	6.439E-05	5.641E-05	3.712E-05		4.223E-05
792	6.512E-05	5.867E-05	3.746E-05		4.072E-05
823	6.239E-05	5.646E-05	3.764E-05		3.854E-05
853	5.611E-05	5.024E-05	3.735E-05		3.818E-05
884	5.829E-05	4.761E-05	3.561E-05		3.914E-05
914	6.159E-05	4.667E-05	3.203E-05		3.962E-05
945	6.106E-05	4.996E-05	3.170E-05		4.005E-05
975	5.609E-05	5.745E-05	3.171E-05		3.989E-05
1006	4.987E-05	5.595E-05	3.151E-05		3.645E-05
1036	4.720E-05	5.074E-05	3.235E-05		3.734E-05
1067	4.705E-05	4.822E-05	3.283E-05		4.070E-05
1097	4.730E-05	4.125E-05	3.307E-05		4.120E-05
1128	4.724E-05	3.822E-05	3.211E-05		4.037E-05
1158	4.742E-05	3.654E-05	3.088E-05		4.090E-05
1189	4.772E-05	4.405E-05	2.984E-05		4.053E-05
1219	4.745E-05	5.316E-05	2.963E-05		4.012E-05
1250	4.760E-05	5.863E-05	3.053E-05		4.008E-05
1280	4.676E-05	5.891E-05	3.077E-05		4.060E-05
1311	4.864E-05	6.210E-05	3.051E-05		4.027E-05
1341	4.892E-05	6.466E-05	3.194E-05		4.047E-05
1372	4.907E-05	6.412E-05	3.272E-05		4.264E-05
1402	4.617E-05	6.367E-05	3.155E-05		3.835E-05
1433	4.462E-05	6.032E-05	2.842E-05		3.654E-05
1463	4.386E-05	5.779E-05	2.673E-05		3.736E-05
1494	4.332E-05	5.526E-05	2.971E-05		3.904E-05
1524	4.649E-05	5.326E-05	3.111E-05		4.243E-05
1554	4.638E-05	5.699E-05	3.163E-05		4.065E-05
1585	5.130E-05	5.835E-05	3.096E-05		4.152E-05
1615	5.479E-05	5.647E-05	3.037E-05		4.126E-05
1646	5.087E-05	5.888E-05	3.010E-05		4.368E-05
1676	5.179E-05	5.733E-05	3.011E-05		3.999E-05
1707	4.608E-05	5.527E-05	3.078E-05		3.760E-05
1737	4.593E-05	5.508E-05	3.068E-05		3.617E-05
1768	4.578E-05	5.490E-05	3.058E-05		3.605E-05
1798	4.563E-05	5.472E-05	3.048E-05		3.593E-05
1829	4.547E-05	5.453E-05	3.037E-05		3.581E-05

FIRST DATA ALT. 6 6 6 6 7  
LAST DATA ALT. 57 57 57 56 8

		FLIGHT NO. 97		FILTER NO. 1				
		BEAM TRANSMITTANCE FROM GROUND TO ALTITUDE		ZENITH ANGLE OF PATH OF SIGHT (DEGREES)				
ALTITUDE	METERS	93	95	100	105	120	150	180
305		.7449758	.8392547	.9158019	.9426961	.9699153	.9825186	.9842428
610		.5232137	.6821893	.8253444	.8791611	.9355085	.9622422	.9672169
914		.3577515	.5479624	.7393548	.8166311	.9004534	.9412569	.9489222
1219		.2606885	.4591770	.6766194	.7694384	.8731307	.9246600	.9344146
1524		.1931697	.3901337	.6234849	.7283558	.8486797	.9096205	.9212381

		FLIGHT NO. 97		FILTER NO. 2				
		BEAM TRANSMITTANCE FROM GROUND TO ALTITUDE		ZENITH ANGLE OF PATH OF SIGHT (DEGREES)				
ALTITUDE	METERS	93	95	100	105	120	150	180
305		.7670312	.8539521	.9238167	.9482233	.9728549	.9842367	.9863341
610		.5474141	.7005976	.8364484	.8870794	.9398605	.9648241	.9694640
914		.3942468	.5801228	.7608662	.8324665	.9094499	.9466750	.9536509
1219		.2934724	.4918003	.7003349	.7874296	.8836398	.9310693	.9400211
1524		.2016120	.3988995	.6304773	.7338262	.8519732	.9116568	.9230739

		FLIGHT NO. 97		FILTER NO. 3				
		BEAM TRANSMITTANCE FROM GROUND TO ALTITUDE		ZENITH ANGLE OF PATH OF SIGHT (DEGREES)				
ALTITUDE	METERS	93	95	100	105	120	150	180
305		.8626079	.9157900	.9568084	.9708117	.9847831	.9911861	.9923624
610		.7375887	.8356352	.9130174	.9413250	.9691849	.9820913	.9844719
914		.6028779	.7435680	.8618160	.9050405	.9496634	.9706214	.9745068
1219		.4957189	.6655816	.8151978	.8718949	.9314981	.9598585	.9651415
1524		.4092553	.5986143	.7729438	.8413092	.9144378	.9496692	.9562624

		FLIGHT NO. 97		FILTER NO. 5				
		BEAM TRANSMITTANCE FROM GROUND TO ALTITUDE		ZENITH ANGLE OF PATH OF SIGHT (DEGREES)				
ALTITUDE	METERS	93	95	100	105	120	150	180
305		.7612832	.8501560	.9217537	.9468718	.9720997	.9837955	.9859512
610		.5703861	.7180446	.8468393	.8944578	.9438890	.9672155	.9715447
914		.4370020	.6166241	.7645294	.8497490	.9191749	.9525064	.9587361
1219		.3436413	.5366329	.7316820	.8109059	.8971801	.9392799	.9471959
1524		.2642552	.4671309	.6624769	.7739011	.8757484	.9262596	.9358143

AZIMUTH OF PATH OF SIGHT = 0								
FLIGHT NO. 97			FILTER NO. 1					
PATH RADIANCE FROM GROUND TO ALTITUDE (WATTS/STER.SQ.M MICRO M.)								
ALTITUDE	ZENITH ANGLE OF PATH OF SIGHT (DEGREES)							
METERS	93	95	100	105	120	150	180	
305	1.425E-05	8.138E-06	3.958E-06	2.512E-06	1.138E-06	6.209E-07	6.282E-07	
610	2.637E-05	1.635E-05	8.378E-06	5.365E-06	2.435E-06	1.288E-06	1.264E-06	
914	3.438E-05	2.299E-05	1.228E-05	8.040E-06	3.671E-06	1.889E-06	1.797E-06	
1219	4.038E-05	2.825E-05	1.557E-05	1.030E-05	4.722E-06	2.389E-06	2.237E-06	
1524	4.862E-05	3.477E-05	1.946E-05	1.292E-05	5.897E-06	2.927E-06	2.713E-06	

FLIGHT NO. 97			FILTER NO. 2					
PATH RADIANCE FROM GROUND TO ALTITUDE (WATTS/STER.SQ.M MICRO M.)								
ALTITUDE	ZENITH ANGLE OF PATH OF SIGHT (DEGREES)							
METERS	93	95	100	105	120	150	180	
305	1.190E-05	6.761E-06	3.261E-06	2.060E-06	9.148E-07	4.805E-07	4.673E-07	
610	2.351E-05	1.445E-05	7.283E-06	4.665E-06	2.084E-06	1.072E-06	1.029E-06	
914	2.923E-05	1.932E-05	1.023E-05	6.678E-06	3.024E-06	1.521E-06	1.411E-06	
1219	3.634E-05	2.491E-05	1.350E-05	8.873E-06	4.013E-06	1.977E-06	1.809E-06	
1524	4.775E-05	3.373E-05	1.863E-05	1.228E-05	5.519E-06	2.668E-06	2.435E-06	

FLIGHT NO. 97			FILTER NO. 3					
PATH RADIANCE FROM GROUND TO ALTITUDE (WATTS/STER.SQ.M MICRO M.)								
ALTITUDE	ZENITH ANGLE OF PATH OF SIGHT (DEGREES)							
METERS	93	95	100	105	120	150	180	
305	7.613E-06	4.186E-06	1.939E-06	1.196E-06	5.074E-07	2.611E-07	2.630E-07	
610	1.346E-05	7.764E-06	3.710E-06	2.317E-06	9.965E-07	5.014E-07	4.850E-07	
914	1.888E-05	1.148E-05	5.680E-06	3.595E-06	1.557E-06	7.532E-07	6.942E-07	
1219	2.569E-05	1.611E-05	8.075E-06	5.130E-06	2.198E-06	1.024E-06	9.156E-07	
1524	3.526E-05	2.253E-05	1.136E-05	7.166E-06	3.014E-06	1.359E-06	1.201E-06	

FLIGHT NO. 97			FILTER NO. 5				
PATH RADIANCE FROM GROUND TO ALTITUDE (WATTS/STER.SQ.M MICRO M.)							
ALTITUDE	ZENITH ANGLE OF PATH OF SIGHT (DEGREES)						
METERS	93	95	100	105	120	150	180
305	1.169E-05	6.626E-06	3.173E-06	1.988E-06	8.554E-07	4.257E-07	4.013E-07
610	2.390E-05	1.437E-05	7.099E-06	4.488E-06	1.938E-06	9.501E-07	8.878E-07
914	3.117E-05	1.987E-05	1.019E-05	6.529E-06	2.845E-06	1.366E-06	1.244E-06
1219	3.755E-05	2.495E-05	1.314E-05	8.493E-06	3.719E-06	1.755E-06	1.570E-06
1524	4.618E-05	3.155E-05	1.684E-05	1.093E-05	4.756E-06	2.193E-06	1.936E-06

AZIMUTH OF PATH OF SIGHT = 90  
 FLIGHT NO. 97      FILTER NO. 1  
 PATH RADIANCE FROM GROUND TO ALTITUDE (WATTS/STER.SQ.M MICRO M.)  
 ALTITUDE      ZENITH ANGLE OF PATH OF SIGHT (DEGREES)  
 METERS      93      95      100      105      120      150      180

305	1.075E-05	6.273E-06	3.190E-06	2.124E-06	1.072E-06	6.624E-07	6.282E-07
610	1.904E-05	1.209E-05	6.474E-06	4.386E-06	2.242E-06	1.365E-06	1.264E-06
914	2.382E-05	1.636E-05	9.247E-06	6.377E-06	3.302E-06	1.972E-06	1.797E-06
1219	2.703E-05	1.944E-05	1.142E-05	7.979E-06	4.178E-06	2.477E-06	2.237E-06
1524	3.061E-05	2.281E-05	1.373E-05	9.685E-06	5.119E-06	3.019E-06	2.713E-06

FLIGHT NO. 97      FILTER NO. 2  
 PATH RADIANCE FROM GROUND TO ALTITUDE (WATTS/STER.SQ.M MICRO M.)  
 ALTITUDE      ZENITH ANGLE OF PATH OF SIGHT (DEGREES)  
 METERS      93      95      100      105      120      150      180

305	8.544E-06	4.957E-06	2.516E-06	1.673E-06	8.414E-07	5.092E-07	4.673E-07
610	1.638E-05	1.024E-05	5.476E-06	3.697E-06	1.881E-06	1.131E-06	1.029E-06
914	2.117E-05	1.362E-05	7.602E-06	5.214E-06	2.677E-06	1.575E-06	1.411E-06
1219	2.383E-05	1.682E-05	9.691E-06	6.721E-06	3.462E-06	2.031E-06	1.809E-06
1524	2.905E-05	2.138E-05	1.273E-05	8.938E-06	4.692E-06	2.735E-06	2.435E-06

FLIGHT NO. 97      FILTER NO. 3  
 PATH RADIANCE FROM GROUND TO ALTITUDE (WATTS/STER.SQ.M MICRO M.)  
 ALTITUDE      ZENITH ANGLE OF PATH OF SIGHT (DEGREES)  
 METERS      93      95      100      105      120      150      180

305	4.944E-06	2.790E-06	1.385E-06	9.119E-07	4.513E-07	2.771E-07	2.630E-07
610	8.697E-06	5.137E-06	2.615E-06	1.735E-06	8.624E-07	5.217E-07	4.850E-07
914	1.187E-05	7.403E-06	3.893E-06	2.609E-06	1.301E-06	7.648E-07	6.942E-07
1219	1.506E-05	9.771E-06	5.262E-06	3.555E-06	1.778E-06	1.023E-06	9.156E-07
1524	1.898E-05	1.267E-05	6.937E-06	4.716E-06	2.371E-06	1.350E-06	1.201E-06

FLIGHT NO. 97      FILTER NO. 5  
 PATH RADIANCE FROM GROUND TO ALTITUDE (WATTS/STER.SQ.M MICRO M.)  
 ALTITUDE      ZENITH ANGLE OF PATH OF SIGHT (DEGREES)  
 METERS      93      95      100      105      120      150      180

305	7.905E-06	4.581E-06	2.315E-06	1.528E-06	7.506E-07	4.362E-07	4.013E-07
610	1.555E-05	9.610E-06	5.043E-06	3.373E-06	1.681E-06	9.763E-07	8.878E-07
914	1.989E-05	1.303E-05	7.093E-06	4.804E-06	2.414E-06	1.385E-06	1.244E-06
1219	2.320E-05	1.589E-05	8.921E-06	6.108E-06	3.096E-06	1.764E-06	1.570E-06
1524	2.686E-05	1.906E-05	1.057E-05	7.583E-06	3.873E-06	2.199E-06	1.936E-06

FLIGHT NO. 97      FILTER NO. 1  
AZIMUTH OF PATH OF SIGHT = 180  
PATH RADIANCE FROM GROUND TO ALTITUDE (WATTS/STER. SQ. M MICRO M.)  
ZENITH ANGLE OF PATH OF SIGHT (DEGREES)

ALTITUDE METERS	93	95	100	105	120	150	180
305	1.056E-05	6.264E-06	3.318E-06	2.289E-06	1.278E-06	9.726E-07	6.282E-07
610	1.890E-05	1.216E-05	6.746E-06	4.734E-06	2.662E-06	1.772E-06	1.264E-06
914	2.392E-05	1.662E-05	9.708E-06	6.910E-06	3.926E-06	2.515E-06	1.797E-06
1219	2.747E-05	2.003E-05	1.211E-05	8.722E-06	5.011E-06	3.134E-06	2.237E-06
1524	3.166E-05	2.382E-05	1.477E-05	1.076E-05	6.275E-06	3.825E-06	2.713E-06

FLIGHT NO. 97      FILTER NO. 2  
PATH RADIANCE FROM GROUND TO ALTITUDE (WATTS/STER. SQ. M MICRO M.)  
ZENITH ANGLE OF PATH OF SIGHT (DEGREES)

ALTITUDE METERS	93	95	100	105	120	150	180
305	8.575E-06	5.042E-06	2.652E-06	1.824E-06	1.004E-06	6.588E-07	4.673E-07
610	1.647E-05	1.048E-05	5.771E-06	4.030E-06	2.247E-06	1.468E-06	1.029E-06
914	2.012E-05	1.375E-05	7.924E-06	5.604E-06	3.137E-06	1.983E-06	1.411E-06
1219	2.406E-05	1.717E-05	1.020E-05	7.298E-06	4.141E-06	2.552E-06	1.809E-06
1524	3.026E-05	2.250E-05	1.361E-05	1.003E-05	5.829E-06	3.476E-06	2.435E-06

FLIGHT NO. 97      FILTER NO. 3  
PATH RADIANCE FROM GROUND TO ALTITUDE (WATTS/STER. SQ. M MICRO M.)  
ZENITH ANGLE OF PATH OF SIGHT (DEGREES)

ALTITUDE METERS	93	95	100	105	120	150	180
305	4.880E-06	2.800E-06	1.459E-06	1.009E-06	5.740E-07	4.112E-07	2.630E-07
610	8.583E-06	5.142E-06	2.728E-06	1.890E-06	1.064E-06	7.428E-07	4.850E-07
914	1.164E-05	7.359E-06	4.015E-06	2.796E-06	1.567E-06	1.043E-06	6.947E-07
1219	1.494E-05	9.825E-06	5.490E-06	3.854E-06	2.185E-06	1.369E-06	9.156E-07
1524	1.913E-05	1.297E-05	7.396E-06	5.245E-06	3.044E-06	1.818E-06	1.201E-06

FLIGHT NO. 97      FILTER NO. 5  
PATH RADIANCE FROM GROUND TO ALTITUDE (WATTS/STER. SQ. M MICRO M.)  
ZENITH ANGLE OF PATH OF SIGHT (DEGREES)

ALTITUDE METERS	93	95	100	105	120	150	180
305	7.940E-06	4.667E-06	2.451E-06	1.678E-06	9.140E-07	6.689E-07	4.613E-07
610	1.570E-05	9.854E-06	5.381E-06	3.739E-06	2.081E-06	1.290E-06	8.878E-07
914	2.001E-05	1.330E-05	7.518E-06	5.279E-06	2.955E-06	1.792E-06	1.244E-06
1219	2.349E-05	1.632E-05	9.496E-06	6.737E-06	3.809E-06	2.248E-06	1.570E-06
1524	2.761E-05	1.985E-05	1.184E-05	8.499E-06	4.866E-06	2.776E-06	1.936E-06

AZIMUTH OF PATH OF SIGHT = 270

FLIGHT NO. 97

FILTER NO. 1

PATH RADIANCE FROM GROUND TO ALTITUDE (WATTS/STER.SQ.M MICRO M.)		ZENITH ANGLE OF PATH OF SIGHT (DEGREES)						
ALTITUDE METERS		93	95	100	105	120	150	180
305	1.046E-05	6.116E-06	3.130E-06	2.092E-06	1.067E-06	6.725E-07	6.282E-07	
610	1.870E-05	1.187E-05	6.365E-06	4.313E-06	2.212E-06	1.464E-06	1.264E-06	
914	2.355E-05	1.615E-05	9.113E-06	6.276E-06	3.247E-06	1.963E-06	1.797E-06	
1219	2.664E-05	1.921E-05	1.124E-05	7.844E-06	4.104E-06	2.463E-06	2.237E-06	
1524	2.995E-05	2.235E-05	1.345E-05	9.489E-06	5.023E-06	3.007E-06	2.713E-06	

FLIGHT NO. 97

FILTER NO. 2

PATH RADIANCE FROM GROUND TO ALTITUDE (WATTS/STER.SQ.M MICRO M.)		ZENITH ANGLE OF PATH OF SIGHT (DEGREES)						
ALTITUDE METERS		93	95	100	105	120	150	180
305	8.463E-06	4.908E-06	2.491E-06	1.653E-06	8.284E-07	5.041E-07	4.673E-07	
610	1.623E-05	1.019E-05	5.411E-06	3.645E-06	1.845E-06	1.114E-06	1.029E-06	
914	1.999E-05	1.348E-05	7.500E-06	5.127E-06	2.614E-06	1.546E-06	1.411E-06	
1219	2.344E-05	1.655E-05	9.511E-06	6.582E-06	3.393E-06	1.997E-06	1.809E-06	
1524	2.822E-05	2.084E-05	1.241E-05	8.725E-06	4.588E-06	2.714E-06	2.435E-06	

FLIGHT NO. 97

FILTER NO. 3

PATH RADIANCE FROM GROUND TO ALTITUDE (WATTS/STER.SQ.M MICRO M.)		ZENITH ANGLE OF PATH OF SIGHT (DEGREES)						
ALTITUDE METERS		93	95	100	105	120	150	180
305	4.863E-06	2.745E-06	1.365E-06	8.981E-07	4.460E-07	2.799E-07	2.630E-07	
610	8.615E-06	5.082E-06	2.580E-06	1.705E-06	8.424E-07	5.162E-07	4.850E-07	
914	1.165E-05	7.257E-06	3.799E-06	2.534E-06	1.252E-06	7.452E-07	6.942E-07	
1219	1.480E-05	9.588E-06	5.137E-06	3.452E-06	1.709E-06	9.961E-07	9.156E-07	
1524	1.830E-05	1.224E-05	6.687E-06	4.535E-06	2.271E-06	1.321E-06	1.201E-06	

FLIGHT NO. 97

FILTER NO. 5

PATH RADIANCE FROM GROUND TO ALTITUDE (WATTS/STER.SQ.M MICRO M.)		ZENITH ANGLE OF PATH OF SIGHT (DEGREES)						
ALTITUDE METERS		93	95	100	105	120	150	180
305	8.231E-06	4.779E-06	2.426E-06	1.607E-06	7.965E-07	4.605E-07	4.013E-07	
610	1.575E-05	9.754E-06	5.131E-06	3.438E-06	1.719E-06	1.000E-06	8.878E-07	
914	1.987E-05	1.304E-05	7.114E-06	4.823E-06	2.429E-06	1.402E-06	1.244E-06	
1219	2.302E-05	1.581E-05	8.886E-06	6.089E-06	3.092E-06	1.775E-06	1.570E-06	
1524	2.825E-05	1.872E-05	1.081E-05	7.484E-06	3.841E-06	2.200E-06	1.936E-06	

AZIMUTH OF PATH OF SIGHT = )  
 FLIGHT NO. 97      FILTER NO. 1  
 DIRECTIONAL PATH REFLECTANCE FROM GROUND TO ALTITUDE  
 ALTITUDE      ZENITH ANGLE OF PATH OF SIGHT (DEGREES)

METERS	93	95	100	105	120	150	180
305	1.427E-01	7.233E-02	3.223E-02	1.988E-02	8.749E-03	4.714E-03	4.758E-03
610	3.760E-01	1.788E-01	7.576E-02	4.552E-02	1.942E-02	9.982E-03	9.748E-03
914	7.168E-01	3.129E-01	1.239E-01	7.344E-02	3.041E-02	1.497E-02	1.412E-02
1219	1.155E 00	4.588E-01	1.716E-01	9.987E-02	4.034E-02	1.927E-02	1.786E-02
1524	1.877E 00	6.648E-01	2.328E-01	1.323E-01	5.182E-02	2.400E-02	2.196E-02

FLIGHT NO. 97      FILTER NO. 2  
 DIRECTIONAL PATH REFLECTANCE FROM GROUND TO ALTITUDE  
 ALTITUDE      ZENITH ANGLE OF PATH OF SIGHT (DEGREES)

METERS	93	95	100	105	120	150	180
305	1.459E-01	7.447E-02	3.320E-02	2.044E-02	8.846E-03	4.592E-03	4.456E-03
610	4.039E-01	1.940E-01	8.190E-02	4.947E-02	2.086E-02	1.045E-02	9.982E-03
914	6.974E-01	3.133E-01	1.265E-01	7.546E-02	3.128E-02	1.511E-02	1.392E-02
1219	1.165E 00	4.765E-01	1.814E-01	1.060E-01	4.272E-02	1.997E-02	1.810E-02
1524	2.228E 00	7.955E-01	2.780E-01	1.574E-01	6.093E-02	2.753E-02	2.481E-02

FLIGHT NO. 97      FILTER NO. 3  
 DIRECTIONAL PATH REFLECTANCE FROM GROUND TO ALTITUDE  
 ALTITUDE      ZENITH ANGLE OF PATH OF SIGHT (DEGREES)

METERS	93	95	100	105	120	150	180
305	6.703E-02	3.472E-02	1.539E-02	9.355E-03	3.913E-03	2.001E-03	2.013E-03
610	1.386E-01	7.056E-02	3.083E-02	1.870E-02	7.809E-03	3.878E-03	3.741E-03
914	2.379E-01	1.173E-01	5.006E-02	3.017E-02	1.245E-02	5.894E-03	5.410E-03
1219	3.937E-01	1.839E-01	7.541E-02	4.468E-02	1.792E-02	8.100E-03	7.205E-03
1524	6.543E-01	2.859E-01	1.116E-01	6.469E-02	2.503E-02	1.087E-02	9.543E-03

FLIGHT NO. 97      FILTER NO. 5  
 DIRECTIONAL PATH REFLECTANCE FROM GROUND TO ALTITUDE  
 ALTITUDE      ZENITH ANGLE OF PATH OF SIGHT (DEGREES)

METERS	93	95	100	105	120	150	180
305	1.836E-01	9.325E-02	4.118E-02	2.512E-02	1.053E-02	5.177E-03	4.871E-03
610	5.013E-01	2.394E-01	1.003E-01	6.003E-02	2.456E-02	1.175E-02	1.093E-02
914	8.534E-01	3.856E-01	1.554E-01	9.193E-02	3.704E-02	1.716E-02	1.552E-02
1219	1.319E 00	5.563E-01	2.149E-01	1.253E-01	4.960E-02	2.236E-02	1.983E-02
1524	2.091E 00	8.081E-01	2.953E-01	1.689E-01	6.498E-02	2.833E-02	2.475E-02



AZIMUTH OF PATH OF SIGHT = 90

FLIGHT NO. 97		FILTER NO. 1						
DIRECTIONAL PATH REFLECTANCE FROM GROUND TO ALTITUDE		ZENITH ANGLE OF PATH OF SIGHT (DEGREES)						
ALTITUDE METERS		93	95	100	105	120	150	180
305	1.077E-01	5.575E-02	2.598E-02	1.681E-02	8.241E-03	5.029E-03	4.758E-03	
610	2.714E-01	1.321E-01	5.851E-02	3.721E-02	1.788E-02	1.058E-02	9.748E-03	
914	4.966E-01	2.227E-01	9.328E-02	5.824E-02	2.735E-02	1.563E-02	1.412E-02	
1219	7.725E-01	3.164E-01	1.259E-01	7.735E-02	3.570E-02	1.998E-02	1.786E-02	
1524	1.182E 00	4.361E-01	1.642E-01	9.918E-02	4.499E-02	2.476E-02	2.196E-02	

FLIGHT NO. 97		FILTER NO. 2						
DIRECTIONAL PATH REFLECTANCE FROM GROUND TO ALTITUDE		ZENITH ANGLE OF PATH OF SIGHT (DEGREES)						
ALTITUDE METERS		93	95	100	105	120	150	180
305	1.048E-01	5.460E-02	2.562E-02	1.660E-02	8.135E-03	4.867E-03	4.456E-03	
610	2.815E-01	1.382E-01	6.158E-02	3.921E-02	1.883E-02	1.102E-02	9.982E-03	
914	4.812E-01	2.208E-01	9.399E-02	5.892E-02	2.768E-02	1.565E-02	1.392E-02	
1219	7.639E-01	3.217E-01	1.302E-01	8.029E-02	3.706E-02	2.052E-02	1.810E-02	
1524	1.355E 00	5.042E-01	1.899E-01	1.146E-01	5.180E-02	2.822E-02	2.481E-02	

FLIGHT NO. 97		FILTER NO. 3						
DIRECTIONAL PATH REFLECTANCE FROM GROUND TO ALTITUDE		ZENITH ANGLE OF PATH OF SIGHT (DEGREES)						
ALTITUDE METERS		93	95	100	105	120	150	180
305	4.353E-02	2.314E-02	1.100E-02	7.134E-03	3.481E-03	2.124E-03	2.013E-03	
610	8.955E-02	4.669E-02	2.174E-02	1.400E-02	6.758E-03	4.035E-03	3.741E-03	
914	1.495E-01	7.562E-02	3.430E-02	2.190E-02	1.040E-02	5.984E-03	5.410E-03	
1219	2.307E-01	1.115E-01	4.902E-02	3.097E-02	1.450E-02	8.098E-03	7.205E-03	
1524	3.522E-01	1.607E-01	6.817E-02	4.257E-02	1.969E-02	1.080E-02	9.543E-03	

FLIGHT NO. 97		FILTER NO. 5						
DIRECTIONAL PATH REFLECTANCE FROM GROUND TO ALTITUDE		ZENITH ANGLE OF PATH OF SIGHT (DEGREES)						
ALTITUDE METERS		93	95	100	105	120	150	180
305	1.242E-01	6.447E-02	3.005E-02	1.931E-02	9.239E-03	5.305E-03	4.871E-03	
610	3.261E-01	1.601E-01	7.126E-02	4.513E-02	2.130E-02	1.208E-02	1.093E-02	
914	5.447E-01	2.528E-01	1.082E-01	6.764E-02	3.142E-02	1.740E-02	1.552E-02	
1219	8.150E-01	3.544E-01	1.459E-01	9.013E-02	4.130E-02	2.247E-02	1.983E-02	
1524	1.210E 00	4.883E-01	1.923E-01	1.172E-01	5.292E-02	2.827E-02	2.475E-02	

AZIMUTH OF PATH OF SIGHT = 180								
FLIGHT NO. 97			FILTER NO. 1					
DIRECTIONAL PATH REFLECTANCE FROM GROUND TO ALTITUDE								
ZENITH ANGLE OF PATH OF SIGHT (DEGREES)								
ALTITUDE	93	95	100	105	120	150	180	
METERS								
305	1.058E-01	5.567E-02	2.703E-02	1.811E-02	9.828E-03	6.624E-03	4.758E-03	
610	2.694E-01	1.330E-01	6.106E-02	4.016E-02	2.123E-02	1.374E-02	9.74E-03	
914	4.987E-01	2.263E-01	9.794E-02	6.312E-02	3.252E-02	1.993E-02	1.412E-02	
1219	7.860E-01	3.253E-01	1.335E-01	8.455E-02	4.280E-02	2.528E-02	1.786E-02	
1524	1.222E 00	4.554E-01	1.767E-01	1.102E-01	5.515E-02	3.136E-02	2.196E-02	

FLIGHT NO. 97			FILTER NO. 2					
DIRECTIONAL PATH REFLECTANCE FROM GROUND TO ALTITUDE								
ALTITUDE	ZENITH ANGLE OF PATH OF SIGHT (DEGREES)							
METERS	93	95	100	105	120	150	180	
305	1.052E-01	5.534E-02	2.701E-02	1.809E-02	9.708E-03	6.296E-03	4.456E-03	
610	2.829E-01	1.407E-01	6.490E-02	4.273E-02	2.249E-02	1.431E-02	9.982E-03	
914	4.800E-01	2.230E-01	9.756E-02	6.333E-02	3.245E-02	1.970E-02	1.392E-02	
1219	7.710E-01	3.285E-01	1.370E-01	8.718E-02	4.408E-02	2.578E-02	1.810E-02	
1524	1.412E 00	5.307E-01	2.061E-01	1.285E-01	6.435E-02	3.586E-02	2.481E-02	

FLIGHT NO. 97			FILTER NO. 3				
DIRECTIONAL PATH REFLECTANCE			FROM GROUND TO ALTITUDE				
ALTITUDE	ZENITH ANGLE		OF PATH OF SIGHT (DEGREES)				
METERS	93	95	100	105	120	150	180
305	4.296E-02	2.322E-02	1.158E-02	7.896E-03	4.427E-03	3.151E-03	2.013E-03
610	8.838E-02	4.673E-02	2.267E-02	1.525E-02	8.335E-03	5.745E-03	3.741E-03
914	1.467E-01	7.517E-02	3.538E-02	2.347E-02	1.253E-02	8.160E-03	5.410E-03
1219	2.289E-01	1.121E-01	5.115E-02	3.357E-02	1.782E-02	1.083E-02	7.205E-03
1524	3.551E-01	1.646E-01	7.267E-02	4.735E-02	2.528E-02	1.454E-02	9.543E-03

FLIGHT NO. 97			FILTER NO. 5				
DIRECTIONAL PATH REFLECTANCE FROM GROUND TO ALTITUDE							
ALTITUDE	ZENITH ANGLE OF PATH OF SIGHT (DEGREES)						
METERS	93	95	100	105	120	150	180
305	1.248E-01	6.569E-02	3.181E-02	2.121E-02	1.125E-02	6.920E-03	4.871E-03
610	3.294E-01	1.642E-01	7.603E-02	5.002E-02	2.638E-02	1.595E-02	1.093E-02
914	5.478E-01	2.581E-01	1.147E-01	7.434E-02	3.847E-02	2.251E-02	1.552E-02
1219	8.250E-01	3.639E-01	1.553E-01	9.941E-02	5.080E-02	2.864E-02	1.983E-02
1524	1.250E 00	5.085E-01	2.076E-01	1.314E-01	6.648E-02	3.587E-02	2.475E-02

AZIMUTH OF PATH OF SIGHT = 270

FLIGHT NO. 97

FILTER NO. 1

DIRECTIONAL PATH REFLECTANCE FROM GROUND TO ALTITUDE								
ALTITUDE	ZENITH ANGLE OF PATH OF SIGHT (DEGREES)							
METERS	93	95	100	105	120	150	180	
305	1.048E-01	5.435E-02	2.549E-02	1.655E-02	8.203E-03	5.106E-03	4.758E-03	
610	2.666E-01	1.297E-01	5.752E-02	3.659E-02	1.763E-02	1.058E-02	9.748E-03	
914	4.910E-01	2.198E-01	9.193E-02	5.733E-02	2.690E-02	1.555E-02	1.412E-02	
1219	7.622E-01	3.120E-01	1.239E-01	7.604E-02	3.506E-02	1.987E-02	1.786E-02	
1524	1.157E 00	4.273E-01	1.609E-01	9.718E-02	4.415E-02	2.466E-02	2.196E-02	

FLIGHT NO. 97

FILTER NO. 2

DIRECTIONAL PATH REFLECTANCE FROM GROUND TO ALTITUDE								
ALTITUDE	ZENITH ANGLE OF PATH OF SIGHT (DEGREES)							
METERS	93	95	100	105	120	150	180	
305	1.038E-01	5.407E-02	2.536E-02	1.640E-02	8.010E-03	4.817E-03	4.456E-03	
610	2.789E-01	1.368E-01	6.086E-02	3.865E-02	1.846E-02	1.086E-02	9.982E-03	
914	4.769E-01	2.186E-01	9.272E-02	5.793E-02	2.703E-02	1.536E-02	1.392E-02	
1219	7.514E-01	3.165E-01	1.278E-01	7.862E-02	3.612E-02	2.017E-02	1.810E-02	
1524	1.317E 00	4.914E-01	1.852E-01	1.118E-01	5.068E-02	2.800E-02	2.481E-02	

FLIGHT NO. 97

FILTER NO. 3

DIRECTIONAL PATH REFLECTANCE FROM GROUND TO ALTITUDE								
ALTITUDE	ZENITH ANGLE OF PATH OF SIGHT (DEGREES)							
METERS	93	95	100	105	120	150	180	
305	4.282E-02	2.277E-02	1.084E-02	7.026E-03	3.440E-03	2.145E-03	2.013E-03	
610	8.871E-02	4.619E-02	2.144E-02	1.376E-02	6.601E-03	3.992E-03	3.741E-03	
914	1.468E-01	7.412E-02	3.348E-02	2.126E-02	1.001E-02	5.831E-03	5.410E-03	
1219	2.263E-01	1.094E-01	4.786E-02	3.007E-02	1.394E-02	7.881E-03	7.205E-03	
1524	3.397E-01	1.552E-01	6.571E-02	4.094E-02	1.886E-02	1.057E-02	9.543E-03	

FLIGHT NO. 97

FILTER NO. 5

DIRECTIONAL PATH REFLECTANCE FROM GROUND TO ALTITUDE								
ALTITUDE	ZENITH ANGLE OF PATH OF SIGHT (DEGREES)							
METERS	93	95	100	105	120	150	180	
305	1.294E-01	6.726E-02	3.149E-02	2.031E-02	9.804E-03	5.601E-03	4.871E-03	
610	3.304E-01	1.625E-01	7.250E-02	4.599E-02	2.179E-02	1.238E-02	1.093E-02	
914	5.440E-01	2.531E-01	1.085E-01	6.791E-02	3.162E-02	1.761E-02	1.552E-02	
1219	8.087E-01	3.525E-01	1.453E-01	8.985E-02	4.124E-02	2.261E-02	1.983E-02	
1524	1.169E 00	4.794E-01	1.895E-01	1.157E-01	5.249E-02	2.842E-02	2.475E-02	

#### FLIGHT 98

**Moonlight.** This flight was made in the Lop Buri area. Away from the city of Lop Buri the ground cover consisted of harvested-crop areas. There was considerable artificial ground lighting in the area. There were high thin cirrus clouds with haze near the ground. Data-taking started at 2112 local time and ended at 2325. The moon phase angle was  $37^\circ$ ; the moon zenith angle during sky radiance data-taking ranged from  $12^\circ$ , to  $1^\circ$  at transit, to  $12^\circ$ .

		FLIGHT NO. 97		FILTER NO. 1					
		IRRADIANCE (WATTS/SQ.M. MICRO M.)							
ALTITUDE	DOWN-	UP-	ALBEDO	SCALAR	SCALAR	SCALAR	SCALAR	SCALAR	SCALAR
(METERS)	WELLING	WELLING		DOWNWELLING	UPWELLING	TOTAL	ALBEDO		
147	8.218E-04	7.061E-05	.086	1.252E-03	1.692E-04	1.422E-03	.135		
439	1.083E-03	7.748E-05	.072	1.522E-03	1.836E-04	1.706E-03	.121		
749	1.173E-03	7.401E-05	.063	1.633E-03	1.955E-04	1.828E-03	.120		
1043	9.861E-04	9.441E-05	.096	1.425E-03	2.455E-04	1.671E-03	.172		
1374	9.437E-04	9.590E-05	.102	1.413E-03	2.544E-04	1.668E-03	.180		
1663	7.603E-04	1.218E-04	.160	1.192E-03	3.077E-04	1.499E-03	.258		

		FLIGHT NO. 98		FILTER NO. 2					
		IRRADIANCE (WATTS/SQ.M. MICRO M.)							
ALTITUDE	DOWN-	UP-	ALBEDO	SCALAR	SCALAR	SCALAR	SCALAR	SCALAR	SCALAR
(METERS)	WELLING	WELLING		DOWNWELLING	UPWELLING	TOTAL	ALBEDO		
146	9.570E-04	7.483E-05	.078	1.405E-03	1.763E-04	1.582E-03	.125		
437	1.090E-03	9.279E-05	.085	1.519E-03	2.135E-04	1.733E-03	.141		
749	1.012E-03	9.510E-05	.094	1.479E-03	2.258E-04	1.705E-03	.153		
1043	1.017E-03	1.084E-04	.107	1.470E-03	2.629E-04	1.733E-03	.179		
1664	1.130E-03	1.198E-04	.106	1.549E-03	2.952E-04	1.844E-03	.191		

		FLIGHT NO. 98		FILTER NO. 3					
		IRRADIANCE (WATTS/SQ.M. MICRO M.)							
ALTITUDE	DOWN-	UP-	ALBEDO	SCALAR	SCALAR	SCALAR	SCALAR	SCALAR	SCALAR
(METERS)	WELLING	WELLING		DOWNWELLING	UPWELLING	TOTAL	ALBEDO		
137	8.274E-04	1.288E-04	.156	1.758E-03	2.808E-04	1.539E-03	.223		
440	1.423E-03	2.748E-04	.193	1.863E-03	6.849E-04	2.548E-03	.368		
749	8.659E-04	1.320E-04	.152	1.303E-03	2.898E-04	1.593E-03	.227		
1043	7.392E-04	1.274E-04	.172	1.163E-03	2.950E-04	1.458E-03	.254		
1375	9.085E-04	1.125E-04	.124	1.321E-03	2.809E-04	1.602E-03	.213		
1664	1.433E-03	1.834E-04	.124	1.869E-03	4.049E-04	2.274E-03	.217		

		FLIGHT NO. 98		FILTER NO. 4					
		IRRADIANCE (WATTS/SQ.M. MICRO M.)							
ALTITUDE	DOWN-	UP-	ALBEDO	SCALAR	SCALAR	SCALAR	SCALAR	SCALAR	SCALAR
(METERS)	WELLING	WELLING		DOWNWELLING	UPWELLING	TOTAL	ALBEDO		
135	6.272E-04	1.843E-04	.294	9.498E-04	1.662E-04	1.316E-03	.386		
439	1.359E-03	2.178E-04	.160	1.696E-03	4.517E-04	2.148E-03	.266		
749	7.802E-04	2.172E-04	.278	1.108E-03	4.484E-04	1.557E-03	.405		
1043	6.433E-04	2.000E-04	.311	9.858E-04	4.049E-04	1.391E-03	.411		
1375	1.134E-03	2.240E-04	.197	1.473E-03	4.553E-04	1.929E-03	.309		
1665	1.087E-03	2.173E-04	.200	1.415E-03	4.464E-04	1.861E-03	.316		

		FLIGHT NO. 98		FILTER NO. 5					
		IRRADIANCE (WATTS/SQ.M. MICRO M.)							
ALTITUDE	DOWN-	UP-	ALBEDO	SCALAR	SCALAR	SCALAR	SCALAR	SCALAR	SCALAR
(METERS)	WELLING	WELLING		DOWNWELLING	UPWELLING	TOTAL	ALBEDO		
133	9.365E-04	7.987E-05	.085	1.387E-03	1.775E-04	1.564E-03	.128		
438	1.149E-03	9.496E-05	.083	1.622E-03	2.262E-04	1.848E-03	.139		
748	8.745E-04	1.036E-04	.118	1.348E-03	2.458E-04	1.594E-03	.182		
1042	8.007E-04	1.138E-04	.142	1.282E-03	2.772E-04	1.555E-03	.216		
1371	1.199E-03	1.279E-04	.107	1.698E-03	3.092E-04	2.007E-03	.182		
1664	9.530E-04	1.629E-04	.171	1.426E-03	3.850E-04	1.811E-03	.270		

FLIGHT NO. 98					
AZIMUTH OF PATH OF SIGHT = 0					
DIRECTIONAL REFLECTANCE OF BACKGROUND					
ZENITH	FILTERS				
ANGLE	1	2	5	3	4
93	.19100	.16999	.19327	.21106	
95	.15213	.13310	.12491	.16919	
100	.09599	.16834	.10337	.34121	
105	.06222	.09804	.08278	.14481	
120	.06729	.07601	.09896	.14434	
150	.07920	.05294	.10787	.14763	
180	.07864	.07640	.08164	.13915	

FLIGHT NO. 98					
AZIMUTH OF PATH OF SIGHT = 90					
DIRECTIONAL REFLECTANCE OF BACKGROUND					
ZENITH	FILTERS				
ANGLE	1	2	5	3	4
93	.17717	.16139	.18491	.38737	
95	.12679	.12693	.11979	.16839	
100	.08938	.10424	.08530	.13791	
105	.08538	.08564	.08566	.14156	
120	.08442	.07925	.07560	.14702	
150	.08633	.06603	.09715	.14883	
180	.07864	.07640	.08164	.13915	

FLIGHT NO. 98					
AZIMUTH OF PATH OF SIGHT = 180					
DIRECTIONAL REFLECTANCE OF BACKGROUND					
ZENITH	FILTERS				
ANGLE	1	2	5	3	4
93	.14375	.16110	.13669	.21305	
95	.12809	.12704	.10667	.18227	
100	.10472	.13167	.09591	.15556	
105	.09627	.09634	.09381	.16717	
120	.08860	.08215	.08074	.19517	
150	.09310	.07876	.09443	.15257	
180	.07864	.07640	.08164	.13915	

FLIGHT NO. 98					
AZIMUTH OF PATH OF SIGHT = 270					
DIRECTIONAL REFLECTANCE OF BACKGROUND					
ZENITH	FILTERS				
ANGLE	1	2	5	3	4
93	.17195	.19871	.14813	.21773	
95	.12445	.12759	.11489	.16871	
100	.11483	.10393	.09812	.14396	
105	.09818	.09711	.09096	.15010	
120	.08740	.05941	.11272	.14595	
150	.10524	.07350	.07962	.18356	
180	.07864	.07640	.08164	.13915	

DATE 33069 FLIGHT NO. 93 GROUND LEVEL ALTITUDE (M.)= 81 IUP=1

ALTITUDE (METERS)	FILTERS	TOTAL SCATTERING COEFFICIENT (PER METER)			
		1	2	3	4
0	6.229E-05	5.201E-05	3.278E-05	5.056E-05	
30	6.208E-05	5.184E-05	3.267E-05	5.040E-05	
41	6.188E-05	5.167E-05	3.256E-05	5.023E-05	
91	6.167E-05	5.150E-05	3.245E-05	5.006E-05	
122	6.147E-05	5.132E-05	3.234E-05	4.989E-05	
152	6.126E-05	5.115E-05	3.224E-05	4.973E-05	
183	5.942E-05	4.915E-05	3.237E-05	4.840E-05	
213	5.822E-05	4.549E-05	3.137E-05	4.824E-05	
244	5.706E-05	4.060E-05	3.093E-05	4.682E-05	
274	5.496E-05	4.051E-05	2.984E-05	4.418E-05	
305	5.176E-05	3.982E-05	2.883E-05	4.255E-05	
335	4.844E-05	4.119E-05	2.654E-05	4.174E-05	
366	4.814E-05	4.248E-05	2.568E-05	4.245E-05	
396	4.878E-05	4.308E-05	2.553E-05	4.246E-05	
427	4.994E-05	4.339E-05	2.651E-05	4.534E-05	
457	5.208E-05	4.398E-05	2.756E-05	4.608E-05	
488	5.218E-05	4.372E-05	2.681E-05	4.316E-05	
518	5.141E-05	4.143E-05	2.591E-05	4.357E-05	
549	5.098E-05	4.002E-05	2.536E-05	4.324E-05	
579	4.964E-05	4.007E-05	2.512E-05	4.242E-05	
610	4.737E-05	4.042E-05	2.489E-05	4.068E-05	
640	4.746E-05	3.906E-05	2.461E-05	3.906E-05	
671	4.707E-05	3.809E-05	2.440E-05	3.989E-05	
701	4.545E-05	3.877E-05	2.519E-05	4.174E-05	
732	4.522E-05	4.042E-05	2.653E-05	4.385E-05	
762	4.644E-05	4.133E-05	2.872E-05	4.607E-05	
792	4.805E-05	4.558E-05	3.027E-05	4.734E-05	
823	5.096E-05	4.882E-05	3.126E-05	4.839E-05	
853	5.745E-05	5.074E-05	3.181E-05	4.902E-05	
884	5.999E-05	5.198E-05	3.259E-05	5.087E-05	
914	6.161E-05	5.396E-05	3.284E-05	5.250E-05	
945	6.222E-05	5.477E-05	3.318E-05	5.361E-05	
975	6.399E-05	5.515E-05	3.366E-05	5.475E-05	
1006	6.583E-05	5.617E-05	3.460E-05	5.459E-05	
1036	6.727E-05	5.765E-05	3.494E-05	5.481E-05	
1067	6.694E-05	5.809E-05	3.487E-05	5.562E-05	
1097	6.828E-05	5.939E-05	3.499E-05	5.568E-05	
1128	6.876E-05	6.029E-05	3.537E-05	5.645E-05	
1158	6.718E-05	6.153E-05	3.558E-05	5.721E-05	
1189	6.860E-05	6.202E-05	3.617E-05	5.775E-05	
1219	7.004E-05	6.162E-05	3.597E-05	5.788E-05	
1250	7.015E-05	6.177E-05	3.616E-05	5.842E-05	
1280	7.015E-05	6.231E-05	3.666E-05	5.819E-05	
1311	7.036E-05	6.206E-05	3.704E-05	5.821E-05	
1341	7.050E-05	6.078E-05	3.713E-05	5.714E-05	
1372	7.054E-05	6.180E-05	3.708E-05	5.678E-05	
1402	7.030E-05	6.078E-05	3.731E-05	5.660E-05	
1433	7.222E-05	5.996E-05	3.726E-05	5.864E-05	
1463	7.296E-05	6.151E-05	3.803E-05	6.008E-05	
1494	7.197E-05	6.171E-05	3.851E-05	6.039E-05	
1524	7.067E-05	6.240E-05	3.794E-05	6.209E-05	
1554	6.940E-05	6.356E-05	3.827E-05	6.295E-05	
1585	6.846E-05	6.452E-05	3.814E-05	6.287E-05	
1615	6.740E-05	6.560E-05	3.813E-05	6.125E-05	
1646	6.911E-05	6.567E-05	3.796E-05	6.334E-05	
1676	6.862E-05	6.545E-05	3.784E-05	6.313E-05	
1707	6.840E-05	6.523E-05	3.771E-05	6.292E-05	
1737	6.817E-05	6.501E-05	3.758E-05	6.271E-05	
1768	6.794E-05	6.480E-05	3.746E-05	6.250E-05	
1798	6.772E-05	6.458E-05	3.733E-05	6.230E-05	
1829	6.749E-05	6.437E-05	3.721E-05	6.209E-05	

FIRST DATA ALT. 6 6 6 5 6  
 LAST DATA ALT. 56 55 55 55 55

FLIGHT NO. 98		FILTER NO. 1						
BEAM TRANSMITTANCE FROM GROUND TO ALTITUDE		ZENITH ANGLE OF PATH OF SIGHT (DEGREES)						
ALTITUDE		93	95	100	105	120	150	180
METERS								
305		.7048935	.8121275	.9008231	.9323232	.9643762	.9792751	.9820266
610		.5217718	.6815665	.8249661	.8788908	.9353595	.9621537	.9671399
914		.5837432	.5717097	.7553079	.8283814	.9071371	.9452849	.9524374
1219		.2549854	.4590967	.6721076	.7659922	.8711042	.9234204	.9333296
1524		.1636947	.3535332	.5934070	.7045902	.8342308	.9006469	.9133623

FLIGHT NO. 98		FILTER NO. 2						
BEAM TRANSMITTANCE FROM GROUND TO ALTITUDE		ZENITH ANGLE OF PATH OF SIGHT (DEGREES)						
ALTITUDE		93	95	100	105	120	150	180
METERS								
305		.7545338	.8457216	.9193270	.9451360	.9712135	.9832779	.9855019
610		.5806800	.7303229	.8540765	.8995793	.9466928	.9688673	.9729814
914		.4481038	.6257278	.7903216	.8539531	.9215261	.9539124	.9599615
1219		.3132793	.5102396	.7133231	.7972503	.8693274	.9345246	.9430416
1524		.2134862	.4115406	.6404274	.7415762	.8566190	.9145237	.9255371

FLIGHT NO. 98		FILTER NO. 3						
BEAM TRANSMITTANCE FROM GROUND TO ALTITUDE		ZENITH ANGLE OF PATH OF SIGHT (DEGREES)						
ALTITUDE		93	95	100	105	120	150	180
METERS								
305		.8297541	.8948832	.9457820	.9632912	.9808268	.9888851	.9903670
610		.7089977	.8165701	.9032930	.9340376	.9652937	.9798129	.9824936
914		.5961765	.7393013	.8593304	.9032884	.9487113	.9700594	.9740181
1219		.4812656	.6546363	.8084415	.8670400	.9288096	.9582580	.9637477
1524		.3813369	.5747496	.7573209	.8298620	.9079760	.9457889	.9528777

FLIGHT NO. 98		FILTER NO. 4						
BEAM TRANSMITTANCE FROM GROUND TO ALTITUDE		ZENITH ANGLE OF PATH OF SIGHT (DEGREES)						
ALTITUDE		93	95	100	105	120	150	180
METERS								
305								
610								
914								
1219								
1524								

FLIGHT NO. 98		FILTER NO. 5						
BEAM TRANSMITTANCE FROM GROUND TO ALTITUDE		ZENITH ANGLE OF PATH OF SIGHT (DEGREES)						
ALTITUDE		93	95	100	105	120	150	180
METERS								
305		.7522101	.8441377	.9184724	.9445395	.9702966	.9830924	.9853409
610		.5805376	.7257508	.8513887	.8976790	.9456571	.9682552	.9724490
914		.4405130	.6194687	.7863435	.8510668	.9199125	.9529477	.9591207
1219		.3128785	.5100172	.7132371	.7971333	.8892596	.9344836	.9430057
1524		.2170372	.4157407	.6436996	.7611113	.8561365	.9154587	.9263566



AZIMUTH OF PATH OF SIGHT = 0								
FLIGHT NO. 98			FILTER NO. 1					
PATH RADIANCE FROM GROUND TO ALTITUDE (WATTS/STER.SQ.M MICRO M.)								
ALTITUDE	ZENITH ANGLE OF PATH OF SIGHT (DEGREES)							
METERS	93	95	100	105	120	150	180	
305	3.226E-05	1.890E-05	9.529E-06	6.245E-06	3.023E-06	1.751E-06	1.691E-06	
610	5.380E-05	3.365E-05	1.768E-05	1.178E-05	5.841E-06	3.490E-06	3.432E-06	
914	7.063E-05	4.687E-05	2.558E-05	1.728E-05	8.712E-06	5.277E-06	5.226E-06	
1219	8.426E-05	6.005E-05	3.447E-05	2.372E-05	1.217E-05	7.391E-06	7.266E-06	
1524	9.423E-05	7.132E-05	4.288E-05	2.998E-05	1.555E-05	9.369E-06	9.098E-06	

FLIGHT NO. 98			FILTER NO. 2					
PATH RADIANCE FROM GROUND TO ALTITUDE (WATTS/STER.SQ.M MICRO M.)								
ALTITUDE	ZENITH ANGLE OF PATH OF SIGHT (DEGREES)							
METERS	93	95	100	105	120	150	180	
305	2.886E-05	1.664E-05	8.294E-06	5.409E-06	2.609E-06	1.530E-06	1.517E-06	
610	4.825E-05	2.957E-05	1.530E-05	1.014E-05	5.000E-06	3.001E-06	2.991E-06	
914	6.363E-05	4.132E-05	2.219E-05	1.490E-05	7.468E-06	4.523E-06	4.467E-06	
1219	7.863E-05	5.451E-05	3.060E-05	2.089E-05	1.064E-05	6.486E-06	6.384E-06	
1524	9.062E-05	6.639E-05	3.880E-05	2.685E-05	1.383E-05	8.423E-06	8.277E-06	

FLIGHT NO. 98			FILTER NO. 3					
PATH RADIANCE FROM GROUND TO ALTITUDE(WATTS/STER.SQ.M MICRO M.)								
ALTITUDE	ZENITH ANGLE OF PATH OF SIGHT (DEGREES)							
METERS	93	95	100	105	120	150	180	
305	2.103E-05	1.186E-05	5.830E-06	3.785E-06	1.810E-06	1.054E-06	1.062E-06	
610	3.858E-05	2.268E-05	1.142E-05	7.492E-06	3.652E-06	2.187E-06	2.287E-06	
914	5.026E-05	3.096E-05	1.602E-05	1.061E-05	5.221E-06	3.125E-06	3.194E-06	
1219	6.015E-05	3.900E-05	2.082E-05	1.394E-05	6.911E-06	4.113E-06	4.120E-06	
1524	7.040E-05	4.767E-05	2.611E-05	1.762E-05	8.762E-06	5.167E-06	5.124E-06	

FLIGHT NO. 98		FILTER NO. 4						
PATH RADIANCE FROM GROUND TO ALTITUDE(WATTS/STER.SQ.M MICRO M.)								
ALTITUDE	ZENITH ANGLE OF PATH OF SIGHT (DEGREES)							
METERS	93	95	100	105	120	150	180	
305								
610								
914								
1219								
1524								

FLIGHT NO. 98			FILTER NO. 5					
PATH RADIANCE FROM GROUND TO ALTITUDE(WATTS/STER.SQ.M MICRO M.)								
ALTITUDE	ZENITH ANGLE OF PATH OF SIGHT (DEGREES)							
METERS	93	95	100	105	120	150	180	
305	2.898E-05	1.672E-05	8.352E-06	5.461E-06	2.651E-06	1.570E-06	1.541E-06	
610	5.024E-05	3.081E-05	1.597E-05	1.060E-05	5.240E-06	3.147E-06	3.103E-06	
914	6.486E-05	4.228E-05	2.278E-05	1.531E-05	7.665E-06	4.595E-06	4.464E-06	
1219	7.912E-05	5.480E-05	3.074E-05	2.096E-05	1.061E-05	6.327E-06	6.047E-06	
1524	9.437E-05	6.847E-05	3.964E-05	2.729E-05	1.388E-05	8.241E-06	7.894E-06	

AZIMUTH OF PATH OF SIGHT = 90		FLIGHT NO. 98		FILTER NO. 1			
PATH RADIANCE FROM GROUND TO ALTITUDE (WATTS/STER.SQ.M MICRO M.)		ZENITH ANGLE OF PATH OF SIGHT (DEGREES)					
ALTITUDE METERS	93	95	100	105	120	150	180
305	5.062E-05	1.901E-05	9.125E-06	6.090E-06	3.052E-06	1.358E-06	1.691E-06
610	5.161E-05	3.240E-05	1.718E-05	1.156E-05	5.892E-06	3.657E-06	3.432E-06
914	6.317E-05	4.537E-05	2.494E-05	1.700E-05	8.775E-06	5.489E-06	5.226E-06
1219	8.174E-05	5.835E-05	3.369E-05	2.335E-05	1.221E-05	7.625E-06	7.266E-06
1524	9.101E-05	6.909E-05	4.182E-05	2.945E-05	1.558E-05	9.638E-06	9.098E-06

FLIGHT NO. 98		FILTER NO. 2					
PATH RADIANCE FROM GROUND TO ALTITUDE (WATTS/STER.SQ.M MICRO M.)		ZENITH ANGLE OF PATH OF SIGHT (DEGREES)					
ALTITUDE METERS	93	95	100	105	120	150	180
305	2.732E-05	1.585E-05	8.020E-06	5.312E-06	2.784E-06	1.659E-06	1.517E-06
610	4.630E-05	2.849E-05	1.490E-05	9.987E-06	5.155E-06	3.180E-06	2.991E-06
914	6.174E-05	4.018E-05	2.173E-05	1.472E-05	7.589E-06	4.712E-06	4.467E-06
1219	7.641E-05	5.308E-05	3.000E-05	2.063E-05	1.070E-05	6.704E-06	6.364E-06
1524	8.691E-05	6.400E-05	3.778E-05	2.639E-05	1.387E-05	8.728E-06	8.277E-06

FLIGHT NO. 98		FILTER NO. 3					
PATH RADIANCE FROM GROUND TO ALTITUDE (WATTS/STER.SQ.M MICRO M.)		ZENITH ANGLE OF PATH OF SIGHT (DEGREES)					
ALTITUDE METERS	93	95	100	105	120	150	180
305	1.998E-05	1.132E-05	5.622E-06	3.689E-06	1.815E-06	1.103E-06	1.062E-06
610	3.746E-05	2.209E-05	1.119E-05	7.395E-06	3.664E-06	2.265E-06	2.287E-06
914	4.895E-05	3.024E-05	1.574E-05	1.050E-05	5.240E-06	3.211E-06	3.194E-06
1219	5.844E-05	3.803E-05	2.044E-05	1.379E-05	6.950E-06	4.221E-06	4.120E-06
1524	6.698E-05	4.563E-05	2.526E-05	1.721E-05	8.742E-06	5.306E-06	5.124E-06

FLIGHT NO. 98		FILTER NO. 4					
PATH RADIANCE FROM GROUND TO ALTITUDE (WATTS/STER.SQ.M MICRO M.)		ZENITH ANGLE OF PATH OF SIGHT (DEGREES)					
ALTITUDE METERS	93	95	100	105	120	150	180
305							
610							
914							
1219							
1524							

FLIGHT NO. 98		FILTER NO. 5					
PATH RADIANCE FROM GROUND TO ALTITUDE (WATTS/STER.SQ.M MICRO M.)		ZENITH ANGLE OF PATH OF SIGHT (DEGREES)					
ALTITUDE METERS	93	95	100	105	120	150	180
305	2.794E-05	1.618E-05	8.145E-06	5.370E-06	2.659E-06	1.615E-06	1.541E-06
610	4.878E-05	3.001E-05	1.566E-05	1.047E-05	5.271E-06	3.236E-06	3.103E-06
914	6.340E-05	4.141E-05	2.241E-05	1.516E-05	7.695E-06	4.690E-06	4.464E-06
1219	7.697E-05	5.346E-05	3.016E-05	2.068E-05	1.061E-05	6.427E-06	6.047E-06
1524	9.028E-05	6.593E-05	3.858E-05	2.681E-05	1.394E-05	8.483E-06	7.894E-06

AZIMUTH OF PATH OF SIGHT = 180		FLIGHT NO. 98 FILTER NO. 1						
PATH RADIANCE FROM GROUND TO ALTITUDE (WATTS/STER.SQ.M MICRO M.)		ZENITH ANGLE OF PATH OF SIGHT (DEGREES)						
ALTITUDE METERS	93	95	100	105	120	150	180	
305	2.964E-05	1.750E-05	8.999E-06	6.018E-06	3.071E-06	1.869E-06	1.691E-06	
610	5.028E-05	3.164E-05	1.688E-05	1.144E-05	5.926E-06	3.687E-06	3.432E-06	
914	6.671E-05	4.447E-05	2.458E-05	1.686E-05	8.821E-06	5.534E-06	5.226E-06	
1219	8.061E-05	5.756E-05	3.335E-05	2.321E-05	1.227E-05	7.675E-06	7.266E-06	
1524	9.003E-05	6.835E-05	4.148E-05	2.932E-05	1.564E-05	9.701E-06	9.098E-06	

FLIGHT NO. 98 FILTER NO. 2		PATH RADIANCE FROM GROUND TO ALTITUDE (WATTS/STER.SQ.M MICRO M.)						
ZENITH ANGLE OF PATH OF SIGHT (DEGREES)								
ALTITUDE METERS	93	95	100	105	120	150	180	
305	2.652E-05	1.543E-05	7.869E-06	5.252E-06	2.677E-06	1.645E-06	1.517E-06	
610	4.508E-05	2.781E-05	1.464E-05	9.879E-06	5.093E-06	3.179E-06	2.991E-06	
914	6.055E-05	3.946E-05	2.145E-05	1.460E-05	7.571E-06	4.721E-06	4.467E-06	
1219	7.568E-05	5.255E-05	2.976E-05	2.053E-05	1.074E-05	6.706E-06	6.384E-06	
1524	8.600E-05	6.333E-05	3.744E-05	2.621E-05	1.369E-05	8.685E-06	8.277E-06	

FLIGHT NO. 98 FILTER NO. 3		PATH RADIANCE FROM GROUND TO ALTITUDE (WATTS/STER.SQ.M MICRO M.)						
ZENITH ANGLE OF PATH OF SIGHT (DEGREES)								
ALTITUDE METERS	93	95	100	105	120	150	180	
305	2.039E-05	1.164E-05	5.891E-06	3.929E-06	1.985E-06	1.169E-06	1.062E-06	
610	3.396E-05	2.317E-05	1.202E-05	8.118E-06	4.182E-06	2.490E-06	2.287E-06	
914	4.979E-05	3.101E-05	1.647E-05	1.119E-05	5.782E-06	3.461E-06	3.194E-06	
1219	5.954E-05	3.895E-05	2.124E-05	1.451E-05	7.506E-06	4.477E-06	4.120E-06	
1524	6.858E-05	4.687E-05	2.621E-05	1.703E-05	9.342E-06	5.571E-06	5.124E-06	

FLIGHT NO. 98 FILTER NO. 4		PATH RADIANCE FROM GROUND TO ALTITUDE (WATTS/STER.SQ.M MICRO M.)						
ZENITH ANGLE OF PATH OF SIGHT (DEGREES)								
ALTITUDE METERS	93	95	100	105	120	150	180	
305								
610								
914								
1219								
1524								

FLIGHT NO. 98 FILTER NO. 5		PATH RADIANCE FROM GROUND TO ALTITUDE (WATTS/STER.SQ.M MICRO M.)						
ZENITH ANGLE OF PATH OF SIGHT (DEGREES)								
ALTITUDE METERS	93	95	100	105	120	150	180	
305	2.700E-05	1.569E-05	7.960E-06	5.290E-06	2.670E-06	1.638E-06	1.541E-06	
610	4.738E-05	2.922E-05	1.535E-05	1.033E-05	5.292E-06	3.279E-06	3.103E-06	
914	6.212E-05	4.062E-05	2.209E-05	1.502E-05	7.727E-06	4.745E-06	4.464E-06	
1219	7.607E-05	5.283E-05	2.908E-05	2.056E-05	1.065E-05	6.483E-06	6.047E-06	
1524	8.894E-05	6.500E-05	3.514E-05	2.650E-05	1.395E-05	8.494E-06	7.894E-06	

AZIMUTH OF PATH OF SIGHT = 270

FLIGHT NO. 98

FILTER NO. 1

PATH RADIANCE FROM GROUND TO ALTITUDE (WATTS/STER.SQ.M MICRO M.)

ALTITUDE METERS	ZENITH ANGLE OF PATH OF SIGHT (DEGREES)						
	93	95	100	105	120	150	180
305	3.142E-05	1.852E-05	9.480E-06	6.294E-06	3.126E-06	1.831E-06	1.691E-06
610	5.211E-05	3.280E-05	1.747E-05	1.178E-05	6.015E-06	3.686E-06	3.432E-06
914	6.835E-05	4.561E-05	2.521E-05	1.723E-05	8.935E-06	5.577E-06	5.226E-06
1219	8.257E-05	5.898E-05	3.413E-05	2.367E-05	1.240E-05	7.710E-06	7.266E-06
1524	9.231E-05	7.009E-05	4.243E-05	2.988E-05	1.580E-05	9.737E-06	9.098E-06

FLIGHT NO. 98

FILTER NO. 2

PATH RADIANCE FROM GROUND TO ALTITUDE (WATTS/STER.SQ.M MICRO M.)

ALTITUDE METERS	ZENITH ANGLE OF PATH OF SIGHT (DEGREES)						
	93	95	100	105	120	150	180
305	2.717E-05	1.574E-05	7.958E-06	5.261E-06	2.626E-06	1.589E-06	1.517E-06
610	4.587E-05	2.824E-05	1.480E-05	9.925E-06	5.058E-06	3.144E-06	2.991E-06
914	6.158E-05	4.006E-05	2.169E-05	1.469E-05	7.540E-06	4.682E-06	4.467E-06
1219	7.727E-05	5.352E-05	3.017E-05	2.070E-05	1.071E-05	6.644E-06	6.384E-06
1524	8.865E-05	6.499E-05	3.816E-05	2.654E-05	1.387E-05	8.592E-06	8.277E-06

FLIGHT NO. 98

FILTER NO. 3

PATH RADIANCE FROM GROUND TO ALTITUDE (WATTS/STER.SQ.M MICRO M.)

ALTITUDE METERS	ZENITH ANGLE OF PATH OF SIGHT (DEGREES)						
	93	95	100	105	120	150	180
305	2.112E-05	1.206E-05	6.112E-06	4.081E-06	2.068E-06	1.189E-06	1.062E-06
610	4.357E-05	2.604E-05	1.309E-05	9.336E-06	4.855E-06	2.674E-06	2.287E-06
914	5.453E-05	3.413E-05	1.833E-05	1.255E-05	6.527E-06	3.661E-06	3.194E-06
1219	6.392E-05	4.198E-05	2.308E-05	1.584E-05	8.213E-06	4.656E-06	4.120E-06
1524	7.315E-05	5.014E-05	2.820E-05	1.945E-05	1.007E-05	5.748E-06	5.124E-06

FLIGHT NO. 98

FILTER NO. 4

PATH RADIANCE FROM GROUND TO ALTITUDE (WATTS/STER.SQ.M MICRO M.)

ALTITUDE METERS	ZENITH ANGLE OF PATH OF SIGHT (DEGREES)						
	93	95	100	105	120	150	180
305							
610							
914							
1219							
1524							

FLIGHT NO. 98

FILTER NO. 5

PATH RADIANCE FROM GROUND TO ALTITUDE (WATTS/STER.SQ.M MICRO M.)

ALTITUDE METERS	ZENITH ANGLE OF PATH OF SIGHT (DEGREES)						
	93	95	100	105	120	150	180
305	2.738E-05	1.590E-05	8.052E-06	5.334E-06	2.682E-06	1.658E-06	1.541E-06
610	4.802E-05	2.961E-05	1.554E-05	1.043E-05	5.335E-06	3.333E-06	3.103E-06
914	6.321E-05	4.130E-05	2.244E-05	1.522E-05	7.805E-06	4.808E-06	4.464E-06
1219	7.769E-05	5.390E-05	3.044E-05	2.091E-05	1.079E-05	6.552E-06	6.047E-06
1524	9.188E-05	6.688E-05	3.906E-05	2.712E-05	1.409E-05	8.510E-06	7.894E-06

AZIMUTH OF PATH OF SIGHT = 0		FLIGHT NO. 98		FILTER NO. 1				
		DIRECTIONAL PATH REFLECTANCE FROM GROUND TO ALTITUDE						
		ZENITH ANGLE OF PATH OF SIGHT (DEGREES)						
ALTITUDE		93	95	100	105	120	150	180
METERS								
305		1.750E-01	8.895E-02	4.044E-02	2.561E-02	1.198E-02	6.835E-03	6.503E-03
610		3.942E-01	1.888E-01	8.192E-02	5.123E-02	2.387E-02	1.387E-02	1.356E-02
914		7.036E-01	3.134E-01	1.295E-01	7.976E-02	3.672E-02	2.134E-02	2.097E-02
1219		1.263E 00	5.066E-01	1.961E-01	1.184E-01	5.339E-02	3.060E-02	2.976E-02
1524		2.201E 00	7.712E-01	2.762E-01	1.626E-01	7.124E-02	3.977E-02	3.808E-02

		FLIGHT NO. 98		FILTER NO. 2				
		DIRECTIONAL PATH REFLECTANCE FROM GROUND TO ALTITUDE		ZENITH ANGLE OF PATH OF SIGHT (DEGREES)				
ALTITUDE		93	95	100	105	120	150	180
METERS								
305		1.256E-01	6.461E-02	2.962E-02	1.879E-02	8.817E-03	5.109E-03	5.055E-03
610		2.700E-01	1.329E-01	5.882E-02	3.699E-02	1.734E-02	1.017E-02	1.009E-02
914		4.661E-01	2.168E-01	9.215E-02	5.728E-02	2.660E-02	1.557E-02	1.528E-02
1219		8.240E-01	3.507E-01	1.408E-01	8.600E-02	3.928E-02	2.279E-02	2.222E-02
1524		1.394E 00	5.296E-01	1.989E-01	1.189E-01	5.299E-02	3.024E-02	2.936E-02

FLIGHT NO. 98				FILTER NO. 3				
DIRECTIONAL PATH REFLECTANCE FROM GROUND TO ALTITUDE								
ALTITUDE	ZENITH ANGLE OF PATH OF SIGHT (DEGREES)							
METERS	93	95	100	105	120	150	180	
305	9.625E-02	5.033E-02	2.341E-02	1.492E-02	7.008E-03	4.046E-03	4.072E-03	
610	2.066E-01	1.055E-01	4.799E-02	3.046E-02	1.437E-02	8.475E-03	8.840E-03	
914	3.201E-01	1.590E-01	7.078E-02	4.461E-02	2.090E-02	1.223E-02	1.245E-02	
1219	4.746E-01	2.262E-01	9.779E-02	6.105E-02	2.825E-02	1.630E-02	1.623E-02	
1524	7.011E-01	3.149E-01	1.309E-01	8.062E-02	3.664E-02	2.075E-02	2.042E-02	

		FLIGHT NO. 98		FILTER NO. 4				
		DIRECTIONAL PATH REFLECTANCE FROM GROUND TO ALTITUDE						
ALTITUDE		ZENITH ANGLE OF PATH OF SIGHT (DEGREES)						
METERS		93	95	100	105	120	150	180
305								
610								
914								
1219								
1524								

FLIGHT NO. 98				FILTER NO. 5				
DIRECTIONAL PATH REFLECTANCE FROM GROUND TO ALTITUDE								
ALTITUDE	ZENITH ANGLE OF PATH OF SIGHT (DEGREES)							
METERS	93	95	100	105	120	150	180	
305	1.292E-01	6.645E-02	3.051E-02	1.940E-02	9.161E-03	5.357E-03	5.246E-03	
610	2.903E-01	1.424E-01	6.294E-02	3.960E-02	1.859E-02	1.090E-02	1.070E-02	
914	4.939E-01	2.290E-01	9.717E-02	6.036E-02	2.795E-02	1.618E-02	1.561E-02	
1219	8.482E-01	3.605E-01	1.446E-01	8.819E-02	4.001E-02	2.271E-02	2.151E-02	
1524	1.459E 00	5.525E-01	2.066E-01	1.230E-01	5.427E-02	3.020E-02	2.858E-02	

AZIMUTH OF PATH OF SIGHT = 90		FLIGHT NO. 98 FILTER NO. 1						
DIRECTIONAL PATH REFLECTANCE FROM GROUND TO ALTITUDE		ZENITH ANGLE OF PATH OF SIGHT (DEGREES)						
ALTITUDE	METERS	93	95	100	105	120	150	180
305		1.660E-01	8.479E-02	3.898E-02	2.497E-02	1.210E-02	7.255E-03	6.503E-03
610		3.782E-01	1.817E-01	7.959E-02	5.027E-02	2.408E-02	1.453E-02	1.386E-02
914		6.791E-01	3.034E-01	1.263E-01	7.847E-02	3.698E-02	2.220E-02	2.097E-02
1219		1.225E 00	4.923E-01	1.916E-01	1.165E-01	5.359E-02	3.157E-02	2.976E-02
1524		2.125E 00	7.471E-01	2.694E-01	1.598E-01	7.139E-02	4.091E-02	3.808E-02

FLIGHT NO. 98 FILTER NO. 2		DIRECTIONAL PATH REFLECTANCE FROM GROUND TO ALTITUDE						
		ZENITH ANGLE OF PATH OF SIGHT (DEGREES)						
ALTITUDE	METERS	93	95	100	105	120	150	180
305		1.189E-01	6.152E-02	2.874E-02	1.845E-02	9.410E-03	5.539E-03	5.055E-03
610		2.591E-01	1.281E-01	5.729E-02	3.645E-02	1.788E-02	1.077E-02	1.009E-02
914		4.523E-01	2.108E-01	9.028E-02	5.659E-02	2.703E-02	1.622E-02	1.528E-02
1219		8.007E-01	3.415E-01	1.380E-01	8.495E-02	3.951E-02	2.355E-02	2.222E-02
1524		1.337E 00	5.105E-01	1.937E-01	1.168E-01	5.314E-02	3.133E-02	2.936E-02

FLIGHT NO. 98 FILTER NO. 3		DIRECTIONAL PATH REFLECTANCE FROM GROUND TO ALTITUDE						
		ZENITH ANGLE OF PATH OF SIGHT (DEGREES)						
ALTITUDE	METERS	93	95	100	105	120	150	180
305		9.144E-02	4.804E-02	2.257E-02	1.454E-02	7.025E-03	4.235E-03	4.072E-03
610		2.006E-01	1.027E-01	4.703E-02	3.006E-02	1.441E-02	8.778E-03	8.840E-03
914		3.118E-01	1.553E-01	6.954E-02	4.412E-02	2.097E-02	1.257E-02	1.245E-02
1219		4.611E-01	2.206E-01	9.603E-02	6.039E-02	2.841E-02	1.673E-02	1.623E-02
1524		6.670E-01	3.015E-01	1.267E-01	7.973E-02	3.656E-02	2.130E-02	2.042E-02

FLIGHT NO. 98 FILTER NO. 4		DIRECTIONAL PATH REFLECTANCE FROM GROUND TO ALTITUDE						
		ZENITH ANGLE OF PATH OF SIGHT (DEGREES)						
ALTITUDE	METERS	93	95	100	105	120	150	180
305								
610								
914								
1219								
1524								

FLIGHT NO. 98 FILTER NO. 5		DIRECTIONAL PATH REFLECTANCE FROM GROUND TO ALTITUDE						
		ZENITH ANGLE OF PATH OF SIGHT (DEGREES)						
ALTITUDE	METERS	93	95	100	105	120	150	180
305		1.246E-01	6.431E-02	2.975E-02	1.907E-02	9.188E-03	5.511E-03	5.246E-03
610		2.819E-01	1.387E-01	6.171E-02	3.912E-02	1.870E-02	1.121E-02	1.070E-02
914		4.828E-01	2.242E-01	9.561E-02	5.974E-02	2.806E-02	1.651E-02	1.561E-02
1219		8.252E-01	3.516E-01	1.418E-01	8.702E-02	4.003E-02	2.307E-02	2.151E-02
1524		1.395E 00	5.320E-01	2.011E-01	1.209E-01	5.449E-02	3.108E-02	2.858E-02

AZIMUTH OF PATH OF SIGHT = 180							
FLIGHT NO. 98				FILTER NO. 1			
DIRECTIONAL PATH REFLECTANCE FROM GROUND TO ALTITUDE							
ALTITUDE	ZENITH ANGLE OF PATH OF SIGHT (DEGREES)						
METERS	93	95	100	105	120	150	180
305	1.607E-01	8.237E-02	3.819E-02	2.468E-02	1.217E-02	7.295E-03	6.583E-03
610	3.684E-01	1.775E-01	7.823E-02	4.976E-02	2.422E-02	1.465E-02	1.356E-02
914	6.645E-01	2.973E-01	1.244E-01	7.779E-02	3.717E-02	2.238E-02	2.097E-02
1219	1.209E 00	4.857E-01	1.897E-01	1.158E-01	5.383E-02	3.177E-02	2.976E-02
1524	2.102E 00	7.391E-01	2.672E-01	1.591E-01	7.168E-02	4.118E-02	3.808E-02

FLIGHT NO. 98			FILTER NO. 2				
DIRECTIONAL PATH REFLECTANCE FROM GROUND TO ALTITUDE							
ALTITUDE	ZENITH ANGLE OF PATH OF SIGHT (DEGRFES)						
METERS	93	95	100	105	120	150	180
305	1.154E-01	5.991E-02	2.810E-02	1.824E-02	9.049E-03	5.493E-03	5.055E-03
610	2.522E-01	1.250E-01	5.629E-02	3.605E-02	1.766E-02	1.077E-02	1.009E-02
914	4.436E-01	2.070E-01	8.908E-02	5.614E-02	2.697E-02	1.625E-02	1.528E-02
1219	7.930E-01	3.381E-01	1.370E-01	8.455E-02	3.966E-02	2.356E-02	2.222E-02
1524	1.322E 00	5.051E-01	1.919E-01	1.160E-01	5.323E-02	3.118E-02	2.936E-02

FLIGHT NO. 98		FILTER NO. 3					
DIRECTIONAL PATH REFLECTANCE FROM GROUND TO ALTITUDE							
ALTITUDE	ZENITH ANGLE OF PATH OF SIGHT (DEGREES)						
METERS	93	95	100	105	120	150	180
305	9.332E-02	4.940E-02	2.365E-02	1.549E-02	7.686E-03	4.488E-03	4.072E-03
610	2.087E-01	1.078E-01	5.054E-02	3.300E-02	1.645E-02	9.650E-03	8.840E-03
914	3.171E-01	1.593E-01	7.278E-02	4.703E-02	2.314E-02	1.355E-02	1.245E-02
1219	4.698E-01	2.259E-01	9.927E-02	6.357E-02	3.069E-02	1.774E-02	1.623E-02
1524	6.829E-01	3.096E-01	1.314E-01	8.251E-02	3.907E-02	2.236E-02	2.042E-02

FLIGHT NO. 98		FILTER NO. 4					
DIRECTIONAL PATH REFLECTANCE FROM GROUND TO ALTITUDE							
ALTITUDE	ZENITH ANGLE OF PATH OF SIGHT (DEGREES)						
METERS	93	95	100	105	120	150	180
305							
610							
914							
1219							
1524							

FLIGHT NO. 98			FILTER NO. 5				
DIRECTIONAL PATH REFLECTANCE FROM GROUND TO ALTITUDE							
ALTITUDE	ZENITH ANGLE OF PATH OF SIGHT (DEGREES)						
METERS	93	95	100	105	120	150	180
305	1.204E-01	6.234E-02	2.907E-02	1.879E-02	9.225E-03	5.590E-03	5.246E-03
610	2.738E-01	1.351E-01	6.050E-02	3.862E-02	1.877E-02	1.136E-02	1.070E-02
914	4.731E-01	2.200E-01	9.425E-02	5.919E-02	2.818E-02	1.670E-02	1.561E-02
1219	8.156E-01	3.475E-01	1.405E-01	8.653E-02	4.019E-02	2.327E-02	2.151E-02
1524	1.375E 00	5.245E-01	1.988E-01	1.199E-01	5.452E-02	3.113E-02	2.858E-02

AZIMUTH OF PATH OF SIGHT = 270

FLIGHT NO. 98

FILTER NO. 1

DIRECTIONAL PATH REFLECTANCE FROM GROUND TO ALTITUDE		ZENITH ANGLE OF PATH OF SIGHT (DEGREES)						
ALTITUDE		93	95	100	105	120	150	180
METERS								
305		1.704E-01	8.710E-02	4.023E-02	2.581E-02	1.239E-02	7.148E-03	6.583E-03
610		3.810E-01	1.840E-01	8.097E-02	5.125E-02	2.458E-02	1.465E-02	1.356E-02
914		6.809E-01	3.050E-01	1.276E-01	7.951E-02	3.766E-02	2.255E-02	2.097E-02
1219		1.238E 00	4.976E-01	1.941E-01	1.181E-01	5.441E-02	3.192E-02	2.976E-02
1524		2.150E 00	7.575E-01	2.734E-01	1.621E-01	7.240E-02	4.133E-02	3.808E-02

FLIGHT NO. 98

FILTER NO. 2

DIRECTIONAL PATH REFLECTANCE FROM GROUND TO ALTITUDE		ZENITH ANGLE OF PATH OF SIGHT (DEGREES)						
ALTITUDE		93	95	100	105	120	150	180
METERS								
305		1.182E-01	6.111E-02	2.842E-02	1.827E-02	8.877E-03	5.306E-03	5.055E-03
610		2.567E-01	1.269E-01	5.690E-02	3.622E-02	1.754E-02	1.065E-02	1.009E-02
914		4.511E-01	2.102E-01	9.008E-02	5.648E-02	2.686E-02	1.611E-02	1.528E-02
1219		8.097E-01	3.444E-01	1.388E-01	8.524E-02	3.954E-02	2.334E-02	2.222E-02
1524		1.363E 00	5.184E-01	1.956E-01	1.175E-01	5.314E-02	3.084E-02	2.936E-02

FLIGHT NO. 98

FILTER NO. 3

DIRECTIONAL PATH REFLECTANCE FROM GROUND TO ALTITUDE		ZENITH ANGLE OF PATH OF SIGHT (DEGREES)						
ALTITUDE		93	95	100	105	120	150	180
METERS								
305		9.668E-02	5.116E-02	2.454E-02	1.609E-02	8.006E-03	4.565E-03	4.072E-03
610		2.334E-01	1.211E-01	5.755E-02	3.796E-02	1.910E-02	1.036E-02	8.840E-03
914		3.473E-01	1.753E-01	8.100E-02	5.274E-02	2.612E-02	1.433E-02	1.245E-02
1219		5.043E-01	2.435E-01	1.084E-01	6.939E-02	3.358E-02	1.845E-02	1.623E-02
1524		7.284E-01	3.313E-01	1.414E-01	8.901E-02	4.212E-02	2.308E-02	2.042E-02

FLIGHT NO. 98

FILTER NO. 4

DIRECTIONAL PATH REFLECTANCE FROM GROUND TO ALTITUDE		ZENITH ANGLE OF PATH OF SIGHT (DEGREES)						
ALTITUDE		93	95	100	105	120	150	180
METERS								
305								
610								
914								
1219								
1524								

FLIGHT NO. 98

FILTER NO. 5

DIRECTIONAL PATH REFLECTANCE FROM GROUND TO ALTITUDE		ZENITH ANGLE OF PATH OF SIGHT (DEGREES)						
ALTITUDE		93	95	100	105	120	150	180
METERS								
305		1.221E-01	6.317E-02	2.941E-02	1.894E-02	9.268E-03	5.657E-03	5.246E-03
610		2.775E-01	1.309E-01	6.124E-02	3.899E-02	1.892E-02	1.155E-02	1.070E-02
914		4.814E-01	2.237E-01	9.571E-02	5.997E-02	2.846E-02	1.693E-02	1.561E-02
1219		8.330E-01	3.545E-01	1.432E-01	8.799E-02	4.072E-02	2.352E-02	2.151E-02
1524		1.420E 00	5.396E-01	2.036E-01	1.222E-01	5.507E-02	3.118E-02	2.858E-02



#### FLIGHT 99

Full moon. This flight was made approximately 60 km east of Khorat. The terrain was relatively flat and forested with deciduous trees and rice paddies. During this season (dry season) the tree foliage was sparse, dry, and yellowed and the rice paddies between the trees were dry. There were a few artificial ground lights. Particularly near the ground the atmosphere was hazy and there were some cirrus clouds remaining after a local thunderstorm had dissipated. Data-taking started at 2039 local time and ended at 2306. The moon phase angle was  $2^\circ$ ; the moon zenith angle was  $54^\circ$  at the start of sky radiance data-taking and  $30^\circ$  at the end.

FLIGHT NO.99				FILTER NO. 1			
IRRADIANCE(WATTS/SQ.M.MICRO M.)							
ALTITUDE (METERS)	DOWN- WELLING	UP- WELLING	ALBEDO	SCALAR DOWNWELLING	SCALAR UPWELLING	SCALAR TOTAL	SCALAR ALBEDO
225	1.665E-03	9.797E-05	.091	3.242E-03	2.959E-04	3.538E-03	.091
527	2.561E-03	1.670E-04	.065	4.905E-03	4.903E-04	5.396E-03	.100
814	2.589E-03	2.349E-04	.091	4.651E-03	6.410E-04	5.292E-03	.138
1123	2.646E-03	2.471E-04	.093	4.577E-03	7.019E-04	5.279E-03	.153
1461	2.534E-03	2.799E-04	.110	4.370E-03	6.144E-04	5.184E-03	.186
1748	3.011E-03	3.524E-04	.110	4.942E-03	9.698E-04	5.912E-03	.196

FLIGHT NO.99				FILTER NO. 2			
IRRADIANCE(WATTS/SQ.M.MICRO M.)							
ALTITUDE (METERS)	DOWN- WELLING	UP- WELLING	ALBEDO	SCALAR DOWNWELLING	SCALAR UPWELLING	SCALAR TOTAL	SCALAR ALBEDO
225	1.606E-03	1.397E-04	.087	3.129E-03	3.729E-04	3.502E-03	.119
527	1.942E-03	1.378E-04	.071	3.689E-03	4.184E-04	4.107E-03	.113
815	2.753E-03	2.088E-04	.076	4.833E-03	6.102E-04	5.443E-03	.126
1129	2.648E-03	2.709E-04	.102	4.574E-03	7.544E-04	5.329E-03	.165
1462	2.967E-03	3.391E-04	.114	4.941E-03	9.271E-04	5.868E-03	.182
1743	2.666E-03	3.807E-04	.154	4.180E-03	1.012E-03	5.192E-03	.242

FLIGHT NO.99				FILTER NO. 3			
IRRADIANCE(WATTS/SQ.M.MICRO M.)							
ALTITUDE (METERS)	DOWN- WELLING	UP- WELLING	ALBEDO	SCALAR DOWNWELLING	SCALAR UPWELLING	SCALAR TOTAL	SCALAR ALBEDO
226	1.861E-03	2.165E-04	.110	3.590E-03	5.158E-04	4.106E-03	.144
528	2.579E-03	2.166E-04	.084	4.495E-03	5.337E-04	5.029E-03	.119
816	2.251E-03	3.052E-04	.136	4.031E-03	7.211E-04	4.752E-03	.179
1131	2.744E-03	3.130E-04	.114	4.647E-03	7.595E-04	5.407E-03	.163
1462	3.029E-03	3.610E-04	.119	4.928E-03	8.952E-04	5.823E-03	.182
1749	2.217E-03	3.437E-04	.155	3.818E-03	9.001E-04	4.718E-03	.236

FLIGHT NO.99				FILTER NO. 4			
IRRADIANCE(WATTS/SQ.M.MICRO M.)							
ALTITUDE (METERS)	DOWN- WELLING	UP- WELLING	ALBEDO	SCALAR DOWNWELLING	SCALAR UPWELLING	SCALAR TOTAL	SCALAR ALBEDO
225	1.215E-03	2.655E-04	.218	2.432E-03	5.938E-04	3.025E-03	.244
528	1.973E-03	3.624E-04	.184	3.465E-03	8.361E-04	4.301E-03	.241
817	1.933E-03	4.758E-04	.246	3.312E-03	1.070E-03	4.382E-03	.323
1131	2.125E-03	5.437E-04	.256	3.534E-03	1.184E-03	4.719E-03	.335
1462	1.610E-03	5.130E-04	.310	2.811E-03	1.139E-03	3.950E-03	.405
1750	1.870E-03	5.162E-04	.270	3.127E-03	1.143E-03	4.269E-03	.365

FLIGHT NO.99				FILTER NO. 5			
IRRADIANCE(WATTS/SQ.M.MICRO M.)							
ALTITUDE (METERS)	DOWN- WELLING	UP- WELLING	ALBEDO	SCALAR DOWNWELLING	SCALAR UPWELLING	SCALAR TOTAL	SCALAR ALBEDO
225	1.780E-03	1.620E-04	.091	3.316E-03	3.614E-04	3.677E-03	.109
527	1.964E-03	2.729E-04	.123	3.683E-03	5.469E-04	4.235E-03	.148
815	2.302E-03	2.181E-04	.092	4.119E-03	6.352E-04	4.755E-03	.154
1129	2.562E-03	3.195E-04	.125	4.372E-03	8.626E-04	5.234E-03	.197
1461	2.242E-03	3.895E-04	.129	4.929E-03	8.434E-04	4.773E-03	.215
1743	2.593E-03	3.419E-04	.132	4.315E-03	8.978E-04	5.212E-03	.208

FLIGHT NO. 99  
AZIMUTH OF PATH OF SIGHT = 0  
DIRECTIONAL REFLECTANCE OF BACKGROUND

ZENITH ANGLE	FILTERS			
	1	2	3	4
93	.52487	.54653	.31432	.39037
95	.33287	.31751	.22109	.25550
100	.11575	.15429	.08951	.17293
105	.07724	.11191	.07675	.12993
120	.05796	.07910	.08947	.11668
150	.05207	.05245	.07575	.06832
180	.04712	.07606	.06667	.04678

FLIGHT NO. 99  
AZIMUTH OF PATH OF SIGHT = 50  
DIRECTIONAL REFLECTANCE OF BACKGROUND

ZENITH ANGLE	FILTERS			
	1	2	3	4
93	.20357	.18100	.23142	.14701
95	.15651	.13739	.13599	.14516
100	.05023	.10418	.08911	.11882
105	.06579	.08421	.07230	.09629
120	.06775	.07867	.05153	.14565
150	.05974	.05731	.08410	.07065
180	.04712	.07606	.06667	.04678

FLIGHT NO. 99  
AZIMUTH OF PATH OF SIGHT = 120  
DIRECTIONAL REFLECTANCE OF BACKGROUND

ZENITH ANGLE	FILTERS			
	1	2	3	4
93	.25183	.21198	.17622	.16414
95	.13622	.15032	.11633	.15043
100	.13331	.13057	.07494	.22795
105	.07771	.14131	.07641	.19630
120	.07586	.12313	.12429	.19781
150	.06606	.11376	.09262	.09722
180	.04712	.07606	.06667	.04678

FLIGHT NO. 99  
AZIMUTH OF PATH OF SIGHT = 170  
DIRECTIONAL REFLECTANCE OF BACKGROUND

ZENITH ANGLE	FILTERS			
	1	2	3	4
93	.24130	.27312	.15666	.20982
95	.17492	.17793	.12249	.14799
100	.08340	.10839	.06794	.14381
105	.06842	.09373	.06816	.13277
120	.05116	.07903	.09907	.13022
150	.05708	.08070	.06939	.07527
180	.04712	.07606	.06667	.04678

DATE 40269 FLIGHT NO. 99 GROUND LEVEL ALTITUDE (M.)= 237 IUP-1

ALTITUDE (METERS)	TOTAL FILTERS	SCATTERING COEFFICIENT (PER METER)			
	1	2	3	4	5
0	6.319E-05	4.666E-05	3.269E-05		5.150E-05
30	6.298E-05	4.650E-05	3.258E-05		5.132E-05
61	6.277E-05	4.635E-05	3.247E-05		5.115E-05
91	6.256E-05	4.619E-05	3.236E-05		5.098E-05
122	6.235E-05	4.604E-05	3.225E-05		5.081E-05
152	6.215E-05	4.589E-05	3.215E-05		5.064E-05
183	6.194E-05	4.573E-05	3.204E-05		5.048E-05
213	6.173E-05	4.558E-05	3.193E-05		5.031E-05
244	5.942E-05	4.543E-05	3.154E-05		5.102E-05
274	5.980E-05	4.617E-05	3.120E-05		5.192E-05
305	6.192E-05	4.501E-05	3.163E-05		5.194E-05
335	6.269E-05	4.377E-05	3.148E-05		5.190E-05
366	6.216E-05	4.329E-05	3.132E-05		5.143E-05
396	6.009E-05	4.158E-05	3.101E-05		5.002E-05
427	6.020E-05	4.127E-05	2.902E-05		4.902E-05
457	5.987E-05	4.201E-05	2.830E-05		4.966E-05
488	5.549E-05	4.349E-05	2.828E-05		4.987E-05
518	5.293E-05	4.344E-05	2.856E-05		4.615E-05
549	5.020E-05	4.405E-05	2.843E-05		4.415E-05
579	5.223E-05	4.663E-05	2.874E-05		4.376E-05
610	5.282E-05	4.837E-05	2.830E-05		4.459E-05
640	5.559E-05	5.303E-05	2.908E-05		4.551E-05
671	5.609E-05	5.925E-05	2.949E-05		4.667E-05
701	5.714E-05	6.166E-05	3.170E-05		4.925E-05
732	6.139E-05	6.180E-05	3.656E-05		4.785E-05
762	6.252E-05	6.288E-05	3.776E-05		4.658E-05
792	6.238E-05	6.343E-05	3.956E-05		4.585E-05
823	6.135E-05	6.226E-05	3.920E-05		4.576E-05
853	6.046E-05	7.026E-05	3.849E-05		4.559E-05
884	5.924E-05	7.225E-05	3.885E-05		4.589E-05
914	5.919E-05	7.301E-05	3.890E-05		4.590E-05
945	5.887E-05	5.811E-05	3.850E-05		4.586E-05
975	6.186E-05	6.656E-05	4.147E-05		4.592E-05
1006	6.329E-05	6.697E-05	4.902E-05		4.559E-05
1036	6.051E-05	6.584E-05	5.607E-05		4.598E-05
1067	6.121E-05	7.417E-05	5.032E-05		4.617E-05
1097	6.407E-05	7.222E-05	4.445E-05		4.862E-05
1128	6.905E-05	7.446E-05	4.117E-05		4.869E-05
1158	7.493E-05	6.711E-05	4.147E-05		4.877E-05
1189	8.536E-05	6.686E-05	4.019E-05		4.856E-05
1219	9.151E-05	6.233E-05	4.146E-05		5.034E-05
1250	8.783E-05	6.087E-05	3.819E-05		5.350E-05
1280	8.445E-05	5.860E-05	3.656E-05		5.486E-05
1311	8.172E-05	5.870E-05	3.347E-05		5.540E-05
1341	8.551E-05	5.227E-05	3.368E-05		5.616E-05
1372	7.607E-05	4.969E-05	3.302E-05		5.449E-05
1402	6.661E-05	5.079E-05	3.260E-05		5.340E-05
1433	6.308E-05	5.397E-05	3.248E-05		5.379E-05
1463	6.883E-05	5.472E-05	3.136E-05		5.556E-05
1494	6.429E-05	4.999E-05	3.166E-05		5.409E-05
1524	5.766E-05	5.055E-05	3.166E-05		5.399E-05
1554	5.703E-05	5.091E-05	3.220E-05		5.494E-05
1585	5.702E-05	5.069E-05	3.216E-05		5.598E-05
1615	5.652E-05	5.113E-05	3.201E-05		5.691E-05
1646	5.777E-05	5.215E-05	3.200E-05		5.798E-05
1676	5.782E-05	5.108E-05	3.208E-05		5.942E-05
1707	5.832E-05	5.035E-05	3.253E-05		5.998E-05
1737	5.470E-05	5.018E-05	3.270E-05		6.117E-05
1768	5.801E-05	5.001E-05	3.259E-05		6.338E-05
1798	5.781E-05	4.985E-05	3.248E-05		6.317E-05
1829	5.762E-05	4.968E-05	3.238E-05		6.296E-05

FIRST DATA ALT. 0 9 8 8 6  
LAST DATA ALT. 59 57 58 59 59

FLIGHT NO. 99		FILTER NO. 1						
BEAM TRANSMITTANCE FROM GROUND TO ALTITUDE		ZENITH ANGLE OF PATH OF SIGHT (DEGREES)						
ALTITUDE		93	95	100	105	120	150	180
METERS								
305		.6993751	.8055579	.8971582	.9297767	.9630117	.9784749	.9813316
610		.4931902	.6592269	.9112620	.8690827	.9299417	.9589322	.9643346
914		.3437433	.5599132	.7211893	.8105395	.8969703	.9391531	.9470851
1219		.2214253	.4174230	.6450056	.7451289	.8587408	.9158308	.9266827
1524		.1311729	.3253189	.5651803	.6819241	.8202296	.8918886	.9056653

FLIGHT NO. 99		FILTER NO. 2						
BEAM TRANSMITTANCE FROM GROUND TO ALTITUDE		ZENITH ANGLE OF PATH OF SIGHT (DEGREES)						
ALTITUDE		93	95	100	105	120	150	180
METERS								
305		.7032861	.8514877	.9224776	.9473010	.9723649	.9839505	.9860857
610		.5878304	.7319123	.8544211	.8998652	.9468485	.9689593	.9730614
914		.4026439	.5869718	.7053616	.8357637	.9113125	.9477939	.9546269
1219		.2638839	.4611311	.6780631	.7705395	.8737773	.9250553	.9347605
1524		.1866155	.3409792	.6160912	.7225495	.8451708	.9074472	.9193317

FLIGHT NO. 99		FILTER NO. 3						
BEAM TRANSMITTANCE FROM GROUND TO ALTITUDE		ZENITH ANGLE OF PATH OF SIGHT (DEGREES)						
ALTITUDE		93	95	100	105	120	150	180
METERS								
305		.8282590	.8949143	.9492079	.9629399	.9806416	.9887773	.9902735
610		.6939918	.8062555	.8975401	.9300478	.9631571	.9785607	.9814057
914		.5594988	.7120524	.8432643	.8919372	.9425212	.9664001	.9708353
1219		.4266025	.6098901	.7802174	.8466127	.9174172	.9514544	.9578190
1524		.3437045	.5415587	.7350452	.8134048	.8986102	.9401441	.9479505

FLIGHT NO. 99		FILTER NO. 4						
BEAM TRANSMITTANCE FROM GROUND TO ALTITUDE		ZENITH ANGLE OF PATH OF SIGHT (DEGREES)						
ALTITUDE		93	95	100	105	120	150	180
METERS								
305								
610								
914								
1219								
1524								

FLIGHT NO. 99		FILTER NO. 5						
BEAM TRANSMITTANCE FROM GROUND TO ALTITUDE		ZENITH ANGLE OF PATH OF SIGHT (DEGREES)						
ALTITUDE		93	95	100	105	120	150	180
METERS								
305		.7409171	.8365403	.9143140	.9416682	.9693678	.9821983	.9845648
610		.5543723	.7062232	.8398128	.8894717	.9411717	.9656010	.9701400
914		.4174356	.6003980	.7740989	.8421525	.9149127	.9499536	.9565104
1219		.3107316	.5050317	.7122640	.7964035	.8888383	.9342278	.9427822
1524		.2207644	.4086003	.6474631	.7470340	.8598766	.9165300	.9272953

AZIMUTH OF PATH OF SIGHT = 0  
 FLIGHT NO. 99 FILTER NO. 1  
 PATH RADIANCE FROM GROUND TO ALTITUDE (WATTS/STER.SQ.M MICRO M.)  
 ZENITH ANGLE OF PATH OF SIGHT (DEGREES)

ALTITUDE METERS	93	95	100	105	120	150	180
305	1.313E-04	7.538E-05	3.574E-05	2.197E-05	8.720E-06	2.803E-06	3.390E-06
610	2.631E-04	1.604E-04	7.861E-05	4.872E-05	1.945E-05	8.466E-06	7.549E-06
914	3.552E-04	2.320E-04	1.192E-04	7.520E-05	3.078E-05	1.368E-05	1.218E-05
1219	4.133E-04	2.918E-04	1.588E-04	1.025E-04	4.325E-05	1.972E-05	1.764E-05
1524	4.417E-04	3.346E-04	1.934E-04	1.281E-04	5.604E-05	2.620E-05	2.353E-05

FLIGHT NO. 99 FILTER NO. 2  
 PATH RADIANCE FROM GROUND TO ALTITUDE (WATTS/STER.SQ.M MICRO M.)  
 ZENITH ANGLE OF PATH OF SIGHT (DEGREES)

ALTITUDE METERS	93	95	100	105	120	150	180
305	9.098E-05	5.582E-05	2.629E-05	1.617E-05	6.483E-06	2.869E-06	2.564E-06
610	1.794E-04	1.072E-04	5.218E-05	3.241E-05	1.313E-05	5.817E-06	5.158E-06
914	2.988E-04	1.902E-04	9.594E-05	6.016E-05	2.452E-05	1.084E-05	9.602E-06
1219	3.798E-04	2.601E-04	1.340E-04	8.516E-05	3.668E-05	1.644E-05	1.458E-05
1524	4.217E-04	3.042E-04	1.683E-04	1.096E-04	4.688E-05	2.154E-05	1.925E-05

FLIGHT NO. 99 FILTER NO. 3  
 PATH RADIANCE FROM GROUND TO ALTITUDE (WATTS/STER.SQ.M MICRO M.)  
 ZENITH ANGLE OF PATH OF SIGHT (DEGREES)

ALTITUDE METERS	93	95	100	105	120	150	180
305	9.155E-05	5.032E-05	2.197E-05	1.383E-05	5.282E-06	2.214E-06	1.948E-06
610	1.671E-04	9.579E-05	4.475E-05	2.711E-05	1.046E-05	4.455E-06	3.974E-06
914	2.371E-04	1.431E-04	6.889E-05	4.216E-05	1.649E-05	7.176E-06	6.354E-06
1219	3.015E-04	1.930E-04	9.656E-05	6.005E-05	2.409E-05	1.069E-05	9.477E-06
1524	3.427E-04	2.282E-04	1.176E-04	7.410E-05	3.040E-05	1.377E-05	1.231E-05

FLIGHT NO. 99 FILTER NO. 4  
 PATH RADIANCE FROM GROUND TO ALTITUDE (WATTS/STER.SQ.M MICRO M.)  
 ZENITH ANGLE OF PATH OF SIGHT (DEGREES)

ALTITUDE METERS	93	95	100	105	120	150	180
305							
610							
914							
1219							
1524							

FLIGHT NO. 99 FILTER NO. 5  
 PATH RADIANCE FROM GROUND TO ALTITUDE (WATTS/STER.SQ.M MICRO M.)  
 ZENITH ANGLE OF PATH OF SIGHT (DEGREES)

ALTITUDE METERS	93	95	100	105	120	150	180
305	1.078E-04	6.111E-05	2.900E-05	1.788E-05	7.375E-06	3.413E-06	3.082E-06
610	1.912E-04	1.157E-04	5.710E-05	3.572E-05	1.483E-05	6.882E-06	6.211E-06
914	2.603E-04	1.602E-04	8.458E-05	5.347E-05	2.233E-05	1.029E-05	9.243E-06
1219	3.170E-04	2.129E-04	1.172E-04	7.192E-05	3.054E-05	1.414E-05	1.284E-05
1524	3.526E-04	2.513E-04	1.367E-04	9.074E-05	3.963E-05	1.863E-05	1.662E-05

AZIMUTH OF PATH OF SIGHT = 90		FLIGHT NO. 99 FILTER NO. 1						
PATH RADIANCE FROM GROUND TO ALTITUDE (WATTS/STER.SQ.M MICRO M.)		ZENITH ANGLE OF PATH OF SIGHT (DEGREES)						
ALTITUDE METERS		93	95	100	105	120	150	180
305		7.820E-05	4.609E-05	2.339E-05	1.537E-05	7.355E-06	3.947E-06	3.390E-06
610		1.495E-04	9.398E-05	4.962E-05	3.309E-05	1.610E-05	8.736E-06	7.549E-06
914		2.093E-04	1.402E-04	7.707E-05	5.212E-05	2.573E-05	1.406E-05	1.218E-05
1219		2.573E-04	1.847E-04	1.067E-04	7.343E-05	3.689E-05	2.033E-05	1.764E-05
1524		2.921E-04	2.229E-04	1.353E-04	9.470E-05	4.868E-05	2.709E-05	2.353E-05

FLIGHT NO. 99 FILTER NO. 2		PATH RADIANCE FROM GROUND TO ALTITUDE (WATTS/STER.SQ.M MICRO M.)						
ZENITH ANGLE OF PATH OF SIGHT (DEGREES)								
ALTITUDE METERS		93	95	100	105	120	150	180
305		5.837E-05	3.379E-05	1.709E-05	1.123E-05	5.464E-06	2.987E-06	2.564E-06
610		1.079E-04	6.611E-05	3.432E-05	2.278E-05	1.108E-05	6.007E-06	5.158E-06
914		1.787E-04	1.169E-04	6.299E-05	4.224E-05	2.061E-05	1.115E-05	9.602E-06
1219		2.366E-04	1.654E-04	9.320E-05	6.339E-05	3.126E-05	1.692E-05	1.458E-05
1524		2.764E-04	2.020E-04	1.178E-04	8.123E-05	4.073E-05	2.230E-05	1.925E-05

FLIGHT NO. 99 FILTER NO. 3		PATH RADIANCE FROM GROUND TO ALTITUDE (WATTS/STER.SQ.M MICRO M.)						
ZENITH ANGLE OF PATH OF SIGHT (DEGREES)								
ALTITUDE METERS		93	95	100	105	120	150	180
305		4.590E-05	2.611E-05	1.306E-05	8.609E-06	4.209E-06	2.291E-06	1.948E-06
610		8.019E-05	5.109E-05	2.602E-05	1.719E-05	8.386E-06	4.592E-06	3.974E-06
914		1.231E-04	7.968E-05	4.153E-05	2.756E-05	1.340E-05	7.309E-06	6.354E-06
1219		1.775E-04	1.160E-04	6.202E-05	4.142E-05	2.015E-05	1.094E-05	9.477E-06
1524		2.114E-04	1.431E-04	7.826E-05	5.267E-05	2.582E-05	1.413E-05	1.231E-05

FLIGHT NO. 99 FILTER NO. 4		PATH RADIANCE FROM GROUND TO ALTITUDE (WATTS/STER.SQ.M MICRO M.)						
ZENITH ANGLE OF PATH OF SIGHT (DEGREES)								
ALTITUDE METERS		93	95	100	105	120	150	180
305								
610								
914								
1219								
1524								

FLIGHT NO. 99 FILTER NO. 5		PATH RADIANCE FROM GROUND TO ALTITUDE (WATTS/STER.SQ.M MICRO M.)						
ZENITH ANGLE OF PATH OF SIGHT (DEGREES)								
ALTITUDE METERS		93	95	100	105	120	150	180
305		6.814E-05	3.961E-05	1.996E-05	1.312E-05	6.374E-06	3.545E-06	3.082E-06
610		1.223E-04	7.579E-05	3.964E-05	2.637E-05	1.292E-05	7.156E-06	6.211E-06
914		1.684E-04	1.096E-04	5.913E-05	3.963E-05	1.941E-05	1.064E-05	9.243E-06
1219		2.121E-04	1.448E-04	8.022E-05	5.424E-05	2.668E-05	1.456E-05	1.264E-05
1524		2.493E-04	1.790E-04	1.029E-04	7.046E-05	3.512E-05	1.919E-05	1.662E-05

--- AZIMUTH OF PATH OF SIGHT = 1-0

FLIGHT NO. 99

FILTER NO. 1

PATH RADIANCE FROM GROUND TO ALTITUDE (WATTS/STER.SQ.M MICRO M.)

ALTITUDE METERS	93	95	100	105	120	150	180
305	8.035E-05	4.816E-05	2.554E-05	1.753E-05	9.390E-06	4.747E-06	3.390E-06
610	1.557E-04	9.966E-05	5.913E-05	3.852E-05	2.112E-05	1.064E-05	7.549E-06
914	2.129E-04	1.454E-04	8.364E-05	5.909E-05	3.266E-05	1.688E-05	1.218E-05
1219	2.571E-04	1.883E-04	1.135E-04	8.135E-05	4.544E-05	2.422E-05	1.764E-05
1524	2.902E-04	2.254E-04	1.424E-04	1.037E-04	5.878E-05	3.219E-05	2.353E-05

FLIGHT NO. 99

FILTER NO. 2

PATH RADIANCE FROM GROUND TO ALTITUDE (WATTS/STER.SQ.M MICRO M.)

ALTITUDE METERS	93	95	100	105	120	150	180
305	6.142E-05	3.616E-05	1.696E-05	1.297E-05	6.894E-06	3.532E-06	2.564E-06
610	1.119E-04	6.971E-05	3.769E-05	2.599E-05	1.388E-05	7.081E-06	5.158E-06
914	1.774E-04	1.185E-04	6.611E-05	4.649E-05	2.514E-05	1.314E-05	9.602E-06
1219	2.290E-04	1.634E-04	9.822E-05	6.789E-05	3.707E-05	1.982E-05	1.458E-05
1524	2.669E-04	1.986E-04	1.204E-04	8.621E-05	4.778E-05	2.621E-05	1.925E-05

FLIGHT NO. 99

FILTER NO. 3

PATH RADIANCE FROM GROUND TO ALTITUDE (WATTS/STER.SQ.M MICRO M.)

ALTITUDE METERS	93	95	100	105	120	150	180
305	4.934E-05	2.866E-05	1.384E-05	1.040E-05	5.722E-06	2.835E-06	1.948E-06
610	9.100E-05	5.517E-05	2.799E-05	2.059E-05	1.154E-05	5.869E-06	3.974E-06
914	1.291E-04	8.222E-05	4.511E-05	3.148E-05	1.759E-05	9.170E-06	6.354E-06
1219	1.703E-04	1.151E-04	6.418E-05	4.493E-05	2.490E-05	1.330E-05	9.477E-06
1524	2.018E-04	1.397E-04	8.091E-05	5.651E-05	3.148E-05	1.730E-05	1.231E-05

FLIGHT NO. 99

FILTER NO. 4

PATH RADIANCE FROM GROUND TO ALTITUDE (WATTS/STER.SQ.M MICRO M.)

ALTITUDE METERS	93	95	100	105	120	150	180
305							
610							
914							
1219							
1524							

FLIGHT NO. 99

FILTER NO. 5

PATH RADIANCE FROM GROUND TO ALTITUDE (WATTS/STER.SQ.M MICRO M.)

ALTITUDE METERS	93	95	100	105	120	150	180
305	6.804E-05	4.027E-05	2.121E-05	1.453E-05	7.798E-06	4.123E-06	3.062E-06
610	1.225E-04	7.114E-05	4.288E-05	2.912E-05	1.579E-05	8.376E-06	6.211E-06
914	1.551E-04	1.011E-04	6.173E-05	4.308E-05	2.324E-05	1.248E-05	9.243E-06
1219	2.041E-04	1.322E-04	8.144E-05	5.748E-05	3.113E-05	1.697E-05	1.264E-05
1524	2.438E-04	1.741E-04	1.031E-04	7.355E-05	4.010E-05	2.218E-05	1.662E-05



AZIMUTH OF PATH OF SIGHT = 270

FLIGHT NO. 99

FILTER NO. 1

ALTIUDE	PATH RADIANCE FROM GROUND TO ALTITUDE(WATTS/STER.SQ.M MICRO M.)							
METERS	ZENITH ANGLE OF PATH OF SIGHT (DEGREES)							
	73	95	100	105	120	150	180	
305	7.559E-05	4.401E-05	2.275E-05	1.503E-05	7.290E-06	3.955E-06	3.390E-06	
10	1.444E-04	9.106E-05	4.837E-05	3.245E-05	1.606E-05	8.821E-06	7.549E-06	
214	2.024E-04	1.359E-04	7.514E-05	5.113E-05	2.568E-05	1.423E-05	1.218E-05	
1219	2.491E-04	1.792E-04	1.040E-04	7.199E-05	3.676E-05	2.056E-05	1.764E-05	
1574	2.839E-04	2.168E-04	1.320E-04	9.304E-05	4.840E-05	2.730E-05	2.353E-05	

FLIGHT NO. 99

FILTER NO. 2

ALTIUDE	PATH RADIANCE FROM GROUND TO ALTITUDE(WATTS/STER.SQ.M MICRO M.)							
METERS	ZENITH ANGLE OF PATH OF SIGHT (DEGREES)							
	73	95	100	105	120	150	180	
305	6.006E-05	3.474E-05	1.747E-05	1.147E-05	5.522E-06	2.986E-06	2.564E-06	
10	1.584E-04	6.652E-05	3.459E-05	2.294E-05	1.118E-05	6.043E-06	5.198E-06	
214	1.745E-04	1.146E-04	6.207E-05	4.180E-05	2.062E-05	1.123E-05	9.607E-06	
1219	2.292E-04	1.609E-04	9.110E-05	6.277E-05	3.109E-05	1.700E-05	1.458E-05	
1574	2.574E-04	1.960E-04	1.140E-04	7.953E-05	4.035E-05	2.232E-05	1.925E-05	

FLIGHT NO. 99

FILTER NO. 3

ALTIUDE	PATH RADIANCE FROM GROUND TO ALTITUDE(WATTS/STER.SQ.M MICRO M.)							
METERS	ZENITH ANGLE OF PATH OF SIGHT (DEGREES)							
	73	95	100	105	120	150	180	
305	4.865E-05	2.759E-05	1.369E-05	8.944E-06	4.275E-06	2.280E-06	1.948E-06	
10	5.702E-05	5.178E-05	2.642E-05	1.748E-05	8.526E-06	4.653E-06	3.974E-06	
214	1.264E-04	7.897E-05	4.135E-05	2.757E-05	1.354E-05	7.429E-06	6.354E-06	
1219	1.714E-04	1.125E-04	6.054E-05	4.065E-05	2.003E-05	1.103E-05	9.477E-06	
1574	2.077E-04	1.361E-04	7.605E-05	5.152E-05	2.566E-05	1.427E-05	1.231E-05	

FLIGHT NO. 99

FILTER NO. 4

ALTIUDE	PATH RADIANCE FROM GROUND TO ALTITUDE(WATTS/STER.SQ.M MICRO M.)							
METERS	ZENITH ANGLE OF PATH OF SIGHT (DEGREES)							
	73	95	100	105	120	150	180	
305								
10								
214								
1219								
1574								

FLIGHT NO. 99

FILTER NO. 5

ALTIUDE	PATH RADIANCE FROM GROUND TO ALTITUDE(WATTS/STER.SQ.M MICRO M.)							
METERS	ZENITH ANGLE OF PATH OF SIGHT (DEGREES)							
	73	95	100	105	120	150	180	
305	6.517E-05	3.810E-05	1.937E-05	1.287E-05	6.344E-06	3.570E-06	3.087E-06	
10	1.192E-04	7.305E-05	3.686E-05	2.599E-05	1.291E-05	7.199E-06	6.211E-06	
214	1.625E-04	1.063E-04	5.763E-05	3.869E-05	1.936E-05	1.073E-05	9.243E-06	
1219	2.020E-04	1.310E-04	7.719E-05	5.288E-05	2.652E-05	1.469E-05	1.264E-05	
1574	2.379E-04	1.715E-04	9.928E-05	6.853E-05	3.478E-05	1.931E-05	1.667E-05	

AZIMUTH OF PATH OF SIGHT = 0		FLIGHT NO. 99		FILTER NO. 1					
DIRECTIONAL PATH REFLECTANCE FROM GROUND TO ALTITUDE		ZENITH ANGLE OF PATH OF SIGHT (DEGREES)							
ALTITUDE		93	95	100	105	120	150	180	
METERS									
305	3.564E-01	1.766E-01	7.518E-02	4.459E-02	1.709E-02	7.336E-03	6.519E-03		
610	1.007E 00	4.592E-01	1.829E-01	1.058E-01	3.948E-02	1.666E-02	1.478E-02		
914	1.950E 00	8.172E-01	3.077E-01	1.751E-01	6.477E-02	2.749E-02	2.427E-02		
1219	3.522E 00	1.320E 00	4.647E-01	2.597E-01	9.513E-02	4.065E-02	3.594E-02		
1524	6.033E 00	1.968E 00	6.457E-01	3.545E-01	1.289E-01	5.545E-02	4.904E-02		

FLIGHT NO. 99		FILTER NO. 2							
DIRECTIONAL PATH REFLECTANCE FROM GROUND TO ALTITUDE		ZENITH ANGLE OF PATH OF SIGHT (DEGREES)							
ALTITUDE		93	95	100	105	120	150	180	
METERS									
305	2.537E-01	1.283E-01	5.576E-02	3.339E-02	1.305E-02	5.705E-03	5.089E-03		
610	5.973E-01	2.870E-01	1.195E-01	7.046E-02	2.714E-02	1.175E-02	1.037E-02		
914	1.452E 00	6.340E-01	2.453E-01	1.409E-01	5.265E-02	2.238E-02	1.968E-02		
1219	2.817E 00	1.104E 00	3.982E-01	2.239E-01	8.214E-02	3.478E-02	3.051E-02		
1524	4.422E 00	1.562E 00	5.346E-01	2.967E-01	1.085E-01	4.644E-02	4.098E-02		

FLIGHT NO. 99		FILTER NO. 3							
DIRECTIONAL PATH REFLECTANCE FROM GROUND TO ALTITUDE		ZENITH ANGLE OF PATH OF SIGHT (DEGREES)							
ALTITUDE		93	95	100	105	120	150	180	
METERS									
305	1.860E-01	9.505E-02	4.103E-02	2.426E-02	9.093E-03	3.780E-03	3.321E-03		
610	4.060E-01	2.006E-01	8.416E-02	4.922E-02	1.833E-02	7.687E-03	6.837E-03		
914	7.156E-01	3.393E-01	1.379E-01	7.981E-02	2.954E-02	1.245E-02	1.105E-02		
1219	1.193E 00	5.343E-01	2.090E-01	1.198E-01	4.434E-02	1.897E-02	1.671E-02		
1524	1.683E 00	7.115E-01	2.701E-01	1.538E-01	5.712E-02	2.473E-02	2.193E-02		

FLIGHT NO. 99		FILTER NO. 4							
DIRECTIONAL PATH REFLECTANCE FROM GROUND TO ALTITUDE		ZENITH ANGLE OF PATH OF SIGHT (DEGREES)							
ALTITUDE		93	95	100	105	120	150	180	
METERS									
305									
610									
914									
1219									
1524									

FLIGHT NO. 99		FILTER NO. 5							
DIRECTIONAL PATH REFLECTANCE FROM GROUND TO ALTITUDE		ZENITH ANGLE OF PATH OF SIGHT (DEGREES)							
ALTITUDE		93	95	100	105	120	150	180	
METERS									
305	2.550E-01	1.283E-01	5.571E-02	3.335E-02	1.327E-02	6.105E-03	5.499E-03		
610	6.050E-01	2.878E-01	1.194E-01	7.054E-02	2.768E-02	1.252E-02	1.125E-02		
914	1.090E 00	4.863E-01	1.919E-01	1.115E-01	4.287E-02	1.902E-02	1.698E-02		
1219	1.792E 00	7.353E-01	2.767E-01	1.566E-01	6.035E-02	2.658E-02	2.354E-02		
1524	2.800E 00	1.049E 00	3.764E-01	2.134E-01	8.095E-02	3.570E-02	3.148E-02		

AZIMUTH OF PATH OF SIGHT = 90

FLIGHT NO. 99      FILTER NO. 1

DIRECTIONAL PATH REFLECTANCE FROM GROUND TO ALTITUDE

ZENITH ANGLE OF PATH OF SIGHT (DEGREES)

ALTITUDE METERS	93	95	100	105	120	150	180
305	2.124E-01	1.080E-01	4.921E-02	3.120E-02	1.442E-02	7.613E-03	6.519E-03
610	5.720E-01	2.691E-01	1.154E-01	7.186E-02	3.268E-02	1.719E-02	1.478E-02
914	1.149E-00	4.937E-01	1.989E-01	1.214E-01	5.414E-02	2.826E-02	2.427E-02
1219	2.193E-00	8.352E-01	3.122E-01	1.860E-01	8.108E-02	4.189E-02	3.594E-02
1524	3.989E-00	1.311E-00	4.518E-01	2.626E-01	1.120E-01	5.732E-02	4.904E-02

FLIGHT NO. 99      FILTER NO. 2

DIRECTIONAL PATH REFLECTANCE FROM GROUND TO ALTITUDE

ZENITH ANGLE OF PATH OF SIGHT (DEGREES)

ALTITUDE METERS	93	95	100	105	120	150	180
305	1.490E-01	7.764E-02	3.616E-02	2.320E-02	1.100E-02	5.941E-03	5.089E-03
610	3.593E-01	1.769E-01	7.860E-02	4.954E-02	2.290E-02	1.213E-02	1.037E-02
914	8.685E-01	3.897E-01	1.610E-01	9.888E-02	4.424E-02	2.301E-02	1.968E-02
1219	1.754E-00	7.019E-01	2.689E-01	1.610E-01	7.001E-02	3.579E-02	3.051E-02
1524	4.090E-00	1.037E-00	3.741E-01	2.203E-01	9.429E-02	4.807E-02	4.098E-02

FLIGHT NO. 99      FILTER NO. 3

DIRECTIONAL PATH REFLECTANCE FROM GROUND TO ALTITUDE

ZENITH ANGLE OF PATH OF SIGHT (DEGREES)

ALTITUDE METERS	93	95	100	105	120	150	180
305	9.357E-02	4.932E-02	2.333E-02	1.509E-02	7.247E-03	3.913E-03	3.321E-03
610	2.097E-01	1.070E-01	4.895E-02	3.121E-02	1.470E-02	7.924E-03	6.837E-03
914	3.867E-01	1.809E-01	8.314E-02	5.217E-02	2.400E-02	1.277E-02	1.105E-02
1219	7.023E-01	3.217E-01	1.342E-01	8.261E-02	3.708E-02	1.941E-02	1.671E-02
1524	1.038E-00	4.462E-01	1.798E-01	1.093E-01	4.851E-02	2.538E-02	2.193E-02

FLIGHT NO. 99      FILTER NO. 4

DIRECTIONAL PATH REFLECTANCE FROM GROUND TO ALTITUDE

ZENITH ANGLE OF PATH OF SIGHT (DEGREES)

ALTITUDE METERS	93	95	100	105	120	150	180
305							
610							
914							
1219							
1524							

FLIGHT NO. 99      FILTER NO. 5

DIRECTIONAL PATH REFLECTANCE FROM GROUND TO ALTITUDE

ZENITH ANGLE OF PATH OF SIGHT (DEGREES)

ALTITUDE METERS	93	95	100	105	120	150	180
305	1.010E-01	5.319E-02	3.235E-02	2.444E-02	1.155E-02	6.341E-03	5.499E-03
610	3.071E-01	1.885E-01	8.291E-02	5.208E-02	2.411E-02	1.305E-02	1.125E-02
914	7.639E-01	2.273E-01	1.347E-01	8.267E-02	3.726E-02	1.968E-02	1.698E-02
1219	1.199E-00	5.002E-01	1.973E-01	1.196E-01	5.272E-02	2.737E-02	2.354E-02
1524	1.980E-00	7.478E-01	2.700E-01	1.657E-01	7.174E-02	3.679E-02	3.148E-02

AZIMUTH OF PATH OF SIGHT = 180								
FLIGHT NO. 99      FILTER NO. 1								
DIRECTIONAL PATH REFLECTANCE FROM GROUND TO ALTITUDE								
ALTITUDE	ZENITH ANGLE OF PATH OF SIGHT (DEGREES)							
METERS	93	95	100	105	120	150	180	
305	2.181E-01	1.128E-01	5.372E-02	3.560E-02	1.840E-02	9.157E-03	6.519E-03	
610	5.957E-01	2.853E-01	1.283E-01	8.365E-02	4.286E-02	2.094E-02	1.478E-02	
914	1.169E-00	5.122E-01	2.159E-01	1.376E-01	6.872E-02	3.393E-02	2.427E-02	
1219	2.192E-00	8.514E-01	3.322E-01	2.061E-01	9.988E-02	4.990E-02	3.594E-02	
1524	3.963E-00	1.326E-00	4.754E-01	2.869E-01	1.352E-01	6.811E-02	4.904E-02	

FLIGHT NO. 99      FILTER NO. 2								
DIRECTIONAL PATH REFLECTANCE FROM GROUND TO ALTITUDE								
ALTITUDE	ZENITH ANGLE OF PATH OF SIGHT (DEGREES)							
METERS	93	95	100	105	120	150	180	
305	1.57E-01	8.308E-02	4.022E-02	2.679E-02	1.387E-02	7.024E-03	5.089E-03	
610	3.726E-01	1.866E-01	8.65E-02	5.652E-02	2.868E-02	1.430E-02	1.037E-02	
914	8.623E-01	3.949E-01	1.703E-01	1.088E-01	5.397E-02	2.714E-02	1.968E-02	
1219	1.798E-00	6.954E-01	2.771E-01	1.724E-01	8.302E-02	4.193E-02	3.051E-02	
1524	2.790E-00	1.020E-00	3.628E-01	2.336E-01	1.106E-01	5.651E-02	4.098E-02	

FLIGHT NO. 99      FILTER NO. 3								
DIRECTIONAL PATH REFLECTANCE FROM GROUND TO ALTITUDE								
ALTITUDE	ZENITH ANGLE OF PATH OF SIGHT (DEGREES)							
METERS	93	95	100	105	120	150	180	
305	1.007E-01	5.413E-02	2.687E-02	1.824E-02	9.852E-03	4.840E-03	3.321E-03	
610	2.214E-01	1.155E-01	5.567E-02	3.737E-02	2.022E-02	1.013E-02	6.837E-03	
914	3.897E-01	1.950E-01	9.032E-02	5.959E-02	3.151E-02	1.602E-02	1.105E-02	
1219	6.747E-01	3.165E-01	1.389E-01	8.961E-02	4.583E-02	2.360E-02	1.671E-02	
1524	9.913E-01	4.356E-01	1.842E-01	1.173E-01	5.914E-02	3.107E-02	2.193E-02	

FLIGHT NO. 99      FILTER NO. 4								
DIRECTIONAL PATH REFLECTANCE FROM GROUND TO ALTITUDE								
ALTITUDE	ZENITH ANGLE OF PATH OF SIGHT (DEGREES)							
METERS	93	95	100	105	120	150	180	
305								
610								
914								
1219								
1524								

FLIGHT NO. 99      FILTER NO. 5								
DIRECTIONAL PATH REFLECTANCE FROM GROUND TO ALTITUDE								
ALTITUDE	ZENITH ANGLE OF PATH OF SIGHT (DEGREES)							
METERS	93	95	100	105	120	150	180	
305	1.614E-01	8.455E-02	4.076E-02	2.711E-02	1.413E-02	7.373E-03	5.499E-03	
610	3.885E-01	1.97E-01	8.803E-02	5.751E-02	2.936E-02	1.524E-02	1.125E-02	
914	6.977E-01	3.27E-01	1.401E-01	8.969E-02	4.462E-02	2.308E-02	1.698E-02	
1219	1.156E-00	4.91E-01	2.021E-01	1.268E-01	6.153E-02	3.192E-02	2.354E-02	
1524	1.893E-00	7.275E-01	2.815E-01	1.729E-01	8.191E-02	4.251E-02	3.148E-02	

AZIMUTH OF PATH OF SIGHT = 270

		FLIGHT NO. 99		FILTER NO. 1					
		DIRECTIONAL PATH REFLECTANCE FROM GROUND TO ALTITUDE		ZENITH ANGLE OF PATH OF SIGHT (DEGREES)					
ALTITUDE	METERS	93	95	100	105	120	150	180	
305		2.052E-01	1.045E-01	4.786E-02	3.050E-02	1.429E-02	7.628E-03	6.519E-02	
610		5.927E-01	2.607E-01	1.125E-01	7.048E-02	3.259E-02	1.736E-02	1.478E-02	
914		1.111E-00	4.757E-01	1.940E-01	1.191E-01	5.403E-02	2.859E-02	2.427E-02	
1219		2.123E-00	8.103E-01	2.043E-01	1.823E-01	8.080E-02	4.236E-02	3.594E-02	
1524		3.878E-00	1.276E-00	4.409E-01	2.575E-01	1.114E-01	5.777E-02	4.904E-02	

		FLIGHT NO. 99		FILTER NO. 2					
		DIRECTIONAL PATH REFLECTANCE FROM GROUND TO ALTITUDE		ZENITH ANGLE OF PATH OF SIGHT (DEGREES)					
ALTITUDE	METERS	93	95	100	105	120	150	180	
305		1.540E-01	7.982E-02	3.705E-02	2.368E-02	1.111E-02	5.939E-03	5.085E-02	
610		3.609E-01	1.781E-01	7.921E-02	4.996E-02	2.311E-02	1.220E-02	1.037E-02	
914		8.471E-01	3.819E-01	1.587E-01	9.786E-02	4.426E-02	2.317E-02	1.968E-02	
1219		1.692E-00	6.826E-01	2.629E-01	1.581E-01	6.962E-02	3.595E-02	3.051E-02	
1524		2.803E-00	1.007E-00	3.646E-01	2.154E-01	9.341E-02	4.813E-02	4.098E-02	

		FLIGHT NO. 99		FILTER NO. 3					
		DIRECTIONAL PATH REFLECTANCE FROM GROUND TO ALTITUDE		ZENITH ANGLE OF PATH OF SIGHT (DEGREES)					
ALTITUDE	METERS	93	95	100	105	120	150	180	
305		9.911E-02	5.211E-02	2.445E-02	1.568E-02	7.360E-03	3.894E-03	3.321E-03	
610		2.119E-01	1.084E-01	4.973E-02	3.174E-02	1.495E-02	8.028E-03	6.837E-03	
914		3.317E-01	1.373E-01	5.279E-02	5.219E-02	2.425E-02	1.298E-02	1.105E-02	
1219		6.782E-01	3.116E-01	1.310E-01	8.107E-02	3.686E-02	1.957E-02	1.671E-02	
1524		9.967E-01	4.305E-01	1.747E-01	1.069E-01	4.822E-02	2.563E-02	2.193E-02	

		FLIGHT NO. 99		FILTER NO. 4					
		DIRECTIONAL PATH REFLECTANCE FROM GROUND TO ALTITUDE		ZENITH ANGLE OF PATH OF SIGHT (DEGREES)					
ALTITUDE	METERS	93	95	100	105	120	150	180	
305									
610									
914									
1219									
1524									

		FLIGHT NO. 99		FILTER NO. 5					
		DIRECTIONAL PATH REFLECTANCE FROM GROUND TO ALTITUDE		ZENITH ANGLE OF PATH OF SIGHT (DEGREES)					
ALTITUDE	METERS	93	95	100	105	120	150	180	
305		1.553E-01	7.017E-02	3.722E-02	2.392E-02	1.150E-02	6.385E-03	5.499E-03	
610		3.777E-01	1.837E-01	7.128E-02	5.133E-02	2.409E-02	1.310E-02	1.125E-02	
914		6.835E-01	3.111E-01	1.306E-01	8.112E-02	3.718E-02	1.985E-02	1.698E-02	
1219		1.145E-00	4.799E-01	1.914E-01	1.166E-01	5.740E-02	2.762E-02	2.354E-02	
1524		1.893E-00	7.105E-01	2.671E-01	1.612E-01	7.104E-02	3.700E-02	3.148E-02	

#### FLIGHT 100I

Moonlight. This flight was made approximately 60 km east of Khorat. The terrain was relatively flat and consisted of deciduous trees and rice paddies. During this season (dry season) the tree foliage was sparse, dry, and yellowed and the rice paddies between the trees were dry. There were a few artificial ground lights. The atmosphere was hazy near the ground, with no clouds except a thunderstorm toward the east. Data-taking started at 2038 local time and continued until 2144. The moon phase angle was  $11^\circ$ ; the moon zenith angle during sky radiance data-taking was  $67^\circ$  at the start and  $53^\circ$  at the end.

FLIGHT NO. 1001				FILTER NO. 1			
IRRADIANCE (WATTS/SQ.M. MICRO M.)							
ALTITUDE (METERS)	DOWN- WELLING	UP- WELLING	ALBEDO	SCALAR DOWNWELLING	SCALAR UPWELLING	SCALAR TOTAL	SCALAR ALBEDO
217	5.577E-04	7.677E-05	.066	1.080E-03	1.109E-04	1.191E-03	.103
536	6.537E-04	5.241E-05	.060	1.230E-03	1.496E-04	1.385E-03	.121
839	6.255E-04	5.343E-05	.065	1.427E-03	2.182E-04	1.645E-03	.153
1124	9.855E-04	9.502E-05	.090	1.924E-03	3.264E-04	2.250E-03	.170

FLIGHT NO. 1001				FILTER NO. 2			
IRRADIANCE (WATTS/SQ.M. MICRO M.)							
ALTITUDE (METERS)	DOWN- WELLING	UP- WELLING	ALBEDO	SCALAR DOWNWELLING	SCALAR UPWELLING	SCALAR TOTAL	SCALAR ALBEDO
217	3.977E-04	4.080E-05	.104	7.283E-04	1.035E-04	8.318E-04	.142
536	7.028E-04	7.435E-05	.106	1.404E-03	1.962E-04	1.601E-03	.140
840	2.332E-04	2.453E-05	.105	4.968E-04	9.100E-05	5.898E-04	.187
1140	7.040E-04	1.061E-04	.151	1.468E-03	3.068E-04	1.775E-03	.209

FLIGHT NO. 1001				FILTER NO. 3			
IRRADIANCE (WATTS/SQ.M. MICRO M.)							
ALTITUDE (METERS)	DOWN- WELLING	UP- WELLING	ALBEDO	SCALAR DOWNWELLING	SCALAR UPWELLING	SCALAR TOTAL	SCALAR ALBEDO
222	5.844E-04	7.395E-05	.127	1.296E-03	1.841E-04	1.480E-03	.142
536	4.109E-04	6.328E-05	.154	9.616E-04	1.822E-04	1.144E-03	.189
839	5.150E-04	6.223E-05	.121	1.017E-03	1.647E-04	1.182E-03	.162
1141	9.374E-04	1.523E-04	.162	1.896E-03	3.668E-04	2.263E-03	.193

FLIGHT NO. 1001				FILTER NO. 4			
IRRADIANCE (WATTS/SQ.M. MICRO M.)							
ALTITUDE (METERS)	DOWN- WELLING	UP- WELLING	ALBEDO	SCALAR DOWNWELLING	SCALAR UPWELLING	SCALAR TOTAL	SCALAR ALBEDO
222	3.792E-04	1.288E-04	.340	6.327E-04	1.861E-04	1.219E-03	.464
537	1.184E-04	3.701E-05	.313	2.874E-04	9.708E-05	3.845E-04	.338
839	5.758E-04	1.966E-04	.341	1.759E-03	4.418E-04	1.700E-03	.351
1141	1.023E-03	2.732E-04	.267	2.049E-03	5.892E-04	2.638E-03	.286

FLIGHT NO. 1001				FILTER NO. 5			
IRRADIANCE (WATTS/SQ.M. MICRO M.)							
ALTITUDE (METERS)	DOWN- WELLING	UP- WELLING	ALBEDO	SCALAR DOWNWELLING	SCALAR UPWELLING	SCALAR TOTAL	SCALAR ALBEDO
222	6.374E-04	5.742E-05	.090	1.276E-03	1.471E-04	1.423E-03	.115
536	4.421E-04	4.920E-05	.111	6.895E-04	1.327E-04	1.022E-03	.149
838	9.057E-04	1.097E-04	.121	1.851E-03	3.357E-04	2.187E-03	.161
1140	1.100E-03	1.191E-04	.108	2.123E-03	3.256E-04	2.449E-03	.153

FLIGHT NO. 1001					
AZIMUTH OF PATH OF SIGHT = 0					
DIRECTIONAL REFLECTANCE OF BACKGROUND					
ZENITH	FILTERS				
ANGLE	1	2	5	3	4
93	.51936	.40561	.32480	.62720	.92567
95	.35092	.23553	.30055	.35719	.80709
100	.17513	.14347	.17144	.17439	4.51987
105	.10250	.11111	.15869	.13945	1.71320
120	.07396	.14633	.08014	.10084	.19993
150	.04740	.07564	.06058	.09830	.19546
180	.05998	.09900	.08944	.15199	.14412

FLIGHT NO. 1001					
AZIMUTH OF PATH OF SIGHT = 90					
DIRECTIONAL REFLECTANCE OF BACKGROUND					
ZENITH	FILTERS				
ANGLE	1	2	5	3	4
93	.19976	.30982	.29265	.31088	.66620
95	.15152	.23147	.20511	.20183	.53755
100	.11253	.11866	.14449	.13656	.42925
105	.08797	.10079	.11462	.10983	.62746
120	.05443	.09315	.07289	.10733	.28876
150	.04373	.07916	.05991	.07975	.20835
180	.05998	.09906	.08944	.15199	.14412

FLIGHT NO. 1001					
AZIMUTH OF PATH OF SIGHT = 120					
DIRECTIONAL REFLECTANCE OF BACKGROUND					
ZENITH	FILTERS				
ANGLE	1	2	5	3	4
93	.17700	.23897	.27280	.19670	.76201
95	.12094	.18129	.21410	.14249	.74966
100	.11569	.11189	.12709	.17308	.75315
105	.10920	.09781	.13591	.18001	.79572
120	.06131	.13665	.10628	.15211	.28366
150	.04826	.07845	.06787	.15300	.16708
180	.05998	.09906	.08944	.15199	.14412

FLIGHT NO. 1001					
AZIMUTH OF PATH OF SIGHT = 270					
DIRECTIONAL REFLECTANCE OF BACKGROUND					
ZENITH	FILTERS				
ANGLE	1	2	5	3	4
93	.25143	.26573	.27297	.28802	.64223
95	.14632	.16594	.15017	.16630	.63716
100	.09753	.11668	.10061	.11541	.60842
105	.09518	.11339	.09015	.13473	.42595
120	.05798	.11037	.08731	.17013	.25857
150	.05167	.07856	.06735	.10012	.18419
180	.05998	.09906	.08944	.15199	.14412



#### FLIGHT 100 II

Overcast moonlight. This flight was a continuation of Flight 100 I, after the formation of a cloud overcast and in the same area approximately 60 km east of Khorat. The terrain was relatively flat and consisted of deciduous trees and rice paddies. During this season (dry season) the foliage was sparse, dry, and yellowed and the rice paddies among the trees were dry. There were a few artificial ground lights. There was a continuous cloud overcast at 1500 m. Data-taking started at 2149 LCT and terminated at 2221. The moon was completely obscured by the overcast.

DATE 40369 FLIGHT NO. 10011 GROUND LEVEL ALTITUDE 231 IUP=1

ALTITUDE (METERS)	FILTER	TOTAL SCATTERING COEFFICIENT (PER METER)	
0	1.611E-04	1.305E-04	9.942E-05
30	1.611E-04	1.361E-04	9.909E-05
61	1.610E-04	1.350E-04	9.876E-05
91	1.605E-04	1.352E-04	9.843E-05
122	1.599E-04	1.347E-04	9.810E-05
152	1.594E-04	1.340E-04	9.777E-05
183	1.589E-04	1.330E-04	9.745E-05
213	1.583E-04	1.334E-04	9.712E-05
244	1.564E-04	1.328E-04	9.508E-05
274	1.563E-04	1.316E-04	9.430E-05
305	1.572E-04	1.327E-04	9.402E-05
335	1.571E-04	1.331E-04	9.445E-05
366	1.571E-04	1.335E-04	9.385E-05
396	1.575E-04	1.325E-04	9.321E-05
427	1.553E-04	1.335E-04	9.249E-05
457	1.557E-04	1.340E-04	9.192E-05
488	1.564E-04	1.339E-04	9.255E-05
518	1.565E-04	1.352E-04	9.193E-05
549	1.570E-04	1.367E-04	9.298E-05
579	1.568E-04	1.390E-04	9.361E-05
610	1.599E-04	1.406E-04	9.285E-05
640	1.594E-04	1.403E-04	9.298E-05
671	1.610E-04	1.417E-04	9.090E-05
701	1.610E-04	1.399E-04	8.976E-05
732	1.604E-04	1.374E-04	8.772E-05
762	1.608E-04	1.374E-04	8.711E-05
792	1.608E-04	1.340E-04	8.861E-05
823	1.610E-04	1.342E-04	8.773E-05
853	1.629E-04	1.336E-04	8.863E-05
884	1.637E-04	1.331E-04	8.897E-05
914	1.645E-04	1.316E-04	8.833E-05
945	1.620E-04	1.320E-04	8.761E-05
975	1.612E-04	1.325E-04	8.714E-05
1006	1.624E-04	1.332E-04	8.898E-05
1036	1.612E-04	1.320E-04	9.175E-05
1067	1.637E-04	1.313E-04	9.115E-05
1097	1.659E-04	1.320E-04	9.136E-05
1128	1.637E-04	1.323E-04	9.193E-05
1158	1.612E-04	1.351E-04	9.235E-05
1189	1.605E-04	1.439E-04	9.407E-05
1219	1.613E-04	1.451E-04	9.355E-05
1250	1.603E-04	1.492E-04	9.646E-05
1280	1.507E-04	1.517E-04	9.535E-05
1311	1.510E-04	1.555E-04	9.756E-05
1341	1.577E-04	1.546E-04	9.570E-05
1372	1.527E-04	1.541E-04	9.538E-05
1402	1.562E-04	1.530E-04	9.507E-05
1433	1.577E-04	1.531E-04	9.475E-05
1463	1.571E-04	1.520E-04	9.443E-05
1494	1.566E-04	1.521E-04	9.412E-05
1524	1.561E-04	1.514E-04	9.381E-05
1554	1.556E-04	1.511E-04	9.349E-05
1585	1.551E-04	1.508E-04	9.318E-05
1615	1.545E-04	1.501E-04	9.287E-05
1646	1.540E-04	1.496E-04	9.256E-05
1676	1.535E-04	1.491E-04	9.226E-05
1707	1.530E-04	1.486E-04	9.195E-05
1737	1.525E-04	1.481E-04	9.164E-05
1768	1.520E-04	1.476E-04	9.134E-05
1798	1.515E-04	1.471E-04	9.103E-05
1829	1.510E-04	1.466E-04	9.073E-05
			1.410E-04
			1.405E-04
			1.400E-04
			1.396E-04
			1.391E-04
			1.386E-04
			1.382E-04
			1.377E-04
			1.371E-04
			1.381E-04
			1.347E-04
			1.348E-04
			1.343E-04
			1.322E-04
			1.302E-04
			1.298E-04
			1.279E-04
			1.279E-04
			1.271E-04
			1.274E-04
			1.271E-04
			1.285E-04
			1.272E-04
			1.276E-04
			1.280E-04
			1.249E-04
			1.251E-04
			1.264E-04
			1.270E-04
			1.314E-04
			1.345E-04
			1.334E-04
			1.303E-04
			1.299E-04
			1.299E-04
			1.308E-04
			1.287E-04
			1.283E-04
			1.294E-04
			1.311E-04
			1.299E-04
			1.313E-04
			1.315E-04
			1.340E-04
			1.389E-04
			1.388E-04
			1.383E-04
			1.379E-04
			1.374E-04
			1.370E-04
			1.365E-04
			1.361E-04
			1.356E-04
			1.352E-04
			1.347E-04
			1.343E-04
			1.338E-04
			1.334E-04
			1.329E-04
			1.325E-04
			1.320E-04
			1.316E-04

FIRST DATA ALT.

LAST DATA ALT.

		FLIGHT NO. 100 II		FILTER NO. 1				
		BEAM TRANSMITTANCE FROM GROUND TO ALTITUDE		ZENITH ANGLE OF PATH OF SIGHT (DEGREES)				
ALTITUDE								
METERS		75	95	100	105	120	150	180
305		.3919001	.5726698	.7559442	.8288496	.9074024	.9454439	.9525767
610		.1533638	.3309477	.5740668	.6890994	.8246858	.8946830	.9081227
914		.0573820	.1902021	.4324410	.5698154	.7474097	.8452771	.8645286
1219		.0209148	.1085901	.3250884	.4705325	.6768928	.7982715	.8227350
1524		.0076404	.0611961	.2460620	.3903342	.6144860	.7549138	.7838916

		FLIGHT NO. 100 II		FILTER NO. 2				
		BEAM TRANSMITTANCE FROM GROUND TO ALTITUDE		ZENITH ANGLE OF PATH OF SIGHT (DEGREES)				
ALTITUDE	METERS	75	95	100	105	120	150	180
305		.4544435	.6253797	.7901007	.8537931	.9214367	.9538589	.9599150
610		.2027344	.3701113	.6234662	.7283412	.8486708	.9096150	.9217333
914		.0801337	.2418476	.4904486	.6200282	.7808080	.8668828	.8836334
1219		.0352766	.1511682	.3874031	.5292834	.7194002	.8268408	.8481746
1524		.0146222	.0886345	.2764319	.4422840	.6555434	.7836368	.8096564

		FLIGHT NO. 100 II		FILTER NO. 3			
		BEAM TRANSMITTANCE FROM GROUND TO ALTITUDE		ZENITH ANGLE OF PATH OF SIGHT (DEGREES)			
ALTITUDE							
METERS.	75	95	100	105	120	150	180
305	.5645945	.7116177	.8430264	.8917538	.9424209	.9663407	.9707837
610	.3234360	.5139618	.7180005	.7992041	.8904549	.9352085	.9436392
914	.1871948	.3758377	.6119109	.7192554	.8431747	.9062093	.9132455
1219	.1084026	.2736299	.5218035	.6463507	.7977947	.8777217	.8931935
1524	.0552191	.1961081	.4414652	.5777662	.7279000	.8487848	.8676347

		FLIGHT NO. 100 II		FILTER NO. 4				
		BEAM TRANSMITTANCE FROM GROUND TO ALTITUDE		ZENITH ANGLE OF PATH OF SIGHT (DEGREES)				
ALTITUDE	METERS	93	95	100	105	120	150	180
	305							
	610							
	914							
	1219							
	1524							

		FLIGHT NO. 100 II		FILTER NO. 5			
		BEAM TRANSMITTANCE FROM GROUND TO ALTITUDE		ZENITH ANGLE OF PATH OF SIGHT (DEGREES)			
ALTITUDE							
METERS	93	95	100	105	120	150	180
305	.4427254	.6157301	.7679583	.8493340	.9189425	.9523674	.9585149
610	.2029096	.3904553	.6237429	.7285580	.8488016	.9096959	.9213041
914	.0930324	.2498298	.4985074	.6268453	.7852401	.8697204	.8861377
1219	.0413194	.1583015	.3964729	.5375655	.7252054	.8306865	.8515899
1524	.0174317	.0982448	.3120545	.4577903	.6673414	.7917486	.8169097

#### FLIGHT 101

Starlight before moonrise. This flight was made over the Gulf of Siam, approximately 95 km south of Rayong, where the depth of the water was 60 m (33 fm). The sky was free of clouds but the atmosphere was very hazy at low altitudes, presumably because of an offshore (north) wind. Data-taking started at 2030 LCT and ended at 2140.

FLIGHT NO. 101				FILTER NO. 1		IRRADIANCE(WATTS/SQ.M. MICRO M.)		SCALAR TOTAL	SCALAR ALBEDO
ALTITUDE (METERS)	DOWN- WELLING	UP- WELLING	ALBEDO	SCALAR DOWNWELLING	SCALAR UPWELLING				
164									
484									
782									
1085									
1399									
1703									

FLIGHT NO. 101				FILTER NO. 2					
IRRADIANCE(WATTS/SQ.M. MICRO M.)									
ALTITUDE (METERS)	DOWN-	UP-	ALBEDO	SCALAR		SCALAR TOTAL	SCALAR ALBEDO		
	WELLING	WELLING		DOWNWELLING	UPWELLING				
164	6.432E-06	9.138E-07	.142	1.206E-05	3.176E-06	1.523E-05	.263		
484	6.954E-06	9.639E-07	.139	1.293E-05	3.198E-06	1.612E-05	.247		
783	7.092E-06	1.059E-06	.149	1.327E-05	3.478E-06	1.674E-05	.262		
1085	7.204E-06	1.183E-06	.164	1.399E-05	4.005E-06	1.799E-05	.236		
1399	7.654E-06	1.414E-06	.185	1.474E-05	4.471E-06	1.921E-05	.303		
1718	7.381E-06	1.509E-06	.204	1.444E-05	4.982E-06	1.942E-05	.345		

FLIGHT NO. 101				FILTER NO. 3		IRRADIANCE(WATTS/SQ.M. MICRO M.)		SCALAR TOTAL	SCALAR ALBEDO
ALTITUDE (METERS)	DOWN- WELLING	UP- WELLING	ALBEDO	SCALAR DOWNWELLING	SCALAR UPWELLING				
164									
484									
782									
1085									
1399									
1713									

FLIGHT NO. 101				FILTER NO. 5					
IRRADIANCE(WATTS/SQ.M. MICRO M.)									
ALTITUDE (METERS)	DOWN- WELLING	UP- WELLING	ALBEDO	SCALAR DOWNWELLING	SCALAR UPWELLING	SCALAR TOTAL	SCALAR ALBEDO		
164	9.576E-06	9.016E-07	.094	1.837E-05	3.049E-06	2.142E-05		.166	
483	1.000E-05	1.012E-06	.101	1.932E-05	3.466E-06	2.279E-05		.179	
783	1.063E-05	1.151E-06	.108	2.073E-05	4.017E-06	2.475E-05		.194	
1086	1.091E-05	1.304E-06	.119	2.182E-05	4.376E-06	2.619E-05		.201	
1399	1.139E-05	1.658E-06	.146	2.303E-05	5.166E-06	2.820E-05		.224	
1719	1.119E-05	1.502E-06	.134	2.239E-05	4.911E-06	2.750E-05		.217	

FLIGHT NO. 101		DIFFUSIONAL REFLECTANCE OF BACKGROUND		FILTERS	
ZENITH ANGLE	2	5	3	4	
93		.42585			
95		.37385			
100		.29002			
105		.22363			
120		.10632			
150		.05081			
180		.04945			

DATE 40669 FLIGHT NO. 101 GROUND LEVEL ALTITUDE (M.)= 9 IUP-1

ALTITUDE (METERS)	TOTAL SCATTERING COEFFICIENT (PER METER)			
	FILTERS 1	2	3	4
0	4.447E-05	3.603E-05	2.556E-05	4.034E-05
30	4.432E-05	3.591E-05	2.547E-05	4.021E-05
61	4.417E-05	3.579E-05	2.539E-05	4.008E-05
91	4.403E-05	3.567E-05	2.530E-05	3.994E-05
122	4.388E-05	3.555E-05	2.522E-05	3.981E-05
152	4.373E-05	3.543E-05	2.514E-05	3.968E-05
183	4.359E-05	3.531E-05	2.505E-05	3.954E-05
213	4.441E-05	3.596E-05	2.481E-05	3.923E-05
244	4.460E-05	3.667E-05	2.462E-05	3.888E-05
274	4.488E-05	3.622E-05	2.476E-05	3.941E-05
305	4.422E-05	3.717E-05	2.503E-05	3.979E-05
335	4.500E-05	3.719E-05	2.498E-05	3.965E-05
366	4.520E-05	3.651E-05	2.506E-05	3.945E-05
396	4.506E-05	3.779E-05	2.517E-05	4.028E-05
427	4.502E-05	3.756E-05	2.504E-05	4.094E-05
457	4.490E-05	3.754E-05	2.535E-05	4.223E-05
488	4.543E-05	3.809E-05	2.519E-05	4.193E-05
518	4.572E-05	3.872E-05	2.511E-05	4.061E-05
549	4.747E-05	3.944E-05	2.512E-05	4.043E-05
579	4.693E-05	4.028E-05	2.530E-05	4.031E-05
610	4.690E-05	4.066E-05	2.534E-05	4.001E-05
640	5.003E-05	4.186E-05	2.513E-05	4.067E-05
671	5.094E-05	4.285E-05	2.507E-05	4.243E-05
701	5.058E-05	4.294E-05	2.544E-05	4.402E-05
732	4.976E-05	4.292E-05	2.559E-05	4.369E-05
762	4.923E-05	4.266E-05	2.577E-05	4.276E-05
792	4.963E-05	4.294E-05	2.541E-05	4.421E-05
823	5.030E-05	4.232E-05	2.574E-05	4.330E-05
853	4.945E-05	4.218E-05	2.567E-05	4.419E-05
884	5.015E-05	4.228E-05	2.533E-05	4.459E-05
914	5.132E-05	4.261E-05	2.613E-05	4.363E-05
945	5.336E-05	4.277E-05	2.626E-05	4.315E-05
975	5.508E-05	4.264E-05	2.677E-05	4.414E-05
1006	5.498E-05	4.481E-05	2.674E-05	4.443E-05
1036	5.590E-05	4.511E-05	2.661E-05	4.508E-05
1067	5.597E-05	4.621E-05	2.700E-05	4.673E-05
1097	5.699E-05	4.550E-05	2.730E-05	4.651E-05
1128	5.814E-05	4.451E-05	2.726E-05	4.823E-05
1158	5.759E-05	4.291E-05	2.738E-05	4.903E-05
1189	5.574E-05	4.186E-05	2.743E-05	4.594E-05
1219	5.418E-05	4.228E-05	2.742E-05	4.323E-05
1250	5.213E-05	4.233E-05	2.757E-05	4.311E-05
1280	5.250E-05	4.178E-05	2.790E-05	4.330E-05
1311	5.256E-05	4.211E-05	2.737E-05	4.223E-05
1341	5.264E-05	4.230E-05	2.726E-05	4.232E-05
1372	5.342E-05	4.225E-05	2.756E-05	4.302E-05
1402	5.423E-05	4.211E-05	2.778E-05	4.350E-05
1433	5.409E-05	4.223E-05	2.772E-05	4.226E-05
1463	5.431E-05	4.190E-05	2.815E-05	4.238E-05
1494	5.428E-05	4.217E-05	2.798E-05	4.266E-05
1524	5.406E-05	4.210E-05	2.829E-05	4.300E-05
1554	5.433E-05	4.175E-05	2.840E-05	4.238E-05
1585	5.443E-05	4.146E-05	2.838E-05	4.172E-05
1615	5.316E-05	4.162E-05	2.800E-05	4.137E-05
1646	5.058E-05	4.248E-05	2.797E-05	4.154E-05
1676	4.986E-05	4.096E-05	2.810E-05	4.218E-05
1707	4.680E-05	4.082E-05	2.862E-05	4.141E-05
1737	4.614E-05	4.069E-05	2.853E-05	4.177E-05
1768	4.593E-05	4.055E-05	2.843E-05	4.114E-05
1798	4.583E-05	4.042E-05	2.834E-05	4.100E-05
1829	4.568E-05	4.029E-05	2.824E-05	4.086E-05

FIRST DATA ALT. 7 7 7 6 7  
LAST DATA ALT. 58 58 57 57 57

FLIGHT NO. 101		FILTER NO. 1						
BEAM TRANSMITTANCE FROM GROUND TO ALTITUDE								
ALTITUDE	ZENITH ANGLE OF PATH OF SIGHT (DEGREES)							
METERS	93	95	100	105	120	150	180	
305	.7713081	.8567960	.9253595	.9492856	.9734189	.9845661	.9866199	
610	.5870489	.7303473	.8540909	.8995895	.9466983	.9688706	.9729842	
914	.4335147	.6133532	.7824379	.8482285	.9183231	.9519967	.9582918	
1219	.3075381	.5047046	.7094985	.7943275	.8876382	.9334994	.9421455	
1524	.2196428	.4186857	.6459847	.7458872	.8591931	.9161093	.9269767	

FLIGHT NO. 101		FILTER NO. 2						
BEAM TRANSMITTANCE FROM GROUND TO ALTITUDE								
ALTITUDE	ZENITH ANGLE OF PATH OF SIGHT (DEGREES)							
METERS	93	95	100	105	120	150	180	
305	.8097851	.8819827	.9389141	.9585924	.9783473	.9874410	.9891144	
610	.6445114	.7716776	.8780171	.9164201	.9558259	.9742528	.9776635	
914	.4978369	.6649560	.8148131	.8716188	.9313494	.9597676	.9650624	
1219	.3794349	.5701570	.7542776	.8276231	.9067071	.9450256	.9522117	
1524	.2907113	.4920002	.7004777	.7875374	.8837024	.9311074	.9400544	

FLIGHT NO. 101		FILTER NO. 3					
BEAM TRANSMITTANCE FROM GROUND TO ALTITUDE							
ALTITUDE	ZENITH ANGLE OF PATH OF SIGHT (DEGREES)						
METERS	93	95	100	105	120	150	180
305	.8628454	.9159453	.9568898	.9708671	.9848122	.9912030	.9923770
610	.7423617	.8388526	.9155816	.9425440	.9698343	.9824712	.9848017
914	.6351775	.7670170	.8753515	.9145528	.9548171	.9736591	.9771474
1219	.5374697	.6979833	.8348804	.8859634	.9392482	.9644612	.9691482
1524	.4514159	.6336309	.7953160	.8575700	.9235445	.9551181	.9610122

FLIGHT NO. 101		FILTER NO. 5						
BEAM TRANSMITTANCE FROM GROUND TO ALTITUDE								
ALTITUDE	ZENITH ANGLE OF PATH OF SIGHT (DEGREES)							
METERS	93	95	100	105	120	150	180	
305	.7918212	.8702927	.9326473	.9542951	.9760745	.9861160	.9879648	
610	.6212629	.7551890	.8685502	.9097791	.9522340	.9721374	.9758248	
914	.4778621	.6493716	.8051718	.8646857	.9275032	.9574797	.9630697	
1219	.3605545	.5537086	.7432763	.8195048	.9020923	.9422456	.9497654	
1524	.2749407	.4767476	.6694929	.7792299	.8788646	.9281611	.9374778	

FLIGHT NO. 101		FILTER NO. 1						
PATH RADIANCE FROM GROUND TO ALTITUDE (WATTS/STER.SQ.M MICRO M.)		ZENITH ANGLE OF PATH OF SIGHT (DEGREES)						
ALTITUDE		93	95	100	105	120	150	180
METERS								
305								
610								
914								
1219								
1524								

FLIGHT NO. 101		FILTER NO. 2						
PATH RADIANCE FROM GROUND TO ALTITUDE (WATTS/STER.SQ.M MICRO M.)		ZENITH ANGLE OF PATH OF SIGHT (DEGREES)						
ALTITUDE		93	95	100	105	120	150	180
METERS								
305	2.318E-07	1.419E-07	7.099E-08	4.649E-08	2.204E-08	1.115E-08	9.210E-09	
610	4.431E-07	2.806E-07	1.449E-07	9.598E-08	4.612E-08	2.361E-08	1.958E-08	
914	6.447E-07	4.234E-07	2.258E-07	1.512E-07	7.346E-08	3.777E-08	3.135E-08	
1219	8.339E-07	5.664E-07	3.113E-07	2.106E-07	1.030E-07	5.276E-08	4.367E-08	
1524	9.959E-07	6.967E-07	3.937E-07	2.690E-07	1.328E-07	6.789E-08	5.605E-08	

FLIGHT NO. 101		FILTER NO. 3						
PATH RADIANCE FROM GROUND TO ALTITUDE (WATTS/STER.SQ.M MICRO M.)		ZENITH ANGLE OF PATH OF SIGHT (DEGREES)						
ALTITUDE		93	95	100	105	120	150	180
METERS								
	305							
	610							
	914							
	1219							
	1524							

FLIGHT NO. 101		FILTER NO. 5						
PATH RADIANCE FROM GROUND TO ALTITUDE(WATTS/STER.SQ.M MICRO M.)		ZENITH ANGLE OF PATH OF SIGHT (DEGREES)						
ALTITUDE		93	95	100	105	120	150	180
METERS								
305	3.538E-07	2.168E-07	1.081E-07	7.042E-08	3.302E-08	1.669E-08	1.383E-08	
610	6.658E-07	4.229E-07	2.177E-07	1.435E-07	6.798E-08	3.445E-08	2.855E-08	
914	9.642E-07	6.343E-07	3.370E-07	2.243E-07	1.071E-07	5.419E-08	4.482E-08	
1219	1.243E-06	8.466E-07	4.640E-07	3.121E-07	1.503E-07	7.583E-08	6.258E-08	
1524	1.479E-06	1.037E-06	5.846E-07	3.972E-07	1.930E-07	9.728E-08	8.011E-08	



FLIGHT NO. 101		FILTER NO. 1						
DIRECTIONAL PATH REFLECTANCE FROM GROUND TO ALTITUDE		ZENITH ANGLE OF PATH OF SIGHT (DEGREES)						
ALTITUDE		93	95	100	105	120	150	180
METERS								
305								
610								
914								
1219								
1524								

FLIGHT NO. 101		FILTER NO. 2					
DIRECTIONAL PATH REFLECTANCE FROM GROUND TO ALTITUDE							
ALTITUDE	ZENITH ANGLE OF PATH OF SIGHT (DEGREES)						
METERS	93	95	100	105	120	150	180
305	1.398E-01	7.857E-02	3.693E-02	2.369E-02	1.100E-02	5.513E-03	4.548E-03
610	3.358E-01	1.776E-01	8.060E-02	5.115E-02	2.357E-02	1.184E-02	9.781E-03
914	6.325E-01	3.110E-01	1.354E-01	8.475E-02	3.853E-02	1.922E-02	1.587E-02
1219	1.073E 00	4.852E-01	2.016E-01	1.243E-01	5.550E-02	2.727E-02	2.240E-02
1524	1.673E 00	5.917E-01	2.745E-01	1.668E-01	7.337E-02	3.561E-02	2.912E-02

FLIGHT NO. 101		FILTER NO. 3						
DIRECTIONAL PATH REFLECTANCE FROM GROUND TO ALTITUDE		ZENITH ANGLE OF PATH OF SIGHT (DEGREES)						
ALTITUDE		73	95	100	105	120	150	180
METERS								
305								
610								
914								
1219								
1524								

FLIGHT NO. 101		FILTER NO. 5					
DIRECTIONAL PATH REFLECTANCE FROM GROUND TO ALTITUDE							
ALTITUDE	ZENITH ANGLE OF PATH OF SIGHT (DEGREES)						
METERS	93	95	100	105	120	150	180
305	1.466E-01	8.174E-02	3.801E-02	2.421E-02	1.110E-02	5.552E-03	4.593E-03
610	3.516E-01	1.837E-01	8.224E-02	5.173E-02	2.342E-02	1.163E-02	9.597E-03
914	6.620E-01	3.204E-01	1.373E-01	8.510E-02	3.789E-02	1.857E-02	1.527E-02
1219	1.131E 00	5.016E-01	2.048E-01	1.249E-01	5.465E-02	2.640E-02	2.162E-02
1524	1.765E 00	7.139E-01	2.781E-01	1.672E-01	7.205E-02	3.438E-02	2.883E-02

#### FLIGHT 102

Starlight before moonrise. The flight pattern was from 15 to 90 km south of Lop Buri. The terrain was flat, cultivated with rice paddies, and included small settlements. During this dry season the rice paddies were dry and other vegetation had lost its lush, green appearance. There were no clouds but the atmosphere was very hazy at low altitude, presumably from the burning off of stubble in the dried rice paddies. Data-taking started at 2034 and ended before moonrise at 2137.

FLIGHT NO. 102		FILTER NO. 1	
IRRADIANCE (WATTS/SQ.M. MICRO M.)			
ALTITUDE (METERS)	DOWN- WELLING	UP- WELLING	ALBEDO
147	7.437E-06	1.474E-06	.191
435	6.749E-06	1.234E-06	.133
757	6.997E-06	9.254E-07	.132
1059	6.771E-06	1.910E-06	.282
1361	6.879E-06	1.190E-06	.173
1670	6.811E-06	1.234E-06	.181
SCALAR		SCALAR	
DOWNWELLING		UPWELLING	
1.422E-05	5.893E-06	2.012E-05	.414
1.252E-05	4.527E-06	1.704E-05	.362
1.309E-05	3.046E-06	1.609E-05	.233
1.260E-05	5.054E-06	1.765E-05	.401
1.295E-05	4.104E-06	1.705E-05	.517
1.288E-05	4.066E-06	1.695E-05	.316

FLIGHT NO. 102		FILTER NO. 2	
IRRADIANCE (WATTS/SQ.M. MICRO M.)			
ALTITUDE (METERS)	DOWN- WELLING	UP- WELLING	ALBEDO
155	7.503E-06	1.753E-06	.234
436	7.117E-06	1.477E-06	.208
757	7.344E-06	1.888E-06	.257
1061	6.823E-06	3.077E-06	.450
1377	7.274E-06	1.653E-06	.232
1669	7.198E-06	2.192E-06	.305
SCALAR		SCALAR	
DOWNWELLING		UPWELLING	
1.442E-05	6.112E-06	2.054E-05	.424
1.355E-05	5.741E-06	1.929E-05	.424
1.403E-05	6.253E-06	2.028E-05	.446
1.245E-05	7.989E-06	2.094E-05	.617
1.399E-05	6.091E-06	2.008E-05	.435
1.387E-05	6.963E-06	2.083E-05	.502

FLIGHT NO. 102		FILTER NO. 3	
IRRADIANCE (WATTS/SQ.M. MICRO M.)			
ALTITUDE (METERS)	DOWN- WELLING	UP- WELLING	ALBEDO
154	1.169E-05	5.328E-06	.456
436	1.048E-05	4.135E-06	.395
757	1.091E-05	3.173E-06	.286
1061	1.102E-05	5.361E-06	.436
1368	1.173E-05	5.624E-06	.479
1669	1.075E-05	5.076E-06	.472
SCALAR		SCALAR	
DOWNWELLING		UPWELLING	
2.519E-05	2.020E-05	4.539E-05	.802
2.177E-05	1.526E-05	3.703E-05	.701
2.263E-05	1.088E-05	3.351E-05	.481
2.355E-05	1.886E-05	4.240E-05	.801
2.460E-05	1.863E-05	4.323E-05	.757
2.268E-05	1.679E-05	3.947E-05	.740

FLIGHT NO. 102		FILTER NO. 5	
IRRADIANCE (WATTS/SQ.M. MICRO M.)			
ALTITUDE (METERS)	DOWN- WELLING	UP- WELLING	ALBEDO
153	1.021E-05	2.646E-06	.259
435	1.033E-05	3.713E-06	.363
757	1.107E-05	1.925E-06	.174
1061	1.180E-05	6.057E-06	.513
1366	1.104E-05	3.128E-06	.283
1669	1.146E-05	3.789E-06	.331
SCALAR		SCALAR	
DOWNWELLING		UPWELLING	
1.994E-05	7.915E-06	2.786E-05	.397
2.026E-05	1.280E-05	3.306E-05	.632
2.180E-05	6.046E-06	2.785E-05	.277
2.344E-05	1.688E-05	4.056E-05	.713
2.190E-05	9.561E-06	3.146E-05	.436
2.325E-05	1.165E-05	3.489E-05	.501

FLIGHT NO. 102		FILTER NO. 5	
DIRECTIONAL REFLECTANCE OF BACKGROUND			
ZENITH ANGLE	1	2	3
93			
95			
100			
105			
120			
150			
180			

DATE 40709 FLIGHT NO. 102 GROUND LEVEL ALTITUDE (M.)= 38 IUP=1

ALTITUDE (METERS)	TOTAL SCATTERING COEFFICIENT (PER METER)				
	FILTER 1	2	3	4	5
0	6.400E-05	4.974E-05	3.098E-05		5.253E-05
30	6.479E-05	4.950E-05	3.666E-05		5.235E-05
61	6.358E-05	4.941E-05	3.674E-05		5.218E-05
91	6.337E-05	4.925E-05	3.602E-05		5.200E-05
122	6.316E-05	4.908E-05	3.649E-05		5.183E-05
152	6.295E-05	4.892E-05	3.637E-05		5.166E-05
183	6.274E-05	4.876E-05	3.534E-05		4.993E-05
213	6.497E-05	4.975E-05	3.440E-05		5.010E-05
244	6.000E-05	4.151E-05	3.500E-05		5.102E-05
274	6.075E-05	4.145E-05	3.522E-05		5.089E-05
305	6.059E-05	4.104E-05	3.420E-05		5.076E-05
335	6.079E-05	5.226E-05	3.375E-05		5.140E-05
366	6.759E-05	5.224E-05	3.409E-05		5.198E-05
396	6.784E-05	5.259E-05	3.339E-05		5.154E-05
427	6.070E-05	5.215E-05	3.256E-05		5.145E-05
457	6.693E-05	5.289E-05	3.267E-05		5.192E-05
488	6.869E-05	5.227E-05	3.193E-05		5.154E-05
518	6.739E-05	5.220E-05	3.090E-05		5.103E-05
549	6.726E-05	5.174E-05	3.022E-05		5.092E-05
579	6.736E-05	5.157E-05	3.076E-05		5.174E-05
610	6.847E-05	5.145E-05	3.105E-05		5.105E-05
640	7.074E-05	5.118E-05	3.143E-05		5.084E-05
671	6.909E-05	5.002E-05	3.443E-05		5.021E-05
701	6.970E-05	4.913E-05	3.436E-05		5.045E-05
732	6.852E-05	5.068E-05	3.263E-05		5.018E-05
762	6.791E-05	5.107E-05	3.247E-05		4.995E-05
792	6.724E-05	5.033E-05	2.350E-05		5.090E-05
823	6.758E-05	4.782E-05	3.117E-05		5.146E-05
853	6.055E-05	4.774E-05	3.372E-05		5.091E-05
884	6.881E-05	4.756E-05	3.419E-05		4.903E-05
914	7.021E-05	4.789E-05	3.466E-05		4.764E-05
945	7.100E-05	4.731E-05	3.384E-05		4.799E-05
975	6.790E-05	4.659E-05	3.392E-05		4.810E-05
1006	7.073E-05	4.663E-05	3.279E-05		4.786E-05
1036	7.123E-05	4.662E-05	3.016E-05		4.730E-05
1067	7.181E-05	4.691E-05	2.930E-05		4.760E-05
1097	7.265E-05	4.630E-05	2.914E-05		4.740E-05
1128	6.954E-05	4.715E-05	2.907E-05		4.728E-05
1158	6.653E-05	4.699E-05	2.894E-05		4.746E-05
1189	6.638E-05	4.630E-05	2.894E-05		4.679E-05
1219	6.543E-05	4.645E-05	2.876E-05		4.604E-05
1250	6.589E-05	4.658E-05	2.873E-05		4.541E-05
1280	6.551E-05	4.609E-05	2.903E-05		4.542E-05
1311	6.730E-05	4.591E-05	2.903E-05		4.517E-05
1341	6.797E-05	4.455E-05	2.895E-05		4.478E-05
1372	6.755E-05	4.541E-05	2.932E-05		4.537E-05
1402	6.777E-05	4.301E-05	2.966E-05		4.542E-05
1433	6.674E-05	4.223E-05	3.023E-05		4.497E-05
1463	6.565E-05	4.327E-05	3.063E-05		4.472E-05
1494	6.552E-05	4.137E-05	3.147E-05		4.414E-05
1524	6.547E-05	4.317E-05	3.168E-05		4.433E-05
1554	6.275E-05	4.367E-05	3.251E-05		4.301E-05
1585	6.245E-05	4.426E-05	3.236E-05		4.238E-05
1615	6.911E-05	4.637E-05	3.214E-05		4.348E-05
1646	6.784E-05	4.512E-05	3.190E-05		4.369E-05
1676	6.730E-05	4.497E-05	3.174E-05		4.389E-05
1707	6.797E-05	4.432E-05	3.174E-05		4.374E-05
1737	6.773E-05	4.467E-05	3.183E-05		4.360E-05
1768	6.799E-05	4.453E-05	3.153E-05		4.345E-05
1798	6.740E-05	4.434E-05	3.142E-05		4.331E-05
1829	6.721E-05	4.423E-05	3.132E-05		4.317E-05

FIRST DATA ALT. 7 7 5 7 7  
LAST DATA ALT. 27 5 46 55 56

FLIGHT NO. 102		FILTER NO. 1						
BEAM TRANSMITTANCE FROM GROUND TO ALTITUDE		ZENITH ANGLE OF PATH OF SIGHT (DEGREES)						
ALTITUDE METERS	93	95	100	105	120	150	180	
305	.6856867	.7988312	.6933906	.9271552	.9616053	.9776496	.9805148	
610	.4584288	.6311805	.7937706	.8564518	.9229209	.9547457	.9606877	
914	.3016732	.4962786	.7035284	.7698369	.8850371	.9319190	.9407641	
1219	.1958894	.3890266	.6225963	.7776592	.8482594	.9093603	.9210100	
1524	.1284038	.3082695	.5539737	.6728224	.8145443	.8883142	.9025211	

FLIGHT NO. 102		FILTER NO. 2						
BEAM TRANSMITTANCE FROM GROUND TO ALTITUDE		ZENITH ANGLE OF PATH OF SIGHT (DEGREES)						
ALTITUDE METERS	93	95	100	105	120	150	180	
305	.7461081	.8400143	.9162178	.9429833	.9700683	.9826080	.9849704	
610	.5459054	.6996909	.8359049	.8866926	.9396484	.9646984	.9693546	
914	.4033967	.5883237	.7662459	.8364109	.9116780	.9480134	.9548183	
1219	.3010738	.4993822	.7057332	.7914968	.8859994	.9325037	.9412754	
1524	.2270289	.4280340	.6531636	.7514543	.8625066	.9181474	.9287123	

FLIGHT NO. 102		FILTER NO. 3						
BEAM TRANSMITTANCE FROM GROUND TO ALTITUDE		ZENITH ANGLE OF PATH OF SIGHT (DEGREES)						
ALTITUDE METERS	93	95	100	105	120	150	180	
305	.8099668	.8821173	.9389260	.9586417	.9783734	.9874562	.9891276	
610	.6673804	.7879063	.8872368	.9228656	.9592997	.9762956	.9794385	
914	.5466788	.7028255	.8377824	.8880283	.9403808	.9651325	.9697323	
1219	.4510600	.6311367	.7937431	.8564318	.9229097	.9547390	.9606819	
1524	.3729544	.5687881	.7533681	.8269535	.9063273	.9447970	.9520122	

FLIGHT NO. 102		FILTER NO. 5						
BEAM TRANSMITTANCE FROM GROUND TO ALTITUDE		ZENITH ANGLE OF PATH OF SIGHT (DEGREES)						
ALTITUDE METERS	93	95	100	105	120	150	180	
305	.7394849	.8355882	.9137916	.9413072	.9691753	.9820857	.9844670	
610	.5435968	.6760110	.8348970	.8859752	.9392547	.9644650	.9691516	
914	.3998899	.5853676	.7643091	.8349919	.9108770	.9475324	.9543988	
1219	.2973636	.4958391	.7032156	.7896013	.8849004	.9318360	.9406915	
1524	.2249041	.4235503	.6497405	.7487943	.8609249	.9171749	.9278664	

FLIGHT NO. 102		FILTER NO. 1						
PATH RADIANCE FROM GROUND TO ALTITUDE (WATTS/STER.SQ.M MICRO M.)		ZENITH ANGLE OF PATH OF SIGHT (DEGREES)						
ALTITUDE METERS	93	95	100	105	120	150	180	
305	5.136E-07	3.253E-07	1.681E-07	1.112E-07	5.215E-08	2.467E-08	1.983E-08	
610	5.033E-07	3.451E-07	2.975E-07	2.066E-07	9.614E-08	4.649E-08	3.764E-08	
914	5.731E-07	7.011E-07	4.032E-07	2.768E-07	1.356E-07	6.727E-08	5.495E-08	
1219	1.116E-06	8.447E-07	5.096E-07	3.567E-07	1.795E-07	9.102E-08	7.460E-08	
1524	1.209E-06	9.509E-07	5.980E-07	4.252E-07	2.175E-07	1.110E-07	9.106E-08	

FLIGHT NO. 102		FILTER NO. 2						
PATH RADIANCE FROM GROUND TO ALTITUDE (WATTS/STER.SQ.M MICRO M.)		ZENITH ANGLE OF PATH OF SIGHT (DEGREES)						
ALTITUDE METERS	93	95	100	105	120	150	180	
305	4.265E-07	2.661E-07	1.357E-07	8.948E-08	4.225E-08	2.015E-08	1.610E-08	
610	7.628E-07	4.996E-07	2.604E-07	1.740E-07	3.292E-08	3.978E-08	3.197E-08	
914	1.002E-06	6.848E-07	3.723E-07	2.522E-07	1.221E-07	5.947E-08	4.803E-08	
1219	1.174E-06	8.328E-07	4.733E-07	3.255E-07	1.611E-07	7.990E-08	6.460E-08	
1524	1.290E-06	9.515E-07	5.589E-07	3.886E-07	1.944E-07	9.658E-08	7.807E-08	

FLIGHT NO. 102		FILTER NO. 3						
PATH RADIANCE FROM GROUND TO ALTITUDE (WATTS/STER.SQ.M MICRO M.)		ZENITH ANGLE OF PATH OF SIGHT (DEGREES)						
ALTITUDE METERS	93	95	100	105	120	150	180	
305	7.658E-07	4.710E-07	2.389E-07	1.571E-07	7.203E-08	3.6E-08	2.390E-08	
610	1.215E-06	7.722E-07	4.023E-07	2.674E-07	1.238E-07	5E-08	4.202E-08	
914	1.552E-06	1.015E-06	5.434E-07	3.636E-07	1.700E-07	8E-08	5.941E-08	
1219	1.925E-06	1.286E-06	7.037E-07	4.747E-07	2.241E-07	1.011E-07	7.891E-08	
1524	2.244E-06	1.532E-06	8.502E-07	5.927E-07	2.781E-07	1.255E-07	9.768E-08	

FLIGHT NO. 102		FILTER NO. 5						
PATH RADIANCE FROM GROUND TO ALTITUDE (WATTS/STER.SQ.M MICRO M.)		ZENITH ANGLE OF PATH OF SIGHT (DEGREES)						
ALTITUDE METERS	93	95	100	105	120	150	180	
305	6.161E-07	3.446E-07	1.963E-07	1.297E-07	6.141E-08	2.964E-08	2.402E-08	
610	1.154E-06	7.509E-07	4.049E-07	2.714E-07	1.299E-07	6.189E-08	5.973E-08	
914	1.513E-06	1.033E-06	5.706E-07	3.872E-07	1.876E-07	9.110E-08	7.369E-08	
1219	1.932E-06	1.359E-06	7.733E-07	5.315E-07	2.625E-07	1.290E-07	1.043E-07	
1524	2.137E-06	1.557E-06	9.764E-07	6.373E-07	3.188E-07	1.580E-07	1.280E-07	

FLIGHT NO. 102		FILTER NO. 1						
DIRECTIONAL PATH REFLECTANCE FROM GROUND TO ALTITUDE								
ALTITUDE	ZENITH ANGLE OF PATH OF SIGHT (DEGREES)							
METERS	93	95	100	105	120	150	180	
305	1.164E-01	1.723E-01	7.949E-02	5.067E-02	2.291E-02	1.066E-02	8.540E-03	
610	7.407E-01	1.648E-01	1.533E-01	9.394E-02	4.401E-02	2.057E-02	1.655E-02	
914	1.363E-00	9.908E-01	2.421E-01	1.480E-01	6.473E-02	3.050E-02	2.468E-02	
1219	2.407E-00	9.173E-01	3.458E-01	2.071E-01	8.941E-02	4.228E-02	3.421E-02	
1524	3.364E-00	1.303E-00	4.560E-01	2.070E-01	1.128E-01	5.279E-02	4.262E-02	

FLIGHT NO. 102		FILTER NO. 2						
DIRECTIONAL PATH REFLECTANCE FROM GROUND TO ALTITUDE								
ALTITUDE	ZENITH ANGLE OF PATH OF SIGHT (DEGREES)							
METERS	93	95	100	105	120	150	180	
305	2.395E-01	1.327E-01	6.202E-02	3.973E-02	1.824E-02	8.587E-03	6.844E-03	
610	5.850E-01	2.959E-01	1.334E-01	8.216E-02	3.695E-02	1.727E-02	1.381E-02	
914	1.040E-00	4.874E-01	2.035E-01	1.262E-01	5.607E-02	2.626E-02	2.106E-02	
1219	1.633E-00	6.982E-01	3.338E-01	1.722E-01	7.614E-02	3.587E-02	2.874E-02	
1524	2.335E-00	9.367E-01	3.582E-01	2.165E-01	9.436E-02	4.404E-02	3.520E-02	

FLIGHT NO. 102		FILTER NO. 3						
DIRECTIONAL PATH REFLECTANCE FROM GROUND TO ALTITUDE								
ALTITUDE	ZENITH ANGLE OF PATH OF SIGHT (DEGREES)							
MET-RS	43	5	100	105	120	150	180	
305	2.534E-01	1.435E-01	6.836E-02	4.405E-02	1.978E-02	8.481E-03	6.493E-03	
610	4.893E-01	2.634E-01	1.220E-01	7.786E-02	3.469E-02	1.496E-02	1.153E-02	
914	7.679E-01	3.882E-01	1.743E-01	1.100E-01	4.857E-02	2.118E-02	1.646E-02	
1219	1.147E-00	5.476E-01	2.332E-01	1.489E-01	6.527E-02	2.845E-02	2.207E-02	
1524	1.617E-00	7.237E-01	3.054E-01	1.594E-01	8.246E-02	3.570E-02	2.757E-02	

FLIGHT NO. 102		FILTER NO. 5						
DIRECTIONAL PATH REFLECTANCE FROM GROUND TO ALTITUDE								
ALTITUDE	ZENITH ANGLE OF PATH OF SIGHT (DEGREES)							
METERS	93	95	100	105	120	150	180	
305	2.563E-01	1.410E-01	6.607E-02	4.238E-02	1.949E-02	9.285E-03	7.507E-03	
610	5.538E-01	3.354E-01	1.492E-01	9.423E-02	4.254E-02	1.974E-02	1.579E-02	
914	1.164E-00	5.429E-01	2.297E-01	1.426E-01	6.341E-02	2.958E-02	2.375E-02	
1219	1.992E-00	8.428E-01	3.383E-01	2.371E-01	9.126E-02	4.240E-02	3.412E-02	
1524	2.949E-00	1.131E-00	4.339E-01	2.618E-01	1.139E-01	5.296E-02	4.242E-02	

## 5.4. DATA INTERPRETATION

### NIGHT SKY IRRADIANCE

A summary of the irradiance from the upper hemisphere calculated from the sky radiances at the lowest altitude of flight is presented in Table 6-3. The flights are arranged in order of increasing irradiance for Filter 5. The range is from overcast starlight Flight 89 at  $6.2 \text{ E-6 watt m}^{-2} \mu\text{m}^{-1}$  to  $1.8 \text{ E-3 watt m}^{-2} \mu\text{m}^{-1}$  for full moon Flight 99, an increase by a factor of 300. The irradiances tabulated in Table 6-3 are those used to obtain the values of  $R_r^*(z, \theta, \phi)$  for each flight. The smaller irradiance for Filter 4 for the overcast Flight 821 is probably real, although the measurement was marginal at that flux level.

The phase angle of the moon is included in the third column of Table 6-3, since for unclouded conditions after moonrise the phase angle of the moon indicates the comparative contribution of the moon to the irradiance level. The relative irradiance as a function of phase angle according to Russel (1916), is presented in Fig. 6-1. This is the relative irradiance on a flat plate normal to the vector from the moon. It is the equivalent of the moon scalar irradiance. In addition to the moon phase angle, the transparency of the atmosphere and the zenith angle of the moon affect the moon contribution to the total downwelling irradiance.

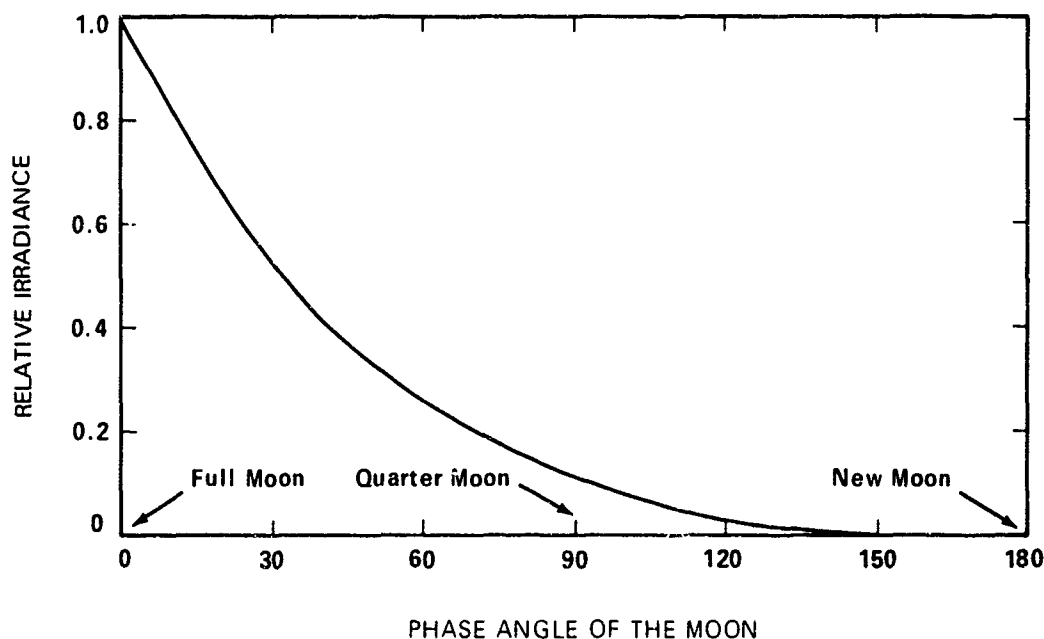


Fig. 6-1. Relative Irradiance Due to the Moon as a Function of Phase Angle

The flights can be easily grouped into three irradiance or flux levels (1) The low flux level flights were those made during starlight, moonlight with moon phase angles between 130 and 150, and overcast. (2) The intermediate flux level flights were those made when the moon phase was quarter moon or 90 phase angle i.e. when it appeared as a half disk. The moon phase angles for flights in this category were between 70° and 102°. (3) The high flux level flights were when the moon phase angles were between 0° and 40°. These flights are described as full or near-full moonlight



Table 6-3. Downwelling Irradiance  $H(z,d)$  watt  $m^{-2} \mu m^{-1}$  for Lowest Flight Altitude

Flux Level	Flight No	Moon Phase Angle (Degrees)	Filters					Avg Alt Above Ground Level (m)
			1	2	5	3	4	
Starlight	89	Before Moonrise	6.20 E-6	5.58 E-6	6.19 E-6	9.71 E-6	-	362
	101	Before Moonrise	-	6.43 E-6	9.58 E-6	-	-	164
	102	Before Moonrise	7.44 E-6	7.50 E-6	1.02 E-5	1.17 E-5	-	152
	88 II	Before Moonrise	8.35 E-6	9.66 E-6	1.12 E-5	1.48 E-5	-	779
	88 I	Before Moonrise	9.08 E-6	1.10 E-5	1.16 E-5	1.54 E-5	-	196
	87	Before Moonrise	8.75 E-6	9.39 E-6	1.33 E-5	1.57 E-5	-	191
	82 I	101	3.14 E-5	3.17 E-5	3.35 E-5	3.31 E-5	1.26 E-5	357
Quarter Moon	93	83	3.54 E-5	4.00 E-5	5.53 E-5	4.87 E-5	-	291
	82 II	102	7.49 E-5	4.90 E-5	9.05 E-5	5.82 E-5	-	332
	92	70	7.94 E-5	8.64 E-5	1.21 E-4	1.08 E-4	-	168
	96	95	1.04 E-4	1.32 E-4	1.25 E-4	1.39 E-4	-	247
	97	71	4.21 E-4	3.34 E-4	2.63 E-4	4.14 E-4	-	164
Full Moon	100 I	11	5.58 E-4	3.94 E-4	6.37 E-4	5.84 E-4	3.79 E-4	220
	98	37	8.22 E-4	9.57 E-4	9.36 E-4	8.27 E-4	6.27 E-4	139
	91	40	8.78 E-4	9.46 E-4	1.00 E-3	1.28 E-3	9.41 E-4	178
	86	14	1.65 E-3	1.89 E-3	1.03 E-3	8.77 E-4	1.60 E-3	184
	99	2	1.66 E-3	1.61 E-3	1.79 E-3	1.86 E-3	1.22 E-3	225

\* Except for Filter 1 at 502 m.

**Variability of Irradiance from Upper Hemisphere.** For the quarter moon and full moon flights downwelling irradiances are often more varied with altitude and less consistent filter-to-filter than for low light level flights. This is because the downwelling irradiance is directly affected when scattered clouds obscure or partially obscure the moon during portions of the flight. The major sources of variability for the low light level flights, artificial lights and lightning, have been largely eliminated during data processing, but no attempt was made to reduce the variability for the moonlight flights.

**Sky Radiance.** The nighttime low flux level sky radiances for Filter 5, from which the downwelling irradiance was computed, are graphed in Fig. 6-2. These are the average sky radiances (for all zenith angles) for the lowest flight altitude (column 9 of Table 6-3). Each curve shape is typical for the flight and

varies very little with altitude or filter. The sky radiance range is small. The exception is Flight 821 which shows the effect of the moon behind the overcast at a zenith angle of 75. For the three flights made before moonrise, 87, 101, and 102, the curve shapes are similar.

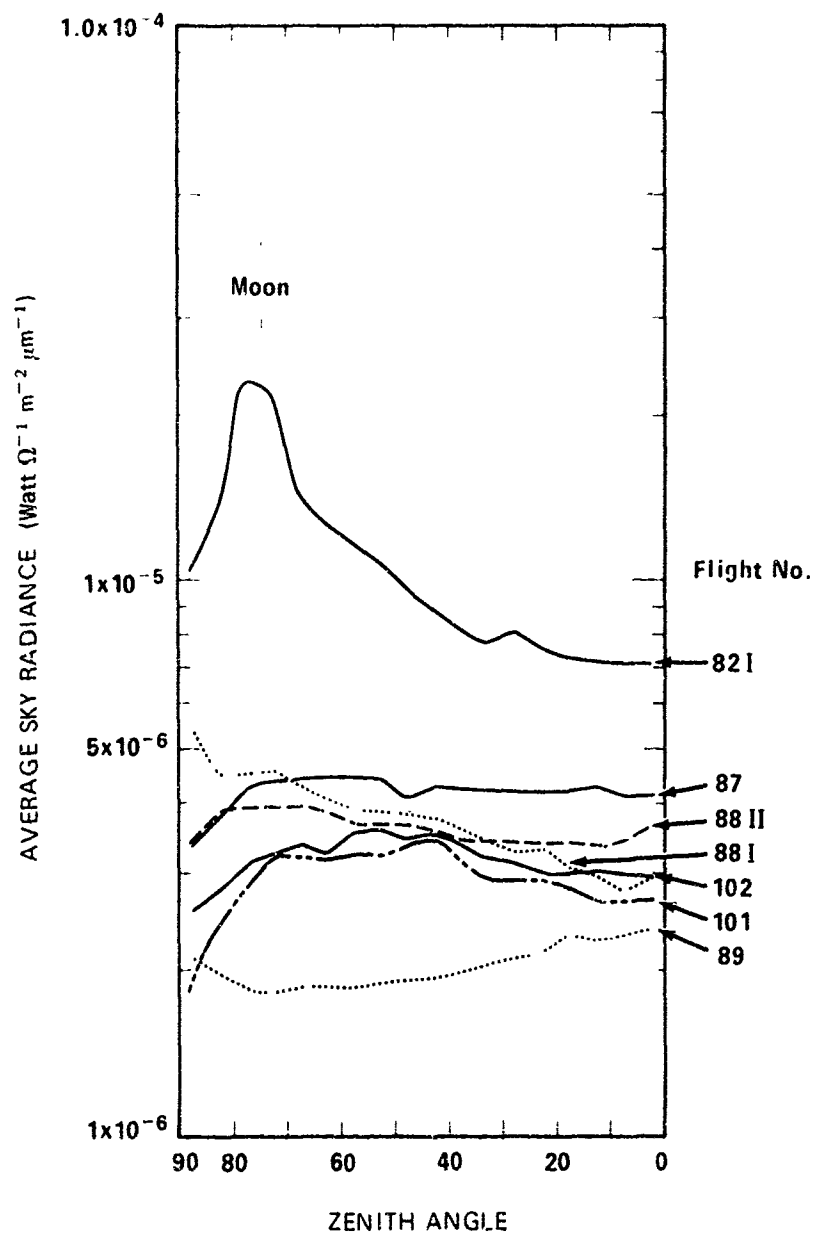


Fig. 6-2. Starlight and Overcast Sky Radiances for Filter 5 at the Lowest Flight Altitude

## DIRECTIONAL REFLECTANCE OF TERRAIN

The tables of directional reflectance of the background (terrain) presented with each flight are derived from data obtained with the lower scanner at the lowest flight altitude. This instrument is a telephotometer with a 5° circular field of view. The tabular values of reflectance therefore relate to an average radiance throughout that field of view. It is completely possible that no part of the terrain has that value of reflectance. Almost certainly objects of interest will be located on a background having a different reflectance than that tabulated for the terrain. That is why this report includes as many directional reflectances of background terrain (airborne measurements) and background reflectances (ground-based measurements [refer to Section 7]) as possible. This provides appropriate values for generating contrast transmittance for a given problem. The effect of background reflectance on the contrast transmittance is not a trivial one. Care should be used in selecting the appropriate value for use in specific problems.

Summary Table 6-4 presents airborne data on the directional reflectance of the terrains for the nadir path of sight. The parenthetical values are derived from the large aperture telephotometer nadir values and the downwelling irradiance computed from the sky scanner data for the lowest flight altitude; the values are not included in the directional reflectance tables provided with each flight.

The reflectance values for the nadir path of sight are presented for conceptual purposes and because of nadir telephotometer data availability. The paths of sight most pertinent to SHED LIGHT are of shallow inclination, i.e., zenith angles between 93° and 105°. Unfortunately, for these paths of sight the terrain reflectances from the airborne data often exceeded unity, thereby indicating the presence of lights from villages over land and fishing boat lanterns over water. The nadir values are more indicative of actual terrain reflectance.

The higher water reflectances for the wet season (Flights 87 and 88I) compared to those of the dry season (Flights 101 and 97) probably indicate the presence of dirt or mud suspended in the water due to runoff from rains. Without suspended matter, the water reflectance should be lower in the red (Filters 3 and 4) than in the green and blue (Filters 1, 2, and 5) as indicated by Flight 97. Water with suspended matter should have spectral reflectance characteristics similar to the characteristics of the matter itself, i.e., muddy water takes on the color of the dirt suspended in it. The increase in overall reflectance for Flights 87 and 88I and the fact that the Filter 3 reflectance is greater than the Filter 1, 2, and 5 reflectances may be attributed to the above phenomenon.

The chlorophyll which is present for growing vegetation shows clearly in the low reflectance measured with Filter 3 and the high reflectance measured with Filter 4 in Flight 82I.

In Table 6-4, columns 2 and 3 present the moon phase angle and zenith angle as information descriptive of the moon contribution to the irradiance.

## TOTAL SCATTERING COEFFICIENT AND BEAM TRANSMITTANCE

A direct measure of air clarity is the atmospheric attenuation coefficient. From this the beam transmittance is calculated. The attenuation coefficient is the sum of the total scattering coefficient and the absorption coefficient. If there is no absorption, the attenuation coefficient is numerically equal to the total scattering coefficient and, in this case, the total scattering coefficient is valid for use in beam trans-

Table 6-4. Directional Reflectance of Terrain for Nadir Path of Sight at Lowest Flight Altitude

Terrain	Moon		Flight No.	Nadir Terrain Reflectance				
	Phase Angle (Degrees)	Avg Zenith Angle (Degrees)		1	2	Filters 5	3	4
Water	(Before Moonrise)		87	0.0790	0.0870	0.103	0.127	-
Water	(Before Moonrise)		88 I	0.0756	0.0781	0.0948	0.129	-
Water	(Before Moonrise)		101	-	-	0.0494	-	-
Water	71	42	97	0.0386	0.0433	0.0560	0.0295	(0.0289)
Cultivation with trees	(Before Moonrise)		88 II	0.0718	0.0845	0.117	0.116	-
Rice paddies & villages Wet	(Before Moonrise)		89	0.0810	0.171	0.194	0.214	-
Rice paddies & villages Brown and dry	(Before Moonrise)		102	-	-	0.148	-	-
Rice paddies & villages Brown and dry*	70	64	92	0.0482	0.0777	0.0598	0.103	(0.230)
Rice paddies & villages Brown and dry	40	14	91	0.0625	0.0723	0.0813	0.121	0.0736
Rice paddies & villages Brown and dry**	37	6	98	0.0786	0.0764	0.0816	0.139	0.250
Grass & deciduous trees Overcast	101	78	82 I	0.0294	0.0495	0.0461	0.0740	0.567
Deciduous trees & scattered rice paddies - wet	102	56	82 II	0.128	0.129	0.0659	0.108	-
Deciduous trees & scattered rice paddies - wet	14	12	86	0.0153	0.0388	0.0649	0.0897	0.275
Deciduous trees & scattered rice paddies - dry	95	54	96	0.0910	0.0889	0.129	0.205	(0.425)
Deciduous trees & scattered rice paddies - dry	83	68	93	(0.045)	(0.047)	0.0678	(0.12)	(0.218)
Deciduous trees & scattered rice paddies - dry	11	60	100 I	0.0600	0.0991	0.0894	0.152	0.144
Deciduous trees & scattered rice paddies - dry	2	42	99	0.0471	0.0761	0.0867	0.0468	0.222

\* In dry season visual report made of moon reflections on water.

\*\* Artificial ground lights noted.

( ) Values in parenthesis are from the large aperture telephotometer values at the nadir and downwelling irradiance.

mittance calculations. If there is absorption, the beam transmittance calculated from the total scattering coefficient will be in error, the error being that the real beam transmittance will be less than the calculated beam transmittance.

The nighttime operations of Project SHED LIGHT precluded the use of an attenuation meter (refer to Appendix A) which in its operation requires a higher level of ambient flux than is available during twilight and nighttime. Accordingly, the scattering meter (integrating nephelometer) described in Section 3 was developed. This instrument has its own light source and operates independently of the ambient flux level. However, it measures only the total scattering coefficient; it does not measure the attenuation coefficient or account for absorption. Examination of data from the field trip made in the Spring of 1969, the dry season, suggests a possibility of atmospheric absorption. An analysis follows.

Table 6-5 is a listing of the total scattering coefficients for zero altitude, obtained by extrapolation from the lowest altitude where data were recorded, and the atmospheric beam transmittance calculated from the total scattering coefficient for the vertical path of sight between 1524 meters and the ground. All these data are Filter 5 data. The flights are arranged in two groups, those made during the wet season and those made during the dry season. The arrangement in each group is by descending values of total scattering coefficients. The spread of the total scattering coefficients within each group is comparable for the two groups. In the first group the spread is from  $2.00 \times 10^{-4} \text{ m}^{-1}$  to  $4.19 \times 10^{-5} \text{ m}^{-1}$ . In the second group the spread is from  $2.19 \times 10^{-4} \text{ m}^{-1}$  to  $4.03 \times 10^{-5} \text{ m}^{-1}$ . These values in the second group appear to be inconsistent with the haze conditions described for those flights. There are two reasons that might explain this inconsistency. As stated, these values are extrapolated from data recorded at the lowest altitudes where the aircraft could fly safely. The haze concentrations were at the lower altitudes, possibly below the lowest recording altitude (it is difficult at night to determine if this is so). Thus, the validity of the extrapolation procedure is questionable.

The second possibility is that the haze particles were absorbing. There was no instrumentation carried in the C-130 aircraft by which this could be determined. If there was absorption, the attenuation coefficients for ground level would be greater than the total scattering coefficients listed in Table 6-5 and transmittances calculated from the total scattering coefficients would be in error by being too high.

All flight operations were conducted under VFR conditions, or better. If "visibility" is defined as a transmittance of 0.05 and if the visibility so defined is 3 statute miles, as required for VFR operation, the attenuation coefficient is  $6.2 \times 10^{-4} \text{ m}^{-1}$ . Thus that attenuation coefficient represents a high limit which would not be exceeded. The largest scattering coefficient in Table 6-5 is for Flight 93 (dry season) and is  $2.19 \times 10^{-4} \text{ m}^{-1}$ , which is about one third of the attenuation coefficient for minimum VFR weather.

The minimum total scattering coefficient  $4.03 \times 10^{-5} \text{ m}^{-1}$  was for Flight 101 made during the dry season over the Gulf of Siam. This is compared to  $1.54 \times 10^{-5} \text{ m}^{-1}$  which is the scattering coefficient for a Rayleigh atmosphere at sea level pressure and  $0^\circ \text{C}$  and which represents a lower limiting value of the scattering coefficient. The value of  $4.03 \times 10^{-5} \text{ m}^{-1}$  is probably not as high as it should be, again because of questionable extrapolation procedure and possible absorption in the atmosphere haze.

Mie volume scattering functions were combined with Rayleigh scattering functions to obtain the proportional directional scattering functions used to compute equilibrium radiance for each path of sight. These Mie volume scattering functions were derived from Barteneva (1960) proportional volume scattering functions by use of the equation

$$M[\sigma(z, \beta)/s(z)] = \left\{ s(z) [\sigma(z, \beta)/s(z)] - R[s(z)] R[\sigma(\beta)/s] \right\} \cdot M[s(z)] \quad (6.2)$$

and were designated by numbers corresponding to the numbered Barteneva volume scattering function from which they were derived. The Filter 5 total scattering coefficient at each data-taking (level flight) altitude was the basis for the selection of the appropriate Mie volume scattering function. These selected functions for the highest and lowest altitudes are listed in columns 4 and 5 of Table 6-5. The Mie proportional directional scattering functions for the range of catalog numbers used for data reduction are graphed in Fig. 6-3.

Table 6-5. Total Scattering Coefficients and Vertical Beam Transmittances (all Filter 5 data)

Flight No	Total Scattering	Vertical Beam Transmittance $T_{1524}(1524,180^\circ)$	Mie Volume Scattering Function**	
	Coefficient $s(0)(m^{-1})$		Minimum Altitude	Maximum Altitude
Wet Season				
82II	2.00 E-4	0.781	5	4
89	1.72 E-4	0.800	4	4
82I	1.59 E-4	0.805	5	4
87	1.10 E-4	0.859	4	4
88I	9.86 E-5	0.877	4	4
88 II	9.11 E-5	0.883	4	4
86	4.19 E-5	0.950	3	2
Dry Season				
93	2.19 E-4	0.724	5	5
92	1.88 E-4	0.794	5	4
100II	1.41 E-4	0.817	-	-
96	1.07 E-4	0.887	3	4
91	9.01 E-5	0.867	4	4
100I	6.24 E-5*	-	4	4
102	5.25 E-5	0.928	3	3
99	5.15 E-5	0.927	3	4
98	5.06 E-5	0.926	3	4
97	4.71 E-5	0.936	3	3
101	4.03 E-5	0.937	3	3

\* This value is not an extrapolated-to-ground-level value. It is, instead, the value recorded during the lowest altitude where level-flight airborne data were recorded.

\*\* The numbers represent the Barteneva volume scattering functions from which these Mie data were derived.

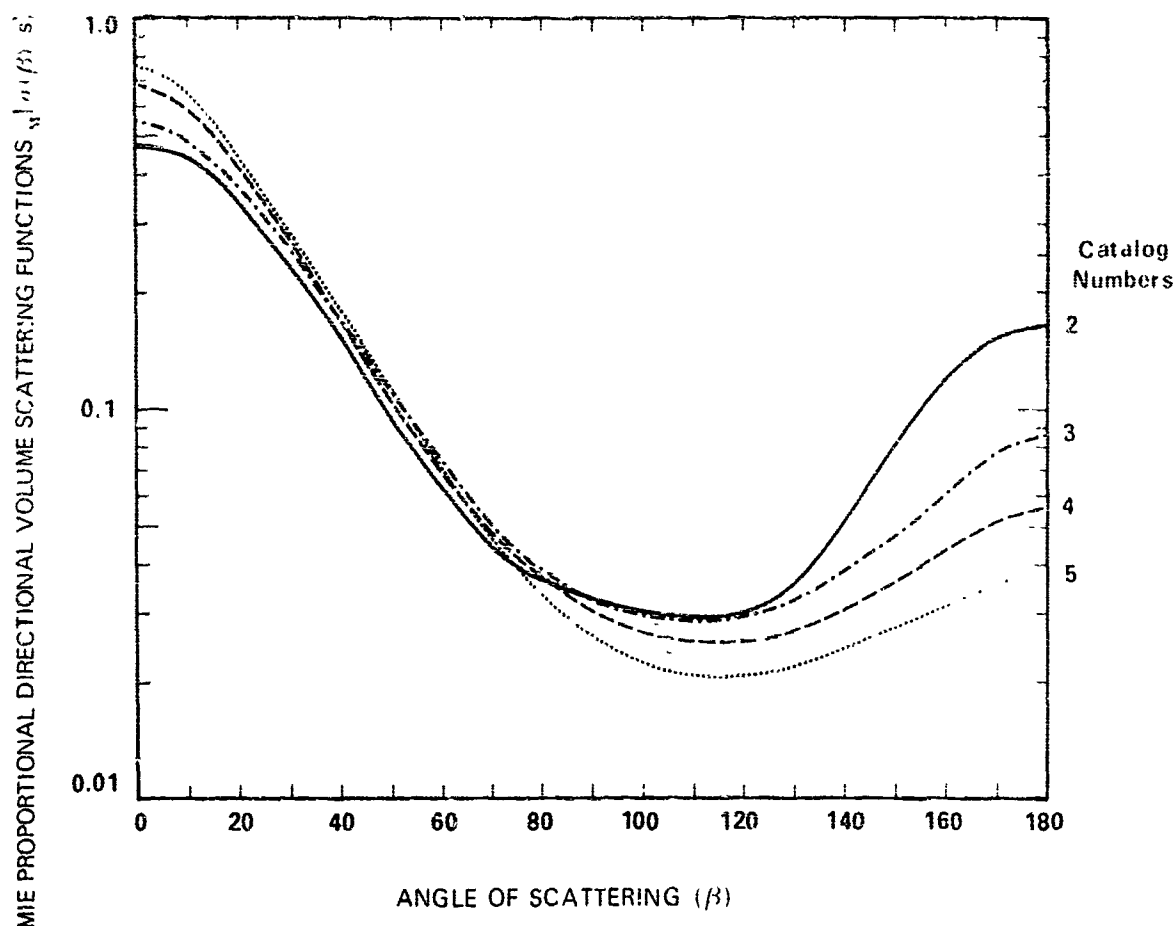


Fig. 6-3. Mie Proportional Directional Volume Scattering Functions Used in the Calculations of Equilibrium Radiance

The total scattering coefficients for the flights during the wet season decreased with increased altitude and were, in general, smoothly changing altitude functions. These coefficients also were greatest for short wavelength and the least with the increase of wavelength. The total scattering coefficients for the dry season flights did not necessarily decrease with altitude and graphs of these functions usually had more structure with change of altitude than those of the wet season. The graphs also show that while the coefficients were usually greatest for short wavelengths and the least with the increase of wavelength, the graphs for data from Filters 1 and 2 crossed and recrossed with change of altitude for Flights 96, 97, and 99.

#### PATH RADIANCE AND EQUILIBRIUM RADIANCE

The path radiance is calculated from the values of equilibrium radiance for a given path of sight by means of Eqs. 2-13 and 2-14. It enters into the equation for contrast transmittance, Eq. 2-2, into the equation for directional path reflectance, Eq. 2-4, and into the equation for computing apparent radiance  $N_r(z, \theta, \phi)$ :

$$N_r(z, \theta, \phi) = N_o(z, \theta, \phi) T_r(z, \theta) + N_r^*(z, \theta, \phi). \quad (6-3)$$

In general, path radiance decreases with increasing wavelength

The apparent radiance of the terrain and other backgrounds or objects tends to approach the equilibrium radiance of that path of sight. Equilibrium radiance generally tends to be relatively invariant with altitude. This is illustrated in Fig. 6-4 using Flight 821 Filter 5 data for the vertical downward path of sight between ground level and altitude. The terrain reflectance measured from the airplane at the lowest altitude was 0.046. The terrain consisted of deciduous trees and tall grass. The apparent radiance of the terrain, as computed with Eq. 6-3 above, is shown on the graph. It increases with altitude always approaching the curve of equilibrium radiance for that path of sight. A second apparent radiance curve is given for a light yellow road surface of 0.50 reflectance. This radiance decreases with altitude as it tends toward the equilibrium radiance. The equilibrium reflectance was 0.264 at ground level and 0.33 at 1585 m. This is about the same reflectance as the beach sand measured at the ground station on 19 October 1968, average reflectance range was 0.28 to 0.33 (assuming the nadir reflectance is similar to the reflectance at zenith angle range of  $92^\circ$  to  $96^\circ$ ). An apparent radiance curve for the beach sand would be nearly equivalent to the equilibrium radiance curve shown in Fig. 6-4.

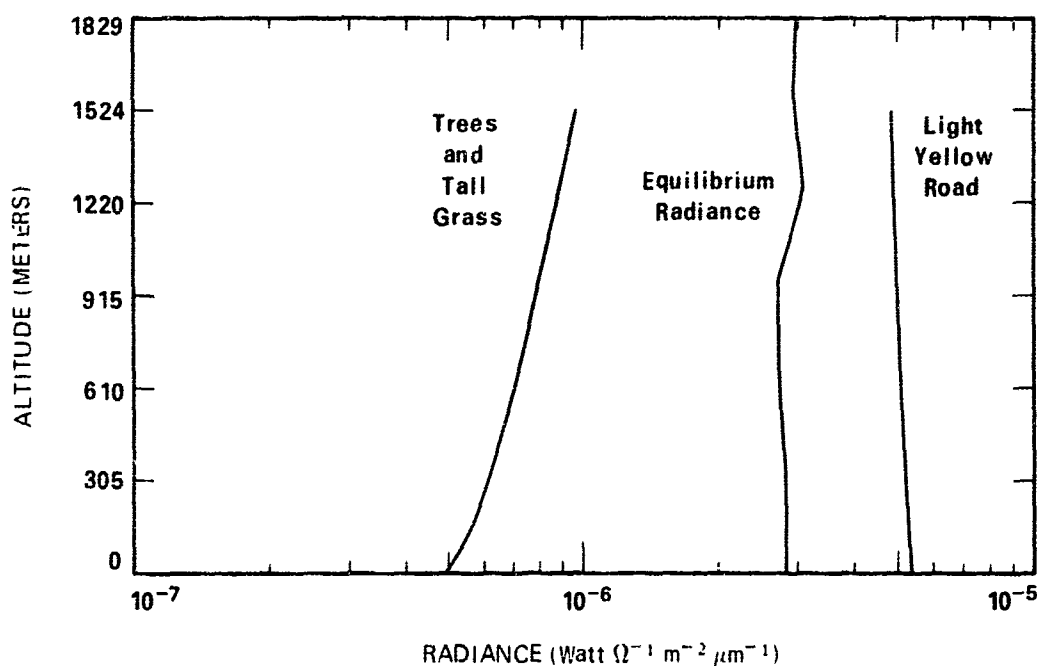


Fig. 6-4. Equilibrium Radiance and Apparent Radiance for the Vertical Downward Path of Sight from Ground Level to Altitude, for Filter 5 Flight 821.

The contrast transmittance can be expressed as the beam transmittance times the ratio of inherent to apparent background radiance

$${}_b\tau_r(z, \theta, \phi) = T_r(z, \theta) {}_bN_o(z, \theta, \phi) / {}_bN_r(z, \theta, \phi) \quad (6-4)$$



When the background reflectance is equal to the equilibrium reflectance, the contrast transmittance is equal to the beam transmittance. This is illustrated in Fig. 6-5. The middle curve is beam transmittance. It might also be the contrast transmittance against a beach sand of 0.29 reflectance. The contrast transmittance for a background lower in reflectance than the equilibrium reflectance will always be smaller than the beam transmittance (shown in Fig. 6-5 for the average terrain, trees, and tall grass). This is true because the ratio of inherent to apparent background radiance will always be less than 1 (since the apparent radiance increases with altitude as shown in Fig. 6-4). On the other hand, the contrast transmittance for a background higher in reflectance than the equilibrium reflectance will have a contrast transmittance greater than the beam transmittance as illustrated in Fig. 6-4.

The above example emphasizes the importance of selecting the appropriate background reflectance for computing valid contrast transmittance values.

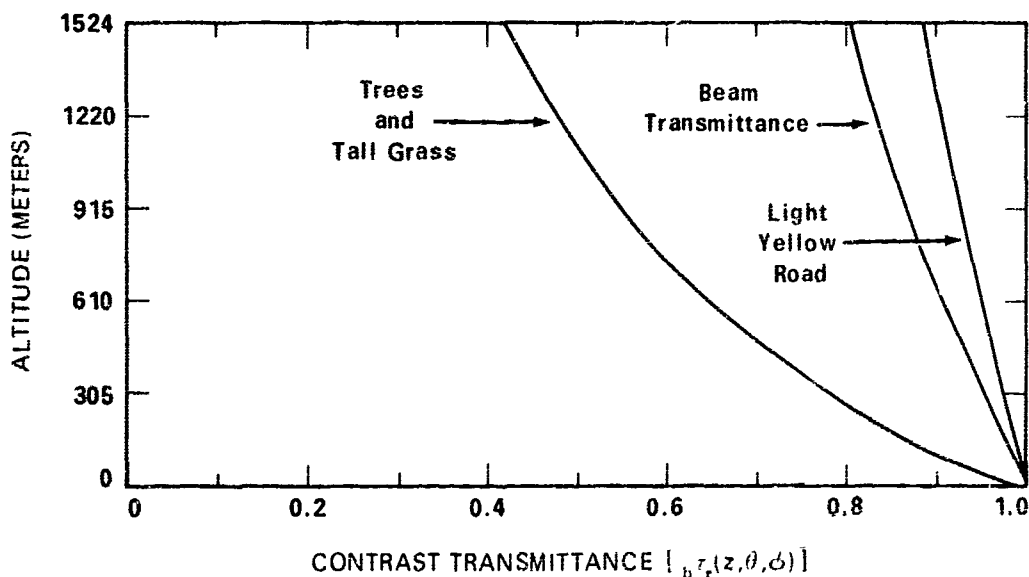


Fig. 6-5. Contrast Transmittance for the Vertical Path of Sight Between Ground Level and Altitude, for Filter 5, Flight 821

**Method of Obtaining Equilibrium Radiance.** Equilibrium radiance (Eq. 2-15) and path radiance (Eqs 2-13 and 2-14) are obtained by using an essentially integrative method. The advantage of this method is being able to handle highly variable data, variable in the sense of changing flux levels due to real changes occurring in space and/or time during the flight. The terrain over which a data flight takes place is chosen for its consistency of terrain appearance. Frequently, however, village lights and fishing boat lanterns are present which change in position relative to the airplane during the flight pattern. Anomalies in the sky lighting distribution occur due to subtle changes in the weather. These may be clouds which alternately cover and uncover the moon, lightning flashes, etc. All these things contribute to the variability of the overall flux level and directional radiance pattern and these two properties define the equilibrium radiance and path function. These derived values are directly descriptive of the real conditions encountered and measured during the flight.

The danger lies in trying to obtain a path radiance by combining data from several altitudes for a given filter. A path radiance is essentially a scattered radiance in a given path at any one instant. Therefore a path radiance during a lightning flash is not compatible with one when lightning is not present. Similarly, a path radiance when the moon is behind a cloud is different from one when the moon is unobscured.

For the starlight flights, the extremely bright close lights or lightning flashes are eliminated but the ubiquitous lower level lights near the horizon are not. Thus the path radiances are reasonable representations of the true path radiances over the terrain (or water) when extraneous lights at ground level are present but not close by.

The intermediate and high flux level flights, however, represent an averaging of the light conditions present during the entire flight (the use of integral Eqs. 2-13 and 2-15 effectively combines the variable data into a crude average of the prevalent condition). The averaging, however, is progressive. The lowest altitude (305m) is not affected by the data variability whereas at the highest altitude (1524 m) all the data are averaged. Thus these intermediate-to-high flux level flights neither represent the clearest nor the cloudiest portion of a flight, but something in between.

#### DIRECTIONAL PATH REFLECTANCE

Using the data from the two scanners to obtain both the path radiance  $N_r^*(z, \theta, \phi)$  and the downwelling irradiance  $H(z, d)$  adds to the reliability of the path reflectance  $R_r^*(z, \theta, \phi)$  since these two quantities are ratioed as shown in Eq. 2-4 repeated below in a slightly different form.

$$R_r^*(z, \theta, \phi) = \frac{\pi}{T_r(z, \theta)} \times \frac{N_r^*(z, \theta, \phi)}{H(z, d)} \quad (6-5)$$

In this way any absolute error in the calibration of the scanners is effectively eliminated. Also since both the path radiance and downwelling irradiance are obtained by integration of a large number of radiance measurements, precision errors tend to cancel or average out.

The directional path reflectance is the most easily utilized form of the atmospheric optical data for obtaining contrast transmittance. (Refer to Section 2.) The path reflectance is used with the directional background reflectance in Eq. 2-3, which is repeated below:

$$t_{br}^*(z, \theta, \phi) = \{ 1 + R_r^*(z, \theta, \phi) \cdot {}_bR_b(0, \theta, \phi) \}^{-1} \quad (6-6)$$

A conceptually valuable graphical representation of the effect of the ratio of path-to-background reflectance on contrast transmittance is provided by Fig 6-6 (Duntley, 1969) (see Appendix D, Fig. 3). It is a nomogram which represents Eq. 6-6 and consists of a diagonal line drawn across a sheet of 2 by 2 cycle log-log graph paper. The path-to-background reflectance ratio is entered on the axis of the abscissa and contrast transmittance is read out on the axis of the ordinate.

Note that when  $R_r^* = {}_bR_b$  the contrast transmittance is 0.50. Smaller values of  $R_r^* / {}_bR_b$  yield higher values of contrast transmittance and vice versa.

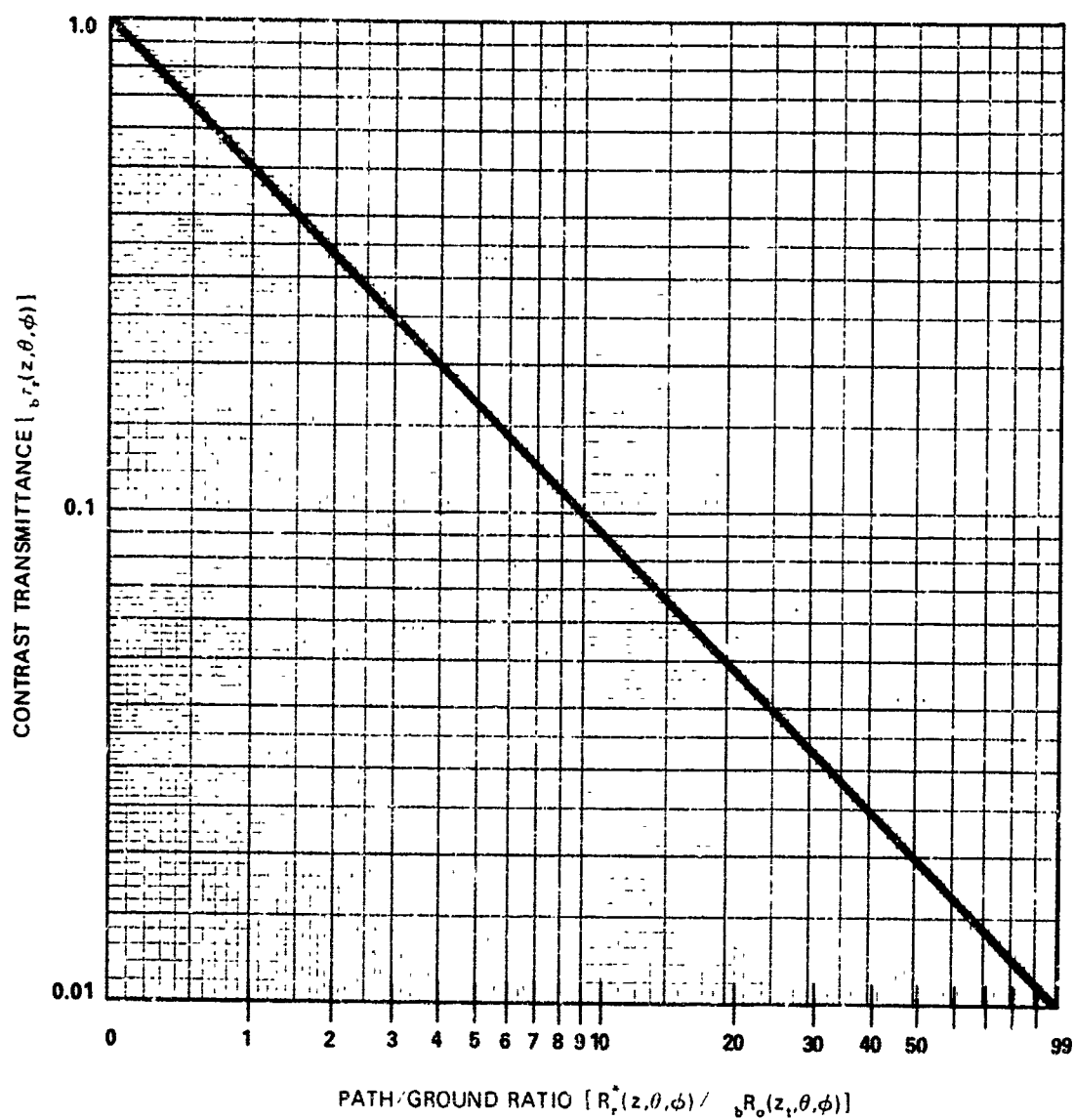


Fig. 6-6. Contrast Transmittance Nomogram

Another form for expressing contrast transmittance as a function of path and background reflectance which is convenient for hand computation is

$${}_b r_r(z, \theta, \phi) = {}_b R_o(0, \theta, \phi) / [{}_b R_o(0, \theta, \phi) + R_r^*(z, \theta, \phi)] . \quad (6-7)$$

Generally speaking the directional path reflectance decreases with wavelength. An exception is seen in Flight 82I. A factor-of-2 decrease in downwelling irradiance from Filter 3 to Filter 4 results in a path reflectance greater for Filter 4 than Filter 3.

# 7. Ground-Based Data

## 7.1 DESCRIPTION OF GROUND OPERATION

The twofold purpose of the ground station was (1) to provide measurements of inherent background radiance and reflectance appropriate for use with airborne measurements, and (2) to provide continuity of measurement by establishing ground level values of downwelling irradiance and the total scattering coefficient. Since the installation of the ground station was an arduous and lengthy task, the station was usually in a given area for one to two weeks before being moved to a new location. Because the mobility of the ground operation was so greatly restricted in comparison to the aircraft movement, the fulfillment of the first purpose was emphasized.

The ground station was employed during each of the two field expeditions to Thailand. Successful operation was achieved during both trips in two locations: Lop Buri and Rayong. A list of the stations with dates (Greenwich), times of measurement (in both Greenwich mean time and local civil time [LCT]), and locations are given in Table 7-1. Data are reported for 19 stations altogether. The moon phase angle and zenith angle are also given in Table 7-1 in order to indicate the contribution of the moon to the total irradiance (refer to Section 6.4, Fig. 6-1 for moon irradiance as a function of phase angle).

On three nights the ground station was in operation in the same area and during the same general time as the airborne operation covering Flights 87, 88I, and 92. This fulfilled the second purpose. The airborne data is compared to the ground-based data in Section 7.3.

Three basic types of information were secured by means of the ground station: (1) atmospheric scattering coefficients, both total and directional, (2) downwelling irradiance, and (3) inherent background radiance. Directional reflectance was then derived by using the data for downwelling irradiance and inherent background radiance in Eq. 2-5. To obtain these data three instruments were employed: (1) an integrating nephelometer, (2) a sky scanning telephotometer with an irradiance cap attachment, and (3) a large aperture telephotometer. (For further details refer to Sections 3 and 4). Each instrument was fitted with the five optical filters used for the airborne operation as described in Section 3.4.

For the first Thailand trip, TDY-1, the downwelling irradiance was measured by the sky scanner with the irradiance cap attached to the scanner. Most of the time the measurements of downwelling irradiance and background radiance were obtained simultaneously. The background radiances for TDY-1 were measured

on backgrounds at a distance so that a change in zenith angle of path of sight also meant a different area (of the same general description) was in the field of view of the telephotometer.

**Table 7-1. Ground Stations for Thailand Field Expeditions: TDY-1, 1968 and TDY-2, 1969**

Station No.	Date 1968	Time of Data Measurement				Site	Phase Angle	Moon Zenith Angle		Concurrent Flight No
		Start		End				Start	End	
1.1	29 Sep	1352	(2052)	1624	(2324)	Lop Buri	85	63	64	
1.2	30 Sep	1443	(2143)	1614	(2314)	Lop Buri	72	58	59	
1.3	3 Oct	1236	(1936)	1617	(2317)	Lop Buri	36	30	28	
1.4	9 Oct	1711	(0011)	1811	(0111)	Rayong	36	26	26	
1.5	10 Oct	1606	(2306)	1715	(0015)	Rayong	46	47	45	
1.6	11 Oct	1619	(2319)	1756	(0056)	Rayong	58	51	48	
1.7	12 Oct	1405	(2105)	1445	(2145)	Rayong	67	Before Moonrise		87*
1.8	13 Oct	1240	(1940)	1418	(2118)	Rayong	78	Before Moonrise		
1.9	19 Oct	1413	(2113)	1552	(2252)	Rayong	152	Before Moonrise		88†
1.10	22 Oct	1332	(2032)	1514	(2214)	Rayong	171	Before Moonrise		
1969										
2.1	23 Feb	1408	(2108)	1439	(2139)	Rayong	97	50	56	
2.2	26 Feb	1422	(2122)	1536	(2236)	Rayong	62	23	37	
2.3	28 Feb	1534	(2234)	1651	(2351)	Rayong	40	16	31	
2.4	2 Mar	1345	(2045)	1427	(2127)	Rayong	18	37	27	
2.5	8 Mar	1651	(2351)	1757	(0057)	Lop Buri	57	69	56	
2.6	9 Mar	1423	(2123)	1614	(2314)	Lop Buri	69	Before Moonrise		
2.7	9 Mar	1815	(0115)	1921	(0221)	Lop Buri	69	65	54	92
2.8	11 Mar	1736	(0036)	1750	(0050)	Lop Buri	95	Before Moonrise		
2.9	12 Mar	1325	(2025)	1546	(2246)	Lop Buri	107	Before Moonrise		

\* Flight 87 was from 1226 to 1337 so the ground station data measurements were after completion of the flight

For the second Thailand trip, TDY-2, the downwelling irradiance was obtained indirectly by measuring the radiance of a horizontally-oriented, calibrated reflectance board. The radiance was measured using the large aperture telephotometer as a nadir telephotometer. Irradiance was derived by solving Eq. 2-5 for irradiance as follows:

$$H(0,d) = \frac{\pi_b N_o(0,180,0)}{b R_o(0,180,0)} \quad (7-1)$$

During TDY-2 the background radiance of a circumscribed area was measured from many paths of sight by rotating the large aperture telephotometer over the area on a large frame. Thus the telephotometer was used as a goniometer.

## 7.2 PRESENTATION OF GROUND-BASED DATA

The scattering coefficient, downwelling irradiance, and background radiance data are presented in order by date in four sections. Each section represents one site during one season. Since it was not always possible to obtain a reflectance value for each of the background radiance measurements, the recoverable reflectances are presented at the end of this section (7.2).

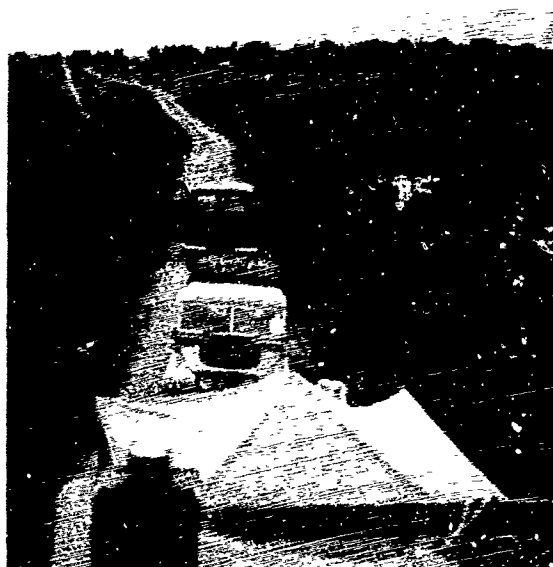
The data for each station are presented in table form. The first column indicates the variable name and columns 2 through 6 are the variables for Filters 1 through 5. The first variable (row) is for the total scattering coefficient  $s(\lambda)$  in units per meter. The second and third variables (rows) are the proportional directional scattering coefficients for the scattering at  $30^\circ$  and  $150^\circ$ :  $\sigma(0,30^\circ)/s(0)$  and  $\sigma(0,150^\circ)/s(0)$ . Fourth is the ratio of the directional scattering at  $30^\circ$  and  $150^\circ$ ,  $\sigma(0,30^\circ)/\sigma(0,150^\circ)$ . The fifth variable is the downwelling irradiance  $H(0,d)$  in units of  $W m^{-2} \mu m^{-1}$ . The remaining rows are for the radiance of a background (such as a rice field) as described in units of  $W \Omega^{-1} m^{-2} \mu m^{-1}$ . The path of sight is specified in each case in terms of zenith angle and azimuth. During moonlight the azimuths are given as azimuths from the moon. For starlight or overcast the azimuths are given as compass points, i.e., north or south, etc.

### TDY-1 STATIONS

*Lop Buri Site.* The first Thailand trip, TDY-1, was during the wet monsoon season. Stations 1.1 through 1.3, 29 September through 3 October 1968, were at the Lop Buri site at latitude  $14.8^\circ N$  and longitude  $100.4^\circ E$ . The ground station was located in the vicinity of Sing Buri near Lop Buri. The truck and instruments were on a dirt road in the midst of a rice field. Radiance measurements of the rice field were made with the telephotometer about 1 m above the top of the rice. A typical view of the rice field is given in Fig. 7-1. The dirt road to the west was also measured on 3 October and is depicted in Fig. 7-1.



Rice Field



Dirt Road (West)

Fig. 7-1. Rice field and dirt road at Lop Buri site during TDY-1.

The approximate position of the ground site for Lop Buri in relation to the flight path for Flights 89, 91, and 92 is depicted in Fig. 7.2. Flight 92 was on the same evening as, but later than, ground station 2.6 and concurrent with station 2.7.

**Station 1.1, 29 September 1968 (Table 7-1A).** Lop Buri in the monsoon season during moonlight. The moon phase angle was  $85^\circ$ , moon zenith angle  $63^\circ$  through  $64^\circ$ , and the moon azimuth  $227^\circ$  through  $228^\circ$  from the north. The weather was initially clear with only a few scattered clouds, but during the evening, clouds built up to a fairly heavy overcast. Data presented are for scattered clouds before the complete overcast. Measurement time span was 2052 through 2324 LCT.

**Table 7-1A. Station 1.1**

Variable Name	Filters				
	1	2	3	4	5
Total Scattering Coefficient ( $\text{m}^{-1}$ )	1.08 E 4	7.91 E 5	5.52 E 5	5.61 E 5	8.08 E 5
$\sigma(0.30^\circ)/s(0)$	0.245	0.287	0.196	0.144	0.198
$\sigma(0.150^\circ)/s(0)$	0.0365	0.0416	0.0226	-	0.0296
$\sigma(0.30^\circ)/\sigma(0.150^\circ)$	6.7	6.9	8.7	-	6.7
Downwelling Irradiance ( $\text{W m}^{-2} \mu\text{m}^{-1}$ ) (After)	1.33 E 4	1.86 E 4	2.38 E 4	1.84 E 4	1.63 E 4

Terrain Description	Path of Sight		Radiance ( $\text{Watt } \Omega^{-1} \text{ m}^{-2} \mu\text{m}^{-1}$ )				
	Zenith Angle	Azimuth	Filters				
			1	2	3	4	5
Rice Field	91	0	-	1.18 E 5	1.18 E 5	3.82 E 5	1.15 E 5
Rice Field	91	90	2.66 E 6	6.68 E 6	4.80 E 6	3.61 E 5	6.82 E 6
Rice Field	91	180	4.39 E 6	9.17 E 6	7.16 E 6	4.48 E 5	9.33 E 6

**Station 1.2, 30 September 1968 (Table 7-2).** Lop Buri in the monsoon season during moonlight. The moon phase angle was  $72^\circ$ , moon zenith angle  $58^\circ$  through  $59^\circ$ , and moon azimuth  $225^\circ$  through  $227^\circ$  from the north. There were many small scattered cumulus. The moonlight was intermittent from 2000 LCT on, but was blacked out severely by clouds toward the end of the evening. Background radiances were measured during 80% cloud cover, with very few instances of clear moon illumination. Measurement time span was 2143 to 2314 LCT.

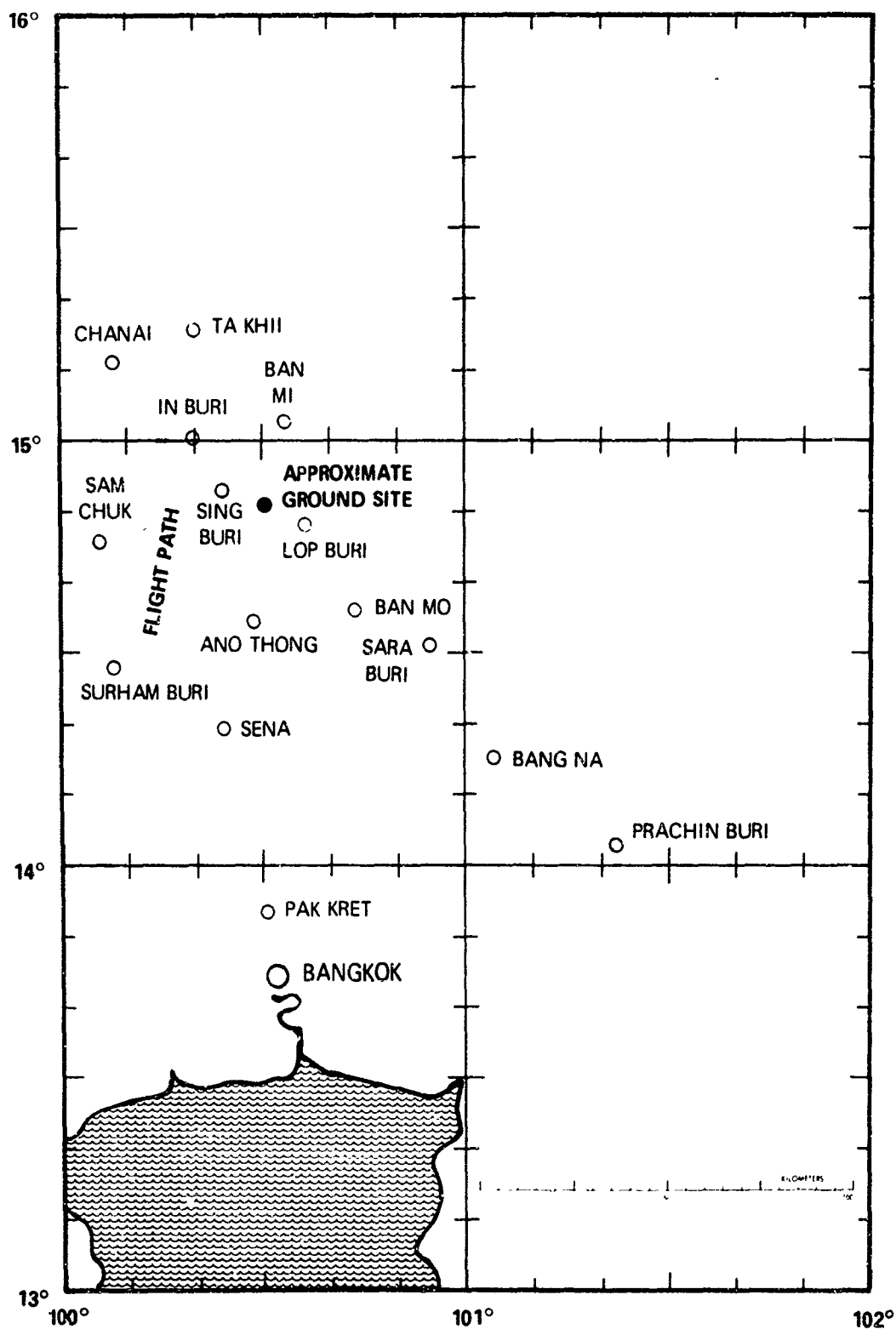


Fig. 7-2. Lop Buri area with location of ground station and flight path.



Table 7-2. Station 1.2

Variable Name	Filters				
	1	2	3	4	5
Total Scattering Coefficient ( $m^{-1}$ )	1.92 E 4	1.48 E 4	1.10 E 4	8.23 E 5	1.62 E 4
$\sigma(0.30) / \sigma(0)$	0.593	0.646	0.526	0.474	0.441
$\sigma(0.150) / \sigma(0)$	0.0434	0.0468	0.0366	0.0329	0.0380
$\sigma(0.30) / \sigma(0.150)$	13.7	13.8	14.4	14.4	11.6
Downwelling Irradiance ( $W m^{-2} \mu m^{-1}$ ) (Average)	2.80 E 4	2.90 E 4	3.62 E 4	2.80 E 4	2.70 E 4

Terrain Description	Path of Sight		Radiance ( $Watt m^{-2} \mu m^{-1}$ )				
	Zenith Angle	Azimuth	Filters				
			1	2	3	4	5
Rice Field	92	0	6.62 E 6	1.54 E 5	1.55 E 5	6.02 E 5	1.67 E 5
Rice Field	92	90	3.28 E 6	7.17 E 6	5.03 E 6	3.32 E 5	6.79 E 6
Rice Field	92	180	5.55 E 6	1.20 E 5	9.34 E 6	5.76 E 5	1.20 E 5

Station 1.3, 3 October 1968 (Table 7-3). Lop Buri in the monsoon season during moonlight. The moon phase angle was  $36^\circ$ , moon zenith angle  $30^\circ$  through  $28^\circ$ , and moon azimuth  $152^\circ$  through  $160^\circ$  from the north. The sky was generally clear, only slightly cloudy from 1900 to 2000 LCT, and clearing to light cloud and horizon haze at 2200 LCT. Measurement time span was 1936 to 2317 LCT.

Table 7-3. Station 1.3

Variable Name	Filters				
	1	2	3	4	5
Total Scattering Coefficient ( $m^{-1}$ )	1.95 E 4	1.67 E 4	1.08 E 4	9.08 E 5	1.75 E 4
$\sigma(0.30) / \sigma(0)$	0.316	0.337	0.290	0.225	0.250
$\sigma(0.150) / \sigma(0)$	0.0253	0.0234	0.0225	0.0138	0.0190
$\sigma(0.30) / \sigma(0.150)$	12.5	14.4	12.9	16.3	13.1
Downwelling Irradiance ( $W m^{-2} \mu m^{-1}$ ) (Average)	1.15 E 3	1.18 E 3	1.33 E 3	1.09 E 3	1.23 E 3

Terrain Description	Path of Sight		Radiance ( $Watt m^{-2} \mu m^{-1}$ )				
	Zenith Angle	Azimuth	Filters				
			1	2	3	4	5
Rice Field	92	0	1.58 E 5	3.93 E 5	4.05 E 5	1.09 E 4	4.07 E 5
Rice Field	92	180	1.21 E 5	2.69 E 5	1.73 E 5	1.34 E 4	2.90 E 5
Rice Field	92	270	1.17 E 5	2.69 E 5	-	1.37 E 4	2.98 E 5
Dirt Road (West)	92	110	4.80 E 5	6.06 E 5	1.06 E 4	1.04 E 4	6.61 E 5

*Rayong Site.* The first Thailand trip, TDY-1, was during the wet monsoon season. Stations 1.4 through 1.10, 9 October through 22 October 1968, were at the Rayong site at latitude 12.7°N and 101.3°E. The ground station was located 16 km west of Rayong in a vegetated area between the beach sand and a road. Backgrounds measured are depicted in Fig. 7-3. Beach sand and the road ran roughly east and west; scrub and sand were to the north; the ocean was south. Vegetation close by was wild sweet peas and grass. Water just offshore was shallow, approximately 3 m in depth.

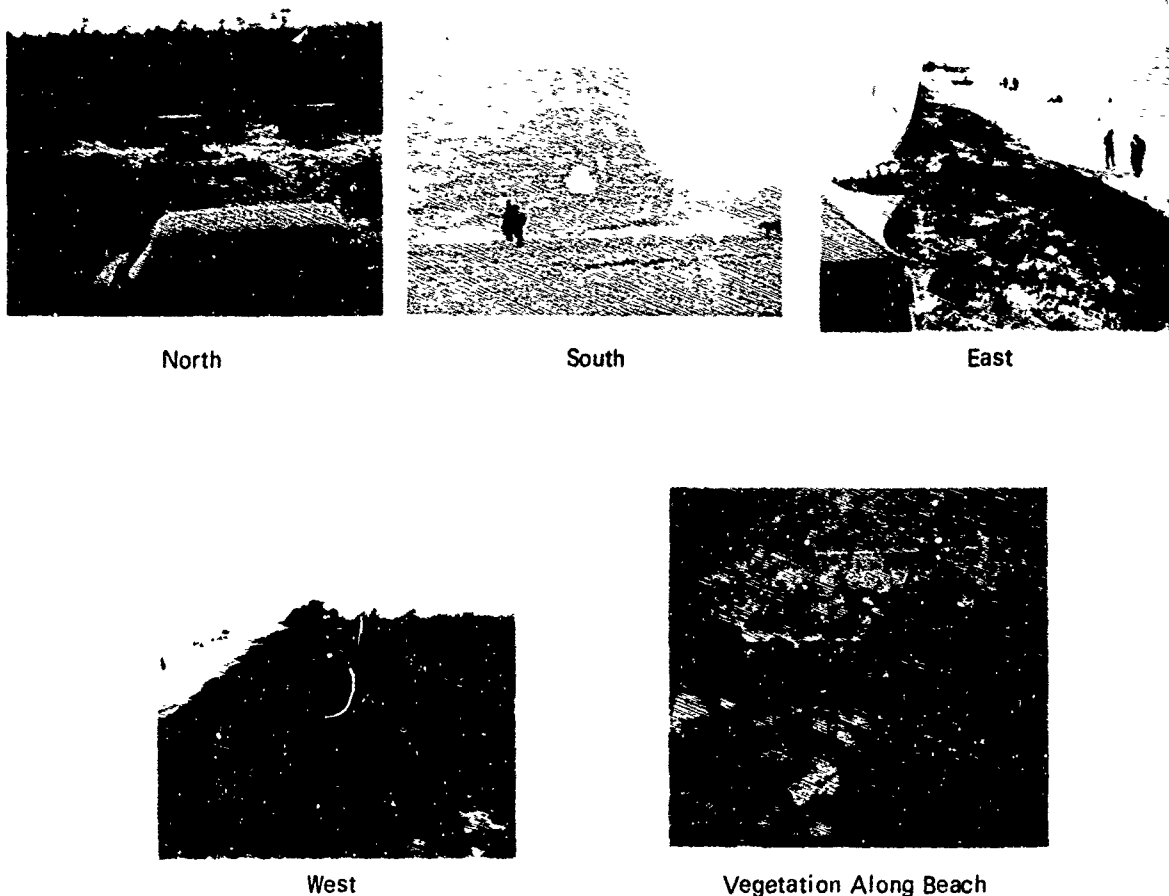


Fig. 7-3. Sandy beach and road (E and W), scrub and sand (N), ocean (S), and wild sweet peas and grass nearby at Rayong site during TDY-1.

The approximate position of the ground station and flight paths for the Rayong site are depicted in Fig. 7-4. The flight path for TDY-1 is for Flights 87 and 88I (the two flights concurrent with ground stations 1.7 and 1.9, respectively). The flight path for TDY-2 is for Flights 97 and 101.

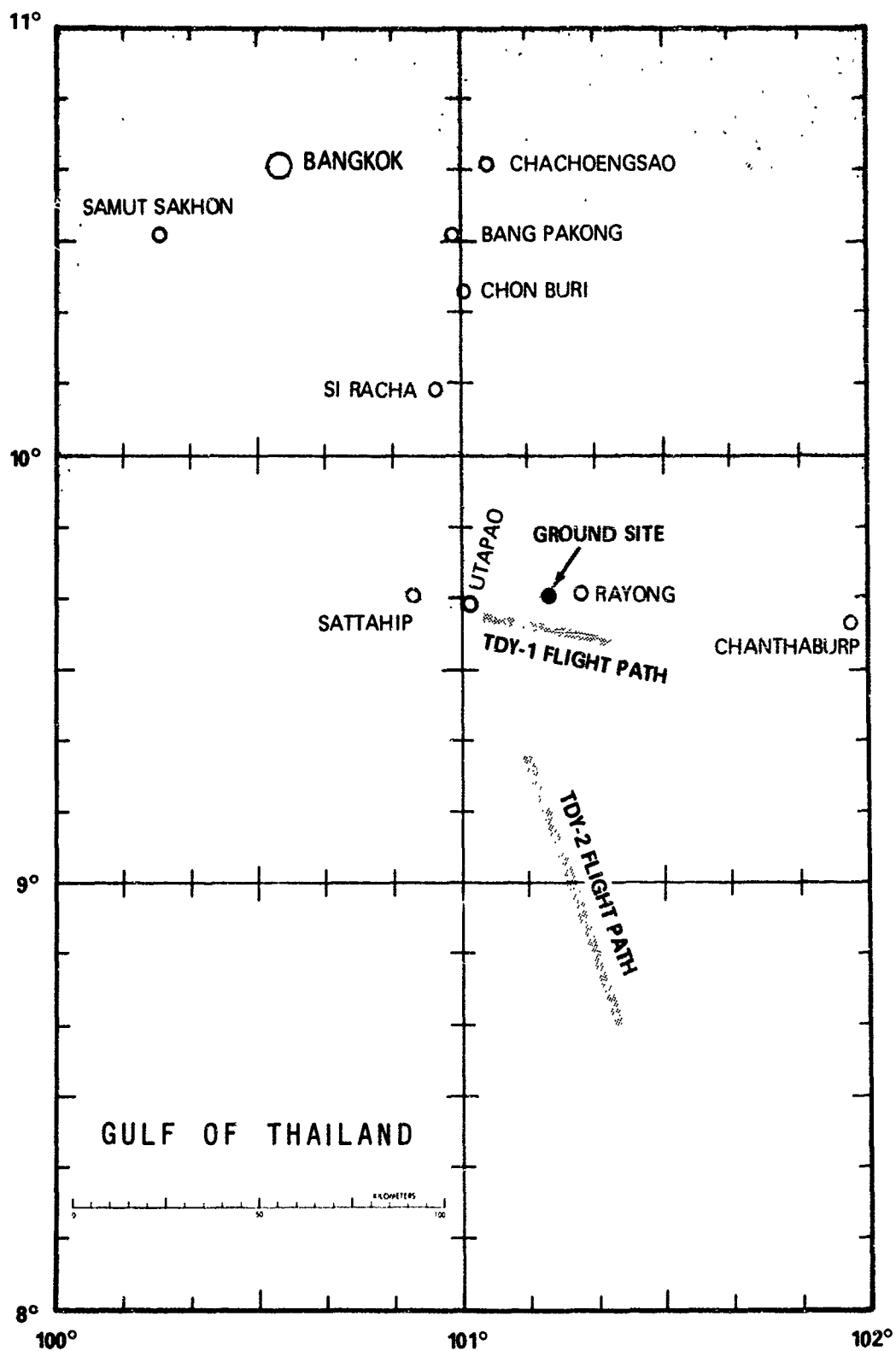


Fig. 7-4. Rayong area with location of ground station and flight paths for TDY-1 and TDY-2.

**Station 1.4, 9 October 1968 (Table 7-4).** Rayong site in the monsoon season during moonlight. The moon phase angle was  $36^\circ$ , moon zenith angle  $26^\circ$ , and moon azimuth  $66^\circ$  from the north. The sky was clear overhead with stars shining; there was a heavy cumulus buildup to the north and west with intermittent lightning flashes in these cloud areas. There were six fishing boats with lanterns about 100 to 200 m off-shore to the south. A couple of small campfires were located approximately 200 to 300 m down the beach to the east. At the end of the data run the moon was almost directly overhead and a slight haze had built up causing slight diffusion of the moon glitter path. There was no wind. Measurement time span was 0011 to 0111 LCT.

**Table 7-4. Station 1.4**

Variable Name	Filters				
	1	2	3	4	5
Total Scattering Coefficient ( $\text{m}^{-1}$ )	1.35 E-4	1.24 E-4	1.04 E-4	1.11 E-4	1.54 E-4
$\sigma(0,30^\circ)/s(0)$	0.381	0.550	0.272	0.167	0.241
$\sigma(0,150^\circ)/s(0)$	0.0449	-	0.0205	0.00864	0.0281
$\sigma(0,30^\circ)/\sigma(0,150^\circ)$	8.5	-	13.2	19.3	8.6
Downwelling Irradiance ( $\text{W m}^{-2} \mu\text{m}^{-1}$ )	9.91 E-4	1.00 E-3	1.14 E-3	9.26 E-4	1.02 E-3

**Station 1.5, 10 October 1968 (Table 7-5).** Rayong site in the monsoon season during moonlight. The moon phase angle was  $46^\circ$ , moon zenith angle  $47^\circ$  through  $45^\circ$ , and moon azimuth  $67^\circ$  from the north. The sky directly overhead was clear. The moon was filtered through a light-to-moderate haze but bright enough to define moderate-to-sharp shadows. The wind was calm and the tide was out. Again there were beach fires and fishing boat lights. Measurement time span was 2306 to 0015 LCT.

**Table 7-5. Station 1.5**

Variable Name	Filters				
	1	2	3	4	5
Total Scattering Coefficient ( $\text{m}^{-1}$ )	1.39 E-4	1.19 E-4	9.05 E-5	7.92 E-5	1.28 E-4
$\sigma(0,30^\circ)/s(0)$	0.410	0.400	0.281	0.217	0.294
$\sigma(0,150^\circ)/s(0)$	0.0615	0.0363	0.0240	0.00660	0.0276
$\sigma(0,30^\circ)/\sigma(0,150^\circ)$	6.7	11.0	11.7	32.9	10.6
Downwelling Irradiance ( $\text{W m}^{-2} \mu\text{m}^{-1}$ )	4.02 E-4	4.03 E-4	4.95 E-4	4.08 E-4	3.84 E-4

**Station 1.6, 11 October 1968 (Table 7-6).** Rayong site in the monsoon season during moonlight. The moon phase angle was  $58^\circ$ , moon zenith angle  $51^\circ$  through  $48^\circ$ , and moon azimuth  $65^\circ$  through  $64^\circ$  from the north. Data were collected after the moon rose above the clouds on the horizon. There were scattered thin clouds but the moonlight was unobscured and there were clear sharp shadows. There was intermittent lightning in the western sky over Utapao. Only two fishing boat lanterns were noticed. Measurement time span was 2319 to 0056 LCT.

Table 7-6. Station 1.6

Variable Name	Filters				
	1	2	3	4	5
Total Scattering Coefficient ( $m^{-1}$ )	1.57 E-4	1.27 E-4	9.77 E-5	8.51 E-5	1.50 E-4
$\sigma(0,30^\circ)/s(0)$	0.431	0.418	0.340		0.336
$\sigma(0,150^\circ)/s(0)$	0.0421	0.0421	0.0307	0.0192	0.0535
$\sigma(0,30^\circ)/\sigma(0,150^\circ)$	10.2	9.9	11.1	-	6.3
Downwelling Irradiance ( $W m^{-2} \mu m^{-1}$ ) (Average)	3.96 E-4	4.10 E-4	4.95 E-4	3.92 E-4	3.86 E-4

Terrain Description	Path of Sight		Radiance ( $Watt \Omega^{-1} m^{-2} \mu m^{-1}$ )				
	Zenith Angle	Azimuth	Filters				
			1	2	3	4	5
Sandy Beach	92	40	3.00 E-5	3.37 E-5	5.11 E-5	3.99 E-5	3.48 E-5
Sandy Beach	94	40	3.67 E-5	4.09 E-5	6.11 E-5	4.58 E-5	4.18 E-5
Sandy Beach	92	210	3.44 E-5	4.03 E-5	6.46 E-5	4.96 E-5	4.29 E-5
Sandy Beach	94	210	3.82 E-5	4.42 E-5	7.11 E-5	5.46 E-5	4.71 E-5
Ocean Water	92	90	3.01 E-5	2.94 E-5	2.57 E-5	1.62 E-5	2.61 E-5

**Station 1.7, 12 October 1968 (Table 7-7).** Rayong site 16 km west of Rayong in the monsoon season during overcast starlight. There was medium-to-full overcast prior to moonrise. Data were measured in conjunction with Flight 87. Flight 87 occurred from 1926 to 2037 LCT in the area 8 km south of Rayong. Station 1.7 began after the flight ended, spanning 2105 to 2145 LCT.

Table 7-7. Station 1.7

Variable Name	Filters				
	1	2	3	4	5
Total Scattering Coefficient ( $m^{-1}$ )	1.63 E-4	1.22 E-4	9.32 E-5	8.04 E-5	1.36 E-4
$\sigma(0,30^\circ)/s(0)$	0.367	0.346	0.298	0.256	0.276
$\sigma(0,150^\circ)/s(0)$	0.0408	0.0404	0.0339	0.0143	0.0401
$\sigma(0,30^\circ)/\sigma(0,150^\circ)$	9.0	8.6	8.8	17.9	6.9
Downwelling Irradiance ( $W m^{-2} \mu m^{-1}$ ) <sup>*</sup>	(9.36 E-6)	(1.06 E-5)	(1.83 E-5)	-	1.59 E-5

Terrain Description	Path of Sight		Radiance ( $Watt \Omega^{-1} m^{-2} \mu m^{-1}$ )				
	Zenith Angle	Azimuth	Filters				
			1	2	3	4	5
Sandy Beach	103	South	6.17 E-7	8.08 E-7	2.14 E-6	2.87 E-6	1.13 E-6

\* Values in parentheses are based on airborne measurements during Flight 87.

**Station 1.8, 13 October 1968 (Table 7-8).** Rayong site in the monsoon season during starlight before moonrise. There was a light haze with clouds around the horizon. The sky glow was clearly visible from Utapao to the west and from the closest village to the northwest. There were eight to ten campfires along the beach to the southeast and one or two fishing boats with lights to the south. Measurement time span was from 1940 to 2118 LCT.

**Table 7-8. Station 1.8**

Variable Name	Filters				
	1	2	3	4	5
Total Scattering Coefficient ( $\text{m}^{-1}$ )	1.62 E-4	1.56 E-4	1.34 E-4	1.11 E-4	1.76 E-4
$\sigma(0,30^\circ)/s(0)$	0.356	0.444	0.386	0.406	0.281
$\sigma(0,150^\circ)/s(0)$	0.0336	0.0296	0.0176	0.00806	0.0228
$\sigma(0,30^\circ)/\sigma(0,150^\circ)$	10.6	15.0	21.9	50.3	12.3
Downwelling Irradiance ( $\text{W m}^{-2} \mu\text{m}^{-1}$ )	(Average) -	-	-	-	1.56 E-5

Terrain Description	Path of Sight		Radiance ( $\text{Watt } \Omega^{-1} \text{ m}^{-2} \mu\text{m}^{-1}$ )				
	Zenith Angle	Azimuth	Filters				
			1	2	3	4	5
Wild sweet peas & grass	92	West	2.63 E-7	4.16 E-7	6.55 E-7	7.09 E-6	7.59 E-7
Sandy Beach	92	West	9.08 E-7	1.16 E-6	3.56 E-6	6.17 E-6	-
Sandy Beach	94	West	8.73 E-7	-	-	-	-
Sandy Beach	100	West	8.78 E-7	1.08 E-6	2.49 E-6	2.94 E-6	1.51 E-6
Ocean water, shallow	92	South	1.38 E-6	1.52 E-6	2.83 E-6	3.91 E-6	1.99 E-6

**Station 1.9, 19 October 1968 (Table 7-9).** Rayong site 16 km west of Rayong in the monsoon season during starlight before moonrise. There were light wisps of clouds scattered overhead. It was cloudy or hazy around the horizon. The offshore windspeed was approximately 6 km/hr. There was typical fishing boat activity and a sky glow in the Utapao direction. Data were taken from 2113 to 2252 LCT in conjunction with Flight 88I from 2111 to 2226 LCT over the ocean 8 km south of Rayong.

**Station 1.10, 22 October 1968 (Table 7-10).** Rayong site in the monsoon season during overcast starlight before moonrise. During the background radiance measurements the sky was almost completely clouded over and only intermittent patches of stars were visible. The offshore windspeed was approximately 10 to 12 km/hr. There were no fishing boat lanterns due to continued small craft warning (there was a storm the night before). There was light surf (normally there was none) and a heavy dew. Measurement time span was 2032 to 2214 LCT.

Table 7-9. Station 1.9

Variable Name	Filters				
	1	2	3	4	5
Total Scattering Coefficient ( $m^{-1}$ )	1.24 E-4	1.09 E-4	8.29 E-5	7.70 E-5	1.13 E-4
$\sigma(0,30^\circ)/s(0)$	0.547	0.446	0.463	0.412	0.298
$\sigma(0,150^\circ)/s(0)$	0.0508	0.0577	0.0348	0.0231	0.0446
$\sigma(0,30^\circ)/\sigma(0,150^\circ)$	10.8	7.7	13.3	17.8	6.7
Downwelling Irradiance ( $W m^{-2} \mu m^{-1}$ ) <sup>*</sup>	(Average) (1.14 E-5)	(1.28 E-5)	(1.78 E-5)		1.45 E-5

Terrain Description	Path of Sight		Radiance ( $Watt \Omega^{-1} m^{-2} \mu m^{-1}$ )				
			Filters				
	Zenith Angle	Azimuth	1	2	3	4	5
Sandy Beach	92	West	8.68 E-7	1.06 E-6	2.19 E-6	2.23 E-6	1.54 E-6
Sandy Beach	94	West	9.59 E-7	1.00 E-6	2.04 E-6	2.07 E-6	1.32 E-6
Sandy Beach	96	West	8.30 E-7	9.87 E-7	2.04 E-6	2.11 E-6	1.30 E-6
Sandy Beach	92	East	9.21 E-7	1.14 E-6	2.50 E-6	3.06 E-6	1.52 E-6
Sandy Beach	94	East	8.36 E-7	9.98 E-7	2.33 E-6	2.32 E-6	1.37 E-6
Sandy Beach	96	East	8.46 E-7	1.05 E-6	-	2.46 E-6	1.40 E-6
Ocean	92	South	1.06 E-6	1.18 E-6	1.75 E-6	1.70 E-6	1.32 E-6

\* Values in parentheses are based on airborne measurements during Flight 881

Table 7-10. Station 1.10

Variable Name	Filters				
	1	2	3	4	5
Total Scattering Coefficient ( $m^{-1}$ )	1.56 E-4	1.20 E-4	1.02 E-4	8.78 E-5	1.35 E-4
$\sigma(0,30^\circ)/s(0)$	0.393	0.443	0.400	0.315	0.314
$\sigma(0,150^\circ)/s(0)$	0.0511	0.0532	0.0269	0.0181	0.0435
$\sigma(0,30^\circ)/\sigma(0,150^\circ)$	7.7	8.3	14.9	17.4	7.2
Downwelling Irradiance ( $W m^{-2} \mu m^{-1}$ )	(Average) -	-	-	-	1.20 E-5

Terrain Description	Path of Sight		Radiance ( $Watt \Omega^{-1} m^{-2} \mu m^{-1}$ )				
			Filters				
	Zenith Angle	Azimuth	1	2	3	4	5
Dirt road	92	West	4.93 E-7	6.43 E-7	1.39 E-6	2.63 E-6	4.60 E-7
Dirt road	96	West	4.42 E-7	5.53 E-7	1.38 E-6	2.78 E-6	3.95 E-7
Dirt road	92	East	4.44 E-7	5.34 E-7	1.26 E-6	2.31 E-6	4.85 E-7
Dirt road	94	East	4.20 E-7	4.68 E-7	1.11 E-6	1.71 E-6	4.90 E-7
Dirt road	96	East	3.39 E-7	4.18 E-7	1.03 E-6	1.62 E-6	4.03 E-7
Scrub and sand	92	North	2.65 E-7	3.30 E-7	6.74 E-7	1.49 E-6	-
Scrub and sand	94	North	2.23 E-7	2.54 E-7	5.34 E-7	1.12 E-6	2.49 E-7
Scrub and sand	96	North	2.03 E-7	2.30 E-7	5.22 E-7	1.05 E-6	2.50 E-7

## TDY-2 STATIONS

**Rayong Site.** The second Thailand trip, TDY-2, was during the relatively dry season. Stations 2.1 through 2.4, 23 February through 2 March 1969, were at the Rayong site at latitude 12.7°N and 101.3°E. The ground station was located on the coast 16 km west of Rayong on the same site used for TDY-1. The site was in a vegetated area between the beach sand and a road. Beach sand and the road ran roughly east and west; there was scrub and sand to the north, the ocean was south. Water just offshore was approximately 3 m in depth. The flight path for Flights 97 and 101 are shown in Fig. 7-4.

**Station 2.1, 23 February 1969 (Table 7-11).** Rayong site in the relatively dry season during moonlight. The moon phase angle was 97°, moon zenith angle 50° to 56°, and moon azimuth 291° from the north. There were clouds and haze on the horizon at sunset. The sky was clear overhead with some scattered clouds during the measurements. A campfire was noticed to the east. The windspeed was 27 km/hr from the south to southwest. Measurement time span was 2108 to 2139 LCT.

Table 7-11. Station 2.1

Variable Name	Filters				
	1	2	3	4	5
Total Scattering Coefficient ( $m^{-1}$ )	-	-	-	-	-
$\sigma(0,30^\circ)/s(0)$	-	-	-	-	-
$\sigma(0,150^\circ)/s(0)$	-	-	-	-	-
$\sigma(0,30^\circ)/\sigma(0,150^\circ)$	-	-	-	-	-
Downwelling Irradiance ( $W m^{-2} \mu m^{-1}$ )	-	-	-	-	-

Terrain Description	Path of Sight		Radiance ( $Watt \Omega^{-1} m^{-2} \mu m^{-1}$ )				
	Zenith Angle	Azimuth	Filters				
			1	2	3	4	5
Dirt Road (West)	92	340	4 01 E 6	5 76 E 6	1 315 E 5	1 39 E 5	7 89 E 6
Dirt Road (West)	94	340	6 09 E 6	6 30 E 6	-	1 29 E 5	8 94 E 6
Dirt Road (West)	96	340	3 94 E 6	4 23 E 6	1 06 E 5	-	-
Dirt Road (West)	100	340	-	1 62 E 6	3 19 E 6	2 19 E 6	2 78 E 6
Dirt Road (West)	105	340	3 37 E 6	3 62 E 6	5 53 E 6	5 91 E 6	-
Dirt Road (East)	92	160	7 86 E 6	1 02 E 5	2 44 E 5	2 44 E 5	1 35 E 5
Dirt Road (East)	94	160	7 22 E 6	8 77 E 6	2 00 E 5	-	1 07 E 5
Dirt Road (East)	96	160	5 93 E 6	7 075 E 6	1 62 E 5	1 60 E 5	9 08 E 6
Dirt Road (East)	100	160	5 22 E 6	6 41 E 6	1 63 E 5	1 26 E 5	2 81 E 6
Dirt Road (East)	105	160	2 12 E 6	2 56 E 6	1 68 E 5	-	9 54 E 6



**Station 2.2, 26 February 1969 (Table 7-12).** Rayong site in the relatively dry season during moonlight. The moon phase angle was  $62^\circ$ , moon zenith angle  $23^\circ$  to  $37^\circ$ , and moon azimuth  $316^\circ$  to  $301^\circ$  from the north. The sky was clear overhead with scattered small clouds and haze on the horizon. The windspeed was 16 to 19 km/hr from the south to southwest. Measurement time span was 2122 to 2236 LCT.

**Table 7-12. Station 2.2**

Variable Name	Filters				
	1	2	3	4	5
Total Scattering Coefficient ( $\text{m}^{-1}$ )	1.42E-4	1.24E-4	6.62E-5	6.34E-5	9.91E-5
$\sigma(0,30^\circ)/s(0)$	0.555	0.400	-	0.341	0.412
$\sigma(0,150^\circ)/s(0)$	0.0349	0.0308	0.0302	0.0227	0.0319
$\sigma(0,30^\circ)/\sigma(0,150^\circ)$	15.9	16.5	-	15.0	12.9
Downwelling Irradiance ( $\text{W m}^{-2} \mu\text{m}^{-1}$ ) (After)	4.35E-4	4.79E-4	6.44E-4	4.80E-4	4.54E-4

Terrain Description	Path of Sight		Radiance ( $\text{Watt } \Omega^{-1} \text{ m}^{-2} \mu\text{m}^{-1}$ )				
	Zenith Angle	Azimuth	Filters				
			1	2	3	4	5
Dirt road (west)	92	320	1.66E-5	2.04E-5	4.49E-5	4.65E-5	2.58E-5
Dirt road (west)	94	320	1.78E-5	2.16E-5	4.86E-5	4.36E-5	2.75E-5
Dirt road (west)	96	320	1.88E-5	2.30E-5	5.31E-5	4.80E-5	2.97E-5
Dirt road (west)	100	320	2.06E-5	2.59E-5	6.22E-5	5.39E-5	3.40E-5
Dirt road (west)	105	320	1.94E-5	2.48E-5	6.14E-5	5.34E-5	3.27E-5
Dirt road (east)	92	140	2.04E-5	2.45E-5	6.02E-5	6.29E-5	3.23E-5
Dirt road (east)	94	140	1.98E-5	2.42E-5	5.38E-5	4.92E-5	3.04E-5
Dirt road (east)	96	140	1.91E-5	2.31E-5	5.26E-5	4.70E-5	2.96E-5
Dirt road (east)	100	140	2.00E-5	2.43E-5	5.90E-5	5.13E-5	3.19E-5
Dirt road (east)	105	140	2.33E-5	2.86E-5	6.03E-5	5.86E-5	3.74E-5

**Station 2.3, 28 February 1969 (Table 7-13).** Rayong site in the relatively dry season during moonlight. The moon phase angle was  $40^\circ$ , moon zenith angle  $16^\circ$  to  $31^\circ$ , and moon azimuth  $321^\circ$  to  $298^\circ$  from the north. The weather was cool with scattered clouds. The windspeed was 16 to 19 km/hr from the south. Measurement time span was 2234 to 2351 LCT.

Table 7-13. Station 2.3

Variable Name	Filters				
	1	2	3	4	5
Total Scattering Coefficient ( $\text{m}^{-1}$ )	-	-	-	-	-
$\alpha(0,30^\circ) \rightarrow s(0)$	-	-	-	-	-
$\alpha(0,150^\circ) \rightarrow s(0)$	-	-	-	-	-
$\alpha(0,30^\circ) \rightarrow \alpha(0,150^\circ)$	-	-	-	-	-
Downwelling Irradiance ( $\text{W m}^{-2} \mu\text{m}^{-1}$ ) (After)	8.75E-4	8.73E-4	1.19E-3	9.07E-4	9.36E-4

Terrain Description	Path of Sight		Radiance ( $\text{Watt } \Omega^{-1} \text{ m}^{-2} \mu\text{m}^{-1}$ )				
	Zenith Angle	Azimuth	Filters				
			1	2	3	4	5
Shrubs and sand (west)	92	320	1.37E-6	2.03E-6	2.60E-6	8.97E-5	2.45E-5
Shrubs and sand (west)	94	320	1.33E-6	1.84E-6	2.32E-6	7.64E-5	2.30E-5
Shrubs and sand (west)	96	320	1.21E-6	1.57E-6	1.21E-6	2.72E-5	9.95E-6
Shrubs and sand (west)	100	320	1.26E-6	1.73E-6	2.68E-6	5.51E-5	1.86E-5
Shrubs and sand (west)	105	320	1.48E-6	1.70E-6	2.93E-6	4.72E-5	1.69E-5
Shrubs and sand (east)	92	140	2.15E-6	2.66E-6	5.48E-5	8.39E-5	3.24E-5
Shrubs and sand (east)	94	140	2.99E-6	3.77E-6	-	-	-
Shrubs and sand (east)	96	140	2.64E-6	3.32E-6	5.91E-5	8.04E-5	3.91E-5
Shrubs and sand (east)	100	140	2.19E-6	2.95E-6	5.12E-5	8.49E-5	3.37E-5
Shrubs and sand (east)	105	140	2.25E-6	2.82E-6	4.73E-5	6.64E-5	3.18E-5

**Station 2.4, 2 March 1969 (Table 7-14).** Rayong site in the relatively dry season during moonlight. The moon phase angle was  $18^\circ$ , moon zenith angle  $37^\circ$  to  $27^\circ$ , and moon azimuth  $78^\circ$  from the north. There were scattered clouds. The windspeed was 19 to 24 km/hr from the south to southwest. Measurement time span was 2045 to 2127 LCT.

**Lop Buri Site.** The second Thailand trip, TDY-2, was during the relatively dry season. Stations 2.5 through 2.10, 7 March through 12 March 1969, were at the Lop Buri site at latitude  $14.8^\circ\text{N}$  and longitude  $100.4^\circ\text{E}$ . The ground station was at the Lop Buri site near Sing Buri. The same general site was used as for TDY-1, except that the truck and instruments were located 13 m south into the field. The rice had been harvested so the field was dirt and stubble during TDY-2. Three views of a typical harvested rice field are shown in Fig. 7-5.

Table 7-14. Station 2.4

Variable Name	Filters				
	1	2	3	4	5
Total Scattering Coefficient ( $m^{-1}$ )					
$\sigma(0.30) \leq (0)$					
$\sigma(0.150) \leq (0)$					
$\sigma(0.30) - \sigma(0.150)$					
Downwelling Irradiance ( $W m^{-2} \mu m^{-1}$ ) (After)	1.57E-3	1.68E-3	2.19E-3	1.60E-3	1.77E-3

Terrain Description	Path of Sight		Radiance ( $Watt m^{-2} \mu m^{-1}$ )				
	Zenith Angle	Azimuth	Filters				
			1	2	3	4	5
Dirt road (west)	92	132	6.12E-5	7.61E-5	1.73E-4	1.59E-4	
Dirt road (west)	34	192	6.72E-5	8.05E-5	1.79E-4	1.45E-4	9.89E-5
Dirt road (west)	96	192	7.23E-5	8.71E-5	1.94E-4	1.61E-4	1.08E-4
Dirt road (west)	100	192	7.83E-5	9.54E-5	2.13E-4	1.73E-4	1.18E-4
Dirt road (west)	105	192	8.17E-5	1.00E-4	2.34E-4	1.87E-4	1.26E-4
Dirt road (east)	92	12	5.77E-5	7.03E-5	1.45E-4	1.21E-4	8.33E-5
Dirt road (east)	94	12	5.57E-5	6.72E-5	1.33E-4	1.17E-4	8E-5
Dirt road (east)	96	12	5.47E-5	6.55E-5	1.39E-4	1.15E-4	7.97E-5
Dirt road (east)	100	12	6.75E-5	8.04E-5	1.88E-4	1.67E-4	1.02E-4
Dirt road (east)	105	12	7.96E-5	9.69E-5	2.23E-4	1.83E-4	

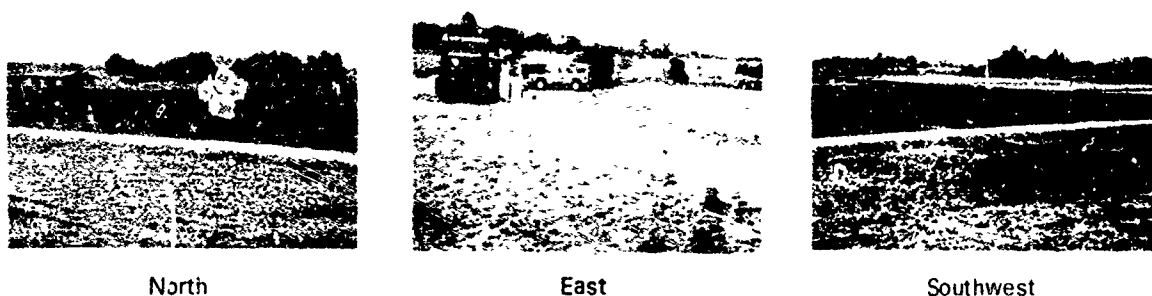


Fig. 7-5. Views of harvested rice fields at Lop Buri site during TDY-2.

**Station 2.5, 8 March 1969 (Table 7-15).** Lop Buri site in the relatively dry season during moonlight. The moon phase angle was  $57^\circ$ , moon zenith angle  $69^\circ$  to  $56^\circ$ , and moon azimuth  $118^\circ$  to  $127^\circ$  from the north. Evening began with haze at the horizon but clear skies overhead and a windspeed of 3 to 8 km/hr from the south to southeast. Then a smoke trail blew in from the south in a very tight smoke layer which occulted the moon. This happened before the nephelometer measurements. By the time the background radiance measurements were being made, the smoke had scattered somewhat. Smoke had completely cleared away by the end of measurements. Measurement time span was 2351 to 0057 LCT.

Table 7-15. Station 2.5

Variable Name	Filters					
	1	2	3	4	5	
Total Scattering Coefficient ( $m^{-1}$ )	2.55 E-4	2.25 E-4	1.48 E-4	1.42 E-4	1.96 E-4	
$\alpha(0.30) : s(0)$	0.370	0.361	0.273	0.196	0.289	
$\alpha(0.150) : s(0)$	0.0223	0.0216	0.0178	0.0137	0.0197	
$\alpha(0.30) : \alpha(0.150)$	16.6	16.7	15.4	14.3	14.7	
Downwelling Irradiance ( $W m^{-2} \mu m^{-1}$ )	(Before)	1.78 E-4	1.92 E-4	2.42 E-4	1.85 E-4	1.90 E-4
	(After)	2.70 E-4	2.95 E-4	4.00 E-4	2.93 E-4	2.80 E-4

**Station 2.6, 9 March 1969 (Table 7-16).** Lop Buri site in the relatively dry season during starlight before moonrise. There was haze on the horizon but the sky was clear overhead. The windspeed was 8 to 11 km/hr from the south to southeast. Measurement time span was 2123 to 2314 LCT. Moonrise was at 2315 LCT. Data were taken just prior to the advent of Flight 92 in the same general area as the ground station.

Table 7-16. Station 2.6

Variable Name	Filters					
	1	2	3	4	5	
Total Scattering Coefficient ( $m^{-1}$ )	2.94 E-4	2.60 E-4	1.70 E-4	1.65 E-4	2.27 E-4	
$\alpha(0.30) : s(0)$	0.327	0.308	0.227	0.166	0.255	
$\alpha(0.150) : s(0)$	0.0215	0.0210	-	0.0137	0.0202	
$\alpha(0.30) : \alpha(0.150)$	15.2	14.7	-	12.1	12.6	
Downwelling Irradiance ( $W m^{-2} \mu m^{-1}$ )	(Before)	5.50 E-6	5.67 E-6	9.42 E-6	1.10 E-5	7.08 E-6
	(After)	8.91 E-6	9.28 E-6	1.34 E-5	1.26 E-5	1.02 E-5

Terrain Description	Path of Sight		Radiance (Watt $\Omega^{-1} m^{-2} \mu m^{-1}$ )				
	Zenith Angle	Azimuth	Filters				
			1	2	3	4	5
Harvested Rice Field	180		1.60 E-7	1.80 E-7	5.21 E-7	5.95 E-7	3.96 E-7
Harvested Rice Field	93	West	1.59 E-7	2.14 E-7	5.07 E-7	8.30 E-7	4.52 E-7
Harvested Rice Field	95	West	1.74 E-7	2.19 E-7	5.65 E-7	8.51 E-7	4.80 E-7
Harvested Rice Field	100	West	1.74 E-7		5.51 E-7	7.57 E-7	4.48 E-7
Harvested Rice Field	105	West	1.70 E-7	1.98 E-7	5.12 E-7	6.11 E-7	4.18 E-7
Harvested Rice Field	120	West	1.45 E-7	1.55 E-7	4.33 E-7	5.46 E-7	
Harvested Rice Field	135	West	1.29 E-7	1.56 E-7	4.13 E-7	5.93 E-7	3.54 E-7
Harvested Rice Field	93	East	1.63 E-7	2.11 E-7	5.56 E-7	7.19 E-7	4.67 E-7
Harvested Rice Field	95	East	1.80 E-7	2.18 E-7	5.79 E-7	7.40 E-7	4.71 E-7
Harvested Rice Field	100	East	1.81 E-7	2.27 E-7	5.83 E-7	6.86 E-7	4.80 E-7
Harvested Rice Field	105	East	2.03 E-7	2.41 E-7	6.36 E-7	6.97 E-7	5.00 E-7
Harvested Rice Field	120	East	2.17 E-7	2.56 E-7	6.31 E-7	6.34 E-7	5.00 E-7
Harvested Rice Field	135	East	2.29 E-7	2.65 E-7	6.39 E-7	5.91 E-7	4.95 E-7
Harvested Rice Field	180		2.40 E-7	2.69 E-7	6.28 E-7	5.86 E-7	4.91 E-7

**Station 2.7, 9 March 1969 (Table 7-17).** Lop Buri site in the relatively dry season during moonlight. The moon phase angle was 69°, moon zenith angle 65° to 54°, and moon azimuth 126° to 136° from the north. This was a continuation of data-gathering after moonrise on the same night as station 2.6. There was haze on the horizon but the sky was clear overhead. The windspeed was 8 to 11 km/hr from the south to southwest. Data were taken from 0115 to 0221 LCT in conjunction with Flight 92 from 0031 to 0253 LCT in the same general area as the ground station.

**Table 7-17. Station 2.7**

Variable Name	Filters				
	1	2	3	4	5
Total Scattering Coefficient ( $m^{-1}$ )	3.23 E 4	2.82 E 4	1.84 E 4	1.76 E 4	2.36 E 4
$\sigma(0.30) / \sigma(0)$	0.330	0.309	0.224	0.159	0.250
$\sigma(0.150) / \sigma(0)$	0.0191	0.0182	0.0151	0.0113	0.0170
$\sigma(0.30) / \sigma(0.150)$	17.1	17.0	14.8	14.1	14.6
Downwelling Irradiance ( $W m^{-2} \mu m^{-1}$ )	(Before)	1.45 E 4	2.03 E 4	1.59 E 4	1.47 E 4
	(After)	1.82 E 4	2.01 E 4	2.77 E 4	2.01 E 4

Terrain Description	Path of Sight		Radiance (Watt $m^{-2} \mu m^{-1}$ )				
	Zenith Angle	Azimuth	1	2	3	4	5
Harvested Rice Field	180		4.86 E 6	6.12 E 6	1.33 E 5	1.36 E 5	
Harvested Rice Field (East)	93	320	6.56 E 6	8.30 E 6	1.63 E 5	1.94 E 5	9.67 E 6
Harvested Rice Field (East)	95	320	6.40 E 6	8.00 E 6	1.59 E 5	1.86 E 5	9.36 E 6
Harvested Rice Field (East)	100	320	6.28 E 6	7.78 E 6	1.56 E 5	1.75 E 5	9.10 E 6
Harvested Rice Field (East)	105	320	6.35 E 6	7.89 E 6	1.61 E 5	1.74 E 5	9.20 E 6
Harvested Rice Field (East)	120	320	6.20 E 6	7.74 E 6	1.60 E 5	1.64 E 5	9.07 E 6
Harvested Rice Field (East)	135	320	5.97 E 6	7.46 E 6	1.55 E 5	1.57 E 5	8.67 E 5
Harvested Rice Field (West)	93	140	8.40 E 6	1.11 E 5	2.28 E 5	2.92 E 5	1.36 E 5
Harvested Rice Field (West)	95	140	9.09 E 6	1.18 E 5	2.53 E 5	2.94 E 5	1.46 E 5
Harvested Rice Field (West)	100	140	9.13 E 6	1.18 E 5	2.55 E 5	2.86 E 5	1.45 E 5
Harvested Rice Field (West)	105	140	9.88 E 6	1.19 E 5	2.55 E 5	3.02 E 5	1.82 E 5
Harvested Rice Field (West)	120	140	8.05 E 6	1.02 E 5	2.08 E 5	2.58 E 5	1.60 E 5
Harvested Rice Field (West)	135	140	9.19 E 6	1.03 E 5	2.15 E 5	2.54 E 5	1.25 E 5
Harvested Rice Field (West)	180		6.45 E 6	8.14 E 6	1.73 E 5		9.63 E 6

**Station 2.8, 11 March 1969 (Table 7-18).** Lop Buri site in the relatively dry season during starlight prior to moonrise. The sky was clear overhead, the horizon was hazy, and the windspeed was 3 to 8 km/hr from the south to southeast. Measurement time span was 0036 to 0050 LCT.

Table 7-18. Station 2.8

Variable Name	Filters				
	1	2	3	4	5
Total Scattering Coefficient ( $m^{-1}$ )	3.40E-4	3.04E-4	2.02E-4	2.06E-4	2.72E-4
$\sigma(0.30) + s(0)$	0.276	0.266	0.197	0.135	0.220
$\sigma(0.150) + s(0)$	0.0170	0.0162	0.0133	0.00975	0.0151
$\sigma(0.30) + \sigma(0.150)$	16.2	16.4	14.9	13.8	14.5
Downwelling Irradiance ( $W m^{-2} \mu m^{-1}$ )					

Station 2.9, 12 March 1969 (Table 7-19). Lop Buri site in the relatively dry season during starlight prior to moonrise. A heavy haze was noticed at sunset which cleared sufficiently so that stars were visible though fuzzy. There was an east wind at 16 to 19 km/hr. Measurement time span was 2025 to 2246 LCT.

Table 7-19. Station 2.9

Variable Name	Filters				
	1	2	3	4	5
Total Scattering Coefficient ( $m^{-1}$ )	2.95E-4	2.43E-4	1.37E-4	1.38E-4	1.99E-4
$\sigma(0.30) + s(0)$	0.277	0.252	0.168	0.132	0.216
$\sigma(0.150) + s(0)$	0.0174	0.0167	0.0138	0.0107	0.0174
$\sigma(0.30) + \sigma(0.150)$	15.9	15.1	12.2	12.4	12.4
Downwelling Irradiance ( $W m^{-2} \mu m^{-1}$ )	(Before)	6.20E-6	6.45E-6	9.28E-6	7.99E-6
	(After)	4.86E-6	5.18E-6	1.10E-5	-

Terrain Description	Path of Sight		Radiance ( $Watt m^{-2} \mu m^{-1}$ )				
	Zenith Angle	Azimuth	Filters				
			1	2	3	4	5
Harvested Rice Field	180		-	2.97E-7	9.49E-7	1.48E-6	3.82E-7
Harvested Rice Field	93	West	3.39E-7	4.42E-7	1.02E-6	2.32E-6	4.05E-7
Harvested Rice Field	95	West	3.50E-7	4.61E-7	9.10E-7	1.80E-6	4.08E-7
Harvested Rice Field	100	West	3.80E-7	4.39E-7	8.42E-7	2.30E-6	3.99E-7
Harvested Rice Field	105	West	4.34E-7	4.99E-7	8.83E-7	1.69E-6	3.48E-7
Harvested Rice Field	120	West	2.37E-7	2.76E-7	6.26E-7	1.17E-6	2.78E-7
Harvested Rice Field	135	West	2.65E-7	3.09E-7	5.73E-7	1.16E-6	2.87E-7
Harvested Rice Field	93	East	2.72E-7	3.03E-7	7.93E-7	1.27E-6	4.30E-7
Harvested Rice Field	95	East	2.83E-7	3.62E-7	3.54E-7	1.23E-6	4.61E-7
Harvested Rice Field	100	East	3.19E-7	4.37E-7	1.11E-6	1.33E-6	4.58E-7
Harvested Rice Field	105	East	3.12E-7	3.33E-7	7.35E-7	1.32E-6	4.44E-7
Harvested Rice Field	120	East	3.24E-7	3.43E-7	6.58E-7	8.93E-7	3.95E-7
Harvested Rice Field	135	East	2.71E-7	3.22E-7	7.56E-7	1.19E-6	4.52E-7
Harvested Rice Field	180		2.65E-7	2.88E-7	8.90E-7	1.61E-6	4.70E-7

#### DIRECTIONAL BACKGROUND REFLECTANCE

The directional background reflectance values  $R_c(0, \theta, \phi)$  are presented in Table 7-20 for the wet season TDY-1. They are given in order by station number with descriptive information on the phase angle and

zenith angle of the moon. The reflectances are obtained from background radiances and irradiances measured concurrently, except as noted.

The reflectances are presented with two significant figures indicating the reliability of the values. It should be kept in mind that there is an expected variability in reflectance for a given background for each path of sight due to the point-to-point differences in the background over a large area.

No reflectances are presented for TDY-2. Reflectances computed using an average of the irradiances measured before and after the background radiances indicated that compensation should be made for the change of irradiance with time. This could be done by assuming that the irradiance changed linearly with time. This will be the topic of a later study.

**Table 7-20. Directional Reflectance, Wet Season TDY-1**

Station	Moon		Description	Path of Sight		Reflectance				
	Phase Angle	Zenith Angle		Zenith Angle	Azimuth	1	2	3	4	5
1 1	85	63 64	Rice Field*	91	0		0 20	0 16	0 65	0 22
					90	0 063	0 11	0 063	0 62	0 13
					180	0 10	0 15	0 095	0 77	0 18
1 2	72	58 59	Rice Field	92	0	0 062	0 14	0 11	0 52	0 15
					90	0 046	0 10	0 060	0 50	0 11
					180	0 063	0 13	0 080	0 62	0 14
1 3	36	30 28	Rice Field	92	0	0 044	0 11	0 097	0 32	0 10
					180	0 033	0 072	0 041	0 39	0 074
					270	0 032	0 072		0 39	0 076
			Dirt Road through Rice Field (West)	92	110	0 13	0 16	0 25	0 29	0 17
1 7	Before Moonrise		Sandy Beach**	103	South	(0 21 )	(0 24 )	(0 37 )		0 22
1 8	Before Moonrise		Sandy Beach	100	West	-				0 32
			Wild Sweet Peas and Grass	92	West				-	0 15
			Ocean, Shallow	92	South			-	-	0 43
1 9	Before Moonrise		Sandy Beach†	92	West	(0 24 )	(0 26 )	(0 39 )		0 33
				94	West	(0 26 )	(0 25 )	(0 36 )		0 29
				96	West	(0 23 )	(0 24 )	(0 36 )		0 28
				92	East	(0 25 )	(0 28 )	(0 44 )		0 33
				94	East	(0 23 )	(0 25 )	(0 41 )		0 30
				96	East	(0 23 )	(0 26 )			0 30
				92	East	(0 29 )	(0 29 )	(0 31 )		0 29
1 10	Before Moonrise		Dirt Road (Near Beach)	92	West	-				0 11
				96	West	-				0 04
				92	East			-	-	0 12
				94	East	-				0 12
				96	East					0 10
			Scrub and Sand	94	North	-				0 074
				96	North	-	-	-	-	0 078

\* Downwelling irradiance measured after, rather than simultaneously with, background radiances

\*\* Values in parenthesis used downwelling irradiance based on airborne values of Flight 87

† Values in parenthesis used downwelling irradiance based on airborne values of Flight 88

### 7.3 GROUND-BASED DATA INTERPRETATION

#### TOTAL AND DIRECTIONAL SCATTERING

The attenuation coefficient is a direct measure of air clarity. In the absence of absorption, the attenuation coefficient and total scattering coefficient are equivalent.

The ground stations are arranged in order of increasing air clarity for Filter 5 (decreasing total scattering coefficients) in Table 7-21. The range of scattering coefficients from  $2.72 \text{E-}4$  to  $8.08 \text{E-}5$  is slightly different than for the airborne data from  $2.19 \text{E-}4$  to  $4.19 \text{E-}5$  (Table 6-5). Seven flights show coefficients less than  $8.08 \text{E-}5$  for Filter 5. Six of those seven flights occurred after 12 March 1969, which is the date of the last ground station with recoverable data. Only three ground stations show total scattering coefficients greater than  $2.19 \text{E-}4$ .

**Table 7-21. Total Scattering Coefficients for Ground Stations Ordered by Increasing Air Clarity for Filter 5**

Station	Date	Total Scattering Coefficient ( $\text{m}^{-1}$ )				
		Filters				
		1	2	5	3	4
2.8	11 Mar 69	$3.40 \text{E-}4$	$3.04 \text{E-}4$	$2.72 \text{E-}4$	$2.02 \text{E-}4$	$2.05 \text{E-}4$
2.7	9 Mar 69	$3.23 \text{E-}4$	$2.82 \text{E-}4$	$2.36 \text{E-}4$	$1.84 \text{E-}4$	$1.76 \text{E-}4$
2.6	9 Mar 69	$2.94 \text{E-}4$	$2.60 \text{E-}4$	$2.27 \text{E-}4$	$1.70 \text{E-}4$	$1.65 \text{E-}4$
2.9	12 Mar 69	$2.95 \text{E-}4$	$2.43 \text{E-}4$	$1.99 \text{E-}4$	$1.37 \text{E-}4$	$1.38 \text{E-}4$
2.5	8 Mar 69	$2.55 \text{E-}4$	$2.25 \text{E-}4$	$1.96 \text{E-}4$	$1.48 \text{E-}4$	$1.42 \text{E-}4$
1.8	13 Oct 68	$1.62 \text{E-}4$	$1.56 \text{E-}4$	$1.76 \text{E-}4$	$1.34 \text{E-}4$	$1.11 \text{E-}4$
1.3	3 Oct 68	$1.95 \text{E-}4$	$1.67 \text{E-}4$	$1.75 \text{E-}4$	$1.08 \text{E-}4$	$9.08 \text{E-}5$
1.2	30 Sep 68	$1.92 \text{E-}4$	$1.48 \text{E-}4$	$1.62 \text{E-}4$	$1.10 \text{E-}4$	$8.23 \text{E-}5$
1.4	9 Oct 68	$1.35 \text{E-}4$	$1.24 \text{E-}4$	$1.54 \text{E-}4$	$1.04 \text{E-}4$	$1.11 \text{E-}4$
1.6	11 Oct 68	$1.57 \text{E-}4$	$1.27 \text{E-}4$	$1.50 \text{E-}4$	$9.77 \text{E-}5$	$8.51 \text{E-}5$
1.7	12 Oct 68	$1.63 \text{E-}4$	$1.22 \text{E-}4$	$1.36 \text{E-}4$	$9.32 \text{E-}5$	$8.04 \text{E-}5$
1.10	22 Oct 68	$1.56 \text{E-}4$	$1.20 \text{E-}4$	$1.35 \text{E-}4$	$1.02 \text{E-}4$	$8.78 \text{E-}5$
1.5	10 Oct 68	$1.39 \text{E-}4$	$1.19 \text{E-}4$	$1.28 \text{E-}4$	$9.05 \text{E-}5$	$7.92 \text{E-}5$
1.9	19 Oct 68	$1.24 \text{E-}4$	$1.09 \text{E-}4$	$1.13 \text{E-}4$	$8.29 \text{E-}5$	$7.70 \text{E-}5$
2.2	26 Feb 69	$1.42 \text{E-}4$	$1.24 \text{E-}4$	$9.91 \text{E-}5$	$6.62 \text{E-}5$	$6.34 \text{E-}5$
1.1	29 Sep 69	$1.08 \text{E-}4$	$7.91 \text{E-}5$	$8.08 \text{E-}5$	$5.52 \text{E-}5$	$5.61 \text{E-}5$

*Airborne and Ground-Based Total Scattering.* The airborne and ground-based measurements of total scattering coefficient for the three nights of near concurrent air and ground operation are tabulated in Table 7-22. The data are given in chronological order. Two values of scattering coefficient per filter are given for each flight. One value is for the measurement during the lowest altitude of level flight. The second value is obtained from the data at the lowest altitude, in parenthesis, of the ascent or descent flight mode. This second value has been extrapolated to ground level by assuming an optical standard atmosphere for the intervening path (Eq. 2-9) which increased the measured value by approximately 2%.

For 9 March 1969 we have data on two ground stations (2.6 during starlight and 2.7 during moonlight) as well as on Flight 92 (during moonlight). Some of the measurements were taken concurrently. Quite



clearly the ground-based data show relatively little change with time. The airborne data, although slightly lower in magnitude than the ground-based data, also indicate relatively little change with time. Clearly, the atmosphere in the interval from ground level to a 168-through-183 m altitude is not well represented by the optical standard atmosphere for Flight 92. It would be more reasonable to extrapolate to the ground-based value measured during station 2.7.

For the two earlier dates, 12 October and 19 October 1968, the airborne scattering coefficient data show a clear change with time, i.e., increased scattering as time progressed. Due to the lack of ground-based data concurrent with or preceding the airborne data, it is not possible to determine whether the ground-based data indicate a further decrease in air clarity with time or also indicate that the ground level to 195 m interval cannot be represented by the optical standard atmosphere.

The Rayong ground station data for station 1.9 are compared to data from Flight 88I since the airplane was in sight from the ground station during the flight pattern. The ground station data are not compared to data from Flight 88II however, since this flight was over land farther east beyond a low range of hills. The airplane was not visible from the ground station during Flight 88II.

The data in Table 7-22 indicate the importance of concurrent air and ground station operation for full documentation of the total scattering coefficient profile with altitude. The ground station provides the anchoring ground level value to complete the profile with any degree of certainty.

**Table 7-22. Airborne and Ground-Based Measurements of Total Scattering Coefficient**

Date	Flight or Station No.	Time LCT		Altitude (Meters)	Mode	Total Scattering Coefficient ( $m^{-1}$ )				
		Start	End			1	2	Filters 3	4	5
12 Oct 68	87	1926	1930	191	L	8.34E-5	6.68E-5	4.87E-5	3.95E-5	1.01E-4
12 Oct 68	87	2013	2035	0(183)	A D	1.23E-4	1.07E-4	9.44E-5	6.65E-5	1.10E-4
12 Oct 68	17	2134	2143	0	GS	1.63E-4	1.22E-4	9.32E-5	8.04E-5	1.36E-4
19 Oct 68	88I	2111	2121	195**	L	8.45E-5	6.97E-5	4.92E-5	3.87E-5	8.14E-5
19 Oct 68	88I	2200	2226	0(183)	A D	1.08E-4	8.00E-5	5.59E-5	4.68E-5	9.86E-5
19 Oct 68	19	2243	2251	0	GS	1.24E-4	1.09E-4	8.29E-5	7.70E-5	1.13E-4
9 Mar 69	26	2123	2314	0	GS	2.94E-4	2.60E-4	1.70E-4	1.65E-4	2.27E-4
9 Mar 69	92	0031	0045	168	L	2.34E-4	1.88E-4	1.11E-4	6.80E-5	1.77E-4
9 Mar 69	2.7	0205	0220	0	GS	3.23E-4	2.82E-4	1.84E-4	1.76E-4	2.36E-4
9 Mar 69	92	0226	0243	0(183)	A D	2.22E-4	1.79E-4	1.13E-4	6.99E-5	1.88E-4

\* Values in parenthesis are lowest altitudes of measurement

\*\* Filter 1 value is for 502 m altitude

L = Level A D = Ascent or Descent GS = Ground Station

**Directional Scattering.** The data on directional scattering are presented in the form of proportional directional scattering coefficients  $\sigma(0,30^\circ)/s(0)$  and  $\sigma(0,150^\circ)/s(0)$ . This form is particularly useful since

$$\int_{4\pi} [\sigma(z,\beta)/s(z)] d\Omega = 1. \quad (7-2)$$

The dimension of the proportional directional scattering coefficient is per steradian. The values for  $\sigma(z, 30^\circ)/s(z)$  should be 0.1 and the values for  $\sigma(z, 150^\circ)/s(z)$  should be 0.1. This latter evaluation comes from inspecting the catalog of proportional directional scattering coefficients published by Barteneva (1960). Refer to Appendix F. All the ground-based directional scattering data meet these criteria. The values of proportional directional scattering coefficients may be converted to directional scattering coefficients in units of  $\Omega^{-1} \text{ m}^{-1}$  by multiplying by the total scattering coefficient.

No valid data on directional scattering are available from the airborne operation. Therefore the ground-based data are all the more valuable as the only measure of the directionality of the volume scattering function.

The ratio of forwardscattering to backscattering at  $30^\circ$  and  $150^\circ$  is a useful indication of the directionality of the scattering. For TDY-1 this ratio generally increased with wavelength. That is reasonable since, although the Mie volume scattering function may show the opposite effect, i.e., decreased ratio with wavelength, the additive Rayleigh component affects the smaller wavelengths to an even greater extent, effectively reversing the ratio with wavelength.

For TDY-2 the ratio is generally reversed. For five of the six TDY-2 stations, the total scattering coefficients are the largest of all the ground station data. These five stations were at Lop Buri where smoke from burning rice fields was commonplace so increased scattering coefficients are not unexpected. The effect of the Rayleigh component on the directional scattering would decrease with the increase in total scattering coefficient. But this would not account for the ratios for station 2.2 at Rayong (with one of the smallest total scattering coefficients), nor would it account for the shift between stations 1.8 and 2.5 (with a small change in total scattering and a reversal of the order of the ratio by wavelength). We are in the process of investigating the TDY-2 directional data and suggest caution in its use.

*Selection of Mie Volume Scattering Function.* A verification of the method of selecting the Mie volume scattering functions for the airborne data was obtained with the directional scattering data measured at the ground station during the three nights of concurrent ground and flight operation.

For both stations 1.7 and 1.9 the  $\sigma(0, 30^\circ)/\sigma(0, 150^\circ)$  ratios (6.9 and 6.7, respectively, for Filter 5) are halfway between the ratios of 5.0 and 8.5, which are for Barteneva function numbers 4 and 5. Since the airborne scattering coefficient at the lowest altitude for both Flights 87 and 88I was lower than the ground station scattering coefficient (refer to Table 7-22), the airborne volume scattering function should be more similar to number 4 than number 5. Number 4 was also the function selected on the basis of the total scattering coefficient for Filter 5 for both flights (refer to Table 6-5).

A similar comparison for the 9 March 1969 data is not as good. This might be expected since the TDY-2 ground station directional scattering data are somewhat suspect due to the decrease of ratio with increased wavelength. The ratios for stations 2.6 and 2.7 (12.6 and 14.6, respectively) indicate a function closest to number 6, whereas number 5 was selected on the basis of the slightly smaller total scattering coefficient at the lowest airborne altitude.

#### DOWNWELLING IRRADIANCE

A summary of downwelling irradiance  $H(0, d)$  measured at ground level is presented in Table 7-23. The stations are arranged in order of increasing irradiance for Filter 5. The range is comparable to the range encountered during the airborne measurements (refer to Table 6-3). The moon phase angle and zenith angle

are given in the second and third columns. They indicate the comparative contribution of the moon to the total irradiance (see Fig. 6-1).

The stations are arranged into three irradiance or flux levels corresponding to the groupings utilized for the airborne data. (1) The low flux level is for starlight. (2) The intermediate flux level is typified by the quarter moon or 90° phase angle. These stations cover moon phase angles from 85° to 46°. (3) The high flux level irradiances are for full or near full moon with phase angles from 18° to 40°.

**Table 7-23. Downwelling Irradiance  $H(z,d)$  Watt  $m^{-2} \mu m^{-1}$  for Ground Stations**

Flux Level	Station No	Moon		1	2	Filters		
		Phase Angle	Zenith Angle			5	3	4
Starlight	2 9	Before Moonrise		6 20 E 6 4.86 E-6	6 45 E 6 5 18 E-6	7 29 E 6 -	9 28 E 6 1 10 E-5	7 99 E-6 -
	2 6	Before Moonrise		5 50 E-6 8 91 E 6	5 67 E-6 9 28 E 6	7 08 E-6 1 02 E 5	9 42 E 6 1 34 E 5	1 10 E-5 1 26 E 5
	1,10	Before Moonrise		-	-	1 20 E-5	-	-
	1 9*	Before Moonrise		(1.14 E-5)	(1 28 E-5)	1 45 E-5	(1 78 E-5)	-
	1 8	Before Moonrise		-	-	1 56 E 5		-
	1 7**	Before Moonrise		(9 36 E 6)	(1 06 E-5)	1 59 E 5	(1 83 E 5)	-
Quarter Moon	2 7	69	65-54	- 1 82 E-4	1 45 E-4 2 01 E-4	1 47 E-4 2 01 E-4	2 03 E 4 2.77 E-4	1 59 E-4 2 07 E-4
	1 1	85	63-64	1 33 E-4	1 86 E-4	1 63 E-4	2 38 E 4	1.84 E 4
	2 5	57	69-56	1 78 E-4 2 70 E-4	1 92 E-4 4 00 E-4	1.90 E-4 2.80 E-4	2 42 E-4 4 00 E 4	1 85 E-4 2 93 E 4
	1 2	72	58-59	2 80 E 4	2 90 E 4	2 70 E-4	3 62 E 4	2.80 E-4
	1 5	46	47-45	4 02 E 4	4 03 E 4	3 84 E-4	4 95 E-4	4 08 E 4
	1.6	58	51-48	3 96 E-4	4 10 E-4	3 86 E-4	4 95 E-4	3 92 E-4
	2 2	62	23-37	4 35 E 4	4 79 E 4	4 54 E-4	6 44 E-4	4 80 E-4
Full Moon	2 3	40	16-31	8 75 E-4	8 73 E-4	9 36 E-4	1 19 F 3	9 07 E-4
	1 4	36	26	9 91 E 4	1 00 E-3	1 02 E-3	1 14 E 3	9 26 E 4
	1 3	36	30-28	1 15 E 3	1 18 E 3	1 23 E 3	1 33 E 3	1 09 E-3
	2 4	18	37-27	1 57 E 3	1 68 E 3	1 77 E-3	2 19 E-3	1.60 E 3

\* Values in parenthesis are based on airborne measurements during Flight 881

\*\* Values in parenthesis are based on airborne measurements during Flight 87

*Concurrent Airborne and Ground-Based Irradiance Measurements.* A comparison is given in Table 7-24 for Filter 5 of the irradiances measured during starlight at the ground station 16 km west of Rayong with the irradiances from the airborne data during flights 8 km south of Rayong. (Data for Filters 1 through 4 were not available for starlight flux levels for TDY-1 ground stations.) Since neither the times nor the locations for the flights and stations were equivalent, the comparison is made for the range of values over the measurement time span in both cases. By using the range of values for all altitudes from the flight data in the comparison, we are interpreting the variability as being primarily a time and horizontal location variability rather than a true function of altitude change. The ranges are reasonably comparable, particularly for 12 October 1968.

Table 7-24. Starlight Airborne and Ground-Based Irradiances

Date	Flight or Station No	Altitude (m)		Time LCT		Downwelling Irradiance (Watt m <sup>-2</sup> μm <sup>-1</sup> )	
		Start	End	Start	End	Minimum	Maximum
12 Oct 68	87	192	1700	1929	2003	1.32 E-5	1.65 E-5
12 Oct 68	17	0	0	2125	2145	1.42 E-5	1.59 E-5
19 Oct 68	881	197	1710	2113	2155	1.16 E-5	1.41 E-5
19 Oct 68	19	0	0	2113	2251	1.42 E-5	1.47 E-5

A comparison of the airborne and ground-based data for moonlight Flight 92 and station 2.7 near Lop Buri is given in Table 7-25. These data were taken during a rising moon with phase angle 70° (zenith angle range from 74° to 54°). Airborne data are taken at approximately the same times as the ground-based irradiance data. In this instance the obvious primary effect is the increase in irradiance as the moon rises. The ground and airborne data are reasonably comparable for all filters at equivalent times.

The comparability of the airborne and ground-based measurements of downwelling irradiance during the three nights of concurrent air and ground operations indicates that the use of the downwelling irradiance from the lowest flight altitude is indeed reasonable for computation of the directional path reflectances (Eq. 2-4).

Table 7-25. Moonlight Airborne and Ground-Based Irradiances

Date	Flight or Station No	Altitude	Time LCT		Downwelling Irradiance (Watt m <sup>-2</sup> μm <sup>-1</sup> )				
			Start	End	Filters				
					1	2	3	4	5
9 Mar 69	92	778	0108	0122	1.35 E-4	1.47 E-4	2.02 E-4	1.09 E-4	1.48 E-4
9 Mar 69	2.7	0	0115	0116		1.45 E-4	2.03 E-4	1.59 E-4	1.47 E-4
9 Mar 69	92	1376	0147	0201	2.18 E-4	2.00 E-4	2.60 E-4	3.05 E-4	2.36 E-4
9 Mar 69	2.7	0	0157	0158	1.82 E-4	2.01 E-4	2.77 E-4	2.07 E-4	2.01 E-4

## TERRAIN RADIANCE AND REFLECTANCE

During TDY-1 the terrain radiances were measured for the shallow paths of sight, zenith angles from 92° to 105°, since these were the angles most pertinent to the SHED LIGHT task. The rice field reflectances clearly show the expected spectral characteristics for the presence of xanthophyll and chlorophyll. There is a small peak in the spectral curve for Filter 2 (mean wavelength λ = 515 nm) lying between the lower reflectances for Filter 1 (λ = 478 nm showing xanthophyll absorption) and Filter 3 (λ = 663 nm showing chlorophyll absorption). The highest reflectance is for Filter 4 (λ = 740 nm). The reflectance for growing rice for Filter 5 (λ = 525 nm) are most similar to those of Filter 2.

During TDY-2 an attempt was made to obtain terrain radiances for both the shallow angles and the steeper paths of sight in order to more fully document the directional reflectance characteristics of the terrain. Unfortunately, due to instrumental difficulties, it was not possible to obtain a direct measure-

ment of downwelling irradiance for the first eight stations of TDY-2, therefore, simultaneity of background radiance and downwelling irradiance was not achieved. Data for the remaining ground stations were not recoverable due to data logger magnetic tape handling difficulties.

Great caution should be exercised in attempting to obtain reflectance values for the TDY-2 terrain radiance data. When only one measurement of downwelling irradiance is available (stations 2.2 through 2.4), there is no way to determine if it was a stable value throughout the period of measurement or a highly variable one. For instance, during TDY-1 at station 1.2, measurements of terrain radiance were made for only three paths of sight. But the downwelling irradiance measurements for Filter 5, made simultaneously with Filter 5 terrain radiance measurements, showed values of  $3.50 \text{ E-4}$ ,  $1.90 \text{ E-4}$ , and  $2.6 \text{ E-4 W } \Omega^{-1} \text{ m}^{-2} \mu\text{m}^{-1}$  in that order over a period of only 8 minutes. Stations 2.6 through 2.8 have two measurements of downwelling irradiance and two measurements of nadir reflectance of the terrain representing the conditions at the beginning and end of the terrain radiance set. If both the nadir terrain radiance and the downwelling irradiance show a consistent shift with time for all filters, it is probably reasonable to use a linear interpolation of irradiance with time. If they indicate a variability filter-to-filter or an inconsistency between nadir radiance change and irradiance shift, the situation is variable and any reflectances derived are relatively unreliable.

The importance of making simultaneous measurements of downwelling irradiance and terrain radiance for obtaining reliable values of terrain reflectance cannot be overemphasized.

#### SUMMARY

The twofold purpose of the ground station was (1) to provide measurements of inherent background radiance and reflectance and (2) to provide continuity of measurement by establishing ground-level values of downwelling irradiance and total volume scattering coefficient.

A particularly excellent job of supplying background radiance measurements was achieved through the ground station. The large aperture telephotometer worked well at even the extremely low flux conditions of starlight with no moon. The measurement method for obtaining reflectances with simultaneous measurements of downwelling irradiance and terrain radiance was also excellent. The need for simultaneity was underscored by the recovery problems encountered due to instrumental difficulties.

The necessity of measuring the total volume scattering coefficient at ground level to provide continuity of measurement for each flight was indicated by the data from the three nights of concurrent air and ground operation. Downwelling irradiance data from these same three nights indicate that it is reasonable to use the airborne downwelling irradiance at the lowest flight altitude to obtain the directional path reflectance. These ground-station data provided a validation of the method used for selecting the shape of the volume scattering functions for the airborne data.

## 8. Royco Data

The data presented in this section were collected by the airborne Royco particle counter. The data collected by the ground-based system, approximately 726 samples, are still being evaluated and will be presented in a separate report.

The analysis of these airborne Royco data will be developed using the ground station data as a statistical base. Of the 726 ground samples available, 566 of them were obtained during TDY-2. These aerosol samples were drawn from inside the integrating nephelometer shroud during each ground-based data set. The comparison of these Royco samples with the simultaneous measurements of total and directional scattering coefficients will provide the base line data for future evaluation and analysis of the Royco system performance.

The data in Table 8.1 lists the particles per cubic meter detected and counted by the Royco system during the flights being reported. The particles included in this total count range in size from  $0.36\mu$  to  $27.0\mu$ . Note that minimum altitudes are not the same for each flight. The altitude increments which are shown as 1000 feet are approximate, the exact value being the altitudes shown in the data tables of Section 6.

The accumulation intervals listed show variation in time from 2 minutes to 10 minutes. The length of the interval is reported because it may be considered as an indication of the measurement reliability, a 10-minute average presumably has a higher reliability than a 4-minute or 2-minute average. In all instances the data are reduced to particles per cubic meter.

Table 8.1 Total Particle Count, Particles per Cubic Meter

Flight No	Minimum Altitude (in 1000 ft)	Minimum Altitude	Minimum Altitude + 1000 ft	Minimum Altitude + 2000 ft	Minimum Altitude + 3000 ft	Minimum Altitude + 4000 ft	Minimum Altitude + 5000 ft	Accumulation Interval (in minutes)
TDY 1								
82I	3.0	4.29E5	3.86E5	5.54E5	5.62E5	1.09E5	9.85E5	2
32II	1.5	1.00E6	5.81E5	3.72E5	3.33E5	1.29E5		4
86	2.2	2.55E6	1.61E6	1.34E6	9.60E5	4.86E5		Variable
87	No Data	-						
88I	0.5	5.84E6	2.50E6	3.68E6	2.67E6	1.87E6	9.85E5	4
88II	2.5	1.89E6	1.01E6	8.56E5	5.92E5			4
89	1.1	9.96E6	8.22E6	4.28E6	3.16E6	-		4
TDY 2								
91	0.7	1.05E8	7.82E7	1.16E8	8.79E7	7.48E7	5.48E7	10
92	0.5	6.83E7	6.03E7	5.67E7	4.93E7	6.95E7	6.21E7	10
93	1.6	1.40E8	1.06E8	1.27E8	1.40E8	8.44E7	7.04E7	10
96	1.3	5.41E8	6.38E7	5.25E7	6.87E7	5.02E7	5.78E7	10
97	0.5	2.21E7	4.09E7	3.61E7	3.14E7	1.41E7	1.90E7	10
98	0.6	5.77E7	5.27E7	5.19E7	7.38E7	6.08E7	7.37E7	10
99	1.3	6.49E7	3.91E7	6.03E7	6.23E7	4.46E7	3.37E7	10
100I	1.3	7.25E7	7.25E7	5.69E7	5.51E7	4.87E7	-	10
101	0.5	4.24E7	3.51E7	3.97E7	5.21E7	4.08E7	2.65E7	4
102	0.5	1.94E6	1.93E6	1.91E6	1.11E6	1.56E6	1.94E6	4

## 9. Acknowledgements

To be conducted successfully, a research program such as Project SHED LIGHT requires the support from many organizations and individuals and their aid in this research is gratefully acknowledged. We especially wish to thank

Lt. Col. James Steeger, USAF, HQ Office of Aerospace Research and Lt. Col. J. H. Jacobsmeyer, USAF, Shed Light Office, for their interest and managerial support of this program.

Mr. Arthur Hasset, Mr. Leo McCaffrey, and other members of the Airborne Research Engineering Branch of the 3245 Air Base Group at Hanscom Field for the engineering work in connection with the aircraft instrumentation.

Mr. Brooks Young and Mr. Payton Lawley of the Hayes International Corporation where the instrumentation was accomplished.

Personnel of Operational Services Division of AFCRL, particularly Mr. James D. Murphy, Mr. Tancredo Maltacea, and Mr. Raymond Silva for the necessary logistical support during the instrumentation and field phases of this project.

Mr. Ernst Corduan, formerly with the Visibility Laboratory, for his liaison work with AFCRL and Hayes International Corp. during the aircraft instrumentation.

Dr. Leonard Wood and Mr. Ronald A. Cummins, Environmental Sciences Division of the ARPA Research and Development Center in Thailand for their technical and logistical advice in planning the program and for their continued efforts in supporting the field measurement program throughout its duration.

Gen. Prasart Mookhaves and Capt. Sonchai Chantiran, Military Research and Development Center, Supreme Command Headquarters, Royal Thai Armed Forces, for providing support of the Royal Thai Government.



Mr. Nirum Suphawong and Mr. Uta Tavinwong, MRDC Royal Thai Armed Forces, for their interest, initiative, and ingenuity with the project in the field.

Mr. George Immisch, station manager, and others of the Applied Scientific Research Corporation of Thailand for making available the facilities of the Tropical Environmental Data (TREND) site near Khorat.

Major Ralph Carboneau, USAF, Major Allen Hinman, USAF, Major A. Luttrell, USAF, and Capt. R. J. MacDonald, USAF, for performing the flight missions for this project.

Additionally, special mention is made of Visibility Laboratory personnel for their continued interest and effort throughout this program. They are:

Mr. John D. Barley, Mr. John J. Edwards, and Mr. Terrance S. Robinson for engineering and design work; Mr. David J. Hoon, Mr. Walter A. Clark, Mr. Marshall C. Randall, and Mr. John LaFon for the construction of the instrumentation.

Mr. Leonard A. Castro, Mr. Kenneth McMaster, Mr. Robert Sydnor, and Mr. George F. Simas for their work as members of the airborne and ground-based scientific parties.

Mr. Nils R. Persson, Jr., Mrs. Alma L. Shaules, and Miss Donna M. Resch, members of the computer programming team.

Miss Sally L. Poor for her work as technical editor, and

Mr. J. C. Brown, Jr., Mrs. Arlene C. Streed, Mr. Louis S. Butler, Mr. Frank J. Campriengo, and Mr. Thomas Hart of the Photo and Reproduction Branch for their effort in producing this report.

We wish also to thank Dr. Robert Fenn and Major Leo Sheehan, USAF, Contract Monitors, for their counsel, advice, and assistance throughout the planning and execution of this project.

## 10. References

1. Barteneva, O. D. (1960), "Scattering Functions of Light in the Atmospheric Boundary Layer," Bull. Acad. Sci. U.S.S.R., Geophysics Series 1237-1244
2. Boileau, A. R. (1964), "VI Atmospheric Properties," Appl. Opt. **3**, 570-581 (Refer to Appendix C.)
3. Boileau, A. R. and J. I. Gordon (1966), "Atmospheric Properties and Reflectances of Ocean Water and Other Surfaces for a Low Sun," Appl. Opt. **5**, 803-813.
4. Boileau, A. R. and F. D. Miller (1967) Appl. Opt. **6**, 7
5. Duntley, S. Q. (1948), "Reduction of Contrast by the Atmosphere," J. Opt. Soc. Am. **38**, 179-191
6. Duntley, S. Q., A. R. Boileau, and R. W. Preisendorfer (1957), "Image Transmission by the Troposphere I," J. Opt. Soc. Am. **47**, 499-506 (Refer to Appendix A.)
7. Duntley, S. Q., et al. (1964) "Visibility," Appl. Opt. **3**, 549-598
8. Duntley, S. Q. (1964), "Visibility. I. Introduction and II. Summary," Appl. Opt. **3**, 550-556. (Refer to Appendix B.)
9. Duntley, S. Q. (1969), "Directional Reflectance of Atmospheric Paths of Sight," Duntley Rep. No. 69-1. (Refer to Appendix D.)
10. Gordon, J. I. (1964), "III Optical Properties of Objects and Backgrounds," Appl. Opt. **3**, 556-562 (Refer to Appendix B.)
11. Gordon, J. I. (1964), "Model for a Clear Atmosphere," J. Opt. Soc. Am. **59**, 14-18. (Refer to Appendix E.)
12. Johnson, J., K. Cooper, E. Brenz, and J. Bunor (Nov. 1965), "Optical Properties of Targets and Backgrounds at Night" (U), CONF. AERDL Rep. 1338
13. Morton, G. A. (1964) "Image Intensifiers and the Scotoscope," Appl. Opt. **3**, 651-672
14. Murray, R. B. and J. J. Manning (1960), Trans. Inst. Radio Engrs **NS-7**, 80
15. Penndorf, R. (1957), "Tables for the Refractive Index for Standard Air and the Rayleigh Scattering Coefficient for the Spectral Region between 0.2 and 20  $\mu$  and Their Application to Atmospheric Optics," J. Opt. Soc. Am. **47**, 176-182
16. Russell, H. N. (1916) Astrophys. J. **43**, 114
17. Tyler, J. E. and R. W. Preisendorfer (1962) "Light" Chap. 8 in *The Sea*, M. N. Hill, Ed (Interscience Publishers, Inc., N.Y.), Vol. 1, pp. 397-451.
18. Wells, M. B., D. G. Collins, and F. A. Hopper (Dec. 1968), "Contrast Transmission Data for Clear and Hazy Model Tropical Atmospheres," Rep. AFCRL-68-0660 (I-III).

SEIBERT Q. DUNTLEY, ALMERIAN R. BOILEAU, AND RUDOLPH W. PREISENDORFER  
*Scripps Institution of Oceanography,† University of California, La Jolla, California*  
(Received November 15, 1956)

## INTRODUCTION

499

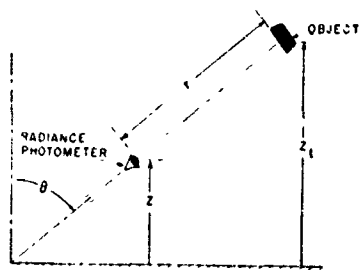


FIG. 1. Illustrating the geometry of the path of sight.

requirements: It is suited to the terrestrially-based system of altitudes and directions in which flight data must be taken and it is fully compatible with the more powerful vector notation required for the generalized theoretical treatments of image transmission and radiative transfer phenomena to follow. It is compatible also with the notation commonly used in several mathematically allied fields of physics, as for example, neutron diffusion theory. It is extendable to hydrological optics, a natural counterpart of meteorological optics, in which the authors of this paper are deeply interested.

The basic symbol employed for the spectral radiance is  $N$ , and the symbol for luminance is  $B$ . The altitude of the photometer is denoted by  $z$ , the height above mean sea level. The direction of any path of sight is specified by a zenith-angle  $\theta$  and an azimuth angle  $\phi$ , the photometer being directed upward when  $0 \leq \theta < \pi/2$ , as in Fig. 1;  $z$ ,  $\theta$ , and  $\phi$  are always written as parenthetic attachments to the parent symbol. When the post subscript  $r$  is appended to any symbol, it denotes that the quantity pertains to a path of length  $r$ . The subscript 0 always refers to the hypothetical concept of a photometer located at zero distance from the object, as, for example, in denoting the *inherent* radiance of a surface. The subscripts identify the object, thus the pre-subscript  $b$  refers to background, and  $i$  to object or visual target. Thus, the (monochromatic) *inherent spectral radiance* of an object  $i$  at altitude  $z_i$  as viewed in the direction  $(\theta, \phi)$  is  $iN_0(z_i, \theta, \phi)$  and the corresponding apparent radiance observed in the direction  $(\theta, \phi)$  at any other altitude  $z$  is  $iN_r(z, \theta, \phi)$  where  $z_i = z + r \cos \theta$ . A post-superscript \*, or post-subscript \*, is employed as a mnemonic symbol signifying that the radiometric quantity has been generated by the scattering of ambient light reaching the path from *all directions*. Thus  $N_r^*(z, \theta, \phi)$  is the spectral path radiance observed at altitude  $z$  in the indicated direction, and  $(N_{*z, \theta, \phi})$  is used to denote *path function*, a quantity defined later in this paper.

The (monochromatic) *apparent visual radiance* of any distant object  $i$  is

$$iN_r(z, \theta, \phi) = T_r(z, \theta, \phi) [iN_0(z_i, \theta, \phi) + N_r^*(z, \theta, \phi)], \quad (1)$$

where the first term on the right is the residual image-forming light from the object and the second term is the path radiance due to scattering processes throughout

the path.  $T_r(z, \theta, \phi)$  is the spectral transmittance of the path for image-forming rays; it includes the factor  $[n(z)/n(z_i)]^2$  required by geometrical optics whenever the index of refraction of the medium at the observer  $[n(z)]$  differs from the index of refraction of the medium at the target  $[n(z_i)]$ . In the case of paths of sight through the troposphere the departure of  $[n(z)/n(z_i)]^2$  from unity is negligible. The transmittance of the path is a property of the atmosphere throughout the path and is independent of the distribution of the ambient lighting; in the case of any path of sight through the troposphere it is the same for upward or downward transmissions, thus  $T_r(z, \theta, \phi) = T_r(z_i, \pi - \theta, \pi + \phi)$  where  $z_i = z + r \cos \theta$ . Because forward scattering generally exceeds backward scattering, reversibility is not true of the path radiance  $N_r^*(z, \theta, \phi)$  except for a few symmetrical lighting conditions, such as (1) horizontal paths of sight under a uniform overcast, and (2) a horizontal path at right angles to the plane of the sun provided both the radiance distributions of the sky above and the earth below the path are symmetrical with respect to the plane.

The image transmitting properties of the atmosphere can be separated from the optical properties of the object by the introduction of the *contrast* concept:

The *inherent spectral contrast*  $C_0(z_i, \theta, \phi)$  of an object is, by definition,

$$C_0(z_i, \theta, \phi) = [iN_0(z_i, \theta, \phi) - bN_0(z_i, \theta, \phi)] / bN_0(z_i, \theta, \phi). \quad (2)$$

The corresponding definition for *apparent spectral contrast* is

$$C_r(z, \theta, \phi) = [iN_r(z, \theta, \phi) - bN_r(z, \theta, \phi)] / bN_r(z, \theta, \phi). \quad (3)$$

The apparent and inherent background radiances are related by the expression

$$bN_r(z, \theta, \phi) = T_r(z, \theta, \phi) bN_0(z_i, \theta, \phi) + N_r^*(z, \theta, \phi). \quad (4)$$

### Theorems

Subtracting Eq. (4) from Eq. (1) yields the relation

$$[iN_r(z, \theta, \phi) - bN_r(z, \theta, \phi)] = T_r(z, \theta, \phi) [iN_0(z_i, \theta, \phi) - bN_0(z_i, \theta, \phi)]. \quad (5)$$

Thus, radiance differences are transmitted along inclined paths with the same attenuation as that experienced by each image-forming ray.

If Eq. (5) is divided by the apparent radiance of the background  $bN_r(z, \theta, \phi)$  and combined with Eq. (3), the result can be written:

$$C_r(z, \theta, \phi) = T_r(z, \theta, \phi) \times [iN_0(z_i, \theta, \phi) / bN_r(z, \theta, \phi) - bN_0(z_i, \theta, \phi) / bN_r(z, \theta, \phi)]. \quad (6)$$

When the inherent radiance of the background is very dark, as in the case of an object at high altitude, the second term in the brackets on the right side of Eq. (6) may be negligible.

Combining Eqs. (2) and (6) yields the expression

$$C_r(z, \theta, \phi) / C_0(z_i, \theta, \phi) = T_r(z, \theta, \phi) + V_0(z_i, \theta, \phi) / b V_r(z, \theta, \phi). \quad (7)$$

The right-hand member of Eq. (7) is an expression for the *contrast transmittance* of the path of sight; it is independent of the optical properties of the object. Equation (7) is the law of contrast reduction by the atmosphere expressed in its most general form.<sup>2</sup>

An interesting variant of Eq. (7) formed by combination with Eq. (4) is the following expression in which *contrast transmittance* is characterized in terms of path radiance and inherent background radiance:

$$C_r(z, \theta, \phi) / C_0(z_i, \theta, \phi) = 1 - [N_r^*(z, \theta, \phi) + V_r(z, \theta, \phi)]. \quad (8)$$

The apparent indeterminateness of Eqs. (7) and (8) when applied to the case of objects outside the atmosphere can be avoided by the use of the limiting form of Eq. (6), as follows:

$$C_r(z, \theta, \phi) = T_r(z, \theta, \phi) + V_0(z_i, \theta, \phi) / b V_r(z, \theta, \phi). \quad (9)$$

It should be emphasized that Eqs. (1) through (9) are completely general; they apply rigorously to any path of sight regardless of the extent to which the scattering and absorbing properties of the atmosphere or the distributions of lighting exhibit nonuniformities from point to point. No theoretical model of the atmosphere is involved and no restrictive assumptions have been made. The equations can be used in treating all real atmospheres and all real lighting conditions. This is in sharp distinction to treatments of the subject which are based upon theoretical models of the atmosphere which invariably involve major assumptions such as horizontal uniformity, exponential lapse rate of air density, vertical uniformity of particle size distribution, negligible earth curvature, etc.

### Equation of Transfer

Image-forming light is lost by scattering and absorption in each elementary segment of the path of sight and contrast-reducing path radiance is generated by the scattering of the ambient light which reaches the segment from all directions. The quantitative description of this scattered component of path-segment radiance involves a quantity called the *path function* and denoted by the symbol  $V_*(z, \theta, \phi)$ , where the mnemonic subscript symbol  $*$  is used both to suggest light reaching the path segment from all directions and to denote that the quantity is a point function. The parenthetical symbols  $(z, \theta, \phi)$  indicate that the path function depends upon the direction of image transmission and upon the location of the segment in the path of sight. The path function depends upon the directional distribution of

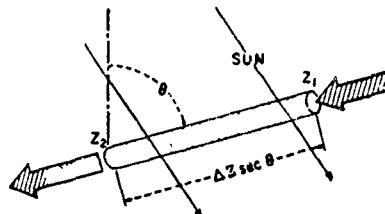


FIG. 2. Illustrating the derivation of the equation of transfer.  $\Delta z$  is defined as  $z_1 - z_2$ , so that  $\Delta r = \Delta z \sec \theta$  is always non-negative. The difference  $\Delta N(z, \theta, \phi)$  between output and input is  $N(z_2, \theta, \phi) - N(z_1, \theta, \phi)$ .

the lighting on the segment due to its surroundings; it can be operationally defined in terms of the (limiting) ratio of the path radiance associated with a short path to the path length by the relation  $N_*(z, \theta, \phi) = \lim(\Delta r \rightarrow 0) \times N_{\Delta r}^*(z, \theta, \phi) / \Delta r$ . In experimental practice, the path length  $\Delta r$  should be sufficiently short that no change in the ratio can be detected if  $\Delta r$  is made shorter. Apparatus for path function measurement has been built and will be described elsewhere.

The loss in image-forming light due to attenuation by scattering and absorption within any path segment is proportional to the amount of image-forming light present; the coefficient of proportionality will be written in the reciprocal form  $1/L(z)$ , and  $L(z)$  will be referred to as the *attenuation length*.  $L(z)$  is a function of position within the path of sight; it does not depend upon the image transmission direction unless the aerosol is anisotropic, as sometimes occurs in the case of falling snow; it is independent of the manner in which the path segment is lighted by the sun or sky; it is a physical property of the atmosphere alone. Attenuation includes loss of image-forming radiance by absorption and by scattering. Absorption refers to any thermodynamically irreversible transformation of monochromatic radiant energy including, primarily, conversion of light into heat but also fluorescence phenomena, photochemical processes, etc. Attenuation by scattering results from any change of direction sufficient to cause the radiation to fall outside the summative radius of the detector mosaic.

In any path segment of length  $\Delta r = \Delta z \sec \theta$ , as illustrated by Fig. 2, the difference  $\Delta V(z, \theta, \phi)$  between output and input radiance is attributable to a gain term  $V_*(z, \theta, \phi) \Delta r$  and a loss term  $V(z, \theta, \phi) \Delta r / L(z)$ , so that  $\Delta V(z, \theta, \phi) = V_*(z, \theta, \phi) \Delta r - V(z, \theta, \phi) \Delta r / L(z)$ . This relation may be rewritten

$$\Delta N(z, \theta, \phi) \Delta z \sec \theta = N_*(z, \theta, \phi) - N(z, \theta, \phi) / L(z). \quad (10)$$

In conformity with usage in other fields of physics Eq. (10) will be referred to as the *incremental form of the equation of transfer*. It is implicit in this equation that  $\Delta z$  must be taken sufficiently small so that over this interval  $L(z)$  and  $N_*(z, \theta, \phi)$  may be regarded as constants within the precision of experimental data.

<sup>2</sup> Equation (7) is a generalization of Eq. (15) on p. 183 of S. Q. Duntley, J. Opt. Soc. Am. 38, 179 (1948).

Equation (10) is a steady-state equation of continuity,<sup>3</sup> based upon the conservation of energy principle; it refers only to nonemitting atmospheres, since an additional term would be needed to represent emission of radiation in the path, as by fluorescence, recombination phenomena, particle excitation, etc. Self-radiosity within the visible spectrum appears to be of negligible importance in the troposphere. Equations (1) and (4) may be regarded as integral forms of the equation of transfer.

The equation of transfer and the concepts of attenuation length and path function share the same generality as the concepts associated with Eqs. (1) through (9). No theoretical model atmosphere has been employed; each of the equations in this paper is applicable to all real isotropic atmospheres, all lighting conditions, and all paths of sight. The use of the equation of transfer in numerical summation procedures involving experimental data will be illustrated in a later section of this paper. Only when Eq. (10) is simulated by a differential equation and an analytic integration performed does the introduction of a theoretical model for the atmosphere become necessary; this will not be done in the present paper.

### Equilibrium Radiance

Many image transmission phenomena are most clearly understandable in terms of the concept of *equilibrium radiance*. This concept is a natural consequence of the equation of transfer, which indicates that some unique *equilibrium radiance*  $N_q(z, \theta, \phi)$  must exist at each point such that the loss of radiance within the path segment is balanced by the gain, i.e.,  $\Delta N_q(z, \theta, \phi) = 0$ . Thus

$$0 = N_*(z, \theta, \phi) - N_q(z, \theta, \phi)/L(z), \text{ so that} \\ N_q(z, \theta, \phi) = N_*(z, \theta, \phi)L(z) \quad (11)$$

and the equation of transfer (10) may be rewritten as follows:

$$\Delta N(z, \theta, \phi)/\Delta z \sec \theta = [N_q(z, \theta, \phi) - N(z, \theta, \phi)]/L(z). \quad (12)$$

Equation (11) shows that each segment of every path of sight has associated with it an equilibrium radiance, and Eq. (12) states that the average space rate of change in image-forming radiance caused by the path segment is in such a direction as to cause the output radiance to be closer to the equilibrium radiance than is the input radiance. This segment-by-segment convergence of the apparent radiance of the object to the dynamic equilibrium radiance is illustrated by the data in Fig. 6 of this paper.

<sup>3</sup> The equation of transfer has been generalized to the transient case, and rigorously derived for an arbitrary optical medium, using the concepts of mesonic theory. R. W. Preisendorfer, "A mathematical foundation for radiative transfer theory," Doctoral dissertation, U.C.L.A., May 1956. An exposition of this theory has been submitted for publication in the Journal of the Optical Society of America.

When the path of sight is horizontal and optically uniform both in terms of the composition of the aerosol and its lighting, the equilibrium radiance is identical with the apparent radiance of the horizon. The apparent radiance of distant objects inherently more radiant than the equilibrium value decreases toward the equilibrium radiance as an asymptote; conversely the apparent radiance of any dark distant object approaches the same asymptote.

### Equilibrium Contrast

Many of the foregoing equations can be rewritten in terms of *equilibrium contrast*,  $C_q(z, \theta, \phi)$ , which is defined by the relation

$$C_q(z, \theta, \phi) = [N_r(z, \theta, \phi) - N_q(z, \theta, \phi)]/N_q(z, \theta, \phi). \quad (13)$$

Notation of the type defined by Eq. (13) enables the equation of transfer (10) to be written

$$\Delta C_q(z, \theta, \phi)/\Delta z \sec \theta = -C_q(z, \theta, \phi)/L(z) \quad (14)$$

or

$$\Delta C_q(z, \theta, \phi)/C_q(z, \theta, \phi) = -\Delta z \sec \theta/L(z), \quad (15)$$

provided that the equilibrium radiance  $N_q(z, \theta, \phi)$  is constant on the segment of path under discussion. In this case the fractional change in equilibrium contrast depends only upon the ratio of the length of the path segment to the attenuation length. The negative signs throughout Eqs. (14) and (15) signify that equilibrium contrast decreases in absolute magnitude in the segment.

## EXPERIMENTAL METHODS

### Introduction

The apparent radiance of any distant object can be computed by means of Eq. (1) if the transmittance of the path of sight and the path radiance are calculated from experimental data. This can be done from profiles of attenuation length and path function for the path of sight by means of the relations

$$T_r(z, \theta, \phi) = [n(z)/n(z_i)]^2 \prod_{i=1}^m \exp\{-\Delta r/L(z_i)\} \\ = [n(z)/n(z_i)]^2 \exp\{-\Delta r \sum_{i=1}^m 1/L(z_i)\} \quad (16)$$

and

$$N_r^*(z, \theta, \phi) = \Delta r \sum_{i=1}^m T_{ri}(z, \theta, \phi) N_{*i}(z_i, \theta, \phi), \quad (17)$$

where the vertical height  $|z_i - z|$  of the path is divided into  $m$  equal segments of length  $\Delta z$ , and  $\Delta r = \Delta z \sec \theta$ .  $L(z_i)$  and  $N_{*i}(z_i, \theta, \phi)$  are the mean values of  $L$  and  $N_*$  in the  $i$ th segment.  $r_i = (i-1)\Delta r$ ,  $i = 1, \dots, m$ .

### Attenuation Profile

An experimental technique for measuring the vertical profile of attenuation length in horizontally uniform atmospheres has been devised around an air-borne version of an instrument based upon principles described earlier.<sup>4,5</sup> Figure 3 shows this attenuation meter mounted on the B-29 aircraft used by the Visibility Laboratory in its flight research program. The optical system is shown diagrammatically in Fig. 4. The for-



Fig. 3. Specially instrumented B-29 aircraft used to collect the data presented in this paper. The long cylindrical apparatus on top of the fuselage is the *attenuation meter*, shown schematically in Fig. 4. The smaller cylindrical device which appears slightly forward of the attenuation meter is the sky scanning telephotometer. It consists of an end-on type multiplier phototube mounted at the focal point of a parabolic front-surfaced mirror 12 in. diam. Scanning is accomplished automatically by means of a turret and trunion mounting, scanning time for the entire hemisphere is 90 sec. Field of view, adjustable by means of interchangeable field stops, was circular, 5° in angular diameter in the case of the data shown in Fig. 6. Sensitivity is sufficient to map even the darkest high altitude night skies. Spectral response is controlled by absorption filters. A similar (downward-viewing) telephotometer is mounted beneath the aircraft but is not shown by this photograph.

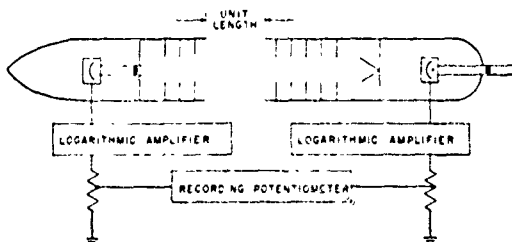


Fig. 4. Schematic diagram of the air-borne attenuation meter. The forward photoelectric telephotometer measures the equilibrium radiance, the rear telephotometer measures the radiance of a path of unit length. The latter radiance is numerically equal to the horizontal path function in the direction of flight. Multiplier phototubes and Sweet type logarithmic circuits enable direct recording of the ratio of these radiances, i.e., of the attenuation length [see Eq. (11)]. Wind tunnel tests of the aerodynamic design showed ambient pressure throughout the unit path. Light trap design, stray light treatment, and photoelectric sensitivity are sufficient to enable measurement of attenuation lengths up to 200 nautical miles when the phototube spectral sensitivity is rendered photopic by means of absorption filters.

<sup>4</sup> S. Q. Duntley, U. S. Patent No. 2,651,650.

<sup>5</sup> S. Q. Duntley, J. Opt. Soc. Am. 39, 630A (1949).

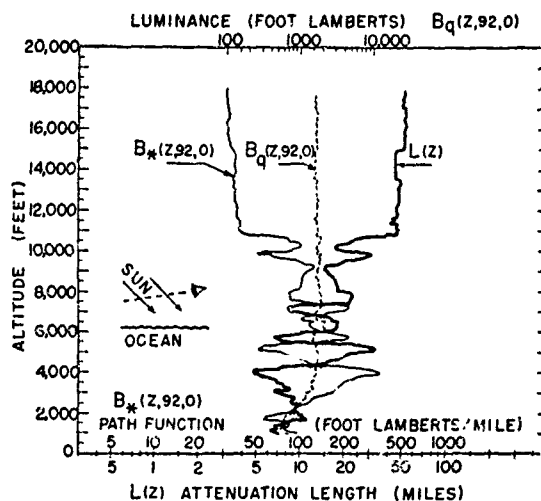


Fig. 5. Measured profiles of path function and attenuation length over the Atlantic Ocean off the coast of Florida, March 10, 1956. Flight 77. Sun position: zenith angle = 48°, azimuth = 140° clockwise from true north. Path function: zenith angle  $\phi = 92^\circ$ ; azimuth  $\theta = 0^\circ$  from the plane of the sun. Sky condition: cloudless, blue. Approximately 36 hr after the passage of a major front. Very light ground haze with top at 4000 ft. The profile of equilibrium luminance was computed by means of Eq. (11).

ward telephotometer is directed toward the horizon and measures the equilibrium radiance of the horizontal path of sight in the direction of flight of the aircraft. The rear telephotometer measures the radiance of a path of unit length; this is numerically equal to the path function. The attenuation length is the ratio of the equilibrium radiance to the path function, as shown by Eq. (11). Recording potentiometers within the aircraft record the outputs of both telephotometers as well as their ratio.

Despite the use of multiplier phototubes, the low level of radiance produced by scattering processes in clear high altitude air precluded the use of narrow-band interference or absorption filters in the airborne attenuation meter. Because it was not possible to measure the spectral radiances called for by the equations given in this paper, each phototube was carefully corrected by means of specially constructed absorption filters to measure luminous quantities. For reasons of rigor the equations in this paper are written with the symbol  $N$ , denoting spectral radiance, but it will be understood that these same equations have been used with  $N$  replaced by  $B$ , denoting luminance, in the treatment of the illustrative data shown in Figs. 5 through 8.

During the flight for which data is given in this paper, the aircraft maintained a constant (southerly) heading and a fixed attitude which held the attenuation meter pointed at the desired portion of the horizon sky while making a controlled, rapid descent from 18,000 ft to 1000 ft at a rate of approximately 1500 ft per min. The resulting profiles of path function, equilibrium luminance, and attenuation length are shown in Fig. 5.

It will be noted that the equilibrium luminance (horizon luminance) was nearly independent of altitude. Repeated descents have demonstrated that the major details of these curves are repeatable.

The transmittance of any inclined path of sight having terminal altitudes between 1000 and 18 000 ft can be calculated from the attenuation profile in Fig. 5 by means of equations corresponding to Eq. (16).

### Path Function Profiles

The aircraft is not equipped for the direct measurement of path functions for vertical and inclined paths of sight. It is capable, however, of measuring the radiance of the sky in any direction, above or below, during flight. A photoelectric telephotometer is located in a trunion mounting on top of the fuselage near the forward end of the attenuation meter, as shown in Fig. 3. This instrument performs an automatic scan of the entire sky above the aircraft in approximately 90 sec. Another telephotometer in a fixed vertical mount provides a continuous record of the radiance of the zenith during the controlled rapid descent described in the preceding section. A corresponding pair of telephotometers is mounted on the bottom of the fuselage. Figure 6 shows zenith luminance data secured by the fixed telephotometer during the same descent to which Fig. 5 applies. Similar profiles of sky luminance for any upward path of sight inclined at angles  $\theta, \phi$  can be constructed from the record of the sky-scanning telephotometer, which is designed to be operated continuously during the descent.

The profile of the path function for any path of sight can be calculated from the sky radiance profile and the attenuation profile by means of Eq. (10) after rearrangement as follows:

$$N_*(z, \theta, \phi) = \Delta V(z, \theta, \phi) / \Delta z \sec \theta + N(z, \theta, \phi) / L(z). \quad (18)$$

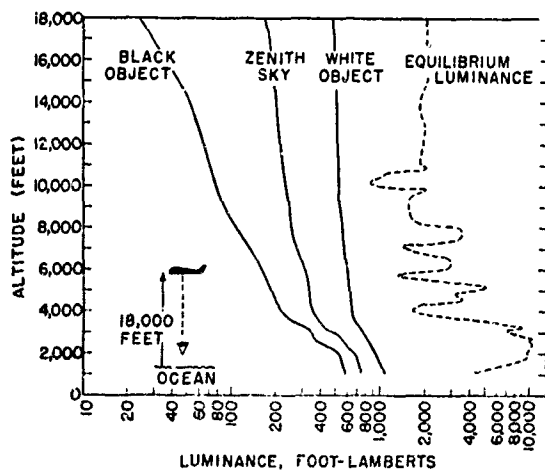


FIG. 6. Measured profile of the luminance of the zenith sky. Flight 77. Calculated profiles of the apparent luminance of black and white objects at 18 000 ft. Calculated profile of vertical equilibrium luminance.

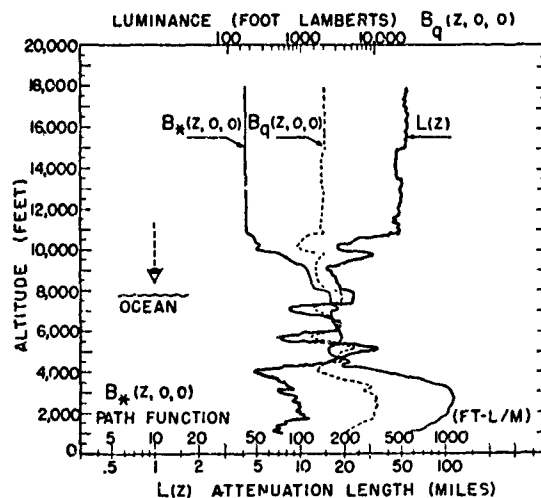


FIG. 7. Calculated profiles of vertical path function and vertical equilibrium luminance. Flight 77. The profile of attenuation length is identical with that in Fig. 5.

Figure 7 shows the result of such a calculation for the vertical path of sight which corresponds with the zenith luminance profile given in Fig. 6.

### Equilibrium Radiance Profiles

An expression for the equilibrium radiance for each element of any path of sight can be found by combining Eqs. (11) and (18) as follows:

$$N_q(z, \theta, \phi) = L(z) (\Delta V(z, \theta, \phi) / \Delta z \sec \theta + N(z, \theta, \phi)). \quad (19)$$

Figure 6 shows the result of the use of Eq. (19) for a calculation of the equilibrium luminance profile for the upward vertical path of sight; the same profile appears in Fig. 7.

In every case the radiance of the sky  $V(z, \theta, \phi)$  as observed from any altitude  $z$  is the path radiance generated by the portion of the path above the observer. That is,  $N(z, \theta, \phi) = N_*(z, \theta, \phi)$ , where  $0 \leq \theta < \pi/2$ . Because  $V(z, \theta, \phi) = 0$  outside the atmosphere (except for light from the stars) and  $V(z, \theta, \phi) > 0$  within, it follows from Eq. (19) that the equilibrium radiance exceeds the apparent radiance of the clear sky and, therefore, the measured radiance of a clear sky increases as the photometer descends.

When clouds are present or when the image transmission direction is upward, the apparent radiance reaching any particular path segment may exceed the equilibrium radiance for that segment, so that a decrease of apparent radiance is possible. In such cases it often happens that the apparent radiance of highly radiant objects decreases while that of objects of small inherent radiance increases. Illustrative data for upward-transmitting paths of sight are planned for presentation in a subsequent paper.



### Profiles of Apparent Object Luminance

Profiles of the apparent luminance of any specific object can be calculated for any path of sight provided that the inherent luminance of the object in the direction of interest is known. Two such profiles appear in Fig. 6; they refer to hypothetical "black" and "white" objects, respectively, located at a fixed altitude of 18 000 ft and viewed from directly below on the occasion to which the data in this paper applies. The profiles were calculated by means of Eq. (1). Alternatively, they could have been generated step-wise by successive applications of either Eq. (10) or Eq. (12). The complexity which characterizes the attenuation, path function, and equilibrium luminance profiles is scarcely noticeable in these vertical profiles of apparent object luminance. In the case of paths of sight inclined at large zenith angles, however, the object luminance profiles exhibit the complexities due to atmospheric structure much more prominently.

### Profiles of Apparent Contrast

Figure 8 shows profiles of apparent object contrast generated by means of Eq. (3) from the apparent luminance profiles in Fig. 6. The same profiles could have been generated by use of the Eq. (7).

### METEOROLOGICAL CORRELATIONS

The complex profiles of attenuation length and path function can only be the result of sharply defined layers of scattering particles. Repeated descents have demonstrated that the major features of the profiles are reproducible in space and time; the layers must, therefore,

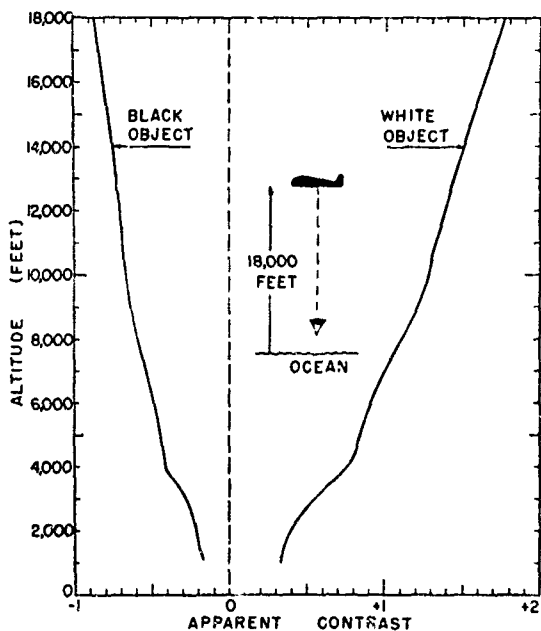


FIG. 8. Calculated profiles of the apparent contrast of black and white objects at 18 000 ft. Flight 77.

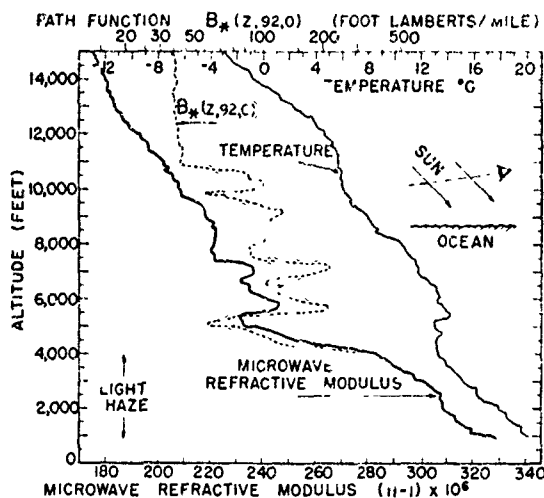


FIG. 9. Profiles of microwave refractive modulus, path function, and free air temperature. Flight 77. Correlations between the profiles of microwave refractive modulus and path function can be noted.

be horizontal strata of great extent which characterize the air mass. Such strata must also be observable in terms of nonoptical meteorological phenomena. Initial attempts to discover correlations with the temperature and humidity profiles produced routinely by the meteorological services from radiosonde observations met with failure. This was attributed to the long time constant associated with the humidity sensing elements carried by the balloons. It was believed necessary to measure the humidity profile during the controlled rapid descent of the B-29 with equipment having a fractional second time constant in order to record faithfully the presence of strata only a few feet in thickness. This was accomplished by means of an airborne microwave refractometer<sup>6</sup> of the type described by Crain and Deam.<sup>7</sup> The microwave refractive index recorded by this instrument is governed primarily by the water vapor concentration in the atmosphere; it is related to pressure, temperature, and the partial pressure of water vapor by an equation derived by Debye and discussed by numerous authors in connection with microwave propagation.<sup>8</sup> An expression for the partial pressure of water vapor obtained from the usual microwave approximation of Debye's equation is:

$$\epsilon = \frac{(\text{microwave refractive modulus})(\text{Kelvin temp.})^2}{(77.6)(4810)} - \frac{(\text{total pressure})(\text{Kelvin temp.})}{4810}$$

<sup>6</sup> The authors are indebted to Mr. Thomas J. Obst, Director of Range Development, Patrick Air Force Base, for suggesting the use of the microwave refractometer and for arranging for the availability of this equipment for the flight experiment described in this paper.

<sup>7</sup> C. M. Crain and A. P. Deam, *Rev. Sci. Instr.* **23**, 149 (1953).

<sup>8</sup> E. K. Smith, Jr., and S. Weintraub, *J. Research Natl. Bur. Standards* **50**, 39 (1953).

A-100000

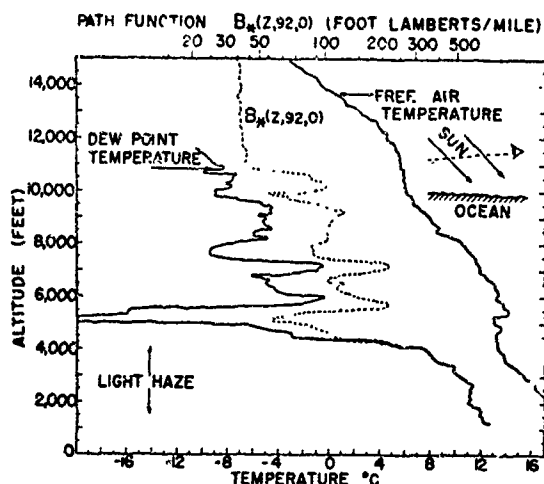


FIG. 10. Profile of dew point temperature calculated by means of Debye's equation from the profile of microwave refractive modulus in Fig. 9. Profiles of path function and free air temperature are identical with those in Fig. 9. Correlations between profiles of dew point temperature and path function are obvious.

In this equation  $\epsilon$  is in millibars, the Kelvin temperature is of the stratum, the total pressure is in millibars, and the microwave refractive modulus of the stratum for microwaves is defined by the expression  $(n-1) 10^6$ , where  $n$  is the refractive index of the stratum.

An Air Force C-131 equipped with a microwave refractometer flew in formation with the B-29 throughout the descent during which the optical data reported in this paper was secured. The resulting profile of microwave refractive modulus is shown in Fig. 9. The profile of horizontal path function from Fig. 5 also appears in Fig. 9 for purposes of comparison.

Debye's equation was used to calculate a humidity profile from the microwave data. This profile, expressed in terms of dew-point temperature, is given in Fig. 10. The close correlation between humidity and path function is obvious.

The following speculations on the reasons for the observed correlation are offered: In terms of visible

light water vapor exhibits virtually no absorption and it contributed only molecular scattering, the magnitude of which is too small to be responsible for the observed effects. The atmosphere invariably contains, however, suspended material such as sea-salt ions, silica, ammonia, or oxides of nitrogen and sulfur which can form condensation nuclei for water droplets. A tenuous haze of these tiny droplets will form in any stratum having a water vapor content above some critical minimum. These droplets will grow until the vapor pressure just outside the curved surface of the drop equals the partial pressure of water vapor in the surrounding air.<sup>9</sup> Liquid droplets ranging from  $4 \times 10^{-7}$  to more than  $10^{-4}$  cm are known to be present in the atmosphere.<sup>10</sup> In the case of spherical water droplets small in diameter compared with a wavelength of light that component of the scattering coefficient which is due to droplets increases as the sixth power of their diameter,<sup>11</sup> assuming the number of droplets per unit of volume to remain fixed. In view of this, the observed correlation between the path function and the humidity within tenuous haze layers appears to be understandable.

#### ACKNOWLEDGMENTS

The number of individuals involved in an experimental program of the complexity, scope, and duration of the flight research partially described by this paper is too great to be listed properly here. Special mention should be made, however, of the technical contributions of Brig. Gen. Victor A. Byrnes, USAF, through whose efforts the program was initiated; Lt. Col. George E. Long, USAF; Major Joseph X. Brennan, USAF; and research pilot Capt. Robert L. Baron, USAF. Important contributions to the detailed design of the apparatus were made by John M. Hood, Roswell W. Austin, W. Joseph Woodside, Thomas H. Glenn, Romuald Anthony, Merrill D. Hobt, and David J. A. Hooton.

<sup>9</sup> W. E. K. Middleton, *Vision through the Atmosphere* (Toronto Press, Toronto, 1952), Chap. 3.

<sup>10</sup> C. Junge, *Nuclei of Atmospheric Condensation*, Compendium of Meteorology (American Society for Metals, Cleveland, 1951).

<sup>11</sup> Lord Rayleigh, *Proc. Roy. Soc. (London)* A90, 219 (1914).

# I. Introduction

Seibert Q. Duntley

Man's ability to see objects through the atmosphere, underwater, or in space by naked eye or with the aid of magnifying and filtering devices is limited by the availability of light, its distribution on the object of regard and its background, the reflective properties of both, the image transmission characteristics of the intervening media, the properties of any magnifying and filtering optical devices employed, and the characteristics of the human visual system. For at least half a century answers have been sought to questions such as the following: Can some particular object of interest be seen? How far can it be seen? How dark may twilight become before the object will be lost to view? How rapidly can it move and yet be visible? What is the effect of object color? Will filters help? How much magnification is necessary to make the object visible at a given distance? What is the optimum procedure for visual search? What is the probability of success in sighting the object searched for? Under what circumstances can it be recognized? Is visual identification possible? How is visual performance affected by fatigue, discomfort, distraction, apprehension, motivation, and kindred factors?

Methods for generating answers to such questions have come into being, particularly during the last twenty years. Specialists in generating these answers refer to their subject as *visibility* and regard it as a professional specialty within optics. They are, however, not alone in the use of the word; meteorologists have long used the term *visibility* as a meteorological parameter, highly restricted in its meaning and greatly limited in its applicability. The word *visibility* has also been used by designers of windows in aircraft, automobiles, and even buildings to denote the field of view which these apertures provide. Despite the universal wish of scientists and engineers for every word to have but a single technical meaning, it seems likely that the term *visibility* will continue to be ambiguous through the foreseeable future. Authors and readers must depend upon context to make clear the school of thought to which the word is applied in each instance. Throughout the remainder of this article, *visibility* will not be used in its meteorological or architectural connotations, but only to denote the human capability to detect, recognize, and identify objects by means of the human visual mechanism used

directly and with the aid of magnifying and filtering devices but without the aid of intervening sensor systems, such as photography, television, image intensifiers, infrared devices, electronic displays, etc. Extension of the use of the term *visibility* to include the performance of the human visual system when aided by such sensors can be made, but will not be attempted in this article.

The limiting performance of the human visual system to detect and recognize distant objects can be predicted by engineering-type calculations, provided adequate input information is available. This form of optical engineering has been severely handicapped, however, by a greater lack of applicable data than has been generally appreciated. It is a purpose of this article to illustrate by example the types of information that are needed and to supply a more complete working sample than has heretofore appeared. Every effort has been made to exclude from the paper all previously published facts and concepts insofar as this can be done without sacrificing viewpoint and clarity. Concise summaries of certain vital concepts and principles are included throughout the account, but the authors have depended heavily upon references and the willingness of the reader to use them. If, in a few instances, paragraphs which summarize known principles or facts seem to go somewhat beyond this criterion, it is because of the belief that the need for such a summary exists.

The authors of this article have shared with many colleagues throughout the world in the development of *visibility* as a science and as an engineering procedure. The paper is intended to provide an overall view of some applied aspects of this subject. Sufficient input data have been included to enable certain sample *visibility* calculations to be carried out by those who wish to explore this branch of optical engineering, but a full professional treatment of the subject would require a book-length treatise. In order to achieve broad coverage and yet adequate technical depth in a compact feature article, it has been deemed best to call upon an integrated team of specialists to produce a unified presentation with each individual contributing in his specialty. Each major section of the present paper, therefore, bears the name of the specialist who prepared it.

550-01-X B

## ii. Summary

**Seibert Q. Duntley**

Calculations of the limiting performance of the human visual systems are based upon the separate properties of all of the physical components which, taken together, comprise a system for the transfer of information from the object to the observer's consciousness by way of the visual pathway. Thus, light reflected or generated by the object forms a body of image-forming flux which, after transmission by the intervening media, forms a retinal image which, in turn, is transmitted to the brain and perceived by the observer. In like fashion, the background against which the object is seen generates flux from a different part of object space, and this signal follows a corresponding path to the perceptual level of the observer. Discrimination of the object from its background depends upon the thresholds of the human visual system.

Prediction of the limiting human visual capability to detect any specific object begins, therefore, with the optical properties of that object and of its background. These, in combination with the nature of the incident lighting, define the inherent optical signal which is available in the direction of the observer. Assessment of the magnitude of this inherent optical signal is the first major step in any visibility calculation. It involves a considerable knowledge of the optical properties of both background and target as well as a detailed specification of their lighting.

## II.1. Backgrounds

The nature of the background against which objects are seen most frequently depends upon whether the path of sight is inclined downward or upward. Some form of natural terrain may provide the background for objects viewed along downward-looking paths of sight, whereas in upward-looking cases the background is usually the sky or a cloud. The following discussion of backgrounds includes these and other cases.

## Natural Terrains

Natural terrains are of wide variety but they can be grossly categorized as vegetated, barren, snowy, and watery. Vegetated terrains, because of shadow minimization and because of reflection from the vertical components of plant surfaces (leaves, stalks, etc.) exhibit a characteristic phenomenon often called *back gloss* (Duntley, 1946) or *negative gloss* (Judd, 1952, p. 303); this means that the directional reflectance of an unresolved vegetated surface is greatest when

viewed by an observer with the sun at his back. Even bare soils, including sand, tend to exhibit back gloss, as is illustrated by Fig. 2.1. Snow covered terrains, nearly matte in their appearance when the snow is freshly fallen, develop gloss upon aging and particularly when they are rain-erusted (Middleton, 1952). Snowy terrains containing outcroppings of vegetation may exhibit a form of back gloss due to the shadows produced by this vegetation whenever these interruptions in the snow surface are unresolved.

Man-made surfaces, such as paints, pavements, or roofs, vary widely in matte-ness but they seldom exhibit back gloss. Their gloss characteristics are usually of the "normal" form, illustrated by the data for a sample of matte brown paint in Fig. 2.1. Typically, therefore, man-made surfaces which match natural terrains when viewed vertically under medium or low sun conditions appear brighter than the terrain when viewed toward the azimuth of the sun but darker than the terrain when the sun is behind the observer.

## Spectral Effects

The reflectance characteristics of many natural terrains vary markedly with wavelength. Inter-reflections between textural elements tend to intensify spectral reflectance effects; thus, as shown by Fig. 2.2, the spectral apparent radiance of a maple tree differs markedly from that of a maple leaf (Duntley, 1946, p. 213).

## Diffuse Reflectors

No natural terrain and no known man-made surface is a perfect diffuse reflector in the sense of appearing equally luminous from all angles of view. A few surfaces, including freshly fallen snow, approximate this condition provided the solar zenith angle is less than  $45^\circ$ , but even fresh snow exhibits marked gloss characteristics when the sun approaches the horizon, an extremely common condition during the snowy season. Man-made surfaces invariably exhibit pronounced gloss characteristics, particularly when the solar zenith angle exceeds  $60^\circ$ . Since large solar zenith angles occur much more commonly than do small ones, very serious errors in visibility calculations can arise from the false assumption that target or background surfaces are perfect diffuse reflectors, i.e., that they obey "Lambert's law of reflection" (O.S.A., 1953, p. 178). In Sec. III of this paper, data are presented on some commonly occurring backgrounds, and techniques for calculating the inherent contrast of objects seen against these surfaces are recommended.

## 11.2. Objects

Objects, or *visual targets* as they are often called, are of every conceivable variety. In general they have complex, three-dimensional shapes producing an in-

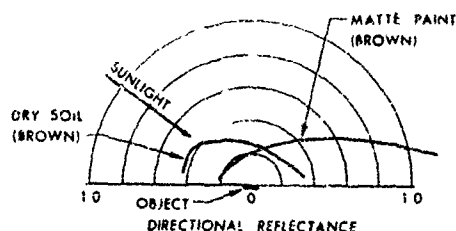


Fig. 2.1. Directional reflectance of dry brown soil and matte brown paint, illustrating typical differences.

tricate pattern of highlights and shadows even if their reflecting characteristics are the same on all of their surfaces, a circumstance which rarely exists. The gloss characteristics of object surfaces show even more variety than do background surfaces. Many glossy objects have mirrorlike surfaces that form virtual images of the sun which are often vastly brighter than any portion of the background and, correspondingly, are visible at much greater range than any other type of surface. Thus, it is a common experience while flying to see rivers and bodies of water in the far distance when no other terrain features of like size are visible; this is a consequence of the large positive contrast presented by these bodies of water owing to the mirrorlike reflections of the sky which they produce.

In virtually every instance of a man-made object viewed against a natural background, the disparate gloss characteristics cause the object to undergo marked changes in its appearance and its conspicuity when viewed from various directions, as has been illustrated in Fig. 2.1. Data for a variety of examples of this sort will be found in Sec. III of this paper.

Obviously, any object is visually detectable only if its photometric properties differ from those of its background in the observer's direction of view. Whatever difference does occur constitutes an optical signal. The detectability of such a signal depends upon the properties of the sensor which, in this article, is the human visual system.

### II.3. Visual Properties

For more than a century, research scientists have produced a voluminous literature concerning the capability of the human visual system to detect minimal optical signals. The discovery that the psychometric function is nearly the same for all visual detection tasks when the photometric nature of the object and its background are specified in terms of contrast (Blackwell, 1946, 1963) enabled the simplification and collation of an enormous body of experimental facts. Without that simplification, visibility calculations would scarcely be practicable as an engineering procedure. The further discovery that the shape of an object is ordinarily of minor consequence compared with the effect of its angular size provided an additional important simplifying approximation. The experi-

mental result that color contrasts ordinarily have an almost negligible effect (MacAdam, 1946) on the detectability of an optical signal, although they affect the noticeability of suprathreshold objects, constitutes yet another important simplification of visual properties. The fact that under virtually all circumstances geometrically identical objects are equally detectable if their universal contrasts are equal in magnitude even if opposite in sign is perhaps the most important of the first-order experimental generalizations; in Secs. III and IX of this paper it is demonstrated that this basic result, a dividend of the definition of universal contrast, is of vital importance in visibility calculations.

Under conditions of high (daylight) level adaptation, visual threshold properties are nearly invariant to adapting luminance, are minimal in the central  $1^\circ$  of the visual field (the foveal region), and increase systematically toward the periphery. The smallest detectable optical signal is one for which all of the object flux is concentrated within a circular area only slightly larger than the anatomical dimensions of the foveal cone receptors. All objects of this angular size or smaller, regardless of their actual angular dimension, shape, or pattern, are equally detectable if their flux content is the same; this is known as Ricco's law, which may be written  $C\omega = \text{constant}$  for the special case of objects having apparent contrast  $C$  and subtending a solid angle  $\omega$  at the eye of the observer but having no angular dimension sufficient to exceed the Ricco domain. The angular diameter within which Ricco's law is obeyed increases somewhat as adaptation luminance is diminished until, in the regions of twilight, moonlight, and starlight the increase is rapid, reaching 15 min of arc at starlight levels of adaptation. Since all objects, regardless of size or shape, which fall within the range of Ricco's law are

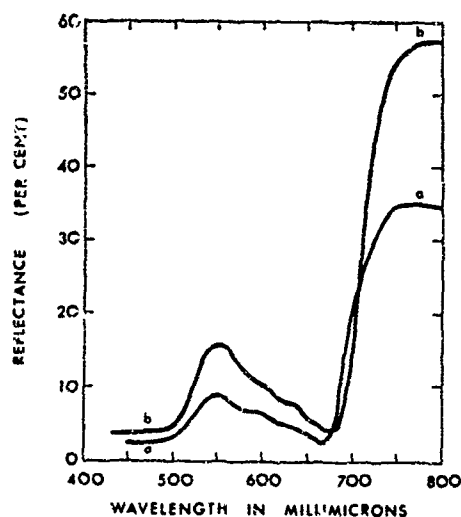


Fig. 2.2. Spectrophotometric curves of a maple tree (curve a) and of a maple leaf (curve b).

indistinguishable if their flux content is equal, the resolving power of the human visual system depends upon adaptation level.

## Peripheral Vision

Maximum object detectability occurs within the rod-free central fovea under conditions of high-level (photopic) daytime adaptation conditions, but at twilight (mesopic) levels, detectability is virtually uniform throughout the fovea, parafovea, and peripheral retina, although resolution diminishes toward the periphery. At low light levels, i.e., scotopic adaptation, the sensitivity of the rod-free central fovea effectively vanishes, and the greatest sensitivity occurs in the ring-shaped parafovea where the population of rod receptors is dense.

## Visual Search

In daytime, optimum detectability occurs when the object is imaged on the foveal portion of the retina, but this circumstance does not always occur. During visual search, in fact, it is relatively improbable that the image will fall on the fovea. The probability of success in searching some prescribed field of view for an object can be computed only if detection thresholds for that object in the peripheral portions of the retina are known. It is as if the eye had associated with it a detectivity lobe, greatest on-axis and falling rapidly toward the periphery. This lobe is not a fixed structure but depends markedly upon the angular size and nature of the object and upon its apparent contrast. Thus, lobe shape is governed by the atmosphere, by the directional reflectance characteristics of both target and background, and by the prevailing distribution of natural lighting; it is, therefore, different for each path of sight and for each visual fixation. Details of visual search calculations in which account is taken of the changing nature of the detectivity lobe are discussed in Sec. X of this article.

## Recognition and Identification

The higher levels of the human visual system are capable of determining object type, class, and identity. Thus, at different levels of visual performance an object may be *detected* as a shapeless spot, *recognized* as a ship, *classified* as a passenger liner, or *identified* as R.M.S. Queen Mary. Although quantitative predictions of the limiting circumstances when the higher-level functions can be performed involve more variables and greater uncertainties with respect to input data, certain approaches to problems of this class have been made (Harris, 1959).

## 11.4. Atmospheric Properties

The appearance of distant objects is affected so profoundly by the optical properties of the atmosphere

that meteorologists include atmospheric clarity among the meteorological parameters to be observed, reported, and forecast. Unfortunately, the meteorological data are seldom of appreciable usefulness in predicting the visual detectability of specific objects. Quite different optical properties of the atmosphere and its lighting must be known before valid predictions can be made. The literature of visibility contains many examples of attempts to calculate the needed information from models of the atmosphere and its lighting. The success of these attempts is difficult to test or judge unless measurements of real atmospheric and lighting conditions have been made for comparison. Such data are difficult to acquire and are, therefore, exceedingly rare. Section VI of this article may be the first publication in a scientific journal of a sufficiently complete set of measured atmospheric properties to enable valid visibility calculations applicable to a real atmospheric condition to be made. Even so, the tables in Sec. VI and the related tabulations in Sec. III relate only to conditions which prevailed at one place on one occasion. They are, moreover, incomplete, since no radiometric or spectroradiometric data are included. Clearly, a complete photometric and radiometric description of the atmosphere at any one time and place involves the measurement and tabulation of a very large quantity of data. The need is, however, for many such bodies of data representing many places at many times of day and under a variety of atmospheric conditions. Such a compilation would be a well nigh hopeless task were it not for the capabilities of large electronic computers for which the required bodies of data can be stored on magnetic tape. The creation of such a computer library of atmospheric and lighting conditions is in prospect and will, when combined with corresponding libraries of visual data, object characteristics, and background information, enable major visibility calculations to be carried through quickly, economically, and automatically. Until sufficient data have been collected and stored in computer format, limited visibility calculation studies will doubtless continue to be carried out by procedures like those described later in this article.

The scientific background which underlies the tables in Secs. III and VI of this article and the equations for their use has been published previously (Duntley *et al.*, 1957). Equation (5) on page 500 of that reference [see also Duntley (1948a), Eq. (12), p. 182] states that all radiance differences are transmitted by the atmosphere with the same attenuation as that experienced by each image-forming ray. This implies that no fine details are obliterated by atmospheric scattering processes. Additional theory by Middleton (1942) and experiments by Duntley (1948a, p. 186) support this implication and the belief that images of distant objects are formed by photons which traverse

the intervening media without being scattered. These concepts can be summarized by the modulation transfer function for atmospheric haze.

### Atmospheric Modulation Transfer Function

In the absence of atmospheric haze, all nonzero spatial frequencies are attenuated equally, by an amount equal to the beam transmittance of the path of sight [see Duntley *et al.* (1957), Eq. (5), p. 500]. The apparent radiance of the zero spatial frequency, however, is, by Eq. (4) of the same reference, the sum of the path radiance and the product of the inherent radiance and beam transmittance. These concepts form the basis of a derivation by James L. Harris of the modulation transfer function for atmospheric haze, as follows: consider the inherent radiance of a scene, such as that on the cover of this issue, to be represented by a radiance distribution  $N_0(\alpha, \beta)$ , where  $N$  denotes spectral radiance, the subscript signifies zero observation distance (i.e., inherent radiance), and  $\alpha, \beta$  are rectangular angular coordinates at the eye of the observer. The field of view is rectangular and bounded by the angles  $-A/2 < \alpha < A/2$  and  $-B/2 < \beta < B/2$ . In terms of a two-dimensional Fourier representation, the inherent radiance is

$$N_0(\alpha, \beta) = a_{00} + \sum_{i=0}^{\infty} \sum_{j=0}^{\infty} a_{ij} \cos \frac{2\pi i \alpha}{A} \cos \frac{2\pi j \beta}{B} \\ + \sum_{i=0}^{\infty} \sum_{j=1}^{\infty} b_{ij} \cos \frac{2\pi i \alpha}{A} \sin \frac{2\pi j \beta}{B} \\ + \sum_{i=1}^{\infty} \sum_{j=0}^{\infty} c_{ij} \sin \frac{2\pi i \alpha}{A} \cos \frac{2\pi j \beta}{B} \\ + \sum_{i=1}^{\infty} \sum_{j=1}^{\infty} d_{ij} \sin \frac{2\pi i \alpha}{A} \sin \frac{2\pi j \beta}{B},$$

where the primes on the first double summation indicate that the term  $i = j = 0$  has been eliminated, where

$$a_{00} = \frac{1}{AB} \int_{-A/2}^{A/2} \int_{-B/2}^{B/2} N_0(\alpha, \beta) d\alpha d\beta. \quad (2.1)$$

The corresponding apparent radiance  $N_r(\alpha, \beta)$ , as seen from observation distance  $r$  is

$$N_r(\alpha, \beta) = a_{00}T_r + T_r \sum_{i=0}^{\infty} \sum_{j=0}^{\infty} g(a_{ij}, b_{ij}, c_{ij}, d_{ij}) + N_r^*,$$

where the double summation symbolizes the four components shown above, provided that the beam transmittance  $T_r \neq f(\alpha, \beta)$  and the path radiance  $N_r^* \neq f(\alpha, \beta)$ . These assumptions are described by saying that  $T_r$  and  $N_r^*$  are decoupled from the scene and represent measures of atmospheric effects.

The nonnormalized modulation transfer function for nonzero spatial frequencies is simply  $a_{ij}T_r / N_r^*$ , and that for the zero spatial frequency is  $(a_{00}T_r + N_r^*) / a_{00}$ . Normalization to unity at zero spatial frequency is

accomplished by dividing each expression by  $(a_{00}T_r + N_r^*) / a_{00}$ . The normalized modulation transfer function for nonzero spatial frequencies, denoted by  $\tau$ , is, therefore,

$$\tau = \frac{T_r}{(a_{00}T_r + N_r^*) / a_{00}} = \frac{1}{1 + N_r^* / a_{00}T_r}. \quad (2.2)$$

The symbol  $a_{00}$ , defined by Eq. (2.1), signifies the average inherent radiance of the field of view. Objects occupying only a minor portion of the field and/or differing but slightly in inherent radiance from their surroundings have a negligible effect on  $a_{00}$ . If the object appears against any uniform area of sufficient angular area to render negligible its effect upon  $a_{00}$  for that area,\* Eq. (2.2) may be written

$$\tau_r = 1 / (1 + N_r^* / N_0 T_r), \quad (2.3)$$

where  $N_0$  is called the inherent radiance of the background against which the object appears. The pre-script  $b$  on  $\tau_r$ , signifies that this modulation transfer function for atmospheric haze applies to the specified background. In this case the object is said to be decoupled from the background. Since  $\tau_r$  applies universally to any decoupled target which may appear against background  $b$ , it has been called the universal modulation transfer function for atmospheric haze; this is the proper factor for use in the modulation transfer function products used to describe the performance of optical and photographic systems used to record decoupled targets.

### Contrast

Throughout the literature of visibility, the ratio of the radiance (or luminance) of any object decoupled from its background to the radiance (or luminance) of its background in the direction of observation, or some function of that ratio, has been referred to as contrast. In this article the ratio just defined will be denoted by  $\rho$  and referred to as ratio contrast. Since any function of  $\rho$  also represents a form of contrast, there are, obviously, a limitless number of possible forms, each of which could be named.

Most of the literature of visibility, both psychophysiological and physical, has made exclusive use of the contrast function  $\rho - 1$ , because it provides important advantages in both disciplines. Fundamentally, the italicized generalization in Sec. II.3, which refers to  $\rho - 1$  or its algebraic equivalent  $\Delta B / B$ , states that flux increments ( $\Delta B$ ) are as detectable as flux decrements ( $-\Delta B$ ). Since negative contrast ( $-\Delta B / B$ ) can never exceed 1 in absolute value, whereas the

\* The area so defined, i.e., the background, often constitutes only a small portion of the field of view. Adjacent areas comprise the surround of the background. The adaptive state of the observer is sometimes affected by a surround which differs markedly in luminance from that of the background.



magnitude of positive contrast is limitless, objects lighter than their backgrounds can be vastly more detectable than otherwise identical objects darker than their backgrounds. Physically,  $\rho - 1$  is relatable to the universal modulation transfer function, as may be seen by combining Eqs. (4) and (7) on p. 500 of the paper by Duntley *et al.* (1957) to produce the equation

$$C_r(z, \theta, \phi) / C_0(z, \theta, \phi) = [1 + N_r^*(z, \theta, \phi) / b N_0(z, \theta, \phi) T_r(z, \theta, \phi)]^{-1} \quad (2.4)$$

in the notation used in that reference as well as in Sec. VI of this article. In Eq. (2.4),  $C_0(z, \theta, \phi)$  denotes the inherent contrast  $\rho - 1$  of an object at altitude  $z$ , when viewed along a path of sight defined by zenith angle  $\theta$  and azimuth angle  $\phi$ ; the subscript zero implies zero observation distance, i.e., inherent contrast. Similarly,  $C_r(z, \theta, \phi)$  denotes the apparent contrast of the target at viewing distance  $r$  from altitude  $z$  along the same path of sight  $\theta, \phi$ . The same parenthetical modifiers denoting altitude and path of sight appear on the path radiance  $N_r^*(z, \theta, \phi)$ , the beam transmittance  $T_r(z, \theta, \phi)$ , and the inherent background radiance  $N_0(z, \theta, \phi)$ . With the incorporation of parenthetical modifiers to specify altitude and path of sight, the right-hand side of Eq. (2.3) is seen to be identical with the right-hand side of Eq. (2.4). Thus, the universal modulation transfer function for atmospheric haze is identically equal to the ratio of apparent to inherent universal contrast when  $C_0 = \rho - 1$ , i.e., in complete notation:

$${}_b\tau_r(z, \theta, \phi) \equiv {}_bC_r(z, \theta, \phi) / {}_bC_0(z, \theta, \phi), \quad (2.5)$$

where the prescript  $b$  specifies that the quantity applies to background  $b$ . The  $\rho - 1$  type of contrasts in Eqs. (2.4) and (2.5) share with  ${}_b\tau_r$ , the unique and valuable property of universal applicability to any object which may appear against background  $b$ .  ${}_bC_r(z, \theta, \phi)$  and  ${}_bC_0(z, \theta, \phi)$  are, therefore, referred to as *universal apparent contrast* and *universal inherent contrast*, respectively. The form  $\rho - 1$  is also referred to as *universal contrast*. The ratio of universal apparent contrast to universal inherent contrast is called universal contrast transmittance and denoted by  ${}_b\mathcal{J}_r(z, \theta, \phi)$ . Because the form  $\rho - 1$  is used exclusively in this article (except in the following paragraph) and throughout virtually the entire literature of visual science and visibility, the adjective *universal* often has been omitted in the later sections of this paper, but the universal form of contrast is to be understood unless some alternate form is mentioned by name.

### Modulation Contrast

Resolution tests and performance analyses of many optical systems, particularly photographic systems, are frequently described in terms of the ratio  $(\rho - 1) / (\rho + 1)$ ; this may be called *modulation contrast* and

denoted by  ${}_mC_r$ . Algebraically, this definition is equivalent to the form  $\Delta N / ({}_1N + {}_2N)$ , a radiometric nonentity in object space, but obviously descriptive of a spatial modulation test object composed of alternating, equally wide bars having radiances  ${}_1N$  and  ${}_2N$ , respectively, and related to the modulation transfer function for atmospheric haze through the relation  $a_{00} = ({}_1N + {}_2N) / 2$ . Modulation contrast  ${}_mC_r$  shares none of the universal properties of  ${}_bC_r$ , but simple algebraic interconnections between it and universal contrast exist because of the respective definitions  ${}_mC_r = (\rho - 1) / (\rho + 1)$  and  ${}_bC_r = (\rho - 1)$ . Simple algebraic relations can readily be found between modulation contrast transmittance  ${}_m\mathcal{J}_r$ , and the pair of universal contrast transmittances  ${}_1\mathcal{J}_r$  and  ${}_2\mathcal{J}_r$ .

Modulation contrast and modulation contrast transmittance have, at present, no usefulness in visibility for at least three reasons: (1) they lack universal applicability to all objects and components of objects, a property essential to the object index concepts described in Sec. IX; (2) they lack the single-valued connection with detection thresholds possessed by the universal forms and without which the techniques dealt with in Secs. III, IV, and X would be vastly more complicated; (3) virtually no visual threshold data exist in spatial frequency form, although research in this direction has begun (De Palma and Lowry, 1962).

### Atmospheric Boil

Image transmission by the atmosphere is affected by atmospheric boil in an entirely different manner than by atmospheric haze. Nonzero spatial frequencies are not attenuated equally, resulting in a true loss of resolution. Visibly noticeable temporal variations are produced in the images of distant objects. The contrast transmittance for objects of small angular subtense varies inversely as the third power of the distance in the presence of boil distributed uniformly throughout the path of sight (Duntley, 1963b). Modulation transfer functions for atmospheric boil have been derived by Hufnagel and Stanley (1964).

### II.5. Water Properties

Visibility by swimmers is limited by contrast attenuation in a manner somewhat similar to that experienced in a foggy atmosphere. Differences between atmospheric effects and corresponding underwater effects are evident along inclined paths of sight, however, because absorption of visible light, ordinarily absent in the atmosphere, plays a prominent role in even the clearest of waters. Underwater sighting ranges are always short compared with sighting ranges in clear air. Nearly all objects, therefore, subtend so large a visual angle when seen underwater that the exact size of the object is of almost no consequence.



Except for very tiny objects or the fine details of larger ones, underwater sighting ranges depend almost entirely upon the contrast transmittance of the path of sight when ample daylight prevails. The fundamentals of this subject have been treated by Duntley (1963a). Additional discussion, chiefly from the standpoint of input data, is given in Sec. VII of this article.

## II.6. Combining Techniques

Data on objects, backgrounds, atmospheres, and observers must be combined if answers are to be generated for the types of questions raised in the first paragraph of Sec. I. Such visibility calculations were made initially by iterative numerical procedures which bracketed the final answer as closely as necessary (Duntley, 1946, 1948a,b). Such calculations are cumbersome, time-consuming, and they invite mistakes. Prior to the advent of fast electronic computers, the most promising method to accelerate the calculations appeared to lie in the use of nomographic charts. A series of nomograms for visibility calculations were published by Duntley (1946, 1948b) and were subsequently republished by Middleton (1952) and by various others.

## Graphical Methods

Alternative graphical procedures have also been devised. One common technique is to prepare a plot of apparent object contrast vs observer distance expressed in terms of the angular diameter of a circular disk having an angular area equal to that of the object. This curve is superimposed upon a plot of threshold contrast for circular objects vs the angular diameter of these objects. The curves intersect at the limiting object diameter and indicate, therefore, the maximum distance at which the object can be visually detected. The steepness of the intersection of the curves and the spread between them at other object distances provide a valuable indication of the varia-

bility of the detection range with observer performance. It must be borne in mind that all of the visual threshold data are averages of the performance of several observers and that there is an important degree of variability throughout the human population (Sec. IV).

## Visual Search

The detection ranges calculated by any of the procedures described in the preceding paragraphs represent the maximum distances achievable. These ranges will only be realized when the object is imaged upon the most sensitive portion of the retina. In most instances the observer is required to search for an object within his field of view. In such a circumstance the chance of the object's being imaged on his optimal retinal area may be small and the probability of detection at any given range will depend upon the peripheral sensitivity of his eye. Calculation of detection probabilities in visual search was pioneered by Lamar (1946), and a valuable compendium on visual search techniques is contained in National Academy of Sciences-National Research Council Publication 712 (1960). Although the principles of visual search calculations have been well known for about twenty years, their practical application has been compromised in virtually every instance by lack of sufficient data on the optical properties of objects and backgrounds, visual properties, ocular behavior, and atmospheric effects. Even when adequate information is available, the computational task is a staggering one if the data are used properly. A new concept of object classification described in Sec. IX may eliminate part of this difficulty. When it is combined with computer techniques, a permanently satisfactory means for visual search calculations should result. Section X of this article contains a numerical example of an advanced type of visual search calculation intended to illustrate more completely than has been done heretofore one technique for incorporating real and complete data into a practical visual search calculation.

# III. Optical Properties of Objects and Backgrounds

Jacqueline I. Gordon

There are two basic approaches to the description of the optical properties of objects and backgrounds. One is to describe the component properties, such as directional reflectance and lighting distribution. These properties may then be combined with information on the shape and orientation of each pattern element in order to determine its inherent luminance in the

direction of any given path of sight. The alternative method is to measure the inherent luminance (or the inherent spectral radiance) under specific natural lighting conditions. It is the latter approach that has been employed almost exclusively in this section, since data in this form are directly usable in practical visibility problems.

Because of space limitations, the data on targets and backgrounds presented in this section will be limited to photopic properties under only one form of natural illumination. Emphasis is placed upon data appropriate for use with the specific atmospheric properties presented in Sec. VI, i.e., a clear day with a moderately high sun at a zenith angle of  $41.5^\circ$ .

### III.1. Natural illumination

The position of the sun and the relative contribution of the sun to the total illuminance have a major effect upon the inherent luminance of objects and backgrounds. The total illuminance on a fully exposed horizontal plane at sea level in clear weather has been tabulated as a function of the zenith angle of the sun by Brown (1952); a curve plotted from these tables is shown in Fig. 3.1. The same figure also contains data points representing data obtained in the desert near Inyokern, California, on 7 August 1962 by means of a photoelectric illuminometer and shadow intensity meter (see Sec. VIII). The measured total illuminance, resulting from both sun and sky, is denoted by crosses, whereas the component of illuminance resulting from the sky alone is shown by circled points. Obviously, the contribution resulting from the sun becomes more important with decreasing solar zenith angle. Figure 3.2 presents the same data as the ratio of the component of illuminance owing to the sky to the total illuminance. The contrast of a shadow on a horizontal, diffusely reflecting background is this ratio minus 1; such contrasts are indicated on the right-hand scale of Fig. 3.2.

On clear days, the total illuminance at a given solar zenith angle shows less variability with air clarity

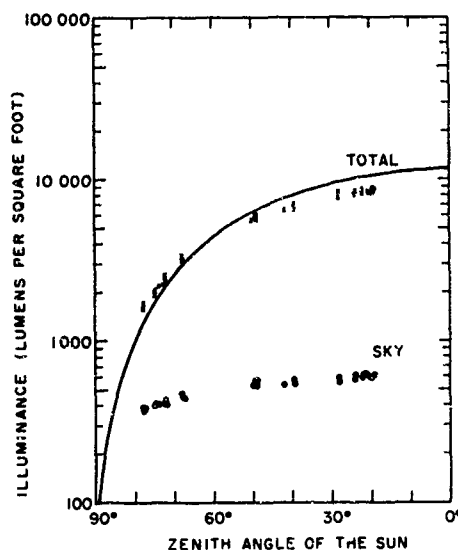


Fig. 3.1. Illuminance as a function of sun position; solid curve is from Brown (1952). A value in  $\text{lm}/\text{ft}^2 \times 10.764$  yields the corresponding value in  $\text{lm}/\text{m}^2$ .

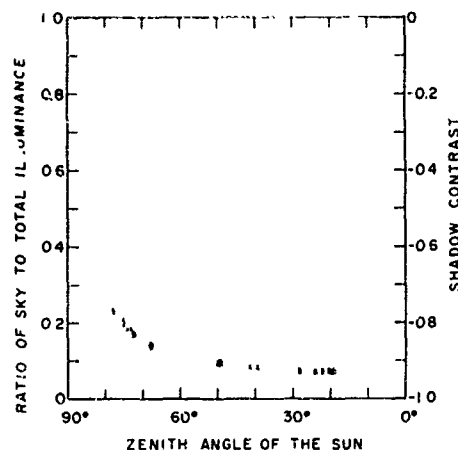


Fig. 3.2. Shadow intensity as a function of sun position; ratio presumably goes to 1 when sun has a zenith angle of  $90^\circ$ .

than does the component of illuminance owing to the sky, presumably because more sunlight is scattered and redistributed when atmospheric clarity decreases, thus increasing the sky illuminance. Since very little visible light is lost by absorption in the atmosphere unless smoke and dust are present, the redistribution may increase the total illuminance at the very large solar zenith angles, and only slightly decrease the total illuminance when the sun is near the zenith. For example, on the day for which the atmospheric properties are given in Sec. VI, the total illuminance on a horizontal plane at ground level was  $5940 \text{ lm}/\text{ft}^2$  ( $64,000 \text{ lm}/\text{m}^2$ ), and the ratio of sky component to the total illuminance was 0.235. Thus the total illuminance was only slightly below that for the clear desert day depicted by the data in Figs. 3.1 and 3.2, but the sky made a much larger relative contribution.

### Moonlight

Measurements of the luminance of objects and backgrounds under moonlight are more difficult to make than under sunlight owing to the large decrease in illumination. The full moon is approximately the same angular size as the sun and, similarly, serves as the principal source of light. Thus, for the same zenith angle of the sun or moon and the same atmospheric conditions, objects and backgrounds will have the same directional reflectances, and contrasts determined in daylight are, therefore, directly applicable. This is as true for upward and horizontal paths of sight as for downward paths of sight. Moreover, the ratio of the luminance of an object under comparable sunlight and full moonlight conditions is equal to the ratio of the inherent luminances of the sun and the moon.

### III.2. Sky Backgrounds

The backgrounds generally encountered on upward-looking paths of sight are skies. Fortunately, the

literature contains numerous measurements of sky luminance under a variety of conditions. A most useful compendium by Hulbert (1957) tabulates clear weather sky luminances for nighttime, twilight, and daytime as a function of solar zenith angle, and path of sight. The luminance of overcast skies was treated by Moon and Spencer (1942).

Sky luminance data as a function of altitude and path of sight for a clear day with a solar zenith angle of  $41.5^\circ$  is given in Sec. VI of this article.

A common background for horizontal paths of sight is the sky near the horizon. Typical horizon sky luminances as a function of time of day or night and type of weather are presented in Table 3.1 from Duntley (1946, 1948b).

Table 3.1. Horizon Sky Luminances

Description	Luminance (ft-L)	Luminance (cd/m <sup>2</sup> )
Full daylight	1000	3,426
Overcast day	100	343
Very dark day	10	34
Twilight	1	3.4
Deep twilight	$10^{-1}$	$3.4 \times 10^{-1}$
Full moon	$10^{-2}$	$3.4 \times 10^{-2}$
Quarter moon	$10^{-3}$	$3.4 \times 10^{-3}$
Starlight	$10^{-4}$	$3.4 \times 10^{-4}$
Overcast starlight	$10^{-5}$	$3.4 \times 10^{-5}$

For horizon sky data for clear weather, nighttime, twilight, and daytime as a function of sun zenith angle and azimuth from the sun, refer to Hulbert (1957). For data coordinated with atmospheric clarity data for sun zenith angle  $41.5^\circ$ , see Sec. VI of this article.

### III.3. Directional Reflectance of Terrains

The characteristic differences in directional reflectance between most man-made surfaces and natural terrains were noted in Sec. II of this article. A further example is provided by Fig. 3.3, which depicts weathered aluminum and hard-packed dirt.

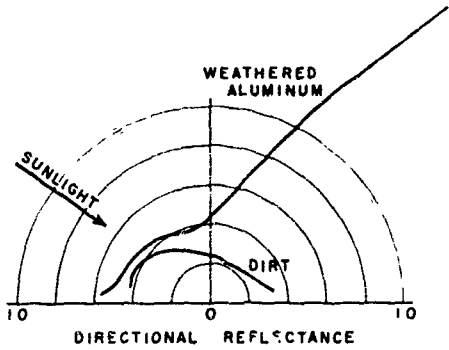


Fig. 3.3. Directional luminous reflectance of weathered aluminum (see Table 3.3, object 1) and hard-packed yellowish dirt (see Table 3.2, terrain 8).

latter exhibits prominent back gloss. Table 3.2 gives luminous directional reflectance data for fourteen terrains. The first five of these terrains were measured simultaneously with the atmospheric data given in Sec. VI of this article and are appropriate for use with those data. The remaining nine sets of terrain data were selected as also appropriate for use in the same way. The data in Table 3.2 are ratios of inherent luminance in the direction of the specified path of sight to the total illuminance on a fully exposed horizontal plane at ground level; this was 5940 lm/ft<sup>2</sup> (64,000 lm/m<sup>2</sup>) when the atmospheric data given in Sec. VI were obtained.

Directional reflectance was chosen for tabulation in Table 3.2 to minimize the effect of the change in total illuminance for small changes in sun zenith angle. Only at the paths of sight where the background exhibits a large specular component does a minor change in solar zenith angle cause an appreciable change in directional reflectance. Specular reflectance tends to be most important at angles which reflect the sun and at grazing incidence to the surface.

All the data in Table 3.2 on various terrain backgrounds and other background surfaces, except those for calm water, exhibit the phenomenon of back gloss: i.e., the highest directional reflectance occurs when the path of sight is away from the azimuth of the sun ( $\phi = 180^\circ$ ).

### III.4. Objects

The most accurate method of determining the optical characteristics of a three-dimensional object is to measure the optical properties of the actual object or a scale model with optically equivalent surface characteristics on the actual background under natural illumination, thus obtaining the effect of the appropriate interreflections between surfaces. A less precise but simpler approach is to measure the directional reflectance of a flat surface oriented in a series of directions appropriate to the object for the paths of sight in question. For the data reported in this section, the latter procedure was utilized. The number of surface orientations was limited to angle increments of  $4.5^\circ$ . Thus, a seventeen-sided figure represents surfaces appropriate for most downward paths of sight, and a twenty-six-sided figure represents surfaces for all paths of sight.

The designation of "object" and "background" is somewhat arbitrary, since what is background in one case may be an object in another. For instance, a road may be the background for a vehicle or it may be the object when viewed against the surrounding terrain. Similarly, what is an object in one case may become a background in another. A vehicle may itself be the object, or some surface of the vehicle may be the background against which lettering is to be

**Table 3.2. Directional Luminous Reflectance of Terrain Backgrounds**

Description	Sun zenith angle	Azimuth of the path of sight relative to the sun	Zenith angle of path of sight							
			180	165	150	135	120	105	100	95
1. Pine trees, small, uniformly spaced. Data are for unresolved terrain over which atmospheric data given in Sec. VI were collected.	41.5	0 45 90 135 180	0.0333	0.0241 0.0222 0.0315 0.0335 0.0402	0.0214 0.0202 0.0311 0.0382 0.0444	0.0214 0.0194 0.0317 0.0392 0.0578	0.0261 0.0210 0.0317 0.0387 0.0640	0.0379 0.0303 0.0337 0.0438 0.0711	0.0463 0.0387 0.0387 0.0463 0.0758	0.0859 0.0549 0.0463 0.0572 0.0825
2. Grass, thick, rather long, pale green, dormant, dryish, little ground showing. <sup>a</sup>	41.5	0 180	0.088	0.081 0.098	0.076 0.119	0.077 0.146	0.088 0.150	0.094 0.153	0.096 0.153	0.094 0.160
3. Asphalt, oily, with dust film blown onto oil. <sup>a</sup>	42.0	0 180	0.061	0.057 0.067	0.058 0.080	0.060 0.101	0.068 0.090	0.090 0.086	0.104 0.086	0.127 0.088
4. "White" concrete, aged. <sup>a</sup>	42.2	0 180	0.266	0.263 0.289	0.254 0.313	0.254 0.343	0.266 0.367	0.298 0.350	0.320 0.343	0.374 0.320
5. Calm water, infinite optical depth. <sup>b</sup>	41.5	0 45 90 135 180	0.0222	0.0234 0.0230 0.0221 0.0213 0.0214	0.0297 0.0240 0.0222 0.0212 0.0212	0.0272 0.0272 0.0234 0.0220 0.0216	0.0569 0.0357 0.0293 0.0270 0.0267	0.139 0.107 0.0711 0.0665 0.0718	0.267 0.199 0.121 0.113 0.125	0.461 0.325 0.214 0.203 0.254
6. Grass, lush green, closely mowed thick lawn. <sup>c</sup>	40.4 39.6 39.6 39.9	0 90 135 180	0.100	0.096 0.103 0.107 0.109	0.098 0.110 0.125 0.109	0.108 0.121 0.148 0.119	0.120 0.138 0.166 0.122	0.149 0.159 0.178 0.125	0.168 0.168 0.178 0.125	
7. Macadam, washed off and scrubbed. <sup>c</sup>	48.5 60.1 46.0	0 90 180	0.113	0.115 0.110 0.126	0.119 0.109 0.141	0.128 0.116 0.156	0.148 0.122 0.166	0.194 0.139 0.172	0.229 0.147 0.176	
8. Dirt, hard packed, yellowish. <sup>c</sup>	53.2 56.5 51.1	0 90 180	0.243	0.230 0.243 0.272	0.229 0.258 0.313	0.239 0.260 0.370	0.252 0.276 0.422	0.300 0.300 0.432	0.330 0.304 0.434	
9. Mixed green forest, deciduous (oak) and evergreen (pine). <sup>d</sup>	39.0 37.0	0 180	0.0360	0.0325 0.0410	0.0291 0.0493	0.0205 0.0493	0.0205 0.0820	0.0342 0.263		
10. Pine forest. <sup>d</sup>	33.5	0	0.0385	0.0385	0.0308	0.0246	0.0246	0.0200		
11. Grass, dry meadow, dense, mid- summer. <sup>e</sup>	45 45 45 45	0 90 180 270	0.0955	0.0897 0.0778 0.116 0.107	0.0960 0.0890 0.131 0.121	0.0952 0.101 0.143 0.134	0.108 0.111 0.153 0.137	0.129 0.130 0.170 0.132		
12. Ilyas, sparse and dry, yellowish grass on sand at end of summer. <sup>e</sup>	40 40 40 40	0 90 180 270	0.231		0.320 0.163 0.295 0.262		0.342 0.176 0.353 0.237	0.356 0.198 0.359 0.229		
13. Sand dunes, sharply expressed micro- relief, dry. <sup>f</sup>	40 40 40 40	0 90 180 270	0.288		0.183 0.284 0.246 0.278		0.337 0.329 0.259 0.410	0.353 0.306 0.276 0.281		
14. Podsol, ploughed, moist. <sup>g</sup>	50 50 50	0 90 270	0.0600	0.0680 0.0682 0.149	0.0646 0.0953 (0.180) <sup>h</sup>		0.0555 0.0814 0.168		0.0761 (0.189) <sup>h</sup>	

\* These terrains were measured on the ground by means of a goniophotometer, beneath and during the collection of the data in Ser. VI.

<sup>b</sup> Computed from equations by Duntley (1952) for the lighting condition prevailing for items 1 and 2 in this table.

\* Data taken with a goniophotometer, 10 October 1956.

\* Data taken with a photoelectric telephotometer from a helicopter at 300 ft (91.4-m) altitude, mountain forested area near Julian, California, 23 September 1959.

\* Luminous directional reflectance for terrains 11 through 14 were computed from spectrophotometric data by Krinov (1947) using C.I.E. Illuminant B. Disparity between data for azimuths 90° and 270° "is explained apparently by the direction of shallow furrows in relation to the sun", (Krinov-Belkov, 1953, p. 75).

/ Parentheses indicate estimates based on incomplete spectral data.

discerned. In Table 3.2 horizontal natural and man-made surfaces are arbitrarily called "background". Just as arbitrarily, man-made surfaces placed in the various orientations described above are termed "objects" in Table 3.3.

The data in Table 3.3 are appropriate for use with the backgrounds in Table 3.2. The three man-made objects are weathered aluminum, an aluminum painted surface, and a glossy white painted surface. Diagrams depicting the orientation of the surfaces and the zenith angle and azimuth ( $\theta, \phi$ ) of the normal from each surface are presented in Fig. 3.4. The top part of the figure is for the path of sight toward the azimuth of the sun,  $\phi = 0^\circ$ ; as shown on the right, the path of sight has various zenith angles from  $180^\circ$  (straight downward) to  $95^\circ$  (nearly horizontal). Similarly, the bottom portion of Fig. 3.4 is for the paths of sight looking away from the sun. These diagrams are to be used as aids in interpreting the data presented in Table 3.3.

### III.5. Inherent Contrast

A graphical method for representing the inherent contrast of objects and backgrounds for various paths of sight is illustrated by Fig. 3.5, wherein data from Tables 3.2 and 3.3 for terrain 8 (dirt) and object 1 (weathered aluminum), respectively, are plotted in semilogarithmic form. Consider first the two solid curves. The (small) vertical separation between

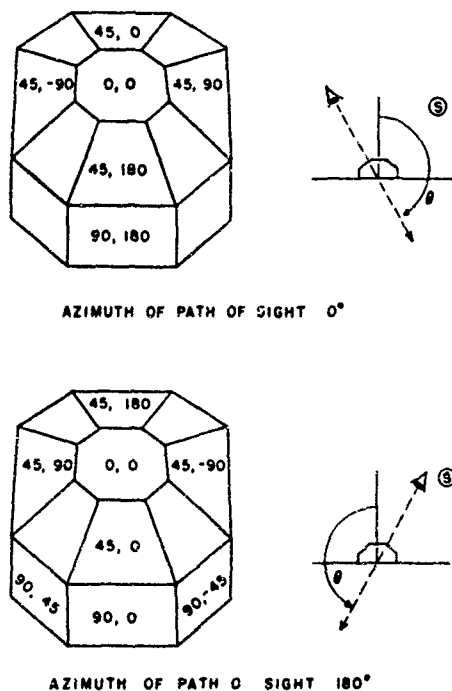


Fig. 3.4. Surfaces of three-dimensional objects; each number pair refers to the zenith angle and azimuth from the plane of the sun of the normal from the surface, respectively.

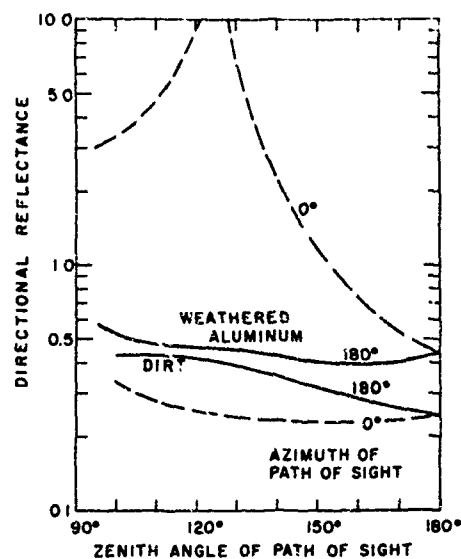


Fig. 3.5. Reflectance of object and background.

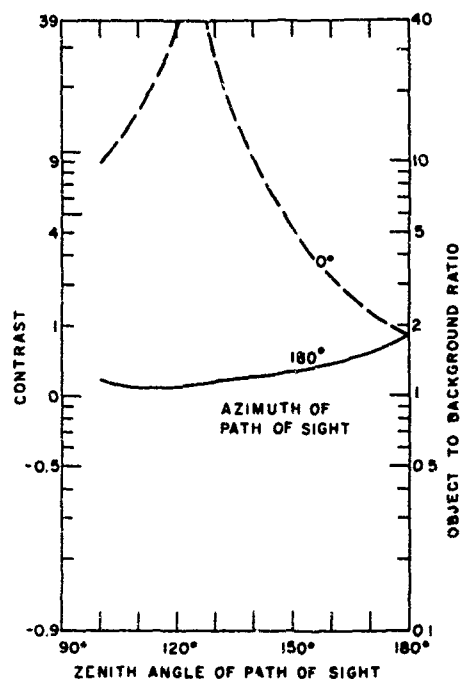


Fig. 3.6. Contrast of object and background.

them is a direct (logarithmic) measure of the ratio of the directional reflectance of the two surfaces along all downward inclined paths of sight in the plane away from the sun. Similarly, the (large) vertical separation between the two dotted curves shows graphically the magnitude of the ratio of the corresponding directional reflectances for paths of sight toward the plane of the sun (azimuth  $0^\circ$ ).

A semilogarithmic plot of the vertical separations between the two pairs of curves in Fig. 3.5 is shown in

Table 3.3. Directional Luminous Reflectance of Objects\*

Object	Sun zenith angle	Azimuth of path of sight relative to sun	Normal from surface		Zenith angle of path of sight								
			Zenith angle	Azimuth	180	165	150	135	120	105	100	95	
1. Weathered aluminum <sup>a</sup>	56.5	0	0	0	0.440	0.62	1.18	3.65	9.2	3.75	3.30	3.03	
	56.2	0	45	180	0.255	0.245	0.245	0.350	1.03	0.86	0.92	1.08	
	56.2	0	45	0	1.00	0.76	0.72						
	57.2	0	45	±90	0.380	0.405	0.51	0.70					
	56.4	0	90	180		0.231	0.269						
	55.8	90	0	0	0.440	0.405	0.445	0.451	0.475	0.52	0.55	0.56	
	56.2	180	0	0	0.440	0.392	0.400	0.440	0.460	0.485	0.52	0.58	
	56.1	180	45	0	1.00	1.80	5.9	3.80	1.62	0.90	0.87	0.80	
	56.1	180	45	180	0.255	0.275	0.328						
	57.2	180	45	±90	0.380	0.380	0.420	0.470					
	57.3	180	90	±45				0.58	0.61	0.64	0.65	0.66	
	56.2	180	90	0		0.455	0.51	0.60	0.70	0.76	0.82	0.88	
	Weathered aluminum (shadowed) <sup>b</sup>	56.0	0	0	0	0.206	0.206	0.245					
		56.0	180	0	0	0.206	0.223	0.261	0.290	0.290	0.310	0.330	0.415
2. Aluminum paint <sup>b</sup>	56.5	0	0	0	0.362	0.420	0.64	1.35	3.45	3.45	3.38	3.45	
	55.9	0	45	180	0.198	0.193	0.220	0.340	0.97	0.83	0.93	1.07	
	55.9	0	45	0	0.77	0.64	0.58						
	57.0	0	45	±90	0.292	0.292	0.345	0.490					
	56.5	0	90	180		0.180	0.222						
	55.8	90	0	0	0.362	0.362	0.370	0.380	0.385	0.420	0.440	0.440	
	56.5	180	0	0	0.362	0.355	0.400	0.460	0.490	0.50	0.50	0.50	
	55.8	180	45	0	0.77	1.06	1.58	1.45	1.20	0.82	0.75	0.68	
	55.8	180	45	180	0.198	0.220	0.270						
	57.0	180	45	±90	0.292	0.310	0.345	0.410					
	57.5	180	90	±45				0.52	0.57	0.56	0.56	0.56	
	56.3	180	90	0		0.460	0.52	0.65	0.71	0.74	0.73	0.72	
	Aluminum paint (shadowed) <sup>b</sup>	56.1	0	0	0	0.180	0.183	0.210					
		56.1	180	0	0	0.180	0.200	0.240	0.246	0.242	0.271	0.285	0.299
3. Glossy white paint <sup>b</sup>	57.2	0	0	0	0.92	0.92	0.95	1.38	4.40	1.85	1.50	1.40	
	55.9	0	45	180	0.248	0.245	0.274	0.395	1.01	0.87	0.99	1.10	
	55.9	0	45	0	1.59	1.49	1.33						
	56.8	0	45	±90	0.72	0.74	0.78	0.82					
	56.3	0	90	180		0.236	0.290						
	55.0	45	0	0	0.92	0.91	0.90	0.89	0.80	0.82	0.79	0.75	
	55.5	90	0	0	0.92	0.91	0.90	0.89	0.86	0.78	0.70	0.64	
	55.0	135	0	0	0.92	0.91	0.90	0.89	0.84	0.72	0.64	0.54	
	57.2	180	0	0	0.92	0.92	0.94	0.99	1.06	0.95	0.89	0.83	
	55.9	180	45	0	1.59	1.08	2.85	1.83	1.60	1.62	1.63	1.63	
	55.9	180	45	180	0.248	0.257	0.315						
	56.9	180	45	±90	0.72	0.74	0.81	0.85					
	57.5	180	90	±45				1.30	1.32	1.33	1.32	1.32	
	56.2	180	90	0		1.20	1.43	1.50	1.50	1.46	1.46	1.42	
	Glossy white paint (shadowed) <sup>b</sup>	56.3	0	0	0	0.223	0.216	0.240					
		56.3	180	0	0	0.223	0.240	0.290	0.285	0.290	0.352	0.400	0.490

\* Sky condition: clear.

<sup>b</sup> Data taken with a goniophotometer, January 1959.

Fig. 3.6. The object-to-background ratios (separations) are plotted on the logarithmic scale at the right in Fig. 3.6. The scale on the left is for contrast, which is simply the object-to-background ratio minus 1.

Practical convenience is often served by a ruler bearing a logarithmic reflectance-ratio scale marked in contrast. When such a ruler is used, zero contrast is always placed on the curve of background reflectance, and contrast is read from the curve of target reflectance

vertically above or below, depending upon whether the contrast is positive or negative.

If, for a given three-dimensional object for one azimuth of the path of sight, the contrasts of all of the surfaces are plotted in similar fashion on one graph, a quick picture is obtained of the range of contrast contained within the complex object. This form for plotting contrast has the additional advantage of duplicating the precision of the initial measurements.

000000-1-X-B

### III.6. Contrast Control

The techniques described above are of direct usefulness to problems of contrast control. Either contrast minimization, or contrast maximization may be desired.

To a first approximation, it can be assumed that a paint can be found with approximately the same directional characteristics as the object surface but lower or higher in reflectance. A reflectance curve of such a paint would have the same characteristics as shown in Fig. 3.5, but displaced above or below the curve depending on whether the reflectance has been raised or lowered. Therefore the contrast curve in Fig. 3.6 can be assumed to depict the contrast of the new paint, but with the curve displaced above or below the present curve. Instead of moving the curve, the zero contrast line may be moved with the same result.

In selecting a new reference line, it is desirable to minimize (or maximize) the absolute value of the contrast, since the human eye responds equally to positive and negative contrast of the same absolute value. Often the best reduction (or increase) in the absolute contrast can be achieved by the minimization (or maximization) of the area between the zero contrast line and the contrast curves when the curve is plotted on a linear contrast scale. One way to achieve minimization is to have as large a portion of the contrast curve lie on or near zero contrast as possible. This also usually means that the areas under the curve are fairly equally divided between positive and negative contrast.

In carrying out these procedures, several cautions should be noted:

First, the coordinates used for plotting the contrast curves in Fig. 3.6 gravely distort the contrast picture. On this grid equal distances above and below the contrast line do not constitute equal absolute contrasts.

The grid completely masks the fact that negative contrast has a maximum value of minus 1, whereas positive contrast can be infinitely large. For this reason, in evaluating a change in reference line it is important to use a movable contrast scale to measure the new absolute values of contrast achieved.

The second factor to be noted while minimizing (or maximizing) contrast is the relative importance of portions of the contrast curves. These must be evaluated in terms of the size of the projected area of the object which has this particular contrast. Consider, for instance, a horizontal surface. The maximum area is seen when the path of sight is normal to the surface, a zenith angle of  $180^\circ$ . At  $120^\circ$  zenith angle the projected area has been reduced to 50% of its maximum. Therefore, for horizontal surfaces, the most important portion of the contrast curve lies on the right-hand side of the graph in Fig. 3.6, and the contrasts for the more slanted paths of sight (zenith angles less than  $120^\circ$ ) can be ignored.

The third caution concerns the achievability of the paint reflectance needed to produce the desired contrast change. The minimum achievable reflectance for black paint depends upon whether a dull or glossy finish is desired.

The reflectance of the desired paint is obtained by dividing the reflectance of the object surface by the factor by which the zero reference line has been raised or multiplying by the factor by which it has been lowered.

The final step necessary to complete the engineering procedure for contrast minimization (or maximization) is to obtain contrast curves for paints believed to have the required directional reflectance characteristics. This requires directional measurements of the paint under appropriate lighting conditions.

## VI. Atmospheric Properties

Almerian R. Boileau

Representative data from Visibility Laboratory Flight 74, south of Crestview, Florida, are shown in Figs. 6.1, 6.2, and 6.3 and Tables 6.1 through 6.12 inclusive. The flight was made midday on 28 February 1956. The day was "clear", that is, cloudless, but with pronounced haze in the first 4000-ft (1.22-km) altitude. Recording of data by airborne photometers was commenced at 1036 Central Standard Time (CST) at an altitude of 20,000 ft (6.1 km) and was terminated at 1326 CST at an altitude of 1000 ft (305 m). Data were recorded simultaneously at sea level by duplicate photometers installed on an instrumented van beneath the flight pattern.

### Beam Transmittance

The measured attenuation length  $L(z)$ , recorded during Flight 74, is plotted as a function of altitude in Fig. 6.1. This shows the laminar structure of the atmosphere.\* Also shown in Fig. 6.1 is a plot of equivalent attenuation length  $\bar{L}(z)$ . This quantity is a pseudo attenuation length which, when combined with its altitude  $z$ , can be used directly in the equation

$$T(z, \theta) = \exp \{ - [z/\bar{L}(z)] \sec \theta \} \quad (6.1)$$

to permit easy calculation of the atmospheric beam transmittance between sea level and altitude  $z$  for a path of sight inclined  $\theta^\circ$  from the vertical.

### Example

What is the beam transmittance for a path of sight between sea level and 5000 ft (1.52 km) when the path of sight is inclined  $60^\circ$  from the vertical, i.e., with a zenith angle of either  $60^\circ$  or  $120^\circ$ ? The equivalent attenuation length  $\bar{L}(z)$  for 5000 ft (1.52 km) is 2.32 naut. miles (4.3 km); the secant of  $60^\circ$  is 2.00 (hence

\* Along inclined paths of sight atmospheric attenuation varies with altitude. This can be taken into account (1) by introducing an optical slant range  $r$  (see Duntley 1946, 1948a), (2) by summation of attenuation length profiles (see Duntley, Boileau, and Eisendorfer, 1957), or (3) by means of an equivalent attenuation length (see Eltermar, 1963).

the path length  $r = z \sec \theta$  is 10,000 ft or 3.05 km); so the beam transmittance found by Eq. (6.1) is

$$\begin{aligned} T_{10,000}(0, 60^\circ) &= \exp \{ -(1.52/4.3) 2.00 \} \\ &= \exp -0.708 \\ &= 0.493. \end{aligned}$$

$T_{10,000}(0, 60^\circ)$  is the notation for the beam transmittance for the upward-looking case. The beam transmittance for the downward-looking case  $T_{10,000}(5000, 120^\circ)$  has the same numerical value.

Table 6.1 is a table of the data shown in Fig. 6.1 augmented by extrapolated values of attenuation length from 20,000 ft to 60,000 ft (6.1 km to 18.3 km). The value of the dimensionless ratio  $z/\bar{L}(z)$  as a function of altitude is also tabulated. Figures 6.2 and 6.3 show beam transmittances computed from the data in Table 6.1. The curves are plotted on log-log graph paper, in the case of the vertical coordinates to expand the data at low altitude and compress the data at the higher altitudes, and, in the case of the horizontal

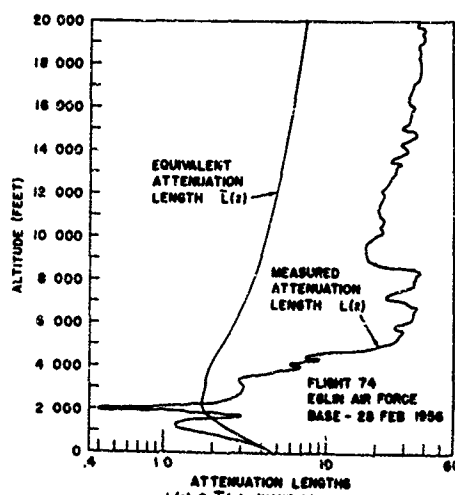


Fig. 6.1. Attenuation length  $L(z)$  was measured continuously during 1000-ft per min descent with aircraft held in level altitude. Equivalent attenuation length  $\bar{L}(z)$  is computed.



coordinate, to permit the curves to be used for graphical determination of beam transmittance between altitudes. An example of how this is done follows.

The beam transmittances given by the curves in Figs. 6.2 and 6.3 are between sea level and the indicated altitude. The beam transmittance between two altitudes is found as the ratio of the two beam transmittances between sea level and the two altitudes. When the data are plotted on a logarithmic scale, the difference between the log values of the beam transmittances

is the log of this ratio. As an example, it is desired to find the beam transmittance between 5000 ft (1.52 km) and 60,000 ft (18.3 km) for a path of sight with a zenith angle of 60° or 120°. The transmittance curve for  $\theta = 60^\circ/120^\circ$  indicates transmittances as

$$T_{120.000}(60,000, 120^\circ) = 0.345,$$

$$T_{10.000}(5000, 120^\circ) = 0.493.$$

Then the ratio of these two is

$$\begin{aligned} T_{120.000}(60,000, 120^\circ)/T_{10.000}(5000, 120^\circ) &= T_{110.000}(60,000, 120^\circ) \\ &= 0.345/0.493 \\ &= 0.700. \end{aligned}$$

This is the beam transmittance between 60,000 ft (18.3 km) and 5000 ft (1.52 km) either upward or downward for a path of sight with a zenith angle of either 60° or 120°. To determine this graphically from Fig. 6.3, the horizontal distance between the intersections of the  $\theta = 60^\circ/120^\circ$  transmittance curve with the 5000-ft (1.52-km) and 60,000-ft (18.3-km) altitude abscissas is transferred to the horizontal base line (preferably with dividers) with the left end of the interval, or difference, placed at the 100% transmittance point, and the right end of the interval will indicate the beam transmittance in question on the base line.

## Path Luminance

Tables 6.2 through 6.6 give the sky luminances for inclined paths of sight ranging from the vertically upward (zenith angle 0°) to horizontal (zenith angle 90°), at azimuths with respect to the sum of 0°, 45°, 90°, 135°, and 180°. For these paths of sight, sky luminance and path luminance are numerically equal, since the stellar contribution to the apparent luminance of the daytime sky is negligible. Tables 6.7 through 6.11 give the path luminances for paths of sight ranging from directly downward (zenith angle 180°) to 5° below the horizontal (zenith angle 95°) for the same azimuths of 0°, 45°, 90°, 135°, and 180°. In Tables 6.2 through 6.6, the luminances are for paths of sight from the observer's altitude to outer space.

In Tables 6.7 through 6.11, the path luminances are for paths of sight from the observer's altitude to sea level, the length of the path indicated by the subscript  $r$  equals  $z \sec \theta$  [see Duntley *et al.*, (1957), p. 501]. The increase in the length of the path of sight resulting from the curvature of the earth is less than 5% in all cases except  $\theta = 95^\circ$ . When  $\theta = 95^\circ$ , the path of sight from 60,000 ft (18.3 km) is increased by earth curvature by 25%. Accordingly, the path luminances for that zenith angle were not extrapolated above 20,000 ft (6.1 km).

Table 6.12 lists the ratios of the pressure at various altitudes  $z$  to the pressure at 20,000 ft (6.1 km). These

Table 6.1. Measured and Equivalent Attenuation Lengths, and Ratio of Altitude to Equivalent Attenuation Length

Altitude, $z$		Measured $L(z)^a$		Equivalent $L(z)^b$		$z/\bar{L}(z)$
(ft)	(km)	(naut. mi)	(km)	(naut. mi)	(km)	
0	0	4.60	8.52	4.60	8.52	0.000
1000	0.305	1.50	2.78	2.65	4.91	0.062
2000	0.610	0.40	0.74	1.75	3.24	0.188
3000	0.914	3.10	5.74	1.71	3.17	0.289
4000	1.219	7.00	12.97	1.90	3.63	0.356
5000	1.524	22.0	40.77	2.32	4.30	0.354
6000	1.820	28.5	52.82	2.74	5.08	0.361
7000	2.134	31.0	57.45	3.15	5.84	0.365
8000	2.438	34.0	63.01	3.55	6.58	0.371
9000	2.743	17.5	32.43	3.92	7.26	0.378
10000	3.048	19.5	36.14	4.25	7.88	0.387
11000	3.353	21.5	39.84	4.58	8.49	0.395
12000	3.658	22.5	41.70	4.90	9.08	0.403
13000	3.962	26.5	49.11	5.22	9.67	0.410
14000	4.267	31.5	58.38	5.54	10.27	0.416
15000	4.572	30.0	55.60	5.86	10.86	0.421
16000	4.877	34.5	63.93	6.18	11.45	0.426
17000	5.182	34.0	63.01	6.48	12.01	0.431
18000	5.486	38.0	70.42	6.80	12.60	0.436
19000	5.791	39.0	72.27	7.10	13.16	0.440
20000	6.096	35.0	64.86	7.40	13.71	0.445
25000	7.620	44.9	83.21	8.85	16.40	0.465
30000	9.144	53.8	99.70	10.3	19.00	0.481
35000	10.668	64.9	120.27	11.6	21.50	0.495
40000	12.192	81.7	151.41	13.0	24.00	0.507
45000	13.716	104	192.73	14.4	26.69	0.515
50000	15.240	132	244.63	15.8	29.28	0.522
55000	16.764	168	311.34	17.1	31.69	0.528
60000	18.288	214	396.58	18.5	34.28	0.533
100000	30.48	262	485.54	29.9	55.41	0.550
200000	60.96	274	597.77	59.3	109.89	0.551 <sup>c</sup>
$\infty$	$\infty$	$\infty$	$\infty$	—	—	0.551 <sup>c</sup>

<sup>a</sup> Attenuation length  $L(z)$  was recorded continuously as a function of altitude from 6.096 km to 0.305 km during descent of airplane at 305 m per min, with the zero altitude value recorded simultaneously in an instrumented van beneath the flight pattern. These data are shown in Fig. 6.1. Attenuation lengths above 6.096 km are extrapolated, using density ratios calculated from Minzner *et al.* (1959).

<sup>b</sup> The quantity  $1/\bar{L}(z)$  is equal to Elterman's mean attenuation coefficient  $K_s(h)$ , and the two quantities  $z/\bar{L}(z)$  and  $K_s(h) \cdot h$  may be used interchangeably in Eq. (6.1). See Elterman (1963).

<sup>c</sup> The value of  $z/\bar{L}(z)$  where  $z = \infty$  was calculated from the sea level to space transmittance obtained from measured and extrapolated attenuation length data.

Table 6.2. Sky Luminance  $B(z, \theta, 0^\circ)$ ,<sup>1</sup> Upper Sky, in Azimuth of Sun<sup>2</sup>

Altitude, $z$		Sky luminance (ft-L) <sup>3</sup> for zenith angle $\theta$ , °							
(ft)	(km)	$\theta = 0^\circ$	$15^\circ$	$30^\circ$	$60^\circ$	$75^\circ$	$80^\circ$	$85^\circ$	$90^\circ$
0	0	950	1300	3000	3850	3500	4350	4600	4600
1000	0.305	820	1200	2500	3400	3400	3500	3600	4000
2000	0.610	680	1180	2250	3200	2900	3100	3200	3300
3000	0.914	600	1150	2050	3100	2650	2750	2920	3000
4000	1.219	536	1120	1900	3000	2400	2500	2700	3500
5000	1.524	510	1100	1810	2900	2200	2300	2530	3300
6000	1.829	490	1090	1720	2850	2010	2150	2400	3200
7000	2.134	475	1050	1650	2800	1900	2000	2300	3100
8000	2.438	465	1000	1620	2750	1820	1920	2220	2980
9000	2.743	450	950	1590	2650	1780	1880	2180	2850
10000	3.048	420	900	1530	2550	1720	1810	2100	2800
11000	3.353	390	840	1500	2480	1690	1770	2050	2750
12000	3.658	365	780	1460	2390	1650	1710	2000	2700
13000	3.962	345	725	1430	2300	1610	1680	1950	2650
14000	4.267	325	680	1400	2250	1590	1650	1930	2650
15000	4.572	305	625	1390	2190	1580	1610	1900	2600
16000	4.877	289	582	1380	2120	1550	1590	1890	2600
17000	5.182	272	539	1350	2090	1530	1570	1850	2550
18000	5.486	260	495	1330	2020	1520	1550	1830	2550
19000	5.791	248	458	1320	2000	1500	1520	1810	2550
20000	6.096	236	420	1300	1950	1500	1500	1810	2550

<sup>1</sup> Parenthetical symbols: photometer altitude  $z$ , zenith angle  $\theta$ , and

table to table.

<sup>2</sup> Average zenith angle of sun during flight was  $41.5^\circ$

<sup>3</sup> The tabulated value in ft-L times 3.426 gives the value in cd/m<sup>2</sup>.

<sup>4</sup> Sky luminances were recorded by airborne equipment during descent, at five altitudes: 20,000, 8500, 7000, 4000, and 1000 ft. Simultaneous records were made in instrumented van. The data for the different azimuths and zenith angles were plotted against altitude and interpolated graphically so that the tabulated values could be read from the graphs.

<sup>5</sup> Extrapolated path luminances for an observer above 20,000 ft may be calculated as the products of 20,000-ft values and appropriate pressure ratio from Table 6.12. This assumes that the character of the aerosol at 20,000 ft and above is unchanged, and that the total number of scattering particles in a vertical path of sight above 20,000 ft is proportional to the pressure.

<sup>6</sup> Sky luminances at zenith angle of  $45^\circ$  were near the sun, exceeded the range of photometer, and hence are not available.

ratios can be used for extrapolating the path luminances listed in Tables 6.2 through 6.6 above 20,000 ft (6.1 km).

The following equation describes the apparent luminances of an object seen through the atmosphere [see Duntley *et al.* (1957), Eq. 1, p. 500]

$$B_A(z, \theta, \varphi) = B_0(z, \theta, \varphi) T_A(z, \theta) + B^*(z, \theta, \varphi). \quad (6.2)$$

From this equation it can be seen that the path luminance  $B^*(z, \theta, \varphi)$  is equal to the difference between the apparent luminance  $B_A(z, \theta, \varphi)$  and the product of the inherent luminance  $B_0(z, \theta, \varphi)$  and the beam transmittance  $T_A(z, \theta)$ . Hence, in all cases the path luminance for a path of sight between two altitudes is the difference between the path luminance at the observer's altitude (obtained from the appropriate table) and the product of the path of sight beam transmittance and the path luminance at the object altitude.

#### Example

Consider a path of sight at  $45^\circ$  from the azimuth of the sun and inclined downward at a zenith angle of  $120^\circ$ . The path luminance between 5000 ft (1.52

km) and 60,000 ft (18.3 km) is the difference between the measured path luminance at 60,000 ft (18.3 km) and the product of the beam transmittance of the path of sight from 5000 ft (1.52 km) to 60,000 ft (18.3 km) and the measured path luminance at 5000 ft (1.52 km). In Table 6.8, for azimuth of  $\pm 45^\circ$ , the path luminance for 60,000 ft (18.3 km) and a zenith angle of  $120^\circ$  is listed as 1230 ft-L (4212 cd/m<sup>2</sup>). The same table gives the corresponding path luminance for 5000 ft (1.52 km) as 444 ft-L (1522 cd/m<sup>2</sup>). The beam transmittance for the path of sight previously determined is 0.700. Hence the path luminance for the downward-looking path of sight between the 60,000-ft (18.3-km) and 5000-ft (1.52-km) altitudes is

$$B^*_{\text{measured}}(60,000, 120^\circ, 45^\circ) = 1230 - (444)(0.700) = 919 \text{ ft-L} \\ = 4212 - (1522)(0.700) = 3148 \text{ cd/m}^2.$$

This is the quantity denoted by  $B^*(z, \theta, \varphi)$  in Eq. (6.2).

#### Apparent Luminance of an Object

Once the beam transmittance and path luminance have been found for the assumed path of sight, the

**Table 6.3. Sky Luminance  $B(z, \theta, \pm 45^\circ)$ ,<sup>a</sup> Upper Sky,  $45^\circ$  from Azimuth of Sun<sup>b</sup>**

Altitude (ft.)	Sky luminance (ft.-L <sub>v</sub> ) for zenith angle $\theta^{\circ}$							
	$\theta = 15^{\circ}$	$30^{\circ}$	$45^{\circ}$	$60^{\circ}$	$75^{\circ}$	$80^{\circ}$	$85^{\circ}$	$90^{\circ}$
0	1180	1410	1760	1740	2000	3190	3220	2400
1000	1030	1230	1550	1520	2080	2220	2520	2400
2000	920	1100	1350	1320	1780	1960	2380	2400
3000	810	985	1280	1260	1530	1740	2160	2400
4000	725	900	1060	1040	1360	1580	1980	2400
5000	678	860	1000	980	1290	1510	1900	2340
6000	645	835	965	945	1230	1460	1830	2290
7000	610	810	930	920	1200	1400	1780	2220
8000	600	795	880	870	1180	1350	1730	2200
9000	590	770	840	840	1130	1310	1690	2150
10000	550	730	800	800	1080	1270	1640	2110
11000	530	690	765	765	1050	1220	1600	2090
12000	500	655	735	735	1010	1180	1550	2060
13000	480	620	700	700	960	1130	1510	2020
14000	455	580	675	675	920	1100	1460	2000
15000	432	550	645	645	880	1060	1420	1980
16000	412	515	620	620	840	1020	1380	1970
17000	390	485	590	590	800	980	1330	1950
18000	370	455	570	570	770	940	1290	1940
19000	352	430	545	545	730	900	1230	1930
20000	332	400	530	530	700	870	1200	1920

<sup>a,b,c,d,e</sup> See footnotes to Table 3.2.

**Table 6.4. Sky Luminance  $B(z, \theta, \pm 90^\circ)$ ,<sup>a</sup> Upper Sky,  $90^\circ$  from Azimuth of Sun<sup>b</sup>**

Altitude (ft)	Sky luminance (ft-L) <sup>c</sup> for zenith angle $\theta^{\circ}$ <sup>a</sup>							
	$\theta = 15^{\circ}$	$30^{\circ}$	$45^{\circ}$	$60^{\circ}$	$75^{\circ}$	$80^{\circ}$	$85^{\circ}$	$90^{\circ}$
0	925	916	990	1110	1580	1850	2090	1450
1000	780	740	780	875	1200	1380	1630	1500
2000	645	615	660	740	1080	1290	1600	1560
3000	545	530	570	660	1000	1270	1580	1600
4000	475	470	495	600	930	1260	1520	1660
5000	450	435	470	575	900	1250	1500	1680
6000	430	410	445	555	880	1220	1480	1700
7000	410	395	425	545	860	1190	1450	1730
8000	400	385	410	530	810	1030	1410	1760
9000	380	365	395	510	775	950	1370	1800
10000	362	345	380	490	750	920	1330	1810
11000	345	328	360	475	715	895	1300	1810
12000	328	310	345	455	695	865	1270	1820
13000	310	295	330	440	670	840	1230	1820
14000	295	280	312	420	645	815	1200	1830
15000	280	265	300	405	625	785	1170	1830
16000	262	252	283	390	605	760	1130	1840
17000	250	240	270	370	590	740	1100	1840
18000	235	230	256	350	570	720	1060	1850
19000	222	219	242	335	555	700	1030	1850
20000	210	210	232	320	540	680	1000	1860

<sup>a,b,c,d</sup> See footnotes to Table 6.2.

apparent luminance  $B(z, \theta, \varphi)$  of an object having an inherent luminance of  $B_0(z, \theta, \varphi)$  can be readily predicted with the aid of Eq. (6.2).

If an aircraft flying at an altitude of 5000 ft (1.52 km) has an inherent luminance of 2500 ft-L (8530 cd/m<sup>2</sup>) in the direction of the path of sight, its apparent luminance at the upper end of the path is

$$\begin{aligned} B_{110,000}(60,000, 120^\circ, 45^\circ) &= (2500)(0.700) + 919 = 2669 \text{ ft-l} \\ &= (8530)(0.700) + 3148 = 9140 \text{ cd/m}^2. \end{aligned}$$

It is interesting to note that if, in this case, the object had an inherent luminance of 3063 ft-L (10,500 cd/m<sup>2</sup>), its apparent luminance would also be 3063 ft-L (10,500 cd/m<sup>2</sup>); this is the effective equilibrium lumi-

Table 6.5. Sky Luminance  $B(z, \theta, \pm 135^\circ)$ ,<sup>a</sup> Upper Sky,  $135^\circ$  from Azimuth of Sun<sup>b</sup>

Altitude (ft)	Sky luminance (ft-L) <sup>c</sup> for zenith angle $\theta$ <sup>d</sup>							
	$\theta = 15^\circ$	$30^\circ$	$45^\circ$	$60^\circ$	$75^\circ$	$80^\circ$	$85^\circ$	$90^\circ$
0	690	640	600	880	1450	1720	1980	1470
1000	610	560	530	740	1220	1410	1820	1570
2000	510	500	530	675	1120	1140	1790	1600
3000	186	150	490	630	1060	1300	1780	1720
4000	410	100	450	595	1000	1290	1780	1780
5000	415	382	435	580	975	1280	1770	1780
6000	395	359	419	570	950	1270	1720	1790
7000	375	355	400	560	940	1260	1690	1800
8000	370	349	395	540	910	1200	1600	1890
9000	358	337	380	520	880	1160	1560	1960
10000	340	319	360	495	860	1130	1550	2000
11000	323	302	342	475	840	1110	1520	2020
12000	306	289	325	460	815	1090	1500	2050
13000	290	275	310	440	790	1060	1480	2100
14000	272	260	292	420	780	1030	1460	2110
15000	251	248	276	400	740	1000	1430	2130
16000	249	235	262	380	715	980	1410	2160
17000	222	222	248	365	690	950	1390	2190
18000	209	210	233	348	665	920	1360	2200
19000	194	198	220	330	615	895	1340	2220
20000	185	189	210	315	625	865	1320	2280

<sup>a,b,c,d,e</sup> See footnotes to Table 6.2.

Table 6.6. Sky Luminance  $B(z, \theta, 180^\circ)$ ,<sup>a</sup> Upper Sky,  $180^\circ$  from Azimuth of Sun<sup>b</sup>

Altitude (ft)	Sky luminance (ft-L) <sup>c</sup> for zenith angle $\theta$ <sup>d</sup>							
	$\theta = 15^\circ$	$30^\circ$	$45^\circ$	$60^\circ$	$75^\circ$	$80^\circ$	$85^\circ$	$90^\circ$
0	700	640	660	950	1600	1900	2500	1500
1000	620	570	600	800	1500	1800	2300	1600
2000	550	510	550	745	1390	1750	2210	1700
3000	490	460	510	710	1310	1710	2150	1780
4000	450	420	480	680	1250	1700	2100	1850
5000	430	405	460	660	1200	1700	2080	1930
6000	415	392	440	640	1180	1690	2030	1980
7000	400	380	420	620	1150	1680	2000	2000
8000	390	365	405	605	1120	1620	1920	2130
9000	370	350	390	590	1080	1590	1900	2230
10000	355	335	370	570	1020	1510	1850	2290
11000	335	320	355	550	980	1450	1810	2300
12000	319	305	340	525	940	1400	1800	2330
13000	300	289	325	500	900	1350	1790	2350
14000	282	272	310	480	860	1300	1750	2380
15000	265	258	295	455	830	1280	1750	2390
16000	250	242	279	435	800	1220	1750	2390
17000	235	230	262	410	770	1200	1750	2400
18000	220	215	249	390	750	1180	1750	2400
19000	208	201	235	370	720	1120	1750	2400
20000	195	190	220	350	700	1100	1750	2400

<sup>a,b,c,d,e</sup> See footnotes to Table 6.2.

nance for this path of sight (Duntley *et al.*, 1957). If, however, the object had an inherent luminance greater than 3063 ft-L (10,500 cd/m<sup>2</sup>), the apparent luminance would be reduced by this path of sight. Thus an object having an inherent luminance of 4000 ft-L (13,700 cd/m<sup>2</sup>) will have an apparent luminance of only 3719 ft-L (12,740 cd/m<sup>2</sup>), since the 1200 ft-L

(4112 cd/m<sup>2</sup>) loss of transmitted inherent luminance exceeds the 919 ft-L (3148 cd/m<sup>2</sup>) path luminance gain.

### Apparent Contrast

Because the detectability of any given object depends on its apparent contrast, the illustrative example from the preceding paragraph should be extended to

Table 6.7. Path Luminance  $B_p(z, \theta, 0^\circ)$ ,<sup>a</sup> Lower Sky, in Azimuth of Sun<sup>b</sup>

Altitude <sup>c</sup> (ft)	Path luminance (ft-L) <sup>d</sup> for zenith angle $\theta$ , <sup>e</sup>							
	$\theta = 180^\circ$	165°	150°	135°	120°	105°	100°	95°
1000	60.9	60.9	81.8	88.7	123	223	398	750
2000	134	132	158	163	214	461	727	1140
3000	192	204	229	236	198	676	998	1400
4000	233	259	298	305	371	868	1210	1500
5000	264	281	318	340	414	973	1300	1690
6000	291	301	344	381	469	1070	1390	1780
7000	313	327	377	434	545	1180	1470	1890
8000	341	366	419	496	671	1290	1530	2020
9000	367	388	445	531	732	1360	1580	2110
10000	388	399	459	545	749	1380	1610	2140
15000	184	457	532	610	823	1510	1780	2310
20000	603	510	604	672	896	1660	1980	2500
25000	710	557	674	731	967	1790	2150	
30000	798	596	731	779	1020	1890	2270	
40000	928	653	815	848	1110	2040	2440	
50000	1010	689	867	891	1150	2120	2540	
60000	1060	710	899	917	1180	2170	2590	

<sup>a</sup> Parenthetical symbols: photometer altitude  $z$ , zenith angle  $\theta$ , and azimuth applicable to table

<sup>b</sup> Average zenith angle of sun during flight 41.5°.

<sup>c</sup> In using these tables, it has been found that above 10,000 ft altitude increments of 5000 ft and 10,000 ft are satisfactory.

<sup>d</sup> The tabulated value in ft-L times 3.426 gives the value in cd/m<sup>2</sup>.

<sup>e</sup> Path luminances from 0 to 20,000 ft altitudes for zenith angles from 95° to 180° were calculated as follows: (1) Path functions for 1000 ft altitude  $B_p(1000, \theta, \varphi)$  were calculated from flight data and Eq. 10 of Duntley *et al.* (1957). (2) Path functions for sea level  $B_p(0, \theta, \varphi)$  were recorded in the van. (3) Path luminances for first 1000 ft altitude  $B_p^*(1000, \theta, \varphi)$  were calculated by means of Eq. 17 of Duntley *et al.* (1957). (4) Inherent background luminances (groundcover luminances)  $B_0(0, \theta, \varphi)$  were calculated by means of Eq. (6.2). See Eq. 4 of Duntley *et al.* (1957). (5) Path luminances for other than first 1000-ft altitude were calculated by means of Eq. (6.2).

<sup>f</sup> Path luminances for altitudes above 20,000 ft were extrapolated as follows: (1) Path functions for 20,000 ft  $B_p(20,000, \theta, \varphi)$  were calculated from flight data and Eq. 10 of Duntley *et al.* (1957). (2) Path functions above 20,000 ft  $B_p(z, \theta, \varphi)$  were calculated, in 100-ft increments, in proportion to atmospheric density. (3) Path luminances above 20,000 ft  $B_p^*(z, \theta, \varphi)$  were calculated by means of Eq. 17 of Duntley *et al.* (1957).

illustrate the calculation of the apparent contrast at the end of the path of sight.

### Example

Let it be assumed that the low-flying aircraft appears against a uniform groundcover of small, fairly closely spaced pine trees on flat terrain. This was the type of groundcover over which Flight 74 took place. Table 3.2 gives the directional luminous reflectance of this groundcover as seen from the assumed direction ( $\theta = 120^\circ$ ;  $\varphi = 45^\circ$ ) as 0.021. During Flight 74 the illumination on a fully exposed horizontal plane at ground level was measured as 5940 lm ft<sup>-2</sup> (64,200 lm/m<sup>2</sup>). Thus the inherent luminance of the groundcover is (5940) (0.021) = 125 ft-L (428 cd/m<sup>2</sup>). Equation (6.2) can now be used with the transmittance from Fig. 6.3 (previously determined to be 0.345) and the path luminance from Table 6.8 (previously determined to be 1230 ft-L; 4212 cd/m<sup>2</sup>) to calculate the apparent luminance of the background against which the aircraft appears. Thus, as seen from an altitude of 60,000 ft (18.3 km), the apparent luminance of the background is

$$\Delta B_{120,000}(60,000, 120^\circ, 45^\circ) = (125)(0.345) + 1230 = 1273 \text{ ft-L} \\ = (428)(0.345) + 4212 = 4360 \text{ cd/m}^2$$

and the apparent contrast of the low-flying aircraft against the pine-covered terrain as seen from 60,000 ft is

$$C_{120,000}(60,000, 120^\circ, 45^\circ) = (2669 - 1273)/1273 = 1.097.$$

### Inherent Contrast

The inherent contrast of the low-flying aircraft against the same groundcover can be found by using the inherent luminance of the aircraft and, as the background luminance, the apparent luminance of the groundcover as seen from 5000 ft (1.52 km) along the assumed directional path of sight.

### Example

The inherent luminance of the groundcover has been determined as 125 ft-L (428 cd/m<sup>2</sup>). The beam transmittance for the appropriate path of sight has already been determined as 0.493. Table 6.8 gives the path luminance for the assumed path of sight as

C 000000-X

Table 6.8. Path Luminance  $B_p^*(z, \theta, \pm 45^\circ)$ ,<sup>a</sup> Lower Sky, 45° from Azimuth of Sun<sup>b</sup>

Altitude <sup>c</sup> (ft)	Path luminance (ft-L) <sup>d</sup> for zenith angle $\theta$ <sup>e</sup>						
	$\theta = 165^\circ$	150°	135°	120°	105°	100°	95°
1000	86.2	103	110	128	259	359	650
2000	159	183	192	241	473	692	961
3000	220	252	262	331	639	837	1190
4000	267	308	318	391	771	1100	1310
5000	299	335	365	441	851	1180	1450
6000	324	356	406	484	935	1270	1570
7000	340	371	441	525	958	1320	1640
8000	375	417	487	606	1020	1390	1700
9000	401	447	518	645	1070	1450	1780
10000	417	463	534	678	1100	1480	1800
15000	495	541	607	755	1280	1600	1920
20000	587	628	689	856	1470	1760	2100
25000	671	707	763	947	1630	1910	
30000	740	772	824	1020	1760	2010	
40000	841	866	912	1130	1930	2160	
50000	903	925	967	1190	2040	2240	
60000	941	961	1000	1230	2110	2280	

<sup>a,b,c,d,e,f</sup> See footnotes to Table 6.7.

Table 6.9. Path Luminance  $B_p^*(z, \theta, \pm 90^\circ)$ ,<sup>a</sup> Lower Sky, 90° from Azimuth of Sun<sup>b</sup>

Altitude <sup>c</sup> (ft)	Path luminance (ft-L) <sup>d</sup> for zenith angle $\theta$ <sup>e</sup>						
	$\theta = 165^\circ$	150°	135°	120°	105°	100°	95°
1000	69.7	77.8	82.8	109	203	359	595
2000	138	156	174	226	389	562	833
3000	195	226	245	325	540	722	990
4000	238	279	298	404	665	867	1110
5000	268	306	339	462	744	975	1190
6000	293	328	372	508	810	1090	1260
7000	321	344	403	549	881	1170	1310
8000	351	383	439	580	932	1190	1380
9000	376	409	463	607	963	1240	1410
10000	393	426	481	628	1000	1270	1450
15000	479	516	571	739	1160	1420	1600
20000	582	609	670	873	1310	1580	1800
25000	675	694	759	993	1450	1730	
30000	751	763	831	1090	1560	1830	
40000	864	864	936	1230	1710	1980	
50000	934	926	1000	1311	1800	2060	
60000	976	964	1040	1370	1860	2100	

<sup>a,b,c,d,e,f</sup> See footnotes to Table 6.7.

444 ft-L (1522 cd/m<sup>2</sup>). Thus the apparent luminance of the background as seen from 5000 ft (1.52 km) along the path of sight would be

$$B_{10,000}(5000, 120^\circ, 45^\circ) = (125)(0.493) + 444 = 506 \text{ ft-L} \\ = (428)(0.493) + 1522 = 1733 \text{ cd/m}^2$$

Then the inherent contrast of the low-flying aircraft would be

$$C_0(5000, 120^\circ, 45^\circ) = (2500 - 506)/506 = 3.941.$$

### Contrast Transmittance

In the preceding illustration, the inherent contrast of 3.941 has been reduced to 1.097 by atmospheric attenuation of the optical signal and the addition of

path luminance. Thus, contrast has been reduced by the factor

$$C_{10,000}(60,000, 120^\circ, 45^\circ)/C_0(5000, 120^\circ, 45^\circ) = 1.097/3.941 \\ = 0.278.$$

The ratio of the apparent contrast to the inherent contrast,  $C_p(z, \theta, \varphi)/C_0(z, \theta, \varphi)$ , is called the contrast transmittance. It is also computable by any of the three following equations:

$$C_p(z, \theta, \varphi)/C_0(z, \theta, \varphi) = T_A(z, \theta) B_p(z, \theta, \varphi)/B_0(z, \theta, \varphi), \quad (6.3)$$

$$C_p(z, \theta, \varphi)/C_0(z, \theta, \varphi) = [1 + B_p^*(z, \theta, \varphi)/T_A(z, \theta) B_0(z, \theta, \varphi)]^{-1}, \quad (6.4)$$

$$C_p(z, \theta, \varphi)/C_0(z, \theta, \varphi) = 1 - B_p^*(z, \theta, \varphi)/B_0(z, \theta, \varphi) \quad (6.5)$$

Table 6.10. Path Luminance  $B_p(z, \theta, \pm 135^\circ)$ ,<sup>a</sup> Lower Sky,  $135^\circ$  from Azimuth of Sun<sup>b</sup>

Altitude <sup>c</sup> (ft)	Path luminance (ft-L) <sup>d</sup> for zenith angle $\theta$ <sup>e</sup>						
	$\theta = 165^\circ$	$150^\circ$	$135^\circ$	$120^\circ$	$105^\circ$	$100^\circ$	$95^\circ$
1000	93.4	120	137	137	336	486	693
2000	161	207	241	282	494	677	951
3000	218	278	315	385	625	813	1100
4000	259	326	375	462	729	910	1230
5000	292	358	414	525	804	1000	1290
6000	323	385	440	573	885	1090	1310
7000	344	401	466	609	936	1170	1400
8000	364	427	497	630	1010	1290	1520
9000	395	458	523	652	1140	1390	1650
10000	417	485	560	694	1170	1450	1700
15000	531	620	691	861	1350	1660	1910
20000	634	724	856	995	1470	1780	2050
25000	725	818	1000	1120	1590	1890	
30000	802	895	1130	1220	1670	1980	
40000	915	1010	1300	1360	1790	2090	
50000	986	1080	1410	1440	1860	2150	
60000	1030	1120	1480	1490	1900	2180	

<sup>a,b,c,d,e,f</sup> See footnotes to Table 6.7.

Table 6.11. Path Luminance  $B_p(z, \theta, 180^\circ)$ ,<sup>a</sup> Lower Sky,  $180^\circ$  from Azimuth of Sun<sup>b</sup>

Altitude <sup>c</sup> (ft)	Path luminance (ft-L) <sup>d</sup> for zenith angle $\theta$ <sup>e</sup>						
	$\theta = 165^\circ$	$150^\circ$	$135^\circ$	$120^\circ$	$105^\circ$	$100^\circ$	$95^\circ$
1000	65.9	94.3	106	144	228	485	860
2000	138	193	227	274	496	763	1140
3000	198	276	327	382	682	935	1270
4000	241	341	407	451	815	1040	1330
5000	264	364	450	512	867	1130	1380
6000	285	386	484	570	920	1230	1450
7000	316	417	515	617	987	1360	1480
8000	387	453	539	659	1110	1450	1680
9000	448	485	558	681	1220	1500	1770
10000	472	509	583	705	1250	1540	1800
15000	575	637	721	816	1420	1750	2000
20000	699	792	867	944	1620	1970	2200
25000	816	943	997	1060	1810	2170	
30000	912	1070	1100	1160	1960	2330	
40000	1050	1250	1260	1300	2160	2530	
50000	1140	1360	1350	1380	2280	2650	
60000	1190	1430	1410	1430	2350	2710	

<sup>a,b,c,d,e,f</sup> See footnotes to Table 6.7.

### Example

Equation (6.3) shows that the contrast transmittance may be calculated from the beam transmittance, and the inherent and apparent background luminances. The beam transmittance has been determined to be 0.700. The inherent background luminance, that is, the background luminance used in the determination

of the *inherent* contrast,  $B_{10,000}$  (5000,  $120^\circ$ ,  $45^\circ$ ), is 506 ft-L (1733 cd/m<sup>2</sup>). The apparent background luminance as seen from 60,000 ft (18.3 km) is 1273 ft-L (4360 cd/m<sup>2</sup>).

Accordingly,

$$C_{110,000}(60,000, 120^\circ, 45^\circ)/C_d(5000, 120^\circ, 45^\circ) \\ = (0.700)(506)/1273 = 0.278.$$

Equation (6.4) relates the contrast transmittance to path luminance, beam transmittance, and inherent background luminance. The path luminance, previously determined, is 919 ft-L (3148 cd/m<sup>2</sup>). The beam transmittance and inherent background luminance are, as before, 0.700 ft-L and 506 ft-L (1733 cd/m<sup>2</sup>), respectively. Then the contrast transmittance is

$$C_{110,000}(60,000, 120^\circ, 45^\circ)/C_0(5000, 120^\circ, 45^\circ) = 1/[1 + 919/(0.700)(506)] = 0.278.$$

When Eq. (6.5) is used to determine the contrast transmittance, only two quantities are required: path luminance and apparent background luminance. These two quantities are 919 ft-L (3148 cd/m<sup>2</sup>) and 1273 ft-L (4360 cd/m<sup>2</sup>). Then

$$C_{110,000}(60,000, 120^\circ, 45^\circ)/C_0(5000, 120^\circ, 45^\circ) = 1 - 919/1273 = 1 - 0.722 = 0.278.$$

It is highly significant and important to note that none of the three equations used to calculate the contrast transmittance involves any photometric property of the object. The contrast transmittance applies, therefore, to *any* object which may appear against the prevailing background and, for this reason, has been specified as the *universal* contrast transmittance. The contrasts, the ratio of which is the universal contrast transmittance, are termed *universal* apparent contrast and *universal* inherent contrast to distinguish them from other forms of contrast, e.g.,  $\rho$  or  $(\rho - 1)/(\rho + 1)$ , which do not share this useful property. It will be shown in Sec. IX that visual object classification techniques are possible only in terms of universal contrast. Throughout this article, the word "contrast" denotes *universal* contrast; all other forms of contrast are specifically identified by name, e.g., ratio contrast  $\rho$  or modulation contrast  $(\rho - 1)/(\rho + 1)$ .

The contrast transmittance nomogram, Fig. 6.4, constructed by Jacqueline I. Gordon, is a device for solving Eq. (6.4) graphically. From this nomogram, one can quickly determine (a) the beam transmittance for a horizontal path of sight from the attenuation length and range, (b) the ratio of path luminance to beam transmittance from the two separate quantities, and (c) the contrast transmittance from this ratio and the inherent background luminance.

### Upward Paths of Sight

The foregoing example concerned a path of sight inclined downward with a zenith angle of 120° and azimuth of 45°. Now let us consider the reciprocal path of sight, the inclined upward path of sight, with a zenith angle of 60° and azimuth of -135°. This would be the path of sight for an observer in the low-flying aircraft looking in the direction of the aircraft

Table 6.12. Pressure Ratios, Pressure at Altitude  $z$  to Pressure at 20,000 ft

Altitude (ft)	Ratio of pressures <sup>a</sup>
20,000	1.000
25,000	0.808
30,000	0.647
40,000	0.404
50,000	0.250
60,000	0.155

<sup>a</sup> Ratios are for pressures given by Minzner *et al.* (1959).

at 60,000 ft (18.3 km). Again, the contrast transmittance can be calculated by Eqs. (6.3), (6.4), or (6.6).

### Example

The beam transmittance of the path of sight as previously determined is 0.700. The inherent background luminance, the product of the 20,000-ft (6.1-km) altitude sky luminance from Table 6.5 and the 60,000-ft (18.3-km) pressure ratio factor from Table 6.12, is 48.8 ft-L (167 cd/m<sup>2</sup>). The apparent background luminance is read directly from Table 6.5 as 580 ft-L (1985 cd/m<sup>2</sup>). The path luminance is the difference between the apparent background luminance and the attenuated inherent background luminance, or is the difference between 580 ft-L and 0.700 × 48.8 ft-L, which is 545.8 ft-L (1870 cd/m<sup>2</sup>). Then the contrast transmittance calculated by Eqs. (6.3), (6.4), and (6.5), respectively, is

$$C_{110,000}(5000, 60^\circ, -135^\circ)/C_0(60,000, 60^\circ, -135^\circ) = (0.700)(48.8)/580 = 0.059,$$

$$C_{110,000}(5000, 60^\circ, -135^\circ)/C_0(60,000, 60^\circ, -135^\circ) = 1/[1 + 545.8/(0.700)(48.8)] = 0.059,$$

$$C_{110,000}(5000, 60^\circ, -135^\circ)/C_0(60,000, 60^\circ, -135^\circ) = 1 - 545.8/580 = 0.059.$$

Inasmuch as the contrast transmittances apply to specific background luminances, the two factors 0.278 and 0.059 calculated in the foregoing examples may, in accordance with Sec. I of this article, be written as

$$0.278_{110,000}(60,000, 120^\circ, 45^\circ) = 0.278 \text{ (path inclined downward),}$$

$$0.059_{110,000}(5000, 60^\circ, -135^\circ) = 0.059 \text{ (path inclined upward).}$$

Note that, although the beam transmittances for the reciprocal paths of sight are identical, the contrast transmittances are not. This is because the path luminances for reciprocal paths of sight may, and usually do, differ greatly.

Material as developed in this section is combined with physiological data of the human eye and other pertinent data, such as search or recognition factors, in the treatment of visibility problems. How this is done is described in another section of this paper.



# DIRECTIONAL REFLECTANCE OF ATMOSPHERIC PATHS OF SIGHT

Seibert Q. Duntley

U. S. Naval Ship Systems Command    Contract NObS-90337    U. S. Air Force Task T-76104  
Air Force Cambridge Research Laboratory

Report No. 69-1    May 1969

## Abstract

The contrast reducing properties of any path of sight inclined downward through the atmosphere can be specified by a single dimensionless number analogous to a reflectance and called the *directional reflectance of the path of sight*  $R^*$ . The contrast transmittance of the path depends solely upon the ratio of the directional path reflectance to the inherent directional reflectance of the background ( $R^*/R_b$ ). Previously published optical atmospheric data derived from in-flight measurements have been used to produce tables of  $R^*$  for two clear-weather conditions. A simple nomograph and numerical examples are included.

## INTRODUCTION

Samples of the data needed for visibility calculations and illustrations of their use are provided in previous papers<sup>1,2,3,4</sup> by the author and his colleagues. These papers include tables of optical atmospheric data for visible light measured from an instrumented aircraft on two typical clear days. Methods for using those data to calculate the contrast transmittance of the atmosphere along any selected path of sight are illustrated by numerical examples<sup>5</sup> using exact equations<sup>6,7,8</sup>. The equations use the ratio of two independent quantities, *path luminance* and *beam transmittance*, to specify the contrast reducing properties of each path. Tables of that ratio could, of course, be made but a more useful descriptor, called the *directional reflectance of the atmospheric path of sight* and denoted by the symbol  $R^*$ , is presented in this paper.

The ratio of  $R^*$  to the inherent directional reflectance of the background  $R_b$  determines the contrast transmittance of the path for any object appearing against that background. Similarly, the ratio of  $R^*$  to the average directional reflectance  $\bar{R}$  of a bar pattern determines the modulation transmittance of the path for that bar pattern. Tables of  $R^*$  for all of the previously published samples of data<sup>1,2,3,4</sup> are given and their use is illustrated.

## CONTRAST REDUCTION BY THE ATMOSPHERE

The reduction of apparent contrast along any path of sight through the atmosphere is discussed in references (1) and (6). The concepts and equations on p. 555 of reference (1) show that the spectral contrast transmittance  $T_s(z, \theta, \phi)$  of a path of sight of length  $r$ , initiating at a background  $b$  and terminating at a receiver which is located at altitude  $z$  and which accepts flux from a direction having zenith angle  $\theta$  and

69-1-1  
D

azimuth  $\phi$  relative to the sun, is

$${}_bT_r(z, \theta, \phi) = \left\{ 1 + \left[ N_r^*(z, \theta, \phi) / {}_bN_o(z, \theta, \phi) T_r(z, \theta, \phi) \right] \right\}^{-1} \quad (1)$$

where  ${}_bN_o(z, \theta, \phi)$  signifies the inherent spectral radiance of the background located at altitude  $z$ , and observed in the direction  $\theta, \phi$  of the path of sight, as shown in Figure 1. The symbols  $N_r^*(z, \theta, \phi)$  and  $T_r(z, \theta, \phi)$  denote, respectively, the spectral path radiance and spectral beam transmittance of the path of sight.

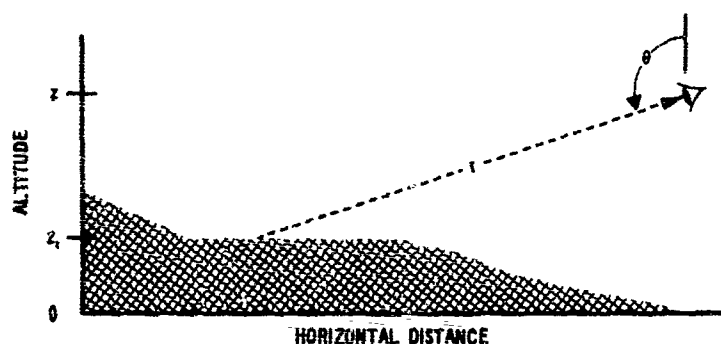


Fig. 1. Illustrating the geometry of a downward inclined path of sight having length  $r$ , zenith angle  $\theta$ , and with the object located at altitude  $z_1$  measured above some datum plane, often mean sea level. The observer is at altitude  $z$ .

In the case of paths of sight which are inclined downward ( $\pi \geq \theta \geq \pi/2$ ) let both numerator and denominator of the term within the square brackets in equation (1) be multiplied by  $\pi/H(z_1, -) T_r(z, \theta, \phi)$ , where  $H(z_1, -)$  is the spectral irradiance on an upward-facing horizontal plane at altitude  $z_1$ . Then equation (1) becomes

$${}_bT_r(z, \theta, \phi) = \left\{ 1 + \left[ \pi N_r^*(z, \theta, \phi) / H(z_1, -) T_r(z, \theta, \phi) \right] / \left[ \pi {}_bN_o(z, \theta, \phi) / H(z_1, -) \right] \right\}^{-1} \quad (2)$$

## DIRECTIONAL REFLECTANCE

The denominator of the second term on the right in eq. (2) can be written  ${}_bN_o(z, \theta, \phi) / [H(z_1, -)/\pi]$ . By established practice<sup>9</sup> this ratio is called the *inherent directional spectral reflectance* of the background; it will be denoted in subsequent equations by the symbol  ${}_bR_o(z, \theta, \phi, \theta', \phi')$  where  $\theta'$  and  $\phi'$  represent, respectively, the zenith angle and the azimuth of the outward normal vector of the reflecting surface.

The factor  $\pi$  is inserted in the definition of directional reflectance in accordance with established practice<sup>9</sup> and to conform with existing bodies of published data, including references (1) and (2), rather

than for any truly fundamental reason. For example, reference (9) states that "the luminance of an imperfectly diffusing surface may be compared with the luminance of a perfectly reflecting, perfectly diffusing surface which is similarly illuminated. The ratio of these luminances is a quantity which frequently differs from luminous reflectance. The corresponding ratio of radiances of surfaces, for homogeneous incident radiant energy and for the same spatial conditions of irradiation and observation, may be called directional spectral reflectance."

Thus, directional spectral reflectance has been defined with reference to the properties of a perfectly reflecting, perfectly diffuse reflector. For a flat surface of this type the total spectral radiant flux reflected per unit of area is found by integration to be  $\pi$  times the radiance. It is the convenient but unnecessary conceptual involvement of a perfectly reflecting, perfectly diffuse reference surface in the definition of directional spectral reflectance that requires the factor  $\pi$  to be inserted in both numerator and denominator of the second term on the right in equation (2). It is an attractive consequence that the directional spectral reflectance of new fallen snow approaches unity whenever such snow approximates a perfectly reflecting, perfectly diffuse reflector.\*†

It is important to note that directional spectral reflectance is a dimensionless ratio which characterizes the reflecting surface in some specified direction of observation and *under a specific lighting condition*.

#### PATH REFLECTANCE

The numerator of the second term on the right in equation (2) has the form of a directional spectral reflectance except for the dimensionless factor  $T_r(z, \theta, \phi)$ . Let the numerator of the second term on the right in equation (2) be symbolized by  $R_r^*(z, \theta, \phi)$  and let it be called the directional spectral reflectance of the path of sight through the atmosphere or, briefly, "*directional spectral path reflectance*." Equation (2) can now be written

$${}_bT_r(z, \theta, \phi) = \left\{ 1 + \left[ R_r^*(z, \theta, \phi) / {}_bR_o(z, \theta, \phi) \right] \right\}^{-1} \quad (3)$$

where, by definition,

$$R_r^*(z, \theta, \phi) \equiv \pi N_r^*(z, \theta, \phi) / H(z) T_r(z, \theta, \phi). \quad (4)$$

\* The directional luminous reflectance of newly fallen snow is ordinarily nearly 1.0 when viewed from any direction unless the incident illumination is nearly grazing incidence. Similarly, the directional reflectance of most matte black surfaces is approximately 0.04. Glossy surfaces may however, have directional reflectances greatly in excess of 1.0 in certain directions. An extreme case of gloss is a perfectly reflecting plane mirror; it may have a directional reflectance of more than 100,000 in the direction in which sunlight is reflected since the solar luminance may exceed  $10^9$  foot lamberts while the illuminance on the mirror produced by the sun and sky is usually less than  $10^4$  lumens per sq. ft.

† If the factor  $\pi$  is not inserted in equation (2) the equally useful but numerically different, nameless, dimensionless ratio of spectral radiance/spectral irradiance appears; in deference to established practice (see reference 9) this ratio should not be called directional spectral reflectance.

## LUMINOUS QUANTITIES

The foregoing discussion and all of the symbols in equations (1) through (4) refer to monochromatic light. The atmospheric optical data in references (1) through (4), however, were measured by means of photoelectric photometers carefully filtered to measure luminance, illuminance, directional luminous reflectance, etc. Under ordinary circumstances equations (1) and (2) are valid approximations for use in visibility calculations if each radiance (N) is replaced by luminance (B) and each irradiance (H) by illuminance (E)<sup>†</sup>. When equations (1) through (4) are used in visibility calculations the symbols  $_bR$ ,  $R^*$ , T, and T must be understood to represent luminous quantities.

## EFFECT OF PATH REFLECTANCE ON CONTRAST TRANSMITTANCE

Contrast transmittance is shown by equation (3) to be a function solely of the ratio of the directional reflectance of the path to the directional reflectance of the background. Ordinarily, path reflectance is affected very little by background and surround properties; it depends chiefly on the atmosphere, its lighting, and the direction of the path of sight. Objects and most non-self-luminous backgrounds have directional reflectances within the rather narrow range 0.8 to 0.04, unless they have prominent gloss. Even glossy surfaces often have directional reflectances within this range except in the direction of specular reflection. Contrast transmittance, however, can vary more widely. To illustrate this, equation (3) has been used to calculate values of contrast transmittance for two background directional reflectances, 0.8 and 0.04, corresponding respectively to a "white" and a "black" background. Decimal values of path reflectance from 0.001 to 100.0 have been assumed. The result is given in Table 1 and Figure 2.

Table 1. Contrast Transmittance

Path Reflectance	Black Background $_bR_o = 0.04$	White Background $_bR_o = 0.80$
0	1.	1.
0.001	0.975	1.
0.01	0.800	0.987
0.1	0.236	0.889
1.0	0.0385	0.445
10.0	0.00398	0.0741
100.0	0.00040	0.00794

<sup>†</sup>The luminance (B) is expressed in candles per unit of area; if lambert units are used, the  $\pi$  is incorporated in the unit and should not appear explicitly in the equations.

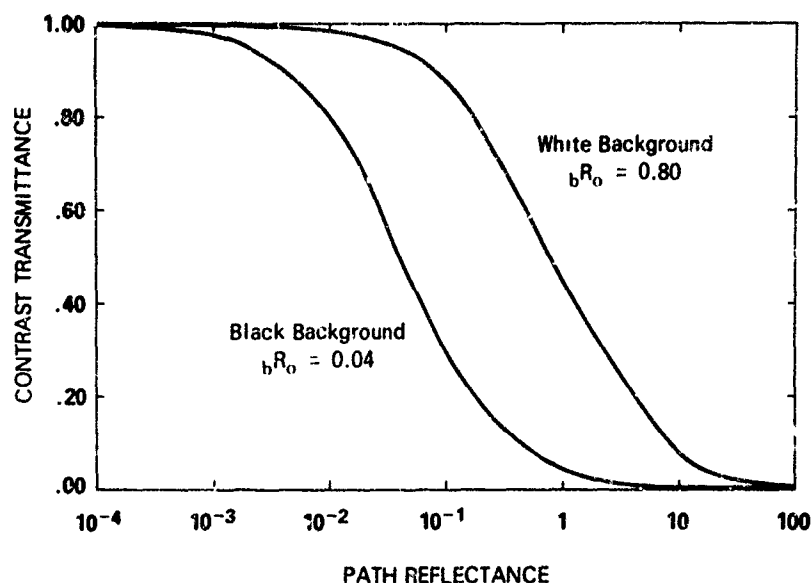


Fig. 2

Contrast transmittance is always 0.50 whenever the directional reflectances of path and background are equal. When the path reflectance ( $R^*$ ) is dominant, contrast transmittance is low, but when background reflectance ( $bR_o$ ) dominates, contrast transmittance is high. For a given path reflectance, contrast transmittance improves as background reflectance increases; this gain may, however, be at least partially offset by a concurrent decrease in inherent contrast.<sup>§</sup>

#### NOMOGRAM

A conceptually valuable graphical representation of the effect on contrast transmittance of the ratio ( $R^* / bR_o$ ) of the path reflectance to background reflectance is provided by Figure 3. It is a nomogram which represents equation (3) and consists merely of a diagonal straight line drawn across a sheet of 2-cycle by 2-cycle log-log graph paper. The path to background reflectance ratio is entered on the axis of abscissa and contrast transmittance is read out on the axis of ordinate.

It will be noted that when  $R^* = bR_o$ , the contrast transmittance is 0.50. Small values of the ratio  $R^* / bR_o$  yield high values of contrast transmittance, and vice versa.

#### PATH-TO-BACKGROUND CONTRAST

Directional path reflectance and directional background reflectance can be combined in the form of a contrast and denoted by  ${}_bC_p^*(z, \theta, \phi)$ , where

$${}_bC_p^*(z, \theta, \phi) = \frac{R_p^*(z, \theta, \phi)}{bR_o(z, \theta, \phi)} - 1 \quad (5)$$

<sup>§</sup> The contrast transmittance of any path of sight is the same for every object which may appear against the specified background.

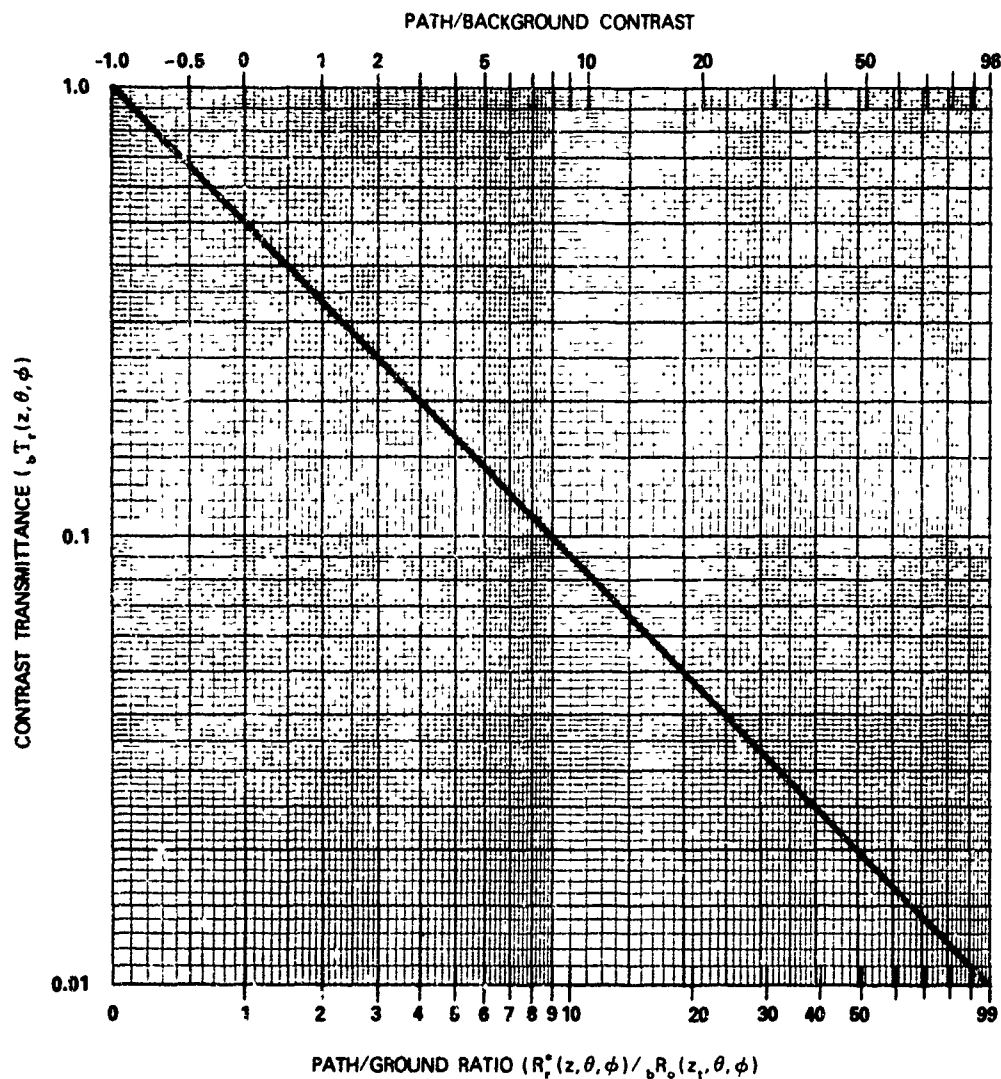


Fig. 3

After combining with equation (3),

$${}_bT_r(z, \theta, \phi) = \left[ 2 + {}_bC_r^*(z, \theta, \phi) \right]^{-1}. \quad (6)$$

When the background directional reflectance is greater than the directional reflectance of the path, the path/background contrast is negative; the contrast transmittance then exceeds 0.5. No particular advantage or convenience seems likely to arise from this formulation. Nevertheless, a scale of path/background contrast has been added along the upper boundary of Figure 3.

## PATH REFLECTANCE FOR A MEDIUM SOLAR ALTITUDE

Directional luminous path reflectance has been calculated for each of the path luminances given in Tables 6.7 through 6.11 in Ref. 1. The results are presented in this report as Tables 2 through 6.

The original data were obtained on 28 February 1956 during a flight (No. 74) of an instrumented B-29 aircraft at Eglin Air Force Base, Florida. On that occasion the zenith angle of the sun was  $41.5^\circ$  and the vertical luminous beam transmittance from space to earth  $T_\infty(0,0)$  was 0.576.<sup>⑥</sup> The nearly uniform terrain beneath the path of flight had small pine trees, uniformly spaced.

Directional reflectance data for various backgrounds which are appropriate for use with the path reflectances in Tables 2 through 6 can be found in Sect. 3 of Ref. 1 and in Ref. 3.

Values of illuminance at ground level are given in both English and metric units for Flight 74 in Table 7A. The ratio of the upwelling to the total downwelling illuminance is 0.034 for the horizontal illuminances. This ratio is sometimes called albedo.

Table 7A gives downwelling scalar (non-directional) illuminance at ground level. The scalar albedo just above the surface is 0.064. Scalar albedo is one of the determinants of the path luminance and downwelling illuminance; see reference 4. It is usually larger than the horizontal surface albedo since the higher directional reflectances at the near horizontal paths of sight are given more weight in the integration.

Table 2. Downward luminous path reflectance  $R_p^*(z, \theta, 0)$  in the azimuth of the sun, for a medium solar zenith angle ( $41.5^\circ$ )

Altitude (z) (feet)	Zenith angle $\theta$ (paths of sight inclined downward)							
	$180^\circ$	$165^\circ$	$150^\circ$	$135^\circ$	$120^\circ$	$105^\circ$	$100^\circ$	$95^\circ$
0								
1,000	0.0109	0.0109	0.0148	0.0163	0.0234	0.0477	0.0959	0.258
2,000	0.0272	0.0270	0.0330	0.0358	0.0524	0.160	0.361	1.66
3,000	0.0432	0.0464	0.0538	0.0598	0.0894	0.348	0.889	6.51
4,000	0.0549	0.0617	0.0739	0.0826	0.122	0.534	1.40	12.6
5,000	0.0633	0.0683	0.0805	0.0945	0.141	0.642	1.68	16.4
6,000	0.0702	0.0736	0.0878	0.107	0.162	0.724	1.86	18.6
7,000	0.0760	0.0804	0.0968	0.122	0.190	0.814	2.03	20.9
8,000	0.0832	0.0905	0.108	0.141	0.237	0.913	2.18	24.0
9,000	0.0901	0.0966	0.116	0.152	0.262	0.983	2.33	27.1
10,000	0.0962	0.100	0.121	0.158	0.274	1.04	2.51	30.5
15,000	0.124	0.119	0.146	0.186	0.322	1.29	3.38	48.7
20,000	0.158	0.136	0.170	0.212	0.367	1.55	4.31	69.0
25,000	0.190	0.152	0.194	0.237	0.412	1.82	5.26	
30,000	0.217	0.165	0.214	0.259	0.450	2.04	6.11	
40,000	0.259	0.186	0.246	0.292	0.515	2.44	7.58	
50,000	0.287	0.199	0.267	0.314	0.550	2.68	8.66	
60,000	0.304	0.208	0.280	0.328	0.576	2.85	9.34	

<sup>⑥</sup>The optical thickness  $t$  of the atmosphere at ground level, derived from measured and extrapolated photopic attenuation lengths by methods described in reference (1), was 0.551. The optical thickness  $t$  above any altitude  $z$  is related to the vertical beam transmittance  $T_\infty(z,0)$  from space to that altitude by the relation  $T_\infty(z,0) = e^{-t}$ .

**Table 3. Downward luminous path reflectance  $R_p^*(z, \theta, 45)$  at  $45^\circ$  from the azimuth of the sun, for a medium solar angle ( $41.5^\circ$ )**

Altitude (z) (feet)	Zenith angle $\theta$ (paths of sight inclined downward)						
	165°	150°	135°	120°	105°	100°	95°
0							
1,000	0.0154	0.0186	0.0202	0.0244	0.0554	0.0865	0.223
2,000	0.0325	0.0383	0.0422	0.0598	0.164	0.344	1.40
3,000	0.0500	0.0593	0.0664	0.0994	0.329	0.746	5.54
4,000	0.0636	0.0764	0.0861	0.129	0.474	1.28	10.4
5,000	0.0726	0.0848	0.101	0.152	0.564	1.53	14.1
6,000	0.0792	0.0908	0.114	0.168	0.632	1.70	16.4
7,000	0.0836	0.0952	0.124	0.183	0.660	1.82	18.2
8,000	0.0927	0.108	0.138	0.214	0.722	1.98	20.2
9,000	0.0999	0.117	0.149	0.231	0.773	2.14	22.9
10,000	0.105	0.122	0.155	0.248	0.827	2.31	25.7
15,000	0.129	0.148	0.185	0.295	1.09	3.04	40.5
20,000	0.157	0.177	0.218	0.351	1.38	3.83	58.0
25,000	0.183	0.203	0.248	0.404	1.65	4.67	
30,000	0.205	0.226	0.274	0.450	1.90	5.41	
40,000	0.239	0.262	0.314	0.524	2.30	6.71	
50,000	0.261	0.285	0.340	0.569	2.58	7.64	
60,000	0.275	0.299	0.358	0.600	2.77	8.22	

**Table 4. Downward luminous path reflectance  $R_p^*(z, \theta, 90)$ , at  $90^\circ$  from the azimuth of the sun, for a medium solar angle ( $41.5^\circ$ )**

Altitude (z) (feet)	Zenith angle $\theta$ (paths of sight inclined downward)						
	165°	150°	135°	120°	105°	100°	95°
0							
1,000	0.0125	0.0141	0.0152	0.0208	0.0434	0.0865	0.204
2,000	0.0282	0.0326	0.0382	0.0554	0.135	0.279	1.21
3,000	0.0443	0.0532	0.0621	0.0976	0.278	0.643	4.60
4,000	0.0567	0.0692	0.0807	0.133	0.409	1.01	8.77
5,000	0.0651	0.0775	0.0942	0.158	0.491	1.26	11.6
6,000	0.0716	0.0837	0.104	0.176	0.548	1.46	13.2
7,000	0.0789	0.0883	0.114	0.192	0.608	1.61	14.5
8,000	0.0868	0.0989	0.125	0.205	0.659	1.70	16.4
9,000	0.0937	0.107	0.133	0.217	0.696	1.83	18.1
10,000	0.0988	0.112	0.140	0.229	0.752	1.98	20.7
15,000	0.125	0.141	0.174	0.289	0.991	2.70	33.7
20,000	0.155	0.171	0.212	0.358	1.22	3.44	49.7
25,000	0.184	0.200	0.246	0.423	1.47	4.23	
30,000	0.208	0.224	0.276	0.481	1.68	4.92	
40,000	0.246	0.261	0.322	0.570	2.04	6.15	
50,000	0.270	0.285	0.352	0.629	2.28	7.02	
60,000	0.285	0.300	0.372	0.669	2.45	7.57	



Table 5. Downward luminous path reflectance  $R_p^*(z, \theta, 135)$ , at  $135^\circ$  from the azimuth of the sun, for a medium solar zenith angle ( $41.5^\circ$ )

Altitude (z) (feet)	Zenith angle $\theta$ (paths of sight inclined downward)						
	$165^\circ$	$150^\circ$	$135^\circ$	$120^\circ$	$105^\circ$	$100^\circ$	$95^\circ$
0							
1,000	0.0168	0.0217	0.0252	0.0261	0.0719	0.117	0.238
2,000	0.0329	0.0433	0.0529	0.0691	0.172	0.336	1.38
3,000	0.0495	0.0654	0.0799	0.116	0.322	0.724	5.12
4,000	0.0617	0.0808	0.102	0.152	0.448	1.06	9.72
5,000	0.0710	0.0907	0.115	0.179	0.531	1.30	12.6
6,000	0.0789	0.0982	0.123	0.198	0.598	1.46	13.7
7,000	0.0846	0.103	0.131	0.213	0.646	1.61	15.5
8,000	0.0900	0.110	0.141	0.223	0.736	1.84	18.0
9,000	0.0984	0.120	0.150	0.234	0.824	2.05	21.2
10,000	0.105	0.128	0.163	0.254	0.879	2.26	24.3
15,000	0.138	0.170	0.211	0.336	1.15	3.15	40.2
20,000	0.169	0.204	0.270	0.408	1.38	3.88	56.5
25,000	0.198	0.235	0.324	0.477	1.61	4.62	
30,000	0.222	0.262	0.376	0.538	1.80	5.32	
40,000	0.260	0.305	0.448	0.631	2.14	6.49	
50,000	0.285	0.332	0.497	0.689	2.35	7.33	
60,000	0.301	0.349	0.529	0.727	2.50	7.86	

Table 6. Downward luminous path reflectance  $R_p^*(z, \theta, 180)$ , at  $180^\circ$  from the azimuth of the sun, for a medium solar zenith angle ( $41.5^\circ$ )

Altitude (z) (feet)	Zenith angle $\theta$ (paths of sight inclined downward)						
	$165^\circ$	$150^\circ$	$135^\circ$	$120^\circ$	$105^\circ$	$100^\circ$	$95^\circ$
0							
1,000	0.0118	0.0170	0.0195	0.0275	0.0488	0.117	0.296
2,000	0.0282	0.0404	0.0498	0.0672	0.172	0.379	1.66
3,000	0.0450	0.0649	0.0829	0.115	0.351	0.833	5.91
4,000	0.0574	0.0846	0.110	0.149	0.501	1.21	10.5
5,000	0.0642	0.0922	0.125	0.175	0.572	1.46	13.4
6,000	0.0696	0.0985	0.136	0.198	0.622	1.64	15.2
7,000	0.0777	0.107	0.145	0.216	0.681	1.88	16.4
8,000	0.0957	0.117	0.153	0.233	0.785	2.07	19.9
9,000	0.112	0.127	0.160	0.244	0.882	2.22	22.8
10,000	0.119	0.134	0.170	0.257	0.940	2.40	25.7
15,000	0.150	0.174	0.220	0.319	1.21	3.33	42.2
20,000	0.186	0.223	0.274	0.387	1.52	4.29	60.7
25,000	0.222	0.271	0.324	0.452	1.84	5.30	
30,000	0.253	0.314	0.366	0.511	2.12	6.27	
40,000	0.299	0.378	0.434	0.603	2.58	7.86	
50,000	0.330	0.419	0.476	0.660	2.89	9.03	
60,000	0.348	0.445	0.504	0.698	3.09	9.77	

0000000000  
X  
D

**Table 7A. Measured illuminance on a horizontal plane at ground level during Flight 74  
(Solar zenith angle = 41.5°)**

	Illuminance	
	lumens/ft <sup>2</sup>	lumens/meter <sup>2</sup>
Illuminance from the sky	1 400	15 100
Illuminance from the sun	4 540	48 900
Total downwelling illuminance	5 940	64 000
Upwelling illuminance	203	2 180

**Table 7B. Scalar illuminance at ground level during Flight 74 (Solar zenith angle = 41.5°)**

	Illuminance	
	lumens/ft <sup>2</sup>	lumens/meter <sup>2</sup>
Illuminance from the sky	3 450	37 100
Illuminance from the sun	6 060	65 200
Total downwelling illuminance	9 510	102 300
Upwelling illuminance	612	6 580
<b>TOTAL</b>	<b>10 122</b>	<b>108 880</b>

#### **PATH REFLECTANCE FOR A LOW SUN**

The path luminances for a low sun given in Tables V through IX in Ref. 2 have been used to compute corresponding directional luminous path reflectances. These are presented in Tables 8 through 12.

The photometric measurements were made during a flight (No. 105) of an instrumented B-29 aircraft over the Atlantic Ocean east of Patrick Air Force Base, Florida on 20 April 1957. The zenith angle of the sun for the data obtained at lowest altitude was 77.3°. The optical thickness at sea level was 0.255 and the luminous vertical beam transmittance through the atmosphere was 0.775. There was a 10 knot (5m/sec) wind. The day was warm with some scattered clouds; the sun was virtually unobscured.

Directional reflectances for backgrounds other than ocean water which are appropriate for use with these path reflectances can be found in Ref. 2.

Sea level illuminance values are given in Table 13. The horizontal surface albedo was 0.055, and the scalar albedo was 0.064.

Table 8. Downward luminous path reflectance  $R_p^*(z, \theta, 0)$  in the azimuth of the sun, for a low sun (maximum solar zenith angle  $77.3^\circ$ )

Altitude (z) (feet)	Zenith angle $\theta$ (paths of sight inclined downward)						
	180°	165°	150°	135°	120°	105°	100° 95°
0							
1,000	0.00143	0.00135	0.00280	0.00780	0.0247		0.0593 0.0994
2,000	0.00341	0.00337	0.00590	0.0182	0.0564		0.130 0.221
3,000	0.00561	0.00575	0.0100	0.0302	0.0924		0.216 0.378
4,000	0.00796	0.00853	0.0145	0.0431	0.131		0.315 0.560
5,000	0.0104	0.0121	0.0196	0.0575	0.178		0.422 0.772
6,000	0.0137	0.0152	0.0244	0.0731	0.228		0.517 0.956
7,000	0.0170	0.0190	0.0300	0.0907	0.282		0.633 1.18
8,000	0.0208	0.0240	0.0362	0.110	0.342		0.762 1.42
9,000	0.0242	0.0291	0.0438	0.129	0.406		0.908 1.75
10,000	0.0283	0.0349	0.0521	0.150	0.475		1.07 2.07
15,000	0.0489	0.0626	0.0969	0.243	0.786		2.20 4.63
20,000	0.0598	0.0927	0.147	0.345	1.11		3.64 8.57
25,000	0.0700	0.122	0.194	0.444	1.43		5.18
30,000	0.0788	0.147	0.236	0.530	1.71		6.61
40,000	0.0930	0.186	0.301	0.668	2.17		9.14
50,000	0.102	0.212	0.346	0.761	2.47		11.1
60,000	0.109	0.230	0.374	0.825	2.67		12.4

Table 9. Downward luminous path reflectance  $R_p^*(z, \theta, 45^\circ)$ , at  $45^\circ$  from the azimuth of the sun, for a low sun (maximum solar zenith angle  $77.3^\circ$ )

Altitude (z) (feet)	Zenith angle $\theta$ (paths of sight inclined downward)						
	165°	150°	135°	120°	105°	100°	95°
0							
1,000	0.00147	0.00186	0.00303	0.00449	0.0123	0.0177	0.0500
2,000	0.00306	0.00424	0.00576	0.00897	0.0271	0.0395	0.102
3,000	0.00530	0.00668	0.00918	0.0149	0.0439	0.0656	0.167
4,000	0.00773	0.00946	0.0126	0.0208	0.0636	0.0955	0.244
5,000	0.0104	0.0125	0.0164	0.0274	0.0856	0.128	0.330
6,000	0.0135	0.0154	0.0211	0.0333	0.106	0.159	0.403
7,000	0.0168	0.0183	0.0256	0.0393	0.131	0.196	0.491
8,000	0.0203	0.0221	0.0320	0.0474	0.158	0.240	0.589
9,000	0.0244	0.0261	0.0386	0.0564	0.191	0.287	0.708
10,000	0.0288	0.0303	0.0451	0.0688	0.225	0.342	0.843
15,000	0.0543	0.0560	0.0786	0.143	0.459	0.768	2.18
20,000	0.0704	0.0840	0.109	0.208	0.769	1.37	4.47
25,000	0.0856	0.111	0.137	0.271	1.09	2.02	
30,000	0.0983	0.134	0.162	0.326	1.38	2.63	
40,000	0.120	0.171	0.202	0.416	1.86	3.71	
50,000	0.133	0.196	0.229	0.478	2.20	4.53	
60,000	0.142	0.212	0.247	0.517	2.43	5.07	



## appendix D

		Zenith angle $\theta$ (paths of sight inclined downward)						
Altitude (z)	(feet)	165°	150°	135°	120°	105°	100°	95°
0								
1,000		0.00186	0.00208	0.00270	0.00507	0.0126	0.0236	0.0369
2,000		0.00408	0.00439	0.00555	0.0105	0.0265	0.0516	0.0856
3,000		0.00635	0.00705	0.00881	0.0162	0.0438	0.0865	0.152
4,000		0.00865	0.00972	0.0124	0.0218	0.0634	0.128	0.238
5,000		0.0112	0.0128	0.0163	0.0292	0.0856	0.179	0.342
6,000		0.0140	0.0159	0.0202	0.0369	0.108	0.229	0.448
7,000		0.0174	0.0198	0.0250	0.0454	0.136	0.288	0.587
8,000		0.0206	0.0246	0.0307	0.0562	0.168	0.354	0.759
9,000		0.0246	0.0298	0.0372	0.0671	0.205	0.431	0.974
10,000		0.0288	0.0360	0.0470	0.0819	0.246	0.509	1.21
15,000		0.0523	0.0693	0.104	0.200	0.532	1.00	2.78
20,000		0.0697	0.102	0.164	0.344	0.929	1.65	5.18
25,000		0.0925	0.133	0.220	0.485	1.34	2.34	
30,000		0.112	0.160	0.270	0.608	1.70	2.99	
40,000		0.143	0.203	0.349	0.808	2.32	4.12	
50,000		0.164	0.232	0.403	0.942	2.76	5.01	
60,000		0.177	0.250	0.437	1.04	3.06	5.58	

**Table 13. Sea level illuminances for Flight 105 (Low Sun)**

	Illuminance	
	lumens/ft <sup>2</sup>	lumens/m <sup>2</sup>
Illuminance on horizontal surface		
Sky	838	9020
Sun	872	9380
Total downwelling	1710	18 400
Upwelling	93.3	1000
Scalar illuminance		
Sky	1940	20 900
Sun	3970	42 700
Downwelling	5910	63 600
Upwelling	375	4000
<b>TOTAL</b>	<b>6285</b>	<b>67 640</b>

## ILLUSTRATIVE EXAMPLE

Reference 5 gives numerical examples of several procedures for calculating the contrast transmittance of a typical inclined path of sight from optical atmospheric data secured during Flight 74 of the instrumented B-29 aircraft. Tables 2 through 7 of this report relate to the same body of basic data. The use of these tables to calculate the contrast transmittance of the same path of sight is illustrated in this section.

Under the heading "EXAMPLE" on page 578 in reference 5 the problem is stated, in part, as follows: "Let it be assumed that the low flying aircraft appears against a uniform ground cover of small, fairly closely spaced pine trees on flat terrain. This was the type of ground cover over which Flight 74 took place. Table 3.2 gives the directional luminous reflectance of this ground cover as seen from the assumed direction ( $\theta = 120^\circ$ ;  $\phi = 45^\circ$ ) as 0.021." The low-flying aircraft in question was at an altitude of 5000 feet and the observer was at 60 000 feet. The downward inclined path of sight had a zenith angle of  $120^\circ$  and an azimuth  $45^\circ$  from the sun. The calculations given in reference 5 led to a contrast transmittance of 0.278 for the path of sight from the low-flying aircraft (5000 feet) to the observer (60 000 feet). The same result can be obtained more easily by means of equation 3 and Table 3 of this report in the following manner.

First, calculate the contrast transmittance of the path of sight from the ground to altitude 5000 feet.

From the preceding paragraph  ${}_bR_o(0, 120^\circ, 45^\circ) = 0.021$

From Table 3:  $R_{10\ 000}^*(5000, 120^\circ, 45^\circ) = 0.152$

From Equation 3:  ${}_bT_{10\ 000}(5000, 120^\circ, 45^\circ) = [1 + (0.152/0.021)]^{-1} = 0.1214$ .

Second, calculate the contrast transmittance of the path of sight from the ground to altitude 60 000 feet.

From Table 3:  $R_{120\ 000}^*(60\ 000, 120^\circ, 45^\circ) = 0.600$

From Equation 3:  ${}_bT_{120\ 000}(60\ 000, 120^\circ, 45^\circ) = [1 + 0.600/0.021]^{-1} = 0.0338$

Third, obtain the contrast transmittance of the path of sight from altitude 5000 feet to altitude 60 000 feet by dividing the contrast transmittance of the portion of the path extending from the ground to altitude 5000 feet by the contrast transmittance of the entire path.

Thus:  ${}_bT_{110\ 000}(60\ 000, 120^\circ, 45^\circ) = 0.0338/0.1214 = 0.278$ .

Alternatively, the same results can be obtained by means of the nomograph (Fig. 3).

## REFERENCES

1. S. Q. Duntley, J. I. Gordon, J. H. Taylor, Carrol T. White, A. R. Boileau, J. E. Tyler, R. W. Austin, and J. L. Harris, "Visibility," *Applied Optics*, 3, 549-598 (1964).
2. A. R. Boileau and J. I. Gordon, "Atmospheric Properties and Reflectances of Ocean Water and Other Surfaces for a Low Sun," *Applied Optics* 5, 803-813 (1966).
3. J. I. Gordon and P. V. Church, "Sky Luminances and the Directional Luminous Reflectances of Objects and Backgrounds for a Moderately High Sun," *Applied Optics* 5, 793-801 (1966).

4. J. I. Gordon, "A Model for a Clear Atmosphere," J. Opt. Soc. Am. **59**, No. 1, 14-18 (1969).
5. A. R. Boileau, "Atmospheric Properties," Applied Optics **3**, 570-581 (1964).
6. S. Q. Duntley, A. R. Boileau, and R. W. Preisendorfer, "Image Transmission by the Troposphere," J. Opt. Soc. Am. **47**, 499-506 (1957).
7. See Eq. 2.3, S. Q. Duntley, Applied Optics **3**, 554 (1964).
8. The equations in References 1 and 6 do not depend upon any form of atmospheric model. They are rigorous for monochromatic light and are ordinarily excellent for engineering use with photopic data.
9. Colorimetry Committee of the Optical Society of America, "The Science of Color," (Thomas Y. Crowell Co., New York (1953) p. 223.

## Model for a Clear Atmosphere\*

JACQUELINE I. GORDON

Visibility Laboratory, Scripps Institution of Oceanography, University of California  
at San Diego, San Diego, California 92152

(Received 19 June 1968)

A model of a clear atmosphere is presented based upon two assumptions: (1) the point-function equilibrium radiance for a given path of sight does not change with altitude; (2) there is no absorption. As a result of these assumptions, the equation of transfer can be integrated. The path radiance for any slant path becomes a function of the equilibrium radiance and the beam transmittance of that path. In addition, the equilibrium radiance is a function of the scalar irradiance from the sun, sky, and earth and the proportional directional scattering coefficient for ground level. Sky radiances, and path radiances through the atmosphere for both upward and downward paths are determined by four parameters; the proportional directional scattering function for ground level, the total vertical beam transmittance of the atmosphere, the scalar albedo, and the solar zenith angle.

There is evidence that the real atmosphere does on some days conform to the above two assumptions to a useful extent for the visible portion of the spectrum.

INDEX HEADINGS: Atmospheric optics; Radiance; Sun; Scattering; Transmittance.

A MODEL of a clear atmosphere for use in the visible region of the spectrum is based upon two assumptions.

(1) The point-function equilibrium radiance for a given path of sight does not change with altitude. Equilibrium radiance is defined as follows. For each segment of every path of sight in any lighted atmosphere there is an equilibrium radiance that will be transmitted unchanged because the loss (attenuation of image-forming light) is exactly counterbalanced by the gain due to the scattering of sunlight and skylight toward the sensor. The equilibrium radiance is a point function of position and direction, which in any real atmosphere may vary from point to point throughout a path of sight. In the model, we are assuming it to be invariant throughout a path of sight.

(2) Absorption is negligible. With only the first assumption it becomes possible to integrate the equation of transfer for the general case of the slant path.

### INTEGRATION OF THE EQUATION OF TRANSFER

The method of integration is similar to the one given by Duntley for slant paths<sup>1</sup> and for the horizontal path,<sup>2</sup> and repeated by Middleton.<sup>3</sup> The difference lies in integrating to get transmittance rather than  $\bar{R}$ . It is not necessary to assume an optical standard atmosphere but merely one in which the equilibrium radiance,  $N_q(z, \theta, \phi)$ , does not change with altitude,

$$N_q(0, \theta, \phi) = N_q(z, \theta, \phi). \quad (1)$$

The parenthetical expression denotes the altitude  $z$ , of

\*Work has been supported under NASA grant NGR-05-009-059.

<sup>1</sup>S. Q. Duntley, J. Opt. Soc. Am. 38, 181 (1948).

<sup>2</sup>S. Q. Duntley, *Visibility Studies and Some Applications in the Field of Camouflage*. Summary Tech. Rept. of Div. 16, NDRC (Columbia University Press, New York, 1946), Vol. 2, p. 20.

<sup>3</sup>W. E. K. Middleton, *Vision Through the Atmosphere* (University of Toronto Press, Canada, 1952), p. 64-68.

the point-function equilibrium radiance, and the zenith angle  $\theta$ , and azimuth from sun  $\phi$ , of the path of sight.

The starting point is the equation of transfer<sup>4</sup> which is applicable to all real atmospheres,

$$\Delta N(z, \theta, \phi) / \Delta z \sec \theta = N_q(z, \theta, \phi) - [N(z, \theta, \phi) / L(z)]. \quad (2)$$

The equation of transfer expresses the change of radiance that occurs in a small segment of the path of sight.  $\Delta N(z, \theta, \phi)$  is the difference between the input and output radiance for the segment. The segment length is  $\Delta z \sec \theta$ . The gain term is the path function,  $N_q(z, \theta, \phi)$ . The loss term is the radiance  $N(z, \theta, \phi)$  divided by the attenuation length,  $L(z)$ . Equation (2) can be rewritten

$$\Delta N(z, \theta, \phi) = [N_q(z, \theta, \phi)L(z) - N(z, \theta, \phi)] \times \sec \theta \Delta z / L(z). \quad (3)$$

From the equation of transfer and the definition of equilibrium radiance [Ref. 4, Eq. (11)]

$$N_q(z, \theta, \phi) = N_q(z, \theta, \phi)L(z). \quad (4)$$

Now, substituting Eqs. (4) and (1) into Eq. (3), we find

$$\Delta N(z, \theta, \phi) = [N_q(0, \theta, \phi) - N_q(z, \theta, \phi)] \sec \theta \Delta z / L(z), \quad (5)$$

or

$$\Delta N(z, \theta, \phi) / [N_q(z, \theta, \phi) - N_q(0, \theta, \phi)] = -\sec \theta \Delta z / L(z). \quad (6)$$

Both sides of the equation can be integrated after passing to the limiting case,  $\lim(\Delta z \rightarrow 0) = dz$ . Integrating both sides, the first between the limits of the inherent radiance  $N_0$  at altitude  $z$  and the apparent radiance  $N_r$ , and the second side between the beginning and end of path length  $r$ , we find

$$\int_{N_0}^{N_r} \frac{dN(z, \theta, \phi)}{N(z, \theta, \phi) - N_q(0, \theta, \phi)} = - \int_0^r \frac{\sec \theta}{L(z)} dz. \quad (7)$$

<sup>4</sup>S. Q. Duntley, A. R. Boileau, and R. W. Preisendorfer, J. Opt. Soc. Am. 47, 501 (1957), Eq. (10).



The results of the integration are

$$\ln \left[ \frac{N_r(z, \theta, \phi) - N_q(0, \theta, \phi)}{N_0(z, \theta, \phi) - N_q(0, \theta, \phi)} \right] = \ln T_r(z, \theta), \quad (8)$$

or

$$\frac{N_r(z, \theta, \phi) - N_q(0, \theta, \phi)}{N_0(z, \theta, \phi) - N_q(0, \theta, \phi)} = T_r(z, \theta), \quad (9)$$

where  $T_r(z, \theta)$  is the beam transmittance for the path of sight of path length  $r$ . Rearranging, we find

$$N_r(z, \theta, \phi) = N_0(z, \theta, \phi) T_r(z, \theta) + N_q(0, \theta, \phi) [1 - T_r(z, \theta)]. \quad (10)$$

The second term in Eq. (10) is the path radiance,  $N_r^*(z, \theta, \phi)$ ,

$$N_r^*(z, \theta, \phi) = N_q(0, \theta, \phi) [1 - T_r(z, \theta)]. \quad (11)$$

Thus in this model atmosphere, the sky radiance and the atmospheric beam transmittance,  $T_\infty(0, \theta)$ , (such as is obtained by a solar transmissometer) can yield a measure of the equilibrium radiance for all upward paths of sight. The sky radiance is the path radiance,  $N_\infty^*(0, \theta, \phi)$ . Substituting into Eq. (11) and rearranging, we find

$$N_q(0, \theta, \phi) = N_\infty^*(0, \theta, \phi) / [1 - T_\infty(0, \theta)]. \quad (12)$$

Although the equations used herein are rigorously true only for monochromatic radiances, they may be used as a reasonable engineering approximation for sensors with a broad pass band in the visible portion of the spectrum. When the sensor has been carefully corrected by means of absorption filters to measure luminous quantities, the equations may be written with the symbol  $N$  replaced by  $B$ , denoting luminance.

Measurements made in real atmospheres for broad pass bands show that the equilibrium radiance computed from sky radiance by means of Eq. (12) or computed from path radiances for shorter upward paths<sup>5</sup> from Eq. (11), is almost solely a function of the angle from the sun,  $\beta$ , of the path of sight. An example is given in Fig. 1 of equilibrium luminances computed from measured sky luminances. This experimental finding makes possible a different and useful expression for equilibrium radiance; it is derived in the following section.

#### DERIVATION OF THE EQUILIBRIUM RADIANCE AS A FUNCTION OF THE SCATTERING LOBE

The derivation of the equilibrium radiance as a function of the scattering lobe is similar to that given by Hulburt<sup>6</sup> for the horizontal case but has been

<sup>5</sup> The path radiance for the upward path between altitude  $z_1$  and  $z$  is found from the experimental data by use of the relation  $N_r^*(z, \theta, \phi) = N_\infty^*(z, \theta, \phi) - N_\infty^*(z_1, \theta, \phi) T_r(z, \theta)$ . For upward-looking paths of sight  $N_\infty^*(z, \theta, \phi)$  is the sky radiance at altitude  $z$ .

<sup>6</sup> E. O. Hulburt, J. Opt. Soc. Am. 31, 474 (1941).

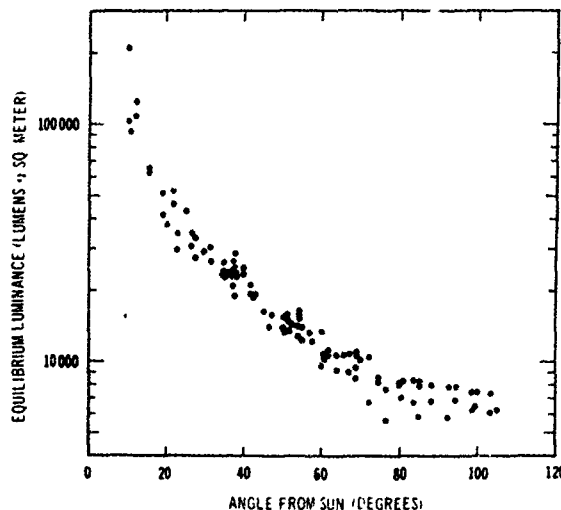


FIG. 1. Equilibrium luminance for many upward-looking paths of sight initiating at an altitude of 6100 m (20 000 ft) and terminating at an altitude of 305 m (1000 ft). Each point plotted in Fig. 1 represents the equilibrium luminance of a different path of sight; all azimuths and zenith angles from 0° to 85° are represented. The data were obtained by A. R. Boileau on Flight 112 of an instrumented B-29 USAF aircraft assigned to the Visibility Laboratory. The flight took place on 16 May 1957 near Eglin Air Force Base, Florida. The measured beam transmittance for the vertical path of sight between altitudes 6100 m and 305 m was 0.897. The solar zenith angle was 25°. These data illustrate that equilibrium luminance depends on angle from the sun but not appreciably upon zenith angle  $\theta$  or azimuth angle  $\phi$ .

extended to equilibrium radiance for all paths of sight. It begins with the definition of path function,

$$N_r(z, \theta, \phi) = N_r(z, \theta, 0) \sigma(z, \beta) d\Omega + \int_{4\pi} N(z, \theta', \phi') \sigma(z, \beta') d\Omega. \quad (13)$$

In the first term, the apparent sun radiance is  $N_r(z, \theta, 0)$ , the directional scattering coefficient at angle  $\beta$  from the sun is  $\sigma(z, \beta)$ , and the angular subtense of the sun is  $d\Omega$ . The second term is the contribution to the path function of the sky and earth radiances,  $N(z, \theta', \phi')$  over the  $4\pi$  solid angle;  $\beta'$  in this case is the angle between the sky (or earth) radiance and the path of sight. The sun radiance times its angular subtense is equivalent to the solar scalar irradiance,

$$h_s(z) = N_r(z, \theta, 0) d\Omega_s. \quad (14)$$

A scalar irradiance is nondirectional, hence its name. Since it has been assumed that there is no absorption,

$$L(z) = 1/s(z), \quad (15)$$

where  $s(z)$  is the total scattering coefficient. Using Eq. (4) and Eq. (15), we can rewrite Eq. (13) in terms of the equilibrium radiance and the directional scattering coefficient divided by the total scattering coefficient,  $\sigma(z, \beta)/s(z)$ , (which will henceforth be called the pro-

portional directional scattering coefficient),

$$N_q(z, \theta, \phi) = h_s(z) \frac{\sigma(z, \beta)}{s(z)} + \int_{4\pi} N(z, \theta', \phi') \frac{\sigma(z, \beta')}{s(z)} d\Omega. \quad (16)$$

Since, as illustrated by Fig. 1,  $N_q(z, \theta, \phi)$  in a clear, real atmosphere is primarily a function of angle from the sun,  $\beta$ , of the path of sight, the effect of directionality in the integral in the second term is small, and an average radiance,  $\bar{N}(z)$ , can be assumed,

$$N_q(z, \theta, \phi) = h_s(z) \frac{\sigma(z, \beta)}{s(z)} + \bar{N}(z) \int_{4\pi} \frac{\sigma(z, \beta')}{s(z)} d\Omega. \quad (17)$$

The scalar irradiance from the sky,  $h_k$ , and the upwelling scalar irradiance from the earth,  $h_u$ , can be expressed as

$$h_k(z) + h_u(z) = \int_{4\pi} N(z, \theta', \phi') d\Omega = \bar{N}(z) \int_{4\pi} d\Omega. \quad (18)$$

Thus

$$\bar{N}(z) = [h_k(z) + h_u(z)] / 4\pi. \quad (19)$$

Also the integral of the proportional directional scattering over the  $4\pi$  solid angle is 1,

$$\int_{4\pi} \frac{\sigma(z, \beta)}{s(z)} d\Omega = 1. \quad (20)$$

Now Eq. (17) may be rewritten

$$N_q(z, \theta, \phi) = h_s(z) \frac{\sigma(z, \beta)}{s(z)} + \frac{h_k(z) + h_u(z)}{4\pi}. \quad (21)$$

From Eq. (21) we note that the equilibrium radiance is solely a function of angle from the sun. Thus, upward and downward paths of sight at the same angle from the sun,  $\beta$ , have equal equilibrium radiances.

If enough equilibrium radiances are available for a good coverage of angles from sun,  $\beta = 0 \rightarrow 180^\circ$ , the scalar irradiance from the lower hemisphere  $h_u(z)$  can be recovered by integrating Eq. (21) when the scalar irradiance from the sun and sky are known,

$$\begin{aligned} \int_{4\pi} N_q(z, \theta, \phi) d\Omega &= h_s(z) \int_{4\pi} \frac{\sigma(z, \beta)}{s(z)} d\Omega + \left[ \frac{h_k(z) + h_u(z)}{4\pi} \right] \int_{4\pi} d\Omega \\ &= h_s(z) + h_k(z) + h_u(z) = h(z), \end{aligned} \quad (22)$$

where  $h(z)$  is the total scalar irradiance. Equation (21) may also be used to recover the proportional directional scattering,  $\sigma(z, \beta)/s(z)$ , by rearrangement of the equation, thus

$$\frac{\sigma(z, \beta)}{s(z)} = \left\{ N_q(z, \theta, \phi) - \left[ \frac{h_k(z) + h_u(z)}{4\pi} \right] \right\} \div h_s(z). \quad (23)$$

We will next show that, conversely, if the atmospheric beam transmittance,  $T_\infty(z, 0)$ , the proportional directional scattering lobe  $\sigma(z, \beta)/s(z)$ , and the scalar reflectance or scalar albedo  $A_s$  are known or can be estimated, the equilibrium radiance can be predicted and hence the sky radiance and downward orbital-path radiances for any solar zenith angle,  $\theta_s$ .

#### EQUILIBRIUM RADIANCE AS A FUNCTION OF BEAM TRANSMITTANCE, THE PROPORTIONAL DIRECTIONAL SCATTERING FUNCTION, SCALAR ALBEDO OF THE EARTH, AND SOLAR ZENITH ANGLE

At any nonzero altitude, the scalar albedo or scalar reflectance of the earth can be defined as the ratio of the upwelling scalar irradiance to the downwelling scalar irradiance.

$$A_s = h_u(z) / [h_s(z) + h_k(z)]. \quad (24)$$

The upwelling scalar irradiance can be broken into two parts,

$$h_u(z) = h_s(z) A_s + h_k(z) A_s. \quad (25)$$

Equation (21) may now be rewritten

$$N_q(z, \theta, \phi) = h_s(z) \left[ \frac{\sigma(z, \beta)}{s(z)} + \frac{A_s}{4\pi} \right] + h_k(z) \left[ \frac{1 + A_s}{4\pi} \right]. \quad (26)$$

The sun scalar irradiance is found by

$$h_s(z) = h_s(\infty) T_\infty(z, \theta_s), \quad (27)$$

where  $h_s(\infty)$  is the scalar solar irradiance out of the atmosphere of the earth.

A first approximation for the scalar irradiance from the sky,  $h_{k1}(z)$ , would be to compute the sky radiance and hence sky irradiance, using the equilibrium radiance from the sun alone [the first term in Eq. (26) above],

$$N_{q1}(z, \theta, \phi) = h_s(z) \left[ \frac{\sigma(z, \beta)}{s(z)} + \frac{A_s}{4\pi} \right]. \quad (28)$$

The sky radiance is

$$N_{r1}^*(z, \theta, \phi) = N_{q1}(z, \theta, \phi) [1 - T_\infty(z, \theta)], \quad (29)$$

and the sky scalar irradiance is

$$h_{k1}(z) = \int_{4\pi} N_{q1}(z, \theta, \phi) [1 - T_\infty(z, \theta)] d\Omega; \quad (30)$$

hence, substituting Eq. (28) into (30), we obtain

$$h_{k1}(z) = h_s(z) \int_{4\pi} \left[ \frac{\sigma(z, \beta)}{s(z)} + \frac{A_s}{4\pi} \right] [1 - T_\infty(z, \theta)] d\Omega. \quad (31)$$

The second approximation for the sky scalar irradiance,  $h_{k2}(z)$ , would be to compute the equilibrium radiance

$N_{q2}(z, \theta, \phi)$  using  $h_{k1}(z)$  in Eq. (26),

$$h_{k2}(z) = \int_{2\pi} N_{q2}(z, \theta, \phi) [1 - T_{\infty}(z, \theta)] d\Omega, \quad (32)$$

$$h_{k2}(z) = h_{k1} + h_{k1} \left( \frac{1 + A_s}{4\pi} \right) \int_{2\pi} [1 - T_{\infty}(z, \theta)] d\Omega. \quad (33)$$

The third approximation for the sky scalar irradiance  $h_{k3}(z)$  would be to compute the equilibrium radiance  $N_{q3}(z, \theta, \phi)$  using  $h_{k2}(z)$  in Eq. (26),

$$h_{k3}(z) = \int_{2\pi} N_{q3}(z, \theta, \phi) [1 - T_{\infty}(z, \theta)] d\Omega, \quad (34)$$

$$h_{k3}(z) = h_{k1} + h_{k1} \left( \frac{1 + A_s}{4\pi} \right) \int_{2\pi} [1 - T_{\infty}(z, \theta)] d\Omega + h_{k1} \left( \frac{1 + A_s}{4\pi} \right)^2 \left\{ \int_{2\pi} [1 - T_{\infty}(z, \theta)] d\Omega \right\}^2. \quad (35)$$

Let

$$B = (1 + A_s)/4\pi \quad (36)$$

and

$$X = \int_{2\pi} [1 - T_{\infty}(z, \theta)] d\Omega. \quad (37)$$

Now Eq. (35) can be written

$$h_{k3}(z) = h_{k1}(1 + BX + B^2X^2). \quad (38)$$

Therefore

$$h_{kn}(z) = h_{k1}(1 + BX + B^2X^2 + \dots + B^{n-1}X^{n-1}). \quad (39)$$

This series is easily evaluated and

$$h_k(z) = h_{k\infty}(z) = h_{k1}/(1 - BX). \quad (40)$$

Substituting Eqs. (31), (36), (37), and (38) into Eq. (26), we find

$$N_q(z, \theta, \phi) = h_s(z) \left\{ \frac{\sigma(z, \beta)}{s(z)} + \frac{A_s}{4\pi} + \left( \frac{1 + A_s}{4\pi} \right) \times \left[ \int_{2\pi} \left[ \frac{\sigma(z, \beta)}{s(z)} + \frac{A_s}{4\pi} \right] [1 - T_{\infty}(z, \theta)] d\Omega / 1 - \left( \frac{1 + A_s}{4\pi} \right) \int_{2\pi} [1 - T_{\infty}(z, \theta)] d\Omega \right] \right\}. \quad (41)$$

The first term in the braces is the direct scattering from the sun. The second term is the portion of the earth scalar irradiance due to the sun. The third term is the sky scalar irradiance and the reflectance from the earth of the light from the sky. Although seemingly complicated, Eq. (41) is quite easily solvable by computer. The scalar albedo has a theoretical range of 0 to 1 and

a practical range of something less than that. It would be easy to assign a series of albedo values to obtain an idea of the effect of different albedos on the sky radiance.

In this model atmosphere, the path radiances for intermediate altitudes would be completely specified if a profile of attenuation length with altitude were known, in addition to the four parameters needed for solution of Eq. (41). Thus, if we assume the structure for an optical standard atmosphere, the only unknowns are the  $\sigma(z, \beta)/s(z)$  functions which are responsible for a given total atmospheric beam transmittance, and the scalar albedos that are appropriate for different types of terrains. The scalar albedo for a given terrain probably varies with solar zenith angle and haziness of the day (ratio of sky scalar irradiance to sun scalar irradiance). For any terrain, however, there is probably a reasonable range of values.

## DISCUSSION

### Related Work on Sky Radiance

Pokrowski<sup>7</sup> expressed sky radiances in a form similar to Eq. (11). He also gave an equation for sky radiance which expressed it as a function of  $\beta$ , and zenith angle,  $\theta$ . Duntley<sup>1</sup> expressed sky luminance in the same form as Eq. (11) for the Optical Standard Atmosphere. The current CIE effort to develop a standard photopic clear sky also uses an equation for sky luminance which is similar to Eq. (11). This is based on work by Kittler.<sup>8</sup> The atmospheric beam transmittance used is 0.71. The equilibrium luminance used by CIE is expressed in equation form as a normalized function of angle from sun,  $\beta$ .

Another group of researchers<sup>9-11</sup> has used sky radiances to obtain a relative measure of the scattering function  $\sigma(z, \beta)$ . Many of these workers have used sky radiances (or luminances) in the same zenith angle as the sun, but none have related the sky radiance to the equilibrium radiance by use of the beam transmittance and the zenith angle of the path of sight.

Both Tousey and Hulburt<sup>12</sup> and Chandrasekhar<sup>14</sup> have developed equations for computing sky radiance which take into account the polarization of the scattered light. These expressions, even when the complications due to polarization are eliminated, are much more complex than the equations given in Sec. I for the model atmosphere. The two assumptions upon which the model is based simplify the relationships between the variables.

<sup>7</sup> G. I. Pokrowski, *Z. Physik* 34, 49, 496 (1925); 53, 67 (1926). *Z. Physik*, 30, 697 (1929).

<sup>8</sup> R. W. Kittler, in *Proceedings of the CIE International Conference on Sunlighting, April 1965 at Newcastle upon Tyne* (Bouwcentrum, Rotterdam, 1967).

<sup>9</sup> R. Anthony, *J. Meteorol.* 10, 60 (1953).

<sup>10</sup> F. E. Volz and K. Bullrich, *J. Meteorol.* 18, 306 (1961).

<sup>11</sup> R. W. Fenn, *Beitr. Physik. Atmosph.* 37, 71 (1964).

<sup>12</sup> R. Tousey and E. O. Hulburt, *J. Opt. Soc. Am.* 37, 78 (1947).

<sup>14</sup> S. Chandrasekhar, *Radiative Transfer* (Clarendon Press, Oxford, England, 1950).

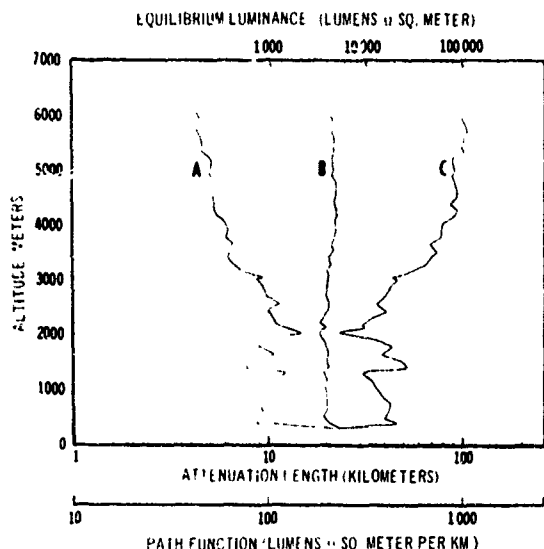


FIG. 2. Measured profiles of path function and horizontal equilibrium luminance over western Florida near Eglin AFB, 16 May 1957, Visibility Laboratory Flight 112, measured by A. R. Boileau. Sun zenith angle is  $25^\circ$ . Path function,  $A_0(2.90, 113)$  is at  $\theta = 100^\circ$ . Sky condition: clear and blue. The profile of attenuation length was computed by means of Eq. (4). Note that the graph has three scales, with the equilibrium luminance scale one half the size of the attenuation-length and path-function scales. Thus the graph is a nomographic expression of the relationship expressed in Eq. (4); that is, equilibrium luminance equals the product of the attenuation length and the path function. A,  $B_0(2.90^\circ, 113^\circ)$ ; B,  $B_0(2.90^\circ, 113^\circ)$ ; C,  $C_0(2.90^\circ, 113^\circ)$ .

#### Comparison of the Real Atmosphere to the Model

The first assumption of the model is that the point function equilibrium radiance for a given path of sight does not change with altitude. A direct measure of the point-function equilibrium radiance is that of the horizon sky. Horizontal equilibrium radiance measurements were made with the forward telephotometer of the attenuation meter mounted on the B 29 USAF aircraft assigned to the Visibility Laboratory (See Ref. 4, p. 503). When the descent of the B 29 from high altitude was made in gradual stages, the horizontal equilibrium radiance in the visible portion of the spectrum remained relatively constant with altitude. See example in Fig. 2. On flights in which the descent

was rapid, the radiance measurements showed a radical decrease at the lower altitudes. It is believed that moisture in the more humid, warmer air at the lower altitudes condensed on the window of the telephotometer, which had become cold during the flight at the upper altitudes. New telephotometers with windows heated to eliminate this effect are soon to be flown. Horizontal equilibrium radiance as a function of altitude measured with these improved instruments should provide additional evidence for use in comparing the real atmosphere to the model.

An additional comparison can be made of the horizontal equilibrium radiance with the slant path equilibrium radiance derived by means of Eq. (12), for the same angle from the sun  $\theta$ . The two equilibrium radiances are equal for the model atmosphere.

The second assumption upon which the model is based is that absorption is negligible. In the visible portion of the spectrum, 0.4 to  $0.7 \mu\text{m}$ , there are 21 absorption bands in the telluric spectrum.<sup>14</sup> These are due to various forms of molecular oxygen ( $\text{O}_2$ ,  $\text{O}^4$ ),<sup>15</sup>  $\text{O}^3$ ,  $\text{O}_3$ ,  $\text{O}_4$  and to water ( $\text{H}_2\text{O}$ ). Of these, 15 are so weak as to be ineffective except in the spectrum of the setting sun. The six remaining bands, for  $\text{O}_2$  and  $\text{H}_2\text{O}$ , lie between 0.5796 and  $0.6981 \mu\text{m}$ . Only one, an  $\text{O}_2$  band at  $0.6884 \mu\text{m}$ , is strong. Thus, for monochromatic light between 0.4 and  $0.57 \mu\text{m}$  and for broad-band visible light detectors (such as photopic vision) the atmospheric absorption can be considered negligible except for a setting sun.

#### SUMMARY

A model for a clear atmosphere applicable to the visible portion of the spectrum has been presented in which the equation of transfer may be integrated. The resultant equations for equilibrium radiance, sky radiance, and proportional directional scattering function are considerably simpler than have been expressed hitherto. Comparisons of the real atmosphere to the model indicate that the two conditions specified by the assumptions are adequately met for visible light on some clear days.

<sup>14</sup> J. Goldberg in *The Earth as a Planet*, G. P. Kuiper, Ed. University of Chicago Press, Chicago, 1954, Ch. 5.

O. D. BARTENEVA

## SCATTERING FUNCTIONS OF LIGHT IN THE ATMOSPHERIC BOUNDARY LAYER\*

Ten classes of scattering functions are presented, corresponding to different conditions in the atmospheric boundary layer. For visibility 220 km and extinction coefficient  $\alpha = 0.0136 \text{ km}^{-1}$  a near-Rayleigh scattering function was obtained. In fogs the scattering functions exhibited peaks near  $140^\circ$ , which corresponds to the primary rainbow region. A correlation was established between visibility and the shape of the scattering function.

The scattering functions of light under different atmospheric conditions must frequently be known in connection with certain theoretical and applied problems in atmospheric optics.

Several disagreements are found among a few investigations [1-6] that have been published. For example, Hulburt [1] obtained a 10:1 forward-to-backward scattering ratio for visibilities from 5 to 20 km, in agreement with Rocard's older data. However, Bullrich [2], Reeger and Siedentopf [3], and Bullrich and Möller [4] have reported the ratio 100:1 for the same transmittance range. Foitzik and Zachaek [5] obtained results close to those given in Refs. [2-4]. The results obtained by V. F. Belov [6] disagree sharply with those given in Refs. [2-5], showing only a very slight dependence of the scattering-curve shape on transmittance.

Scattering measurements were confined, as a rule, to small transmittance ranges and were then extrapolated to the entire transmittance range. The disagreement of Refs. [1-6] can be attributed not so much to the inadequacies of any particular procedures, as to different conditions for observation under which the quantity, character and size distribution of particles suspended in the air were never known. Reliable data regarding the scattering function of light require a large number of observations at different geographical locations under different meteorological conditions.

It was therefore of interest to supplement and improve data on the atmospheric scattering of light by means of systematic observations of scattering functions over the entire range of visibilities. Our measurements have shown that the shape of the scattering curve is strongly dependent on transmittance. In addition, curves of different shapes can be obtained for the same visibility.

From 1955 to 1958 scattering functions were measured under different meteorological and geographical conditions, using a nephelometer with variable observation angle, which had been developed by Rityn' and Lazarev [7].

The nephelometer consists of an illuminator, visual photometer and recording device. The illuminator emits a directed light beam. The brightness of a given air layer is measured by the photometer at different angles  $\varphi$  from the illuminator axis. These measurements yield curves

characterizing the spatial distribution of scattered light - the scattering functions or angle-dependent scattering coefficients  $\rho(\varphi)$ . The total scattering coefficients  $\rho$  or extinction coefficients  $\alpha$  are then calculated by means of the equality

$$\rho = \alpha = 2\pi \int_0^\pi \rho(\varphi) \sin \varphi d\varphi. \quad (1)$$

Scattering was measured in an open volume of air. The apparatus was designed for field work during non-daylight hours and can measure scattering at angles from  $16^\circ$  to  $164^\circ$ . ( $\varphi = 0^\circ$  is the direction of the projected beam.)

Scattering functions were measured at intervals of  $10^\circ$  in the given angular range. As a control, at the end of a run the first point was remeasured; the difference between the first and last measurement should not exceed the error in measuring  $\rho(\varphi)$ .

Simultaneous measurements of scattering functions by several observers showed that the r.m.s. error of a single measurement of  $\rho(\varphi)$  fluctuates from  $\pm 5$  to  $\pm 15\%$ , depending on the brightness levels of the compared photometric fields. For each angle  $\varphi$  photometric balance was established three times. The number of readings was increased to five or more when the photometric fields were not bright and measurements became difficult. Most measurements were obtained by two observers who recorded the distribution curves successively. This made it possible to eliminate subjective visual errors, and considerably increased the accuracy of  $\rho(\varphi)$ .

Scattering observations in fogs required great care because of variations in fog density and in the aerosol size distribution. In order to provide certainty that a given measured scattering function pertains to a single fog condition, we considered only curves that had been obtained either by two observers in succession or from several runs by a single observer.

The average time required for measuring a single scattering function was 15-20 min for non-automatic recording, and 5 min for automatic recording of photometer readings. Under fog conditions all readings were recorded automatically.

Curves were plotted from average measurements. Omitted regions from  $0^\circ$  to  $16^\circ$  and from

\*Reported at the All-Union Conference on Actinometry and Atmospheric Optics in Leningrad, January, 1955. Izv. Geophys. Ser., 19(1), pp. 1852-1865, translated by Irving Emin.

164° to 180° were extrapolated graphically. Functional coordinates were used, with the axes representing  $x = \cos \varphi$  and  $y = \log \rho(\varphi)$ . Smooth curves were drawn through the experimental points. On the assumption that the number of points was adequate for determining the shape of a scattering curve, in addition to interpolation between points, extrapolation was extended to  $\varphi = 0^\circ$  and  $180^\circ$ . It appeared that a sufficient number of scattering measurements had been performed, since the value of

$$\rho = 2\pi \int_{-1}^1 f(x) dx$$

that was calculated from the smooth curve agreed with the value of  $\alpha$  as measured by different methods [8]. It was convenient to use the indicated coordinates for plotting the scattering functions, since the requirement

$$\frac{d\rho(\varphi)}{d\varphi} = 0$$

is easily satisfied for  $\varphi = 0^\circ$  and  $\pi$ .

#### MEASUREMENTS OF SCATTERING FUNCTIONS

During the period 1955-1958, 715 scattering functions were measured under different meteorological and geographical conditions and with visibility  $S (=3/\alpha)$  varying from 0.4 to 220 km.

Measurements were performed (a) in the Lenin-grad region at the field base of the Main Geophysical Observatory in Voeikovo for three years, and at the Toksovo weather station; (b) at Odesa on land and at sea during October (in collaboration with G. Ya. Bashilov); (3) during the Mt. Elbrus expedition of the USSR Academy of Sciences, at 3200 m (Terskol Peak) and at 4000 m (glacier base), during September, (d) in the central portion of the Atlantic Ocean far from any land (38-43°N, 45-47°W) on the steamship Lomonosov during April (under the direction of G. Ya. Bashilov).

The extinction coefficient  $\alpha$  was measured at the same time but independently of the scattering

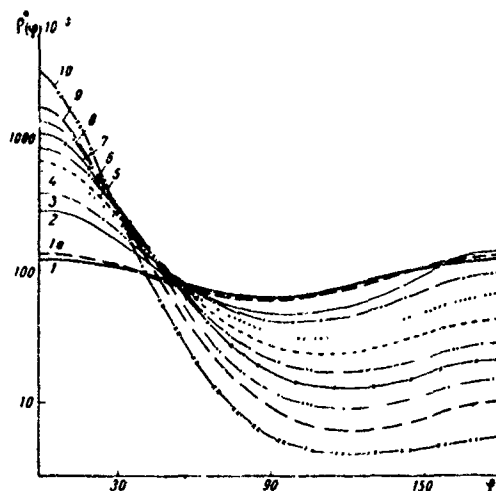


Fig. 1. Scattering functions of light in air - gradual type  
1a - curve registered at Mt. Elbrus; 1 - Rayleigh function for pure dry air; 2 - class 2, gradual type; 3 - class 3, gradual type, etc.

functions. Under certain conditions in a highly transparent atmosphere ( $S > 50$  km)  $\alpha$  was determined by numerical integration of the scattering coefficient  $\rho(\varphi)$  (Eq. (1)).

In conjunction with scattering measurements in fogs transmittance was always measured by an M-37 transmittometer [11]. In the processing of the data only those scattering functions were retained for which the extinction coefficient derived by numerical integration of the scattering curve agreed, within error limits, with the extinction coefficient  $\alpha$  derived from transmittometer measurements.

Visibility was computed from the formula  $S = 3/\alpha$ . All scattering-curve measurements were accompanied by notations of pressure, temperature and relative humidity.

The large amount of experimental material permitted a rigorous evaluation procedure and rejection of

Table 1

Class and type of scattering function	$K$	$S$ , km	Number of measured functions and station
1	1	220	13 (E)
2	1.2-1.5	180-100	33 (E, V)
3	1.6-2.5	150-50	138 (E, V)
4	2.6-3.5	100-20	94 (E, V, T, O, L)
5	3.6-5.5	50-10	101 (E, V, T, C)
5'		20-10	17 (L, O, V)
6		20-4	70 (V, T, O)
6'	5.6-7.4	10-4	8 (V, O)
6''		0.8-0.4	7 (T)
7		10-2	64 (V, T, O)
7''	7.5-11	0.8-0.4	14 (V, T)
8		4-0.6	25 (V)
8''	11.1-16.5	0.5-0.4	6 (V)
9		2-0.6	20 (V)
9''	16.6-25	0.8-0.4	6 (V)
10		1.5-0.7	4 (V)
10''	25-35	0.5-0.4	4 (V)

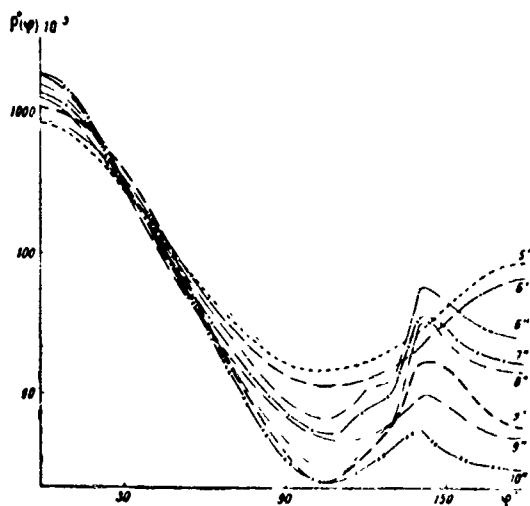


Fig. 2. Scattering functions of light in air - steep type

5' - class 5, steep type; 6' - class 6, steep type; 6'' - class 6, steep type with peak, etc.

tion of doubtful cases. Only 624 out of 715 scattering curves were retained.

The parameter used to characterize a family of curves representing scattering under different conditions was the so-called light-flux asymmetry coefficient  $K$  (the Richtungsquotient of Foitzik and Zschaek [5]), which is the ratio of the forward-scattered flux  $\Phi_1$  to the backward-scattered flux  $\Phi_2$ .

$$K = \frac{\Phi_1}{\Phi_2} = \frac{\int_0^{\pi/2} p(\varphi) \sin \varphi d\varphi}{\int_{\pi/2}^{\pi} p(\varphi) \sin \varphi d\varphi}.$$

$K$  was determined for each scattering function, and all curves with values of  $K$  in the same range were grouped together to form a single class.

The values of  $K$  in adjacent classes differed by a factor of about 1.5, 10 different classes were discriminated in this manner. Besides the division into classes, the scattering functions were designated as either "gradual" or "steep" with a deep minimum at  $\varphi = 110-120^\circ$ .

The results are given in Table 1, where the class numbers and types are listed in the first column, steep types are denoted by single or double primes. The second column gives corresponding values of  $K$ , and the third column gives the visibility  $S$  with which each class is associated. The fourth column gives the number of measured curves in each class and the station (V - Voikovo, T - Toksovo, O - Odessa, E - Mt. Elbrus, L - Lomonoosov).

Figs. 1 and 2 show the different classes of scattering curves, with abscissas denoting the scattering angle  $\varphi$  in degrees and the ordinates denoting normalized values

$$p^*(\varphi) = \frac{p(\varphi)}{2\pi \int_0^{\pi} p(\varphi) \sin \varphi d\varphi}. \quad (2)$$

In Fig. 1, curve 1a, representing  $K = 1$ , is the average of 13 curves measured at various times during the night of September 21-22, 1957 on Terskol Peak. Associated values of parameters are  $a = 0.0136 \text{ km}^{-1}$  and  $S = 220 \text{ km}$ . At the time of observation the air temperature was  $+5^\circ$ , relative humidity 26% and pressure 704 mb. The r.m.s. error of  $p(\varphi)$  was  $\pm 5\%$ .

Curve 1a in Fig. 1 is close to the Rayleigh function (curve 1), for which the normalized function is

$$p^*(\varphi) = \frac{3}{16\pi} (1 + \cos^2 \varphi).$$

The maximum discrepancy of  $p^*(\varphi)$  between curve 1a and the Rayleigh function was  $+4\%$  at  $\varphi = 16^\circ$  and  $164^\circ$ , which is within the limits of error.

Each additional curve in Figs. 1 and 2, representing the different classes and types, is the average of a large number of observations at different geographical locations (Table 1).

The curves were found to depend on more than one parameter. Some classes included both the gradual type, represented by the Rayleigh function (Fig. 1, curves 1 and 1a), and the steep type, represented in Fig. 2 by greatly extended curves with steep maxima at  $\varphi = 0^\circ$  and pronounced minima at  $110-120^\circ$ . The gradual curves differ in that they lack pronounced minima.

Classes 1-4 for  $K \leq 3.5$  contain curves of only a single (gradual) type. For  $K > 3.5$ , i.e., beginning with class 5, for a single value of  $K$  we find both the gradual type (Fig. 1, curves 5, 6, etc.) and the steep type (Fig. 2, curves 5', 6'). The steep type begins to appear in class 4, but the difference between the two types is very small there, and is within the limits of error.

For  $K > 5.6$  (beginning with class 6) steep curves exhibit a peak near  $140^\circ$ , which remains in all subsequent classes but with some reduction of peak height (Fig. 2, curves 6'', 7'', etc.).

The shapes of both types vary with  $K$ . With increasing  $K$  the curves are stretched and the maximum at  $\varphi = 0^\circ$  becomes more pronounced.

The highest values of  $K$  are represented by the gradual type in class 10. The steep type in class 10 includes four curves with  $K = 40$ . However, according to the calculations of Shifrin [9], our value  $K = 40$  probably results from errors of measurement and should be reduced to 35.

Fig. 3 shows scattering curves corresponding to transmittance varying from that of a pure Rayleigh atmosphere with  $S = 220 \text{ km}$  to a fog with  $S = 0.4-0.5 \text{ km}$ . The shape of the scattering function was not observed to depend uniquely on transmittance. For any given visibility, scattering curves are observed to differ considerably in shape as well as in scale of magnitude. (In Figs. 1-3 all curves have been reduced to the same flux.) For high transmittance with  $S \geq 50 \text{ km}$  only gradual scattering curves are observed. In the remaining major portion of the visibility range both types of curves are observed.

The shape of a scattering curve is strongly dependent on atmospheric conditions, and is stretched out more and more as visibility is reduced. We can therefore not limit ourselves to a single average curve for scattering such as the Rocard scattering function.

The scattering curve for a fog can differ considerably from that for a haze. In classes 6, 7, 8, 9, and 10 we recorded the steep type with a peak

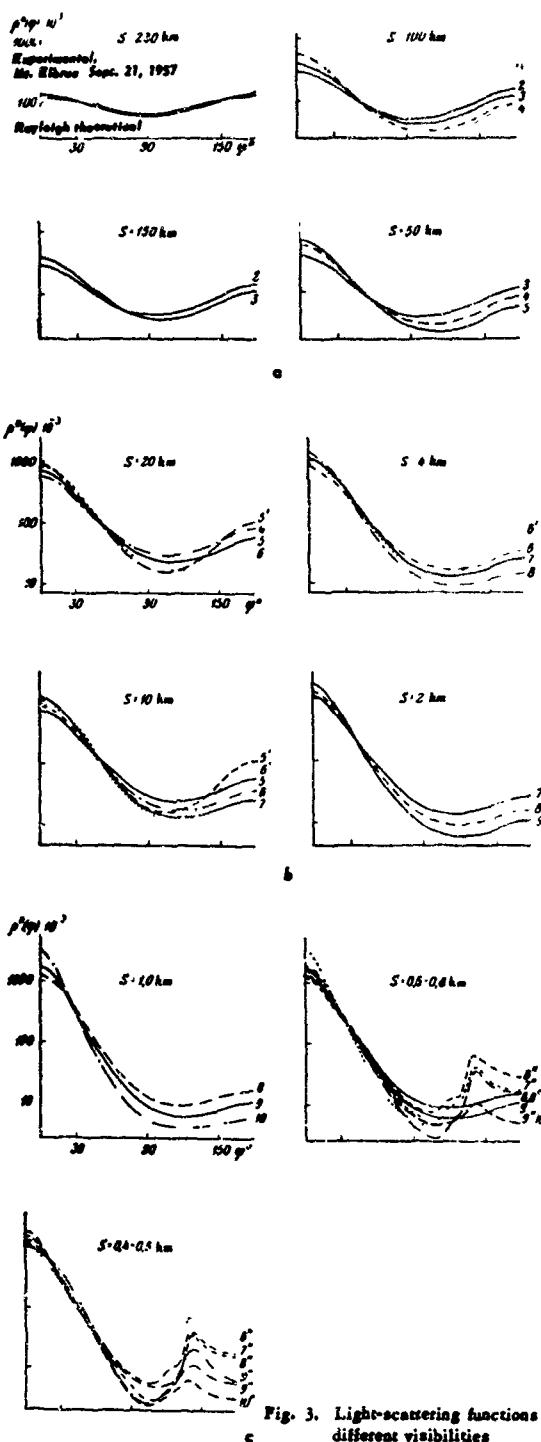


Fig. 3. Light-scattering functions for different visibilities

near  $\phi = 140^\circ$ , which is observed only in fogs; in Fig. 2 this type is represented by curves 6"-10". In the higher-numbered classes, i.e., with increasing asymmetry coefficient of the light flux, the peak is reduced. In classes 6, 7 and 8 the

curve shape remains unchanged within the limits of error and it was possible to average the measurements obtained on different days. In class 9 two different curves (9" in Fig. 2) were obtained with peaks of different heights near  $140^\circ$ . Class 10 was limited to four curves of identical shape (within the limits of error) and with a low peak around  $140^\circ$ .

Fig. 3c shows our scattering curves in fogs. Both gradual and steep curves are observed for  $S = 0.6-0.8$  km, while only a steep curve with a peak near  $140^\circ$  is observed for  $S = 0.4-0.5$  km.

The peak near  $\phi = 140^\circ$  in fogs corresponds to the primary rainbow region; the bend of the curves for classes 6", 7" and 8" at  $120-130^\circ$  corresponds to the secondary rainbow region. According to the calculations of Shifrin [10], a rainbow results from the presence of large water drops in a fog. The height of the peak evidently depends on the relative number of large drops in the total number of all particles suspended in the air. The intensity of the rainbow may possibly provide a basis for determining the size distribution of particles in fogs. However, all of these hypotheses require further checking and, primarily, knowledge of the fog-particle size distribution at the time of measurement. Bullrich [13] also recently observed a fog rainbow.

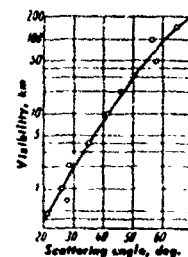


Fig. 4. Intersection point of light-scattering curves as a function of visibility

It must also be noted that, in accordance with Fig. 3a-c the point of intersection of scattering curves observed for any given visibility depends on the visibility. The curves observed for high visibility ( $S > 50$  km) intersect near  $\phi = 60^\circ$ .

With increasing turbidity the intersection point begins to move toward smaller angles  $\phi$ ; in a highly turbid atmosphere the curves intersect near  $30^\circ$  and  $20^\circ$ . Fig. 4 shows how the intersection point of scattering functions depends on visibility.

Pyaskovskaya-Fessenkova [12] measured scattering functions by observing sky brightness during high visibility, and obtained an intersection point near  $\phi = 60^\circ$ , in agreement with our results. The mean value of  $\mu/\tau$  (corresponding to our  $\rho(\phi)$ ) obtained by the same investigator from a large amount of data was 0.076 for  $0.05 \leq \tau \leq 0.30$  (Ref. [12], Table 46). Our data show that this transmittance range furnishes scattering curves of classes 1 to 5; the corresponding values of  $\rho(\phi)$  for  $\phi = 60^\circ$  (Table 2) fluctuate from 0.075 to 0.068 and are close to the values of  $\mu/\tau$  given in Ref. [12].

For the purpose of comparing our scattering functions with the results obtained by Foitzik and Zachaeck (Ref. [5], Table 3), the scattering curves were normalized in accordance with Eq. (2), after which our classification based on the values of  $K$  was used.

Fig. 5 shows scattering curves for our classes 3 to 9, together with points obtained by Foitzik and



Table 2

Class and type of scattering function	Gradual 1		Gradual 2	Gradual 3	Gradual 4	Gradual 5	Steep 5'	Gradual 6	Steep 6'	Steep with peak c max 6°	Gradual 7	Steep with peak c max 7°	Gradual 8	Steep with peak c max 8°	Gradual 9	Steep with peak c max 9°		Gradual 10	Steep with peak c max 10°
	Rayleigh	Experimental														1780·10 <sup>-3</sup>	1050·10 <sup>-3</sup>		
0	119·10 <sup>-3</sup>	130·10 <sup>-3</sup>	282·10 <sup>-3</sup>	385·10 <sup>-3</sup>	564·10 <sup>-3</sup>	681·10 <sup>-3</sup>	820·10 <sup>-3</sup>	834·10 <sup>-3</sup>	831·10 <sup>-3</sup>	1200·10 <sup>-3</sup>	1100·10 <sup>-3</sup>	1300·10 <sup>-3</sup>	1320·10 <sup>-3</sup>	1520·10 <sup>-3</sup>	1760·10 <sup>-3</sup>	1780·10 <sup>-3</sup>	1050·10 <sup>-3</sup>	2500·10 <sup>-3</sup>	1810·10 <sup>-3</sup>
10	118	126	270	350	499	594	712	727	748	992	935	1090	1080	1270	1380	1500	928	1680	1440
20	112	114	216	272	354	410	445	498	541	525	548	628	597	617	618	637	658	700	680
30	104	105	162	196	234	269	280	295	333	289	299	307	302	312	274	264	299	280	305
40	94.7	94	123	139	152	168	168	171	175	151	161	150	150	141	124	125	200	100	135
50	84.4	84	87.7	98.0	101	106	97.3	98.8	90.6	81.5	90.6	78.1	78.2	71.7	67.0	61.0	81.0	46.0	64.5
60	76.6	75	69.0	71.4	70.0	68.4	66.7	58.8	50.4	45.2	53.1	39.8	42.8	30.0	35.0	33.0	36.0	22.0	29.0
70	66.7	65	55.4	54.8	50.5	45.8	35.3	38.1	30.4	25.0	33.1	21.2	25.6	15.5	20.2	19.0	16.0	12.0	13.5
80	61.5	61	48.5	45.1	39.6	34.0	22.9	26.9	18.8	14.1	22.6	12.1	16.8	7.9	12.7	10.8	7.0	7.2	6.2
90	59.7	60	46.7	40.9	34.2	26.9	17.3	20.6	13.8	9.1	16.9	7.6	12.5	4.6	9.1	6.9	3.6	5.3	3.4
100	61.5	62	46.7	40.0	32.0	24.1	15.2	17.8	11.8	7.1	14.1	5.6	10.1	3.1	7.1	5.2	2.3	4.5	2.4
110	66.7	67	49.0	41.3	31.8	23.2	15.7	16.7	12.4	7.3	12.9	5.4	9.3	2.7	6.2	4.7	2.6	4.2	2.5
120	76.6	72	53.4	44.5	33.2	23.6	17.6	16.7	13.0	11.3	12.8	8.2	9.1	4.4	5.9	5.0	3.8	4.0	3.1
130	84.4	80	61.2	50.0	36.2	25.4	22.0	17.4	16.0	13.1	13.4	11.2	9.4	6.5	6.1	6.4	4.5	4.0	4.3
140	94.7	92	74.0	57.9	41.0	28.7	30.1	18.4	22.8	61.5	14.0	34.7	10.2	34.7	6.6	10.2	16.0	4.2	6.0
150	104	104	94.0	66.3	46.7	31.7	46.5	20.6	37.4	90.0	15.9	31.5	11.5	25.0	7.5	8.8	16.0	4.6	4.1
160	112	115	115	77.8	54.3	35.8	69.5	23.4	50.2	36.8	18.4	21.5	12.9	18.0	8.5	6.6	11.0	4.8	3.4
170	118	126	133	91.0	62.4	40.6	91.2	27.0	72.2	30.1	20.7	18.5	14.3	16.0	9.8	5.4	6.7	5.3	3.0
180	119	130	139	96.0	65.3	42.6	99.0	28.0	78.2	28.5	21.3	17.8	15.0	15.5	10.2	5.2	6.1	5.5	3.0

X-00000000

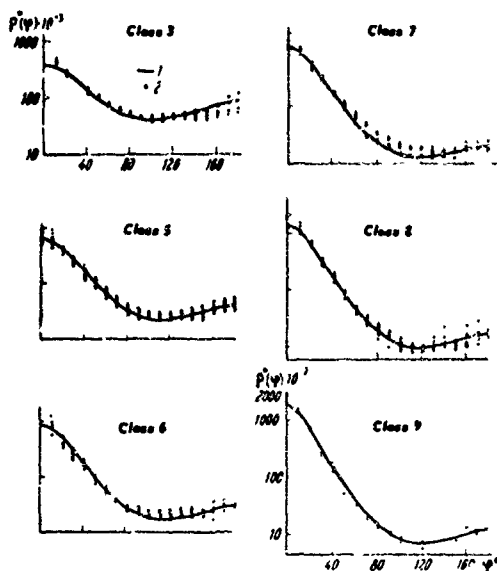


Fig. 5. Comparison of scattering functions obtained in the present investigation with those of Foitzik and Zschack [5]  
1 - classes 3 to 9 (our classification); 2 - corresponding data in Ref. [5]

Zschack which represent these same classes. These data are seen to be in good agreement with our results. The data given in Ref. [5] are quite uniformly distributed around our curves. The somewhat higher values of  $\rho^*(\phi)$  in the region  $90-130^\circ$  for classes 3, 5, 6 and 7, compared with our data, can probably be accounted for by the fact that the observations of scattered light which are reported in Ref. [5] were performed against the background of a wooded hill with sufficient brightness to increase appreciably the value of  $\rho^*(\phi)$  at the scattering-curve minimum. For low visibility (classes 8 and 9,  $S = 0.6-6$  km) when the brightness of the hill was also very small compared with the observed scattered light the points of Foitzik and Zschack were uniformly distributed around curves 8 and 9. Our measurements were performed against an ideal black-body background.

The visibility associated with each given class of scattering functions reported in Ref. [5] corresponded to our limit of visibility for the same class.

The agreement of scattering measurements obtained with different independent techniques suggests that our data for the visibility range  $S = 220$  km to 1 km are quite reliable. The steep scattering curves with peaks near  $140^\circ$  (curves 6"-10"), observed in a fog, were based on meager data and are therefore only provisional.

Table 2 gives values of the normalized scattering functions  $\rho^*(\phi)$  for different classes at intervals

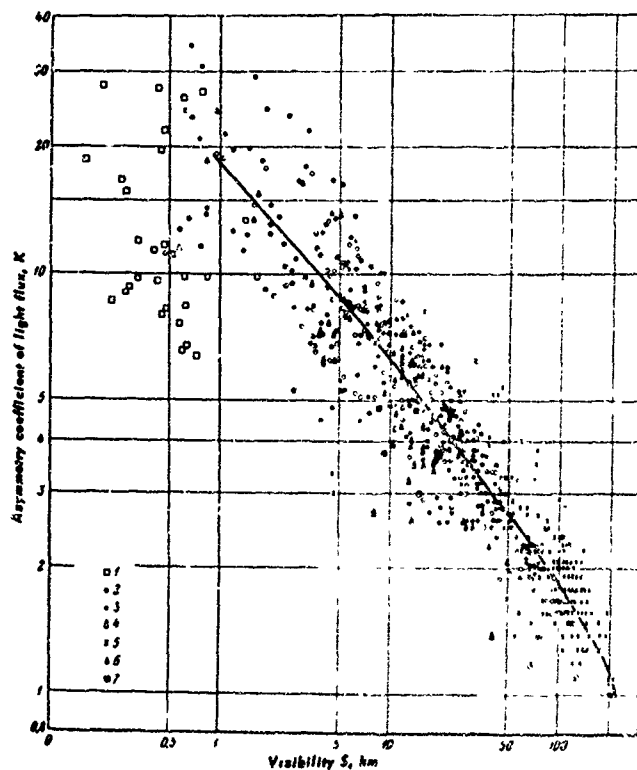


Fig. 6. Asymmetry coefficients  $K$  of light flux as a function of visibility  
1 - Voikov, fogs with peaks; 2 - Voikov; 3 - Toksovo; 4 - Odessa; 5 - Mt. Elbrus; 6 - Potsdam [5]; 7 - Lomonosov

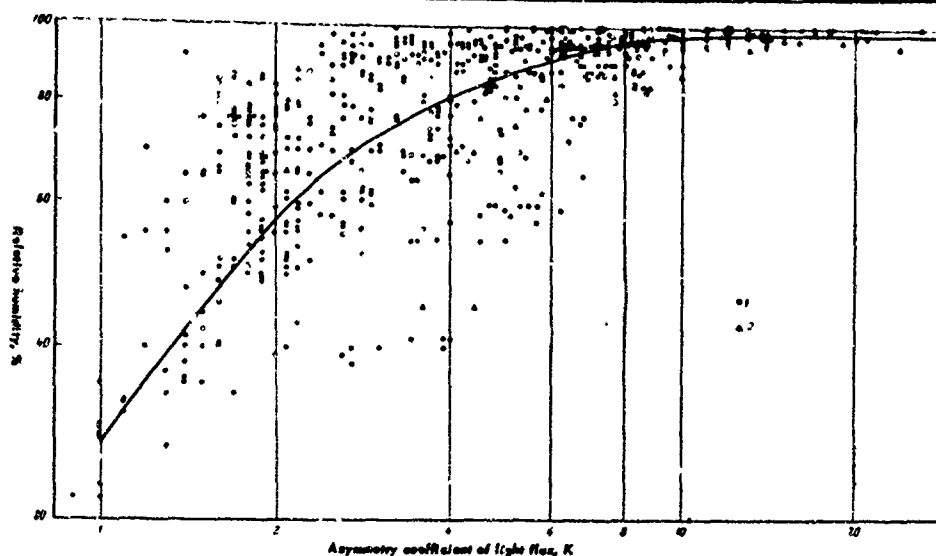


Fig. 7. Asymmetry coefficient  $K$  of light flux as a function of relative humidity

1 - Present investigation; 2 - Ref. [5]

of  $10^\circ$ . Absolute values  $p(\theta)$  are obtained through multiplication by appropriate values of the extinction coefficient  $\alpha$ .

#### ASYMMETRY COEFFICIENT OF LIGHT FLUX

Fig. 6 shows the correlation between the forms of scattering curves characterized by  $K$ , and visibility  $S$ . The observation stations are denoted by different symbols. The results given in Ref. [5] are included.

A large spread of the experimental values is observed. Visibilities ranging over two points of the international scale correspond to the same value of  $K$ . For a single value of the visibility,  $K$  can vary by a factor of 2.5, including three different curve classes, with increasing turbidity the range of fluctuation of  $K$  increases. The correlation  $R$  between the form of scattering curve characterized by  $K$  and visibility  $S$  is  $R = 0.77 \pm 0.02$  for  $10 \text{ km} \leq S \leq 220 \text{ km}$ ,  $R = 0.69 \pm 0.02$  for  $4 \text{ km} \leq S \leq 220 \text{ km}$ , and  $R = 0.50 \pm 0.08$  for  $1 \text{ km} \leq S < 10 \text{ km}$ .

The quantity and properties of aerosols are affected by the geographical location of the observation station, synoptic conditions, the ground surface and other factors. However, it was not observed that the form of the scattering function depends on geographical location.

Table 1 and Fig. 6 show that the same form of scattering function for a given visibility range was recorded at Odessa, Mt. Elbrus, and Potsdam, depending on the character of the air masses at the observation times.

Measurements by other investigators confirm these results. Ref. [12] furnishes the best approximation to the Rayleigh function in a desert, rather

than on mountains, where greater air purity is assumed. Somewhat different results can be expected over a water surface far from land, with steep functions predominating in hazes. Such curves were partially obtained on the Atlantic Ocean, although the data are still insufficient to permit definite conclusions.

Fig. 7 shows the correlation between the form of scattering function, characterized by  $K$ , and relative humidity. A very large spread of the experimental values is seen in the figure. The r.m.s. deviation of  $\Delta K/K$  from the curve in Fig. 7 is  $\pm 0.45$  for a single value of the relative humidity. The correlation coefficient  $R = 0.58 \pm 0.03$  is obtained between the scattering functions, characterized by  $K$ , and relative humidity.

#### CONCLUSIONS

1. 10 classes of light-scattering functions were obtained, corresponding to different values of the light-flux asymmetry coefficient  $K$  and different conditions in the atmospheric boundary layer. For  $K > 3.5$  each class includes both gradual and steep curves.
2. The shape of scattering functions does not depend uniquely on visibility, functions of markedly different shapes are observed for the same visibility. As visibility diminishes, the curves are stretched increasingly away from the Rayleigh function.
3. For  $\alpha = 0.0136 \text{ km}^{-1}$  a near-Rayleigh function was recorded. In fogs scattering functions were found with a peak near  $\theta = 140^\circ$ , corresponding to the primary rainbow region, as a consequence of large fog drops.
4. Correlation has been established between the shape of the scattering function, characterized by the parameter  $K$ , and visibility  $S$ . For  $10 \text{ km} \leq S \leq 220 \text{ km}$  we have the correlation coefficient

$R = 0.77 \pm 0.02$ , and for  $1 \text{ km} \leq S < 10 \text{ km}$ ,  $R = 0.56 \pm 0.08$ .

In conclusion the author wishes to thank N. G. Boldyrev for a discussion of the results, K. S. Shifrin for valuable suggestions, G. Ya. Bashilov

for the furnishing of oceanic scattering data, and A. N. Boyarova for assistance in the investigation.

Voeikov Main Geophysical  
Observatory

Received  
2/8/1960

#### REFERENCES

1. Hulburt, E. O., Optics of Atmospheric Haze, J. Opt. Soc. Am. 31, 467, 1941.
2. Bullrich, K., Durchlässigkeitszahl und Zerstreuungsfunktion in dunstiger Luft, Meteorol. Z. 61, 1944.
3. Reeger, E. and H. Siedentopf, Die Streufunktion des atmosphärischen Dunstes nach Scheinwerfermessungen, Optik 1, 1946.
4. Bullrich, K. and F. Möller, Die Streuung des Lichtes in trüber Luft, Optik 2, 1947.
5. Foitzik, L. and H. Zschaeck, Messungen der spektralen Zerstreuungsfunktion bodennaher Luft bei guter Sicht in Dunst und Nebel, Z. Meteorol. 1, 1953.
6. Belov, V. F., Measurement of the Principal Optical Characteristics of the Atmospheric Boundary Layer, Hydrometeopress, Moscow, 1956.
7. Rityn', N. E. and V. P. Lazarev, An Instrument for Measuring Scattering Functions of Light in Air, Optiko-mekh. prom. (Opto-Mechanical Industry) No. 2, 1959.
8. Barteneva, O. D., G. Ya. Bashilov, and N. G. Boldyrev, The Use of an IF-14 Nephelometer with Variable Observation Angle, Optiko-mekh. prom., No. 2, 1959.
9. Shifrin, K. S., The Effect of Fog on Radiation Balance, Trans. (Trudy) Main Geophysical Observatory, No. 27(89), 1951.
10. Shifrin, K. S., The Scattering of Light in a Turbid Medium, Gostekhteorizdat, Moscow, 1951.
11. Goryshin, V. I., Apparatus for Measuring and Registering Horizontal Visibility in the Atmosphere, Trans. (Trudy) Main Geophysical Observatory, No. 100, 1959.
12. Pyaskovskaya-Fessenkova, E. V., An Investigation of Light Scattering in the Earth's Atmosphere, Acad. Sci. USSR Press, 1957.
13. Bullrich, K., Streulichtmessungen in Dunst und Nebel, Meteorol. Rundschau 13, H. 1, 1960.

# Glossary And Notation

The notation used in reports and journal articles produced by the Visibility Laboratory staff follow, in general, the rules set forth in Appendix A, pages 499-500 (Duntley *et al*, 1957). These rules are:

Each optical property is indicated by a basic (parent) symbol.

A presubscript may be used with the parent symbol as an identifier, e.g.,  $b$  indicates background while  $t$  denotes an object.

A postsubscript may be used to indicate the length of a path of sight, e.g.,  $r$  denotes an *apparent* property as measured at the end of a path of sight of length  $r$ , while  $o$  denotes an *inherent* property based on the hypothetical concept of a photometer located at zero distance from an object.

A postsuperscript  $*$ , or a postsubscript  $*$ , is employed as a mnemonic symbol signifying that the radiometric quantity has been generated by the scattering of ambient light reaching the path from all directions.

The parenthetical attachments to the parent symbol denote altitude and direction. The letter  $z$  indicates altitude in general;  $z_o$  is used to specify the altitude of an object. The direction of a path of sight is specified by the zenith angle  $\theta$  and the azimuth  $\phi$ . In the case of irradiances, the downwelling irradiance is designated by  $d$ , the upwelling by  $u$ .

$A(z)$	Albedo at altitude $z$ , defined by the equation $A(z) \equiv H(z,u)/H(z,d)$ . ( <i>Scalar Albedo</i> , at altitude $z$ , is the ratio $h(z,u)/h(z,d)$ .)	$N(z,\theta,\phi)$
$C_o(z_t,\theta,\phi)$	Inherent universal contrast determined for a path of sight of zero length at altitude of the object $z_t$ in the direction of zenith angle $\theta$ and azimuth $\phi$ . This property is defined by the equation	${}_bN_o(z_t,\theta,\phi)$
	$C_o(z_t,\theta,\phi) \equiv \frac{{}_tN_o(z_t,\theta,\phi) - {}_bN_o(z_t,\theta,\phi)}{{}_bN_o(z_t,\theta,\phi)}$	${}_bN_r(z,\theta,\phi)$
$C_r(z,\theta,\phi)$	Apparent universal contrast as determined at altitude $z$ from the end of path of sight of length $r$ in the direction of the zenith angle $\theta$ and azimuth $\phi$ . This property is defined by the equation	${}_tN_o(z,\theta,\phi)$
	$C_r(z,\theta,\phi) \equiv \frac{{}_tN_r(z,\theta,\phi) - {}_bN_r(z,\theta,\phi)}{{}_bN_r(z,\theta,\phi)}$	${}_tN_r(z,\theta,\phi)$
${}_bC_r^*(z,\theta,\phi)$	Path-to-background contrast. This property may be defined by the equation	
	${}_bC_r^*(z,\theta,\phi) \equiv \frac{R_r^*(z,\theta,\phi) - {}_bR_o(z_t,\theta,\phi)}{{}_bR_o(z_t,\theta,\phi)}$	$N_q(z,\theta,\phi)$
$H(z,d)$	Irradiance produced by downwelling flux as determined on a horizontal flat plate at altitude $z$ . In this report $d$ is used in place of the minus sign in the notation $H(z,-)$ which appears in Appendix D. This property may be defined by the equation $H(z,d) \equiv \int_{2\pi} N(z,\theta',\phi') \cos\theta' d\Omega$ .	$N_*(z,\theta,\phi)$
$H(z,u)$	Irradiance produced by upwelling flux as determined on a horizontal flat plate at altitude $z$ . Here $u$ is substituted for the plus sign formerly used in the notation $H(z,+)$ .	$N_r^*(z,\theta,\phi)$
$h(z)$	Scalar irradiance. This may be defined as the radiant flux arriving at a point, from all directions about that point, at altitude $z$ (Tyler and Preisendorfer, 1962).	psia
	$h(z) = h(z,d) + h(z,u)$	psid
$h(z,d)$	Scalar irradiance produced by downwelling flux. This may be defined as the radiant flux from the upper hemisphere arriving at a point at altitude $z$ .	${}_bR_o(z_t,\theta,\phi)$
${}_k h(z,d)$	Scalar irradiance defined as the radiant flux from the upper hemisphere sky (flux from the sun is not included) arriving at a point at altitude $z$ .	${}_bR_r(z,\theta,\phi)$
${}_s h(z)$	Scalar irradiance defined as the radiant flux from the sun arriving at a point at altitude $z$ .	$R_r^*(z,\theta,\phi)$
$h(z,u)$	Scalar irradiance produced by upwelling flux. This may be defined as the radiant flux from the lower hemisphere arriving at a point at altitude $z$ .	$\overline{S_\lambda T_\lambda}$
$I$	Luminous intensity of a photometric standard, usually incandescent, in the direction normal to the plane of the filament.	$S_\lambda T_\lambda$
$L(z)$	Attenuation length at altitude $z$ . This property is the reciprocal of attenuation coefficient, that is,	
	$L(z) \equiv \alpha(z)^{-1}$	

A

- $N(z, \theta, \phi)$  Radiance as determined from altitude  $z$  in the direction specified by zenith angle  $\theta$  and azimuth  $\phi$ .
- ${}_bN_o(z_t, \theta, \phi)$  Inherent background radiance as determined at altitude of the photometer  $z_t$  at zenith angle  $\theta$  and azimuth  $\phi$ .
- ${}_bN_r(z, \theta, \phi)$  Apparent background radiance as determined at altitude  $z$  from the end of a path of sight of length  $r$  at zenith angle  $\theta$  and azimuth  $\phi$ . This property may be defined by the equation

$${}_bN_r(z, \theta, \phi) \equiv {}_bN_o(z_t, \theta, \phi) T_r(z, \theta) + N_r^*(z, \theta, \phi).$$

- ${}_iN_o(z_t, \theta, \phi)$  Inherent radiance of an object as determined at altitude of the photometer  $z_t$  at zenith angle  $\theta$  and azimuth  $\phi$ .
- ${}_iN_r(z, \theta, \phi)$  Apparent radiance of an object as determined at altitude  $z$  from the end of a path of sight of length  $r$  at zenith angle  $\theta$  and azimuth  $\phi$ . This property may be defined by the equation

$${}_iN_r(z, \theta, \phi) \equiv {}_iN_o(z_t, \theta, \phi) T_r(z, \theta) + N_r^*(z, \theta, \phi).$$

- $N_q(z, \theta, \phi)$  Equilibrium radiance at altitude  $z$  with the direction of the path of sight specified by by zenith angle  $\theta$  and azimuth  $\phi$ . This property is a point function of position and direction.
- $N_*(z, \theta, \phi)$  Path function at altitude  $z$  with the direction of the path of sight specified by zenith angle  $\theta$  and azimuth  $\phi$ . This property is defined by the equation

$$N_*(z, \theta, \phi) \equiv \int_{4\pi} \sigma(z, \beta') N(z, \theta', \phi') d\Omega.$$

This property also is a point function of position and direction.

- $N_r^*(z, \theta, \phi)$  Path radiance as determined at altitude  $z$  at the end of a path of sight of length  $r$  in the direction specified by zenith angle  $\theta$  and azimuth  $\phi$ .

psia Pressure, absolute, pounds per square inch.

psid Pressure, differential, pounds per square inch.

${}_bR_o(z_t, \theta, \phi)$  Inherent background reflectance as determined at altitude of an object  $z_t$  and viewed at zenith angle  $\theta$  and azimuth  $\phi$ .

${}_bR_r(z, \theta, \phi)$  Apparent background reflectance determined at altitude  $z$  from the end of a path of sight of length  $r$  specified by zenith angle  $\theta$  and azimuth  $\phi$ .

$R_r^*(z, \theta, \phi)$  Directional path reflectance as determined at altitude  $z$  at the end of a path of sight of length  $r$  in the direction specified by zenith angle  $\theta$  and azimuth  $\phi$ .

$\overline{S_\lambda T_\lambda}$  Standardized relative spectral response of filter-cathode combination where  $S_\lambda$  is spectral sensitivity of the multiplier phototube cathode and  $T_\lambda$  is spectral transmittance of optical filter.

$S_\lambda T_\lambda$  Relative spectral response of an individual filter-phototube system.

B

$s(z)$  Total volume scattering coefficient as determined at altitude  $z$ . This property may be defined by the equation

$$s(z) \equiv \int_{4\pi} \sigma(z, \beta) d\Omega.$$

In the absence of atmospheric absorption, the total volume scattering coefficient is numerically equal to the attenuation coefficient.

$s_M(z)$  Total volume scattering coefficient for Mie scattering at altitude  $z$ .

$s_R(z)$  Total volume scattering coefficient for Rayleigh scattering at altitude  $z$ .

$T_r(z, \theta)$  Beam transmittance as determined at altitude  $z$  for a path of sight of length  $r$  at zenith angle  $\theta$ . This property is independent of azimuth in atmospheres having horizontal uniformity. It is always the same for the designated path of sight or its reciprocal.

$\tau_r(z, \theta, \phi)$  Contrast transmittance as determined at altitude  $z$  at the end of a path of sight of length  $r$  and specified by zenith angle  $\theta$  and azimuth  $\phi$ . This property is *not* independent of azimuth and is *not* the same for the designated path of sight and its reciprocal.

$W_\lambda$  Spectral emittance (power/unit of area) of electromagnetic flux from a plane surface.

$\bar{y}$  Symbol for visual efficiency function.

ZSV Zero scale value. The zero point on the linear scale when the radiometric or photometric quantity  $x$  is equal to a reference radiometric or photometric quantity  $x_0$  as shown in equation

$$\log [x_0/x] = 0.$$

$\alpha(z)$  Volume attenuation coefficient as determined at altitude  $z$ . In the absence of atmospheric absorption, the attenuation coefficient is numerically equal to the volume scattering coefficient.

$\beta$  Symbol for scattering angle of flux from a light source. It is equal to the angle between the line from the source to the observer and the path of sight

$\beta'$  Symbol for scattering angle of flux from a discrete part of the sky. It is equal to the angle between the direction specified by  $\theta'$  and  $\phi'$  and the path of sight.

$\Delta$  Symbol to indicate incremental quantity and used with  $r$  and  $z$  to indicate small, discrete increments in path length  $r$  and altitude  $z$ .

$\epsilon_\lambda$  Spectral emissivity of tungsten filament.

$\zeta$  Symbol for radius of the earth in Eqs. 2-11 and 2-12 and Fig. 2-2.

$\theta$  Symbol for zenith angle. This symbol is usually used as one of two coordinates to specify the direction of a path of sight.

A



defined by  $\theta'$  Symbol for zenith angle usually used as one of two coordinates to specify the direction of a discrete portion of the sky.

$\phi$  Symbol for azimuth. The azimuth is the angle in the horizontal plane of the observer between a fixed point and the path of sight. The fixed point may be, for example, true north, the bearing of the sun, or (as in this report) the bearing of the moon. This symbol is usually used as one of two coordinates to specify the direction of a path of sight.

ally equal  $\phi'$  This symbol for azimuth is usually used as one of two coordinates to specify the direction of a discrete portion of the sky.

h angle  $\theta$ .  $\sigma$  Symbol for volume scattering function. Parenthetical symbols may be added; for example,  $\beta$  may be always the used to designate the scattering angle from a source. In Appendix E the parenthetical symbols are  $z$  and  $\beta$  for altitude and scattering angle.

r and  $\sigma(z,\beta)/s(z)$  Proportional directional volume scattering function. This may be defined by the equation and is not

$$\int_{4\pi} [\sigma(z,\beta)/s(z)] \equiv 1.$$

$\lambda$  Symbol for wavelength.

tric quan-  $\Omega$  Symbol for solid angle. For a hemisphere

$\Omega = 2\pi$  steradians;

for a sphere

$\Omega = 4\pi$  steradians.

c absorp-

line from

between

ete incre-

the direc-

B

UNCLASSIFIED

Security Classification

DOCUMENT CONTROL DATA - R&D		
<i>(Security classification of body of abstract and indexing and data on the basis of the security classification of the report)</i>		
1. ORIGINATING ACTIVITY (Corporate author)		2. SECURITY CLASSIFICATION
Visibility Laboratory University of California, San Diego San Diego, California 92152		UNCLASSIFIED
3. REPORT TITLE		
AIRBORNE MEASUREMENTS OF OPTICAL ATMOSPHERIC PROPERTIES AT NIGHT		
4. DESCRIPTIVE NOTES (Type of report and inclusive dates)		
Scientific. Final 19 January 1967 - 30 April 1970 Approved 10 Apr 70		
5. AUTHOR (Corporate author, individual, and organization)		
Seibert O. Duntley      Jacqueline I. Gordon Richard W. Johnson      Almerian R. Boileau		
6. REPORT DATE	7a. TOTAL NUMBER	7b. NUMBER
May 1970	387	18
8a. CONTRACT OR GRANT NO.	9a. ORIGINATOR'S REPORT NUMBER	
F 19628-67-C-0181	SIO Ref. 70-7	
11. Project, Task, Work Unit Nos.		
7621-07-01		
12. DoD Element      62101F	9b. OTHER REPORT NUMBER (Other number assigned to this report)	
13. Dod Subelement      681000	AFCRL-70-0137	
10. AVAILABILITY LIMITATION NOTICE		
2 - This document is subject to special export controls and each transmittal to foreign governments or foreign nationals may be made only with prior approval of AFCRL (CROA), L. G. Hanscom Field, Bedford, Massachusetts 01730.		
11. SUPPLEMENTARY NOTES	12. SPONSORING MILITARY ACTIVITY	
Multiple Reprints Included	Air Force Cambridge Research Laboratories (CRO) L. G. Hanscom Field Bedford, Massachusetts 01730	
13. ABSTRACT		
<p>This report presents atmospheric optical data collected at night in Thailand chiefly with airborne instruments during two field expeditions, one trip made during the wet monsoon season and one during the dry season. Results from eighteen flights are presented. The data include irradiance, directional reflectance of backgrounds, total scattering coefficients, atmospheric beam transmittance, path radiance, and directional path reflectance. Data for starlight, moonlight, and overcast conditions were derived for downward-looking paths of sight inclined at seven zenith angles (93°, 95°, 100°, 105°, 120°, 150°, and 180°) from altitudes of 1524 m and lower in five spectral regions, as follows: four narrow band optical filters with maximum transmittances at 475, 515, 660, and 745 nm; one broad band sensitivity representing the S-20 multiplier phototubes fitted with UV reflection filter. Simultaneous photoelectric (Royco) measurements of the distributions of atmosphere particle sizes are reported.</p>		

DD FORM 1473  
1 JAN 64UNCLASSIFIED  
Security Classification

UNCLASSIFIED  
Security Classification

14 KEY WORDS	LINK A		LINK B		LINK C	
	ROLE	WT	ROLE		ROLE	WT
Albedos Atmospheric Optics Atmospheric Scattering Coefficient Atmospheric Beam Transmittance Atmospheric Contrast Transmittance Nighttime Irradiance Nighttime Radiance Nighttime Optical Properties Path Reflectance Radiometry Terrain Reflectance						

UNCLASSIFIED  
Security Classification